

P • A • R • T • 6

# **SOIL IMPROVEMENT AND STABILIZATION**



---

# SECTION 6A

# NONGROUTING TECHNIQUES

---

EVERT C. LAWTON

<b>6A.1 INTRODUCTION</b>	<b>6.3</b>
<b>6A.2 OVEREXCAVATION/ REPLACEMENT</b>	<b>6.4</b>
<b>6A.2.1 Ultimate Bearing         Capacity</b>	<b>6.6</b>
<b>6A.2.2 Settlement</b>	<b>6.14</b>
<b>6A.2.3 Usefulness and Limitations         of the Finite Element         Method</b>	<b>6.30</b>
<b>6A.2.4 Limitations of the         Overexcavation/         Replacement Method</b>	<b>6.31</b>
<b>6A.3 NEAR-SURFACE         COMPACTION</b>	<b>6.37</b>
<b>6A.3.1 Equipment</b>	<b>6.39</b>
<b>6A.3.2 Moisture-Density         Relationships</b>	<b>6.53</b>
<b>6A.3.3 Laboratory Compaction and         Testing</b>	<b>6.54</b>
<b>6A.3.4 Engineering Properties and         Behavior of Compacted         Soils</b>	<b>6.69</b>
<b>6A.3.5 Quality Control and         Assurance</b>	<b>6.162</b>
<b>6A.4 DEEP COMPACTION</b>	<b>6.193</b>
<b>6A.4.1 Dynamic Compaction</b>	<b>6.193</b>
<b>6A.4.2 Vibro-Compaction</b>	<b>6.209</b>
<b>6A.4.3 Blast Densification</b>	<b>6.211</b>
<b>6A.5 GRANULAR COLUMNS</b>	<b>6.214</b>
<b>6A.5.1 Types of Granular         Columns</b>	<b>6.215</b>
<b>6A.5.2 Engineering         Characteristics, Response,         and Behavior</b>	<b>6.224</b>
<b>6A.6 PRECOMPRESSSION</b>	<b>6.250</b>
<b>6A.6.1 Types of Preloads</b>	<b>6.250</b>
<b>6A.6.2 Simple Precompression</b>	<b>6.251</b>
<b>6A.6.3 Precompression with         Additional Surcharge</b>	<b>6.255</b>
<b>6A.6.4 Precompression with         Vertical Drains</b>	<b>6.259</b>
<b>6A.6.5 Strength         Considerations</b>	<b>6.271</b>
<b>6A.6.6 Monitoring Field         Performance</b>	<b>6.271</b>
<b>6A.7 CHEMICAL STABILIZATION</b>	<b>6.271</b>
<b>6A.7.1 Chemicals and Reactions</b>	<b>6.272</b>
<b>6A.7.2 Engineering Properties and         Behavior of Chemically         Stabilized Soils</b>	<b>6.291</b>
<b>6A.7.3 Construction Methods</b>	<b>6.317</b>
<b>6A.8 MOISTURE BARRIERS</b>	<b>6.326</b>
<b>6A.8.1 Horizontal Barriers</b>	<b>6.327</b>
<b>6A.8.2 Vertical Barriers</b>	<b>6.329</b>
<b>REFERENCES</b>	<b>6.329</b>

---

## 6A.1 INTRODUCTION

---

Increasing urbanization continues to occur throughout much of the world, and at this time this trend appears likely to continue for at least the near future. As the population grows in any metropolitan area, a variety of additional facilities are needed to serve these people. Many of these facilities are in the form of structures—such as houses, apartment buildings, restaurants, and office buildings—that occupy areas within the metropolis. The additional space required for these structures is generally obtained in three ways: (a) Existing structures are torn down to make room for new structures; (b) new structures are built on land within the existing metropolitan boundaries that were previously “unimproved” (relative term); and (c) the boundaries of the metropolis are expanded to provide additional land for development.

One of the primary criteria used to select a site for development is the suitability of the ground for supporting the structure to be built. In most urban areas, the best sites were developed first, and, as urbanization continues, when a previously undeveloped site is purchased, the engineering properties of the existing near-surface materials are often such that the structure cannot be supported by

**6.4 SOIL IMPROVEMENT AND STABILIZATION**

shallow foundations. The traditional solution for these situations is to support the structures on deep foundations—typically piles or drilled piers—where a small portion of the load is transmitted to the poorer near-surface materials and a large portion of the load is transmitted to better bearing materials deeper within the ground. However, even with the development and use of more economical types of deep foundations such as auger-cast piles, the demand has increased for more economical solutions to the unsuitability of near-surface soils for shallow foundations.

To meet this demand, numerous soil stabilization and improvement techniques (also commonly called *ground modification techniques*) have been developed within the past 25 years or so. These techniques involve modifying the engineering properties and behavior of the near-surface soils at a site so that shallow foundations can be used where they previously could not or in some instances so that more economical shallow foundations can be used. The state of the art in this field is currently changing so fast that it is difficult, if not impossible, for any one person to keep up with it. It is likely that significant new technologies or modifications to existing technologies will have occurred between the time of writing and the time of publication of this handbook. Therefore, it is incumbent upon the reader to review the literature frequently to keep up with developments and changes in ground modification techniques.

Many of the techniques described in this section have proprietary restrictions to their use. In many instances, the restrictions are not in the use of the method itself but in other areas such as in the manufacture of a material or product used in the technique or in equipment used to perform the modifications to the soil or to install a particular product. Because patents associated with ground improvement techniques are continuously expiring and new patents are being obtained, it would be onerous and unfruitful to attempt to describe all these restrictions. Few patents are worldwide, and certain restrictions that apply in one country may not apply in the country where the project is being undertaken. Therefore, anyone who wishes to use or recommend the use of a particular soil improvement technique for a project should first perform a thorough examination of all potential proprietary restrictions associated with that technique.

Although many techniques are currently available, and more are likely to become available, not all techniques are appropriate for every project. The primary responsibilities of the foundation engineer, therefore, are to (a) determine which techniques can be used to safely support the structure; (b) determine which of the suitable methods is most economical for the project; (c) design or supervise the design of the details for the technique that best meets criteria (a) and (b); and (d) ensure that the actual modifications produce the desired result. In some instances, especially where proprietary restrictions are involved, the company or individuals who developed a particular method may require that they perform the design themselves, so that the project foundation engineer's responsibility is to ensure that the design prepared by the company meets criteria (a) and (b) and that the final product achieves the desired objectives stated in the specifications.

In keeping with the goals of this handbook, soil improvement and stabilization techniques that are applicable to buildings are discussed in this chapter. The chapter is divided into two main sections—nongrouting and grouting techniques. These two sections are organized according to type of technique. In building applications, the most important static properties for bearing soils are strength, compressibility, drainage characteristics (permeability), and potential for wetting- and drying-induced volume changes. In seismically active regions, liquefaction potential of saturated silty sands and sands is extremely important. The discussions in this chapter are primarily aimed at showing how each technique can be used to improve one or more of these properties.

**6A.2 OVEREXCAVATION/REPLACEMENT**

The technique of overexcavation/replacement is one of the oldest, most intuitive, and simplest methods for modifying bearing materials to increase support for shallow foundations. The method consists of excavating poor or inadequate bearing material and replacing it with a stiffer and stronger material (see Fig. 6A.1). As long as the in-place replacement material is stiffer and stronger than the

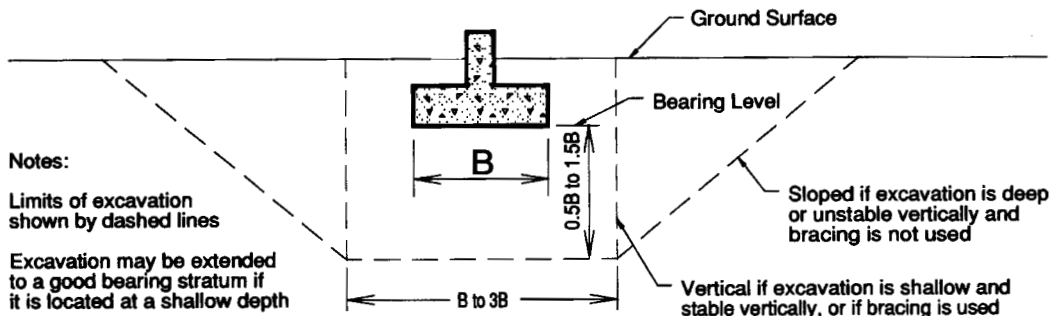


**FIGURE 6A.1** Typical dimensions of excavation for overexcavation/replacement.

excavated bearing soil, the settlement that the foundation undergoes when loaded is reduced and the factor of safety against ultimate bearing capacity failure is increased. The greater the stiffness and strength of the replacement material, the greater the reduction in settlement and increase in ultimate bearing capacity.

Overexcavation/replacement is most commonly used when the bearing soils are very weak and highly compressible. The replacement material can be the excavated material that has been modified in some way, or it can be borrow material (obtained from another location on or off the site). The replacement material is usually sand, gravel, or a sand-gravel mixture, especially in situations where the ground-water table is high or when it is desirable to have a free-draining bearing material. To obtain the stiffest and strongest material possible, the replaced sand or gravel is usually compacted in lifts during the replacement process. If good-quality sands and gravels are not readily or economically available, the excavated soils can be chemically stabilized and used as the replacement material. However, chemically stabilized soils are generally not free-draining (they have relatively low permeabilities), so their use as a replacement material may change the local or regional ground-water seepage and precipitation infiltration patterns, which may be an environmental consideration in some instances. It is also possible to use the excavated soil as the replacement material without chemically modifying it, although this is seldom done. If the inadequate bearing soil is cohesionless, several techniques are available for densifying in situ soil that are more economical than removing, drying or wetting, replacing, and compacting it. Cohesive soils can be excavated, dried, and compacted at an appropriate water content to produce a material that is initially stiff and strong, but these soils may be susceptible to wetting-induced volume changes and reductions in stiffness and strength from wetting (see Sec. 6A.3.4).

The excavation is deeper and often wider than is needed to place the foundation, hence the term overexcavation. Typical dimensions for an overexcavation are shown in Fig. 6A.1. The width of the bottom of the excavation typically varies from one to three times the width of the foundation ( $B$  to  $3B$  in Fig. 6A.1), and the depth below the bearing level is generally about  $\frac{1}{2}$  to  $1\frac{1}{2}$  times the foundation width ( $0.5B$  to  $1.5B$ ). If a good bearing stratum (medium dense sand, dense sand, gravel, or bedrock) exists close to the bearing level, the excavation is usually taken to the top of the bearing stratum or a shallow depth into it.

The replacement material is usually compacted so that the replaced zone is as stiff and strong as possible. A variety of compaction procedures can be used. If the excavation is narrow and shallow, hand-operated compaction equipment appropriate for confined areas is used, including rammers, tampers, vibrating plates, and small rollers (see Sec. 6A.3.1). For deep, narrow excavations, backhoes or hydraulic excavators with special compaction attachments can be used. Other techniques include pounding the material with the bucket of a backhoe and dropping a weight from a crane. For wide excavations, full-size compaction rollers are normally used.

## 6.6 SOIL IMPROVEMENT AND STABILIZATION

### 6A.2.1 Ultimate Bearing Capacity

When the overexcavation/replacement process is properly designed and implemented, it results in a composite bearing zone that is stronger and stiffer than the unreinforced material. An increase in ultimate bearing capacity occurs because the potential failure surface must pass either through or around the stronger replaced zone. Three possible failure methods are shown in Fig. 6A.2 for a foundation bearing on a strong replaced zone of finite width and depth. It is possible (but unlikely) that the most critical failure surface is a general bearing failure surface that develops through the replaced zone and into the in situ soil [Fig. 6A.2(a)]; a theoretical solution for this case where the foundation bears on a long (continuous) granular trench within a soft saturated clay matrix immediately after loading (the clay is undrained) has been given by Madhav and Vitkar (1978). Their solution is presented in the form of charts from which modified bearing capacity factors ( $N_{ct}$ ,  $N_{qt}$ , and  $N_{\gamma}$ ) can be obtained (Fig. 6A.3). These factors are valid for the following conditions:

1. The width of the granular trench ( $W$ ) varies from zero (no trench) to twice the foundation width ( $2B$ ).
2. The friction angle for the granular trench material ( $\phi_1$ ) varies from  $20^\circ$  to  $50^\circ$ , and the cohesion intercept ( $c_1$ ) varies from zero to the same value as for the clay matrix ( $c_2$ ).
3. The clay matrix is undrained ( $\phi_2 = 0$ ,  $c_2$  = undrained shear strength =  $s_u$ ).
4. The unit weights of the granular trench material and the clay matrix are the same ( $\gamma_1 = \gamma_2$ ).

With these factors, the ultimate bearing capacity ( $q_{ult}$ ) can be predicted from the following equation, which has the same form as the general bearing capacity equations for homogeneous bearing soil:

$$q_{ult} = c_2 N_{ct} + q N_{qt} + 0.5 \gamma_2 B N_{\gamma} \quad (6A.1)$$

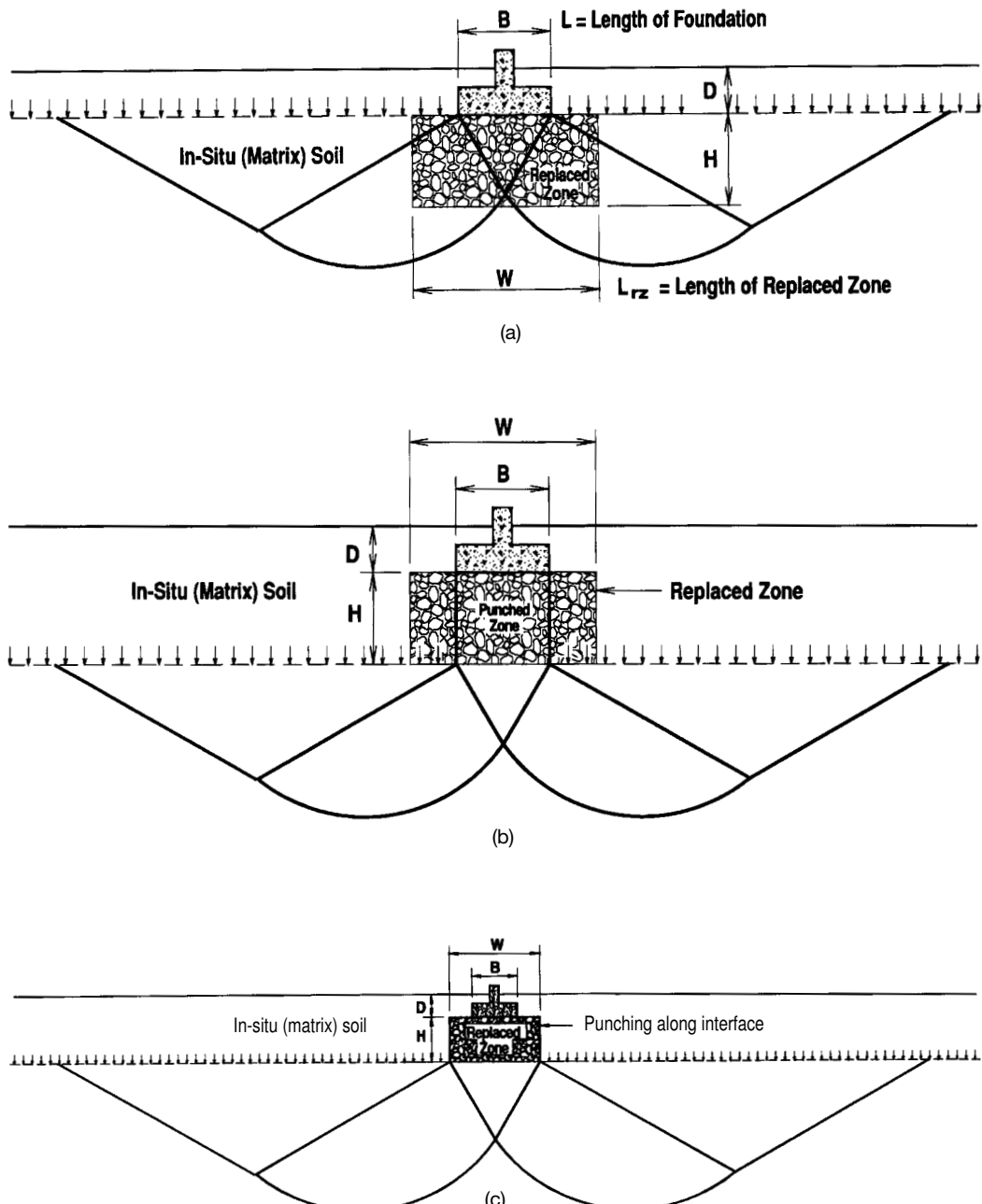
Hamed and coworkers (1986) conducted laboratory model tests to determine the variation in  $q_{ult}$  for a continuous foundation bearing on a granular trench ( $W = B$ ) constructed within a soft clay matrix. By comparing their experimental values of  $q_{ult}$  with values predicted from Eq. (6A.1) (see Fig. 6A.4), Hamed and colleagues concluded that Madhav and Vitkar's theory overpredicts  $q_{ult}$ . In addition, they found that the minimum height of the granular trench necessary to obtain the maximum value of  $q_{ult}$  is about  $3B$ . Hamed and colleagues also developed their own theory for  $q_{ult}$  based on the following assumptions:

1. Failure occurs by bulging at the bearing level along the interface between the trench and matrix materials.
2. Undrained conditions exist at failure in the saturated clay matrix.
3. The principal planes at the failure point are horizontal and vertical in both the trench and matrix materials.
4. The horizontal stress ( $\sigma_h$ ) in the trench material is the minor principal stress ( $\sigma_3$ );  $\sigma_h$  in the matrix material is the major principal stress ( $\sigma_1$ ). These two values of  $\sigma_h$  are equal.

From these assumptions, the following equation for  $q_{ult}$  was derived:

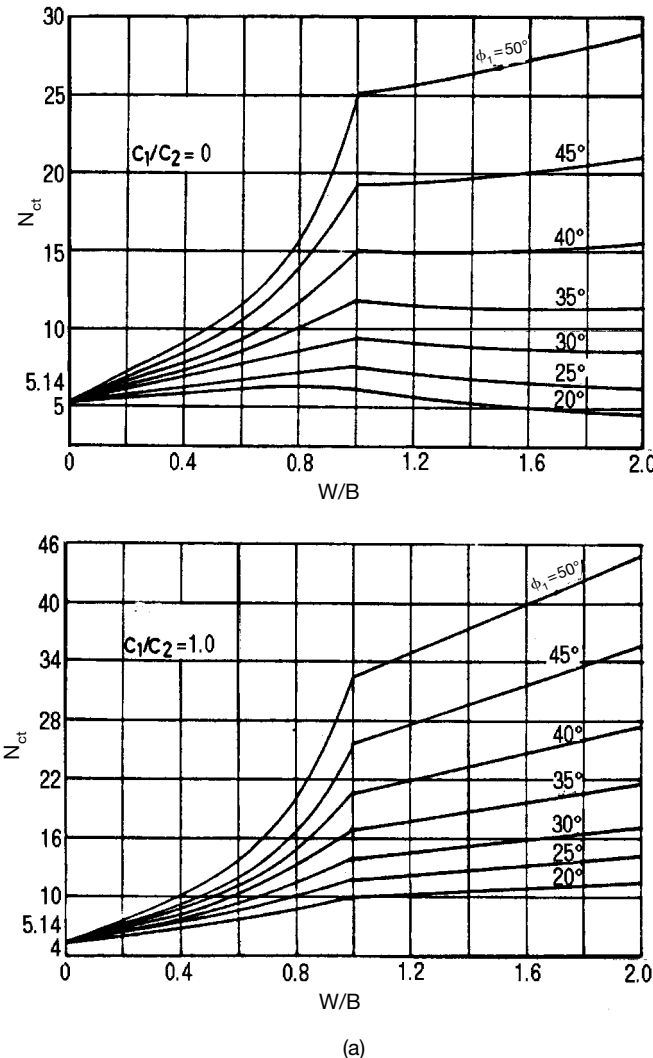
$$q_{ult} = (\gamma_2 D + 2s_u) \tan^2 \left( 45^\circ + \frac{\phi_1}{2} \right) \quad (6A.2)$$

A comparison of the maximum experimental values of  $q_{ult}$  with values calculated from Eq. (6A.2) (Fig. 6A.4) suggests that this theory provides a reasonable (but probably somewhat conservative) estimate of  $q_{ult}$  for  $W = B$  and  $H/B \geq 3$ .



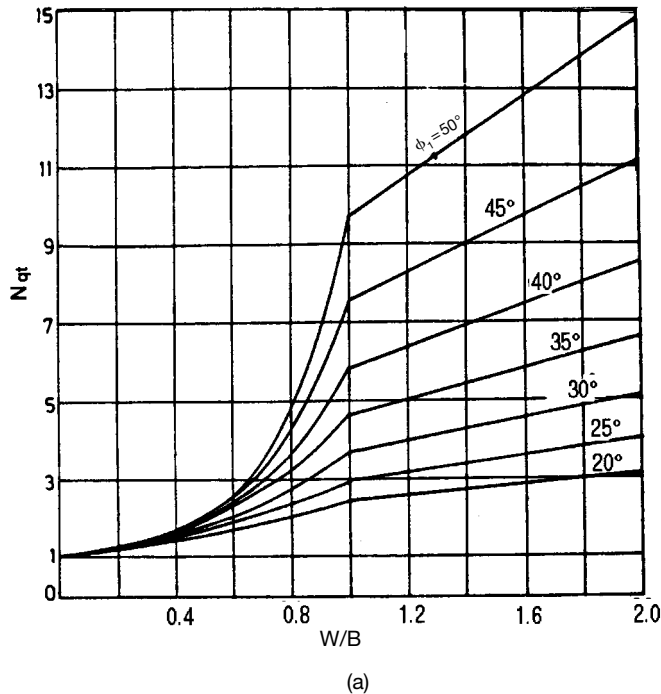
**FIGURE 6A.2** Potential bearing shear failure mechanisms for foundation supported by overexcavated and replaced zone: (a) general shear failure through replaced zone and in situ soil; (b) punching failure through replaced zone; (c) punching failure of replaced zone through in situ soil.

## 6.8 SOIL IMPROVEMENT AND STABILIZATION



**FIGURE 6A.3** Bearing capacity factors for general shear failure in a weak clay stabilized with a granular trench (from Madhav and Vitkar, 1978): (a)  $N_{cP}$  (b)  $N_{qP}$  (c)  $N_{\gamma P}$ .

If the in situ soil is a moderate or stiff clay or a granular soil, it is likely that failure would occur by punching through or around the perimeter of the replaced zone combined with general shear failure in the underlying in situ soil [Fig. 6A.2(b) and (c)]. The wider the replaced zone is, the more likely that punching failure would occur through it rather than around it. If it is not apparent which punching mechanism is more likely to occur, estimates of  $q_{ult}$  for both types can be determined and the lesser value used for design. It is also possible that general shear failure would occur completely within the replaced zone ( $q_{rz}$ ), but this is not likely unless the replaced zone is deep and wide. It is

**FIGURE 6A.3 (Continued)**

prudent, however, to calculate  $q_{rz}$  in all cases to ensure that the computed values of  $q_{ult}$  for the two punching cases are less than  $q_{rz}$ .

For punching through the replaced zone [Fig. 6A.2(b)], the following equation based on Meyerhof and coworkers (Meyerhof and Hanna, 1978; Valsangkar and Meyerhof 1979) and Bowles (1988) can be used to estimate  $q_{ult}$ :

$$q_{ult} = q_b + \frac{pP_h \tan \phi_1 + pHc_1 - W_{pz}}{A_f} \leq q_{rz} \quad (6A.3a)$$

where  $q_b$  = ultimate bearing capacity of the in situ soil beneath the replaced zone based on the dimensions of the foundation

$p$  = perimeter length of the punched zone =  $2(B + L)$  for a rectangular foundation or  $\pi d_0$  for a circular foundation (where  $d_0$  diameter)

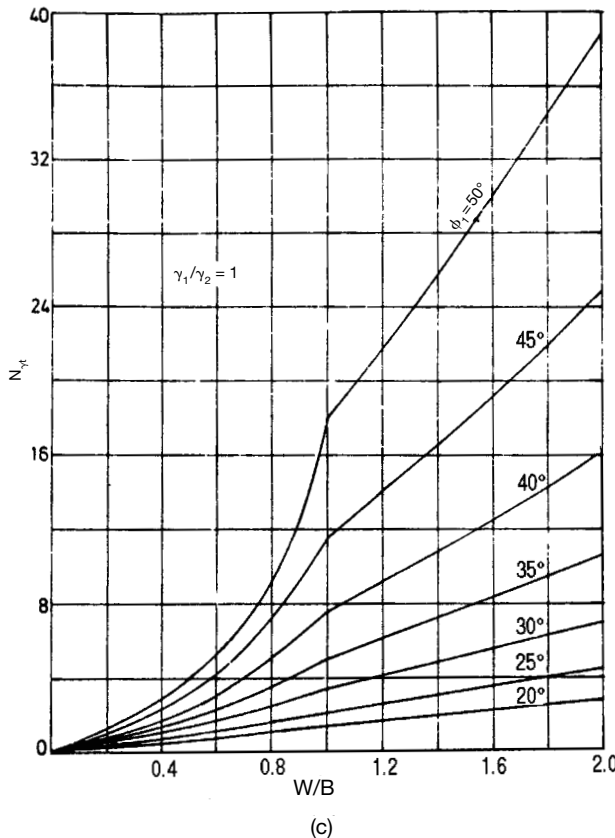
$P_h$  = lateral earth pressure thrust (force per unit horizontal length) acting along the perimeter surface of the punched zone at failure =  $\int_0^H K_s \sigma_v dH$

$K_s$  = lateral earth pressure coefficient along the perimeter surface of the punched zone at failure

$W_{pz}$  = weight of the material in the punched zone

$A_f$  = area of the foundation =  $BL$  for rectangular and  $0.25\pi d_0^2$  for circular

$q_{rz}$  = ultimate bearing capacity for general shear failure within the replaced zone

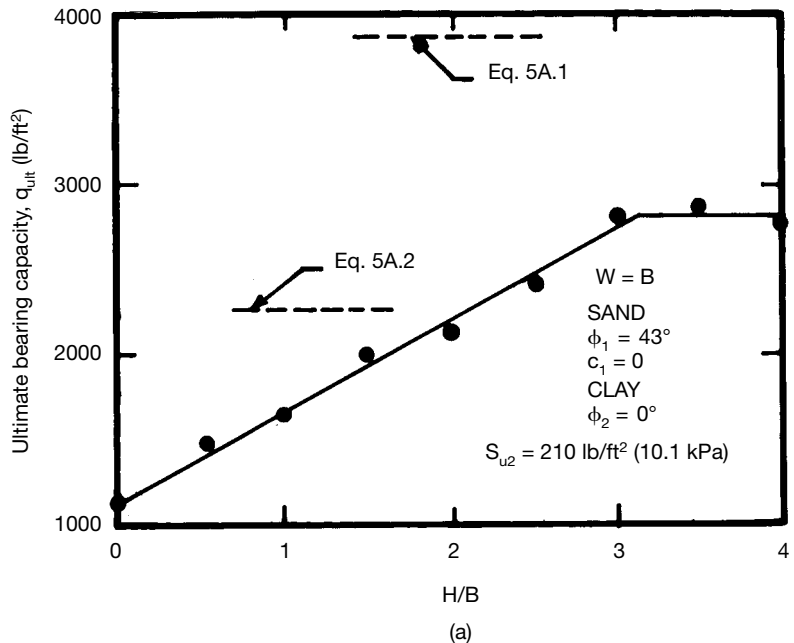
**6.10** SOIL IMPROVEMENT AND STABILIZATION**FIGURE 6A.3** (Continued)

If the ground-water table is below the lowest point on the potential failure surface, the following equations apply:

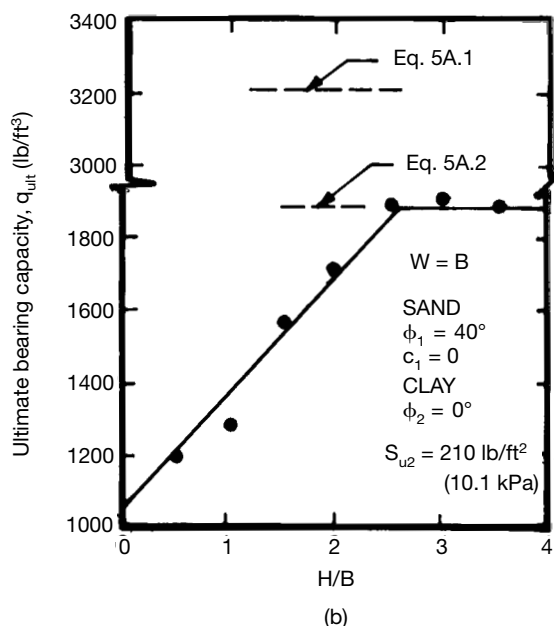
$$q_b = c_2 N_{c2} S_{c2} D_{c2} + \gamma_2 (D + H) N_{q2} S_{q2} D_{q2} + 0.5 \gamma_2 B N_{\gamma2} S_{\gamma2} D_{\gamma2} \quad (6A.3b)$$

where  $N_{c2}$ ,  $N_{q2}$ ,  $N_{\gamma2}$  are bearing capacity factors (see Sec. 2B) for general shear failure in the in situ soil beneath the punched zone based on  $\phi_2$  and  $S_{c2}$ ,  $S_{q2}$ ,  $S_{\gamma2}$  are shape factors and  $D_{c2}$ ,  $D_{q2}$ ,  $D_{\gamma2}$  are depth factors (see Sec. 2B) based on the dimensions of the foundation and an embedded depth of  $(D + H)$ .

The use of  $\gamma_2$  for the  $N_{q2}$  term in Eq. (6A.3b) is conservative if  $W$  is greater than  $B$ , because a portion of the surcharge soil for the general failure surface beneath the punched zone consists of the replacement material ( $\gamma_1$ ), which in most cases is denser than the in situ soil ( $\gamma_1 > \gamma_2$ ). The wider the replaced zone, the more conservative is the use of  $\gamma_2$  in the  $N_{q2}$  term. If desired, an equivalent unit weight can be calculated that accounts for the relative portions of the replacement material and in situ soil that are in the surcharge zone, but this refinement is probably not necessary in most instances.



(a)



(b)

**FIGURE 6A.4** Ultimate bearing capacity of a model continuous foundation on a granular trench within a soft clay matrix (from Hamed and coworkers, 1986): (a) trench material is dense sand. (b) Trench material is medium dense sand.

## 6.12 SOIL IMPROVEMENT AND STABILIZATION

$$q_{rz} = c_1 N_{c1} S_{c1} D_{c1} + \gamma_2 D N_{q1} S_{q1} D_{q1} + 0.5 \gamma_1 B N_{y1} S_{y1} D_{y1} \quad (6A.3c)$$

where  $N_{c1}$ ,  $N_{q1}$ ,  $N_{y1}$  are bearing capacity factors for general shear failure within the replaced zone based on  $\phi_1$  and  $S_{c1}$ ,  $S_{q1}$ ,  $S_{y1}$  are shape factors and  $D_{c1}$ ,  $D_{q1}$ ,  $D_{y1}$  are depth factors based on the dimensions of the foundation and an embedded depth of  $D$ . In addition,

$$W_{pz} = BLH\gamma_1 \quad \text{for a rectangular foundation} \quad (6A.3d.1)$$

$$W_{pz} = 0.25\pi d_0^2 H\gamma_1 \quad \text{for a circular foundation} \quad (6A.3d.2)$$

If  $K_s$  is assumed to be constant at all depths along the perimeter surface of the punched zone, the following equation applies for  $P_h$ :

$$P_h = K_s(\gamma_2 DH + 0.5\gamma_1 H^2) \quad (6A.3e)$$

If the ground-water table is within the potential failure zone, its influence on the effective stresses and unit weights (and hence  $q_b$ ,  $q_{rz}$ ,  $W_{pz}$ , and  $P_h$ ) must be considered, which may alter Eqs. (6A.3b), (6A.3c), (6A.3d), and (6A.3e).

Selection of a value for  $K_s$  is not necessarily simple.  $K_s$  probably varies along the depth of the punched zone, so if one value is selected, it constitutes an average or equivalent value. Meyerhof and Hanna (1978) provided values of  $K_s$  as a function of  $\phi_1$  and  $q_2/q_1$  for the case of a continuous foundation bearing on a strong layer of infinite horizontal extent overlying a weak layer (Fig. 6A.5);  $q_1$  and  $q_2$  are the ultimate bearing capacities for a continuous foundation of width  $B$  under a vertical centric load on the surfaces of homogeneous thick deposits of the strong and weak soils and can be calculated from the following equations:

$$q_1 = c_1 N_{c1} + 0.5 \gamma_1 B N_{y1} \quad (6A.4a)$$

$$q_2 = c_2 N_{c2} + 0.5 \gamma_2 B N_{y2} \quad (6A.4b)$$

Thus, the term  $q_2/q_1$  represents the relative strengths of the weaker and stronger materials, with  $q_2/q_1 = 1$  representing soils of the same strength and  $q_2/q_1 = 0$  corresponding to a strong soil that is infinitely stronger than the weak soil.

Values for  $K_s$  can be selected from Fig. 6A.5 but should be used with caution, since these values do not strictly apply to either finite length foundations or a replaced zone of finite width. The reader should also note that  $K_s$  does not equal Rankine's  $K_p = \tan^2(45^\circ + \phi_1/2)$  for two reasons: (a) Shear stresses develop along the vertical punched perimeter, and therefore  $\sigma_h$  and  $\sigma_v$  cannot be principal stresses as was assumed by Rankine; and (b) values of  $\sigma_v$  along the punched perimeter are likely to be higher than calculated from the weights of the overburden material owing to the application of the foundation load and the shearing action along the punched perimeter which therefore increases  $\sigma_h$ . Item (a) tends to reduce the value of  $K_s$ , whereas item (b) tends to raise it. Hence,  $K_s$  may be either greater or lesser than  $K_p$  when  $K_p$  is based on  $\sigma_v$  calculated from the weights of the overburden materials [as in Eq. (6A.3e)]; for example, the values of  $K_s$  for  $\phi_1 = 30^\circ$  in Fig. 6A.5 range from about 1.0 for  $q_2/q_1 = 0$  to about 5.6 for  $q_2/q_1 = 1$ , while  $K_p = 3.0$ . If a conservative value is desired,  $K_s$  can be assumed equal to the at-rest coefficient for normally consolidated soils ( $K_{0-nc}$ ):

$$K_s = K_{0-nc} = 1 - \sin \phi_1 \quad (6A.5)$$

It is unlikely that  $K_s$  would ever be less than  $K_{0-nc}$ . For a design situation, a better estimate of  $K_s$  can be obtained from Fig. 6A.5 than from Eq. (6A.5) so long as a reasonable factor of safety is applied to  $q_{ult}$ .

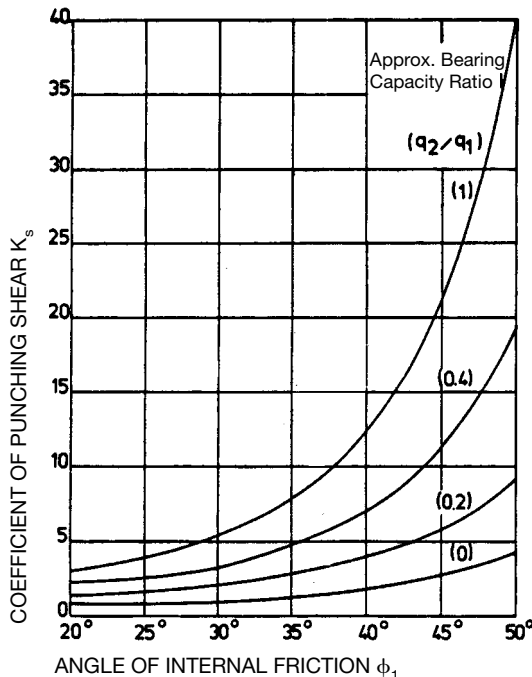


**FIGURE 6A.5** Coefficients of punching shear resistance under vertical load (from Meyerhof and Hanna, 1978).

If the replaced zone punches through the matrix soil [Fig. 6A.2(c)], punching resistance will develop within the in situ soil adjacent to the vertical perimeter surface of the replaced zone. The following equation applies to this case:

$$q_b = q_b \cdot \frac{A_{rz}}{A_f} + \frac{pP_h \tan \phi_2 + pHc_2 - W_{rz}}{A_f} \leq q_{rz} \quad (6A.6a)$$

where  $q_b$  = ultimate bearing capacity of the in situ soil beneath the replaced zone based on the dimensions of the replaced zone

$p$  = perimeter length of the replaced zone =  $2(W + L_{rz})$  for a rectangular replaced zone  
(where  $L_{rz}$  is the length of the replaced zone) and  $\pi d_{rz}$  for a circular replaced zone  
(where  $d_{rz}$  is the diameter of the replaced zone)

$P_h$  = lateral earth pressure thrust (force per unit length) acting along the perimeter surface of the replaced zone at failure =  $\int_0^H K_s \sigma_v dH$

$K_s$  = lateral earth pressure coefficient along the perimeter surface of the replaced zone at failure

$W_{rz}$  = weight of the material in the replaced zone

$A_{rz}$  = area of the replaced zone =  $WL_{rz}$  for a rectangular zone and  $0.25\pi d_{rz}^2$  for a circular zone

$q_{rz}$  = ultimate bearing capacity for general shear failure within the replaced zone [from Eq. (6A.3c)]

## 6.14 SOIL IMPROVEMENT AND STABILIZATION

If the ground-water table is below the lowest point on the potential failure surface, the following equations apply:

$$q_b = c_2 N_{c2} S_{c2} D_{c2} + \gamma_2 (D + H) N_{q2} S_{q2} D_{q2} + 0.5 \gamma_2 W N_{\gamma2} S_{\gamma2} D_{\gamma2} \quad (6A.6b)$$

where  $N_{c2}$ ,  $N_{q2}$ ,  $N_{\gamma2}$  are bearing capacity factors for general shear failure in the in situ soil beneath the replaced zone based on  $\phi_2$  and  $S_{c2}$ ,  $S_{q2}$ ,  $S_{\gamma2}$  are shape factors and  $D_{c2}$ ,  $D_{q2}$ ,  $D_{\gamma2}$  are depth factors based on the dimensions of the replaced zone and an embedded depth of  $(D + H)$ . In addition,

$$W_{rz} = WL_{rz}H\gamma_1 \quad \text{for a rectangular replaced zone} \quad (6A.6c.1)$$

$$W_{rz} = 0.25\pi d_{rz}^2 H\gamma_1 \quad \text{for a circular replaced zone} \quad (6A.6c.2)$$

If  $K_s$  is assumed to be constant at all depths along the perimeter surface of the replaced zone, the following equation applies for  $P_h$ :

$$P_h = K_s (\gamma_2 DH + 0.5 \gamma_2 H^2) = K_s \gamma_2 (DH + 0.5H^2) \quad (6A.6d)$$

Values for  $K_s$  can be obtained from Fig. 6A.5 for  $q_1 = q_2$  (since passive resistance develops within the in situ soil) or by assuming  $K_s = K_{0-nc}$  and using the following equation:

$$K_s = K_{0-nc} = 1 - \sin \phi_2 \quad (6A.7)$$

The method employed to obtain the friction angles used in Eqs. (6A.3) through (6A.7) should model the type of failure assumed in each equation. Values of  $\phi_1$  in Eq. (6A.3a) and  $\phi_2$  in Eq. (6A.6a) obtained from direct shear tests would be appropriate. Values of  $\phi_1$  or  $\phi_2$  used to calculate factors in the other equations should be axisymmetric (triaxial) values if the foundation or replaced zone is square or circular or plane-strain if rectangular and  $L/B$  or  $L_{rz}/W$  is greater than about 5. Most values for  $\phi$  found in tables based on relative density or Standard Penetration Test (SPT) blow-counts are correlated to triaxial values. Conservative values for plane-strain friction angle ( $\phi_{ps}$ ) can be estimated from triaxial values ( $\phi_{tx}$ ) using the following equations (Lade and Lee, 1976):

$$\phi_{ps} = \phi_{tx} \quad \text{for } \phi_{tx} \leq 34^\circ \quad (6A.8a)$$

$$\phi_{ps} = 1.5\phi_{tx} - 17^\circ \quad \text{for } \phi_{tx} > 34^\circ \quad (6A.8b)$$

Values of  $\phi$  from direct shear tests are usually about  $1^\circ$  or  $2^\circ$  greater than  $\phi_{tx}$  for the same range of confining stresses.

### 6A.2.2 Settlement

When properly designed and implemented, overexcavation and replacement results in reduced settlement owing to one or both of the following factors: (a) The replaced zone is stiffer so it settles less than the replaced in situ soil would have, and (b) the vertical stresses induced in the in situ soil beneath the replaced zone may be less than without the replaced zone, so the settlement of this underlying soil may also be less. As will be discussed subsequently, the vertical stresses induced in the underlying in situ soil may be greater with a replaced zone than without it, so care must be exercised when using overexcavation/replacement where saturated fine-grained soils are within the zone of influence for settlement.

Several solutions are available in the literature to calculate settlement for a uniform, circular load on the surface of two- and three-layer elastic systems (e.g. Burmister, 1945; Burmister, 1962; Thenn de Barros, 1966; Ueshita and Meyerhof, 1967). The solutions for two-layer systems take the following general form:

$$S_i = \frac{q_0 d_0}{E_2} I_s \quad (6A.9)$$

where  $q_0$  = uniform stress applied to the surface of the uppermost layer

$d_0$  = diameter of the loaded area

$E_2$  = stress-strain modulus for the lower layer

$I_s$  = influence factor for settlement beneath the center of the loaded area

The magnitude of  $I_s$  depends on the height of the stiff layer relative to the diameter of the loaded area ( $H/d_0$ ), the modulus ratio for the two layers ( $E_2/E_1$ ), and the Poisson's ratios for the two layers ( $\nu_1, \nu_2$ ). Values of  $I_s$  for a two-layer system with  $\nu_1 = 0.2$  and  $\nu_2 = 0.4$  are given in Fig. 6A.6 (Burmister, 1962), from which it can be seen that settlement decreases as  $E_1/E_2$  increases or  $H/d_0$  increases.

The applicability of charts such as Fig. 6A.6 for estimating the settlement of a foundation bearing on a replaced zone is limited in the following ways:

1. The charts are not applicable to replaced zones of finite width unless the replaced zone is wide enough to get the full reduction in settlement.
2. Embedment of the foundation, which results in reduced settlement, is not considered.
3. The possible existence of a rigid base (such as bedrock) within the zone of influence, which also reduces settlement, is not considered.
4. The charts apply only to foundations with circular or square shapes. (Square foundations can be considered by converting to an equivalent circle with the same area.)

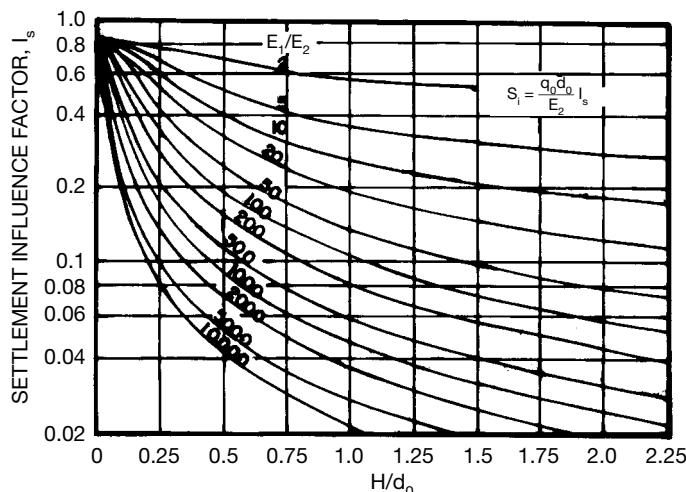


**FIGURE 6A.6** Settlement influence factors for a circular, uniform load on the surface of a two-layer elastic system ( $\nu_1 = 0.2, \nu_2 = 0.4$ ) (from Burmister, 1962).

## 6.16 SOIL IMPROVEMENT AND STABILIZATION

No solutions are available in the literature to estimate settlement for a replaced zone of finite width or for infinitely wide layered soils when the foundation is either embedded or rectangular. Solutions are available for calculating immediate settlement for semi-infinite, homogeneous soils that consider the effect of depth of embedment for both circular and rectangular foundations [Nishida (1966) for circular and E. Fox (1948) for rectangular]. Settlement of a circular foundation bearing on the *surface* of a two-layer system underlain by a rough, rigid base can be estimated from the influence chart or tables given in Uzan and coworkers (1980). An extensive collection of elastic solutions for stresses and displacements of geologic materials can be found in Poulos and Davis (1974).

The induced vertical stresses ( $\Delta\sigma_z$ ) in a two-layer elastic system subjected to a uniform, circular stress on the surface of the upper layer are shown in Fig. 6A.7 for  $v_1 = v_2 = 0.5$  and the following two

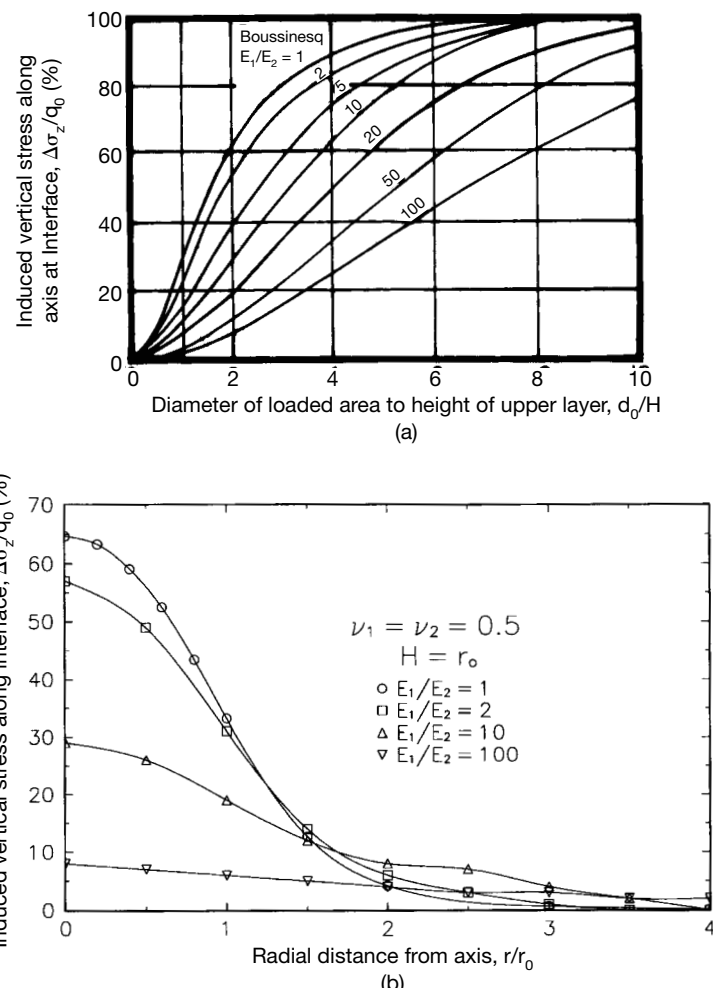


**FIGURE 6A.7** Induced stresses along the interface of a two-layer elastic system subjected to a circular, uniform load on the surface ( $v_1 = v_2 = 0.5$ ): (a) along axis for varying  $d_0/H$  and  $E_1/E_2$  (from Burmister, 1958); (b) as a function of  $r/r_0$  and  $E_1/E_2$  for  $H = r_0$  (data from L. Fox, 1948).

distributions: (a) Along the axis at the interface between the two layers as a function of  $d_0/H$  and  $E_1/E_2$ , and (b) horizontal distribution along the interface for  $H = r_0$  and varying  $E_1/E_2$ . Figure 6A.7 shows that increasing either the height or the stiffness of the upper layer distributes the load over a larger area and reduces the maximum  $\Delta\sigma_z$  (along the axis of the loaded area). To obtain an estimate of the approximate slope of the vertical stress distribution [ $\alpha$ (vertical):1(horizontal)] as a function of  $E_1/E_2$ , the curves in Fig. 6A.7 were integrated numerically by the author to determine the radial distance within which 95% of the applied load is distributed, with the results shown in Fig. 6A.8. This technique is similar in concept to the 2:1 or 60° stress distribution methods. Thus, an estimate of the minimum dimensions of the replaced zone needed to obtain the full reduction in settlement can be determined with the aid of Fig. 6A.8 and the following equations. For a rectangular foundation use

$$W \geq B + \frac{2H}{\alpha} \quad (6A.10a.1)$$

$$L_{rz} \geq L + \frac{2H}{\alpha} \quad (6A.10a.2)$$

For a circular foundation use

$$d_{rz} \geq d_0 + \frac{2H}{\alpha} \quad (6A.10b)$$

In many cases where overexcavation/replacement is used, the replaced zone is not wide enough to develop the full reduction in settlement. As an example, consider the case of a circular foundation bearing on a cylindrical replaced zone with  $H = d_0$ , and  $E_1/E_2 = 20$ . From Fig. 6A.8:

$$\alpha \approx 0.42$$

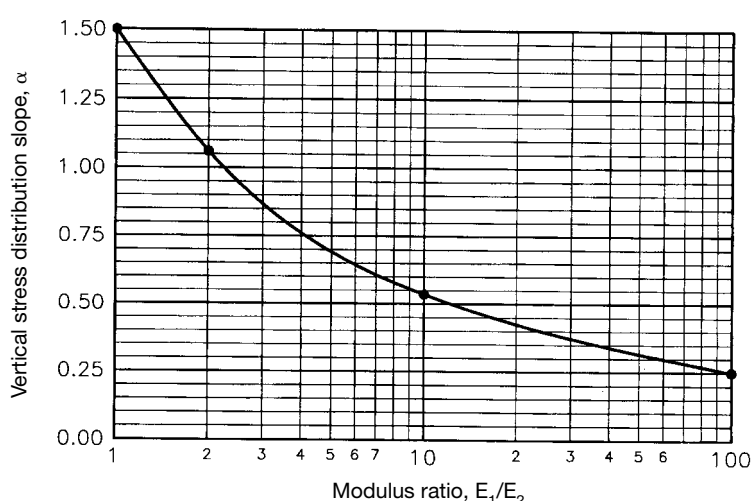


**FIGURE 6A.8** Vertical stress distribution slope for a two-layer elastic system.

**6.18** SOIL IMPROVEMENT AND STABILIZATION

From Eq. (6A.10b):

$$d_{rz} \geq d_0 + \frac{2d_0}{0.42} = 5.8d_0$$

$d_{rz}$  is typically in the range of  $d_0$  to  $3d_0$ , which is less than the minimum diameter of about  $5.8d_0$  required for full reduction in settlement. Estimating  $S_i$  from Fig. 6A.6 and Eq. (6A.9) for this case would therefore tend to underestimate the settlement.

To determine the influences of depth of embedment and width, height, and stiffness of the replaced zone on  $S_i$ , a parametric finite element study was performed by the author for a flexible, uniform, circular stress applied to the surface of a cylindrical replaced zone ( $v_1 = 0.2$ ) within an otherwise homogeneous, isotropic, elastic soil mass ( $v_2 = 0.4$ ). In this investigation, the following values of parameters were used:

$$\frac{E_1}{E_2} = 5, 10, 20, 50, \text{ and } 100$$

$$\frac{D}{d_0} = 0, 0.5, 1.0, \text{ and } 1.5$$

$$\frac{H}{d_0} = 0.5, 1.0, \text{ and } 1.5$$

$$\frac{d_{rz}}{d_0} = 0.25, 0.5, 0.75, 1, 2, 3, 4, 6, 8, \text{ and } 10$$

The results are presented in Table 6A.1 in the form of settlement influence factors ( $I_s$ ), which can be used in Eq. (6A.9) to estimate  $S_i$  for an embedded circular or square foundation bearing on a finite-width replaced zone within a relatively homogeneous in situ soil. Values of  $I_s$  are given for settlement at the center of the loaded area and the mean settlement over the entire loaded area. The values of mean  $I_s$  represent a better estimate for real foundations, which are neither perfectly flexible nor perfectly rigid. The values of  $I_s$  at the center of the loaded area for  $d_{rz}/d_0 = 10$  in Table 6A.1 match the corresponding theoretical values for an infinitely wide upper layer obtained from Fig. 6A.6. In addition, the values of central  $I_s$  for a homogeneous soil ( $E_1/E_2 = 1$ ) are within 2% of the theoretical values obtained from Nishida's (1966) equations for a uniform, circular stress embedded within a homogeneous half-space. These comparisons indicate that the finite element results are reasonable.

The values of  $v_1 = 0.2$  and  $v_2 = 0.4$  used in the parametric study were selected as reasonable estimates for most overexcavation/replacement cases. For other values of  $v_1$  and  $v_2$ , adjustments may be needed to the values shown in Table 6A.1. A limited investigation has indicated that  $v_2$  has a significant influence on  $S$  but that  $v_1$  has very little effect. This can be illustrated by the following finite element results for  $E_1/E_2 = 20$ ,  $D/d_0 = 1$ ,  $H/d_0 = 1$ , and  $d_{rz}/d_0 = 2$ :

$v_1$	$v_2$	$I_s$ center	$I_s$ mean
0.2	0.4	0.24	0.23
0.3	0.4	0.23	0.23
0.4	0.4	0.23	0.23
0.2	0.3	0.29	0.28
0.3	0.3	0.28	0.28
0.4	0.3	0.28	0.28

$v_1$	$v_2$	$I_s$ center	$I_s$ mean
0.2	0.2	0.31	0.31
0.3	0.2	0.31	0.31
0.4	0.2	0.31	0.30

Therefore, values of  $I_s$  from the above table can be used for  $v_2 = 0.4$  and any reasonable value of  $v_1$ . Preliminary results suggest that for  $v_2 \neq 0.4$ , a rough estimate for  $I_s$  can be obtained from the following equation:

$$I_{s(v_2 \neq 0.4)} = \frac{1 - v_2}{1 - 0.4} \cdot I_{s(v_2=0.4)} \quad (6A.11)$$

For homogeneous soils,  $I_s$  is proportional to  $(1 - v_2)$ , so the immediate settlement for overexcavated and replaced soils appears to be affected more by the Poisson's ratio of the matrix soil than are homogeneous soils.

$I_s$  also depends on the shape of the loaded area. Reasonable values of  $I_s$  for square foundations and rectangular foundations with IJB less than about 1.5 can be obtained by converting to an equivalent circle with the same area. However, this method is not applicable to higher  $L/B$  ratios. To illustrate the effect that shape of the loaded area has on  $I_s$ , results from plane-strain finite element analyses (strip loading on an infinitely long replaced zone) are compared with axisymmetric results for the case of  $v_1 = 0.2$ ,  $v_2 = 0.4$ ,  $E_1/E_2 = 20$ ,  $D/d_0 = D/B = 1$ , and  $H/d_0 = H/B = 1$  as follows:

Axisymmetric [ $S_i = (q_0 d_0 / E_2) I_s$ ]			Plane-Strain [ $S_i = (q_0 B / E_2) I_s$ ]		
$d_{rz}/d_0$	$I_s$ center	$I_s$ average	$W/B$	$I_s$ center	$I_s$ average
0.25	0.41	0.44	0.25	0.16	0.16
0.5	0.38	0.40	0.5	0.15	0.15
0.75	0.35	0.35	0.75	0.15	0.15
1	0.32	0.32	1	0.14	0.14
1.5	0.27	0.26	1.5	0.14	0.14
2	0.24	0.23	2	0.13	0.13
3	0.21	0.20	3	0.13	0.13
4	0.20	0.19	4	0.12	0.12
6	0.19	0.18	6	0.12	0.12
8	0.19	0.18	8	0.12	0.12
10	0.18	0.18	10	0.12	0.12

Therefore, for comparable conditions, a long rectangular foundation will settle substantially less than a circular foundation with the same width ( $d_0 = B$ ). No additional information is currently available for estimating  $S_i$  for rectangular foundations of finite length bearing on replaced zones of finite extent, so engineering judgment is required for these cases. A very conservative estimate for  $I_s$  could be obtained by using Table 6A.1 with  $D/d_0 = D/B$ ,  $D/d_0 = H/B$ , and  $d_{rz}/d_0 = W/B$ . One could also perform plane-strain finite element analyses for comparable conditions to obtain a lower-bound value for  $S_i$ , with  $S_i$  from the axisymmetric case as an upper-bound value, and use engineering judgment to estimate  $S_i$  for the actual  $L/B$  ratio. A better method would be to perform a three-dimensional finite element analysis for the actual conditions; unfortunately, few engineers have ready access to a three-dimensional finite element code suited to this type of problem.

If the in situ bearing soils within the depth of influence for settlement are highly stratified with

**TABLE 6A.1** Settlement Influence Factors for a Flexible, Uniform, Circular Stress Applied to the Surface of a Cylindrical Replaced Zone within an Otherwise Homogeneous, Isotropic, Elastic Half-Space ( $v_1 = 0.2$ ,  $v_2 = 0.4$ )

$E_1/E_2$	$D/d_0$	$H/d_0$	$d_{rz}/d_0$	$I_s$ center	$I_s$ mean	
1	0	0	0	0.84	0.71	
1	0.5	0	0	0.65	0.59	$S_i = \frac{q_0 d_0}{E_2} I_s$
1	1	0	0	0.54	0.50	
1	1.5	0	0	0.50	0.46	
5	0	0.5	0.25	0.71	0.69	
5	0	0.5	0.5	0.65	0.65	
5	0	0.5	0.75	0.61	0.59	
5	0	0.5	1	0.57	0.54	
5	0	0.5	1.5	0.53	0.49	
5	0	0.5	2	0.51	0.47	
5	0	0.5	3	0.50	0.46	
5	0	0.5	4	0.50	0.46	
5	0	0.5	6	0.50	0.46	
5	0	0.5	8	0.50	0.46	
5	0	0.5	10	0.50	0.46	
5	0	1	0.25	0.67	0.67	
5	0	1	0.5	0.60	0.60	
5	0	1	0.75	0.54	0.53	
5	0	1	1	0.49	0.47	
5	0	1	1.5	0.43	0.41	
5	0	1	2	0.39	0.37	
5	0	1	3	0.37	0.35	
5	0	1	4	0.37	0.34	
5	0	1	6	0.36	0.34	
5	0	1	8	0.36	0.34	
5	0	1	10	0.36	0.33	
5	0	1.5	0.25	0.66	0.66	
5	0	1.5	0.5	0.57	0.58	
5	0	1.5	0.75	0.51	0.50	
5	0	1.5	1	0.46	0.44	
5	0	1.5	1.5	0.40	0.38	
5	0	1.5	2	0.36	0.34	
5	0	1.5	3	0.33	0.31	
5	0	1.5	4	0.32	0.30	
5	0	1.5	6	0.31	0.29	
5	0	1.5	8	0.31	0.29	
5	0	1.5	10	0.31	0.28	
5	0.5	0.5	0.25	0.57	0.56	
5	0.5	0.5	0.5	0.54	0.53	
5	0.5	0.5	0.75	0.51	0.49	
5	0.5	0.5	1	0.48	0.46	
5	0.5	0.5	1.5	0.44	0.42	
5	0.5	0.5	2	0.43	0.40	
5	0.5	0.5	3	0.42	0.39	
5	0.5	0.5	4	0.42	0.39	
5	0.5	0.5	6	0.42	0.39	
5	0.5	0.5	8	0.42	0.39	
5	0.5	0.5	10	0.42	0.39	
						5
						1
						10
						0.29
						0.28









**TABLE 6A.1** (*Continued*)

$E_1/E_2$	$D/d_0$	$H/d_0$	$d_{r2}/d_0$	$I_s$ center	$I_s$ mean	$E_1/E_2$	$D/d_0$	$H/d_0$	$d_{r2}/d_0$	$I_s$ center	$I_s$ mean
100	0	0.5	0.25	0.63	0.65	100	0.5	1.5	0.25	0.38	0.44
100	0	0.5	0.5	0.58	0.59	100	0.5	1.5	0.5	0.35	0.38
100	0	0.5	0.75	0.52	0.51	100	0.5	1.5	0.75	0.32	0.32
100	0	0.5	1	0.44	0.44	100	0.5	1.5	1	0.28	0.28
100	0	0.5	1.5	0.34	0.34	100	0.5	1.5	1.5	0.23	0.23
100	0	0.5	2	0.28	0.28	100	0.5	1.5	2	0.19	0.19
100	0	0.5	3	0.23	0.23	100	0.5	1.5	3	0.15	0.15
100	0	0.5	4	0.22	0.21	100	0.5	1.5	4	0.13	0.13
100	0	0.5	6	0.21	0.21	100	0.5	1.5	6	0.11	0.11
100	0	0.5	8	0.21	0.20	100	0.5	1.5	8	0.11	0.10
100	0	0.5	10	0.20	0.19	100	0.5	1.5	10	0.10	0.10
100	0	1	0.25	0.50	0.57	100	1	0.5	0.25	0.44	0.46
100	0	1	0.5	0.46	0.49	100	1	0.5	0.5	0.42	0.43
100	0	1	0.75	0.41	0.41	100	1	0.5	0.75	0.39	0.39
100	0	1	1	0.36	0.36	100	1	0.5	1	0.35	0.35
100	0	1	1.5	0.28	0.28	100	1	0.5	1.5	0.28	0.28
100	0	1	2	0.23	0.23	100	1	0.5	2	0.24	0.24
100	0	1	3	0.18	0.18	100	1	0.5	3	0.21	0.21
100	0	1	4	0.15	0.15	100	1	0.5	4	0.20	0.20
100	0	1	6	0.13	0.13	100	1	0.5	6	0.19	0.19
100	0	1	8	0.13	0.13	100	1	0.5	8	0.19	0.19
100	0	1	10	0.12	0.12	100	1	0.5	10	0.18	0.18
100	0	1.5	0.25	0.43	0.52	100	1	1	0.25	0.38	0.42
100	0	1.5	0.5	0.39	0.43	100	1	1	0.5	0.36	0.38
100	0	1.5	0.75	0.35	0.35	100	1	1	0.75	0.33	0.33
100	0	1.5	1	0.31	0.31	100	1	1	1	0.30	0.30
100	0	1.5	1.5	0.25	0.24	100	1	1	1.5	0.24	0.24
100	0	1.5	2	0.20	0.20	100	1	1	2	0.20	0.20
100	0	1.5	3	0.16	0.16	100	1	1	3	0.16	0.16
100	0	1.5	4	0.13	0.13	100	1	1	4	0.14	0.14
100	0	1.5	6	0.11	0.11	100	1	1	6	0.13	0.13
100	0	1.5	8	0.11	0.11	100	1	1	8	0.12	0.12
100	0	1.5	10	0.10	0.10	100	1	1	10	0.12	0.12
100	0.5	0.5	0.25	0.52	0.53	100	1	1.5	0.25	0.34	0.39
100	0.5	0.5	0.5	0.48	0.49	100	1	1.5	0.5	0.32	0.34
100	0.5	0.5	0.75	0.44	0.44	100	1	1.5	0.75	0.29	0.29
100	0.5	0.5	1	0.39	0.39	100	1	1.5	1	0.26	0.26
100	0.5	0.5	1.5	0.31	0.30	100	1	1.5	1.5	0.22	0.21
100	0.5	0.5	2	0.26	0.26	100	1	1.5	2	0.18	0.18
100	0.5	0.5	3	0.22	0.22	100	1	1.5	3	0.15	0.15
100	0.5	0.5	4	0.21	0.21	100	1	1.5	4	0.13	0.13
100	0.5	0.5	6	0.20	0.20	100	1	1.5	6	0.11	0.11
100	0.5	0.5	8	0.20	0.19	100	1	1.5	8	0.11	0.10
100	0.5	0.5	10	0.19	0.19	100	1	1.5	10	0.10	0.10
100	0.5	1	0.25	0.43	0.47	100	1.5	0.5	0.25	0.41	0.43
100	0.5	1	0.5	0.40	0.42	100	1.5	0.5	0.5	0.39	0.41
100	0.5	1	0.75	0.37	0.37	100	1.5	0.5	0.75	0.37	0.37
100	0.5	1	1	0.33	0.32	100	1.5	0.5	1	0.33	0.32
100	0.5	1	1.5	0.26	0.26	100	1.5	0.5	1.5	0.26	0.26
100	0.5	1	2	0.22	0.22	100	1.5	0.5	2	0.23	0.22
100	0.5	1	3	0.17	0.17	100	1.5	0.5	3	0.20	0.20
100	0.5	1	4	0.15	0.15	100	1.5	0.5	4	0.19	0.19
100	0.5	1	6	0.13	0.13	100	1.5	0.5	6	0.19	0.18
100	0.5	1	8	0.13	0.12	100	1.5	0.5	8	0.18	0.18
100	0.5	1	10	0.12	0.12	100	1.5	0.5	10	0.18	0.17

(continued)

**6.26** SOIL IMPROVEMENT AND STABILIZATION**TABLE 6A.1** (Continued)

$E_1/E_2$	$D/d_0$	$H/d_0$	$d_{rz}/d_0$	$I_s$ center	$I_s$ mean	$E_1/E_2$	$D/d_0$	$H/d_0$	$d_{rz}/d_0$	$I_s$ center	$I_s$ mean
100	1.5	1	0.25	0.35	0.39	100	1.5	1.5	0.25	0.32	0.37
100	1.5	1	0.5	0.34	0.36	100	1.5	1.5	0.5	0.30	0.33
100	1.5	1	0.75	0.31	0.31	100	1.5	1.5	0.75	0.28	0.28
100	1.5	1	1	0.28	0.28	100	1.5	1.5	1	0.25	0.25
100	1.5	1	1.5	0.23	0.23	100	1.5	1.5	1.5	0.21	0.20
100	1.5	1	2	0.19	0.19	100	1.5	1.5	2	0.18	0.18
100	1.5	1	3	0.16	0.16	100	1.5	1.5	3	0.14	0.14
100	1.5	1	4	0.14	0.14	100	1.5	1.5	4	0.13	0.12
100	1.5	1	6	0.13	0.12	100	1.5	1.5	6	0.11	0.11
100	1.5	1	8	0.12	0.12	100	1.5	1.5	8	0.11	0.10
100	1.5	1	10	0.12	0.11	100	1.5	1.5	10	0.10	0.10

widely varying stiffnesses, or if there is one or more layers of saturated clay within the zone of influence, more involved techniques are needed. The increased stiffness of a replaced zone that is sufficiently wide to develop the full reduction in settlement [Eq. (6A.10)] can be readily incorporated into most methods for calculating immediate settlement (e.g., Bowles, 1987; Schmertmann, 1970 and Schmertmann et al., 1978; Burland and Burbidge, 1985; Meyerhof, 1956, 1965). If either the Bowles or Schmertmann method is used, a value of equivalent stress-strain modulus ( $E$ ) for the replaced soil is needed and can be estimated in a variety of ways (see Sec. 2B.4). If a method based on SPT blowcounts ( $N$ ) is used (Burland and Burbidge or Meyerhof), SPT tests can be conducted within the replaced zone to obtain  $N$  values for estimating  $S_i$ .

For a replacement zone of finite width within highly stratified matrix soils, Eq. (6A.9) and Table 6A.1 can be used to estimate  $S_i$  if an average or equivalent value for  $E_2$  is calculated for the settlement influence zone. A weighted average modulus based on the thicknesses of the layers may be appropriate and can be calculated from the following equation (Bowles, 1987):

$$E_{2-av} = \frac{\sum_{i=1}^{i=n} H_i \cdot E_i}{\sum_{i=1}^{i=n} H_i} \quad (6A.12)$$

where  $n$  = number of layers within the settlement influence zone

$H_i$  = thickness of layer  $i$

$E_i$  = stress-strain modulus for layer  $i$

If certain strata are deemed to be more critical than others, additional weighting factors can be applied. For example, if a stratum is considered to be twice as critical as the other strata, its height can be multiplied by two, with the weighted height used in both the numerator and denominator of Eq. (6A.12).

When a saturated clay layer is within the depth of influence for settlement,  $S_i$  for a wide replaced zone can be calculated using the undrained modulus for the clay and any appropriate method based on elastic theory. An estimate of  $\Delta\sigma_z$  throughout the height of the clay layer is needed to estimate primary consolidation settlement ( $S_c$ ). Many engineers use Boussinesq-type analyses based on a

uniform stress applied to the surface of a homogeneous half-space to estimate  $\Delta\sigma_z$  in the clay layer; however, if the replaced zone is much stiffer than the undrained clay, or if the foundation bears below the ground surface, Boussinesq-type analyses are overly conservative and should not be used. Thus, it is better to use a method that considers the effects of the stiffer upper layer and the depth of embedment. A simple method for a wide replaced zone is to determine an equivalent uniform stress induced at the top of the lower zone ( $q_{LZ}$ ) and dimensions of the loaded area ( $B_{LZ}$  and  $L_{LZ}$  or  $d_{LZ}$ ) using the following equations:

$$B_{LZ} = B + \frac{2H}{\alpha} \quad \text{for a rectangular foundation} \quad (6A.13a.1)$$

$$L_{LZ} = L + \frac{2H}{\alpha} \quad \text{for a rectangular foundation} \quad (6A.13a.2)$$

$$d_{LZ} = d_0 + \frac{2H}{\alpha} \quad \text{for a circular foundation} \quad (6A.13b)$$

$$q_{LZ} = q \cdot \frac{BL}{B_{LZ}L_{LZ}} \quad \text{for a rectangular foundation} \quad (6A.14a)$$

$$q_{LZ} = q \cdot \frac{d_0^2}{d_{LZ}^2} \quad \text{for a circular foundation} \quad (6A.14b)$$

Methods for estimating  $\Delta\sigma_z$  for foundations embedded within homogeneous, semi-infinite soils [Nishida (1966) for circular; Skopek (1961) for rectangular] can be used with Eqs. (6A.13) and (6A.14) to estimate  $\Delta\sigma_z$  beneath the replaced zone.

An alternate method for a wide replaced zone is to estimate  $\Delta\sigma_z$  using the average bearing stress applied to surface of the replaced zone and solutions for layered elastic systems. All available methods for layered systems are for a circular load on the ground surface, so the effect of embedment is ignored, and square foundations must be converted to equivalent circles. If the replaced zone bears directly on a saturated clay layer and the clay layer is thick (extends to the bottom of the settlement influence zone or deeper), a two-layer analysis is appropriate, and Table 6A.2 can be used to estimate  $\Delta\sigma_z$  beneath the center of the loaded area at various depths within the clay layer. If the replaced zone is underlain by a thin clay layer, or if the clay layer is the second layer beneath the replaced zone, a three-layer analysis is appropriate, and  $\Delta\sigma_z$  can be estimated from the tables given in Jones (1962) or the charts provided in Peattie (1962).

If the width of the replaced zone is less than the minimum required for full reduction in settlement, the stresses induced within the underlying in situ soil may be either lesser or greater than for the same foundation in a homogeneous soil. The finite element results provided in Fig. 6A.9 illustrate this concept for a cylindrical replaced zone of varying diameter with  $E_1/E_2 = 20$ ,  $D/d_0 = 1$ , and  $H/d_0 = 1$ . Along a vertical profile near the axis [Fig. 6A.9(a)], the induced vertical stress near the interface between the replaced zone and the underlying in situ soil decreases as the diameter of the replaced zone increases. For a replaced zone with  $d_{rz}/d_0 \leq 1$ , the induced vertical stresses near the interface are greater than for the homogeneous case ( $d_{rz}/d_0 = 0$ ), and the induced stresses are lesser for  $d_{rz}/d_0 \geq 1.5$  than for the homogeneous case. At greater depths, the trends are different. The induced vertical stresses do not change much for  $d_{rz}/d_0 \geq 6$ ; this result is consistent with the approximate value of  $d_{rz}/d_0 = 5.8$  calculated previously for minimum diameter required for full reduction in settlement when  $H/d_0 = 1$  and  $E_1/E_2 = 20$ .

The induced vertical stresses along a horizontal profile located a short distance below the bot-

**6.28** SOIL IMPROVEMENT AND STABILIZATION

tom of the replaced zone are shown in Fig. 6A.9(b). For any replaced zone with  $d_{rz}/d_0 \leq 2$ ,  $\Delta\sigma_z/q_0$  increases from the axis to the edge of the footprint for the replaced zone and then decreases with distance from the footprint. For  $d_{rz}/d_0 \geq 3$ ,  $\Delta\sigma_z/q_0$  decreases gradually with distance from the axis. The induced vertical stresses for a homogeneous soil fall within the range for replaced zones with  $0.25 \leq d_{rz}/d_0 \leq 10$  at all distances from the axis. To obtain an estimate of the relative magnitudes of settlement that would occur in the soil underlying the replaced zone, an estimate of the force transmitted to the underlying soil within the footprint of the loaded area ( $Q_{tr}$ ) was obtained for each  $d_{rz}/d_0$  by numerically integrating the curves for  $\Delta\sigma_z/q_0$  in Fig. 6A.9 from  $r/r_0 = 0$  to  $r/r_0 = 1$ . Values of  $Q_{tr}$  are shown as a percentage of the applied load in the table below, along with  $Q_{tr}$  for each  $d_{rz}/d_0$  divided by  $Q_{tr}$  for a homogeneous soil:

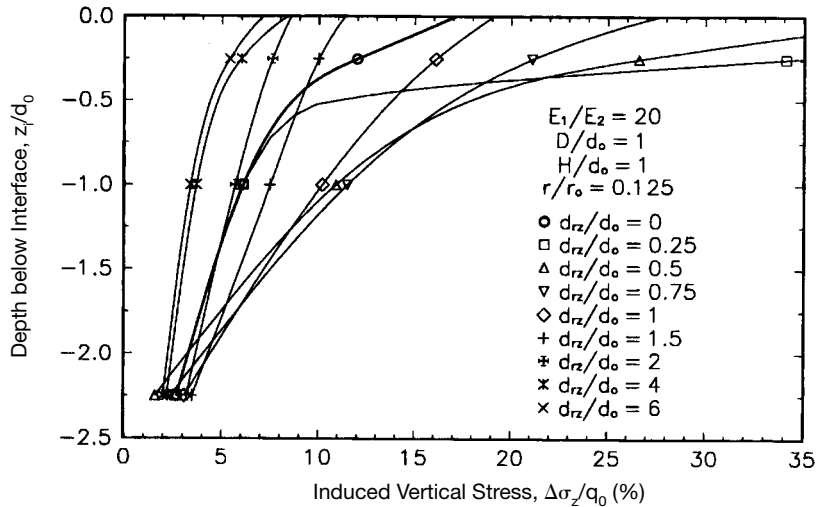
$\frac{d_{rz}}{d_0}$	$Q_{tr}(\%)$	$\frac{Q_{tr}}{Q_{tr}(d_{rz}/d_0=0)}$
0	10.9	1.00
0.25	14.5	1.34
0.50	18.3	1.68
0.75	21.1	1.94
1.00	18.4	1.69
1.50	10.3	0.95
2.00	7.5	0.69
3.00	5.8	0.53
4.00	5.3	0.49
6.00	5.1	0.47

**TABLE 6A.2**  $\Delta\sigma_z/q_0$  beneath the Center of a Uniform Circular Stress Applied to the Surface of a Two-Layer System with a Perfectly Rough Interface and  $v_1 = v_2 = 0.5$

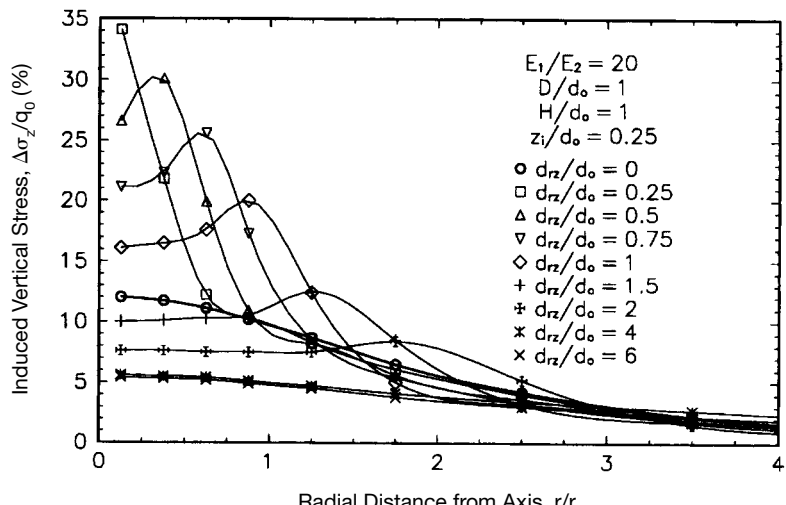
$H/d_0$	$z_i/H$	$\Delta\sigma_z/q_0 (\%)$			
		$E_1/E_2 = 1$	$E_1/E_2 = 10$	$E_1/E_2 = 100$	$E_1/E_2 = 1000$
0.25	0	91.1	64.4	24.6	7.10
	1	64.6	48.0	20.5	6.06
	2	42.4	34.0	16.5	5.42
	3	28.4	24.4	13.3	4.80
	4	20.0	18.1	10.8	4.28
0.5	0	64.6	29.2	8.1	1.85
	1	28.4	16.8	6.0	1.62
	2	14.5	10.5	4.6	1.43
	3	8.70	7.0	3.6	1.24
	4	5.70	5.0	2.9	1.10
1	0	28.4	10.1	2.38	0.51
	1	8.70	4.70	1.58	0.42
	2	4.03	2.78	1.17	0.35
	3	2.30	1.84	0.91	0.31
	4	1.48	1.29	0.74	0.28

Note:  $z_i$  = depth below the interface between the two layers

Source: After L. Fox (1948).



(a)



(b)

**FIGURE 6A.9** Vertical stresses induced in underlying matrix soil by a uniform circular stress applied to the surface of an embedded replaced zone of varying diameter within an otherwise homogeneous half-space as predicted by finite element analysis: (a) vertical profile near axis; (b) horizontal profile near interface.

**6.30 SOIL IMPROVEMENT AND STABILIZATION**

Thus, the settlement in the underlying soil would be greater for a replaced zone with  $d_{rz}/d_0$  less than about 1.5 than for the homogeneous case, and is a maximum for  $d_{rz}/d_0 \approx 0.75$ . Where the induced vertical stresses in the underlying clay matrix are greater for overexcavation/replacement than without it, either a net increase or decrease in settlement could occur depending on whether the increase in primary consolidation settlement is greater or lesser than the decrease in immediate settlement. Thus, more involved analyses such as these are warranted when overexcavation/replacement is being considered for foundations underlain by one or more layers of saturated clay. For cases where a granular replaced zone is constructed within a saturated clay matrix, the replaced zone will act as a drainage well, and the rate of consolidation will be increased owing to increased horizontal drainage.

**6A.2.3 Usefulness and Limitations of the Finite Element Method**

On many projects where one or more of the ground modification techniques described in this handbook are used to increase bearing support for building foundations, the availability of reliable theoretical or empirical methods for estimating settlement or bearing capacity for the improved ground are either limited or nonexistent. In these cases, the finite element method—if used properly—can provide valuable insight into how ground modification affects settlement and bearing capacity. There are currently several axisymmetric and plane-strain finite element software packages available at relatively low cost that run on microcomputers and are capable of modeling the stress-strain-strength behavior of soils. Thus, the finite element technique is now readily available to many practicing engineers and should be used more frequently in foundation engineering practice than it is. Although it is not a cure-all, the finite element method is a powerful tool that all foundation engineers should consider using when available theoretical or empirical techniques are inadequate.

If the results of finite element analyses are to be meaningful, sufficient data are needed to determine reliable stress-strain-strength parameters for the bearing soils (replaced zone material and in situ soils for overexcavation/replacement). However, even under the best of circumstances, finite element analyses for soils seldom give reliable quantitative predictions for settlement or bearing capacity unless the input parameters for the stress-strain-strength characteristics of the soils are adjusted until the finite element results match the known or expected values. Therefore, an appropriate procedure for using the finite element method to estimate the bearing capacity or settlement of a foundation bearing on a replaced zone is as follows:

1. Calculate the estimated settlement or ultimate bearing capacity for the foundation with and without the replaced zone using the theories given in this section and Sec. 2B.4.
2. Obtain reliable values for the stress-strain-strength parameters for the replacement material and the in situ soils within the zone of influence. For the hyperbolic finite element model (Duncan and Chang, 1970), which is the most frequently used model for soils, the stress-strain-strength parameters are obtained from triaxial tests conducted on specimens of the soils or are estimated from published data on similar soils (e.g., Duncan et al., 1980).
3. Perform finite element (FE) analyses for the foundation without the replaced zone (in situ geologic profile). Compare the FE values for settlement or  $q_{ult}$  with those obtained from theoretical analyses (step 1). If the FE results are comparable to the theoretical results, proceed to step 4. If not, adjust the input soil parameters until the FE results are comparable.
4. Conduct finite element analyses for the foundation with the replaced zone. The input parameters for the replaced zone should be adjusted in a manner similar to that used for the in situ soils. These FEM results should provide reasonable estimates for settlement or ultimate bearing capacity.

In many projects, settlement must be estimated from limited soil data. In the United States it is

fairly common to have only SPT blowcounts from which to estimate the settlement of granular soils, and the use of nonlinear stress-strain parameters for the finite element analyses is not justified in these cases. Therefore, it is better to estimate a reasonable range in values of elastic stress-strain modulus for the replacement material and each in situ soil and to perform a parametric study to estimate the probable percentage reduction in settlement which would occur from overexcavation/replacement. To provide an estimate of the settlement that would occur with the replaced zone, the range of values for percentage reduction in settlement can be applied to estimated values of settlement for the same foundation without the replaced zone.

#### **6A.2.4 Limitations of the Overexcavation/Replacement Method**

Although the overexcavation/replacement method has been used for centuries to improve bearing soils, it has the following limitations (Lawton et al., 1994):

1. Expensive bracing or sloping of the excavation is required if it is deep.
2. The excavation may cause settlement of adjacent existing structures.
3. High ground water may cause instability of the excavation and difficulties in compacting the replacement material. Therefore, bracing may be required to support the sides of the excavation, and pumping may be needed to lower the ground-water level within the excavation.
4. Sufficient high-quality replacement material may not be readily or economically available.
5. The densification that can be achieved in cohesionless replacement soils is sometimes limited to low levels, owing to lack of confinement in wide excavations and limited access in narrow excavations.

**Example Problem 6A.1** A 1-m (3.28-ft) diameter footing will support a centric vertical load at the bearing level of 471 kN (106 kips) and will bear at a depth of 1 m (3.28 ft) below the ground surface. The in situ soil consists of a thick deposit of fairly homogeneous sandy micaceous silt. The overexcavation/replacement technique will be used to improve the bearing soils. A replacement zone 1 m (3.28 ft) in height and 2 m (6.56 ft) in diameter is being considered. The replacement material will be compacted gravelly sand. Relevant properties of the in situ and replacement soils are given below:

Replacement soil	In situ soil
Gravelly sand	Sandy micaceous silt
$\phi_1 = 45^\circ$	$\phi_2 = 28^\circ$
$c_1 = 0$	$c_2 = 0$
$E_1 = 100 \text{ MPa (2090 ksf)}$	$E_2 = 5 \text{ MPa (104 ksf)}$
$v_1 = 0.2$	$v_1 = 0.4$
$\gamma_1 = 22 \text{ kN/m}^3 (140 \text{ pcf})$	$\gamma_2 = 16.5 \text{ kN/m}^3 (105 \text{ pcf})$

Estimate the ultimate bearing capacity, factor of safety against bearing capacity failure, immediate settlement, and vertical stresses induced in the underlying in situ soil. Compare results with those for the same footing without the replaced zone.

**Solution: Ultimate bearing capacity without replaced zone.** Use Meyerhof's (1951, 1963) equations and an equivalent square foundation:

$$B_{\text{eq}} = L_{\text{eq}} = (0.25\pi d_0^2)^{1/2} = [0.25\pi(l)^2]^{1/2} = 0.8862 \text{ m (2.91 ft)}$$

**6.32** SOIL IMPROVEMENT AND STABILIZATION

For  $c_2 = 0$ ,

$$\begin{aligned}
 q_{\text{ult}} &= \gamma_2 D N_{q2} S_{q2} D_{q2} + 0.5 \gamma_2 B_{\text{eq}} N_{\gamma2} S_{\gamma2} D_{\gamma2} \\
 S_{q2} = S_{\gamma2} &= 1 + 0.1 \tan^2 \left( 45^\circ + \frac{\phi_2}{2} \right) \cdot \frac{B_{\text{eq}}}{L_{\text{eq}}} \\
 &= 1 + 0.1 \tan^2(59^\circ)(1) = 1.277 \\
 D_{q2} = D_{\gamma2} &= 1 + 0.1 \tan \left( 45^\circ + \frac{\phi_2}{2} \right) \cdot \frac{D}{B_{\text{eq}}} \\
 &= 1 + 0.1 \tan(59^\circ) \frac{1}{0.8862} = 1.188 \\
 N_{q2} &= e^{\pi \tan \phi_2} \cdot \tan^2 \left( 45^\circ + \frac{\phi_2}{2} \right) = e^{\pi \tan(28^\circ)} \cdot \tan^2(59^\circ) = 14.72 \\
 N_{\gamma2} &= (N_{q2} - 1) \tan(1.4 \phi_2) = (14.72 - 1) \tan(39.2^\circ) = 11.19 \\
 q_{\text{ult}} &= (16.5)(1)(14.72)(1.277)(1.188) + 0.5(16.5)(0.8862)(11.19)(1.277)(1.188) = 493 \text{ kPa (10.3 ksf)}
 \end{aligned}$$

Calculate the average applied stress at bearing level:

$$q_0 = \frac{471}{0.25 \pi (1)^2} = 600 \text{ kPa (12.5 ksf)}$$

$$F_s \text{ (bearing capacity failure)} = \frac{493}{600} = 0.82$$

**Solution: Ultimate bearing capacity with replaced zone—punching through replaced zone  $q_b$** , is calculated for  $B_{\text{eq}}$ ,  $L_{\text{eq}}$ , and an embedded depth of 2 m.  $N_{q2}$ ,  $N_{\gamma2}$ ,  $S_{q2}$ , and  $S_{\gamma2}$  are the same as before.

$$D_{q2} = D_{\gamma2} = 1 + 0.1 \tan(59^\circ) \cdot \frac{2}{0.8862} = 1.376$$

From Eq. (6A.3b):

$$\begin{aligned}
 q_b &= (16.5)(2)(14.72)(1.277)(1.376) + 0.5(16.5)(0.8862)(11.19)(1.277)(1.376) \\
 &= 997 \text{ kPa (20.8 ksf)}
 \end{aligned}$$

Calculate the perimeter length based on a circular rather than a square punching area, because the perimeter length for an equivalent square based on area is not the same as for the circle.

$$p = \pi d = \pi(l) = 3.142 \text{ m (10.3 ft)}$$

From Eq. (6A.4) with  $c_1 = c_2 = 0$ :

$$\frac{q_2}{q_1} = \left( \frac{\gamma_2}{\gamma_1} \right) \left( \frac{N_{\gamma_2}}{N_{\gamma_1}} \right)$$

$$N_{\gamma_1} = e^{\pi \tan(45^\circ)} \cdot \tan^2(67.5^\circ) = 134.9$$

$$N_{\gamma_1} = (134.9 - 1)\tan(63^\circ) = 262.7$$

$$\frac{q_2}{q_1} = \left( \frac{16.5}{22} \right) \left( \frac{11.19}{262.7} \right) = 0.032$$

From Fig. 6A.5 for  $q_2/q_1 = 0.032$  and  $\phi_i = 45^\circ$

$$K_s \equiv 3.2$$

From Eq. (6A.3e):

$$\begin{aligned} P_h &= (3.2)[(16.5)(1)(l) + 0.5(22)(l)^2] \\ &= 88.0 \text{ kN/m (6.03 kips/ft)} \end{aligned}$$

From Eq. (6A.3d):

$$\begin{aligned} W_{pz} &= 0.25\pi(l)^2(1)(22) = 17.28 \text{ kN (3.88 kips)} \\ A_f &= \pi \frac{d_0^2}{4} = \pi \frac{(1)^2}{4} = 0.7854 \text{ m}^2 (8.454 \text{ ft}^2) \end{aligned}$$

From Eq. (6A.3a):

$$q_{ult} = 997 + \frac{(3.142)(88.0)\tan(45^\circ) + 0 - 17.28}{0.7854} = 1327 \text{ kPa (27.7 ksf)}$$

**Solution: Ultimate bearing capacity with replaced zone—punching of replaced zone through in situ soil**

$$\begin{aligned} W_{eq} &= [0.25\pi(2)^2]^{1/2} = 1.772 \text{ m (5.82 ft)} \\ D_{q2} &= D_{\gamma_2} = 1 + 0.1 \tan\left(45^\circ + \frac{\phi_2}{2}\right) \cdot \frac{D + H}{W} \\ &= 1 + 0.1 \tan(59^\circ) \cdot \frac{1 + 1}{1.772} = 1.188 \end{aligned}$$

From Eq. (6A.6b):

$$q_b = (16.5)(2)(14.72)(1.277)(1.188) + 0.5(16.5)(1.772)(11.19)(1.277)(1.188) = 985.1 \text{ kPa (20.6 ksf)}$$

**6.34 SOIL IMPROVEMENT AND STABILIZATION**

$$p = \pi d_{rz} = \pi(2) = 6.283 \text{ m (20.6 ft)}$$

From Fig. 6A.5 for  $q_2/q_1 = 1$  and  $\phi_1 = \phi_2 = 28^\circ$ :

$$K_s \equiv 4.5$$

From Eq. (6A.6d):

$$P_h = 4.5(16.5)[(1)(1) + (1)^2/2] = 111.4 \text{ kN/m (7.63 kips/ft)}$$

From Eq. (6A.6c):

$$W_{rz} = 0.25\pi(2)^2(1)(22) = 69.12 \text{ kN (15.5 kips)}$$

$$A_{rz} = 0.25\pi(2)^2 = 3.142 \text{ m}^2 (33.8 \text{ ft}^2)$$

From Eq. (6A.6a):

$$q_{ult} = 985.1 \cdot \frac{3.142}{0.7854} + \frac{(6.283)(111.4)\tan(28^\circ) + 0 - 69.12}{0.7854} = 4326 \text{ kPa (90.4 ksf)}$$

**Solution: Ultimate bearing capacity with replaced zone—general shear failure within replaced zone.** Because of the limited horizontal extent of the replaced zone, it is unlikely that general shear failure would occur within this zone. However,  $q_{rz}$  is calculated here to ensure that it is greater than either of the two values of  $q_{ult}$  computed for the punching cases.  $N_{q1}$  and  $N_{\gamma1}$  were calculated previously.

$$S_{q1} = S_{\gamma1} = 1 + 0.1 \tan^2(67.5^\circ)(1) = 1.583$$

$$D_{q1} = D_{\gamma1} = 1 + 0.1 \tan(67.5^\circ)(1/0.8862) = 1.272$$

From Eq. (6A.3c):

$$q_{rz} = (16.5)(1)(134.9)(1.583)(1.272) + 0.5(22)(0.8862)(262.7)(1.583)(1.272) = 9638 \text{ kPa (201 ksf)}$$

Comparing  $q_{rz}$  with  $q_{ult}$  for the two punching cases, it is seen that the value of  $q_{ult}$  for punching through the replaced zone controls. Now calculate the factor of safety against bearing capacity failure:

$$F_s = \frac{q_{ult}}{q_0} = \frac{1327}{600} = 2.2$$

Most engineers would prefer a higher factor of safety, preferably in the range of 3 to 4. According to Vesic (1975), a minimum factor of safety of 2.0 is acceptable for apartment and office buildings if a thorough and complete soil exploration has been completed, but higher factors of safety are required for other structures and conditions. Thus, for most situations  $F_s = 2.2$  is unacceptable. The ultimate bearing capacity could be increased for this case by deepening the replacement zone. A second option would be to use a stronger replacement material, which in this case would likely necessitate chemically stabilizing the replacement material (see Sec. 6A.7) since the replacement material currently selected is a strong granular soil.

**Solution: Settlement without replaced zone.** From Table 6A.1 for  $E_1/E_2 = 1$  and  $D/d_0 = 1$ , mean  $= I_s = 0.50$ . From Eq. (6A.9):

$$S_i = \frac{(600)(1)}{5000} \cdot 0.50 = 0.060 \text{ m} = 60 \text{ mm (2.4 in)}$$

**Solution: Settlement with replaced zone.** From Fig. 6A.9 for  $E_1/E_2 = 20$ ,  $\alpha \approx 0.42$ . The minimum diameter required to obtain the full reduction in settlement can be estimated from Eq. (6A.10b):

$$d_{rz}(\min) = 1 + \frac{(2)(1)}{0.42} = 5.8 \text{ m (19 ft)}$$

Since the actual  $d_{rz}$  is less than  $d_{rz}(\min)$ , the full reduction in settlement will not be achieved. From Table 6A.1 for  $E_1/E_2 = 20$ ,  $D/d_0 = 1$ ,  $H/d_0 = 1$ , and  $d_{rz}/d_0 = 2.0$ , the mean  $I_s \approx 0.23$ . From Eq. (6A.9):

$$S_i = \frac{(600)(1)}{5000} (0.23) = 0.028 \text{ m} = 28 \text{ mm (1.1 in)}$$

The effect of the replaced zone is to reduce the estimated immediate settlement from 60 mm (2.4 in) to 28 mm (1.1 in). A maximum tolerable settlement of 25 mm (1.0 in) is frequently specified for buildings by the structural engineer or architect, so this value of immediate settlement may not be acceptable. Since there may be some additional long-term settlement in granular soils (see Burland and Burbidge 1985), a lower estimated value for  $S_i$  may be preferable, perhaps in the range of 13 to 19 mm (0.5 to 0.75 in). In this situation the settlement could be reduced by deepening or widening the replaced zone, using a stiffer replacement material, chemically stabilizing the replacement material before placement (see Sec. 6A.7), increasing the diameter of the footing, increasing the depth of embedment, or by some combination of these factors.

A design value of  $S_i = 19 \text{ mm (0.75 in)}$  will be used. A number of changes could be made to reduce estimated  $S_i$  to the design value, including the following.

If footing size and depth of embedment remain the same:

$$d_0 = D = 1 \text{ m} = 3.3 \text{ ft} \Rightarrow \frac{D}{d_0} = 1$$

The required value of  $I_s$  can be calculated by rearranging Eq. (6A.9) as follows:

$$I_s \leq \frac{S_i E_2}{q_0 d_0} = \frac{(0.019)(5000)}{(600)(1)} = 0.16$$

For the same replacement material,  $E_1/E_2 = 20$

$$H = 1.5 \text{ m (4.9 ft)}, d_{rz} = 4 \text{ m (13.1 ft)} \Rightarrow \frac{H}{d_0} = 1.5, \frac{d_{rz}}{d_0} = 4, \text{ and } I_s = 0.16.$$

If the replacement material is chemically stabilized to give  $E_1 = 250 \text{ MPa (5,220 ksf)}$   $\Rightarrow E_1/E_2 = 50$ :

$$H = 1 \text{ m (3.3 ft)}, d_{rz} = 4 \text{ m (13.1 ft)} \Rightarrow \frac{H}{d_0} = 1, \frac{d_{rz}}{d_0} = 4, \text{ and } I_s = 0.16$$

$$H = 1.5 \text{ m (4.9 ft)}, d_{rz} = 3 \text{ m (9.8 ft)} \Rightarrow \frac{H}{d_0} = 1.5, \frac{d_{rz}}{d_0} = 3, \text{ and } I_s = 0.16$$

**6.36** SOIL IMPROVEMENT AND STABILIZATION

If the diameter of the footing is increased to 2 m (6.6 ft) with the same  $D = 1$  m (3.3 ft)  $\Rightarrow D/d_0 = 0.5$ :

$$q_0 = \frac{\frac{471}{\pi}}{\frac{4}{4}(2)^2} = 150 \text{ kPa (3.1 ksf)}$$

$$I_s \leq \frac{S_i E_2}{q_0 d_0} = \frac{(0.019)(5000)}{(150)(2)} = 0.32$$

For the same replacement material ( $E_1/E_2 = 20$ ), the following dimensions of the replaced zone will work:

$$H = 1 \text{ m (3.3 ft)}, d_{rz} = 3.6 \text{ m (11.8 ft)} \Rightarrow \frac{H}{d_0} = 0.5, \frac{d_{rz}}{d_0} = 1.8, \text{ and } I_s \cong 0.32$$

$$H = 2 \text{ m (6.6 ft)}, d_{rz} = 2.4 \text{ m (7.9 ft)} \Rightarrow \frac{H}{d_0} = 1, \frac{d_{rz}}{d_0} = 1.2, \text{ and } I_s \cong 0.32$$

**Solution: Stress distribution, in situ soil beneath replaced zone** Although not needed to estimate settlement in this example problem, the stresses along the axis of the applied load are calculated for various depths below the interface to illustrate the procedure. The following four methods are used to calculate values of  $\Delta\sigma_z$ :

1. Values of  $\Delta\sigma_z$  for an infinitely wide replaced zone are calculated from Table 6A.2 for  $H/d_0 = 1$ . Manual curve fitting is used to interpolate values of  $\Delta\sigma_z/q_0$  for  $E_1/E_2 = 20$  at each level of  $z_i/H$ .
2. Values of  $\Delta\sigma_z$  for  $d_{rz}/d_0 = 2$  are obtained by interpolation from a curve of  $\Delta\sigma_z/q_0$  versus  $z_i/d_0$  [similar to Fig. 6A.9(a)] drawn from results of finite element analyses.
3. Values of  $\Delta\sigma_z$  for an embedded load within a homogeneous half-space are obtained from the equation given in Nishida (1966).
4. Values of  $\Delta\sigma_z$  for a surface-loaded homogeneous half-space (ignoring the embedment) are obtained from the equation given in Foster and Ahlvin (1954).

The results are summarized in the following table:

Induced vertical stress beneath axis, $\Delta\sigma_z$									
$z_i$ (m)	$z_i/H$	Wide replaced zone*		$d_{rz}/d_0 = 2^\dagger$		Homogeneous considering $D^\ddagger$		Homogeneous ignoring $D^\$$	
		$E_1/E_2 = 20$	$E_1/E_2 = 20$	$E_1/E_2 = 20$	$E_1/E_2 = 1$	$E_1/E_2 = 1$	$E_1/E_2 = 1$	$E_1/E_2 = 1$	$E_1/E_2 = 1$
0	0	41	0.86	50	1.0	98	2.0	171	3.6
1	1	20	0.42	34	0.71	35	0.73	52	1.1
2	2	14	0.29	21	0.44	18	0.38	24	0.50
3	3	9.6	0.20	15	0.31	11	0.23	14	0.29
4	4	7.0	0.15	11	0.23	7.3	0.15	8.9	0.19

\*Interpolated by manual curve fitting from Table 6A.2.

$^\dagger$ From results of finite element analyses.

$^\ddagger$ Nishida (1966).

$^\$$ Foster and Ahlvin (1954).

The induced vertical stresses for an infinitely wide replaced zone are less than for the case of  $d_{rz}/d_0 = 2$  by an average of 33%. The induced stresses for the embedded homogeneous case are greater by 96% at the inter-

face and lesser by 34% at  $z/H = 4$ . For the homogeneous case where embedment is ignored, the values of  $\Delta\sigma_z$  are greater by 242% at the interface and less by 19% at  $z/H = 4$ .

### **6A.3 NEAR-SURFACE COMPACTION**

---

The density of a soil is one of the primary factors that influences its compressibility and strength. So long as all other characteristics of the soil remain unchanged—such as state of stress, moisture condition, fabric, and physical and chemical nature of the soil particles and pore fluid—the densification of a soil will generally result in a stronger, less compressible material. However, it is generally neither desirable nor possible to densify a soil without changing one or more of these other characteristics. Therefore, the process of densifying a soil to achieve desired engineering characteristics is more complicated than it seems because many other factors will affect the engineering properties of the soil after densification. In addition, these other factors generally vary with time, which not only may affect the density of the soil (resulting in settlement or heave of the soil) but also may substantially alter the strength and compressibility of the soil.

Compaction is the process by which mechanical energy is applied to a soil to increase its density. At the time of compaction, the void spaces of the soil are occupied by air, water, and various chemicals and substances, or some combination thereof. For simplicity, it will be assumed in this discussion that the voids are occupied by air, water, or both. The soil is said to be *dry* if the voids are completely filled with air (water content,  $w$ , is 0 and degree of saturation,  $S_r$ , is 0) and *saturated* (also called *wet* by some engineers) if entirely occupied by water ( $S_r$  is 100%). In the more general case where both water and air occupy the voids ( $0 < S_r < 100\%$ ), the moisture condition of the soil is described as *partially saturated* or *moist*. In reality soils are never dry, so the term *unsaturated* is sometimes used for soils that are not completely saturated ( $S_r < 100\%$ ).

The total volume of the soil is decreased during densification; because the volume of the soil solids remains essentially unchanged, the volume of the voids decreases by the same amount that the total volume decreases. The result is that air, water, or both are expelled from the void spaces of the soil. The soil is usually partially saturated when compaction is initiated. Because the air permeability of a soil is typically much greater than the water permeability, air is expelled from the voids of a partially saturated soil during compaction. If the soil is initially saturated or becomes saturated or essentially saturated during the compaction process, water will be expelled.

Numerous methods and types of equipment are used to apply mechanical energy to soil during compaction. The methods and equipment used on any particular project depend on several factors, including cost, availability of equipment, the contractor's experience and preference, regional practices, volume and types of soil to be compacted, and conditions under which the compaction occurs (such as weather conditions, proximity to structures and utilities, and availability of water). In the following sections, the discussion of compaction is organized according to the equipment and method used to effect the densification of the soil.

The most common type of compaction, and what most engineers and contractors think of when the term compaction is used, is *near-surface* or *shallow compaction*. In open areas where the size of the equipment is not a consideration, near-surface compaction is generally accomplished using self-propelled or towed compaction rollers, although rubber-tired and tracked construction vehicles, sheep, elephants (Meehan, 1967), and human feet (Kyulule, 1983) have also been used. Hand-held compactors, tampers, or rammers are used in confined areas such as narrow trenches and small excavations, around pipes, behind retaining and basement walls, and adjacent to buildings, bridges, and other structures.

Near-surface compaction can be performed on unexcavated site soils or on fill materials placed in thin layers called *lifts* (Fig. 6A.10). Near-surface compaction of unexcavated site soils is usually done to increase the stiffness and strength of granular soils for support of lightly loaded (residential and light commercial) shallow foundations. Two common types of fills—embankments and fills produced from cut-and-fill operations—are illustrated in parts (b) and (c) of Fig. 6A.10.

## 6.38 SOIL IMPROVEMENT AND STABILIZATION

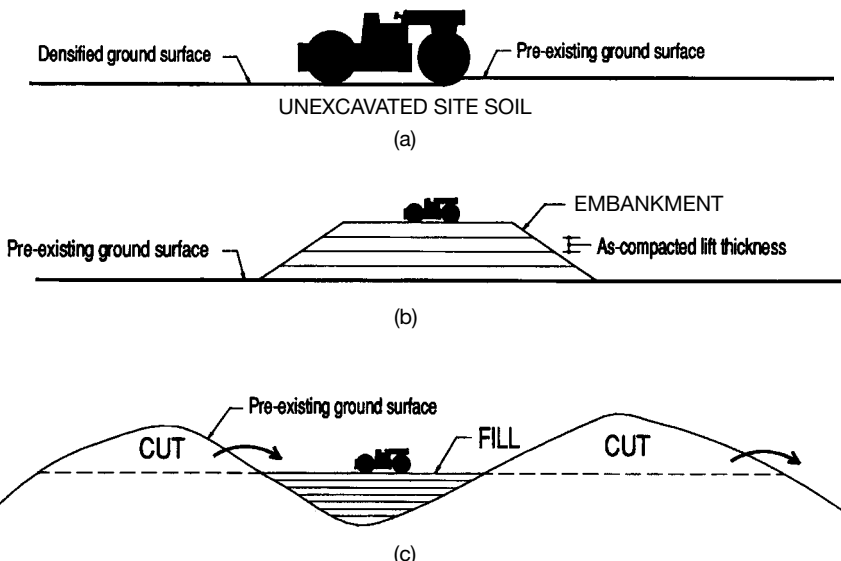


**FIGURE 6A.10** Common types of near-surface compaction: (a) compaction of unexcavated site soil; (b) construction of embankment; and (c) cut-and-fill operations.

Embankments may be used to impound water (earth dams, levees, and so on) or to support structures such as highways, buildings, and abutments for bridges. Cut-and-fill operations are conducted in hilly areas to provide relatively flat grades primarily for highways and residential developments.

Fill materials can consist of on-site soils that have been excavated and replaced in the same location (called *overexcavation/replacement*—see Sec. 6A.2) or borrow materials obtained from either on-site or off-site borrow pits. Soils to be used in fills are frequently moisture conditioned, pulverized, chemically modified, blended with other materials, or otherwise modified before compaction. The maximum depth to which soil can be densified using rollers or hand-held equipment is about 6 ft (2 m) and usually is much less (hence the term *near-surface*), depending on the compaction equipment used and the type of soil compacted. Substantial densification generally occurs only to a depth of about 6 to 24 in (150 to 610 mm). The degree of densification of a dune sand with depth as a function of the number of passes of a vibratory roller is illustrated in Fig. 6A.11 (D'Appolonia et al., 1969). Because of the shallow depth to which substantial densification occurs, compaction of unexcavated site soils is generally limited to situations where either the applied loads are light or the depth of influence of the applied load is shallow (the width of the loaded area is small). As a rule of thumb, the depth of substantial densification decreases as the cohesiveness of the soil increases. Lift thicknesses in fill operations range from about 3 to 36 in (75 to 910 mm), with the smallest values for highly plastic (fat) clays and the largest values for select coarse-grained soils.

Engineering properties of the soil that can be affected by compaction and that can be controlled to some extent during the compaction process include the following:

1. Density
2. Strength
3. Compressibility

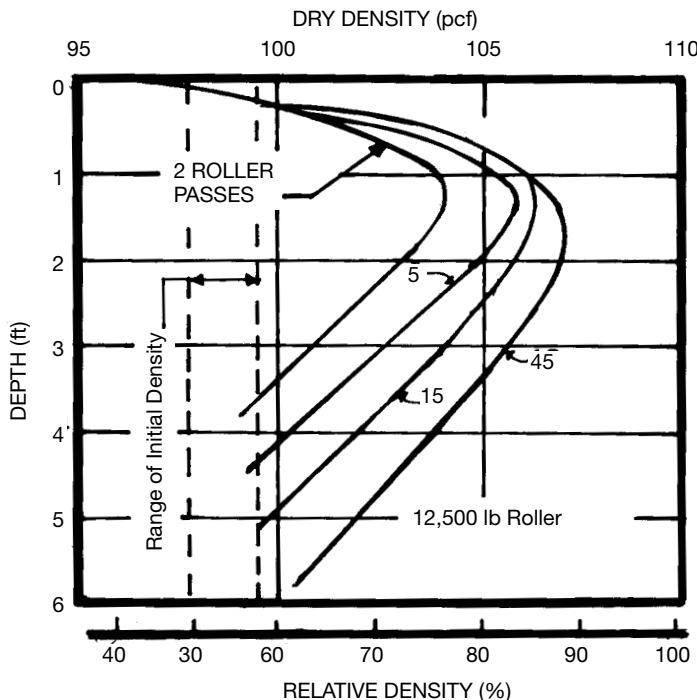


**FIGURE 6A.11** Relationship between as-compacted dry density and depth for an increasing number of passes from a 12,500-lb (56-kN) vibratory smooth-drum roller on an 8-ft (2.4-m) lift height of a dune sand (from D'Appolonia et al., 1969).

4. Potential for volume changes caused by changes in moisture condition (swell, collapse, shrinkage)
5. Potential for frost heave
6. Permeability

### 6A.3.1 Equipment

A variety of construction equipment is used in a near-surface compaction process. For borrow materials, equipment is needed to excavate the material at the borrow location, transport it to the site, place it in lifts, and compact it. If in situ soils are to be compacted in place, only compaction equipment is required. A detailed discussion of the wide variety of methods and equipment used on compaction projects is beyond the scope of this book, so only a general overview is given here.

#### 6A.3.1.1 Excavation, Hauling, Spreading

Borrow materials are usually excavated using some combination of power shovels, draglines, scrapers (pans), loaders, backhoes, and hydraulic excavators (see Figs. 6A.12 to 6A.15). Scrapers are multipurpose vehicles that can also be used to transport the soil and spread it in lifts on the fill area. If scrapers are not used, borrow materials are usually transported to the fill area in haul trucks (Fig. 6A.13) and spread in lifts using graders (Fig. 6A.16), loaders (Fig. 6A.13), or bulldozers (Fig.

**6.40** SOIL IMPROVEMENT AND STABILIZATION



**FIGURE 6A.12** Scraper (courtesy of Caterpillar Inc., Peoria, IL).



**FIGURE 6A.13** Loader dumping soil into a haul truck (courtesy of Caterpillar Inc., Peoria, IL).



**FIGURE 6A.14** Backhoe (courtesy of Deere & Company, Moline, IL).

6A.17). Some compaction rollers have a blade on the front that allows the soil to be spread and compacted in the same process. If the borrow material consists of dry, cohesive soils, it may need to be pulverized using a pulverizer or pugmill prior to spreading. Depending on the application, it may also be necessary to remove cobbles, boulders, undecomposed organic parts, or other undesirable components prior to hauling or spreading.

Moisture conditioning is frequently required to bring the soil to the desired compaction water content. This process consists of either drying or wetting the soil, reworking (mixing) the soil, and allowing the soil sufficient time to achieve relatively uniform moisture distribution. This can be accomplished either after the soil is spread in a loose lift using a water truck and discing equipment or in a stockpile located in a designated processing area. The conditioning time required to achieve moisture equilibrium in a soil after either wetting or drying depends on the soil type, varying from a few minutes for clean coarse sands and gravels to several days or weeks for highly plastic clays. When dry cohesive soils are wetted, the required moisture conditioning time depends primarily on the time required for the water to penetrate the hard clods and is therefore a function of clod size—larger clods need more conditioning time. At least 24 to 72 h are generally needed for proper moisture conditioning of cohesive soils, and more time usually is desirable.

#### **6A.3.1.2 Compaction**

Near-surface compaction is accomplished using a variety of equipment that can be classified into two primary categories depending on whether the general shape of the portion of the equipment that contacts the soil is round or flat. The major types of compactors are listed in Fig. 6A.18.

The types of equipment used on any compaction project depend on the grain-size distribution and mineralogy of the soils being compacted, the engineering properties that need to be controlled during the compaction process, and the equipment readily available to the compaction contractor. In some instances the type of equipment to be used is designated in the compaction specifications (usually just general type but sometimes more specifically, including type, weight, length of feet, vibration frequencies, and so on), but more commonly the choice of equipment is left to the compaction contractor. This will be discussed in more detail in Sec. 6A.3.5.

**6.42** SOIL IMPROVEMENT AND STABILIZATION

**FIGURE 6A.15** Hydraulic excavator (courtesy of Deere & Company, Moline, IL).

*Smooth-drum or smooth-wheel rollers* (Fig. 6A.19) have smooth steel drums that provide 100% areal coverage over the width of the drum, and compaction occurs primarily from static pressures generated by the weight of the roller. A conceptual drawing illustrating the forces generated by a moving smooth-drum roller is given in Fig. 6A.20. The peripheral force ( $U$ ) generated by the rotating drum acts horizontally but opposite in direction to the tractive force ( $Z$ ) generated by the momentum of the roller. Because the peripheral and tractive forces tend to negate each other (although a small net horizontal force may result in either direction), the primary force generated upon the soil results from the weight of the roller ( $W$ ).

The vertical contact pressure generated by a roller depends on  $W$  and the magnitude of the contact area. The shape of the contact area can be approximated by a rectangle whose length is equal to the length of the drum and whose width depends on the magnitude of vertical deflection, which in turn depends on the magnitude of  $W$  and the stiffness of the soil. During the initial pass of the roller on a loose lift, the vertical deflection (and hence the width of the contact area) is greatest; during subsequent passes of the roller, the soil is stiffer and the contact area is less, which produces higher contact stresses.

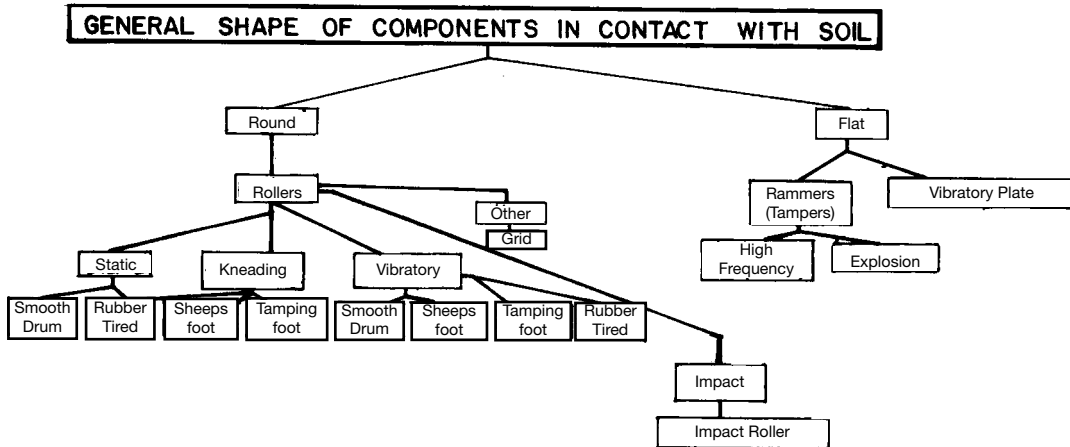
Smooth drum rollers have been used historically to compact soils of all types, but their usefulness in current practice is generally limited to proofrolling (smoothing) the surface of lifts compacted by other types of rollers and compacting granular soils and asphaltic pavements. Their usefulness



**FIGURE 6A.16** Grader (courtesy of Caterpillar Inc., Peoria, IL).



**FIGURE 6A.17** Tracked bulldozer towing a sheepsfoot roller (courtesy of Case Corporation, Racine, WI).

**6.44** SOIL IMPROVEMENT AND STABILIZATION

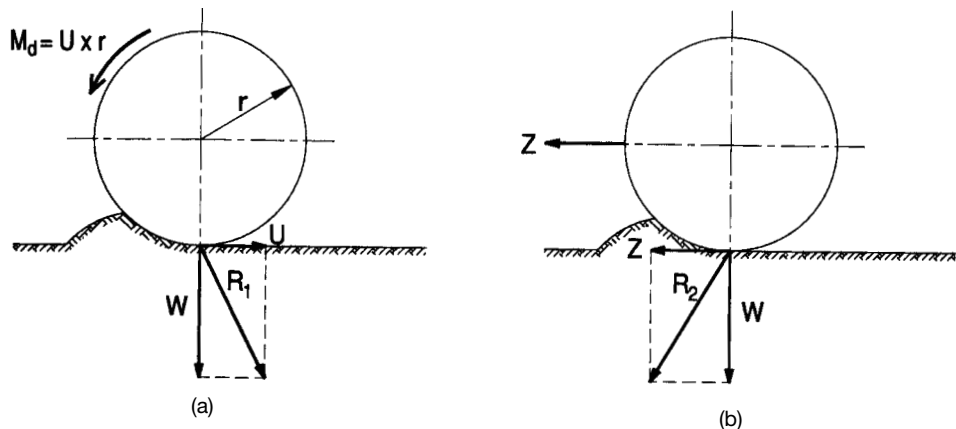
**FIGURE 6A.18** Classification of near-surface compaction equipment (modified after Poesch and Ikes, 1975).

for compacting relatively soft cohesive soils is limited owing to poor traction and a “plowing” effect in which soil is displaced laterally without significant compaction (Hausmann 1990). Smooth drum rollers are also typically very slow compared to newer types of rollers.

A wide variety of *rubber-tired* or *pneumatic rollers* (Fig. 6A.21) are available. Most contain a series of tires closely spaced at regular intervals across the width of the roller. The areal coverage is typically about 80%, and tire pressures up to about 100 psi (700 kPa) are used (Holtz and Kovacs,



**FIGURE 6A.19** Vibratory smooth-drum roller (courtesy of Vibromax 2000 USA Inc., Racine, WI).



Note: The shifts in the points of application of the horizontal forces during travel of the roller are neglected in this analysis.

**FIGURE 6A.20** Forces applied to the ground by a static smooth-drum roller (after Poesch and Ikes, 1975): (a) drum rotating in place; (b) drum pulled by a tractive force ( $Z$ ).



**FIGURE 6A.21** Rubber-tired roller (courtesy of Caterpillar Inc., Peoria, IL).

**6.46** SOIL IMPROVEMENT AND STABILIZATION

1981). Compaction occurs by a combination of static pressure (approximately equal to the inflation pressure of the tires) and kneading action of the tires. *Wobble-wheel rollers* have the wheels mounted such that the tires wobble laterally as the roller is towed forward, which imparts additional kneading action to the soil that facilitates compaction in cohesive soils (Spangler and Handy, 1982). The factors that influence the compactive effort include gross weight of the roller; wheel diameter and load; and tire width, size, and inflation pressure (Hausmann, 1990). Rubber-tired rollers are effective compactors of a wide range of soil types. Large-size tires are desirable in cohesionless soils to avoid shear and rutting. In general, low inflation pressures of 20 to 40 psi (140 to 275 kPa) are desirable for clean sands and gravelly sands with low gravel content, whereas inflation pressures greater than 65 psi (425 kPa) are desirable for cohesive soils and very gravelly soils (Spangler and Handy, 1982). Although not technically classified as compaction equipment, standard rubber-tired and tracked construction vehicles are sometimes used for compaction but are inefficient compared to rubber-tired or other rollers designed specifically for compaction.

In *sheepsfoot rollers* (Fig. 6A.17) and *tamping foot or padfoot rollers* (Fig. 6A.22), protrusions or "feet" of various lengths, sizes, and shapes (Fig. 6A.23) extend outward from a steel drum. Although tamping foot rollers are considered by some to be sheepsfoot rollers, they are categorized separately here because the effectiveness of each type can vary for different cohesive soils and compaction conditions. Sheepsfoot and tamping foot rollers are most effective in cohesive soils and are the best rollers currently available for compacting most cohesive soils. The results from model studies simulating the action of a sheepsfoot in clay and in sand are shown in Fig. 6A.24 (Spangler and Handy, 1982). These results were obtained by photographing the soil movements in a Plexiglas-fronted box caused by vertical penetration of a spherically tipped device and indicate a much larger zone of compaction in clay than in sand.



**FIGURE 6A.22** Self-propelled tamping foot roller with leveling blade on front (courtesy of Caterpillar Inc., Peoria, IL).

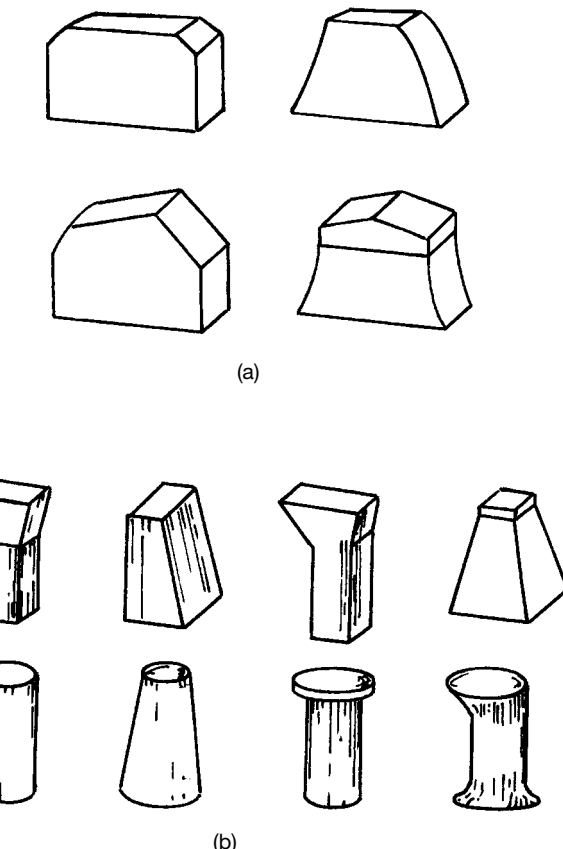


**FIGURE 6A.23** Some typical shapes of feet for compaction rollers (from Poesch and Ikes, 1975): (a) tamping foot; and (b) sheepsfoot.

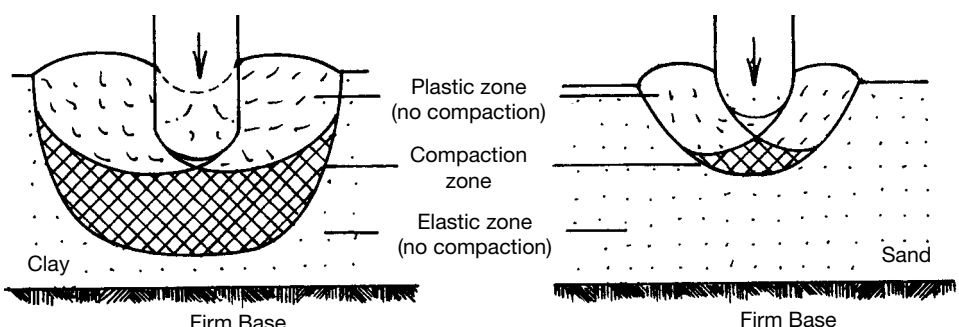


**FIGURE 6A.24** Results of model studies simulating the action of a sheepsfoot roller in clay and sand (from Spangler and Handy, 1982; after Butt et al., 1968).

**6.48** SOIL IMPROVEMENT AND STABILIZATION

Sheepsfoot rollers generally have feet about 6 to 10 in (150 to 250 mm) long with tip areas from 5 to 12 in<sup>2</sup> (30 to 80 cm<sup>2</sup>), provide an areal coverage of 8 to 12%, with contact pressures ranging from about 200 to 1000 psi (1400 to 7000 kPa) (Holtz and Kovacs, 1981). Compaction occurs as a combination of static pressure from the weight of the roller and kneading action of the feet as they penetrate the soil and are rotated through it. In cohesive soils, the high contact pressures permit crushing or breaking of dry clods and remolding of wet clods into a denser soil mass. If the lift thickness is smaller than the length of the feet, densification first occurs along the interface between the previously compacted lift and the new lift as the loose soil along the bottom of the new lift is pushed into and molded with the upper portion of the underlying lift. In this manner a good bond is developed between lifts, which helps prevent sloughing along lift interfaces in fills constructed on slopes and reduces preferential drainage paths for contaminant migration in compacted clay. It is therefore important to compact cohesive soils in thin lifts to promote good interfacial bonding. The upper surface of a newly completed lift is sometimes scarified using discing or other equipment before the next lift is placed to promote better bonding between the lifts. As compaction continues, the soil in the new lift is densified from the bottom upward, and the roller is said to "walk out" of the soil as the upper portion of the lift becomes densified.

The feet on tamping foot rollers are typically shorter, less than 6 in (150 mm), but have greater contact area [20 to 30 in<sup>2</sup> (130 to 190 cm<sup>2</sup>)] than those on sheepsfoot rollers. The areal coverage is also much greater, typically about 40%, with contact pressures ranging from about 200 to 1200 psi (1400 to 8400 kPa) (Holtz and Kovacs, 1981). Some tamping foot rollers have hinged feet for greater kneading action. Like sheepsfoot rollers, tamping foot rollers are most effective in compacting cohesive soils. Tamping foot rollers are generally more effective than sheepsfoot rollers in compacting softer, wetter cohesive soils in which the clods need to be remolded rather than crushed or broken; the larger foot contact area and areal coverage of the tamping foot roller provides better and more uniform remolding of the clods. For the same lift thickness, however, the shorter tamping feet are less effective than sheepsfeet in producing interfacial bonding of lifts; therefore, thinner lift thicknesses or scarification of the lift surfaces is needed when using tamping foot rollers if good bonding between lifts is required.

The drums on *grid rollers* consist of heavy steel mesh that provides about 50% coverage and contact pressures from about 200 to 900 psi (1400 to 6200 kPa) (Holtz and Kovacs, 1981). The moderate areal coverage of the mesh allows high contact pressures while helping to prevent excessive shear deformation responsible for producing plastic waves in front of the roller (Hausmann, 1990). Grid rollers are effective in breaking and rearranging gravel and cobble-sized particles and are primarily used in weathered rocks and rocky soils containing large sand, gravel, and cobble fractions. Cohesive soils tend to clog the mesh, rendering it ineffective by essentially changing the roller into a smooth drum roller. By varying the operating speed of the grid roller, more effective compaction can be obtained; faster speeds can be used in the initial passes to break down the material, and lower speeds can be used in the final passes to produce greater densification (Hausmann, 1990).

Smooth-drum, rubber-tired, sheepsfoot, and tamping foot rollers can have vibrators attached to make them *vibratory rollers*. The vibration is typically produced by rotating eccentric weights. Vibratory rollers are the most effective method for near-surface compaction of cohesionless soils. The vibration produces cyclic deformation of the soil, which can result in significant densification beyond that provided by the static weight of the roller, as shown in Fig. 6A.25. Vibration can, in some instances, produce additional densification in soils with some cohesion (Selig and Yoo, 1977). The effectiveness of vibratory compaction on any given project is a function of the characteristics of the compactor, the properties of the soil, and the construction procedures used. The variables that influence vibratory compaction include the following (Forssblad, 1981; Holtz and Kovacs, 1981):

1. Characteristics of the compactor
  - a. Static weight
  - b. Vibration frequency and amplitude
  - c. Ratio between frame mass and drum mass
  - d. Drum diameter

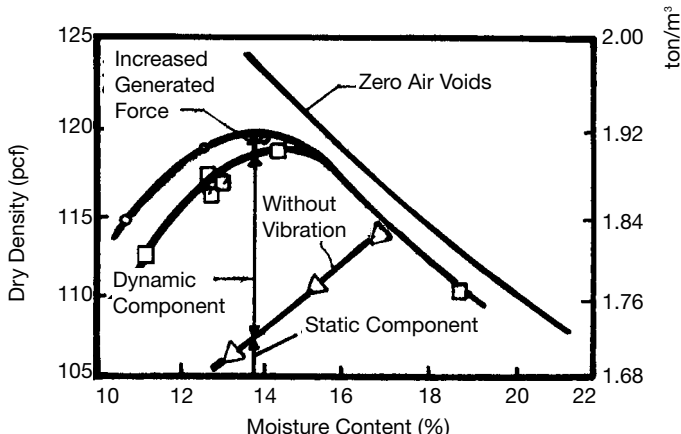


**FIGURE 6A.25** Compaction results on 12-in (305-mm) layers of silty sand with and without vibration using a 17,000-lb (76-kN) towed vibratory roller (after Parsons et al. 1962 as cited in Selig and Yoo, 1977).

2. Properties of the soil
  - a. Initial density (density prior to compaction)
  - b. Grain-size distribution
  - c. Shapes of particles
  - d. Compaction (molding) water content
3. Construction procedures
  - a. Number of passes of the roller per lift
  - b. Lift thickness
  - c. Speed at which the roller is operated

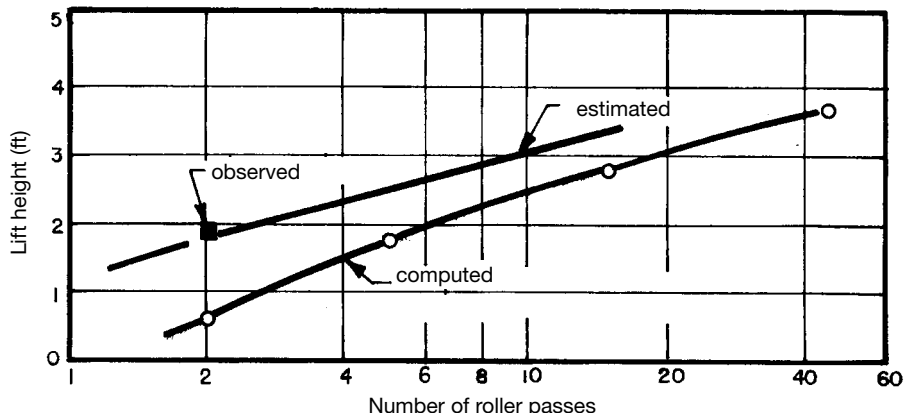
The relationship between lift thickness and number of passes for a given roller and desired soil density is illustrated in Fig. 6A.26. By decreasing the lift thickness, the number of passes needed to achieve the desired density is reduced; conversely, a thicker lift can be used if the number of passes is increased.

The vibration frequency of the compactor has been shown to affect the as-compacted dry density of a wide variety of soil types. As indicated in Fig. 6A.27, in most soils a peak dry density is achieved at an optimum vibration frequency. However, the differences in dry density achieved at various frequencies are relatively small. Better compaction (higher density and greater depth of influence) results from a combination of a large amplitude and a frequency just over the resonance frequency (usually about 25 Hz) than a combination of high frequency and small amplitude (Forssblad, 1981).

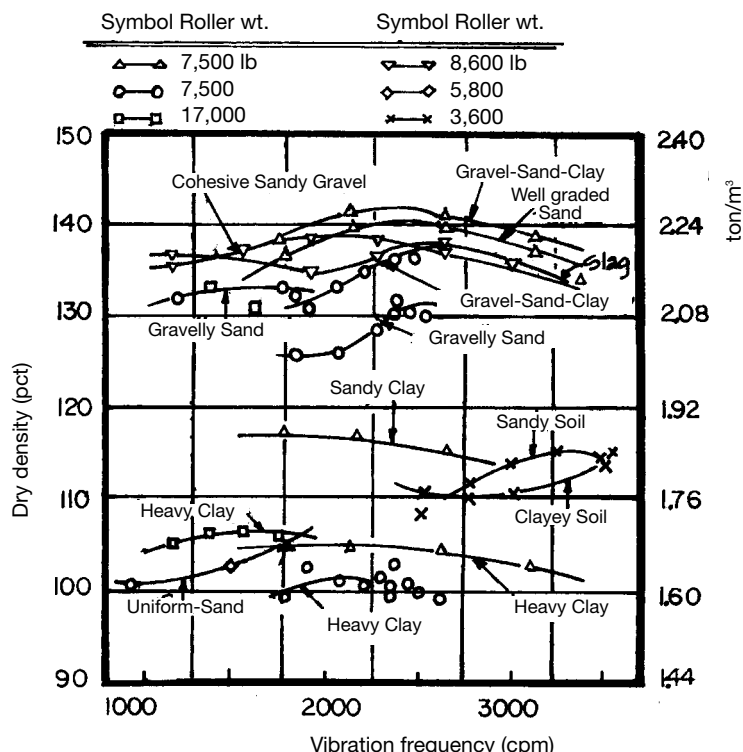
The effect of roller speed and number of passes on the as-compacted dry density of a well-graded sand and a highly plastic clay are shown in Fig. 6A.28. It is apparent from this figure that the dry density increases with increasing number of passes up to a certain point, beyond which little additional densification is achieved from more passes. The influence of roller speed is also obvious; for comparable conditions, reducing the travel speed results in higher as-compacted dry density.

The *impact roller* was developed in the 1950s in South Africa for in situ densification of collapsible sands (see Sec. 6A.3.4.2) (Clifford, 1980). An impact roller typically consists of a four-faced rolling mass that delivers four impact blows per revolution and is towed at an ideal speed of about 6 to 9 mi/h (10 to 14 km/h). The typical shape of an impact roller is shown in Fig. 6A.29 and

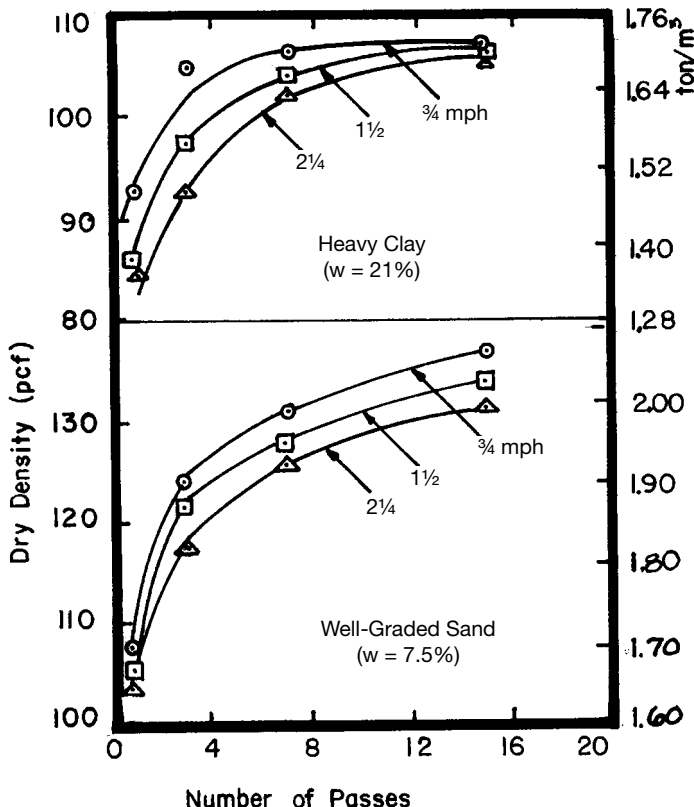
## 6.50 SOIL IMPROVEMENT AND STABILIZATION



**FIGURE 6A.26** Relationship between lift height and number of passes of a 12,500-lb (56-kN) vibratory smooth-drum roller required to achieve a minimum relative density of 75% in a dune sand (from D'Appolonia et al., 1969).



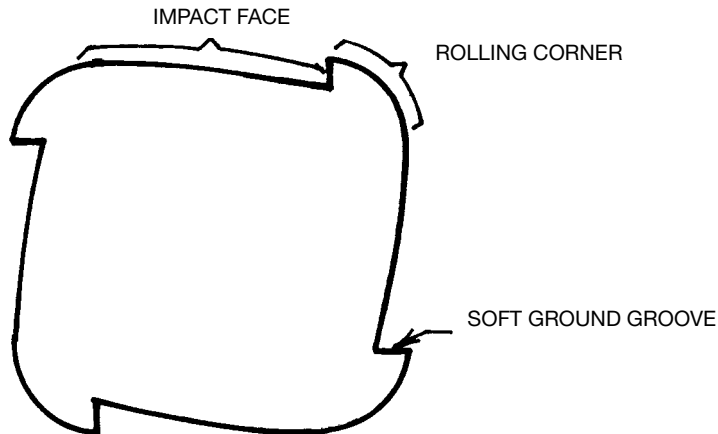
**FIGURE 6A.27** Effect of vibration frequency on the as-compacted dry density of different soils (from Selig and Yoo, 1977).



**FIGURE 6A.28** Influence of travel speed and number of passes on the as-compacted dry densities of a clay and a sand (from Parsons et al., 1962 as cited in Selig and Yoo, 1977).

includes rounded corners to simplify transition from one lift and fall cycle to the next. A groove is incorporated behind each rolling corner to allow the roller mass to revolve freely during impact even in soft ground when the corner penetrates some distance into the surface of the soil. The impact faces of the roller are rounded so that as the soil densifies, the impact blow is dissipated over a smaller and smaller area, effecting compaction to greater depth. The high energy delivered by an impact roller compacts materials up to about 10 ft (3 m) thick. A corrugated surface is left by the impact roller, which has been found to produce good interfacial bonding of lifts and to reduce potential interfacial shear movements. If a smooth final surface is desired, the top lift must be proofrolled with a smooth-drum roller.

Most *vibratory plate compactors* (Fig. 6A.30) are self-propelled and hand-guided and are used primarily for base and subbase compaction for streets, sidewalks, and the like; street repairs; fills behind bridge abutments, retaining walls, basement walls, and so on; fills below floors; and trench fills (Broms and Forssblad, 1969). Tractor-mounted and crane-mounted models are also available. Compaction is achieved by the application of high-frequency (10 to 80 Hz), low-amplitude vibrations (Wacker, 1987). Vibratory plates are usually powered by gasoline or diesel engines and are used mainly for compacting granular and low-cohesion soils. The hand-guided vibratory plate com-

**6.52** SOIL IMPROVEMENT AND STABILIZATION

**FIGURE 6A.29** Typical shape of an impact roller (from Clifford, 1980).

actors generally weigh between 100 and 6000 lb (0.4 to 27 kN) and come in a wide variety of plate sizes.

Hand-guided *rammers* or *tampers* densify the soil by a combination of impact and vibratory compaction. The most common applications for rammers are for street repairs; fill behind bridge abutments, retaining walls, basement walls, and so on; and trench fills (Broms and Forssblad, 1969). In *explosion* or *combustion rammers* (Fig. 6A.31), a mixture of either diesel fuel or gasoline and air is ignited in an internal chamber that simultaneously forces the rammer against the ground and lifts



**FIGURE 6A.30** Vibratory plate compactor (courtesy of Wacker Corporation, Menomonee Falls, WI).

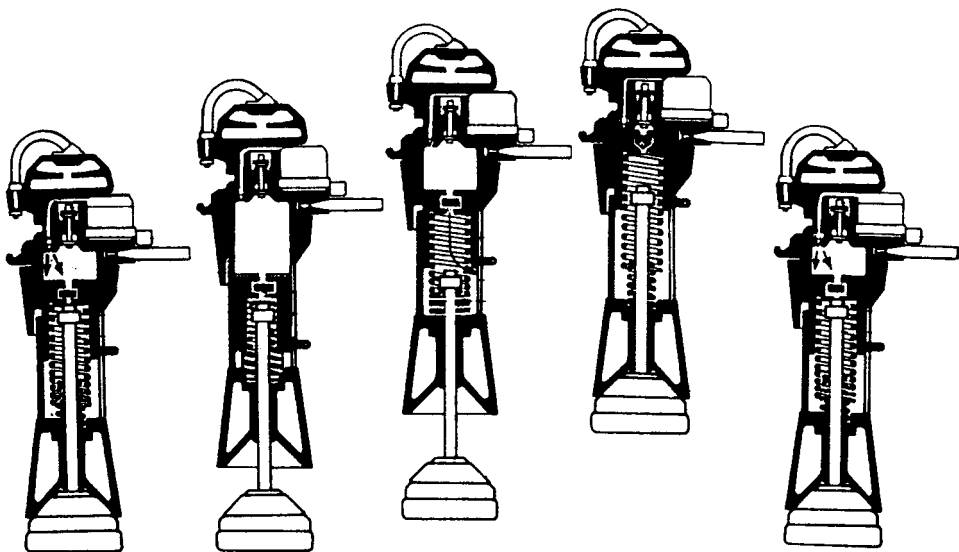


**FIGURE 6A.31** Typical action of an explosion rammer (modified after Poesch and Ikes, 1975).

the casing off the ground. After the casing has moved upward a short distance independent of the rammer, the piston rod (which is attached to the rammer) is pulled upward with the casing until the maximum trajectory reached. The casing and rammer then fall freely to the ground, where a second impact occurs. Thus, two impacts are produced from one explosion. Explosion rammers typically weigh about 200 to 2000 lb (1 to 10 kN), with impact surface areas of about 80 to 930 in<sup>2</sup> (500 to 6000 cm<sup>2</sup>) (Poesch and Ikes, 1975). *High-frequency rammers* (Fig. 6A.32) are usually powered by gasoline or diesel engines and produce high-frequency impacts through a piston/spring system connected to the engine via a gear transmission system (Wacker, 1987). Typical characteristics of high-frequency rammers are as follows (Broms and Forssblad, 1969; Wacker, 1987):

Frequency: 6 to 14 Hz

Weight: 100 to 300 lb (450 to 1300 N)

Impact area of ramming shoe: 100 to 500 in<sup>2</sup> (650 to 3200 cm<sup>2</sup>)

Maximum height rammer comes off ground: 1 to 3 in. (25 to 75 mm)

High-frequency rammers can be used on granular and cohesive soils.

### 6A.3.2 Moisture-Density Relationships

The quality of a compacted soil is frequently correlated with the dry density of the as-compacted soil; that is, a greater dry density is commonly assumed to mean a better soil. Although this correlation is generally valid for many soils in terms of their strength and compressibility, other parameters (especially water content) may have an important effect, especially in cohesive soils. In addition, some engineering properties of certain soils are only slightly influenced by dry density, and other parameters such as moisture condition have a greater effect. These relationships will be discussed in more detail in Sec. 6A.3.4. Despite these other considerations, the fact remains that dry density is

**6.54** SOIL IMPROVEMENT AND STABILIZATION

**FIGURE 6A.32** High-frequency rammer.

the property used most often to determine whether a compacted soil will exhibit the desired engineering behavior.

The primary factors that influence the value of dry density obtained by compacting a specific soil are as follows:

1. Moisture condition of the soil during compaction (molding or compaction water content)
2. Compactive energy or effort per unit volume of soil (lift thickness and number of passes, blows, or tamps of the equipment)
3. Method of compaction (compaction equipment)
4. Rate of compaction (rate of travel, frequency of impact, or frequency of vibration of the equipment)

For a given situation in which factors 2, 3, and 4 are held constant, the as-compacted dry density of the soil may vary significantly depending on the molding water content. For many soils, the

moisture–density relationship for a given method of compaction and compactive effort can be described by a single peak curve similar to that shown in Fig. 6A.33. The water content and dry density corresponding to the highest peak in the moisture–density curve for one method of compaction and one level of compactive effort are referred to as the *optimum* water content and *maximum* dry density. If the method of compaction or the compactive effort is varied, the moisture–density curve for the same soil will be different. For example, the effect of varying the compactive effort for the same soil and the same method of compaction is illustrated in Fig. 6A.34; similarly, the influence of method of compaction is shown in Fig. 6A.35. Therefore, for a specific soil there are an infinite number of optimum water contents and maximum dry densities, and the terms optimum and maximum are relative rather than absolute and should be used in proper contexts.

For a given method of compaction, the optimum moisture condition for achieving the maximum dry density is represented by the locus of points corresponding to the peak points for various compactive efforts (Fig. 6A.34). This locus of points is known as the *line of optimums* or the *locus of optimums*. Analysis of the general trend of the line of optimums shows that the maximum dry density increases and the optimum water content decreases as the compactive effort is increased. This trend is not without bounds, however, as a point is reached where applying additional compactive effort produces no measurable increase in dry density and in some instances may produce a decrease in dry density.

The line of optimums is generally approximately parallel to the zero air voids line (ZAVL), which represents a degree of saturation of 100%, and as such the line of optimums is approximately a line of constant degree of saturation. In the author's experience, the degree of saturation represented by the line of optimums varies from about 60 to 95%, with the lower values for clean sands and higher values for highly plastic clays; for most soils this value ranges between 70 and 85%. This correlation is important with respect to the engineering behavior of many soils (to be discussed in Sec. 6A.3.4) and suggests that the moisture condition of a soil may, in some circumstances, be better represented by degree of saturation rather than by water content. The approximate degree of saturation represented by the line of optimums is referred to as optimum saturation ( $S_{opt}$ ). The line of optimums may vary for a given soil depending on the method of compaction, as shown in Figure 6A.36 for a lean clay. The range in degree of saturation for each of the four lines of optimums shown in Fig. 6A.36 are summarized as follows (assuming  $G_s = 2.70$ ):

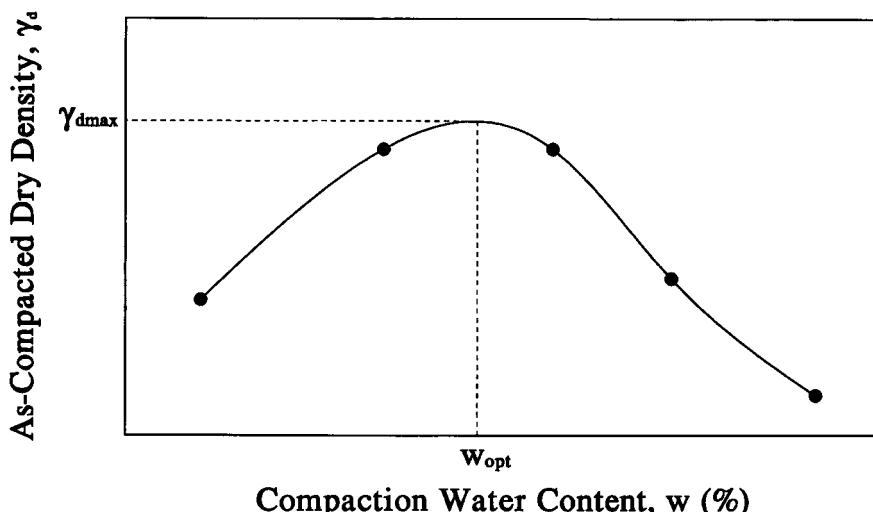
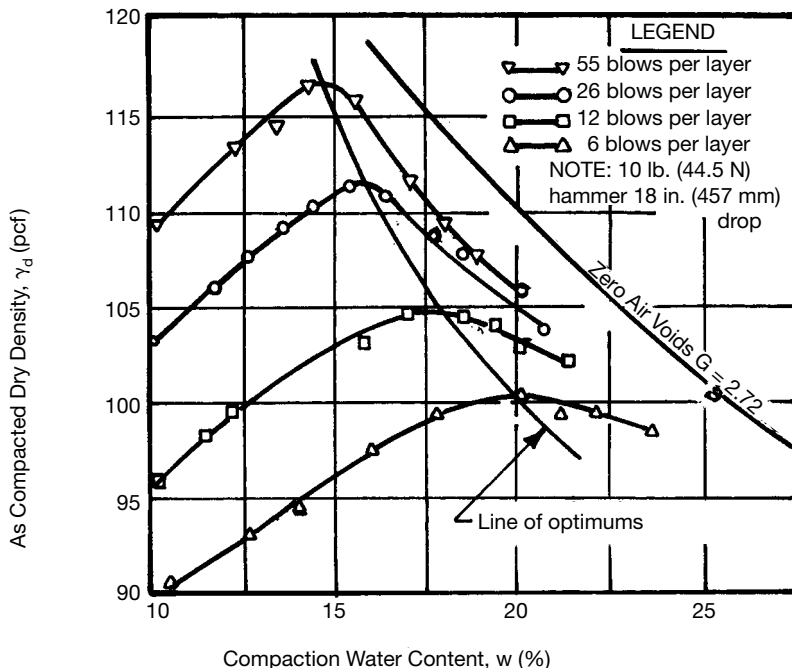


FIGURE 6A.33 Typical moisture–density relationship for compacted soil.

## 6.56 SOIL IMPROVEMENT AND STABILIZATION



**FIGURE 6A.34** Effect of compactive effort on the moisture–density relationship of an impact-compacted soil (from Foster, 1962).

Method of Compaction	Approximate Range of $S_{opt}$
Sheepsfoot roller	73–83%
Laboratory impact	77–86%
Laboratory static	80–81%
Rubber-tired roller	89–90%

For each method of compaction,  $S_{opt}$  varies within a fairly narrow range ( $\leq 10\%$ ). Although the lines of optimums vary somewhat from each other, the line of optimums from the laboratory impact (Proctor) tests provides a reasonable approximation of the line of optimums for the two field-compacted soils, and this is generally true for most soils.

The ZAVL varies as a function of specific gravity of the soil solids, and the ZAVL can be found from the following equation by setting  $S_r = 100\%$ :

$$w = \left( \frac{\gamma_w}{\gamma_d} - \frac{1}{G_s} \right) \cdot S_r \quad (6A.15)$$

where  $\gamma_d$  = dry density (by mass or weight) of the soil

$\gamma_w$  = density (by mass or weight) of water

w = water content

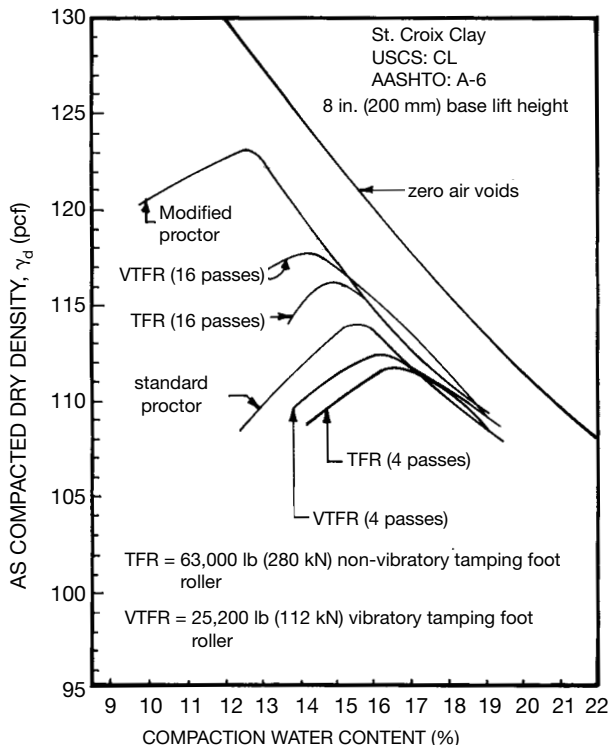


**FIGURE 6A.35** Comparison of laboratory and field moisture-density relationships for St. Croix clay (modified after Lin and Lovell, 1981; data from Terdich, 1981).

$S'$  = degree of saturation

$G_s'$  = average specific gravity of the soil solids

Any line of constant saturation (e.g., 60%, 70%, 80%) can be found using Eq. (6A.15).

Although the single peak curve is most common, an extensive laboratory study by Lee and Suedkamp (1972) showed that three irregularly shaped curves can also occur, as illustrated in Fig. 6A.37. The results from their research indicate that (1) soils with a liquid limit between 30 and 70 typically exhibited a single-peak moisture-density curve; (2) both double-peak and oddly shaped curves were present in soils with a liquid limit greater than 70; (3) soils with a liquid limit less than 30 usually produced either a double-peak or a one-and-one-half peak curve; and (4) the length of the moisture conditioning period substantially affected the moisture-density relationships in high-plasticity (high-liquid-limit) soils but had little influence on low-plasticity or nonplastic soils.

The moisture-density curves for free-draining sands and sandy gravels typically have  $1\frac{1}{2}$  peaks, as illustrated in Figure 6A.38 (Foster, 1962). The maximum dry density for these soils is obtained in either the air-dried or saturated condition. In the partially saturated state, capillary suction increases the effective stresses in the soil and produces a resistance to compaction called *bulking*. Because it is difficult to keep large quantities of borrow materials in the air-dried condition, sands and sandy gravels are usually placed saturated. Keeping free-draining soils saturated is not easy and generally requires continuous wetting of the soil in front of the compaction equipment.

## 6.58 SOIL IMPROVEMENT AND STABILIZATION

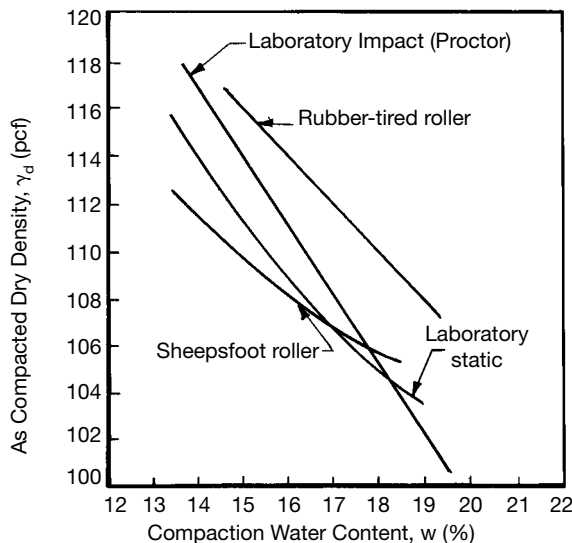


**FIGURE 6A.36** Comparison of lines of optimums for four methods of compaction (Foster, 1962).

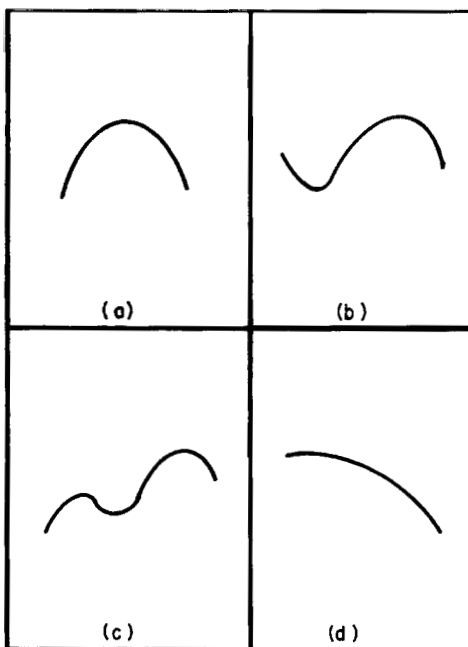


**FIGURE 6A.37** Types of moisture-density curves: (a) single peak; (b) one-and-one-half peaks; (c) double peak; and (d) oddly shaped (Lee and Suedkamp, 1972).

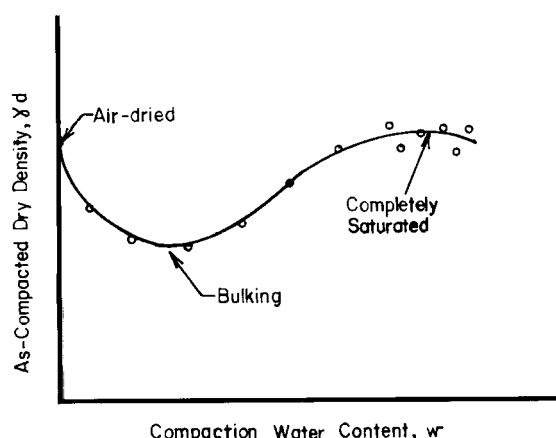


**FIGURE 6A.38** Typical compaction curve for free-draining sands and sandy gravel (Foster, 1962).

The temperature of the soil during compaction has a noticeable effect on as-compacted dry density when the temperatures are above freezing—the same compactive effort produces a lower dry density at the same compaction water content (Waidelich, 1990). Thus, more compactive effort is needed to obtain the same value of dry density at lower temperatures. If the temperature of the soil is below freezing, it is extremely difficult, uneconomical, and virtually impossible under some circumstances to obtain the densities required for proper performance of a compacted fill. The influence of temperatures below freezing on the standard and modified Proctor moisture–density relationships of a sand with a trace of silt is illustrated in Fig. 6A.39. At a temperature of 30°F ( $-1^{\circ}\text{C}$ ) standard Proctor  $\gamma_{d\max}$  was 94% of the value at 74°F ( $23^{\circ}\text{C}$ ), and increasing the compactive effort to modified Proctor (4.5 times that of standard Proctor) at 30°F ( $-1^{\circ}\text{C}$ ) only increased  $\gamma_{d\max}$  to 98% of standard Proctor  $\gamma_{d\max}$  at 74°F ( $23^{\circ}\text{C}$ ). An additional problem with fills compacted at temperatures below freezing is that the interior portions of the fill may take several years to thaw, depending on the type of fill and its dimensions. For these reasons, it is highly recommended that compaction not be conducted during freezing weather; in fact, many government agencies located in freezing climates that engage in earthwork construction do not permit the construction of fills during winter months.

### 6A.3.3 Laboratory Compaction and Testing

The best method for predicting the engineering behavior of compacted soil is to conduct full-scale field testing on the soil that simulates as closely as possible the actual service conditions. For exam-

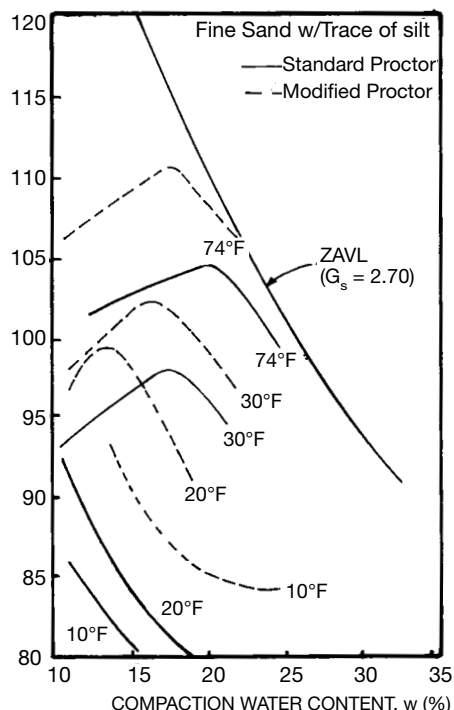


**FIGURE 6A.39** Influence of temperature on the moisture–density relationships of a sand with a trace of silt (from Waidelich, 1990).

**6.60** SOIL IMPROVEMENT AND STABILIZATION

ple, if the compacted soil is to support shallow foundations for a building, full-scale load tests can be conducted on all footings prior to any construction of the superstructure to ensure that the compacted soil can support the footings without excessive settlement or failure. This method is rarely used in practice for obvious reasons—the cost is extremely high, and a long time is required for testing. For a compacted fill, a test pad is sometimes constructed using the actual soil and compaction equipment, and appropriate tests (field, laboratory, or both) are conducted on the test pad to determine the important engineering properties. For example, many state and federal regulatory agencies currently require that a test pad be constructed to simulate a compacted clay liner for waste containment systems. In situ permeability tests (usually double-ring infiltration tests, ASTM D5093) are then conducted on the test pad to verify that the permeability of the test pad is less than the maximum allowable value (usually  $1.0 \times 10^{-7}$  cm/s =  $2.8 \times 10^{-4}$  ft/day). However, laboratory tests are used on many projects as the primary method for predicting, controlling, and verifying the engineering properties and behavior of compacted soil because laboratory tests generally cost much less than comparable field tests.

It is important to model field conditions as closely as possible when conducting moisture–density tests and when preparing samples to be used in other types of laboratory tests. For example, recent research on compacted soils has shown that clod size and percentage of large-size particles (gravel and larger) have an important effect on the engineering properties of compacted soils (e.g., Benson and Daniel, 1990; Day, 1989, 1991; Houston and Randeni, 1992; Houston and Walsh, 1993; Larson et al., 1993; Shelley and Daniel, 1993). A general rule of thumb for laboratory testing is that the maximum particle or clod size should be less than one-sixth to one-tenth the smallest dimension of the sample. It is therefore important to test samples that are large enough to obtain results that are representative of field behavior. Several methods are available for correcting for oversize particles, where the term oversize refers to particles that are too large to be included in a particular testing apparatus (see ASTM D698, D1557, D4253, and D4718; Hausmann, 1990; Houston and Walsh, 1993; Fragaszy et al., 1992; Siddiqi et al., 1987).

When preparing soils for moisture–density determination or when making specimens for laboratory testing, the soil should be brought to the desired water content and double-sealed in airtight containers for a sufficient time to allow the soil to come to moisture equilibrium (called the *moisture conditioning period*). For proper modeling of field compaction techniques, this moisture conditioning period should duplicate that to be used in the field. As noted previously, for cohesive soils a minimum of 24 h is desirable, and for highly plastic soils 72 h or more may be needed for proper moisture conditioning. When preparing samples for testing at specific values of water content and density, a method of compaction should be used that simulates as closely as possible the field compaction method. A comparison of the most common laboratory and field compaction methods is provided in Table 6A.3, and additional details on laboratory compaction methods are given below.

#### **6A.3.3.1 Static Compaction**

For all laboratory compaction methods, the soil is placed loosely into a compaction mold (usually cylindrical with a base plate and generally made of steel or aluminum), and the surface of the soil is leveled as well as possible using a spatula or similar device. In static compaction, a loading plate slightly smaller than the inner diameter of the mold (usually with an attached piston) is placed gently onto the surface of the loose soil and a compressive force is applied to the soil via the loading plate in one of several ways (see Fig. 6A.40). The most common methods are (1) slowly pushing the loading plate using a speed-regulated compression machine; (2) jacking against a reaction frame using a hydraulic jack; or (3) applying constant force using a dead-weight reaction frame. The compressive stress is increased until the desired density has been achieved or a predetermined energy has been applied. A diagram of a mold used by the writer to prepare statically compacted oedometer specimens is shown in Fig. 6A.41. Compactive energy can be determined by numerically integrating the load-deformation curve (Fig. 6A.42). It is difficult to apply a predetermined magnitude of compactive effort, especially if a speed-regulated compression machine is used, as the energy must be calculated immediately after each set of load and deformation readings and the test stopped when the desired energy level has been reached.

**TABLE 6A.3** Comparison of Common Laboratory and Field Compaction Methods

Type of Compaction	Laboratory methods	Field methods
Static	Loading plate with outer diameter slightly smaller than inner diameter of mold is pushed onto soil using a speed-regulated compression machine, a hydraulic jack within a loading frame, or a dead weight loading system (Fig. 6A.40).	Smooth drum roller (nonvibratory) Rubber-tired roller*
Impact	Impact hammer is used to drop a rammer with a diameter about one-third to one-half the diameter of the mold from a given height onto the soil (Fig. 6A.43). In some setups, the diameter of the rammer is slightly smaller than the diameter of the mold.	Impact roller Hand-guided rammer† Dynamic compaction
Kneading	Harvard miniature tamper is pushed into the soil until the spring deflects (Fig. 6A.44).	Sheepsfoot roller Tamping foot roller Rubber-tired roller*
Vibratory	California kneading compactor is used to push a compaction foot into the soil at constant pressure for a given time (Fig. 6A.45).  Mold containing soil plus surcharge weight on top of the soil is placed on vibrating table and vibrated (Fig. 6A.47).  High-frequency rammer compacts the soil within a mold (Fig. 6A.48). The ramming plate has a diameter slightly smaller than the diameter of the mold	Vibratory rollers‡ Vibrating plates Hand-guided rammers†

\*Combination static and kneading compaction.

†Combination impact and vibratory compaction.

‡Some vibratory rollers, such as vibratory sheepsfoot and vibratory rubber-tired rollers, compact by using a combination of vibration and kneading action, and require more sophisticated tools to model.

## 6.62 SOIL IMPROVEMENT AND STABILIZATION

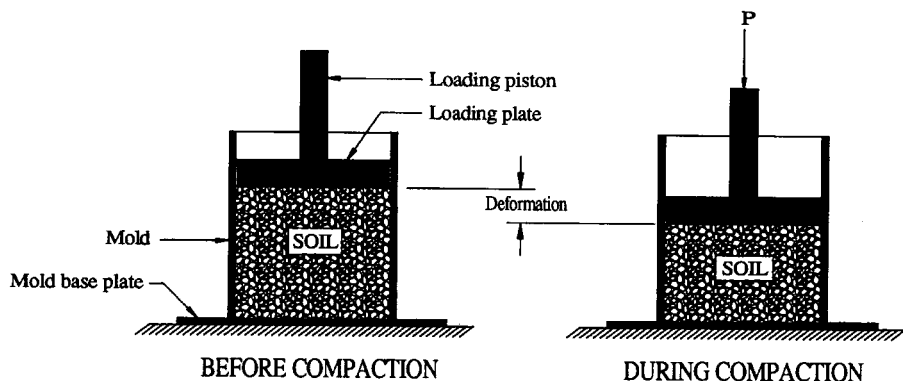


FIGURE 6A.40 Schematic illustration of laboratory static compaction.

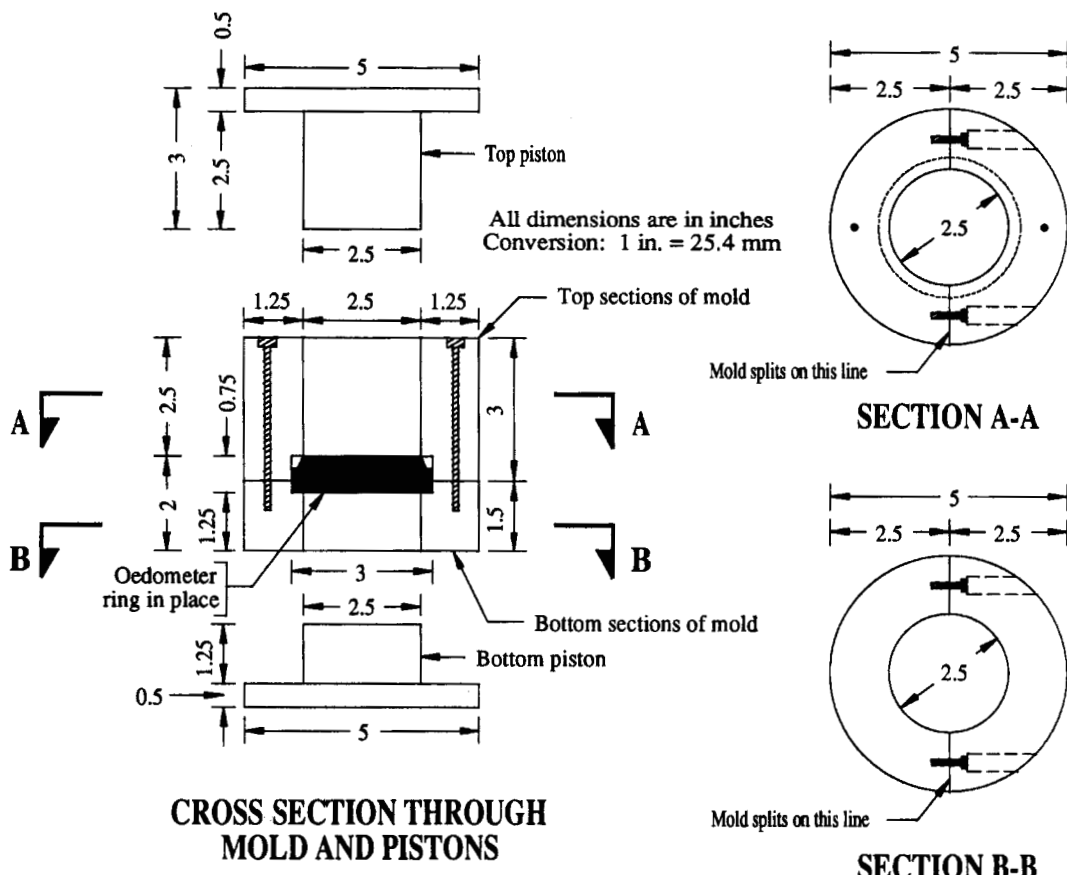
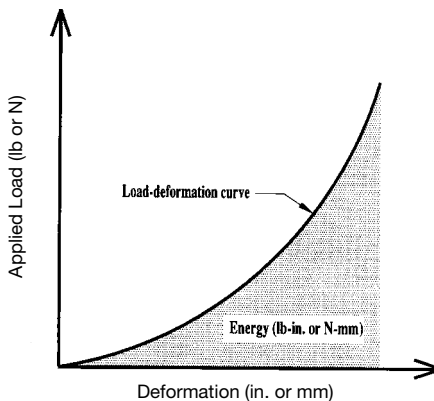


FIGURE 6A.41 Schematic diagram of mold for laboratory static compaction of oedometer specimens.



**FIGURE 6A.42** Typical load-deformation curve from laboratory static compaction illustrating energy of compaction.

Static compaction is a relatively inefficient laboratory compaction method, because for any given type of soil and compaction water content, the same density can be achieved with less effort using another compaction method. Most samples need to be compacted in thin lifts because the force required to obtain a given density can be enormous. For example, the author once attempted to use static compaction to prepare a 6-in (152-mm) diameter sample of clayey sand in 2-in (50.8-mm) thick lifts to modified Proctor maximum dry density at the modified Proctor optimum water content. Using a 250,000-lb (1.1-MN) capacity compression machine normally used for structural engineering testing, the capacity of the machine was reached before the desired density was achieved. However, static compaction is commonly used in parametric studies because the reproducibility of nominally identical fine-grained specimens is greater than for the other methods. Because the method of compaction can have a significant influence on the as-compacted fabric of soils—and hence their engineering properties (see Sec. 6A.3.4)—static compaction should be used with caution.

#### 6A.3.3.2 Impact Compaction

Impact compaction, usually in the form of Proctor tests, is the most commonly used method for estimating the moisture–density relationships of compacted soil. Of all the types of compaction rollers described in Sec. 6A.3.1, only the impact roller can be classified as an impact method. Therefore, the use of impact tests to predict field behavior of most compaction rollers may create some problems because of differences in moisture–density relationships between the laboratory and field compaction methods. A comparison of the differences in moisture density curves for two compaction rollers and laboratory impact compaction was given previously (Fig. 6A.35). Furthermore, differences in compaction method can have an important effect on the fabric of fine-grained soils and therefore the engineering behavior of compacted soils. Impact methods are used so frequently primarily because of their relatively low cost and the ease and accuracy in calculating compactive effort. However, the potential differences in moisture–density relationships and other engineering characteristics must be considered when deciding which compaction method to use for laboratory and field testing of compacted soils.

The standard test for determining the moisture–density relationships of compacted soils are impact tests in which rammers of a given weight are dropped from a constant height onto soil contained within a mold (Fig. 6A.43). Either hand-held or automatic hammers may be used. These tests are routinely conducted in the laboratory and the field and are commonly referred to as the *Proctor tests* in honor of R. R. Proctor, who in 1933 introduced the principles of modern compaction in a series of

## 6.64 SOIL IMPROVEMENT AND STABILIZATION

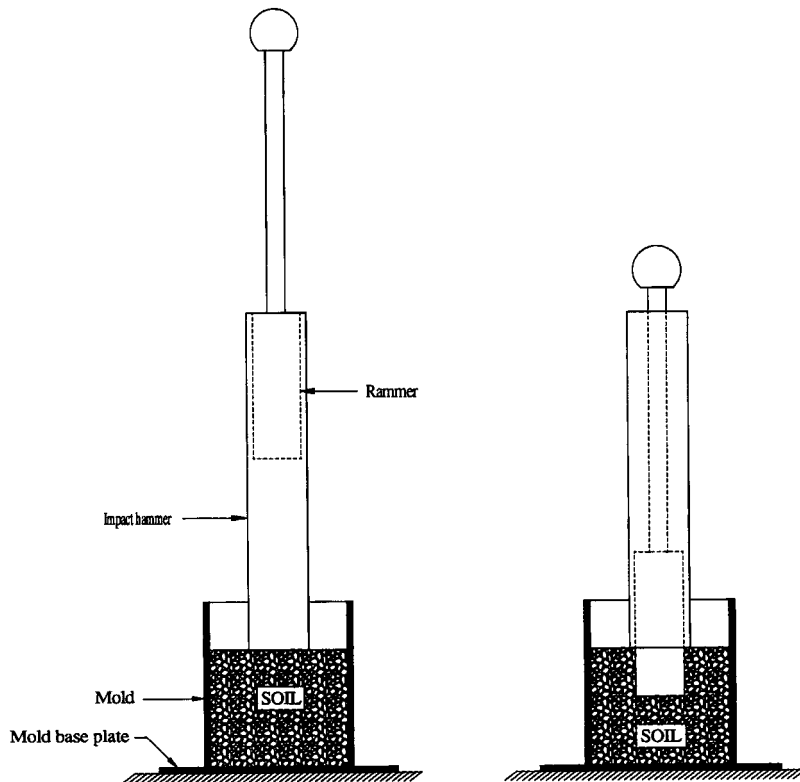


**FIGURE 6A.43** Schematic illustration of laboratory impact compaction.

four articles in the *Engineering News-Record* (Proctor, 1933). Two variations of the Proctor test are used—the *standard* and *modified* tests (ASTM D698 and D1557). The basic procedures for the two tests are the same, but the compactive efforts are considerably different. The variation in details for the two tests are outlined in Table 6A.4. The original (standard) Proctor test was developed to model the compactive effort of light rollers in use at that time. The modified Proctor test was developed later to simulate the compactive effort of heavier compaction equipment that subsequently became common.

Two types of procedures can be used to prepare impact-compacted specimens for oedometric, triaxial, and other types of testing. One method involves compacting oversize specimens using a Proctor hammer and mold and trimming the specimens to the desired shape and dimensions. This method is applicable only to cohesive soils and is often difficult to perform on compacted specimens because they do not trim easily at low to moderate water contents (owing to the stiff, brittle nature of the compacted soil). A second procedure involves compacting a specimen in a mold or ring with the desired shape and dimensions using a properly sized impact hammer. For some applications, stock or special order molds and hammers are available from various geotechnical equipment suppliers. If the impact face of the hammer has a diameter that is smaller than the diameter of the confining ring or mold, it is impossible to get the surface of the specimen perfectly flush with the top of the confining ring or exactly perpendicular to the axis of the specimen at the desired height by compaction with the hammer alone. To compensate for this unevenness, the surface of the specimen must be left slightly above the top of the ring or the desired height and brought to the appropriate level in one of the following ways:

**TABLE 6A.4** Comparison of Standard and Modified Proctor Tests

Detail	Standard Proctor	Modified Proctor
Rammer		
Diameter*	2.0 in (50.8 mm)*	2.0 in (50.8 mm)*
Drop height	12.0 in (304.8 mm)	18.0 in (457.2 mm)
Weight (mass)	5.5 lb (2.49 kg)	10.0 lb (4.54 kg)
Mold		
Option 1		
Diameter	4.0 in (101.6 mm)	4.0 in (101.6 mm)
Height	4.584 in (116.4 mm)	4.584 in (116.4 mm)
Volume	1/30 ft <sup>3</sup> (994 cm <sup>3</sup> )	1/30 ft <sup>3</sup> (994 cm <sup>3</sup> )
Option 2		
Diameter	6.0 in (152.4 mm)	6.0 in (152.4 mm)
Height	4.584 in (116.4 mm)	4.584 in (116.4 mm)
Volume	1/13.333 ft <sup>3</sup> (2124 cm <sup>3</sup> )	1/13.333 ft <sup>3</sup> (2124 cm <sup>3</sup> )
No. of soil layers	3	5
Blows per layer		
Mold Option 1	25	25
Mold Option 2	56	56
Compactive effort	12,375 ft-lb/ft <sup>3</sup> (593 kJ/m <sup>3</sup> )	56,250 ft-lb/ft <sup>3</sup> (2693 kJ/m <sup>3</sup> )

\*Diameter shown is for a hand-held hammer or an automatic compactor used with a 4.0-in (101.6-mm) mold. If an automatic compactor is used with a 6.0-in (152.4-mm) mold, a foot in the shape of a sector of a circle with a radius of 2.90 in (73.7 mm) is used.

1. If the specimen is contained within a confining ring, the specimen can be trimmed level with the top of the ring using a stiff, sharpened, metal trimming bar. For cohesive specimens that will be removed from the mold—such as for unconfined compression or triaxial testing—the specimens can be cut to the proper height using a miter box and wire saw. However, if the specimen is brittle, as is the case for compacted specimens at low to moderate compaction water contents, this method will not work because the specimen will crumble or chunks will break off the specimen, leaving the end uneven and unsuitable for testing.
2. The preferred method is to complete the specimen using static compaction, which involves removing the impact hammer and replacing it with a loading plate that has a diameter slightly smaller than the inside diameter of the ring or mold. The loading plate is then pushed to the top of the ring or to the desired height of specimen via a loading piston (Fig. 6A.40).

#### 6A.3.3.3 Kneading Compaction

Two types of kneading apparatuses are commonly used to compact soils in the laboratory—the Harvard miniature tamper (Wilson, 1970) and the California kneading compactor (ASTM D1561, D2844). The Harvard miniature tamper consists of a 0.5-in (12.7-mm) diameter piston attached to a spring contained within an otherwise hollow handle (Fig. 6A.44). An adjusting nut is used to preset the compression of the spring to a specified force, commonly 40 lb (178 N). Springs of different stiffnesses can be used to provide various values of preset force. The tamper is inserted into the mold and pushed firmly into the soil until the spring just begins to compress; at this point, a force equal to the preset value has been applied to the soil. The tamper is then pulled from the soil, and one “tamp” has been completed.

Specimens for testing can be made in layers within a mold by applying a sufficient number of tamps to each layer to obtain the desired density. Moisture-density relationships can be obtained by

## 6.66 SOIL IMPROVEMENT AND STABILIZATION

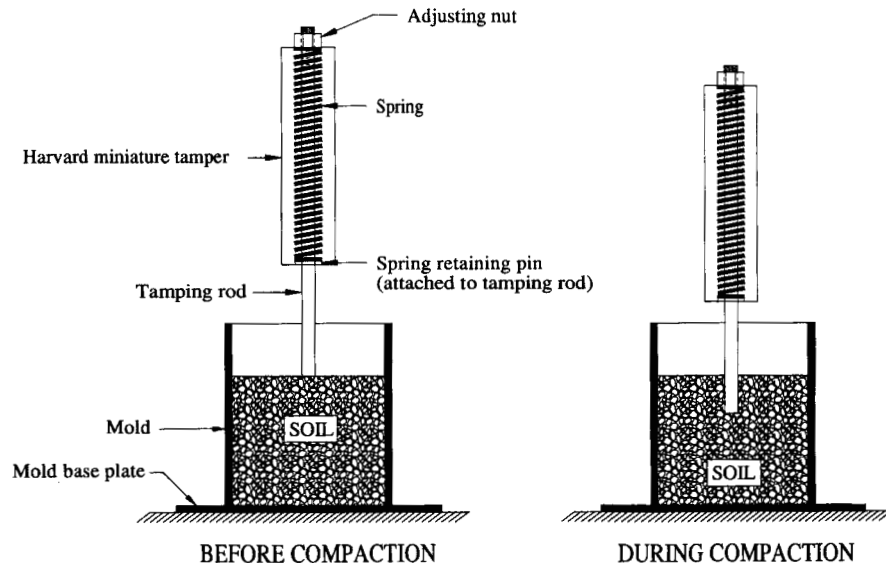


**FIGURE 6A.44** Schematic illustration of laboratory kneading compaction using a Harvard miniature tamper.

varying the water content of the soil and applying a predetermined level of compactive effort. Compactive effort is controlled by the volume of soil in the layer and the number of tamps per layer. A standard procedure for conducting moisture-density tests using the Harvard miniature tamper is given in Wilson (1970).

With the California kneading compactor, the soil is compacted within a 4-in (102-mm) diameter mold by applying a constant pressure to the soil via a pie-shaped tamper foot (see Figs. 6A.45 and 6A.46). When each tamp is completed, the mold is rotated an equal angle (usually 5 to 7 tamps per revolution), and another tamp is applied. This process is continued until a given number of tamps

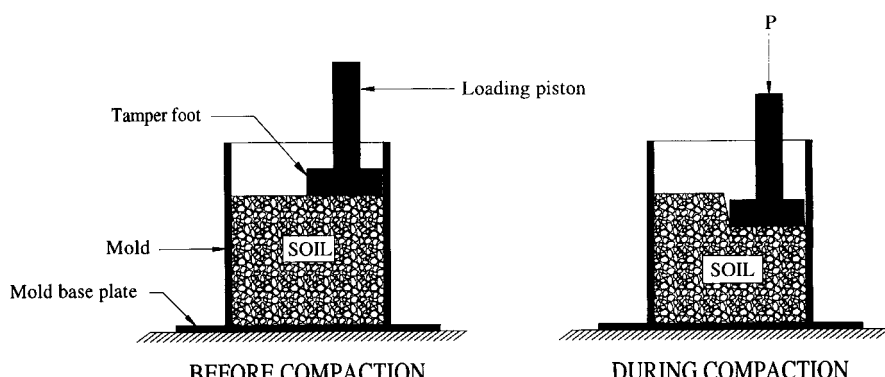


**FIGURE 6A.45** Schematic illustration of laboratory compaction using a California kneading compactor.

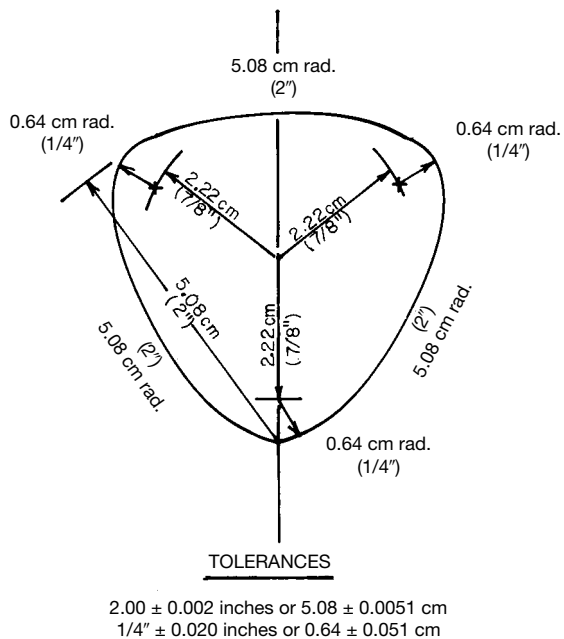


**FIGURE 6A.46** Characteristics of pie-shaped tamper foot for California kneading compactor (from ASTM D2844).

have been applied or until additional tamps produce no additional compaction in the lift. The compactive effort applied to the soil can be changed by varying the pressure of application, the lift height, or both. Specimens that will be subjected to additional testing are usually trimmed from the 4-in (102-mm) diameter specimen created during the compaction process.

The top surface of specimens prepared using either the Harvard miniature tamper or the California kneading compactor are generally neither level nor square (perpendicular to the axis). If the specimens are to be tested without being trimmed, a final application of static compaction is needed to provide a level and square surface. Procedures similar to those described for impact compacted specimens in Sec. 6A.3.3.2 can be used.

#### 6A.3.3.4 Vibratory Compaction

In the United States, vibratory compaction of cohesionless soils is most commonly conducted in the laboratory using a vibratory table (Fig. 6A.47). To simulate field compaction, soil at an appropriate water content is placed loosely in a mold, a surcharge weight corresponding to the expected surcharge pressure in the field is placed gently on top of the loose soil, and the mold containing the soil and surcharge weights is secured to a vibratory table and vibrated at a given amplitude and frequency for a period. The soil to be densified can be dry, wet, or moist depending on the field conditions to be modeled. Vibration is continued until the desired density is achieved. If no further densification can be achieved but the desired density has not been obtained, the amplitude of vibration can, in some instances, be varied to achieve a greater densification.

Standard test methods are also available for determining the maximum index density of free-draining soils using a vibratory table (ASTM D4253). Because capillary tension in partially saturated soils creates a resistance to compaction called *bulking* (see Fig. 6A.38), the maximum index den-

## 6.68 SOIL IMPROVEMENT AND STABILIZATION

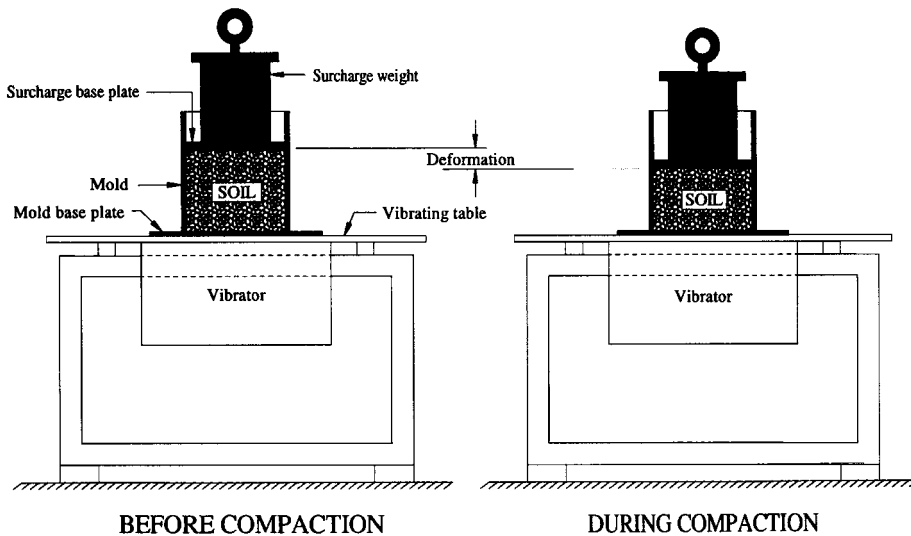


**FIGURE 6A.47** Schematic illustration of laboratory compaction using a vibratory table.

sity test is performed on either oven-dried or saturated soil. A surcharge weight corresponding to a pressure of 2 psi (14 kPa) is applied to the soil contained within a mold, and the mold, soil, and surcharge are vibrated vertically at a double amplitude of vertical vibration of 0.013 in (0.33 mm) for 8 min at 60 Hz or at 0.019 in (0.48 mm) for 10 min at 50 Hz. Because the peak density for various soil types and gradations can vary as a function of double amplitude of vibration, ASTM D4253 permits the use of amplitudes other than those given above in special circumstances. It is important to note that an absolute maximum density is not necessarily obtained by these test procedures, rather they provide a standard method for obtaining reproducible values of "maximum" density. The relative density of a compacted soil can be calculated from the actual density of the soil in relation to the minimum (ASTM D4254) and maximum index densities.

Other vibratory methods can be used in the laboratory to compact soils and to determine the maximum index density (Forssblad, 1981). These methods include a vibrating rammer used in Sweden (Fig. 6A.48), a vibrating hammer used in England, and a manually operated steel fork used in Germany.

#### 6A.3.3.5 Special Considerations for Confined-Ring Specimens

When tests are to be conducted on specimens within small confining rings, such as for one-dimensional compression or wetting-induced volume change tests, the samples can be prepared in four ways:

1. The soil can be compacted directly into the confining ring using any of the four laboratory methods of compaction discussed above.
2. A sample can be compacted into an oversize mold in the laboratory using static, impact, or kneading compaction, and the specimen can be trimmed into the ring from the oversize specimen.
3. The ring can be pushed into the field-compacted soil, trimmed, sealed in an air-tight container, and then brought to the laboratory for testing.

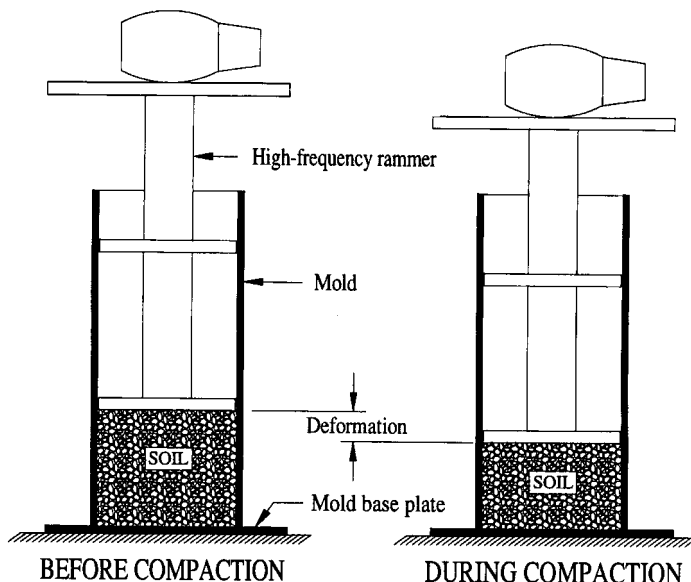


**FIGURE 6A.48** Schematic illustration of laboratory compaction using a high-frequency rammer (after Forssblad, 1981).

4. A chunk sample of the field-compacted soil can be brought into the laboratory and a specimen trimmed into the ring from the chunk sample.

For laboratory-compacted specimens, compaction directly into the ring is preferable to trimming an oversize sample because disturbance to the specimen caused during the trimming procedure is eliminated. Typical procedures for compacting specimens directly into confining rings using different methods of compaction can be found in Lawton (1986), Lawton and coworkers (1993), and Booth (1976).

Confined cohesive specimens obtained from the field-compacted soil (methods 3 and 4) are theoretically better than those prepared by either of the two laboratory methods (1 and 2) because the specimens ideally have the same fabric, density, and water content as the soil being modeled (that is, the field-compacted soil). Sometimes, however, the field-compacted soil cannot be trimmed into a confining ring without substantial disturbance, especially if the soil is dry to moderately dry or contains a significant fraction of oversize particles. In addition, a long time may elapse from removal in the field to testing in the laboratory, during which time the specimen may either dry out or bond to the ring. In these instances, laboratory compaction directly into the ring may produce a specimen more representative of the field-compacted soil if a laboratory compaction technique is used that closely simulates the field compaction.

#### **6A.3.4 Engineering Properties and Behavior of Compacted Soils**

The engineering behavior and properties of compacted soils are discussed here according to type of soil. For convenience, the soil types are divided into three general categories that differentiate the behavior of most compacted soils: clean coarse-grained soils (those containing less than about 2% fines), granular (cohesionless) soils with fines, and cohesive soils. The reader should bear in mind, however, that deviations from the typical engineering behavior described in the following sections

## 6.70 SOIL IMPROVEMENT AND STABILIZATION

may occur for each type of soil, and it is incumbent upon the engineer for a particular project to determine the relevant engineering properties of the soils to be compacted.

### 6A.3.4.1 Granular (Cohesionless) Soils

In building applications, the most important static properties for the bearing soil are strength, compressibility, permeability, and potential for volumetric changes induced by variations in available moisture. The engineering behavior of granular soils depends mainly on the relative density of the soil, although cementation of the particles upon aging after compaction may also play an important role. In seismically active regions, liquefaction potential of saturated silty sands and sands is extremely important.

*Static Stress-Strain-Strength Behavior.* The static settlement of a building to be founded on granular soils can be substantially reduced by compacting the soil to a greater density (lower void ratio) before constructing the building. The influence of relative density on the one-dimensional and isotropic compressibility of sand is shown in Figs. 6A.49 and 6A.50. For example, according to the

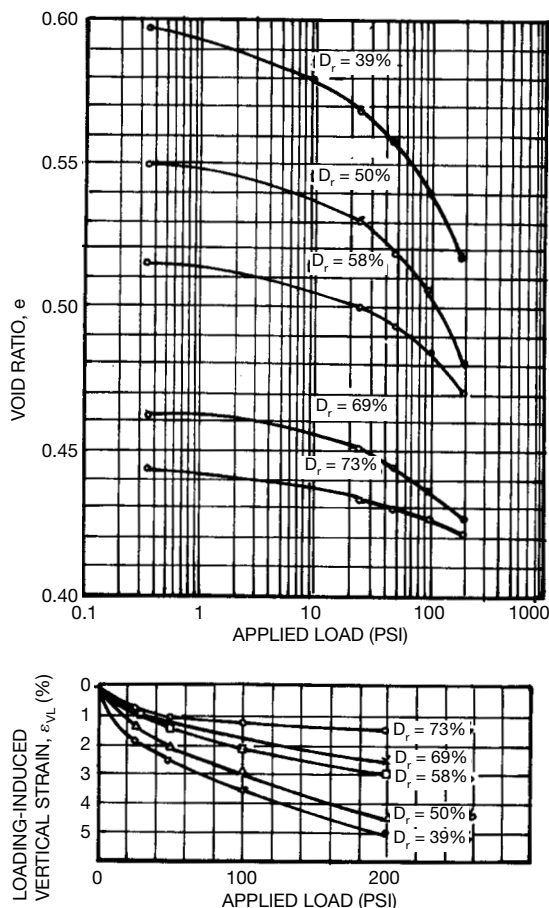


**FIGURE 6A.49** Compressibility of a clean medium sand at various relative densities (from Hilf, 1991).

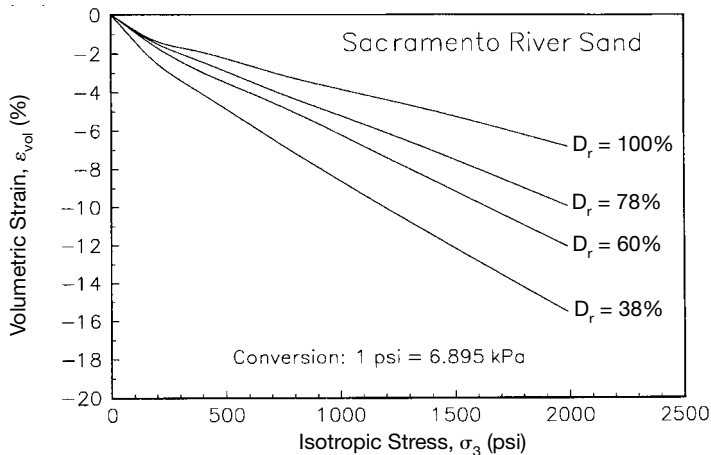


**FIGURE 6A.50** Influence of density on the isotropic compressibility of Sacramento River sand (data from Lee and Seed, 1967b).

data shown in Fig. 6A.49, the one-dimensional loading-induced vertical strain for Platte River sand (a clean, medium sand) at an applied stress of 25 psi (172 kPa) was about 58% less for  $D_r = 73\%$  ( $\varepsilon_{VL} = 0.8\%$ ) than for  $D_r = 39\%$  ( $\varepsilon_{VL} = 1.9\%$ ). Similar trends are shown in Fig. 6A.50 for the isotropic compressibility of Sacramento River sand (fine, uniform sand). The  $\varepsilon_{vol} - \sigma_3$  plots for all four relative densities are reasonably straight for  $u_3$  greater than about 350 psi (2400 kPa), so a measure of the increased stiffness of the soil with increased density can be obtained by calculating values for bulk compressive modulus ( $M_B = -\Delta\sigma_3/\Delta\varepsilon_{vol}$ ), with the following results:

Bulk modulus, $M_B$		
$D_r$ , %	ksi	MPa
38	13.9	96
60	17.4	120
78	21.2	146
100	32.5	224

Thus,  $M_B$  for  $D_r = 100\%$  is more than twice the value of  $M_B$  for  $D_r = 38\%$ .

For foundation conditions in which the width of the foundation is small compared to the total thickness of the compressible strata beneath the bearing level, the strains induced by loading will be three-dimensional, and the magnitudes of the horizontal stresses within the zone of influence for settlement are important. Compaction increases both the density and horizontal stresses within the compacted soil, and both effects increase the stiffness of the soil, as shown by the results in Fig. 6A.51 for drained triaxial tests on Sacramento River sand. Thus, compaction is especially effective in reducing settlement for situations in which horizontal strains contribute significantly to vertical settlement.

The strength and hence ultimate bearing capacity of a granular bearing stratum can be substantially enhanced by a reduction in void ratio produced by compaction. The variation in angle of internal friction between the loose and dense conditions for most naturally occurring granular soils is about 4 to 10°. The influence of density on the drained shearing strength of Sacramento River sand

## 6.72 SOIL IMPROVEMENT AND STABILIZATION

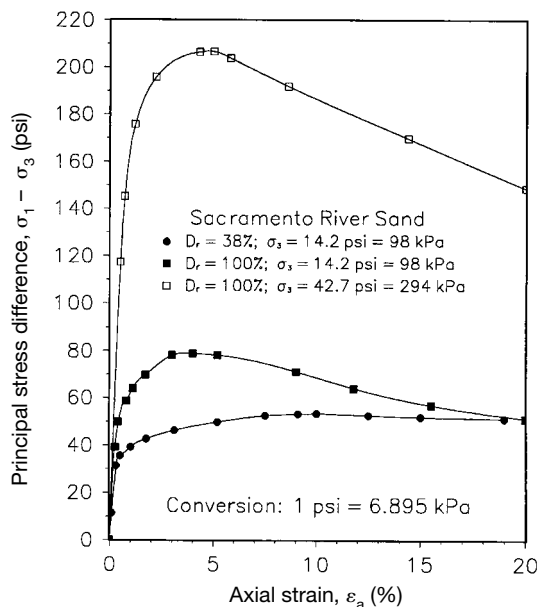


**FIGURE 6A.51** Effect of density and confining pressure on the drained triaxial stress-strain behavior of Sacramento River sand (data from Lee and Seed, 1967b).

is illustrated in Fig. 6A.52, for which the angle of internal friction at low confining pressures increased from  $34^\circ$  in the loose condition ( $D_r = 38\%$ ) to  $41^\circ$  in the dense condition ( $D_r = 100\%$ ). The magnitude of potential increase in ultimate bearing capacity can be measured by the change in the bearing capacity factors [using Meyerhof's (1951, 1963) factors]:

Condition	$D_r$ , %	$\phi'$ , degrees	$N_q$	$N_y$
Loose	38	34	29.4	31.1
Dense	100	41	73.9	114.0

It can be seen that  $N_q$  and  $N_y$  are 151 and 267% greater, respectively, in the dense condition than in the loose condition, indicating that the increase in ultimate bearing capacity would be within this range.

Contrary to common perception, the fabric of coarse-grained soils may have an important effect on compressibility and strength. Thus, method of compaction may affect the fabric of a compacted coarse-grained soil and hence its stress-strain-strength behavior. The effects of fabric anisotropy are greater in coarse-grained soils with elongated grains than in those with more spherical grains (Mitchell, 1993). Fabric anisotropy produces differences in volume change (dilatancy) tendencies for different directions of loading, which results in differences in stress-deformation and strength behavior. This effect is illustrated in Fig. 6A.53 for specimens of crushed basalt tested in direct shear (Mahmood and Mitchell, 1974). At relative densities less than about 90%, specimens sheared along the plane of preferred orientation (along the long axis of most particles) were weaker than

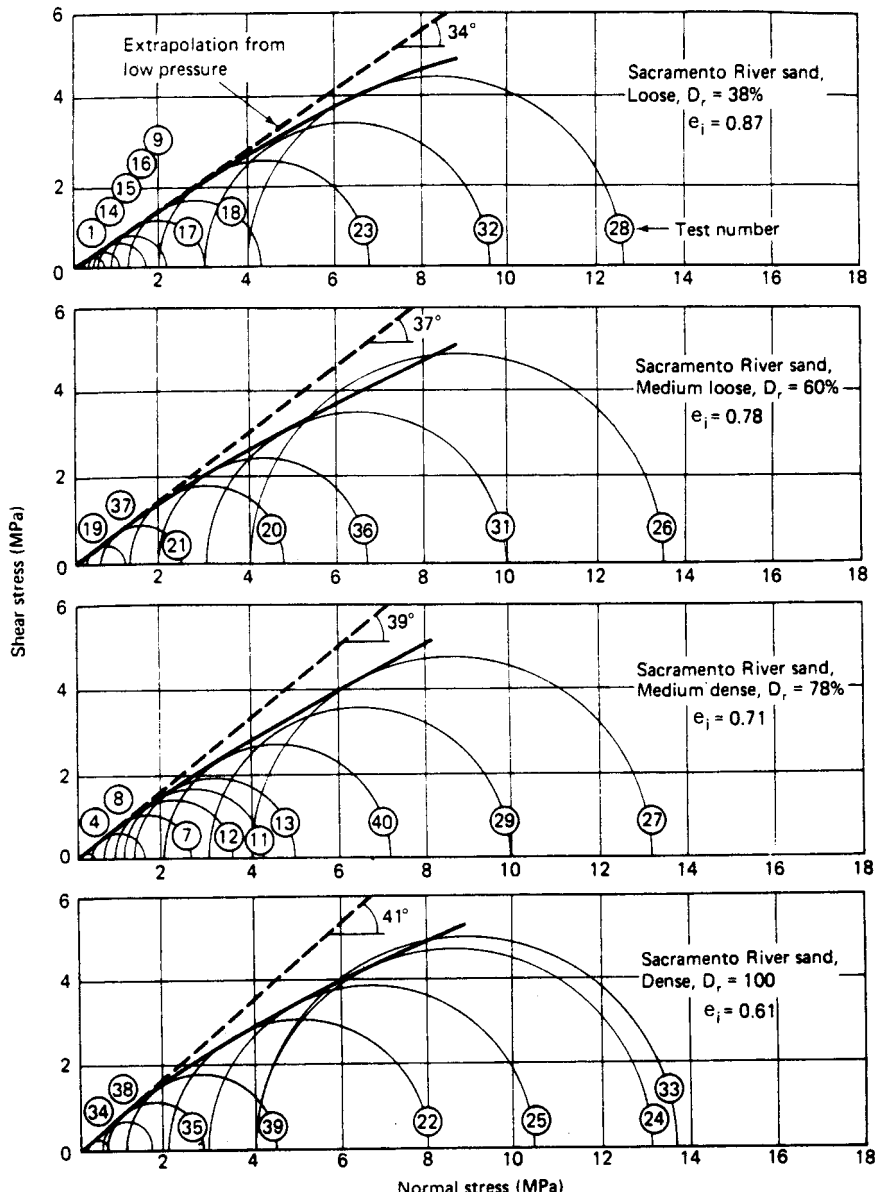


**FIGURE 6A.52** Influence of relative density on the drained triaxial shear strength of Sacramento River sand (from Holtz and Kovacs, 1981; data from Lee, 1965 and Lee and Seed, 1967b).

## 6.74 SOIL IMPROVEMENT AND STABILIZATION

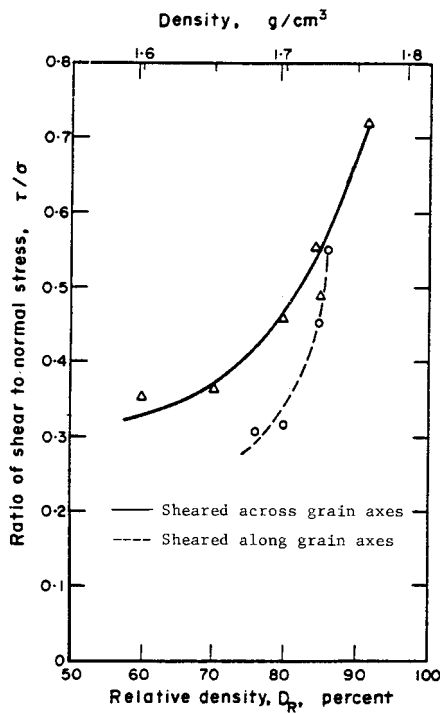


**FIGURE 6A.53** Effect of shear direction on the strength of specimens of crushed basalt prepared by pouring into a shear box (from Mahmood & Mitchell 1974).

comparable specimens sheared across the plane of preferred orientation. This difference in strength decreased with increasing density, and the strengths were about the same for relative densities above 90%. These results were consistent with the finding that the intensity of preferred orientation decreased as relative density increased.

The influence of laboratory method of compaction on the triaxial stress-strain and volume-change behavior of a uniform sand with rounded to subrounded grains and a mean axial length ratio of 1.45 is shown in Fig. 6A.54. In these tests, oven-dried soil was poured into a cylindrical mold and then compacted to a dense void ratio of 0.64 by two methods: (1) plunging a hand-held tamper into the sand, and (2) tapping the side of the mold with the hand tamper (vibration). The method of compaction had a significant influence on both the volume-change and stress-deformation characteristics. The specimen compacted by tapping dilated more and was substantially stiffer than the specimen compacted by tamping. These differences in behavior were attributed to differences in fabric—the specimens prepared by tapping tended toward some preferred orientation of long axes parallel to the horizontal plane, and the intensity of orientation increased slightly during deformation; specimens prepared by tamping initially had weak preferred orientation in the vertical direction, and this disappeared with deformation. These results illustrate the importance of using a method of compaction in the laboratory that closely simulates the method to be used in the field, as discussed in Sec. 6A.3.3.

The influence of fabric anisotropy on stress-strain-strength properties of compacted granular soils can be summarized as follows (Mitchell, 1993):

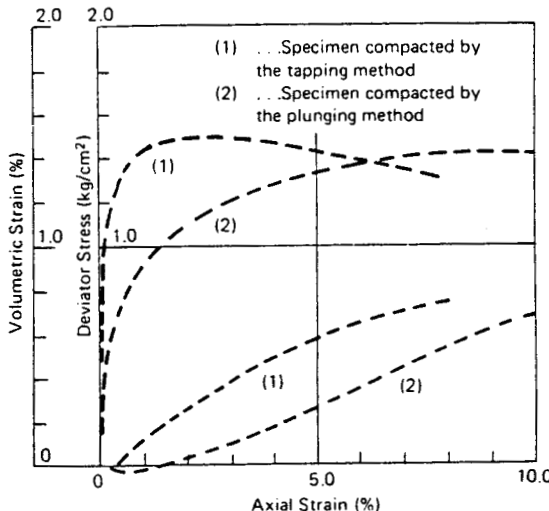


**FIGURE 6A.54** Influence of compaction method on the triaxial stress-strain and volume change behavior of a uniform sand (from Mitchell, 1993; data from Oda, 1972).

1. Anisotropic fabric and anisotropic mechanical properties are likely to occur in compacted soils.
2. The magnitude of strength and modulus anisotropy depends on density and the extent to which particles are platy and elongated. When axial ratios of particles are 1.6 or greater, differences in peak strength on the order of 10 to 15% may exist. Stress-strain moduli in different directions may vary by a factor of two or three.

### Effect of Moisture on Compressibility and Strength

*CLEAN COARSE-GRAINED SOILS* Moisture has little effect on the static stress-strain-strength behavior of most coarse-grained soils, although clean, very fine sands are generally slightly stiffer and stronger in the partially saturated condition than in either the dry or saturated condition owing to matric suction (all other factors being the same). The compressibility and strength of some coarse-grained soils, however, are substantially affected by moisture condition. For example, Bishop and Eldin (1953) showed that the angle of internal friction of a fine to medium clean sand tested in drained triaxial compression was consistently higher in the dry condition than in the saturated condition—about 5° higher for dense condition and 2° higher for loose condition. Triaxial compression tests conducted by Lee and Seed (1967c) on a fine uniform sand indicated that the friction angle, stress-strain behavior, and creep behavior were substantially affected by moisture condition. This sand was stronger, less compressible, and exhibited less creep in the oven-dried condition than the saturated condition, with air-dried behavior intermediate between the two extreme states. Increased moisture also caused a decrease in dilatant volume change behavior and an increase in particle crushing during shearing. The moisture sensitivity was therefore attributed to the presence of cracks in some of the particles, into which water infiltrated and weakened those particles so that they crushed during shearing. Moisture sensitivity has also been found in some gravels and rockfills (e.g., Zeller and Wulliman, 1957).

Based on evidence found in the literature and their own work, Lee and Seed (1967c) came to the following conclusions regarding moisture sensitivity of granular soils:

## 6.76 SOIL IMPROVEMENT AND STABILIZATION

From the available information it would appear that moisture sensitivity is likely to be greatest in granular soils whose particles either contain cracks or are susceptible to the formation of fine cracks as a result of loading. Such soils would be those derived from weathered rock, and angular material such as broken rock in which low contact areas would lead to high contact stresses and the formation of minute cracks at the contact points. Furthermore, it would also appear that water sensitivity may be greater at high pressures since fracturing of particles will be facilitated under these conditions.

In light of the available evidence, therefore, it would seem to be desirable to check the nature of the component particles in investigating the strength of cohesionless soils and ascertain their sensitivity to moisture changes.

*GRANULAR SOILS WITH FINES* Any granular soil containing particles that are cracked or that develop cracks when loaded may be susceptible to loss of strength and stiffness with increasing moisture content, as discussed in the previous section. Granular soils with a substantial nonplastic fines fraction may also be susceptible to loss of strength and stiffness with increasing moisture owing to a reduction in suction. The total suction in an unsaturated soil can be subdivided into the osmotic suction and the matric suction. Osmotic suction arises from differences in ionic concentrations at different locations in the soil water within a soil. *Osmotic suction* is of significance primarily in cohesive soils where the cations in the soil water are electrochemically attracted to the clay particles, with the result that the concentration of cations is greatest near the surface of the clay particles and decreases with distance from the particles. *Matric suction* is the difference between the pore air pressure and the pore water pressure ( $u_a - u_w$ ) in a partially saturated soil and reflects both the capillary forces and the electrochemical forces between the soil particles and the water molecules in the soil water (adsorptive forces).

In granular soils, the adsorptive forces are small, and thus the matric suction is predominately associated with the capillary menisci that occur in the partially saturated condition owing to *surface tension* that develops along the air-water interface (also called the *contractile skin*). Surface tension is a tensile force per unit length that is tangential to the contractile skin and results from a difference in intermolecular attractions between water molecules along the air-water interface and those within the interior of the water. Within the interior of the water, the water molecules are attracted to neighboring water molecules, and there is no net force acting on any of the water molecules because the molecules are distributed equally in all directions (see Fig. 6A.55). The water molecules along the

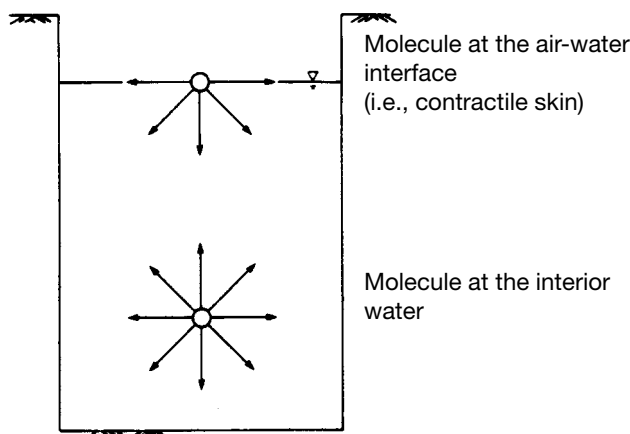


**FIGURE 6A.55** Intermolecular forces along the air-water interface and within the interior of water (from Fredlund and Rahardjo, 1993).

air-water interface are attracted to neighboring molecules within the interior and those along the interface, which results in a net attraction into the bulk of the water. Thus, the surface layer of water molecules is pulled toward the interior until the contractile skin assumes a spherical shape, which is the most stable configuration from an energy standpoint because the surface area is minimal (Davis et al., 1984). Surface tension develops, therefore, to overcome the net inward intermolecular force and to provide equilibrium to the contractile skin.

In partially saturated granular soils,  $u_a$  is usually zero (atmospheric) or compressive (positive), and  $u_w$  is tensile (negative). Kelvin's capillary model equation can be used to relate the matric suction to the curvature of a spherical contractile skin and the surface tension:

$$(u_a - u_w) = \frac{2T_s}{r_m} \quad (6A.16)$$

where  $T_s$  = surface tension

$r_m$  = radius of the meniscus (contractile skin)

Theoretical values of  $(u_a - u_w)$  from Eq. (6A.16) for a contact angle of zero are shown in Fig. 6A.56 for saturated soils as a function of pore radius, such as might occur at the top of a saturated capillary zone or in a saturated soil as it dries.

The influence of moisture condition on matric suction is illustrated in Fig. 6A.57 using the capillary model. In drier soils (lower degree of saturation), the capillary menisci have smaller radii and higher values of  $(u_a - u_w)$ . Note, though, that the contact area between the pore water and the soil particles is less for drier soils, as indicated by the parameter  $\chi$  in the following equation for effective stress in unsaturated soils proposed by Bishop (1959):

$$\sigma' = (\sigma - u_a) + \chi(u_a - u_w) \quad (6A.17)$$

$\chi$  relates the portion of  $(u_a - u_w)$  that is transmitted to the soil in terms of a change in effective stress.  $\chi = 0$  for a completely dry soil and  $\chi = 1$  for a saturated soil, and the relationship between  $\chi$  and de-

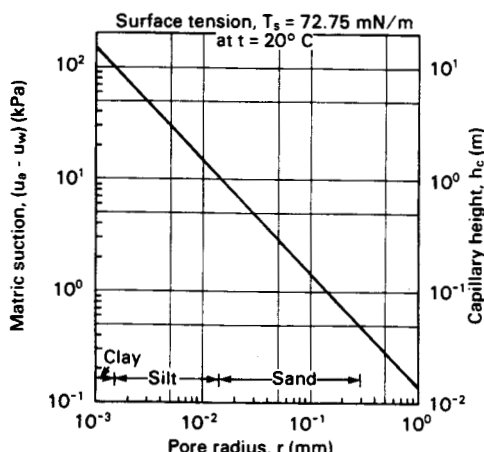


**FIGURE 6A.56** Relationships among pore radius, matric suction, and capillary height for saturated soils (from Fredlund and Rahardjo, 1993).

## 6.78 SOIL IMPROVEMENT AND STABILIZATION

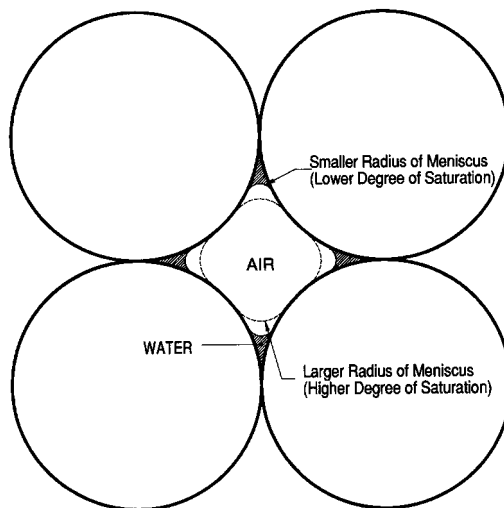


**FIGURE 6A.57** Influence of moisture condition on the capillary menisci in an unsaturated soil according to the capillary model.

gree of saturation for a silt is shown in Fig. 6A.58. In granular soils,  $\chi$  depends primarily on the ratio of area of pore water in contact with the soil particles to the total surface area of the particles but also on factors such as the fabric and stress history of the soil.  $\chi$  has also been found to differ when determined for volume change behavior and shear strength for the same soil under otherwise identical conditions (Morgenstern 1979).

The net effect of a lower water content may be either to decrease or increase the effective stress in a soil depending upon the combined effect of increased suction and decreased contact area—that is, how the combined factor  $\chi(u_a - u_w)$  varies as a function of water content. The relation between matric suction and change in effective stress is shown in Fig. 6A.59 for a clayey sand. This concept is also illustrated for three types of soils in Fig. 6A.60, which shows the unconfined compressive strength as a function of water content. It is clear from Fig. 6A.60 that even perfectly cohesionless soils (e.g., very fine clean sand) can have an unconfined compressive strength greater than zero owing to matric suction, which provides some effective stress in the soil even at essentially zero total stress. The effective stress induced by matric suction in cohesionless soils is sometimes referred to as *apparent cohesion*.

Because the strength of finer-grained soils is not negligible at very low water contents (silty sand and clay in Fig. 6A.60), the capillary model obviously cannot be used by itself to describe the changes in matric suction that result from changes in moisture condition. Thus, the influence of adsorptive forces on matric suction is significant for cohesive soils and will be discussed in more detail in Sec. 6A.3.4.2.

In most granular soils the values of matric suction are small, and the stress-strain-strength behavior of these soils is generally little affected by changes in moisture condition. In current “standard” geotechnical engineering practice, the effect of partial saturation on granular soils is generally ignored for three primary reasons:

1. Ignoring the effect is simpler.
2. The effect is nearly always conservative.
3. There is always a chance the soil will become saturated at some later point.

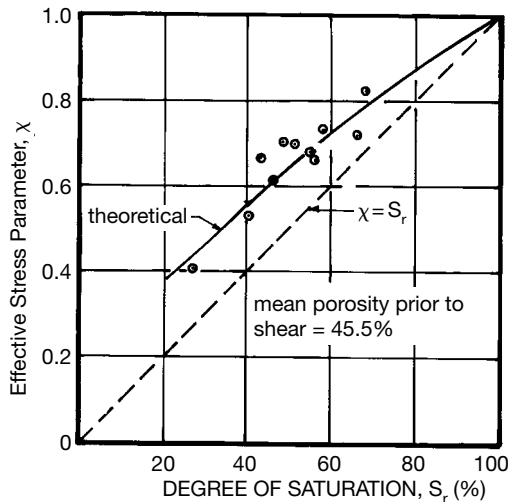


**FIGURE 6A.58** Relationship between effective stress parameter  $\chi$  and degree of saturation for Braehead silt (from Bishop et al., 1960).

Techniques for including the effect of partial saturation are considered to be too difficult to implement in practice.

Thus, most laboratory tests on granular soils are conducted on either dry or saturated specimens, and stress-strain-strength analyses are performed on the basis of total stresses, which are assumed to be equal to effective stresses. In a similar manner, the results of field tests are used to determine appropriate stress-strain-strength parameters based on total stresses, assuming that the total stresses are equal to the effective stresses.

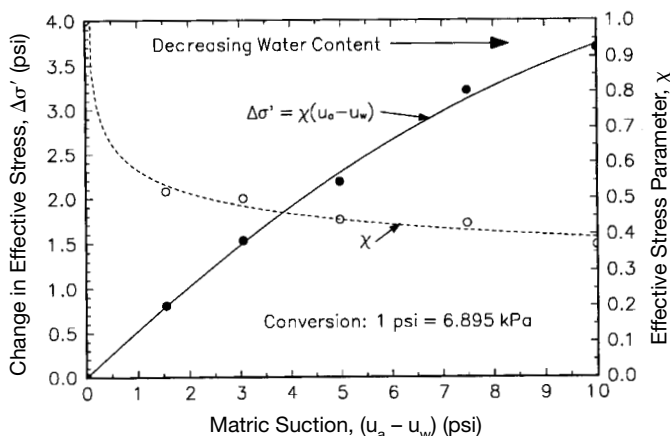


**FIGURE 6A.59** Relationship between matric suction and change in effective stress for a clayey sand (data from Blight, 1965).

## 6.80 SOIL IMPROVEMENT AND STABILIZATION

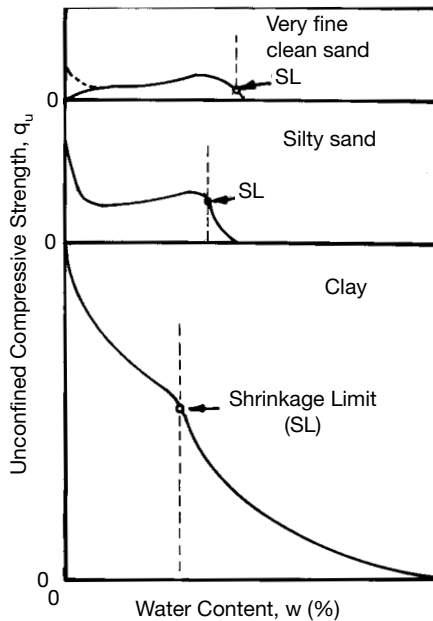


**FIGURE 6A.60** Unconfined compressive strength as a function of water content for three types of soils (from Terzaghi and Peck, 1967).

Although ignoring the effects of partial saturation usually has no practical consequence in granular soils, in some instances doing so is uneconomical. Bishop's effective stress equation for unsaturated soils—Eq. (6A.17)—has proved to have little practical use primarily because of difficulties in obtaining values of  $\chi$  that adequately predict field behavior. These difficulties stem from the fact that stress-strain-strength behavior cannot be uniquely defined in terms of a single effective stress variable (Morgenstern, 1979). Thus, modern methods of predicting the stress-strain-strength behavior of unsaturated soils use two independent stress variables, usually  $(\sigma - u_a)$  and  $(u_a - u_w)$ . Although the use of these more sophisticated techniques is slowly becoming more common in geotechnical engineering practice, most geotechnical engineers prefer to use traditional total stress analyses. Because these techniques have limited application in granular soils, they will not be discussed any further here but will be discussed in more detail in Sec. 6A.3.4.2.

**Permeability.** Although the terms *permeability* and *hydraulic conductivity* are often used interchangeably in engineering practice, they have different meanings. The *intrinsic permeability* of a soil is independent of the fluid which may flow through it, and the relationship between intrinsic permeability ( $K$ ) and coefficient of permeability ( $k$ ) can be described by the following equation (Das, 1983):

$$k = \frac{K \cdot \gamma_f}{\mu_f} \quad (6A.18)$$

where  $\gamma_f$  = weight density (unit weight) of the fluid

$\mu_f$  = absolute viscosity of the fluid

Thus, the coefficient of permeability depends on the density and viscosity of the fluid flowing through the soil. The terms *hydraulic conductivity* and *water permeability* describe the same characteristic of a soil—the relative ease with which water can flow through the voids in the soil. In soils, the two most common fluids that flow through the soil in foundation engineering contexts are water and air. For simplicity, the term *permeability* will be used to mean water permeability or hydraulic conductivity, and the permeability with respect to other types of fluids will be differentiated as required.

The coefficient of permeability of clean, coarse-grained soils increases as void ratio ( $e$ ) increases. Several correlations have been proposed to describe this relationship, including the following (Das, 1983):

$$k \propto \frac{e^3}{1+e} \quad (6A.19a)$$

$$k \propto \frac{e^2}{1+e} \quad (6A.19b)$$

$$k \propto e^2 \quad (6A.19c)$$

Permeability is important in granular soils with respect to their drainage characteristics. It is advantageous in most instances for granular bearing soils to be free-draining, that is, any significant accumulation or introduction of moisture should drain rapidly through the granular layer. Although compaction results in somewhat lower permeability, the permeability of even dense coarse-grained soils is generally still high enough to permit free drainage under most conditions.

$k$  decreases with decreasing grain size, as illustrated by the typical values for various types of granular soils given in Table 6A.5. Casagrande (1938) has established the boundary between good drainage and poor drainage as  $1 \times 10^{-4}$  cm/s ( $3 \times 10^{-1}$  ft/day). Thus, granular soils with a large percentage of fines may not be free-draining soils and may require a perimeter or interior drainage system to prevent unwanted buildup of moisture in situations where moisture accumulation may have a deleterious effect on the load-carrying capacity of the foundation soil.

### **Wetting-Induced Volume Changes**

*CLEAN COARSE-GRAINED SOILS* Coarse-grained soils will not swell (increase in volume) when wetted because they contain no expansive clay minerals. However, all compacted soils are susceptible to *wetting-induced collapse* or *hydrodensification* (decrease in volume when wetted) under some conditions (Lawton et al., 1992). The magnitude of collapse depends on the state of the soil at the time of wetting; in general, collapse increases with increasing mean normal total stress, decreasing water content or degree of saturation, and decreasing dry density (Lawton et al., 1989, 1991). Therefore, one must consider the potential changes in these properties that may occur between the end of

**TABLE 6A.5** Typical Values of Coefficient of Permeability for Granular Soils

Type of soil	$k$	
	cm/s	ft/day
Clean gravel	$1 \times 10^0$ to $1 \times 10^2$	$3 \times 10^3$ to $3 \times 10^5$
Clean sand	$1 \times 10^{-3}$ to $1 \times 10^0$	$3 \times 10^0$ to $3 \times 10^3$
Silty sand/sandy silt	$1 \times 10^{-4}$ to $1 \times 10^{-2}$	$3 \times 10^{-1}$ to $3 \times 10^1$
Silt	$1 \times 10^{-6}$ to $1 \times 10^{-4}$	$3 \times 10^{-3}$ to $3 \times 10^{-1}$

**6.82** SOIL IMPROVEMENT AND STABILIZATION

compaction and the time when wetting may occur. Examples of changes that may occur include the placement of additional fill or structures above a given lift, which increases the stresses acting on that lift and densifies the soil (thereby changing both the state of stress and density); drying of the exposed surfaces of the soil from evaporation or transpiration (which changes the moisture condition); and redistribution of moisture throughout the partially saturated soil as it tries to achieve hydraulic, thermal, chemical, and electrical equilibrium.

The addition of water necessary for collapse in compacted soil may occur in a variety of ways, including precipitation, irrigation, regional ground-water buildup, broken water pipes, moisture buildup beneath covered areas, ponding, inadequate or ineffective drainage, and flooding (Lawton et al., 1992). Some of these methods are difficult to predict or foresee, so it is prudent to consider the wetting-induced collapse potential for all compacted soils.

Although some notable exceptions have occurred, compacted coarse-grained soils will not collapse significantly upon wetting under most circumstances. Some examples of clean coarse-grained soils that have collapsed are provided below to illustrate the potential problems.

Jaky (1948) reported that apartment houses and other structures along the banks of the Danube suffered extensive damage and cracking when the level of the Danube rose 2 m (6.2 ft) above the flood stage. The results from one-dimensional collapse tests on specimens made from six different granular soils indicated that the collapse potential could be high for all the soils under certain conditions. Grain-size distribution properties and USCS classification for the six soils studied are summarized in Table 6A.6, and the effect of relative density on measured wetting-induced collapse strains is shown in Fig. 6A.61. As would be expected, the collapse potential decreased as the relative density of each soil increased. The optimal or critical relative density (the minimum relative density for which the collapse was zero) varied from 69 to 97%.

Collapse settlements have also been observed in rockfill dams. Sowers and colleagues (1965) reported that the Dix River dam was accidentally flooded during construction, with a wetting-induced vertical strain of about 0.5%. They also conducted one-dimensional wetting tests on specimens of freshly broken rocks of various types and found that additional (collapse) settlements occurred rapidly when the dry specimens were wetted. These collapse settlements were attributed to water entering microfissures in the particles that were produced at highly stressed contact points, with the water causing local increases in stress and additional crushing of particles at the contact points. Collapse settlements were also observed during filling of the El Infiernillo dam (Marsal and Ramírez de Arellano, 1967).

The results of triaxial collapse tests on specimens of Antioch sand and Ottawa sand were reported by Lee and Seed (1967c). In these tests, oven-dried or air-dried dense ( $D_r = 100\%$ ) specimens of both soil types were first loaded to an axisymmetric state of stress with the sustained deviator stress ( $\sigma_1 - \sigma_3$ ) equal to 76 or 83% of the maximum deviator stress for Antioch sand and 90% of the maximum deviator stress for Ottawa sand. To ensure that the pore water pressures

**TABLE 6A.6** Grain Size Properties and Classification of Six Granular Soils Investigated by Jaky (1948)

Soil	Grain size distribution by weight, %*					USCS Classification*	
	Gravel	Sand	Silt	$D_{50}$ , mm	$D_{10}$ , mm	Symbol	Descriptive name
Fine sand	0	97	3	0.14	0.10	SP	Poorly graded sand
Coarse sand	0	100	0	0.28	0.15	SP	Poorly graded sand
Danube gravel 1	43	57	0	3.0	0.19	SW	Well-graded sand with gravel
Danube gravel 2	31	52	17	2.2	0.041	SM	Silty sand with gravel
Pea gravel	20	80	0	1.6	0.29	SW	Well-graded sand with gravel
Slag	N.A.	N.A.	N.A.	N.A.	N.A.	—	—

\*ASTM D-2487

N.A. = not available

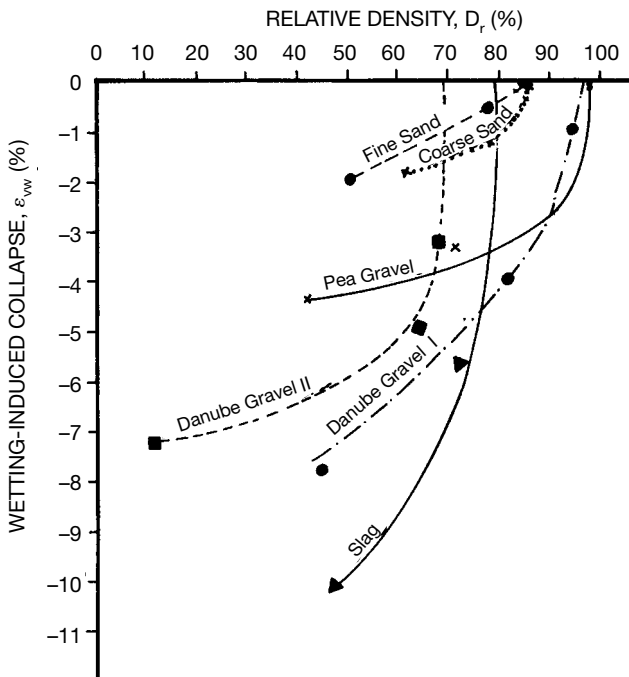


**FIGURE 6A.61** Influence of relative density on the one-dimensional collapse of six granular soils (from Jaky, 1948).

were maintained at a very low level during wetting, water was introduced into the specimens by gravity flow through the bottom drainage line under a head of less than 1.0 in (25 mm). Upon wetting, the Antioch sand specimens first underwent substantial collapse strains before culminating in a sudden large deformation along a well-developed shear plane. In contrast, the addition of water to the Ottawa sand specimens produced virtually no collapse. The differences in collapse behavior for these two types of soils were attributed to differences in the soundness of the particles—a significant number of the Antioch sand particles contained small cracks, whereas the Ottawa sand grains were essentially sound.

Hellweg conducted more than 300 one-dimensional collapse tests on specimens of various sands from northern Germany with different densities, moisture contents, and applied loads (Rizkallah and Hellweg, 1980). The results from these tests indicated that uniform fine sands can only be compacted with extraordinary difficulties and that such soils collapse about 8% when wetted. Based on these results, it was concluded that compacting uniform fine sands to a high relative compaction based on the standard Proctor maximum dry density does not necessarily ensure low collapse potential.

It has been recognized for a long time that fill materials containing soft rock fragments—such as shales, mudstones, siltstones, chalks, and badly weathered igneous and metamorphic rocks—can deform significantly upon wetting when used in embankment dams and should be avoided where possible (Sherard et al. 1963). That excessive wetting-induced settlement can also occur in buildings founded on compacted fills containing soft rock fragments has been reported by Wimberley and coworkers (1994). In this project, the excessive settlement (>12 in = 30 cm) of a one-story building founded on a 50-ft (15-m) deep compacted fill occurred. The compacted fill consisted of fine-grained fill with rock fragments (siltstone, limestone, claystone, and sandy shale) and some rocky

**6.84** SOIL IMPROVEMENT AND STABILIZATION

layers. Much of the settlement was believed to relate to the introduction of moisture into the fill by precipitation and watering of plants, which caused softening of highly stressed contact points between coarser particles and degradable coarse particles (e.g., poorer shales).

In summary, the collapse potential of compacted clean coarse-grained soils under most conditions is insignificant. However, substantial collapse potentials can exist if one or more of the following factors are present in the compacted soil: (1) The compaction is poor or insufficient; (2) defects exist within some of the particles; (3) some of the particles are water soluble or degradable; or (4) the soil is subjected to very high stress levels. The types of granular soils that have defects sufficient to cause potentially high wetting-induced collapse potentials include those derived from highly weathered rock and blasting. Angular particles with low contact areas and high applied stresses seem to be more susceptible to the formation of minute cracks at contact points. Compacted soils containing substantial amounts of soft rock fragments may also be susceptible to wetting-induced collapse. Structures founded on deep fills are especially susceptible to damage resulting from collapse settlements because of the high stresses generated at lower portions of the fill from the weight of the overlying material.

Because potential problems from wetting-induced collapse can be detected by performing one-dimensional collapse tests on representative compacted specimens, it is recommended that collapse tests be conducted in all situations where collapse is possible. Granular soils containing medium and fine sand particles only can be tested in standard consolidometers; soils containing larger particles require special testing equipment that can be found in some universities and other research institutes. For example, San Diego State University has the facilities to test compacted specimens 4 ft (1.2 m) in diameter (Noorany, 1987).

*GRANULAR SOILS WITH FINES* There are several cases described in the literature of damage resulting from wetting-induced collapse of compacted granular soils containing fines. Examples include severe cracking of two earth dams in California (Leonards and Narain, 1963), and deformation, cracking, and failure of numerous highway embankments in South Africa (Booth, 1977). The earth dams were constructed of sand/silt mixtures, and silty sands and wetting occurred during filling of the reservoirs. The highway embankments were composed of silty sands, with wetting generally resulting from infiltration of water following periods of heavy rainfall.

Collapse settlements in compacted granular soils generally occur because the soils are too dry, not dense enough, or both. For Woodcrest dam (Leonards and Narain, 1963), which suffered severe cracking, the average compaction water content was 1.7% below standard Proctor optimum, the average degree of saturation was 30% below optimum saturation, and the average standard Proctor relative compaction was 94%. The highway embankments reported by Booth (1977), which suffered extensive damage from collapse settlements, were loosely compacted (modified Proctor relative compaction,  $R_m = 80\%$ ) and were very dry (estimated degree of saturation,  $S_r < 10\%$  in some instances). It was not known whether the embankments were compacted dry (no compaction water content records were available) or whether substantial moisture loss occurred between compaction and wetting.

Recent research (Alwail et al. 1992) has shown that the amount of silt and shape of the silt particles has an important influence on the collapse potential of granular soils. These effects are shown in Fig. 6A.62 for compacted mixtures of uniform silica sand and two different silts compacted to  $R_m = 90\%$  at water contents 3% dry of modified Proctor optimum water content ( $w_{om}$ ). For both silts, the maximum one-dimensional collapse potential for applied vertical stresses ranging from 0.52 to 33.4 ksf (25 to 1600 kPa) increased as the percentage of silt was increased. It is also evident that the group 2 soils had substantially higher collapse potentials than the group 1 soils. Scanning electron micrographs taken on samples of the two groups of soils showed that the group 1 silt grains were rounded to subrounded, whereas the group 2 silt grains were flaky and angular. Thus, the greater collapse potential for the group 2 soils was attributed to a more open structure resulting from the angular and flaky shapes of the silt grains.

*Shrinkage.* Shrinkage (decrease in volume induced by drying) is not a problem in granular soils because by definition granular soils are cohesionless, and thus they contain no appreciable amount of expansive minerals.

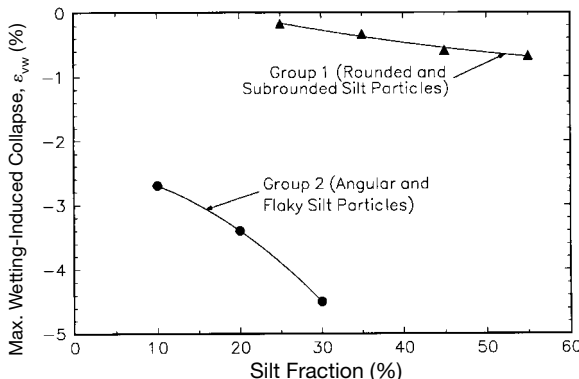


**FIGURE 6A.62** Effect of silt content and shape on one-dimensional collapse of sand-silt mixtures (from Alwail et al., 1992).

*Liquefaction Potential.* Liquefaction occurs in a saturated sandy soil when deformation during undrained or partially drained conditions produces a buildup in pore water pressure to a level that approaches or equals the total confining pressure. At this point the effective confining pressure is zero or near zero, and the soil will continue to deform until enough water has been squeezed from the soil to dissipate a substantial portion of the excess pore water pressure. Liquefaction may occur from either statical strains induced from monotonic loading (e.g., Casagrande 1936a) or from cyclic strains induced by dynamic or vibratory loading (e.g., Lee and Seed, 1967a). Damage to buildings caused by static liquefaction is rare, so only liquefaction caused by cyclic loadings (also called *cyclic mobility*) will be considered herein.

Extensive damage can occur to buildings and other engineering structures during earthquakes owing to liquefaction in saturated sandy soils beneath the structures. For example, hundreds of buildings were severely damaged as a result of liquefaction during the 1964 earthquake in Niigata, Japan (Seed and Idriss, 1967). Many structures settled more than 3 ft (0.9 m), and the settlement was frequently accompanied by severe tilting (up to 80°). Lateral ground displacements generated during earthquakes by liquefaction-induced lateral spreads and flows have also caused severe damage to structures and their appurtenances (Youd, 1993). Furthermore, liquefaction can occur from lower levels of excitation produced by other phenomena, including blasting, pile driving, construction equipment, road and train traffic, and dynamic compaction (Carter and Seed, 1988). Thus all structures underlain by saturated sand deposits may be susceptible to liquefaction-induced damage, and it is imperative that liquefaction potential be considered for these cases even when the site is not located in a seismically active region.

Three definitions differentiate the possible states of liquefaction (Lee and Seed, 1967a):

*Complete liquefaction*—when a soil exhibits no resistance or negligible resistance over a wide range of strains (e.g., a double amplitude of 20%).

*Partial liquefaction*—when a soil exhibits no resistance to deformation over a strain range less than that considered to constitute failure.

*Initial liquefaction*—when a soil first exhibits any degree of partial liquefaction during cyclic loading.

The following characteristics are known with respect to liquefaction in saturated sandy soils (Lee and Seed, 1967a; Seed, 1986):

## 6.86 SOIL IMPROVEMENT AND STABILIZATION

- Application of cyclic stresses or strains will induce liquefaction or partial liquefaction over a considerable range of densities, even in moderately dense sands.
- If the generated pore pressures do not exceed about 60% of the confining pressure, liquefaction will not be triggered in the soil, and there is no serious deformation problem.
- The smaller the cyclic stress or strain to which the soil is subjected, the higher is the number of stress cycles required to induce liquefaction (Fig. 6A.63).
- The higher the confining pressure acting on a soil, the higher the cyclic stresses, strains, or number of cycles required to induce liquefaction (Fig. 6A.64).
- The higher the density of a soil, the higher the cyclic stresses, strains, or number of cycles required to induce liquefaction (Figs. 6A.63 and 6A.64).
- When loose sandy soils liquefy under cyclic stresses of constant amplitude, deformations immediately become very large (complete liquefaction occurs quickly—see Fig. 6A.65).
- When dense sandy soils liquefy under cyclic stresses of constant amplitude, deformations are initially small (partial liquefaction occurs) and gradually increase with increasing number of cycles (Fig. 6A.66). Even when the pore water pressure becomes equal to the confining pressure in dense sands, it is often of no practical significance because the strains required to eliminate the condition are very small. Thus, dense cohesionless soils do not normally present problems with regard to the design of foundations.

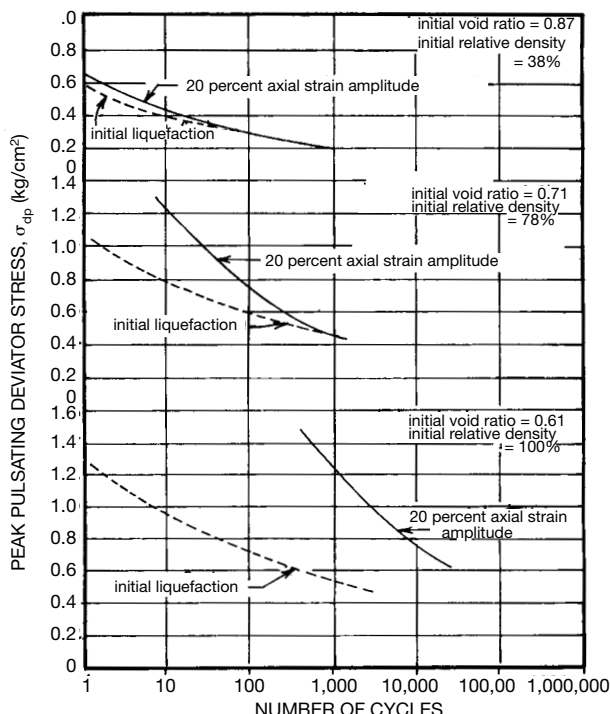


**FIGURE 6A.63** Effect of density, number of cycles, and failure criterion on the cyclic stress required to cause liquefaction of Sacramento River sand at  $\sigma_3 = 1.0 \text{ kg/cm}^2$  (from Lee and Seed, 1967a).

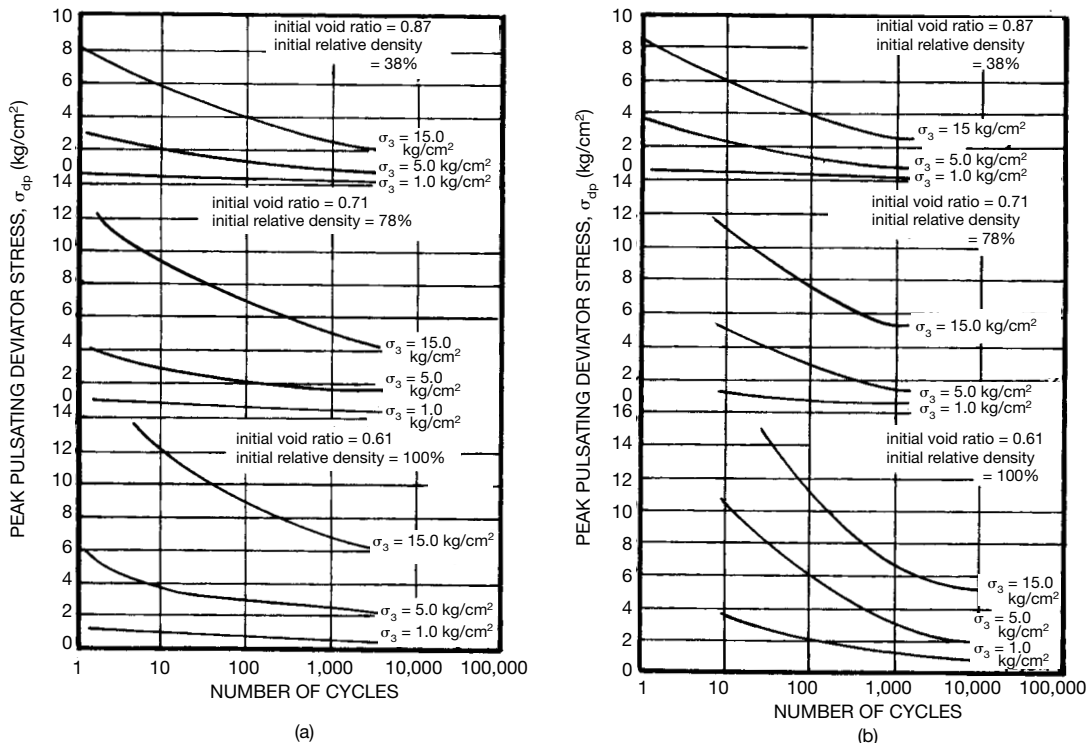


**FIGURE 6A.64** Influence of confining pressure, density, and number of cycles on the cyclic stress required to cause (a) initial liquefaction and (b) 20% strain in Sacramento River sand (from Lee and Seed, 1967a).

8. Numerous structures built on liquefiable soils have stood for hundreds of years without liquefaction occurring, simply because there has been no triggering mechanism strong enough to induce liquefaction. Therefore, liquefaction can be prevented by designing to keep the pore pressures well below the confining stresses.

It is evident from the preceding information that the liquefaction potential of any saturated sandy soil depends on both the properties of the soil (density, permeability, and lengths of drainage paths) and the characteristics of the cyclic loading (magnitude of stress and strain, duration). Three possible methods have been used to various extents for estimating liquefaction potential (Youd, 1993): (1) analytical methods, (2) physical modeling, and (3) empirical procedures. Because it is difficult to model the soil conditions at liquefiable sites either analytically or physically, empirical procedures are commonly used in routine engineering practice. A complete discussion of methods for evaluating liquefaction potential for all types of cyclic loading is beyond the scope of this presentation, so details are given below only for earthquake-induced liquefaction. Methods for evaluating liquefaction for cyclic loads from other sources (blasting, pile driving, construction equipment, road and train traffic, and dynamic compaction) are given in Carter and Seed (1988).

The factor of safety against the occurrence of earthquake-induced liquefaction is commonly defined as the available soil resistance to liquefaction (expressed in terms of the cyclic stresses required to cause liquefaction) divided by the cyclic stresses generated by the design event (Youd, 1993). Both factors are usually normalized with respect to the preevent effective overburden stress at the depth being analyzed. In equation form, the factor of safety is defined as

## 6.88 SOIL IMPROVEMENT AND STABILIZATION

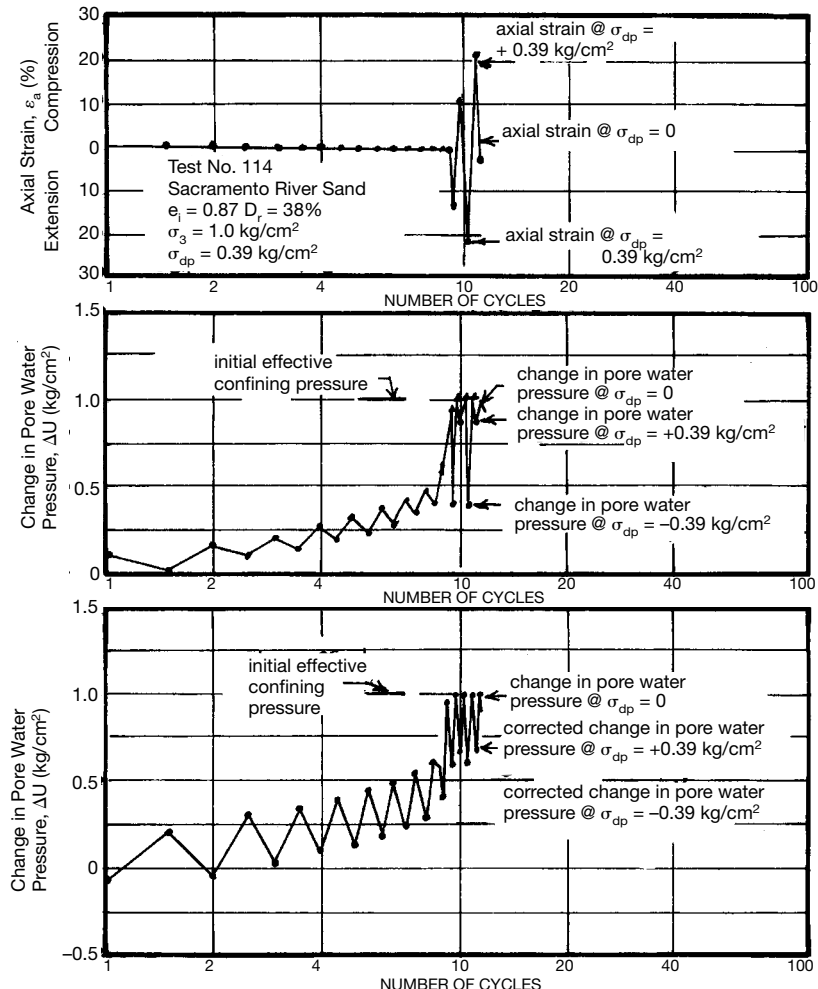


**FIGURE 6A.65** Results from pulsating load test on loose Sacramento River sand (from Seed and Lee, 1966).

$$F_s = \frac{\text{CSRL}}{\text{CSRE}} \quad (6A.20)$$

where CSRL = cyclic stress ratio required to generate liquefaction

CSRE = cyclic stress ratio generated by the design earthquake =  $\tau_{av}/\sigma'_{v0}$

$\tau_{av}$  = average earthquake-induced cyclic shear stress

$\sigma'_{v0}$  = preearthquake effective overburden stress at the depth under consideration

CSRE can evaluated either by using a computer code (such as SHAKE or DESRA) to estimate  $\tau_{av}$  or by estimating it directly from the following equation (Seed & Idriss 1971):

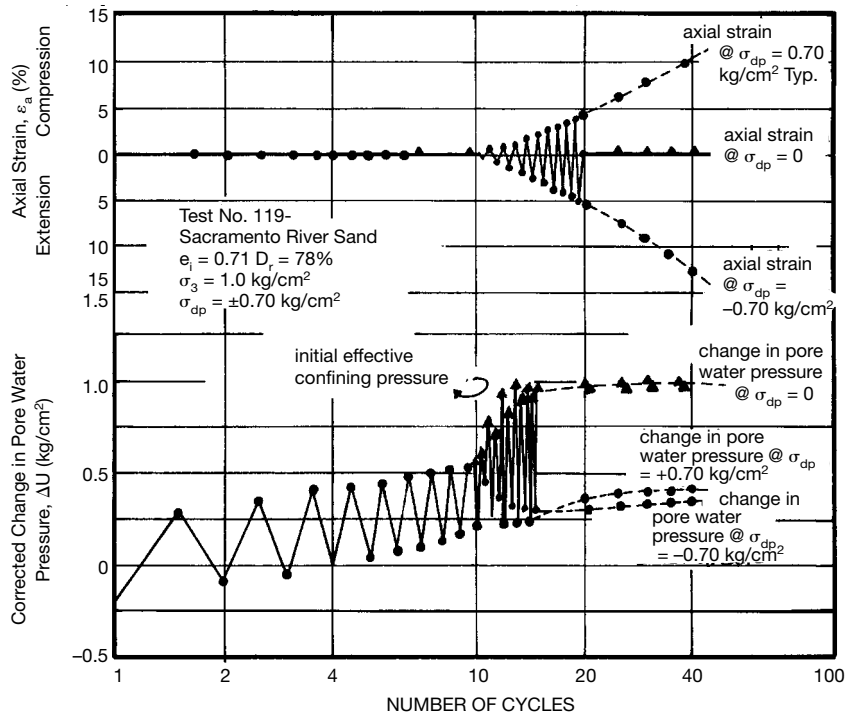


**FIGURE 6A.66** Results from pulsating load test on dense Sacramento River sand (from Seed and Lee, 1966).

$$\text{CSRE} = 0.65 \cdot \frac{a_{\max}}{g} \cdot \frac{\sigma_{v0}}{\sigma'_{v0}} \cdot r_d \quad (6A.21)$$

where  $a_{\max}$  = maximum acceleration at the ground surface that would occur in the absence of liquefaction

$g$  = acceleration caused by gravity

$\sigma_{v0}$  = total overburden stress at the depth under consideration

$r_d$  = depth-related stress reduction factor that varies with depth ( $z$ ) from the ground surface

$r_d$  can be estimated from the following equation for noncritical projects (NCEER 1997):

$$r_d = 1.0 - 0.00765 z \quad \text{for } z \leq 9.15 \text{ m} \quad (6A.21a)$$

$$r_d = 1.174 - 0.0267 z \quad \text{for } 9.15 \text{ m} < z \leq 23 \text{ m} \quad (6A.21b)$$

$$r_d = 0.744 - 0.008 z \quad \text{for } 23 \text{ m} < z \leq 30 \text{ m} \quad (6A.21c)$$

$$r_d = 0.50 \quad \text{for } z > 30 \text{ m} \quad (6A.21d)$$

where  $z$  is the depth below the ground surface in meters.

## 6.90 SOIL IMPROVEMENT AND STABILIZATION

Estimated values for  $a_{\max}$  are usually determined using one of the following three methods (Youd, 1993): (1) standard peak acceleration attenuation curves that are valid for comparable soil conditions; (2) standard peak acceleration attenuation curves for bedrock sites, with correction for local site effects using standard site amplification curves or computerized site response analysis; and (3) probabilistic maps of  $a_{\max}$ , with or without correction for site attenuation or amplification depending on the rock or soil conditions used to generate the map.

CSRL is most commonly estimated from empirical correlations with corrected SPT blowcount [ $(N_1)_{60}$ ] such as those shown in Fig. 6A.67, which are valid for magnitude 7.5 earthquakes and sands and silty sands with up to 35% fines. Open symbols represent sites where surface liquefaction did not develop, and filled symbols are from sites where surface liquefaction did occur. Curves are given in the figure for varying percentage of fines that represent the boundary between the liquefaction and no liquefaction zones. Youd (1993) recommends using a factor of safety of 1.2 for engineering design based on this chart because it is possible that liquefaction may have occurred at some sites.

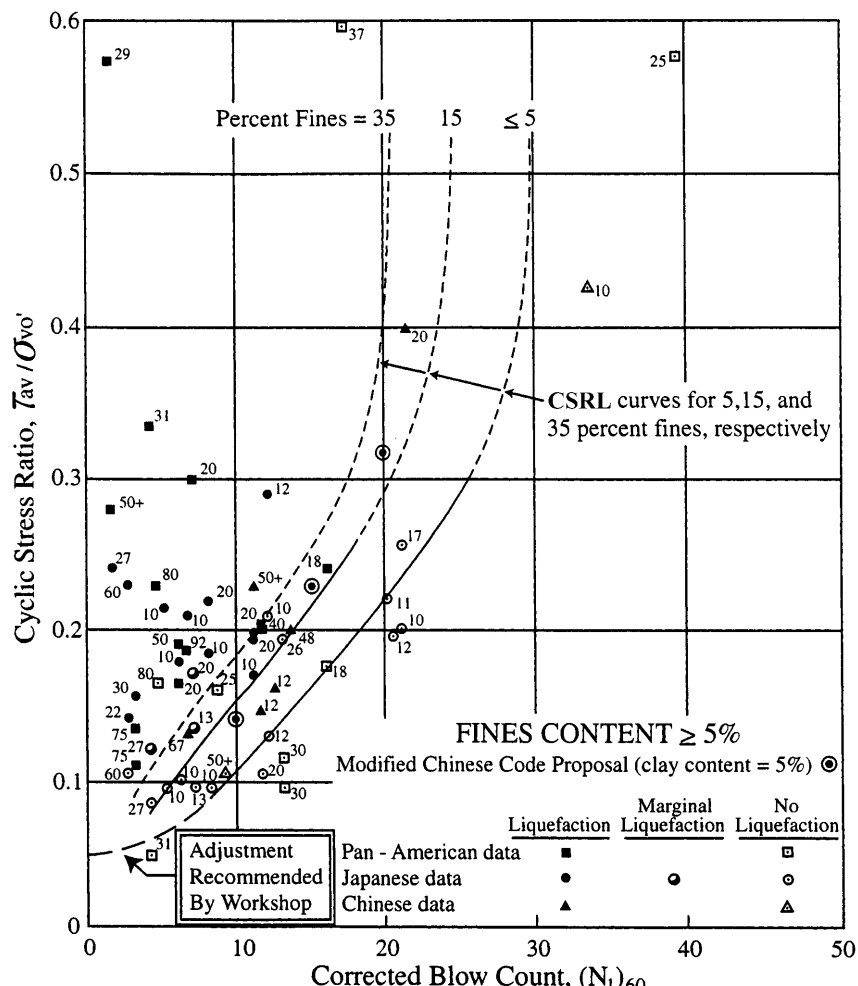


**FIGURE 6A.67** Relationship between CSRL and  $(N_1)_{60}$  values for silty sands and magnitude 7.5 earthquakes (from NCEER 1997, modified from Seed et al. 1985).

but was not detected at the ground surface. One should exercise care when using the curves in Fig. 6A.67 for soils containing substantial gravel fractions because verified corrections for gravel content have not been established (Youd, 1993).

Correlations between CSRL and a number of other parameters besides SPT blowcount have recently been developed and are summarized in NCEER (1997). These other parameters include tip resistance ( $q_c$ ) from the Cone Penetration Test, shear wave velocity, and blowcount from the Becker Penetration Test. Details of these correlations are beyond the scope of this handbook and can be found in NCEER (1997).

$(N_1)_{60}$  is the field SPT blowcount corrected for overburden pressure (reference stress = 1 tsf = 95.8 kPa), energy efficiency, length of drill rod, and characteristics of sampling barrel (Seed et al., 1985) and can be represented by the following equation:

$$(N_1)_{60} = N_{\text{field}} \cdot C_E \cdot C_N \cdot C_L \cdot C_S \cdot C_B$$

where  $N_{\text{field}}$  = SPT blowcount measured in the field

$C_E$  = correction factor for energy ratio

$C_N$  = correction factor for overburden pressure

$C_L$  = correction factor for length of drill rod

$C_S$  = correction factor for sampling barrel

$C_B$  = correction factor for borehole diameter

$(N_1)_{60}$  is standardized to an energy ratio (actual energy divided by theoretical free-fall energy) of 60%, so the energy ratio correction can be calculated as

$$C_E = \frac{E_r}{60} \quad (6A.23)$$

where  $E_r$  = energy ratio for the equipment being used

$E_r$  can be either measured during use of the actual equipment (preferred) or estimated from the type of equipment (e.g., Table 6A.7).  $C_N$  can be obtained from Fig. 6A.68 or the following equation suggested by Liao and Whitman (NRC, 1985):

$$C_N = \left( \frac{2}{\sigma'_{v0}} \right)^{1/2} \leq 2 \text{ for } \sigma'_{v0} \text{ in units of ksf} \quad (6A.24a)$$

$$C_N = \left( \frac{95.76}{\sigma'_{v0}} \right)^{1/2} \leq 2 \text{ for } \sigma'_{v0} \text{ in units of kPa} \quad (6A.24b)$$

$C_L$  is 0.75 for drill rod shorter than 13 ft (4 m); 0.85 for drill rod lengths of 13 to 20 ft (4 to 6 m); 0.95 for drill rod lengths of 20 to 33 ft (6 to 10 m); 1.0 for drill rod lengths of 33 to 100 ft (10 to 30 m) and > 1.0 for drill rod lengths greater than 100 ft (30 m).  $C_S$  is 1.0 for a constant-barrel diameter (that is, with a liner); if a liner is not used,  $C_S$  is 1.1 for loose sands and 1.25 to 1.30 for dense sands.  $C_B$  is 1.0 for borehole diameters less than 4.5 in. (115 mm) or if the test is conducted through the stem of a hollow-stem auger; 1.05 for a 6 in. (150 mm) diameter borehole; and 1.15 for an 8 in. (200 mm) diameter borehole.

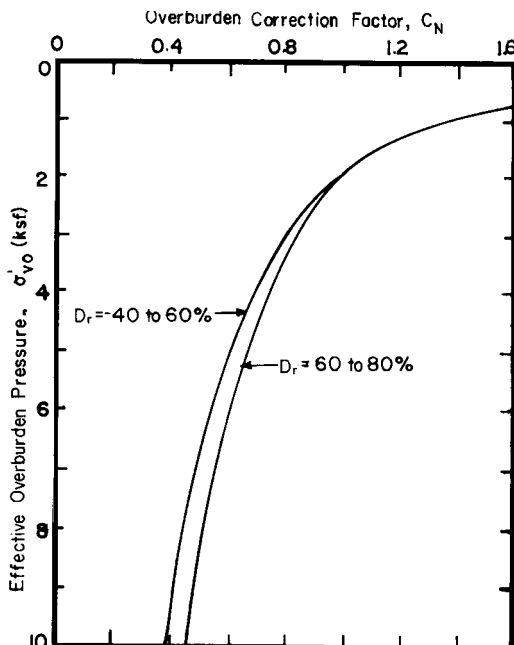
The following SPT procedure is recommended by Seed and colleagues (1985) for use in liquefaction correlations:

1. *Borehole.* 4- to 5-in (102- to 127-mm) diameter rotary borehole with bentonitic drilling mud to stabilize borehole.
2. *Drill bit.* Upward deflection of drilling mud (tricone or baffled drag bit) to prevent erosion of soil below the cutting edge of the bit.

**6.92** SOIL IMPROVEMENT AND STABILIZATION**TABLE 6A.7** Estimated Energy Ratios for SPT Procedures (from Seed et al., 1985)

Country	Hammer type	Hammer release	Estimated rod energy, %	Correction factor for 60% rod energy
Japan	Donut	Free-fall	78	1.30
	Donut	Rope and pulley with special throw release	67	1.12
United States	Safety	Rope and pulley	60	1.00
	Donut	Rope and pulley	45	0.75
Argentina	Donut	Rope and pulley	45	0.75
China	Donut	Free-fall	60	1.00
	Donut	Rope and pulley	50	0.83

3. *Sampler*. 2.00-in (50.8-mm) outer diameter, 1.38-in (35.0-mm) constant inner diameter.
4. *Drill rods*. A or AW for depths less than 50 ft (15 m); N or NW for greater depths.
5. *Energy ratio*. 60% of theoretical free-fall energy.
6. *Blowcount rate*. 30 to 40 blows per minute.
7. *Penetration resistance count*. Measured over depth of 6 to 18 in (152 to 457 mm) below the bottom of the borehole.

**FIGURE 6A.68** Chart for values of overburden correction factor,  $C_N$  (from Seed et al., 1985).

If the design earthquake has a magnitude other than 7.5, the value of CSRL obtained from Fig. 6A.67 must be multiplied by a magnitude scaling factor (MSF) to obtain the adjusted CSRL. Values of MSF provided by Seed and Idriss (1982) are commonly used and are summarized in Table 6A.8. A panel of experts convened to discuss liquefaction (NCEER 1997) determined that Seed and Idriss' values are probably too conservative for magnitudes less than 7.5 and probably not sufficiently conservative for magnitudes greater than 7.5. The panel's recommended values are also given in Table 6A.8. It is preferable to use moment magnitude in liquefaction analyses, but surface-wave magnitude or local (Richter) magnitude may also be used for magnitudes less than 7.5 (Youd, 1993).

The previous discussions clearly establish that density plays an important role in the liquefaction potential of a saturated sandy soil. Therefore, the liquefaction potential of a compacted granular fill that may become saturated can be reasonably controlled in many instances by ensuring that the fill soil is highly densified. Reducing the liquefaction potential of an existing saturated granular soil deposit can be more difficult. Near-surface compaction is not a viable alternative in many cases because it is effective only to a maximum depth of about 5 to 10 ft (1.5 to 3.0 m) from the ground surface, and many potentially liquefiable deposits extend to much greater depths. In these instances, several types of deep compaction techniques have been successfully used. Liquefaction potential can also be controlled by shortening the drainage path within the liquefiable deposit, which prevents the excess pore pressure from building to a level where liquefaction can occur. This can be accomplished by the inclusion of granular columns (usually gravel or stone columns) with much higher permeability than the existing deposit.

*Effects of Cementation.* Many soils contain carbonates, iron oxide, alumina, and organic matter that may precipitate at interparticle contacts and act as cementing agents (Mitchell, 1993). The effect of cementation is to increase the stiffness and strength of the soil while reducing the permeability and liquefaction potential somewhat. For highly cemented coarse-grained soils, the increase in stiffness and strength and the decrease in liquefaction potential can be significant, whereas the reduction in permeability is generally small, so that the overall effect is beneficial for bearing soils. Cemented granular soils that are densified in place by near-surface or dynamic compaction may lose most of or all their natural cementation during the compaction process. The net effect may be either an increase or a decrease in stiffness and strength depending on which mechanism predominates—the increase produced by densification or the decrease resulting from loss of cementation. Therefore, compaction should be used with caution in naturally cemented soils.

Any cementation of borrow materials will also likely be substantially destroyed during the excavation and compaction procedures. However, borrow soils that were cemented before excavation

**TABLE 6A.8** Correction Factors for Influence of Earthquake Magnitude on Liquefaction Resistance

Earthquake magnitude, M	Magnitude Scaling Factor, MSF	
	Seed & Idriss (1982)	Recommended by NCEER (1997)
5.5	1.43	2.20 to 2.80
6.0	1.32	1.76 to 2.10
6.5	1.19	1.44 to 1.60
7.0	1.08	1.19 to 1.25
7.5	1.00	1.00
8.0	0.94	0.84
8.5	0.89	0.72

**6.94** SOIL IMPROVEMENT AND STABILIZATION

contain minerals that will cement, and therefore it is likely they will develop new cementation with time after compaction. The effect of this postcompaction cementation on the engineering properties of compacted soils is commonly ignored in foundation engineering practice primarily because it is difficult or impractical to determine both the rate at which the cementation will occur and what effect this cementation will have at critical stages of construction and loading of the structure being built. In addition, since cementation has a positive effect on compressibility, strength, and liquefaction potential, and little effect on the permeability, it is conservative to use the as-compacted properties in design and analysis.

In some instances neglecting the postcompaction cementation of fills may be highly uneconomical. For example, in southeastern Florida a common borrow material is carbonate sand that either is a residual soil from the oolitic limestone found near the ground surface or is excavated and crushed from rock deposits of the same material. It is common knowledge among engineers in the area that recementing of the carbonate sand occurs after compaction so that the resulting fill behaves more like a soft rock than a soil. A significant improvement in the postcompaction stress-strain-strength characteristics of the compacted fills often occurs, so that the stiffness and strength of the fills commonly continue to increase during their service life. This improvement is sometimes included in a qualitative way in the design of the foundations for structures constructed on fills composed of these carbonate materials, but more in-depth studies of this phenomenon would surely result in more economical foundation designs. The effects of aging on the engineering properties and behavior of compacted soils are discussed in more detail in Sec. 6A.3.4.3.

#### **6A.3.4.2 Cohesive Soils**

The engineering characteristics of compacted cohesive soils are strongly influenced by the as-compacted structure, moisture condition, and density of the soil; by the method used to compact the soil; and by any postcompaction changes in structure, moisture condition, and density that may occur.

*Fabric and Structure.* Although the terms *fabric* and *structure* are sometimes used interchangeably, it is preferable to define *fabric* as the arrangement of particles, particle groups, and pore spaces within a soil, and to use *structure* to refer to the combined effects of fabric, composition, and interparticle forces. The structure of cohesive soils is extremely complex, and the reader is referred to Mitchell (1993) for a comprehensive discussion. Therefore, only fabric will be discussed here. The fabric of a soil can be considered to consist of the following three components (Mitchell, 1993):

1. *Microfabric.* The microfabric consists of the regular aggregations of particles and the very small pores between them. Typical fabric units are up to a few tens of micrometers across.
2. *Minifabric.* The minifabric contains the aggregations of the microfabric and the interassemblage pores between them. Minifabric units may be a few hundred micrometers in size.
3. *Macrofabric.* The macrofabric may contain cracks, fissures, root holes, laminations, and so on.

For a given cohesive borrow material, the fabric of the as-compacted soil can vary widely depending on the compaction water content and the method of compaction. Conventional descriptions of the fabric of compacted cohesive soils assume that the soil is composed entirely of plate-shaped clay particles and are based on the microfabric of the soil, that is, how the individual clay particles are arranged (Lambe, 1958). If most of the particles are oriented parallel to each other, the fabric is said to be *dispersed* or *oriented* (Fig. 6A.69). In clays where most of the particles are arranged perpendicular to each other, the fabric is considered to be *flocculated* or *random*. Compaction dry of optimum or with low effort tends to produce a more flocculated fabric, whereas compaction wet of optimum or with high effort generally yields a more dispersed fabric (Fig. 6A.70).

Although the engineering behavior of pure clay samples compacted in the laboratory can be adequately explained on the basis of the microfabric, it is difficult to justify its use for field compacted

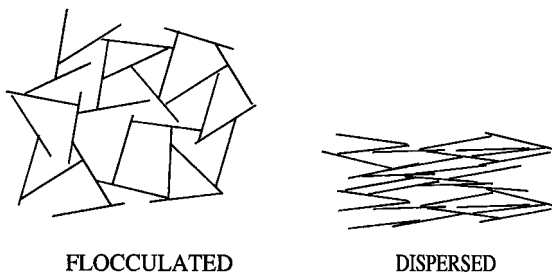


**FIGURE 6A.69** Microfabrics for individual particle interaction in pure clays.

cohesive soils for two reasons: (1) Most of the soils contain a variety of particles, including both coarse-grained and fine-grained particles; and (2) the minifabric and macrofabric have a predominant influence in many cases on the engineering characteristics. Excellent reviews of models for compacted soil behavior can be found in Hausmann (1990) and Hilf (1991). A practical theory that considers both microfabric and minifabric is the *clod model*, a slightly modified version of the model proposed by Hodek and Lovell (1979), which built upon the basic concepts developed by others (e.g., Barden and Sides, 1970; Mitchell et al., 1965; Olsen, 1962). In this model, the borrow soil consists of aggregations of particles held together by cohesive (clay) particles and separate granular particles. These aggregations (called *clods*), may contain particles as coarse as gravel-sized, but their behavior during compaction is dominated by the clay particles. The granular particles are generally brittle, but the clods may be either brittle or plastic depending on their moisture condition. The total void space within the soil consists of *intraclod pores* (voids within the clods) and *interclod pores* (void spaces between bulky units, either clods or separate granular particles). The interclod pores are considerably larger than the intraclod pores.

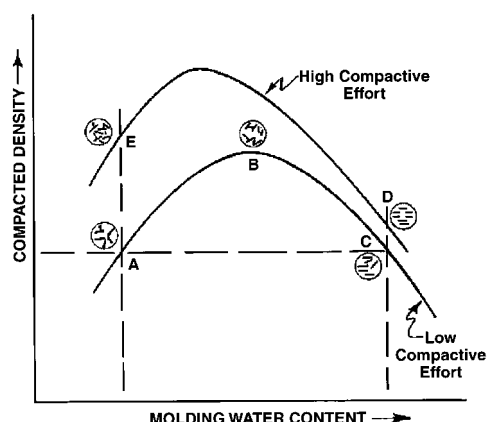


**FIGURE 6A.70** Effects of molding water content and compactive effort on the microfabric of pure clays (from Lambe, 1958).

**6.96** SOIL IMPROVEMENT AND STABILIZATION

Densification is achieved during compaction by one or more of the following three mechanisms: (1) Pushing the clods and granular particles closer together; (2) breaking brittle clods; and (3) deforming plastic clods. The moisture condition of the clods during compaction is the key factor that determines the density, fabric, and behavior of the as-compacted soil. The granular particles are generally little affected by moisture within the soil. At relatively low compaction water contents, the capillary (matric) suction within the clods is very large, and the clods are dry, strong, and brittle and behave as discrete units. During compaction these clods may be either broken or moved as a unit, but they deform very little, and thus behave essentially as granular particles. Compaction reduces the interclod space but does not affect the intraclod space, which is relatively small because the clods are shrunken (Fig. 6A.71). Thus, the as-compacted fabric of dry cohesive soil essentially consists of discrete, hard clods. Sheepsfoot and tamping foot rollers are generally more effective in densifying dry cohesive soils because the higher contact pressures break down more of the hard clods.

At relatively high water contents, the suction is small, and the clods are plastic and may be remolded into almost any shape. As the clods are deformed during compaction, the interclod space can be nearly eliminated without affecting the intraclod space, which is relatively large because the aggregates are swollen. Depending on the amount of remolding of clods that occurs during compaction, the as-compacted fabric may vary. Owing to their high contact pressures and large induced shearing strains, sheepsfoot rollers tend to remodel the clods into a relatively homogeneous fabric. Smooth-drum rollers remold the clods primarily by compressive forces, resulting in a fabric that retains to some extent the identity of the individual clods.

The engineering behavior and properties of compacted cohesive soils often vary with time as changes occur in moisture condition, stress state, and fabric. The as-compacted characteristics of cohesive soils, and how these properties may change as other parameters change, is discussed in the following sections.

*Stress-Strain-Strength Behavior:* The discussion in this section on the stress-strain-strength be-

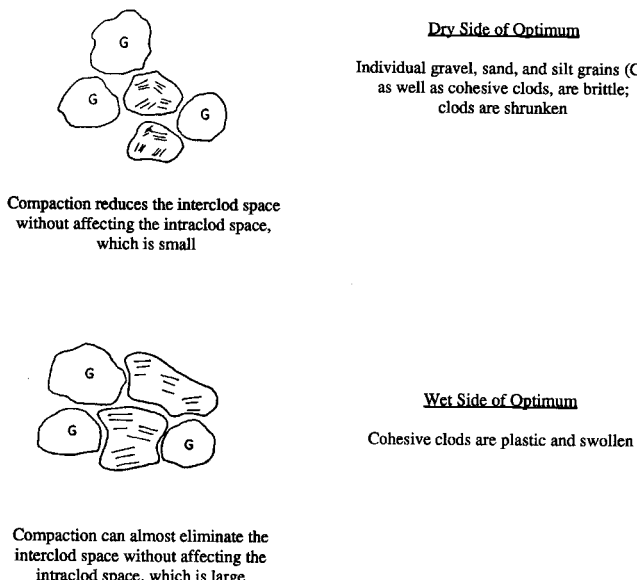


**FIGURE 6A.71** Schematics of compaction according to the clod model (modified from Hodek and Lovell, 1979).

havior of compacted cohesive soils is divided into two primary classifications based on the moisture condition of the soil at the time of loading: (1) Soils that remain at their as-compacted water content up to and throughout the loading, and (2) soils that become soaked prior to loading. These two moisture conditions represent the limiting cases usually considered for compacted cohesive soils. Although some compacted cohesive soils dry out during their service life, the drying generally results in a stiffer and stronger soil (unless substantial cracking occurs), so it is usually conservative to ignore the effects of drying and use the compressibility and strength characteristics of the soil at its as-compacted moisture content. However, drying of the soil may result in shrinkage and settlement of any structures founded on that soil. In addition, the loss of moisture increases the potential for subsequent wetting-induced volume changes (swelling or collapse), and this increased potential for volume changes should also be considered (see Sec. 6A.3.4.2).

The term “as-compacted” will be used throughout the next section to refer to a compacted cohesive soil that has remained at its compaction water content up to the time of loading. Thus, *as-compacted* refers to no change in moisture content but does not preclude changes in void ratio, for example, owing to compression under the weight of fill placed on top of the soil prior to the inducement of shearing stresses by a structure constructed on or within the fill. This definition of *as-compacted* is somewhat different than that given by others (for example, Seed et al., 1960), who have defined as-compacted soils as those in which no change in either moisture condition or void ratio occurs prior to or during loading.

### **As-compacted moisture content**

**Compactive Prestress** The as-compacted compressibility and strength of compacted cohesive soils are influenced by the moisture condition and density of the soil, as well as method and effort of compaction. The cyclic application and removal of mechanical energy during compaction prestresses the soil, and the stress-strain behavior of an as-compacted cohesive soil is similar to that of an overconsolidated, saturated clay. A typical strain-stress plot for one-dimensional compression of an as-compacted cohesive soil is shown in log  $\sigma_v - \varepsilon_{VL}$  space in Fig. 6A.72, in which the recompression and virgin compression portions of the loading curve are evident. The vertical stress at which the behavior changes from recompression to virgin compression is called the *compactive prestress* ( $\sigma_{vc}$ ) and is analogous to the effective preconsolidation pressure ( $\sigma'_p$ ) in saturated clays. Casagrande's (1936b) graphical procedure for estimating  $\sigma'_p$  of saturated clays can also be used to approximate  $\sigma_{vc}$  for compacted cohesive soils.  $\sigma_{vc}$  for a particular soil increases with increasing dry density and decreasing water content (Lin and Lovell, 1983). Method of compaction also has a significant influence on  $\sigma_{vc}$ , as indicated in Fig. 6A.73 for specimens of a clayey sand compacted at two water contents to the same dry density using kneading, static, and impact compaction. For both compaction water contents,  $\sigma_v$  for static compaction is greater than for kneading compaction because static compaction is much less efficient in cohesive soils than kneading compaction. Thus, for the same compaction water content, higher pressures are needed in static compaction to produce the same density.  $\sigma_v$  for impact compaction is less than for static compaction at both water contents but is greater than for kneading compaction at  $w = 10\%$  and less than for kneading compaction at  $w = 16\%$ . This suggests that impact compaction is less efficient than kneading compaction for compaction below optimum moisture condition (as-compacted  $S_r < S_{opt}$ ) but more efficient above optimum moisture condition (as-compacted  $S_r > S_{opt}$ ). The apparent anomalies in the behavior of impact-compacted cohesive soils will be discussed in more detail in a subsequent section.

**Influence of Moisture Condition** Moisture condition has a dramatic influence on the compressibility and strength of compacted cohesive soils owing to changes in suction. As discussed previously (Sec. 6A.3.4.1), the total suction in an unsaturated soil consists of two components—osmotic suction and matric suction. Values of total, matric, and osmotic suction are shown in Fig. 6A.74 for specimens of a glacial till compacted with modified Proctor effort at various water contents. Matric suction is the largest component of suction in unsaturated soils. Because osmotic suction varies lit-

## 6.98 SOIL IMPROVEMENT AND STABILIZATION

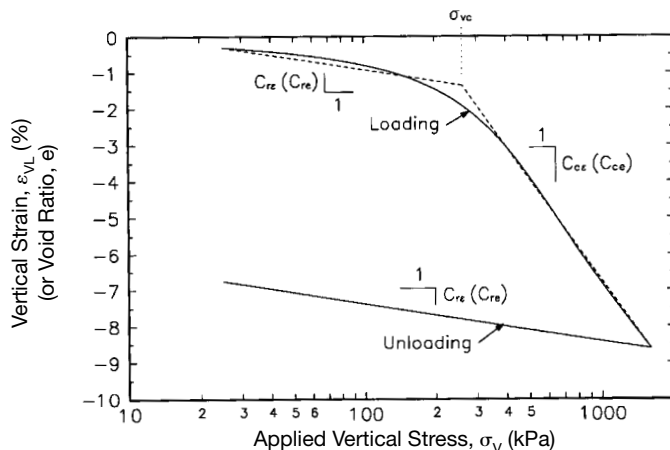


**FIGURE 6A.72** Typical strain-stress curve for one-dimensional loading-induced compression of a compacted cohesive soil.

tle for the normal variation in water contents for most compacted soils, changes in suction are primarily related to changes in matric suction, which can be substantial. For example, for the glacial till shown in Fig. 6A.74, the matric suction decreased from about 900 kPa (131 psi) at  $w = 11\%$  to about 200 kPa (29 psi) at  $w = 17\%$ , a 78% reduction in matric suction for a 6% increase in water content.

The effect of moisture condition on the one-dimensional compressibility of a compacted clayey sand is illustrated in Fig. 6A.75. At low water contents the clods are hard and the compacted soil is relatively stiff. Well-compacted, highly plastic, dry soils can be nearly incompressible under stress levels encountered in some projects. For the same method of compaction and as-compacted density, the compressibility of the soil increases as the water content increases, owing to the reduction in suction described previously. Similar trends are seen in Fig. 6A.76 for triaxial stress-strain-strength behavior. An increase in compaction moisture content at constant energy level results in a weaker, more compressible soil. Note also the reduction in brittleness as water content is increased.

The shear strength of an unsaturated soil is commonly formulated in terms of the stress-state variables net normal stress ( $\sigma - u_a$ ) and matric suction ( $u_a - u_w$ ). The resulting shear strength equation, which takes the form of a three-dimensional extension of the Mohr-Coulomb failure criterion (see Fig. 6A.77), is as follows (Fredlund et al., 1978):

$$\tau_{ff} = c' + (\sigma_f - u_a)_f \cdot \tan \phi' + (u_a - u_w)_f \cdot \tan \phi^b \quad (6A.25)$$

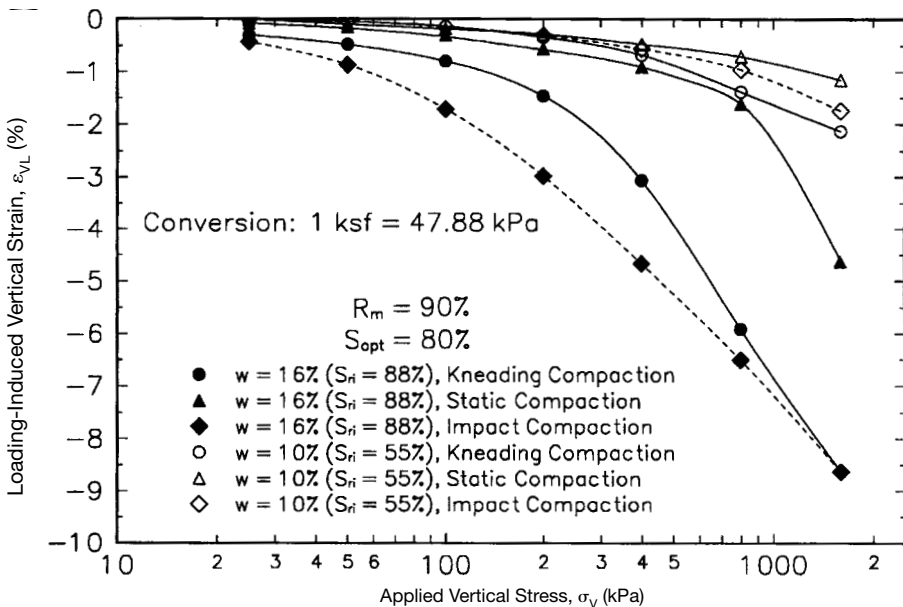
where  $\tau_{ff}$  = shear stress on the failure plane at failure (shear strength)

$c'$  = intercept of the extended Mohr-Coulomb failure envelope on the shear stress axis where the net normal stress and the matric suction at failure are equal to zero (commonly referred to as the *effective cohesion intercept*)

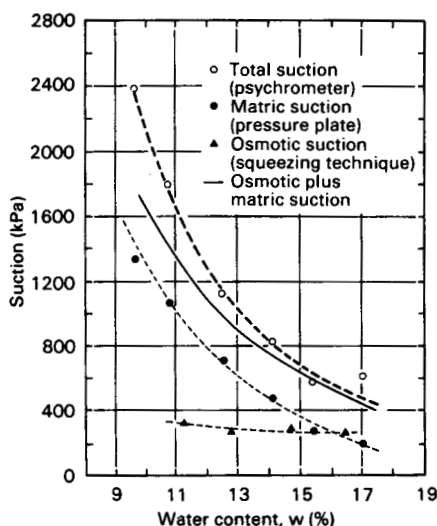
$(\sigma_f - u_a)_f$  = net normal stress state on the failure plane at failure

$u_{af}$  = pore air pressure on the failure plane at failure

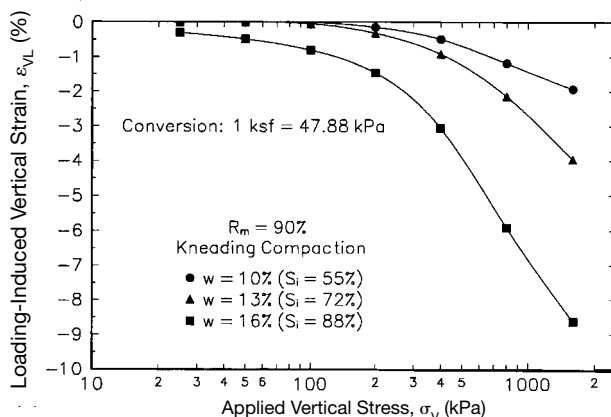
$\phi'$  = angle of internal friction associated with the net normal stress variable



**FIGURE 6A.73** Effect of compaction method on one-dimensional compressibility of compacted clayey sand (data from Lawton, 1986).



**FIGURE 6A.74** Total, matric, and osmotic suctions for glacial till (Fredlund and Rahardjo, 1993, data from Krahm and Fredlund, 1972).

**6.100** SOIL IMPROVEMENT AND STABILIZATION

**FIGURE 6A.75** Influence of moisture condition on one-dimensional compressibility of compacted clayey sand (data from Lawton, 1986).

$(u_a - u_{w_f})_f$  = matric suction on the failure plane at failure

$\phi^b$  = angle indicating the rate of increase in shear strength relative to the matric suction,  
 $(u_a - u_{w_f})_f$

The effect of changes in matric suction on the shear strength of an unsaturated soil is illustrated in Fig. 6A.78(a). The projections of the three-dimensional failure envelope on the shear stress-net normal stress plane are shown in Fig. 6A.78(b). Thus, the effect of wetting an unsaturated cohesive soil is to reduce its shear strength owing to a reduction in matric suction. This loss of shear strength upon wetting can be considered to result from a reduction in cohesion intercept, where the cohesion intercept is defined as

$$c = c' + (u_a - u_{w_f})_f \cdot \tan \phi^b$$

Values of  $\phi'$  and  $c'$  can be measured using saturated soil specimens and conventional triaxial and direct shear testing equipment. Tests on unsaturated specimens using specialized triaxial or direct shear testing apparatuses are needed to obtain values of  $\phi^b$  and the reader is referred to Fredlund and Rahardjo (1993) for details of these tests and equipment. Experimentally determined values of  $\phi^b$  have ranged from about 7 to 26°, with most values in the range of about 13 to 18°.

**Effect of Density** In general, an increase in density of a compacted cohesive soil for the same method of compaction and water content results in an increase in stiffness and strength. The decrease in as-compacted one-dimensional compressibility of a compacted clayey sand with increasing density at the same water content is shown in Fig. 6A.79. Note also that the compactive prestress increases with increasing density, as would be expected because more energy is required, at the same compaction water content, to achieve a greater density.

The effects of density on the unconsolidated, undrained triaxial compressive strength of two cohesive soils at small and large strains are shown in Figs. 6A.80 and 6A.81. In these graphs, the strength is defined as the maximum stress that the sample sustained to reach the designated value of strain and thus is not necessarily the point on the stress-strain graph corresponding to that value of

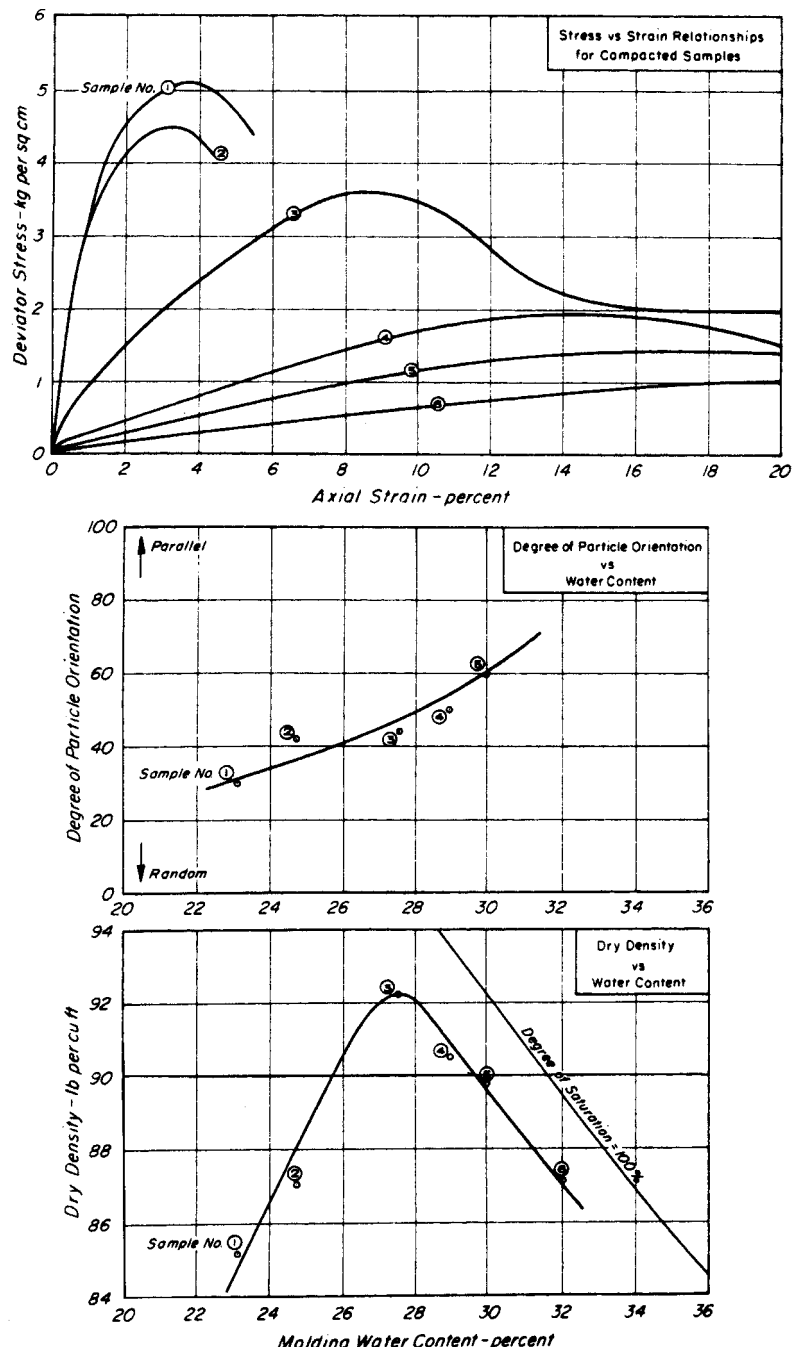
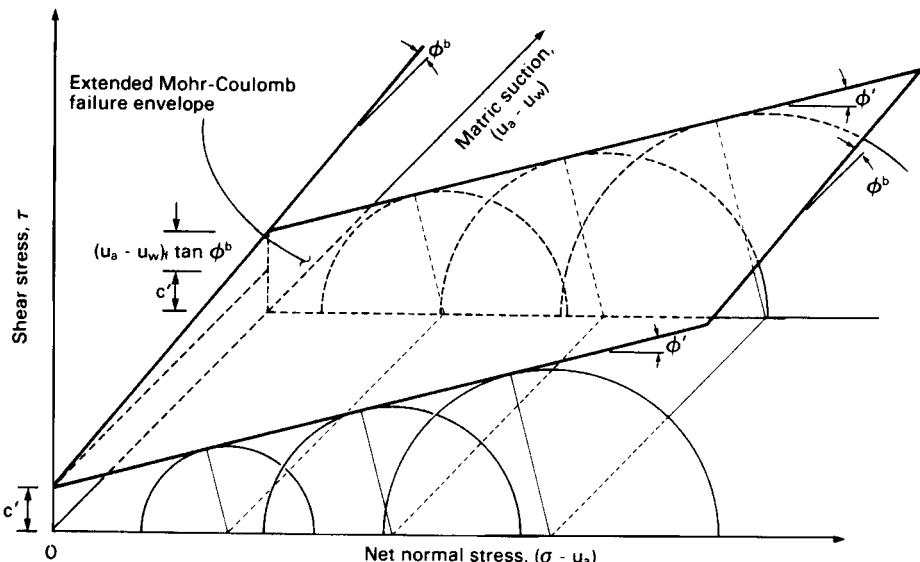


FIGURE 6A.76 Influence of molding water content on structure and triaxial stress-strain relationship for as-compacted samples of Kaolinite (from Seed and Chan, 1959a).

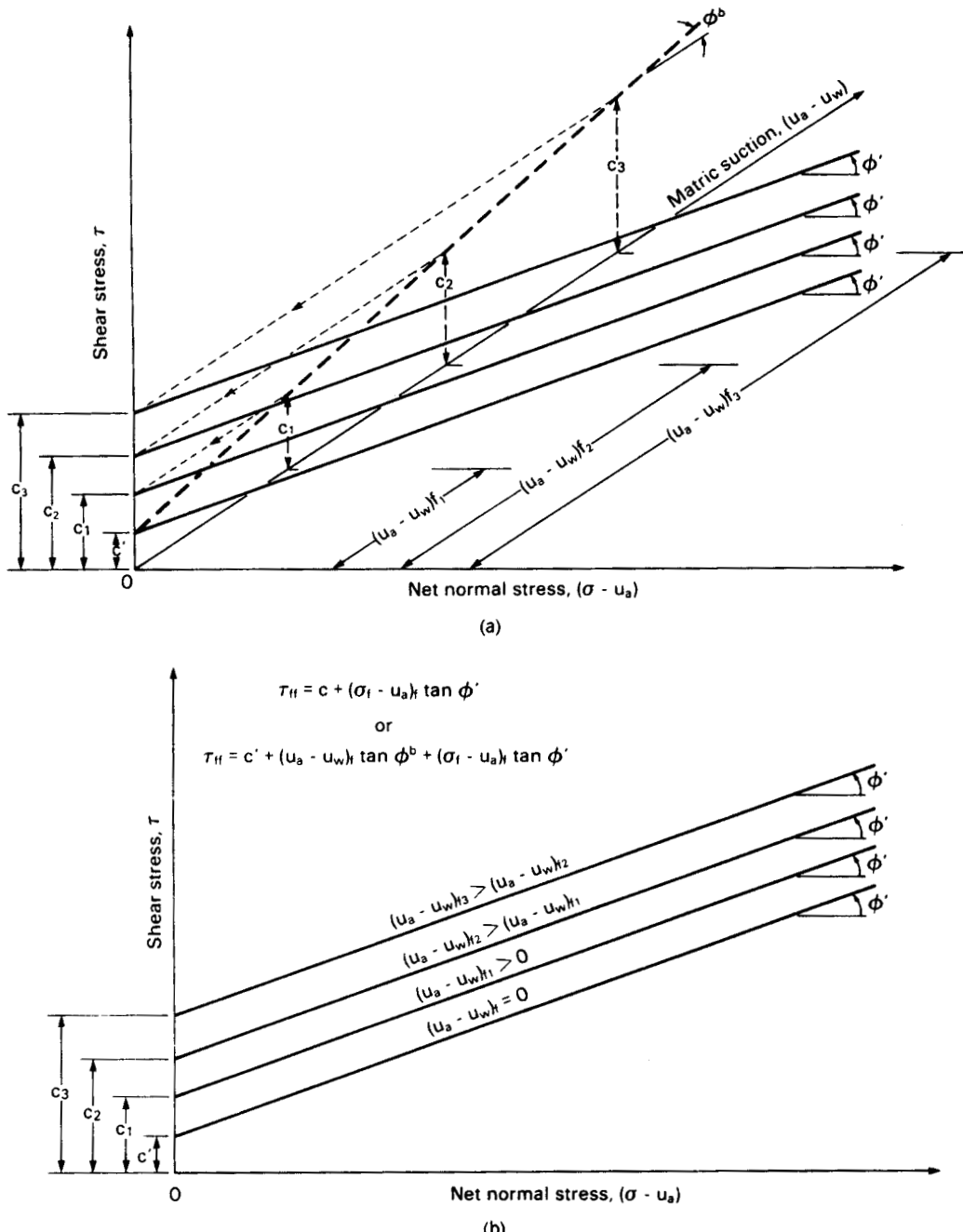
## 6.102 SOIL IMPROVEMENT AND STABILIZATION



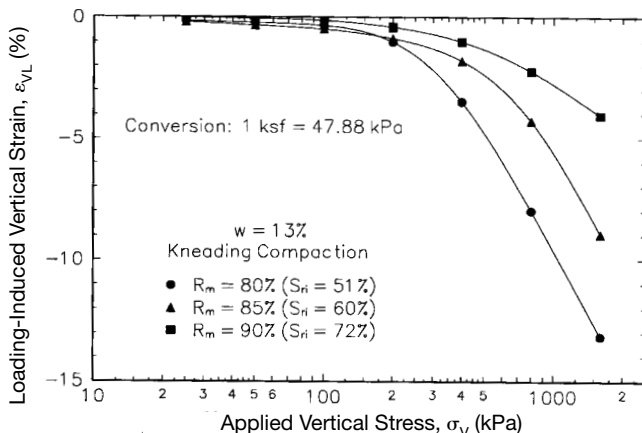
**FIGURE 6A.77** Extended Mohr-Coulomb failure envelope for unsaturated soils (from Fredlund and Rahardjo, 1993).

strain. The strength at large strain (20 or 25%) is applicable to situations where large deformations are tolerable, such as a flexible (wet) core of a high earth dam. The strength at small strain (5%) is appropriate for bearing soils where only small deformations are tolerable, such as for a building founded on a compacted fill, or where the soil is brittle (dry) and may crack at small strains.

At large strains, the strength of the sandy clay and the silty clay either increased or remained constant as the dry density increased. At low strains, the strength of both soils increased with increased density at low water contents, but at high water contents the strength peaks at a given density and then decreases with increased density beyond the peak. This loss of strength at high water contents is especially pronounced in the silty clay; for example, at a water content of 16% the strength peaks at about  $5.2 \text{ kg/cm}^2$  ( $10.7 \text{ ksf} = 510 \text{ kPa}$ ) for  $\gamma_d = 112.5 \text{ pcf}$  ( $17.7 \text{ kN/m}^3$ ) but drops to  $2.0 \text{ kg/cm}^2$  ( $4.1 \text{ ksf} = 200 \text{ kPa}$ ) for  $\gamma_d = 114.9 \text{ pcf}$  ( $18.0 \text{ kN/m}^3$ ), a reduction of 62%. The rapid decrease in strength at low strains near optimum water content can be seen in the left side of Fig. 6A.81 for each of the three compactive energy levels. At the same water content of 16%, the sample compacted with lower energy [ $\gamma_d = 112.5 \text{ pcf}$  ( $17.7 \text{ kN/m}^3$ )] is dry of optimum ( $S_r < S_{opt}$ ) and therefore stronger than the sample compacted with higher energy [ $\gamma_d = 114.9 \text{ pcf}$  ( $18.0 \text{ kN/m}^3$ )] that is denser but wet of optimum ( $S_r > S_{opt}$ ). The same trend can be seen in the right side of Fig. 6A.81, where the author has added the line of optimums. Seed and coworkers (1960) attributed this marked decrease in strength near optimum moisture condition to differences in fabric—higher pore water pressures develop in undrained cohesive soils compacted wet of optimum owing to a greater degree of dispersion of the microfabric. An alternative interpretation of this phenomenon can be given in terms of the air/water phases and their pressures. For  $S_r < S_{opt}$ , the air phase is continuous, and the matric suction likely remains positive even under undrained loading conditions because the air is somewhat compressible, and therefore only small values of positive air pressure are likely to develop compared to the negative water pressures. This suction adds to the strength and stiffness of the soil. As  $S_r$  approaches  $S_{opt}$ , there is a transition from a continuous to an occluded air phase, which changes the pore water pressures from negative to positive during undrained loading, with a corresponding reduction in strength and stiffness of the soil.



**FIGURE 6A.78** Horizontal projection of the failure envelope onto the  $\tau$  versus  $(\sigma - u_a)$  plane, viewed parallel to the  $(u_a - u_w)$  axis (from Fredlund and Rahardjo, 1993): (a) failure envelope projections onto the  $\tau$  versus  $(\sigma - u_a)$  plane; and (b) contour lines of the failure envelope onto the  $\tau$  versus  $(\sigma - u_a)$  plane.

**6.104** SOIL IMPROVEMENT AND STABILIZATION

**FIGURE 6A.79** Effect of density on as-compacted one-dimensional compressibility of a compacted clayey sand (data from Lawton, 1986).

**Method of Compaction** Method of compaction can have an important influence on the fabric of as-compacted cohesive soils, which in turn can have a substantial effect on their stress-strain-strength characteristics. For dry cohesive borrow materials, the clods are hard, and densification occurs either by rearrangement of the clods, which retain their basic shape, or by breaking of the clods into smaller (but still hard) pieces. During static compaction (smooth-drum roller), the induced stresses are primarily compressive and of relatively low magnitude compared to other types of rollers of comparable weight, so little breakage of dry clods occurs, and densification results mainly from rearrangement of clods. In contrast, kneading compaction (sheepsfoot and padfoot rollers) induces both shear stresses and compressive stresses in the soil that are of relatively high magnitude owing to the smaller contact areas of the feet, which results in densification from both rearrangement and breakage of particles. Thus, the microfabric of dry clods for both types of compaction is the same because it is essentially unaffected by the compaction, but the minifabric of the compacted soil is different—larger clods and larger intraclod pores for statically compacted soils, and smaller clods and smaller intraclod pores for soils compacted by kneading compaction. If the clods are very hard or the compactors are light, little breakage of clods will occur even for kneading compactors, and the method of compaction used will have little effect on the fabric of the compacted soil. Whether breakage occurs during compaction has little effect on the strength and stiffness of the as-compacted soil for the applied stress levels normally encountered in engineering practice because both characteristics depend on the strength and stiffness of the clods, which are independent of their size. At very high applied stress levels where some breakage might occur, a soil with a fabric consisting of small, hard clods might be stronger and stiffer than one at the same density but with larger clods because of the higher number of interclod contacts, which would result in less force being carried per clod and therefore less breakage of particles. This tendency toward greater stiffness may be offset to some degree by the possibility of more cracks being induced in the smaller clods during compaction, which would make the smaller clods more susceptible to breakage for the same applied force.

Wet cohesive borrow materials are soft, and clods are easily remolded during compaction. Static compaction tends to flatten the clods from the applied compressive stresses, but little change occurs to the microfabric of the clods. The resulting compacted soil mass tends to consist of relatively large interclod pore spaces and clods with flocculated microfabrics that retain to some extent their individual identity. Kneading compaction results in a more homogeneous fabric owing

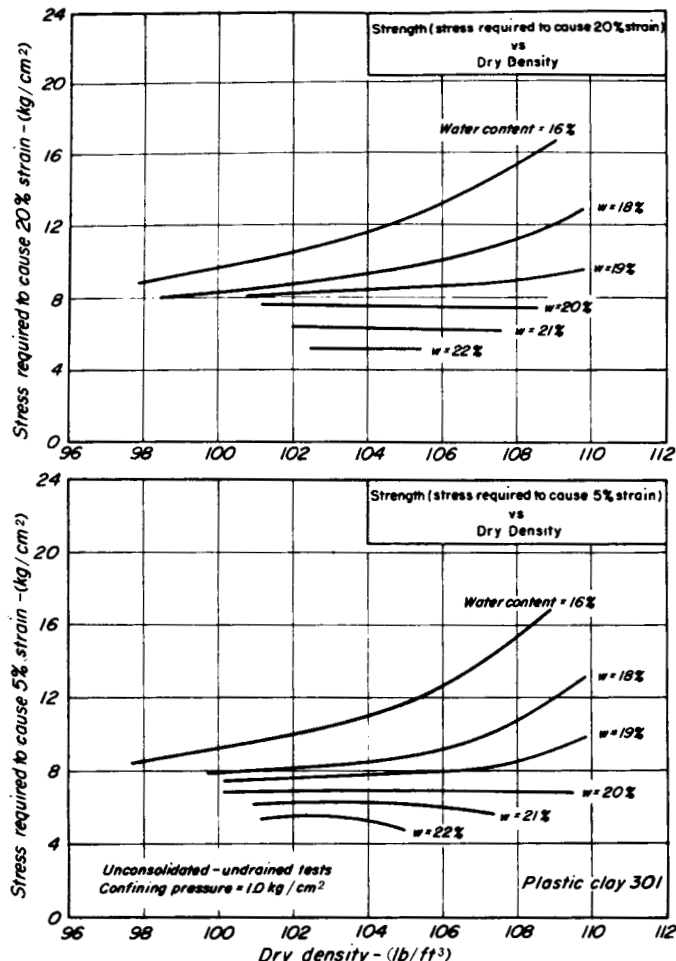


**FIGURE 6A.80** Relationships among dry density, water content, and triaxial strength for as-compacted specimens of highly plastic clay prepared by kneading compaction (from Seed et al., 1960).

to the shearing stresses induced during kneading, and the microfabric tends to be more dispersed than for static compaction. For the same moisture content and density, a cohesive soil with a flocculated fabric is less compressible and stronger than the same soil with a dispersed fabric. Thus, static compaction at high water contents produces a stronger and stiffer soil than does kneading compaction. The reasons for this difference in strength and stiffness for differing fabric are quite complex (see Lambe, 1958 for details). Simplified explanations for differences in strength and stiffness for the same soil, water content, and density but different methods of compaction can be given as follows:

**Compression.** Compression from an applied load tends to align the particles in a parallel array perpendicular to the direction of the applied load. Applying a load to particles that are already parallel merely brings them closer together. Applying the same load to particles that are random-

## 6.106 SOIL IMPROVEMENT AND STABILIZATION

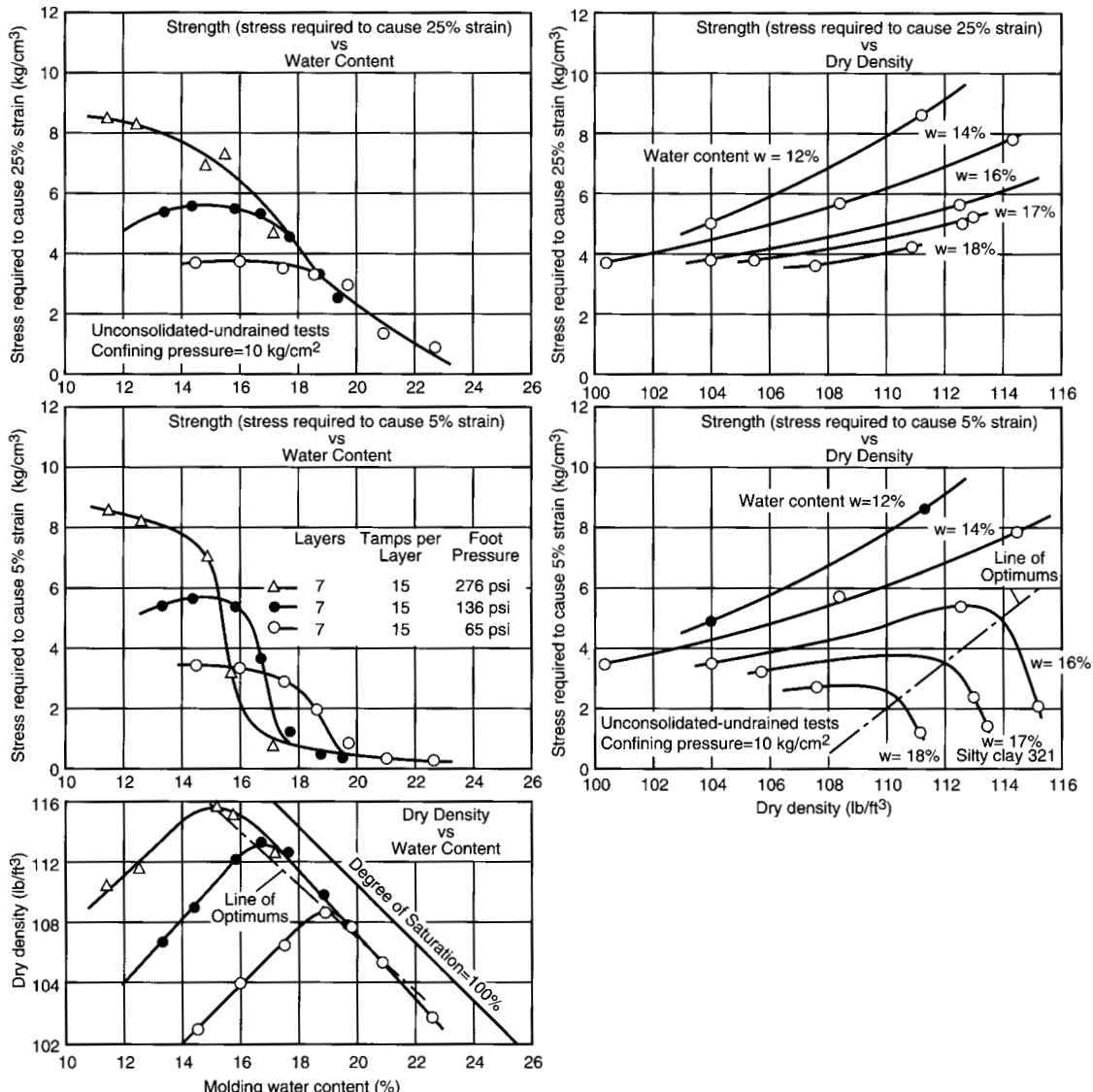


**FIGURE 6A.81** Relationships among dry density, water content, and triaxial strength for as-compacted specimens of silty clay prepared by kneading compaction (from Seed et al., 1960).

ly oriented requires that a portion of the load be spent reorienting the nonaligned particles to a more parallel arrangement before any reduction in average void ratio occurs.

**Shear Strength.** For the same water content and average spacing between clay particles (same void ratio), increasing the angle between particles increases the net attractive force between the particles, and hence increases the shear stress required to cause sliding of the particles relative to one another.

It is unlikely that field compaction would be undertaken on a cohesive borrow material so dry that no remolding would occur during compaction. Therefore, it is reasonable that method of compaction will have some effect on the compressibility and strength of all field-compacted cohesive soils.

Typical results from a series of laboratory one-dimensional compression tests conducted on specimens of a clayey sand compacted directly into the confining rings using static, impact, and kneading methods are shown in Fig. 6A.73. Two sets of results are provided—those for  $w = 16\%$  and  $R_m = 90\%$  corresponding to a wet of optimum moisture condition (as-compacted degree of saturation,  $S_{ri}$ , greater than optimum saturation,  $S_{opt}$ ), and those for  $w = 10\%$  and  $R_m = 90\%$  corresponding to a dry of optimum moisture condition ( $S_{ri} < S_{opt}$ ). In both cases, the statically compacted specimens are less compressible than the kneading-compacted specimens. For the dry of optimum specimens at low stresses [ $\sigma_v < 200$  kPa (4.2 ksf)], there is little discernible difference in the results. Isograms of loading-induced vertical strain ( $\epsilon_{VL}$ ) for kneading and statically compacted specimens loaded to  $\sigma_v = 400$  kPa (8.4 ksf) are shown in dry density-water content space in Fig. 6A.82. Note that  $\epsilon_{VL}$  is greater for kneading compaction than for static compaction for the entire ranges of dry densities and water contents studied. It is interesting that the isograms of  $\epsilon_{VL}$  for kneading compaction and  $S_i$  greater than about 70% are approximately horizontal, indicating that the compressibility of the specimens at these higher values of  $S_i$  is essentially independent of the water content and suggesting that the air phases become occluded in this soil after kneading compaction at about  $S_r = 70$  to 80% for  $R_m = 80$  to 90%. In contrast, the isograms  $\epsilon_{VL}$  for the statically compacted specimens in the same region indicate that compressibility is a function of both water content and density, which suggests that occlusion of the air phases has not occurred.

One-dimensional compression results are also shown in Fig. 6A.73 for specimens compacted directly into oedometer rings using a specially designed impact hammer. At both water contents, the impact-compacted soil was more compressible than the statically compacted soil. However, the comparison between the effects of kneading and impact compaction is not as straightforward—im-

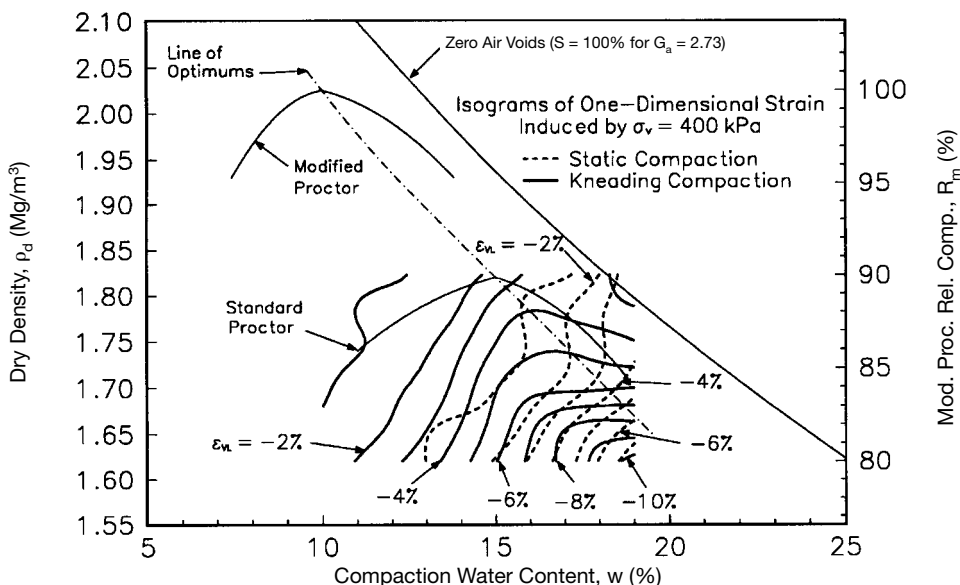


**FIGURE 6A.82** Isograms of one-dimensional as-compacted compressibility of clayey sand for specimens prepared by static and kneading compaction (data from Lawton, 1986).

**6.108** SOIL IMPROVEMENT AND STABILIZATION

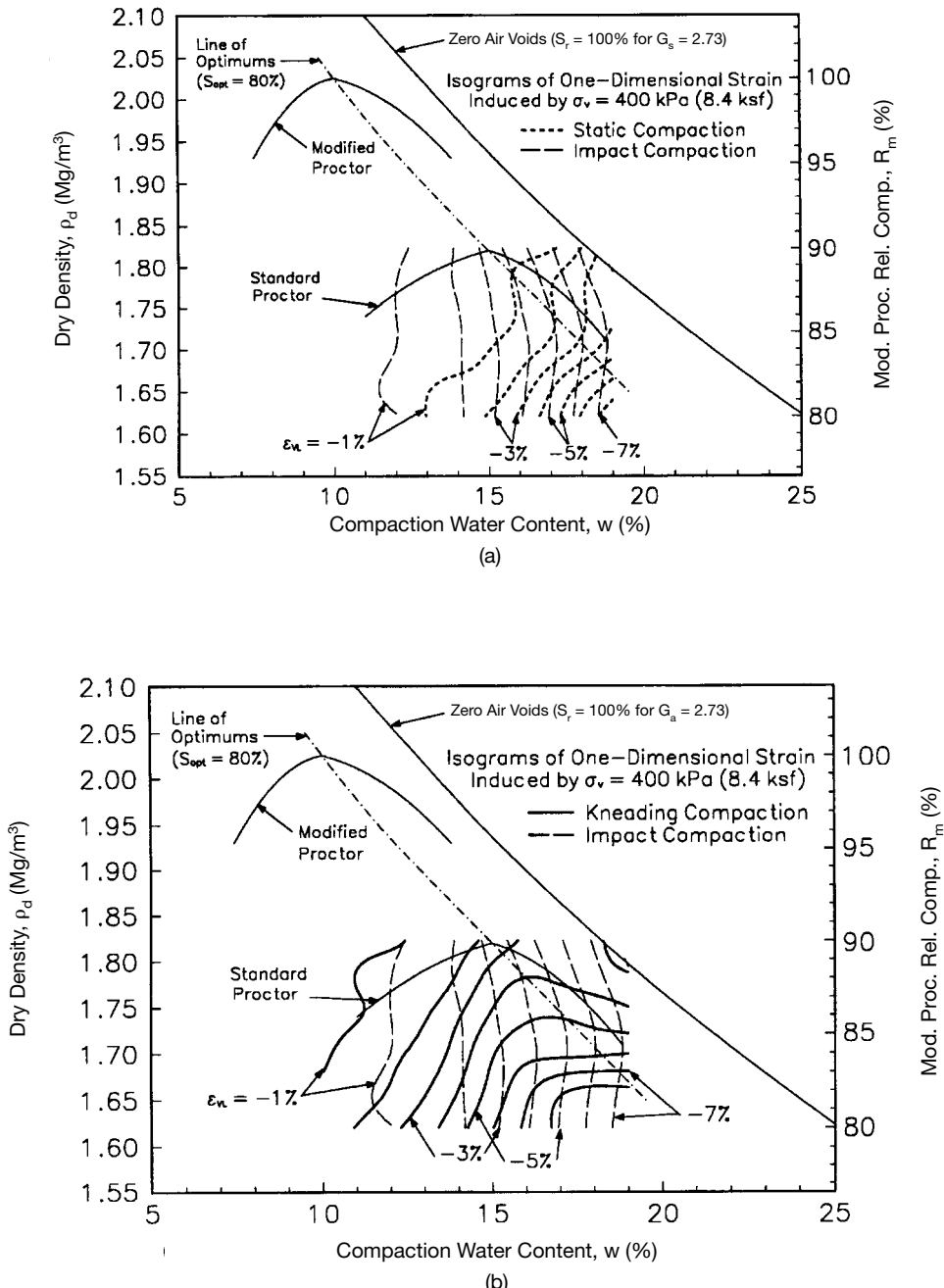
pact compaction produced a less compressible soil at  $w = 10\%$  but a more compressible soil at  $w = 16\%$ . To provide additional insight into the differences in compressibility produced by impact compaction compared to static and kneading compaction, isograms of  $\varepsilon_{vL}$  at  $\sigma_v = 400$  kPa for the same clayey sand are given in Fig. 6A.83(a) for static and impact compacton, and Fig. 6A.83(b) for kneading and impact compaction. It can be seen in Fig. 6A.83(a) that static compaction produced a stiffer soil than kneading compaction at all values of  $\rho_d$  and  $w$  studied. In Fig. 6A.83(b), the equivalent isograms for kneading and impact compaction intersect, with the kneading-compacted soil tending to be more compressible than the impact-compacted soil at low densities and less compressible at high densities. Also note that the isograms for the impact-compacted soil are nearly vertical, suggesting that the as-compacted compressibility of the impact-compacted soil is highly dependent on water content and nearly independent of density for the ranges studied.

Similar results have been found with respect to the effect of method of compaction on the unconsolidated-drained shear strength of a silty clay (Seed and Chan, 1959a). Values of relative unconsolidated, undrained triaxial strength at 5% strain, based on the strength for kneading compaction, are shown in Fig. 6A.84 for specimens prepared to nominally identical values of  $(\gamma_d, w)$  at various points along the standard Proctor moisture-density curve. The method of compaction had little influence on the strength dry of optimum but had a substantial influence on the strength wet of optimum. Note that the strength of the statically compacted soil was equal to or greater than the strength of the kneading-compacted and impact-compacted soil at all water contents. Impact compaction produced a weaker soil than kneading compaction at low water contents ( $<18.5\%$ ) and a stronger soil at high water contents ( $>18.5\%$ ). For purposes of further analysis, the strength results shown in Fig. 6A.84 for the silty clay are subdivided into three regions:

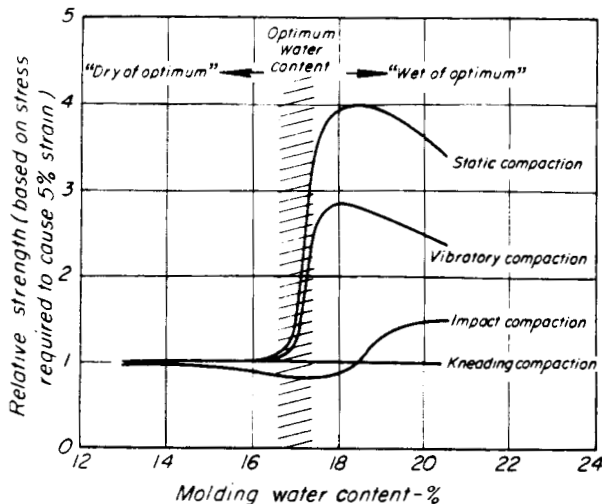
1. At the low end of the compaction water contents (13 to 14%), the soil was very dry, and the strengths of the soil for both impact and static compaction were about the same.
2. Around optimum water content (15.5 to 17.5%), the specimens were dense (standard Proctor relative compaction,  $R_s \cong 99$  to 100%), and impact-compacted specimens were about 80 to 90% as strong as the kneading-compacted specimens.
3. At the upper end of the compaction water content range for the silty clay (19.5 to 20.5%), the densities are lower ( $R_s \cong 94$  to 96%), and impact compaction produced soil that was about 1.4 to 1.5 times stronger than the soil prepared by kneading compaction.

The reasons for the differences in stress-strain-strength behavior of impact-compacted and kneading-compacted cohesive soils are not completely understood, and further research is needed in this area. A preliminary explanation for these differences can be given as follows (modified from Seed and Chan, 1959a):

1. For cohesive borrow materials that are very dry, no method of compaction produces any appreciable shear deformation, and consequently the method of compaction has no appreciable effect on the fabric and hence the stress-strain-strength characteristics of the as-compacted soil.
2. For the water contents at which cohesive borrow soils are usually compacted, impact compaction causes somewhat less shearing strain during compaction than does kneading compaction. At the same density, the as-compacted fabric for impact compaction tends to have larger but fewer intraclocl voids and less dispersion within the clods than for kneading compaction. The larger intraclocl voids tend to decrease the strength and increase the compressibility of the impact-compacted soil, but the lesser degree of dispersion tends to increase the strength and decrease the compressibility. Whether the impact-compacted soil is stronger and stiffer than the kneading-compacted soil or vice versa depends on which characteristic dominates the stress-strain-strength behavior—larger intraclocl voids or decreased dispersion. At high densities, the fabric of impact-compacted cohesive soil apparently has a degree of dispersion that is close to that of kneading-compacted soil but still has larger intraclocl voids. In this case, the larger intraclocl voids dominate, resulting in a more compressible soil. At low densities, the increased stiffness produced by the more flocculated fabric of the impact-compacted soil is greater than the reduction in stiffness resulting from the larger intraclocl voids.



**FIGURE 6A.83** Isograms of one-dimensional as-compacted compressibility of clayey sand for specimens prepared by (a) static and impact compaction; and (b) kneading and impact compaction (data from Lawton, 1986).

**6.110** SOIL IMPROVEMENT AND STABILIZATION

**FIGURE 6A.84** Influence of compaction method on the triaxial strength of silty clay (from Seed and Chan, 1959a).

The results presented in this section provide salient evidence to substantiate that the methods and procedures used to prepare laboratory-compacted specimens for testing should simulate as closely possible the methods and procedures used in the field compaction process. It is also apparent that specimens obtained for stress-strain-strength testing by trimming Proctor samples—a routine practice in some testing laboratories—are unlikely to have stress-strain-strength characteristics representative of the soil as compacted in the field using most types of rollers. The following procedure is the best way to ensure that the fabrics of cohesive specimens to be tested in the laboratory are similar to those of the field-compacted soil:

1. Construct several lifts of the borrow soil in a test pad in which the actual compaction procedure is simulated, that is, using the same compaction roller, lift thicknesses, and construction techniques that will be employed in the field compaction process.
2. Obtain samples of the compacted soil from the test pad that are several times larger than the sizes of the specimens to be tested in the laboratory.
3. Carefully trim laboratory specimens to the appropriate sizes for testing from within the interior portions of the larger samples obtained from the field.

Unfortunately, this procedure is not economically feasible for many projects, and thus test specimens are commonly prepared using laboratory compaction procedures.

**Time Rate of Settlement** As with saturated naturally deposited cohesive soils, the settlement of compacted cohesive soils can be considered to consist of three parts: immediate settlement, primary compression settlement, and secondary compression settlement. *Primary compression* is defined herein for compacted cohesive soils as the loading-induced compression that occurs until either the matric suction reaches a steady-state value under the applied load (unsaturated soil where the air phase is continuous), or the pore water pressure reaches a steady-state value under the applied load (soil is unsaturated but the air phase is occluded or becomes occluded during compression). Primary compression in unsaturated compacted cohesive soils generally occurs much more quickly than does primary consolidation in the same cohesive soil that is saturated (all other factors being the

same), owing to differences in water permeability and air permeability. Coefficients of air permeability ( $k_a$ ) and water permeability ( $k_w$ ) for a compacted cohesive soil (10% clay) as a function of water content are shown in Fig. 6A.85 (Barden and Pavlakis, 1971). At degrees of saturation less than about  $S_{opt}$ , the air phase is continuous, and loading-induced compression expels air from the voids rather than water. For  $S_r \ll S_{opt}$ , the portion of the void through which air can flow (the area not occupied by water) is large and primary compression occurs very quickly because of the high value of  $k_a$ . As  $S_r$  increases,  $k_a$  decreases owing to a decrease in the size of the air phase, with a concomitant decrease in the rate of primary compression. For  $S_r < S_{opt}$ , the air phase becomes occluded, water rather than air is expelled during compression, and the rate of primary compression (consolidation) is controlled by  $k_w$ .

The effect of moisture condition on the time rate of one-dimensional compression in a compacted clayey sand is illustrated in Fig. 6A.86. The total compressive strains are shown in Fig. 6A.86(a), and the time-dependent strains (after the first reading at 0.25 min) are plotted in Fig. 6A.86(b). In these tests, oedometer specimens were compacted at different water contents to the same nominal dry density ( $R_m = 80\%$ ) and then loaded incrementally in a standard one-dimensional compression test. The results shown in Fig. 6A.86 are for the loading increment from 200 to 400 kPa (4.2 to 8.4 ksf). During the previous loading increments, the magnitudes of the strains produced in the specimens were different, so the void ratios of the specimens at the beginning of the 200 to 400 kPa loading increment ( $e_{200}$ ) varied somewhat, but the influence of these small differences in void ratio on the loading-induced compression was negligible compared to the effect produced by the differences in degree of saturation ( $S_{r-200}$ ). It can be seen in Fig. 6A.86(b) that the magnitude of the time-dependent strains increased substantially with increasing degree of saturation. It is also apparent that the strain-log time plot for the wettest sample ( $S_{r-200} > S_{opt}$ ) has the classical "backward S" shape associated with saturated cohesive soils; in contrast, the plot for the driest sample ( $S_{r-200} \ll S_{opt}$ ) is essentially linear, suggesting that primary compression was completed prior to the first reading (0.25 min).

Differentiating between primary and secondary compression in compacted cohesive soils is not easy unless tests are conducted in which the pore air and pore water pressures are simultaneously measured during compression, which requires special testing equipment. Tests of this type are rarely conducted in geotechnical engineering practice. Details of equipment and methods that can be used to measure or control  $u_a$  and  $u_w$  in unsaturated samples are given in Fredlund and Rahardjo (1993). Simultaneous measurement of  $u_a$  and  $u_w$  is further complicated by the fact that the air phase in the

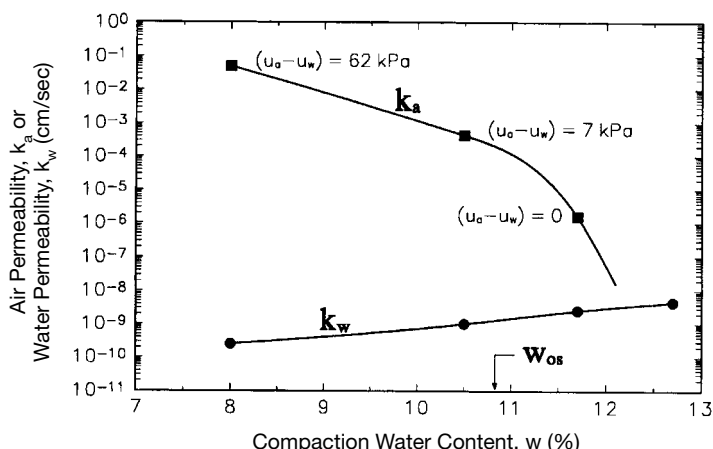
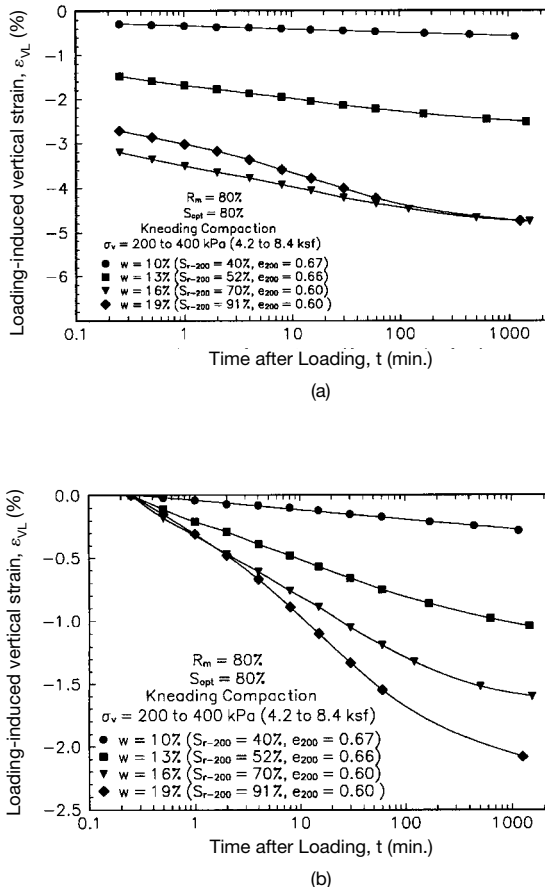


FIGURE 6A.85 Effect of compaction water content on air and water permeability of Westwater soil (from Barden and Pavlakis, 1971).

## 6.112 SOIL IMPROVEMENT AND STABILIZATION



**FIGURE 6A.86** Effect of moisture condition on the time rate of one-dimensional loading-induced compression of a compacted clayey sand (data from Lawton, 1986): (a) total vertical strain; and (b) time-dependent vertical strain.

compacted specimen may change from continuous to occluded during the compression. For example, the specimen with  $w = 16\%$  in Fig. 6A.86 was loaded incrementally from the as-compacted state ( $\sigma_v \approx 0$ ) to  $\sigma_v = 1600$  kPa (33.4 ksf), which increased  $S_r$  from 63% (17% below  $S_{opt}$ ) to nearly 100%, and it is likely that the air phase changed from continuous to occluded. [Note that  $S_r$  increased from 70 to 81% during the loading increment from 200 to 400 kPa (4.2 to 8.4 ksf) shown in Fig. 6A.86.] Although the air phase was continuous, the pore air pressures were either positive or zero during loading, whereas the pore water pressures were negative [ $u_w \approx -80$  kPa (-1.7 ksf)] in the as-compacted state determined from suction measurements. After the air phase became occluded, the pore water pressures were positive (perhaps as much as 800 kPa during the 800–1600-kPa loading increment) or zero, and the pore air pressures in the occluded bubbles could not have been measured but probably had little effect on the behavior during compression. To have measured both the pore air and pore water pressures throughout this test would have required the following setup:

1. A sealed sample with a low air entry porous disk at the top of the sample (for measuring or controlling  $u_a$ ) and a high air entry porous disk at the bottom of the sample (for measuring  $u_w$ ).
2. A pressure transducer for measuring positive air pressures up to perhaps 800 kPa (16.7 ksf = 116 psi).
3. A pressure transducer for measuring  $u_w$  from about -80 kPa (-1.7 ksf = -12 psi) to perhaps + 800 kPa (16.7 ksf = 116 psi).

Because high air entry ceramics usually have low permeabilities, the response time is generally slower than desired for rapidly changing pore water pressures so that there may be somewhat of a difference between measured and actual pore water pressures at any time.

Owing to the difficulty and expense associated with measuring  $u_a$  and  $u_w$  during compression tests on compacted cohesive soils, the delineation between primary and secondary compression is usually accomplished by visually examining the strain-log time curves in the same manner as for saturated cohesive soils. The following guidelines are provided for conducting an immediate/primary/secondary compression analysis for a compacted cohesive soil:

1. The values for immediate strain can be calculated from the first readings taken after applying any loading increment (usually 6 or 15 s). From the data in Fig. 6A.86(a), the immediate strains for the 200–400-kPa (4.2–8.4-ksf) loading increment would be 0.29, 1.5, 3.2, and 2.7% for  $w = 10, 13, 16$ , and 19%, respectively.

2. Primary and secondary (creep) compression occur during the phase called *primary compression*, but there is no method currently available to separate the two components other than to assume that the secondary compression that occurs during primary compression is the same as (or similar to) that measured after primary compression has ended. In typical geotechnical engineering practice, the secondary compression component is not differentiated from the primary compression component, and the two components together are considered to constitute primary compression.

3. When the strain-log time plot has the classical backward S shape [e.g.,  $w = 19\%$  in Fig. 6A.86(b)], the time to the end of primary compression is estimated to occur at the point of intersection of a straight line extended forward from the central (steepest) portion of the backward S (some judgment involved) and a best-fit straight line extended backward from the tail of the backward S. Secondary compression is assumed to begin when primary compression ends. The secondary compression index,  $C_{ae}$  (or  $C_{ae}$  from void ratio-log time plot), can be determined from the slope of the best-fit straight line through the tail, and settlement estimated using the following equations:

$$C_{ae} = -\frac{d\varepsilon_v}{d(\log t)} \quad (6A.27a)$$

$$C_{ae} = -\frac{de}{d(\log t)} \quad (6A.27b)$$

$$S_s = \int_{z=0}^{z=H} \int_{t=t_p}^{t=t_{\text{design}}} C_{ae} \cdot d(\log t) \cdot dz \quad (6A.28a)$$

$$S_s = \int_{z=0}^{z=H} \int_{t=t_p}^{t=t_{\text{design}}} \frac{C_{ae}}{1+e_p} \cdot d(\log t) \cdot dz \quad (6A.28a)$$

where  $\varepsilon_v$  = vertical strain

$e$  = void ratio

$z$  = depth from bearing level

**6.114** SOIL IMPROVEMENT AND STABILIZATION

$H$  = height of the compacted soil layer

$e_p$  = void ratio at the end of primary compression

$t_{\text{design}}$  = design life of the structure

If  $C_{ae}$  (or  $C_{ae}$ ) is assumed to be independent of time and stress level, and  $e_p$  is assumed to be approximately constant with depth, Eq. (6A.28) reduces to the form more commonly seen in the literature:

$$S_s = C_{ae} \cdot H_0 \cdot \log \frac{t_{\text{design}}}{t_p} \quad (6A.29a)$$

$$S_s = \frac{C_{ae}}{1 + e_p} \cdot H_p \cdot \log \frac{t_{\text{design}}}{t_p} \quad (6A.29b)$$

The height of the compacted soil layer is shown as  $H_0$  in Eq. (6A.29a) because strain is generally plotted as engineering strain ( $\Delta H/H_0$ ). In Eq. (6A.29b)  $e_p$  and  $H_p$  are used because secondary compression is assumed to begin when primary compression ends ( $t_p$ ). However, for one-dimensional compression the ratio  $H/(1 + e)$  is a constant, so  $e_0$  with  $H_0$  can also be used, which is the form more commonly seen in the literature, but the equation as shown is the strictly correct form. If the soil is highly layered or if  $C_{ae}$  (or  $C_{ae}$ ) varies significantly as a function of stress level, the depth integral in Eq. (6A.28) can be approximated by a summation:

$$S_s = \sum_{i=1}^{i=n} C_{aen} \cdot \log \frac{t_{\text{design}}}{t_p} \cdot \Delta z_n \quad (6A.30a)$$

$$S_s = \sum_{i=1}^{i=n} \frac{C_{aen}}{1 + e_{pn}} \cdot \log \frac{t_{\text{design}}}{t_p} \cdot \Delta z_n \quad (6A.30b)$$

The coefficient of primary compression,  $c_v$ , can be calculated from the same techniques used for saturated cohesive soils. A more direct method for extrapolating one-dimensional laboratory results to field time scale is to assume that the time rate of compression is proportional to  $H_{dp}^2$ , where  $H_{dp}$  is the height of the longest drainage path. For example,  $\varepsilon_{VL}$  after 1 h in a 1-in (25-mm) high, doubly drained laboratory specimen can be extrapolated to field time scale for a 20-ft (6.1-m) thick, singly drained compacted fill in the following manner:

$$H_{dp-\text{lab}} = 0.5 \text{ in (13 mm)}$$

$$H_{dp-\text{field}} = 20 \text{ ft (6.1 m)} = 240 \text{ in}$$

$$t_{\text{field}} = t_{\text{lab}} \cdot \frac{H_{dp-\text{field}}^2}{H_{dp-\text{lab}}^2} = (1 \text{ h}) \cdot \frac{(240 \text{ in})^2}{(0.5 \text{ in})^2} = 230,400 \text{ h} = 9600 \text{ day} = 26.3 \text{ yr}$$

Although this method is crude, it is similar in concept to the methods commonly used for saturated cohesive soils and is simple enough to use in routine practice. More sophisticated methods are available for estimating the time rate of compression for unsaturated soils (see Fredlund and Rahardjo, 1993), but these techniques are beyond the scope of this handbook. An alternative method for establishing the effect of  $H_{dp}$  on the time rate of compression is to conduct a series of one-dimensional compression tests on specimens compacted at the same water content to the same density but of varying thicknesses, and then comparing the values of strain for the same loading increments and time after loading.

4. If the strain-log time plot can be approximated quite closely with a straight line [e.g., plot for  $w = 10\%$  in Fig. 6A.86(b)], it can be assumed that primary compression was complete and secondary compression began before the first reading was taken. Thus, the strain at the first reading can be conservatively used as the immediate plus primary compression strain. In this case, the approach for estimating settlement is similar to that used for sands wherein the primary compression settlement occurs so quickly that it cannot be separated from the immediate (distortion) settlement, so both components are included in a single component called *immediate settlement*.

5. For time-rate plots that are neither straight lines nor backward S shapes [e.g.,  $w = 13$  and  $16\%$  in Fig. 6A.86(b)], the time to the end of primary compression can be estimated as the point of intersection between a straight line extended forward for the initial (steeper) portion of the plot and a straight line extended backward from the tail (flatter) portion of the plot. Some judgment is commonly required to draw these straight lines, especially the line drawn through the initial portion of the plot, because this part is generally curved.

6. For loading and field conditions that cannot be reasonably approximated by one-dimensional compression tests, more sophisticated laboratory testing techniques—such as the stress path method (Lambe and Whitman, 1979)—are needed to model the field compression in a reasonable way.

**Total Settlement** It is difficult to differentiate between immediate compression and secondary compression in the laboratory and even more difficult to extrapolate this difference to field time scale. Using a traditional dead-weight consolidometer setup, the first reading commonly taken in a one-dimensional compression test is either 6 s or 15 s. Using the method given in the previous section, these two laboratory times are extrapolated to field scale for a 1.0-in (25-mm) high, doubly drained laboratory specimen and various singly drained fill thicknesses in the following table:

Singly drained field thickness		$H_{dp-field}$	$t_{field}$ (days)	
ft	m		$H_{dp-lab}$	$t_{lab} = 6$ s
1	0.3	24	0.04	0.1
5	1.5	120	1	2.5
10	3.0	240	4	10
20	6.1	480	16	40
50	15.2	1200	100	250
100	30.5	2400	400	1000
200	61.0	4800	1600	4000

Thus, it is clear that extrapolating laboratory immediate settlement to field time scale depends on the relative values of  $H_{dp-lab}$  and  $H_{dp-field}$  and is not easy to do for large values of  $H_{dp-lab}/H_{dp-field}$ . Because of these difficulties, it is common in geotechnical engineering practice to perform a combined settlement analysis for the immediate and primary compression components,  $S_{ic}$ . It should be recognized, though, that usually a significant portion of the settlement that occurs at the first reading is immediate settlement that would occur regardless of when the first reading is taken. Thus, the author recommends taking readings as quickly as possible and assigning the value of strain at the first reading to immediate strain, with the time-dependent strains assumed to occur after the first reading.

The results from one-dimensional compression tests are commonly plotted as either a  $\log \sigma_v - \varepsilon_v$  or  $\log \sigma_v - e$  plot, as shown in Fig. 6A.72. In either case, the plot can be approximated by two straight lines (dashed lines in Fig. 6A.72) as is commonly done for saturated clays, with the slopes of the recompression and virgin compression lines designated  $C_{re}$  and  $C_{ce}$ , respectively (or  $C_{re}$  and  $C_{ce}$  if plotted in  $\log \sigma_v - e$  space). Because the initial portion of the strain-stress plot is curved, some judgment is needed to establish  $C_{re}$ . The method preferred by the author is to use the aver-

**6.116** SOIL IMPROVEMENT AND STABILIZATION

age slope for the rebound curve obtained by unloading the specimen after the loading portion is completed, as shown in Fig. 6A.72.  $C_{ce}$  is obtained by approximating the virgin compression curve with a straight line. The intersection of the two straight lines representing initial recompression and virgin compression establishes the value of  $\sigma_{vc}$ . With the calculated values for  $C_{re}$ ,  $C_{ce}$ , and  $C_{vc}$ , one-dimensional settlement for a shallow foundation can be estimated from the following equation:

$$S_{ic} = \int_{z=0}^{z=\infty} \varepsilon_{VL} dz \quad (6A.31)$$

where  $z = 0$  corresponds to the bearing level, with  $z$  increasing with depth below the bearing level.

The symbol for settlement in Eq. (6A.31) is designated  $S_{ic}$  because the results from one-dimensional compression tests include both the immediate and primary compression components of the settlement. The loading-induced, one-dimensional vertical strain for any point within a compacted soil mass can be expressed by one of the following equations:

For  $\sigma_{v1} \leq \sigma_{vc}$ :

$$\varepsilon_{VL} = C_{re} \cdot \log \frac{\sigma_{v1}}{\sigma_{v0}} \quad (6A.32a)$$

For  $\sigma_{v1} > \sigma_{vc}$ :

$$\varepsilon_{VL} = C_{re} \cdot \log \frac{\sigma_{vc}}{\sigma_{v0}} + C_{ce} \cdot \log \frac{\sigma_{v1}}{\sigma_{vc}} \quad (6A.32b)$$

where  $\sigma_{v0}$  = initial total vertical stress

$\sigma_{v1}$  = total vertical stress after loading

If true one-dimensional compression is closely approximated—such as a wide foundation bearing on a relatively thin and homogeneous compacted soil layer overlying a thick, incompressible layer—and  $\sigma_{v1} \leq \sigma_{vc}$  at all depths, Eq. (6A.31) can be used directly to estimate settlement:

$$S_{ic} = \int_{z=0}^{z=H} C_{re} \cdot \log \frac{\sigma_{v1}}{\sigma_{v0}} \cdot dz \quad (6A.33)$$

where  $H$  = the height from the bearing level to the bottom of the compacted soil layer

$$\sigma_{v0} = \gamma D + z$$

$$\sigma_{v1} = \sigma_{v0} + q_0$$

$\gamma$  = average unit weight of the compacted soil

$D$  = depth of embedment of the foundation

$q_0$  = applied uniform, centric bearing stress

Assuming that  $C_{re}$  is constant throughout  $H$ ,  $C_{re}$  can be pulled out of the integrand, and the solution for  $S_{ic}$  is as follows:

$$S_{ic} = C_{re} \left\{ \frac{\gamma(H+D) + q_0}{\gamma} \cdot \log[(\gamma(H+D) + q_0)] - (H+D) \cdot \log[(\gamma(H+D))] - \frac{\gamma D + q_0}{\gamma} \cdot \log(\gamma D + q_0) + D \cdot \log(\gamma D) \right\} \quad (6A.34)$$

A similar equation can be derived for  $\sigma_{v1} > \sigma_{vc}$ . In Eqs. (6A.33) and (6A.34), the settlement term  $S_{ic}$  is used because  $C_{ce}$  and  $C_{re}$  are commonly calculated based on laboratory data that include both immediate and primary compression strains. If the time rate of settlement is an important consideration, a preferred alternative is to separate the immediate and primary compression components, with values of  $C_{cei}$  and  $C_{rei}$  determined separately for immediate compression and primary compression (that is,  $C_{cei}$  and  $C_{rei}$ , for immediate compression and  $C_{cec}$ , and  $C_{rec}$  for primary compression).

Equation (6A.34) is valid if the excavation is backfilled after construction of the foundation, and if no rebound occurs from the time of excavation to the completion of backfilling (which depends on time rate of rebound for the soil versus the elapsed time between excavation and construction of the foundation). If the foundation is not backfilled, or if the soil rebounds completely before the backfill is placed, the initial stress at the bearing level is zero, and  $S_{ic}$  should be calculated based on  $\sigma_{v0} = \gamma z$ . For this case, Eq. (6A.34) simplifies to

$$S_{ic} = C_{rei} \left\{ \frac{\gamma(H + D) + q_0}{\gamma} \cdot \log[(\gamma(H + D) + q_0)] - H \cdot \log(\gamma H) \right. \\ \left. - \frac{\gamma D + q_0}{\gamma} \cdot \log(\gamma D + q_0) \right\} \quad (6A.35)$$

It is assumed in Eq. (6A.35) that the total weight of the foundation, the portion of the wall or stem below the ground surface, and the backfilled soil above the foundation is about the same as the weight of the excavated soil within the footprint of the foundation.

In many situations the width of the foundation is small in comparison to  $H$ , which means that the equation for  $\sigma_{v1}$  is much more complex than that given in Eq. (6A.33), and the  $\log(\sigma_{v1}/\sigma_{v0})$  term in Eq. (6A.33) cannot be easily integrated. For these cases, the integration must be approximated with a summation, and the appropriate equations for  $S_{ic}$  using the one-dimensional compression indices are

$$S_{ic} = \sum_{i=1}^{i=n} S_{ici} \quad (6A.36a)$$

For  $\sigma_{v1} \leq \sigma_{vc}$ :

$$S_{ici} = C_{rei} \cdot \log \frac{\sigma_{v1i}}{\sigma_{v0i}} \cdot \Delta z_i \quad (6A.36b)$$

For  $\sigma_{v1} > \sigma_{vc}$ :

$$S_{ici} = \left( C_{rei} \cdot \log \frac{\sigma_{vci}}{\sigma_{v0i}} + C_{cei} \cdot \log \frac{\sigma_{vli}}{\sigma_{vci}} \right) \cdot \Delta z_i \quad (6A.36c)$$

where  $n$  = the number of sublayers into which the bearing soil is subdivided for purposes of settlement analysis

$i$  = subscript added to each parameter indicating the value of that parameter for the  $i$ th sublayer

$$\sigma_{v1} = \sigma_{v0} + \Delta\sigma_v$$

$\Delta\sigma_v$  = increase in total vertical stress caused by the foundation load

$\Delta z_i$  = height of the  $i$ th layer

The greater the value of  $n$ , the more closely the integration is approximated. Values of  $\sigma_{v0}$  and  $\sigma_{v1}$  at the center of each sublayer are used as "average" values.  $\Delta\sigma_v$  can be estimated for each sublayer us-

## 6.118 SOIL IMPROVEMENT AND STABILIZATION

ing an appropriate stress distribution method. If the soil within the settlement influence zone is relatively homogeneous, the Boussinesq-type equations can be used for foundations bearing on the ground surface. For foundations embedded within a relatively homogeneous soil, Skopek's (1961) and Nishida's (1966) solutions can be used for rectangular and circular foundations, respectively. For layered soils and other conditions, refer to the discussion in Sec. 6A.2.2. Spreadsheet programs are ideally suited for estimating settlement in this manner.

If one-dimensional strain conditions are closely approximated but the soil within the settlement influence zone is layered, the settlement can be calculated by integrating the strains for each layer using Eq. (6A.33) (or a comparable equation for  $\sigma_{v1} > \sigma_{vc}$ ) and the appropriate value of  $H$  for each layer. As an alternative, the settlement can be estimated using Eq. (6A.36) and subdividing each layer into a number of sublayers.

**Three-Dimensional Settlement** It is important to note that for small-width foundations relative to the thickness of the compressible zone (a common situation), the use of Eqs. (6A.32) to (6A.36) would be inconsistent, because one-dimensional compression indices ( $C_{ce}$  and  $C_{re}$ ) would be used to estimate settlement for conditions of three-dimensional strain. The influence of principal stress ratio on the compression characteristics of a clayey sand compacted at  $w_{om}$  to  $R_m = 85\%$  is shown in Fig. 6A.87. These results were determined from a series of tests conducted in a triaxial cell in which an initial vertical stress of 25 kPa (3.6 psi) was applied to four identically compacted specimens, and the initial radial (horizontal) stress was varied to provide ratios of  $\sigma_r/\sigma_v = 1/3, 1/2, 2/3$ , and 1. The vertical strain induced in each sample by the application of the initial stresses was very small and could not be accurately measured, and thus are shown as zero in Fig. 6A.87. The stresses on the specimens were then increased incrementally, while maintaining the appropriate value of lateral stress coefficient ( $\sigma_r/\sigma_v$ ), up to the controlling capacities of the equipment (a maximum cell pressure of 690 kPa = 100 psi or a maximum vertical stress of 1600 kPa = 232 psi). Therefore, the maximum value of  $\sigma_r$  for each test varied.

The results from these triaxial compression tests are compared in Fig. 6A.87 with those from one-dimensional compression tests conducted in an oedometer on specimens compacted directly into the oedometer ring at the same water content using the same compaction method to the same relative compaction. At low stresses the strains are small and the effect of  $\sigma_r/\sigma_v$  is small, and it is difficult to determine a consistent relationship. At the higher stresses, it is clear that the stress ratio

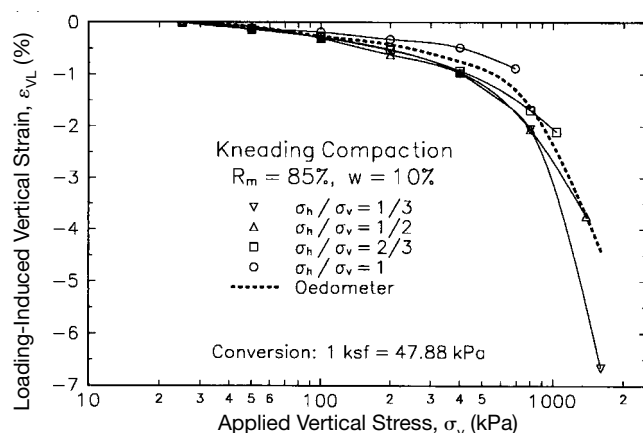


**FIGURE 6A.87** Influence of stress ratio on vertical compressibility of compacted clayey sand (data from Lawton 1986).

has a significant influence on the loading-induced strain, with  $\varepsilon_{YL}$  increasing with decreasing  $\sigma_r/\sigma_v$ . Thus, the lower the confining pressure, the greater the induced vertical strain. Comparing the position of the curve for the oedometer test with those from the triaxial test indicates that the value of  $\sigma_r/\sigma_v$  in the oedometer sample was consistently between  $\frac{1}{3}$  and 1 for stresses below the compactive prestress ( $\sigma_{vc} \approx 600$  kPa = 87 psi) but decreased at stresses above  $\sigma_{vc}$  to a value of about 0.5 at  $\sigma_v = 1600$  kPa (232 psi).

These results suggest that the results of oedometer tests can be used to estimate three-dimensional settlements for dry, stiff compacted cohesive soils at low applied stresses but that more sophisticated techniques are needed for higher stresses or wet, soft soils. Some methods that might be used include the following:

1. The Skempton and Bjerrum (1957) method for correcting one-dimensional settlement of saturated cohesive soils for three-dimensional conditions might be used for soils with  $S_r > S_{opt}$  because the induced pore pressures in the compacted soil may be similar to those for saturated soil. However, as noted by Lambe and Whitman (1979), Skempton and Bjerrum's method assumes a discontinuous—and therefore incorrect—stress path and tends to underestimate settlement.
2. The stress-path method (Lambe, 1967) could be employed and would involve conducting stress-path triaxial tests on a number of samples that duplicate the expected stress paths in the soil at various depths beneath the foundation. The major problem with using the stress-path method is that the induced changes in vertical and horizontal stress must be predicted, and the predicted values may vary substantially from the actual changes in stress.
3. A series of plate-load tests using at least three sizes of plates could be conducted in the field-compacted soil at the expected bearing level, and the results could be extrapolated to full field scale.
4. A finite element settlement analysis could be performed (see Sec. 6A.2.3 for recommended procedures).

**Ultimate Bearing Capacity Analyses** Any appropriate method for estimate ultimate bearing capacity can be used (see Sec. 2B). It is important that the strength parameters (friction angle and cohesion intercept) be consistent with the desired analysis, that is, undrained strength parameters for short-term bearing capacity and drained strength parameters for long-term bearing capacity.

**Final Comments** One might conclude from the previous discussions that it is best to compact cohesive bearing soils at low water contents to maximize strength and minimize loading-induced settlement. Although dry cohesive soils are stronger and stiffer than wet (all other factors being the same), the potential for wetting-induced and drying-induced volume changes must also be considered, as will be discussed. Thus, a settlement analysis for a foundation bearing on a compacted cohesive soil must consider the potential for settlement or heave from loading, wetting, and drying throughout the design life of the structure.

### Soaked

In some instances it is highly likely that compacted cohesive soils will become wetter at some time during the design life of the structure founded on these soils. Wetting may occur from obvious sources such as precipitation (rainfall and snowmelt) and changes in regional or local groundwater conditions (rising of the ground-water table, diversion of runoff, and so on). Wetting may also result from less obvious sources, including broken or leaking water pipes, landscape irrigation, and clogged drainage systems. Therefore, it is nearly impossible to ensure that wetting will not occur in cohesive bearing soils, which prompts many engineers to estimate settlement and ultimate bearing capacity based on soaked compressibility and strength characteristics of the soil.

**Compressibility** Wetting of a compacted cohesive soil generally results in some volume change (swelling or collapse, as will be discussed), which must be considered in the overall settlement/heave analysis, and which also changes the compressibility and strength of the soil. The

**6.120** SOIL IMPROVEMENT AND STABILIZATION

changes in compressibility and strength depend on the prewetting moisture condition and the magnitude and sign of the wetting-induced volume change (if any). For example, a soil that swells when wetted becomes more compressible owing to both the reduction in suction and the increase in void ratio. The significant increase in one-dimensional compressibility caused by wetting a high-density ( $R_m = 90\%$ ), dry ( $S_r = 55\%$ ) compacted clayey sand is illustrated in Fig. 6A.88. After inundation at a very low applied stress ( $\sigma_v = 1 \text{ kPa} = 0.02 \text{ ks}$ ), the specimen swelled 14.4%, which changed the void ratio from 0.51 in the as-compacted condition ( $e_i$ ) to 0.66 at the beginning of the loading process ( $e_L$ ). In addition, the matric suction in the specimen was reduced by soaking from about 800 kPa (16.7 ks) to essentially zero. At an applied stress of 1600 kPa (33.4 ks), the soaked sample compressed 14.5%—about 7 times as much as the as-compacted sample (2.1%). Soaking the specimen eliminated the prestressing induced during compaction, as indicated by the essentially linear strain-log stress relationship for the soaked sample.

Cohesive soils compacted to high degrees of saturation will undergo little or no wetting-induced volume change and their compressibility will not be appreciably affected by soaking. This is illustrated in Fig. 6A.89 for a compacted clayey sand with  $S_r \approx S_{opt}$  that swelled only 0.4% after soaking. The compressibility of this soaked specimen did not differ significantly from that of the as-compacted specimen. In addition, the soaking had no noticeable effect on the compactive prestress.

Soaking can also induce a decrease in void ratio (collapse) in the soil. This decrease in void ratio tends to reduce the compressibility, but in most instances this reduction is more than offset by the increase in compressibility produced by the reduction in matric suction.

**Strength** The soaked strength of compacted cohesive soils depends on many factors, including the following:

1. Fabric (microfabric, minifabric, and macrofabric)
2. Method of compaction
3. Compaction water content
4. Soaked water content and degree of saturation
5. Volume change induced by the soaking

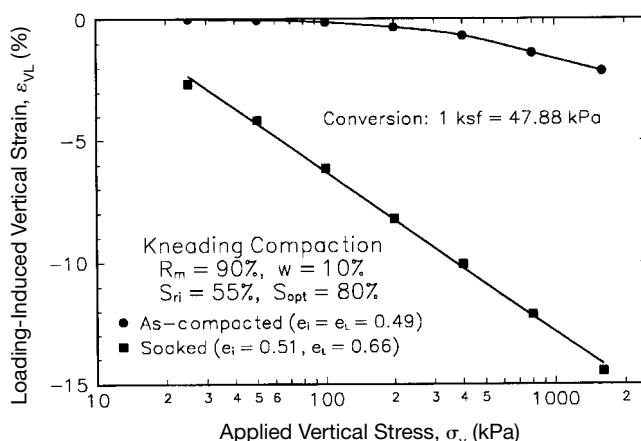


**FIGURE 6A.88** Effect of soaking on one-dimensional compressibility of dry compacted clayey sand (data from Lawton, 1986).

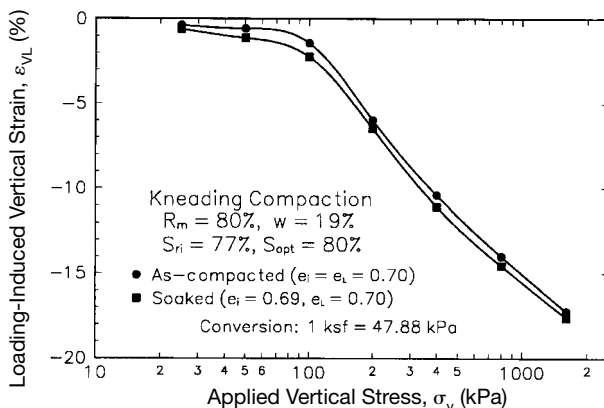


**FIGURE 6A.89** Influence of soaking on one-dimensional compressibility of wet compacted clayey sand (data from Lawton, 1986).

6. Dry density or void ratio after soaking

7. Magnitude and sign of the pore water pressures that develop during loading

Most of these factors are interdependent. Because these interrelationships are quite complicated, only general discussions will be given below. Further details can be found in Seed and Chan (1959b) and Yi (1991).

**Effect of fabric** The fabric of the soaked soil at the initiation of loading can have a substantial effect on the strength. It is generally assumed that the fabric of the soaked soil is essentially the same as that of the as-compacted soil, but some changes in fabric may occur because of soaking, and further study is needed of this issue. There is no doubt, however, that the soaked fabric depends to some extent on the as-compacted fabric.

The fabric affects the undrained strength of soaked soil primarily in terms of the developed pore pressures. The results from consolidated-undrained triaxial compression tests on two specimens of compacted silty clay are given in Fig. 6A.90. The two specimens were prepared by kneading compaction to different as-compacted states—one dry of optimum and one wet of optimum, but after soaking the specimens had the same composition ( $\gamma_d, w$ ). The dry-of-optimum specimen had an initially flocculated microfabric and developed a high strength at low strain ( $\approx 2\%$ ) and thereafter showed only a small increase in strength with additional deformation. The wet-of-optimum specimen had an initially dispersed microfabric, and at strains less than about 12.5%, appreciably larger pore water pressures were developed than in the dry-of-optimum specimen, with the result that the wet-of-optimum specimen was weaker. These differences in developed pore water pressures result from the different shapes of the pore spaces in the microfabric. The magnitude of developed pore water pressure in any void space is inversely related to the permeability of that void space, and the permeability of a void space depends to a great extent on its smallest dimension. Thus, for two void spaces with the same volume and identical loading conditions, greater pore water pressures will be induced in a void space with a long, narrow shape (dispersed microfabric) than in a more equidimensionally shaped void space (flocculated microfabric). At strains greater than 12.5%, the differences in pore water pressures were small and the strengths of the two specimens were nearly the same, suggesting that the microfabric in the zones of the failure planes for the two specimens were essentially the same (dispersed). The effective principal stress ratios for both specimens were nearly

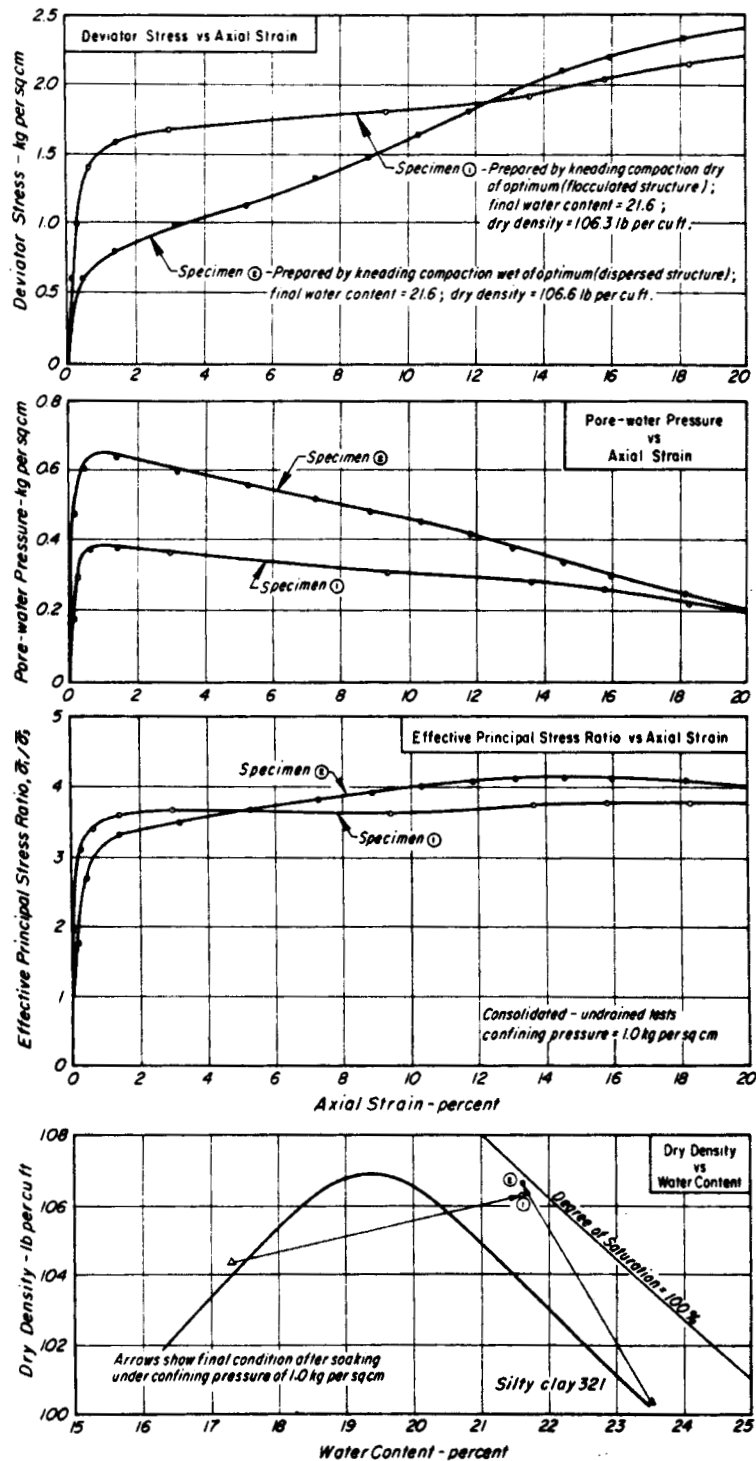


**FIGURE 6A.90** Effect of microfabric on pore water pressure and strength from triaxial consolidated-undrained tests on a silty clay (from Seed et al., 1960).

the same at all strains, suggesting that the effective stress strengths were similar for the two specimens so that the differences in total stress strengths (load-carrying capacity) were primarily the result of differences in developed pore water pressures.

Yi (1991) conducted a similar study on soils that collapsed when wetted. The results of consolidated-undrained simple shear tests conducted on specimens of a clayey sand that were compacted to two different as-compacted states and then soaked to the same  $\gamma_d$  and  $w$  are shown in Fig. 6A.91. The dry-of-optimum specimens collapsed on wetting, whereas the wet-of-optimum specimens underwent no volume change. The results clearly show that at all three vertical confining pressures, the dry-of-optimum specimens developed higher pore water pressures and were weaker than the wet-of-optimum specimens. Similar results were obtained for three other soils. These results cannot be explained in terms of flocculated versus dispersed microfabric and are opposite to those found by Seed and Chan (1959b) for the silty clay discussed above. It is not known if these differences in results are related to differences in types of soils, type of wetting-induced volume change (swelling versus collapse), or perhaps differences in sample preparation (although kneading compaction was used in both studies). Scanning electron micrographs of the dry-of-optimum clayey sand specimens showed that the effect of collapse on fabric was to reduce the size of the interclod pores without any apparent change to the microfabric. Unfortunately, no micrographs of the wet-of-optimum specimens were taken, so the characteristics of the fabric for these specimens are not known. Yi assumed both that the soaked fabrics of the wet- and dry-of-optimum specimens were similar, with the wet-of-optimum specimens containing larger interclod pores and therefore denser microfabric, and that the strengths of these specimens were governed by the density of their microfabric. The author believes that the soaked fabrics of the wet- and dry-of-optimum specimens were probably not as similar as assumed by Yi, so that the explanation for the differences in strength is probably quite complex and cannot be determined from the available information.

Clearly, fabric can play an important role in the soaked strength of compacted cohesive soils. However, with our present knowledge and the uncertainty regarding the relative importance of microfabric and minifabric, additional research is needed before a reasonable explanation can be given for the influence of fabric on soaked strength.

**Influence of wetting-induced volume change** The volume changes that occur from soaking a compacted cohesive soil can be summarized as (a) no change in volume, (b) an increase in volume (swelling), and (c) a decrease in volume (collapse). Compacted cohesive soils that undergo no volume change after soaking are a special case and may be of two types—nonexpansive soils that are soaked under a low surcharge pressure and expansive soils soaked under a surcharge pressure sufficiently high to prevent swelling.

The undrained strength of a compacted cohesive soil that has been soaked depends on the characteristics of the soil in the soaked condition—dry density, water content, and fabric. These soaked characteristics depend on the as-compacted characteristics of the soil ( $\gamma_d$ ,  $w$ , and fabric) as well as the stress state of the soil at the time of soaking, as discussed previously.

The influence of soaking at constant volume on the unconsolidated-undrained (UU) triaxial compressive strength at low strain ( $\epsilon_{VL} = 5\%$ ) of a silty clay prepared by kneading compaction is shown in Fig. 6A.92. At all densities and water contents, the soaked soil is weaker than the comparable as-compacted soil, with the differences decreasing with increasing compaction water content.

Isograms of triaxial UU triaxial compressive strength at low strain are shown in Fig. 6A.93 for kneading-compacted specimens of sandy clay soaked under two different surcharge loads. Under the low surcharge pressure (1 psi = 7 kPa), the soaked strength depended significantly on the compaction water content owing to the differences in swelling that occurred upon soaking. At lower water contents the soil swelled more than at higher water contents, and thus for the same as-compacted dry density, the dry density after soaking was less and the water content was more for the initially dryer soil. Thus, for the same dry density, the soaked strength increased significantly with increasing compaction water content. Note that this relationship is the opposite of that for as-compacted strength, which decreases with increasing compaction water content at the same dry density (see Fig. 6A.92).

## 6.124 SOIL IMPROVEMENT AND STABILIZATION

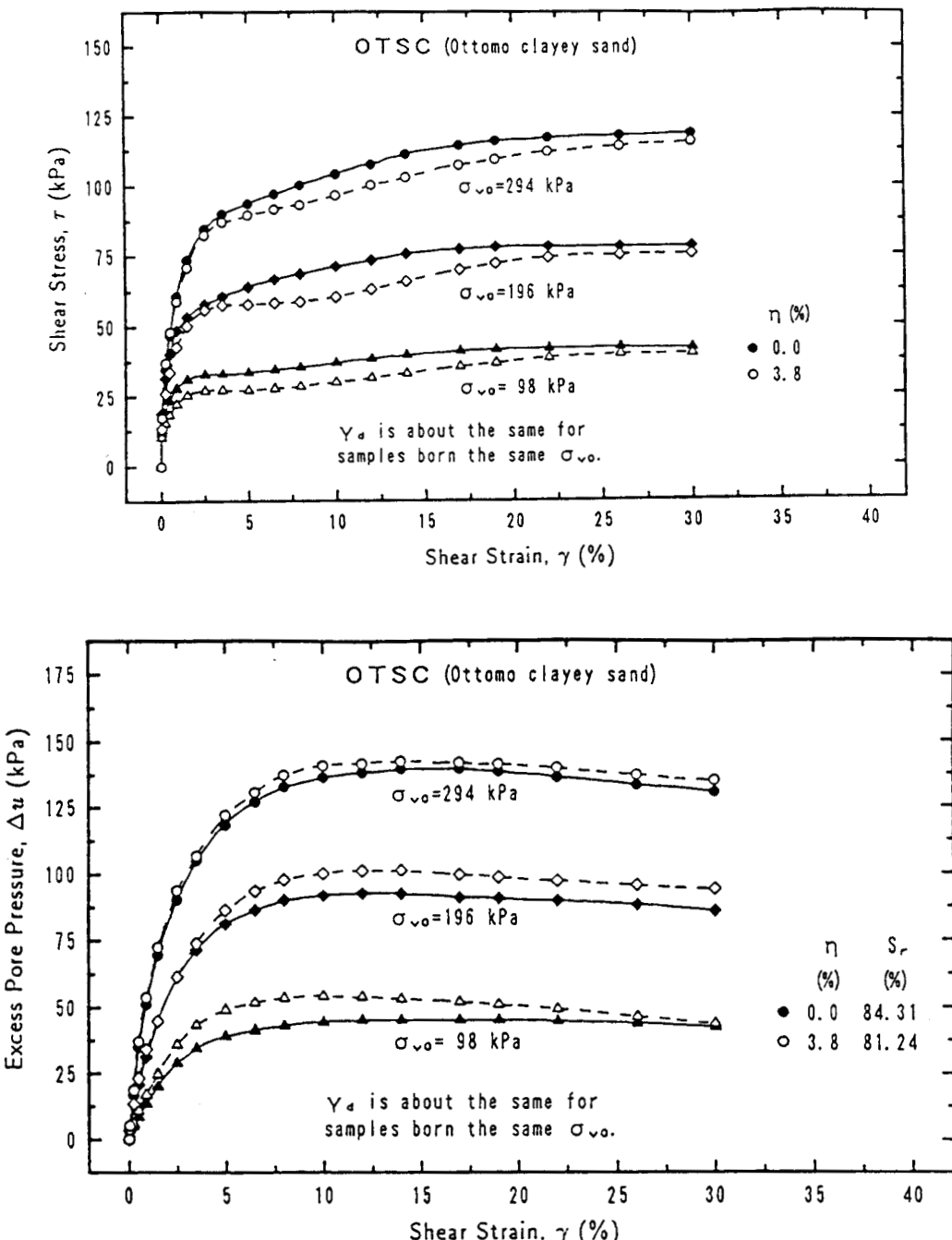
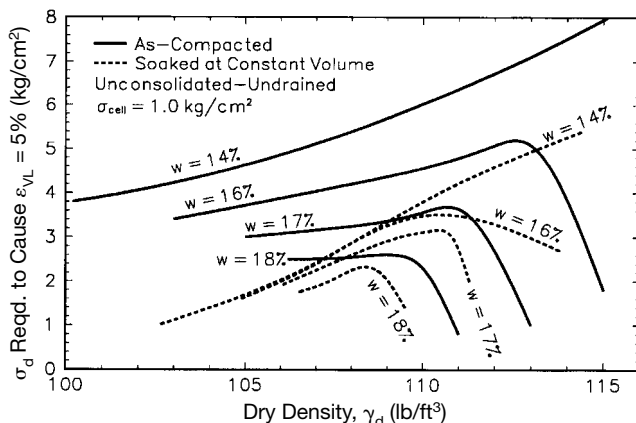


FIGURE 6A.91 Results from consolidated-undrained simple shear tests on specimens of a clayey sand which underwent different amounts of collapse (from Yi, 1991).



**FIGURE 6A.92** Influence of soaking on the triaxial compressive strength of kneading-compacted silty clay (data from Seed and Chan, 1959a,b).

The high-surcharge specimens underwent little swelling, and the corresponding soaked-strength isograms are nearly horizontal, indicating that the strength depended primarily on as-compacted density and was nearly independent of compaction water content. Dry of optimum ( $S_r < S_{opt}$ ) the strength at constant as-compacted dry density increases slightly with increasing compaction water content owing to slightly more swelling at the lower compaction water contents. Note, though, that the strength decreases slightly with increasing water content wet of optimum ( $S_r > S_{opt}$ ) because the microfabric became increasingly more dispersed but no swelling occurred.

There is no information available with regard to the influence of the magnitude of collapse on the soaked strength of compacted cohesive soils. For a given composition and fabric, increasing the

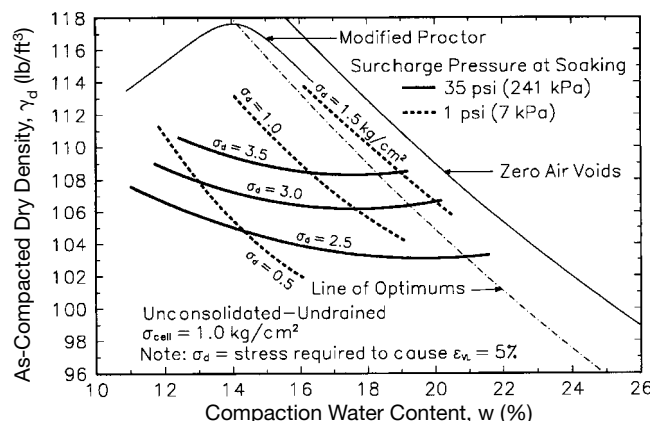


**FIGURE 6A.93** Influence of surcharge pressure at soaking on the triaxial compressive strength at low strain for kneading-compacted sandy clay (data from Seed and Chan, 1959a,b).

**6.126** SOIL IMPROVEMENT AND STABILIZATION

applied stresses causes greater wetting-induced collapse and thus increases the density of the soil, which likely increases the soaked strength of the soil. However, differences in magnitude of collapse may produce variations in fabric, which in turn may affect the soaked strength of the soil.

**Method of compaction** For a cohesive soil compacted to the same composition, varying the method of compaction may alter the soaked strength in two ways: (a) The as-compacted fabric (and hence the soaked fabric) may be different, and (b) the wetting-induced volume change may vary. As noted previously, flocculated microfabrics are stronger than dispersed microfabrics, so, other than very dry of optimum where compaction method has little effect on fabric, static compaction would be expected to produce a stronger soil than kneading compaction. However, the wetting-induced volume change also affects the soaked strength. Static compaction induces a higher swelling potential or a higher collapse potential in the soil than does kneading compaction, depending on the applied stress level (see discussion below). As discussed above, greater swelling reduces the soaked strength of the soil while greater collapse likely increases it. Thus, for conditions where swelling is likely to occur (highly expansive soils and low stresses), static compaction may result in greater or lesser soaked strength than kneading compaction depending on which mechanism controls. For nonexpansive soils or high surcharge pressures, either no volume change or collapse is likely to occur from wetting, and static compaction will probably produce a stronger soaked soil.

*Wetting-Induced Volume Changes.* *Swelling*, which is an increase in total volume of a soil upon wetting, and *collapse*, which is a decrease in total volume upon wetting, are considered separate and distinct phenomena by many engineers and researchers. Recent research has shown, however, that any unsaturated cohesive soil may either collapse, swell, or not change volume when wetted, depending on the condition of the soil at the time of wetting. Thus, swelling and collapse in unsaturated cohesive soils are associated aspects of the general phenomenon of wetting-induced volume changes.

The magnitude and sign of the volume change that occurs when an unsaturated cohesive soil is wetted are primarily related to changes in matric suction. As suction decreases during wetting, the change in pore water pressure is positive (the pore water pressure becomes less negative), which reduces both the effective stresses acting on the soil and the stiffness of the soil structure. The decrease in effective stress results in an increase in volume (swelling), whereas the reduction in stiffness produces a decrease in volume (collapse). The net change in volume may be positive, negative, or zero depending on the condition of the soil at the time of wetting.

The primary factors that affect the wetting-induced volume change in a compacted cohesive soil are as follows (Lawton et al., 1992, 1993):

1. Gradation of the soil and mineralogy of the clay particles
2. State of stress at the time of wetting
3. Void ratio or dry density at the time of wetting
4. Moisture condition at the time of wetting
5. Degree of wetting
6. Fabric of the soil at the time of wetting
7. Chemistry of the water that is introduced into the soil

*SOIL TYPE* The effect of clay content on the one-dimensional wetting-induced volume change of compacted silt-clay and sand-clay mixtures was studied by El Sohby and Rabbaa (1984), with the results shown in Fig. 6A.94. The clay was highly expansive, with calcium montmorillonite the predominant mineral (45% by weight). For any given soil type (same silt or sand and clay fraction), the net collapse increased or the net swelling decreased with increasing applied vertical stress. For the applied stress levels studied ( $\sigma_v = 400, 800$ , or  $1600$  kPa or  $8.4, 16.7$ , or  $33.4$  ksf), the specimens containing low clay fractions collapsed and those containing high clay fractions swelled. The magnitude of swelling at high clay fractions increased with increasing clay content. At low clay contents, the silt-clay collapsed more than the sand-clay; at moderate to high clay contents, the silt-clay col-

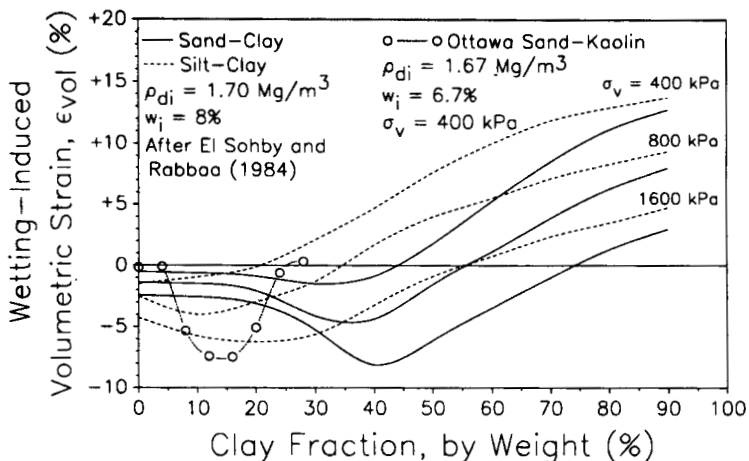


**FIGURE 6A.94** Influence of clay fraction on potential for wetting-induced volume change of clay-sand and clay-silt mixtures (from Lawton et al., 1992).

lapsed less or swelled more than the sandy clay. The maximum collapse occurred at clay contents of 10 to 20% for the silt-clay and 30 to 40% for the sand-clay.

A similar study was conducted by the author to determine the influence of clay content on the wetting-induced volume change of mixtures of uniform sand and slightly expansive clay (kaolin). The results from this study are also shown in Fig. 6A.94 and can be summarized as follows:

1. At very low clay contents (<5%), little or no wetting-induced volume change occurred.
2. At clay contents from between 5 and 25%, collapse occurred, reaching a maximum between 12 and 16%.
3. At clay contents greater than 25%, a small amount of swelling occurred.

The effects of soil type on the potential for wetting-induced volume change in cohesive soils can be summarized as follows (Lawton et al., 1992):

1. *Very low clay contents.* The clay acts as a binder between silt and sand particles. When wetted, the clay binders soften and lubricate the intergranular contacts, thereby facilitating collapse at high applied stresses. If the clay is highly expansive, there may be some swelling at low pressures and high densities, but the magnitude will likely be small because the clay content is too low for the soil to have appreciable swelling. Silts tend to collapse more than sands.
2. *Low to moderate clay contents.* With increasing clay content, more clods are present in the borrow material, and for the compaction water contents at which significant collapse and swelling potentials exist, the as-compacted soil retains to some extent the identities of the individual clods. Upon wetting, the clods swell but also soften and distort under the applied load, so that the net volume change depends on the stress state and the expansiveness of the clay minerals. Swelling tends to occur at low stresses and for expansive clay minerals, and collapse tends to occur at high stresses and for nonexpansive clay minerals.
3. *Moderate to high clay contents.* Although some collapse occurs during wetting, swelling generally predominates over collapse, especially for highly expansive clay minerals and low stresses. For highly expansive clay minerals and high clay contents, swelling can occur at overburden pressures as great as 1600 kPa (33.4 ksf).

**6.128** SOIL IMPROVEMENT AND STABILIZATION

*DENSITY AND MOISTURE CONDITION* The effects of prewetting density and prewetting moisture condition on the one-dimensional wetting-induced volume change of a compacted clayey sand subjected to an applied total vertical stress ( $\sigma_v$ ) of 200 kPa (4.2 ksf) are shown in Fig. 6A.95. The prewetting dry density is represented as a percentage of modified Proctor maximum dry density,  $R_{mw}$ , and the prewetting moisture condition is expressed as degree of saturation,  $S_{rw}$ . The values of wetting-induced volumetric strain,  $\varepsilon_{vw}$ , shown in Fig. 6A.95 are for complete inundation with water and therefore represent the maximum potential for wetting-induced volume change. For the same  $S_{rw}$ ,  $\varepsilon_{vw}$  is more positive (greater swelling) or less negative (less collapse) as  $R_{mw}$  increases because the stiffness of the soil increases with increasing dry density. Thus, for the same moisture condition and total vertical stress, the swelling resulting from the reduction in effective stresses would be the same, although the collapse resulting from the reduction in stiffness would be less, with a net increase in swelling or decrease in collapse. For the same  $R_{mw}$ , the matric suction in the soil decreases with increasing moisture, with the result that the net swelling or net collapse decreases as  $S_{rw}$  increases up to the value of  $S_{rw}$  at which the suction is zero (typically in the range of 70 to 90%). Therefore, for the same dry density and total vertical stress, the net wetting-induced volume change—whether positive or negative—will be less for an initially wetter soil because the magnitude of the dominating mechanism—reduction in effective stress for net swelling or reduction in stiffness for net collapse—will be less for lower values of prewetting suction.

For the same prewetting moisture condition ( $S_{rw}$ ), an increase in dry density either reduces the collapse potential or increases the swelling potential. Collapse in most compacted cohesive soils seems

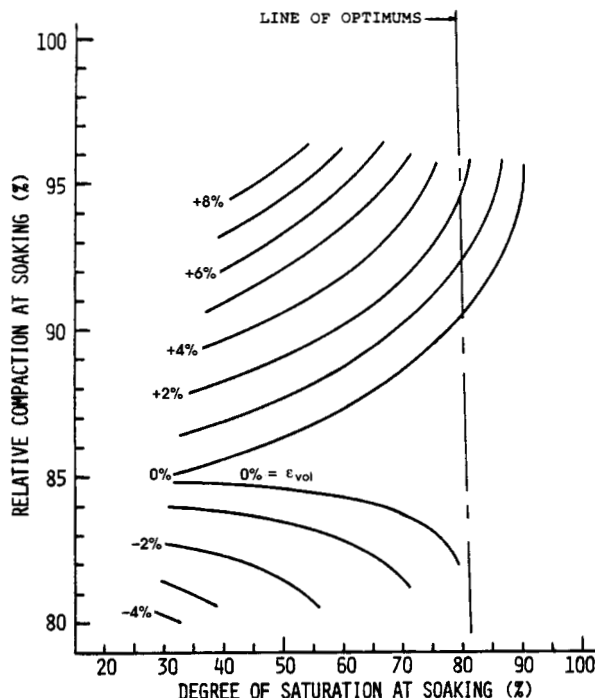


**FIGURE 6A.95** Isograms of one-dimensional wetting-induced vertical strain for an applied vertical stress of 200 kPa (4.2 ksf) as a function of prewetting relative compaction and prewetting degree of saturation (from Lawton, 1986).

to occur primarily as a reduction in volume of the interclod voids (Yi, 1991). In a denser soil, the interclod voids are smaller. After wetting, the soil will come to an equilibrium density based on the state of stress. Therefore, less reduction in volume will occur for a denser soil with the same prewetting moisture condition. Swelling is a complex phenomenon that cannot be easily characterized. A greatly simplified explanation for the influence of density on swelling potential can be given as follows:

1. For a given saturated cohesive soil with the same soil fabric and water chemistry, there is a unique relationship between void ratio and state of stress.
2. For the same fabric and moisture condition of the prewetting soil, when soaked the soil will come to an equilibrium void ratio that depends on the state of stress acting on the soil but is independent of the prewetting density. Therefore, the increase in void ratio caused by soaking will be greater for an initially denser soil.

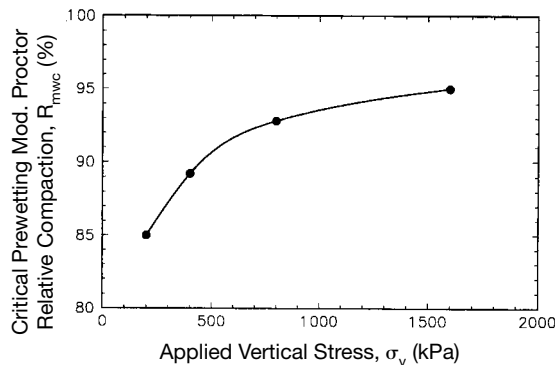
The wetting-induced volume change in compacted cohesive soils can also be zero. In compacted cohesive soils, this can occur in three ways: (a) The swelling and collapsing components are equal and therefore offset each other; (b) the prewetting suction in the soil is small enough that no significant reduction in effective stress or stiffness will occur upon wetting; or (c) cementation of particles is strong enough to preclude any wetting-induced volume change. Cementation of particles may exist in clods prior to compaction and may survive the compaction process to some extent. Cementation may also occur naturally with time after compaction or may be intentionally induced in the soil by chemical stabilization prior to compaction. These latter two possibilities are discussed in more detail in subsequent sections.

For a cohesive soil loaded and wetted shortly after compaction (before any significant post-compaction cementation occurs), there is a range of prewetting dry densities and degrees of saturation for which there is no wetting-induced volume change, as illustrated by the zone in Fig. 6A.95 bounded by the two isograms for  $\varepsilon_{vw} = 0$ . No wetting-induced volume change occurs at low degrees of saturation because the swelling and collapsing components offset each other, and in Fig. 6A.95 this occurs at  $R_{mw} \approx 85\%$ . At degrees of saturation equal to or greater than a critical value ( $S_{rc}$ ), the prewetting suction is small, and  $\varepsilon_{vw} \approx 0$ . This phenomenon is indicated in Fig. 6A.95 by the increase in distance between the two isograms for  $\varepsilon_{vw} = 0$  at higher values of  $S_{rw}$ .  $S_{rc}$  varies as a function of soil type, prewetting dry density, and prewetting state of stress. For a given soil, the influence of density and state of stress is small, and  $S_{rc}$  can be approximated as  $S_{opt}$  obtained from Proctor tests or can be determined more accurately by conducting a series of one-dimensional wetting-induced volume change tests.

Another important characteristic illustrated by the isograms of Fig. 6A.95 is that for any soil and any value of  $\sigma_v$ , there is a range in values of  $R_{mw}$  for which  $\varepsilon_{vw} = 0$  regardless of moisture condition. The value of  $R_{mw}$  at the middle of this range is called the *critical prewetting relative compaction* ( $R_{mwc}$ ), and for a given soil  $R_{mwc}$  increases as  $\sigma_v$  increases (Fig. 6A.96).

*STATE OF STRESS* The effect of increased stress for the same prewetting density, moisture condition, and fabric is to reduce the swelling potential or increase the collapse potential. This relationship is illustrated in Fig. 6A.97, where isograms of one-dimensional wetting-induced strain are given for a compacted clayey sand at two levels of overburden pressure. At each point in  $R_{mw} - S_{rw}$  space,  $\varepsilon$  is less positive or more negative at  $\sigma_v = 800$  kPa than at  $\sigma_v = 400$  kPa.

For three-dimensional strain conditions, the total wetting-induced volume change is uniquely related to the mean normal total stress (Lawton et al. 1991) and thus is independent of the principal stress ratio, as illustrated in Fig. 6A.98 for wetting tests on kneading-compacted specimens of a compacted clayey sand conducted under axisymmetric loading conditions. However, the individual components of wetting-induced volume change depend significantly on the stress ratios. For a given magnitude of stress in a direction of interest, the swelling increases or the collapse decreases in that direction as the perpendicular stresses increase. This concept is illustrated in Fig. 6A.99, where vertical and radial wetting-induced strains are plotted as a function of vertical stress. An increase in lateral stress ratio ( $\sigma_r/\sigma_v$ ) for any given value of vertical stress results in an increase in vertical strain (increase in swelling or decrease in collapse) and a decrease in radial strain (decrease in swelling or increase in collapse).

**6.130** SOIL IMPROVEMENT AND STABILIZATION

**FIGURE 6A.96** Effect of vertical stress on critical prewetting density (data from Lawton, 1986).

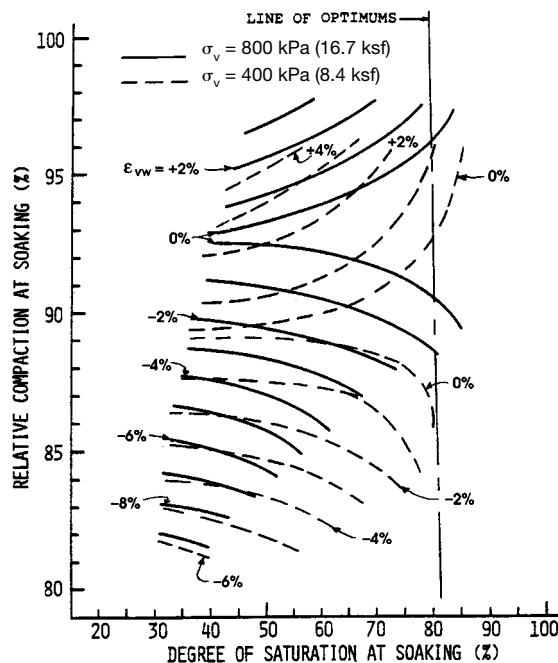


**FIGURE 6A.97** Influence of applied vertical stress on iso-grams of wetting-induced volume change as a function of prewetting relative compaction and prewetting degree of saturation for a compacted clayey sand (data from Lawton, 1986).

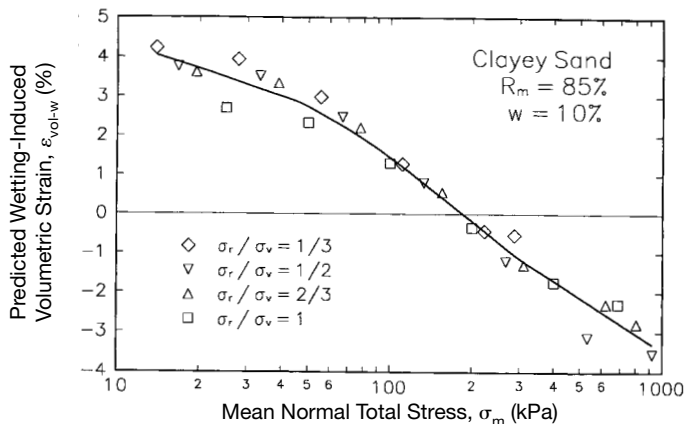


**FIGURE 6A.98** Predicted wetting-induced volumetric strain as a function mean normal total stress from double triaxial tests on kneading-compacted specimens of a clayey sand (from Lawton et al., 1991).

Results from wetting tests on oedometer specimens compacted at the same water content to the same density using the same method of compaction are also shown in Fig. 6A.99(a) for comparison with the triaxial results. This comparison clearly indicates that the one-dimensional wetting tests may not give reliable predictions for situations where three-dimensional strains occur. It is also apparent that for the range of lateral stress ratios studied ( $\sigma_r / \sigma_v = 1/3$  to 1), collapse was affected more by the stress ratio than was swelling. In addition, the results appear to indicate that the oedometer tests significantly overestimate the swelling for three-dimensional volume change. However, the process of application and removal of loads during compaction can result in significant lateral earth pressures, which can be many times greater than the theoretical at-rest values and may approach limiting passive earth pressure values (Duncan and Seed, 1986). Thus, the values of  $\sigma_r / \sigma_v$  for as-compacted soils may be much greater than the maximum value of 1.0 shown in Fig. 6A.99. In addition, for a constant vertical stress, the horizontal stresses may vary substantially as the soil undergoes wetting-induced volume change. Preliminary research indicates that the horizontal stress in a compacted soil increases with increasing vertical collapse and decreases with increasing vertical swelling, that the limiting passive horizontal pressure may be approached for large vertical collapse, and that limiting active horizontal pressure may be achieved for large vertical swelling (Lawton et al., 1991). Thus, laboratory tests in which  $\sigma_r / \sigma_v$  is kept constant do not accurately model the stress path of soils in the field that undergo three-dimensional wetting-induced volume change, and additional research is needed to clarify the interdependence of horizontal stress and wetting-induced volume change of soil.

*METHOD OF COMPACTION* The influence of compaction method on the one-dimensional wetting-induced volume change of a clayey sand is shown in Fig. 6A.100 for three different as-compacted compositions and can be summarized as follows:

1. For the same water content, density, and state of stress, the statically compacted specimens swelled more than the kneading-compacted specimens.
2. Within the lower range of stresses at which collapse occurred, the magnitude of collapse was less for the statically compacted specimens than for the kneading-compacted specimens.
3. At stresses near or greater than the stresses at which maximum collapse would occur for any given composition, the statically compacted specimens collapsed more than the kneading-compact-

## 6.132 SOIL IMPROVEMENT AND STABILIZATION

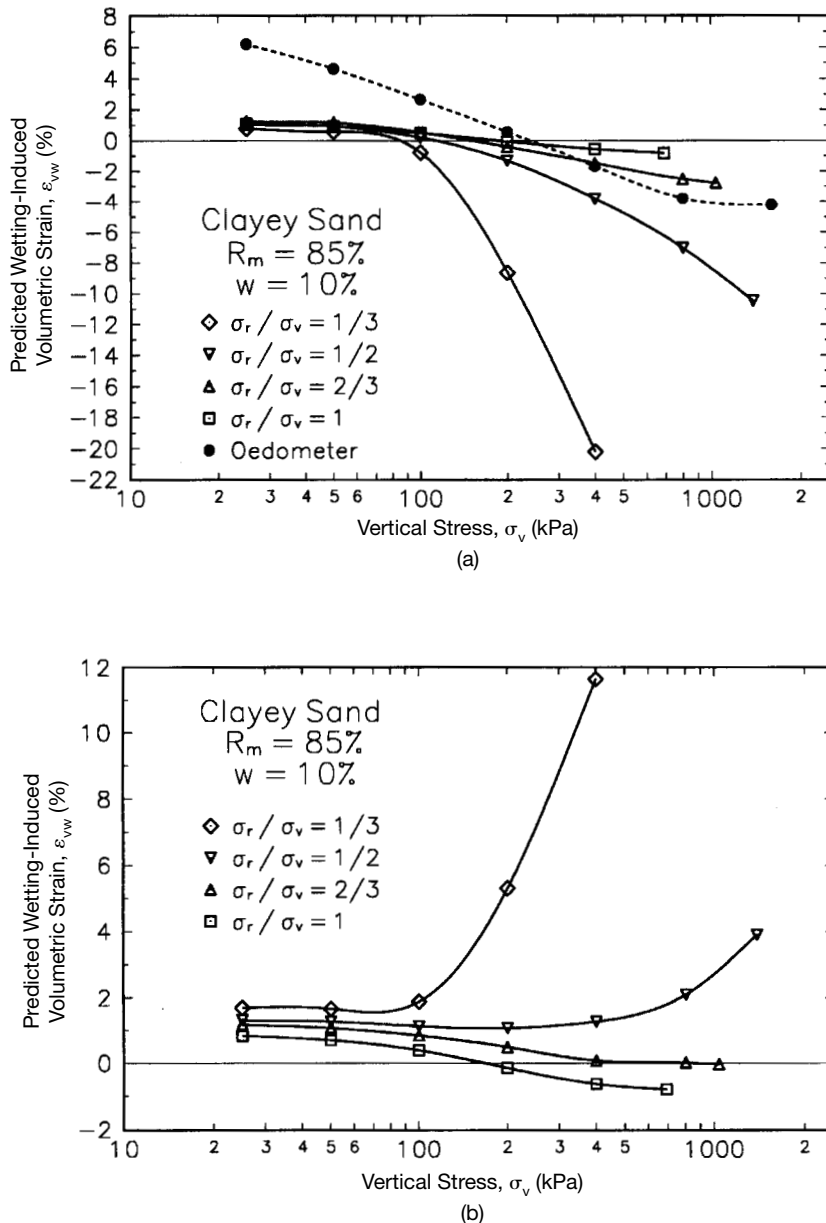


**FIGURE 6A.99** Comparison of predicted wetting-induced (a) vertical strain, and (b) radial strain versus vertical stress curves from double triaxial and double oedometer tests on kneading-compacted specimens of a clayey sand (from Lawton et al., 1991).

ed specimens. This trend is not observed for  $R_m = 90\%$  and  $w = 10\%$  because the maximum stress on the specimens was less than the stress at which maximum collapse would occur.

Statically compacted cohesive soil can be either more or less collapsible than the comparable kneading-compacted soil because static compaction tends to produce a fabric that is susceptible to both more swelling and more collapse. Recall from previous discussions that both swelling and collapse occur when an expansive soil is wetted. At low stresses, the swelling component clearly dominates, and swelling is greater for static compaction than for kneading compaction. At high stresses, the collapsing component dominates and the statically compacted soil collapses more than the kneading-compacted soil. There is a transition zone for moderate stresses wherein the net wetting-induced volume change is negative (collapse) but the tendency for greater swelling in the statically-compact ed soil results in less collapse than for the kneading-compacted soil.

Although method of compaction can have a measurable effect on  $\varepsilon_{vw}$ , it is apparent from the results in Fig. 6A.100 that  $w$  and  $\sigma_v$  influence  $\varepsilon_{vw}$  to a much greater degree than method of compaction. To illustrate this point, examples of changes in  $\varepsilon_{vw}$  produced by changes in  $w$ ,  $\sigma_v$ ,  $R_m$ , and method of compaction using  $\varepsilon_{vw} = +8.6\%$  (static compaction,  $R_m = 90\%$ ,  $w = 10\%$ ,  $\sigma_v = 25$  kPa) as the base are as follows:

Change	$\varepsilon_{vw}$ , %	$\Delta \varepsilon_{vw}/\varepsilon_{vw\text{-base}}$ , %
Increase $w$ to 16%	+1.4	-84
Increase $\sigma_v$ to 200 kPa	+3.1	-64
Decrease $R_m$ to 80%	+4.4	-49
Change to kneading compaction	+7.0	-19

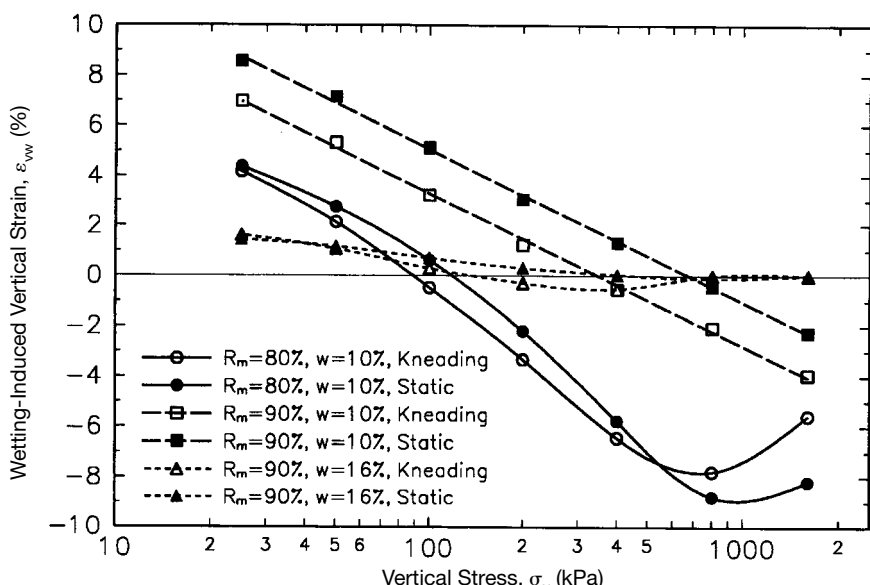


**FIGURE 6A.100** Influence of compaction method on one-dimensional wetting-induced strain for a clayey sand (data from Lawton, 1986).

**6.134** SOIL IMPROVEMENT AND STABILIZATION

This discussion is not meant to imply that method of compaction is unimportant; rather that with respect to wetting-induced volume change in cohesive soils, it is a relatively minor factor compared to  $w$  and  $\sigma_v$ . In addition, it should be borne in mind that specimens which will be tested in the laboratory should always be prepared with a method of compaction that simulates as closely as possible the method of compaction to be used in the field compaction process.

*DEGREE OF WETTING* The degree of wetting has a substantial influence on the wetting-induced volume change; that is, the results of wetting tests in which the specimen is inundated with water represent the maximum wetting-induced volume change for the conditions under which the specimen was tested. Partial wetting reduces the matric suction somewhat but to a lesser degree than full wetting. Thus, the magnitude of wetting-induced volume change, which is significantly influenced by the changes in suction, will be less for partial wetting than for full wetting. This is illustrated in Fig. 6A.101 for collapse of three naturally deposited soils. Note that the collapse for the three soils shown in Fig. 6A.101 is essentially completed at degrees of saturation less than 100%, typically about 80%. Similar trends have been noted by the author for the wetting-induced volume change (both collapse and swelling) of compacted cohesive soils. In general, little or no wetting-induced volume change occurs in compacted cohesive soils for additional wetting above  $S_{opt}$ .

*Oversize particles* When tests are conducted in the laboratory to estimate the potential for wetting-induced volume changes in field-compacted soils, the specimens used for testing are generally small, and the maximum particle size that can be used in a specimen is limited to approximately one-sixth the least dimension of the specimen. In this context, the term *oversize* refers to sizes of particles that are larger than the maximum size that can be used in a specimen for any particular test, and the maximum size will therefore vary depending on the test being performed and the size of the sample being tested. In general, the oversize particles are gravel size and larger. As with other types of tests, the results from laboratory wetting-induced volume change tests should be corrected to account for the effects of the oversize particles that are present in the field-compacted soil but not in the specimens tested in the laboratory.

A common method of correcting for the lack of oversize particles in laboratory wetting tests is based on the following two assumptions:

1. The oversize particles are inert and therefore do not change volume when wetted.
2. The presence of the oversize particles in the borrow material during field compaction does not influence the potential for wetting-induced volume change within the matrix soil (the soil exclusive of the oversize particles).

With these two assumptions, the results from laboratory tests on specimens prepared at the same compaction water content as the field matrix soil to the same dry density as the field matrix soil us-

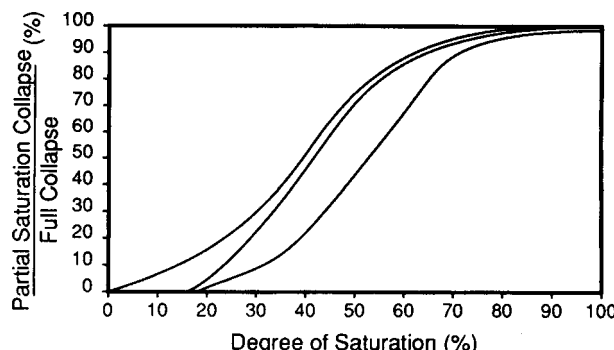


**FIGURE 6A.101** Partial collapse curves for three collapsible silts (from Walsh et al., 1993).

ing the same (or similar) method of compaction and loaded to the same state of stress can be used to predict the potential for wetting-induced volume change of the field-compacted soil. The dry density and water content of the field matrix soil ( $\gamma_{dm}$  and  $w_m$ ) can be calculated from the following equations, which are derived from phase relations:

$$\gamma_{dm} = \frac{(1 - P_{ow}) \cdot G_{so} \cdot \gamma_w \cdot \gamma_d}{G_{so} \cdot \gamma_w - P_{ow} \cdot \gamma_d(1 + G_{so} \cdot w_o)} \quad (6A.37)$$

$$w_m = \frac{w - w_o \cdot P_{ow}}{1 - P_{ow}} \quad (6A.38)$$

where  $w$  = water content of the field-compacted soil

$\gamma_d$  = dry density of the field-compacted soil

$P_{ow}$  = fraction of the soil that is oversized particles, by dry weight, expressed as a decimal

$G_{so}$  = specific gravity of the oversize particle solids

$w_o$  = water content of the oversize particle fraction

$\gamma_w$  = density of water

$w_o$  can be estimated by removing the oversize particles from a sample of the field-compacted soil and scraping the surfaces of the oversize particles to remove any cohesive material that is adhered to them. This can be a cumbersome task, and a value for  $w_o$  is usually estimated in the range of 0.5 to 2%. The following example illustrates the calculation of  $\gamma_{dm}$  and  $w_m$  for the preparation of laboratory specimens for wetting tests (after Noorany and Stanley, 1994): Given that  $w = 11.7\%$ ,  $\gamma_d = 112.1$  pcf (17.61 kN/m<sup>3</sup>),  $P_{ow} = 15\%$ ,  $G_{so} = 2.66$ , and  $w_{os}$  assumed to be 1%, calculate values of  $\gamma_{dm}$  and  $w_m$  for the field-compacted soil

$$\gamma_{dm} = \frac{(1 - 0.15)(2.66)(62.43)(112.1)}{(2.66)(62.43) - (0.15)(112.1)[1 + (2.66)(0.01)]} = 106 \text{ pcf} \left( 16.7 \frac{\text{kN}}{\text{m}^3} \right)$$

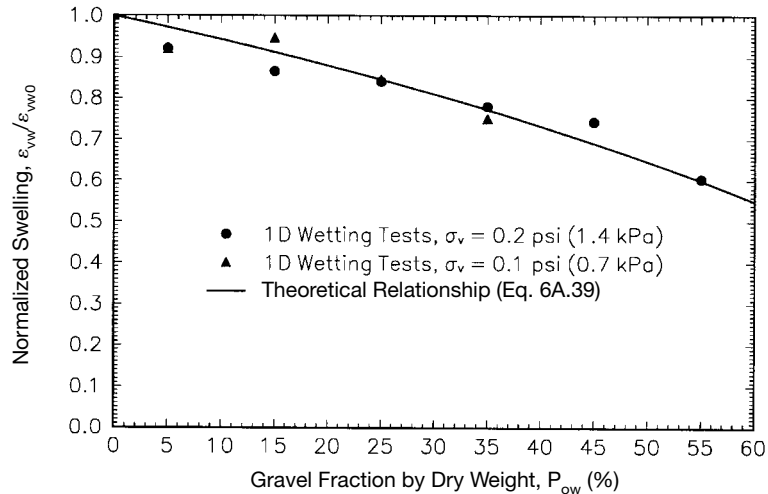
$$w_m = \frac{0.117 - (0.01)(0.15)}{1 - 0.15} \cdot 100 = 13.6\%$$

Some preliminary research has been conducted to determine the validity of this method for predicting wetting-induced volume change of field-compacted soil. Day (1991) studied the effect of gravel content on the magnitude of one-dimensional swelling of specimens with an expansive silty clay matrix. The wetting tests were conducted at low stresses— $\sigma_v = 0.1$  to 0.2 psi (0.7 to 1.4 kPa)—and swelling occurred in all tests. The results from these tests are given in Fig. 6A.102 in the form of the wetting-induced strain for the specimens containing gravel normalized with respect to the wetting-induced strain for the comparable specimen with no gravel at the same applied stress ( $\varepsilon_{vw}/\varepsilon_{vw0}$ ). Also shown in Fig. 6A.102 is the theoretical relationship for  $\varepsilon_{vw}/\varepsilon_{vw0}$  obtained from the following equation, which was derived from the same assumptions discussed above except that the gravel was assumed to be dry:

$$\frac{\varepsilon_{vw}}{\varepsilon_{vw0}} = \frac{(1 - P_{ow}) \cdot G_{so} \cdot \gamma_w}{(1 - P_{ow}) \cdot G_{so} \cdot \gamma_w + P_{ow} \cdot \gamma_{dm}} \quad (6A.39)$$

A comparison of the experimental and theoretical results suggests that this method provides a reasonable estimate for predicting the one-dimensional swelling potential of compacted cohesive soils.

A similar study was conducted by the author and his associates (Larson et al., 1993) with regard to the influence of oversize particles on the one-dimensional collapse of compacted clayey sands.

**6.136** SOIL IMPROVEMENT AND STABILIZATION

**FIGURE 6A.102** Effect of gravel content on one-dimensional swelling of a compacted silty clay (modified from Day, 1991).

Experimental values of  $\varepsilon_{vw} / \varepsilon_{vw0}$  from this study are plotted in Fig. 6A.103 as a function of percentage of oversize particles by volume ( $P_{ov}$ ). The experimental results are compared with the following theoretical equation, which is equivalent to Eq. (6A.39) except that  $\varepsilon_{vw} / \varepsilon_{vw0}$  is given in terms of  $P_{ov}$  rather than  $P_{ow}$ :

$$\frac{\varepsilon_{vw}}{\varepsilon_{vw0}} = 1 - P_{ov} \quad (6A.40)$$

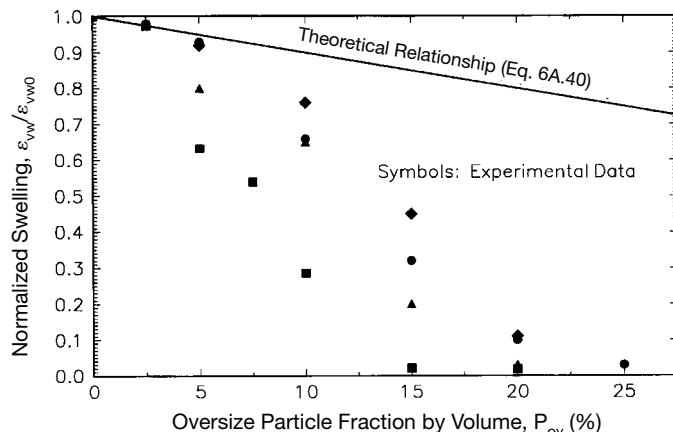


**FIGURE 6A.103** Influence of oversize particles on the collapse of compacted clayey sands (from Larson et al., 1993).

For the soils and conditions studied, the theoretical relationship is valid only for small oversize fractions ( $P_{ov} \approx 2.5$  to 5%;  $P_{ow} \approx 4$  to 8%), thus indicating that at higher contents of oversize particles, the presence of the oversize particles changes the fabric of the matrix soil, the manner in which collapse occurs, or both. The magnitudes of collapse for the five specimens with  $P_{ov} \geq 20\%$  ( $P_{ow} \geq 28\%$ ) were less than 11% of the values for the comparable specimens without any oversize particles.

Why this method of correcting for oversize particles apparently works for swelling but not for collapse is not well understood. We know that the oversize particles affect the fabric of the as-compacted soil (e.g., Siddiqi et al., 1987; Fragaszy et al., 1990). In soils with  $P_{ow}$  less than about 40%, the oversize particles "float" in the matrix soil, as shown in Fig. 6A.104; therefore, there is little or no interaction between oversize particles, and the behavior of the soil is controlled by the matrix soil. Soils with the same overall matrix density and water content but varying amounts of oversize particles will have different fabrics, with the matrix soil adjacent to the surfaces of the oversize particles (near-field matrix) having higher void ratios than the matrix soil that is distant from the oversize particles (far-field matrix soil). For conditions where net swelling occurs, the amount of swelling in the near and far-field matrices is different, but the overall magnitude of swelling for the soil is about the same. Because the oversize particles move farther apart as the swelling occurs, they do not interact, and their presence does not appreciably affect the swelling process. The influence of the oversize particles on the collapse process is less well understood. For the results shown in Fig. 6A.103, as little as 5% oversize particles (by volume) decreased the collapse by as much as 37%. At this low-oversize particle content, appreciable interaction among the oversize particles is unlikely, so the reduction in collapse must be primarily related to changes in fabric. Apparently little additional collapse occurs within the looser near-field matrix compared to the soil without any oversize particles, and collapse within the denser far-field matrix is substantially reduced. Some of the reduction may occur from the oversize particles bridging the near-field matrix zones that underlie the particles so that even if collapse occurs in these areas, it may not decrease the total volume of the soil.

*TIME RATE OF WETTING-INDUCED VOLUME CHANGE* The time rate of one-dimensional wetting-induced volume change for two specimens of a clayey sand with the same as-compacted condition but loaded to a low and a high vertical stress and then soaked are shown in Fig. 6A.105. The specimen loaded to  $\sigma_v = 1$  kPa swelled, and the specimen loaded to  $\sigma_v = 400$  kPa collapsed. When plotted versus the log of time, the wetting-induced strain curves are similar in shape to those for loading-induced strain of saturated fine-grained soils. In Fig. 6A.105, three distinct regions of wetting-in-

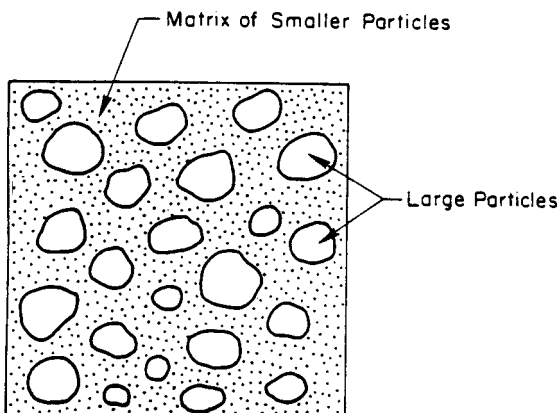


**FIGURE 6A.104** Schematic representation of large particles floating in a matrix of smaller particles (from Siddiqi et al., 1987).

## 6.138 SOIL IMPROVEMENT AND STABILIZATION

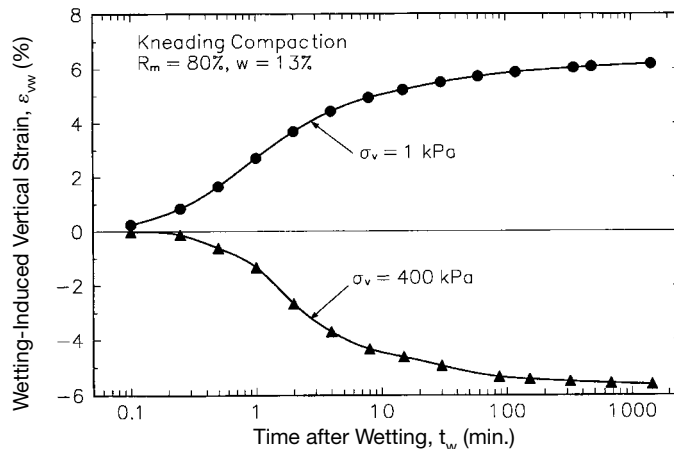


**FIGURE 6A.105** Time rate of one-dimensional wetting-induced volume change for compacted clayey sand (data from Lawton, 1986).

duced strain are evident. Each curve is initially flat as the water flows through the porous stones and enters the specimen. As water infiltrates the specimen, the majority of the wetting-induced strain occurs and the curve is relatively steep. After the matric suction in the specimen is eliminated, the wetting-induced strain is nearly complete, and the curve again becomes flat. At some time after wetting, the effective stress in the specimen becomes constant, but secondary compression will continue to occur. This region of secondary compression is apparent in the specimen that collapsed but not in the specimen that swelled because the magnitude of the secondary compression for the low applied stress level is too small to be measured. Eventually, the secondary compression will become negative.

Wetting-induced volume changes occur quickly in oedometer specimens inundated in the laboratory, usually within a few hours or less, which suggests that the wetting-induced volume change at any location in a field-compacted soil takes place within a few hours of sustained wetting (Lawton et al., 1992). Thus, the time required for complete wetting-induced volume change to occur in a field-compacted soil depends on (a) the method by which wetting occurs, and (b) the rate of water infiltration, which is a function of the permeability of the soil.

*CONTROL OF WETTING-INDUCED VOLUME CHANGE* The potential for wetting-induced volume change can be maintained within acceptable limits (a) before compaction by changing the engineering properties of the borrow material, (b) during design and construction by properly written compaction specifications and adequate supervision and inspection of the compaction process, or (c) after the compaction process by preventing water from infiltrating the soil or by modifying the properties of the soil. Preventing the infiltration of water into a compacted soil over a long period is nearly impossible and is not a viable alternative. Modifying the properties of the soil after compaction is generally difficult and expensive. Thus, the preferred alternatives are a and b, and they will be discussed in detail below.

From the data shown in Fig. 6A.97, there are two ways in which the potential for wetting-induced volume changes in a fill consisting of expansive compacted soil can be theoretically eliminated or substantially reduced during the compaction process without modifying the borrow soil: (a) by compacting the soil to a degree of saturation greater than the optimum saturation or (b) by compacting the soil at any depth within the fill to a dry density corresponding to the appropriate critical relative compaction based on the anticipated value of  $\sigma'_v$  at that level in the fill. However, both methods have practical limitations that may preclude their use on any project. If the borrow materials are

highly variable—and they usually are on large fills—determining appropriate values of  $S_{rwc}$  and  $R_{mwc}$  for the different materials would be difficult or very expensive. In addition, the quality control procedures required to ensure that the compacted soil has the desired properties are much more extensive and stringent than typically used for most projects. Some potential drawbacks to compacting to a high degree of saturation include:

1. The degree of saturation changes from the as-compacted condition owing to compression caused by placement of additional fill or structures built on or within the fill. However, compression causes an increase in  $S_r$ , so that a fill constructed with  $S_r \geq S_{rwc}$  will meet the requirements as long as the soil does not dry out so much that  $S_r$  drops below  $S_{rwc}$ .

2. Postcompaction wetting or drying of the soil may occur, especially for shallow depths along the exposed surfaces of the fill. Continuous or intermittent wetting wherein the moisture content increases gradually over a long period constitutes part of the wetting process and will not result in any significant volume change if the as-compacted soil is properly compacted ( $S_r \geq S_{rwc}$ ). Cyclic wetting and drying can be troublesome, especially near the top of the fill, where the stress levels are low and cyclic swelling/shrinkage may occur. Swelling and shrinkage are primarily elastic phenomena and will continue to occur so long as the wetting/drying cycles occur, although recent research suggests that the magnitude of the swelling and shrinkage may decrease somewhat for the first few cycles and then remain constant thereafter. Wetting-drying cycles at depths within the fill where the stress levels are high enough to result in collapse are unusual, but these cycles may occur near the bottom of moderately deep to deep embankments along the exposed surfaces. Wetting-drying cycles are generally less of a problem for collapsible conditions than for swelling conditions because collapse is primarily plastic, and any shrinkage caused by drying is small and decreases the potential for further collapse. Drying of the soil produces an increase in density owing to shrinkage and an increase in suction, which can be a major problem at low stress levels in an expansive fill because both phenomena increase the swelling potential. At high stress levels, the increase in density decreases the collapse potential, but this decrease is usually more than offset by the increase in collapse potential resulting from the reduction in suction. Thus, post-compaction drying at all depths within a compacted cohesive soil can be important, because it increases either the collapse potential or the swelling potential depending on the stress level. Postcompaction drying commonly occurs in embankments located in regions with semiarid and arid climates.

3. Compacted cohesive soils with high degrees of saturation have more time-dependent compression than the same soil at low degrees of saturation (for the same stress level and dry density), as discussed previously. For  $S_r > S_{opt}$ , the air phase is probably occluded and the time-dependent compression behavior may be similar to that for the same soil in the saturated condition.

Swelling of the bearing soils for a foundation can be eliminated by ensuring that the applied bearing stress from the foundation is greater than the *swelling pressure* of the bearing soil. *Swelling pressure* is defined as the pressure needed to prevent swelling of a soil as it takes on moisture from its *in situ* condition to its stable moisture level. Swelling pressure is usually determined in the laboratory on a specimen contained within a cylindrical mold that is subjected to water and is nominally prevented from swelling. A calibrated steel bar or a strain gauge is commonly used to measure the force that develops in the specimen because it is prevented from expanding. However, in both types of devices, the developed force is determined from a calibration factor or curve that is based on that amount of deformation that occurs in the bar or the gauge. Thus, some upward movement of the specimen does occur, with the magnitude of movement depending on the stiffness of the force measuring device, and the calculated swelling pressure (measured force divided by the area of the specimen) is less than the actual swelling pressure by some unknown amount. An alternative method for determining swelling pressure is to perform a series of oedometric wetting tests on nominally identical specimens subjected to increasing applied stresses and to determine graphically the swelling pressure from a plot of  $\varepsilon_{vw}$  versus  $\sigma_v$  as the value of  $\sigma_v$  at which the wetting-induced volume change is zero. The results from such a series of tests would be similar to any one of the curves shown in Fig. 6A.100. For example, the swelling pressure is about 340 kPa (7.1 ksf) for the specimen in Fig. 6A.100 prepared by kneading compaction at  $w = 10\%$  to  $R_m = 90\%$ . One must make

**6.140** SOIL IMPROVEMENT AND STABILIZATION

sure, however, that the applied bearing stress is not so high that an unacceptable potential for wetting-induced collapse exists.

If the borrow soil is nonexpansive or slightly expansive, swelling potential is not a concern, and collapse potential can be controlled by compacting the soil to a high density. The critical relative compaction above which little or no collapse occurs for any reasonable compaction water content varies considerably from soil to soil but is typically in the range of  $R_m = 85$  to 100% ( $R_s = 90$  to 110%). The value for any soil can be estimated from a series of one-dimensional laboratory tests performed on specimens prepared at the driest water content to be used in the field compaction to various densities.

Chemical stabilization of expansive borrow soils prior to compaction has been used successfully for many years to control the swelling potential of the as-compacted soil. The most commonly used stabilizing agents are Portland cement, hydrated lime, and fly ash. Chemical stabilization can also be used to control the collapse potential of compacted soils but to date has been little used for this purpose. The primary advantage to using chemical stabilization to control wetting-induced volume change is that the potential for swelling or collapse is unaffected by post-compaction drying of the soil. Other advantages include increased stiffness and strength of the as-compacted soil and little or no reduction in stiffness and strength if the soil becomes soaked. Potential disadvantages include increased brittleness and decreased permeability.

As shown previously, the addition of gravel to a cohesive borrow material may substantially reduce the potential for collapse but not swelling. Thus, for nonexpansive or slightly expansive soils, blending gravel with the cohesive borrow material may be an economically viable method for controlling collapse potential if sufficient quantities of inexpensive gravel are available.

*Shrinkage.* Expansive soils are also susceptible to shrinkage (decrease in total volume) caused by drying, which is also known as *desiccation shrinkage* to differentiate it from other phenomena that produce a decrease in volume. During drying, the matric suction increases, which in turn increases the effective stresses acting on the soil, resulting in a decrease in volume that may be accompanied by cracking. In general, the trends of factors that affect shrinkage potential are opposite to the trends of the same factors for swelling, that is, if increasing a certain factor tends to increase the swelling potential of a compacted soil, increasing that same factor tends to decrease the shrinkage potential. The most important factors that affect the shrinkage potential of compacted cohesive soils are as follows:

1. *Soil type.* The more expansive a soil is, the more susceptible it is to shrinkage. Soils that have high shrinkage potentials generally contain some highly active clay minerals such as montmorillonite.
2. *Moisture condition.* The drier a soil is prior to desiccation, the greater its matric suction and the lesser the increase in effective stress for complete drying. Thus, shrinkage potential decreases with decreasing moisture condition (see Fig. 6A.106).
3. *Dry density.* For the same moisture condition and fabric, denser soils shrink less than looser soils.
4. *Fabric.* The influence of fabric on the axial shrinkage of a silty clay is shown in Fig. 6A.107 for three pairs of specimens where each pair had the same density and water content but different fabrics when shrinkage was initiated. For each pair of specimens, one specimen was compacted dry of optimum and the other was compacted wet of optimum, and then both specimens were soaked to the same composition. In each case the dry-compacted specimen (flocculated microfabric) shrank substantially less than the wet-compacted specimen (dispersed microfabric). The greater resistance to shrinkage for the flocculated microfabric can be attributed to two factors: (a) The flocculated microfabric contains more interparticle contacts that resist shrinkage, and (b) a portion of the load must be spent reorienting the nonaligned particles in the flocculated fabric to a more parallel arrangement before any reduction in average void ratio occurs.

During drying of compacted expansive soils with occluded air phases, the increase in suction resulting from drying acts on the entire surface area of all soil particles and thus produces an increase

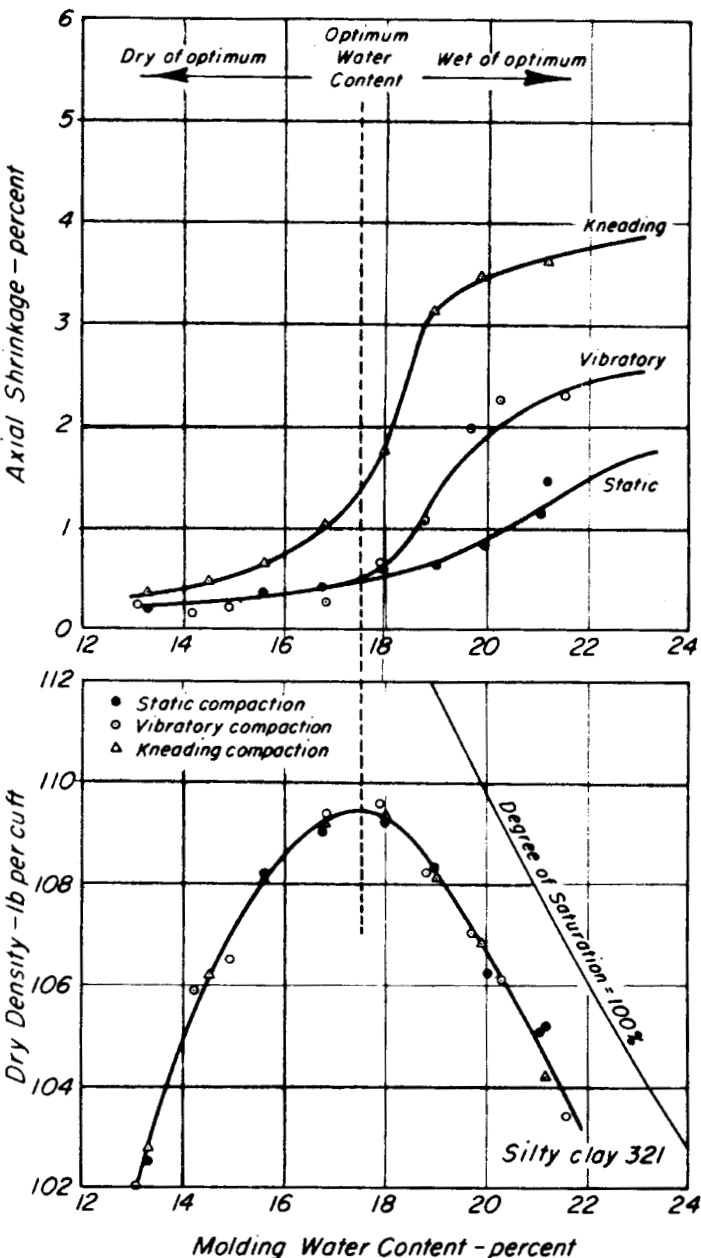


FIGURE 6A.106 Influence of method of compaction and molding water content on axial shrinkage of a silty clay (from Seed et al., 1960).

## 6.142 SOIL IMPROVEMENT AND STABILIZATION

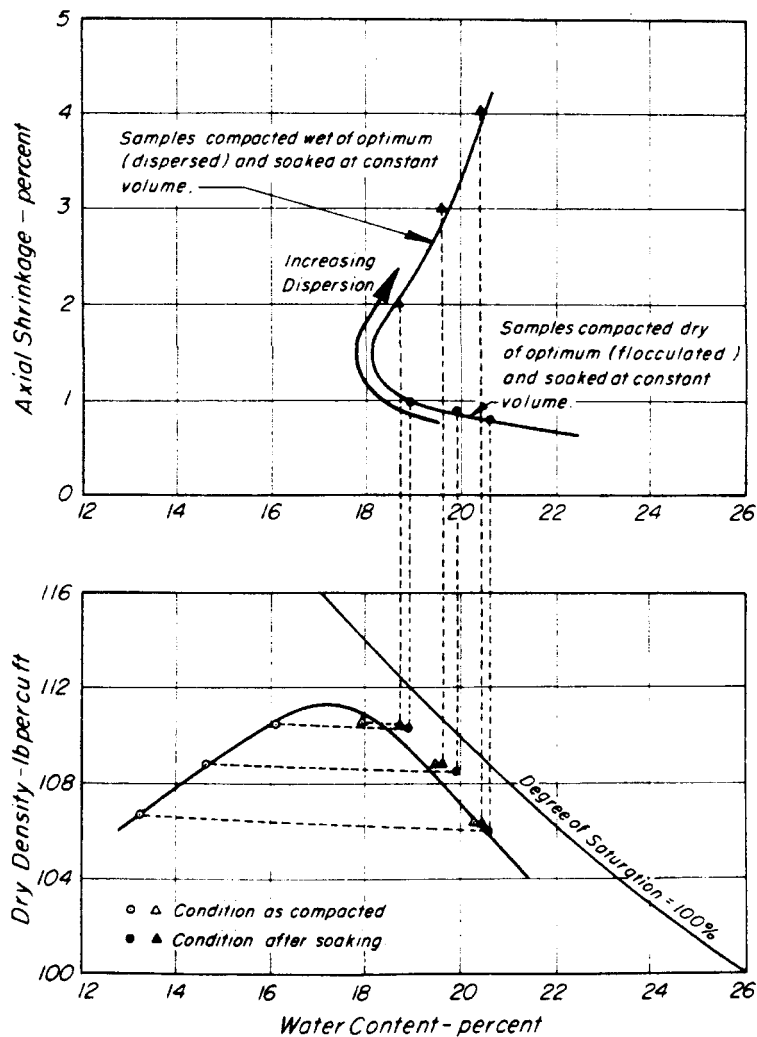


FIGURE 6A.107 Effect of fabric on the axial shrinkage of a silty clay (from Seed and Chan, 1959a).

in effective stress equal to the increase in suction. When some of the pore air spaces become continuous through adjacent void spaces, the suction no longer acts on the total surface area of the particles, and not all the increase in suction is transmitted to the soil as effective stress. As drying continues to occur, the portion of the increase in suction that is transmitted to the soil as effective stress decreases (see Fig. 6A.59). Shrinkage also produces an increase in stiffness of the soil owing to both the increase in density and the increase in suction. Shrinkage ceases when the increase in effective stress resulting from desiccation is no longer sufficient to produce a measurable decrease in volume. The water content of the soil when the shrinkage stops is called the *shrinkage limit*, which generally decreases with increasing plasticity of the soil. Partial drying of the soil to a water content above the

shrinkage limit results in less shrinkage than drying to or below the shrinkage limit. The shrinkage limit of the soil as it dries from an as-compacted, partially saturated state, may be a somewhat different value than that determined by the standard shrinkage limit test (ASTM D427) where the soil is dried from a loose, saturated state. The shrinkage limit for compacted cohesive soils may also vary somewhat depending on the density and water content at which drying initiates.

It is important to note that shrinkage of an expansive soil may also occur from moisture use by vegetation (transpiration). However, according to Brown (1992), the potential for foundation distress relative to transpiration is probably much less than normally assumed, and as long as the moisture loss is confined to capillary water, the soil itself is not particularly affected. However, at some point other moisture may be pulled from the clay and may result in shrinkage and potential foundation settlement. The greatest potential for transpiration-induced settlement is from trees located close to shallow foundations. However, tree roots can be beneficial to foundation stability, since they tend to act as soil reinforcement and increase the soil's stiffness and shearing resistance. Thus, the practical result of a tree located close to a shallow foundation may be to impede foundation settlement, even though the roots remove moisture from the soil (refer to Sec. IA).

Available data indicate that significant structural distress occurs much more frequently from swelling-induced heave than from shrinkage-induced settlement. Of the 502 foundation inspections in Dallas County, Texas, reviewed by Brown (1992) during a particular study period, 216 showed some movement but did not warrant repairs. Of the 286 cases that did warrant foundation repairs, 87 resulted from settlement and 199 resulted from heave. Because it is likely that nearly all of the heave cases were caused by swelling, and the settlement cases could have resulted from a number of phenomena other than shrinkage (e.g., loading-induced compression, marginal bearing capacity, or erosion of supporting soil), it is clear that structural distress is much more likely to occur from swelling than from shrinkage.

*Cyclic Swelling and Shrinkage.* Cyclic swelling and shrinkage of expansive bearing soils is a serious problem that introduces two issues that are not a concern for a single cycle of either swelling or shrinkage: (a) Cyclic swelling and shrinkage may cause fatigue cracking or failure in the foundation or structure for situations where the same amount of movement in one cycle of swelling or shrinkage would not, and (b) the magnitude of cyclic swelling and shrinkage cannot be controlled by compaction alone. Cyclic swelling and shrinkage is of most concern in regions where expansive surficial soils are prevalent and therefore might commonly be used as borrow material, where the summers are hot and dry, and where there is a substantial rainy season in the winter (e.g., southern California and Texas).

As discussed in the two previous sections, the potential for either swelling or shrinkage can be kept to acceptable levels by proper compaction of the soil—compaction wet of optimum to control swelling, and compaction dry of optimum to control shrinkage. However, both swelling and shrinkage potential cannot be controlled by compaction moisture content alone because reducing the potential for either phenomenon increases the potential for the other. In addition, the beneficial effect of compaction moisture control is eliminated by subsequent cycles of wetting and drying. For example, Day (1994) showed that the one-dimensional swelling of a silty clay compacted wet of optimum ( $R_m = 92\%$ ,  $S_{ri} = 89\% > S_{opt} = 80\%$ ) was only 1.0% for the first cycle of wetting (after an aging period of 21 days) but increased to 8.0% for the second and subsequent cycles of wetting after drying.

Because problems from cyclic swelling and shrinkage cannot be eliminated by compaction moisture control alone, alternative methods must be used. It is theoretically possible to reduce substantially postcompaction wetting or drying of the bearing soil, but this is difficult to accomplish in practice over a long period of time. Blending gravel with the borrow material may effectively eliminate the shrinkage potential if a sufficient amount is used, but swelling potential will only be reduced in proportion to the volume of gravel added; thus, this method is unlikely to be economical in many instances. Therefore, chemical stabilization is the preferred alternative on most projects.

*Permeability.* Compacted cohesive soils have low permeabilities, with values of coefficient of permeability ( $k$ ) for small specimens tested in the laboratory typically within the range of  $1 \times 10^{-4}$  cm/s to  $1 \times 10^{-11}$  cm/s ( $3 \times 10^{-1}$  to  $3 \times 10^{-8}$  ft/day). The low permeability of compacted cohesive soils generally causes two types of concerns in applications for building foundations:

**6.144** SOIL IMPROVEMENT AND STABILIZATION

1. Rainfall and snowmelt tend to pond on the surface or run off the surface rather than infiltrate the compacted soil. Thus, more extensive drainage systems are required around buildings founded in compacted cohesive soils than are needed for more permeable granular soils.
2. Local or regional ground-water aquifers and flow patterns may be affected by compacting an existing cohesive soil or by constructing a compacted cohesive fill. This factor may require extensive (and expensive) measures to mitigate potential problems or to compensate adjacent property owners who may be adversely affected. Potential problems include reduction in available water supplies for nearby landowners and damage from diversion of additional water onto adjacent properties because of erosion or wetting-induced volume changes.

The low permeability nature of compacted cohesive soils can be put to productive engineering use in the form of compacted clay liners, which are used to impound water, hazardous waste, and other liquids. Some information on compacted clay liners is given below, but because they are used infrequently in building projects, an in-depth discussion of this topic is beyond the scope of this book. A good reference for additional details on compacted clay liners is Daniel (1993).

The in situ permeability of a compacted cohesive soil is generally controlled by the macrofabric, which may include macroscopic characteristics such as cracks, fissures, root holes, animal burrow holes, and flow channels between lifts that increase the permeability of the in situ soil. Because laboratory specimens are typically quite small, these macroscopic features are generally not included in laboratory specimens. Therefore, laboratory specimens contain only the microfabric and minifabric features of the in situ soil, so that values of  $k$  obtained from laboratory testing represent lower-bound values. To obtain a realistic estimate of the in situ permeability, field tests—such as the sealed double ring infiltration test (see Sec. 6A.3.5)—should be conducted over an area of the compacted soil that is large enough to represent the macrofabric of the soil. The following factors can have a major influence on the field permeability of a compacted cohesive soil:

*1. Soil gradation and mineralogy.* The permeability of any soil depends on the size distribution and shape of the portions of the voids through which water can flow. In cohesionless soils, the water essentially can flow through the entire voids. In cohesive soils, the adsorbed (double-layer) water is strongly attracted to the clay particles, and the flow of water is limited to the portions of the voids outside the boundaries of the double layers. Thus, the permeability of a cohesive soil depends on the clay content as well as the size distribution and activity of the clay particles. In general, the permeability of a cohesive soil decreases with increasing clay content and activity and decreasing size of the clay particles. Because activity of the clay minerals is inversely related to particle size, plasticity index is a general indicator of relative permeability, with  $k$  decreasing with increasing plasticity of the soil. For clay contents greater than about 30% by weight, the clay fraction dominates the permeability to the extent that the gradation of the rest of the soil has little influence on the permeability unless there is a high percentage of particles gravel size or larger. Laboratory tests on uniformly blended mixtures of gravel and cohesive soils have shown that gravel contents less than about 60% have little effect on permeability (Fig. 6A.108) because the gravel floats in the finer matrix (see Fig. 6A.104). At higher gravel contents, the finer particles exist within the void spaces of a skeleton formed by the gravel particles, and the finer soil may not completely fill the voids of the skeleton. Thus, the permeability of the soil decreases rapidly with increasing gravel content above 60%. In the field, the borrow materials cannot be blended as uniformly as in the laboratory so that some segregation of the gravel particles occurs, with the result that gravel skeletons may form at gravel contents as small as 30%. For compacted clay liners where very low permeability is required, it is recommended that the gravel content of the borrow soil be limited to a maximum of 30%.

Large particles (coarse gravel, cobbles, and boulders) inhibit the compaction of the near-field matrix soil (finer soil close to the particles), whereas the far-field matrix soil is unaffected by the presence of the large particles. This produces zones of near-field matrix soil that may be significantly less dense and much more permeable than the far-field matrix soil. These relatively high permeability zones provide a preferential path for water flow through the soil and hence substantially increase its overall permeability. Thus, for low-permeability applications, all particles larger than

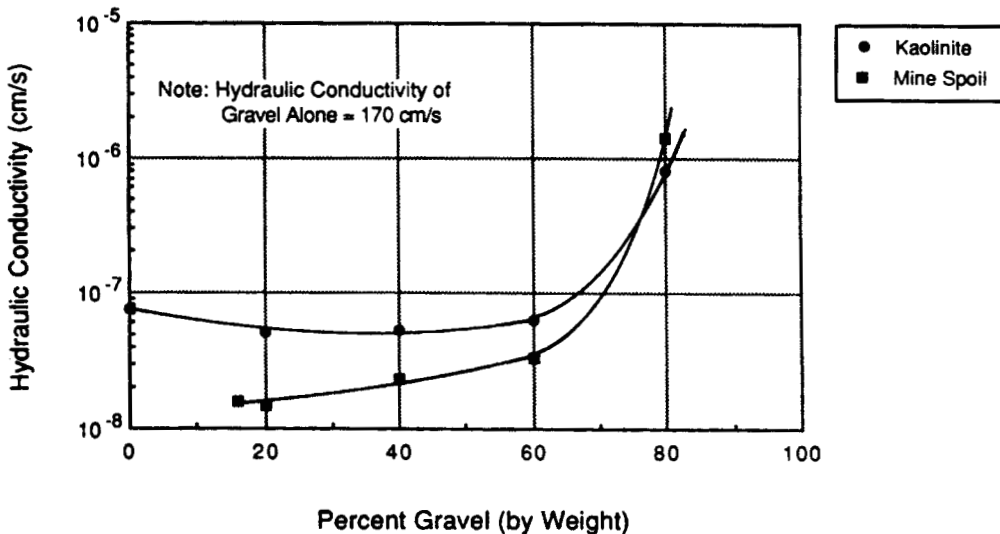


**FIGURE 6A.108** Influence of gravel content on hydraulic conductivity of kaolinite/gravel and mine spoil gravel mixtures (from Shellel and Daniel, 1993).

about 1 to 2 in (25 to 50 mm) should be removed from the borrow material prior to moisture conditioning and compaction.

2. *Fabric.* The ease with which water can flow through any void in a given soil depends on the smallest dimension of the void in the direction perpendicular to the flow. The voids in flocculated microfabrics may be irregular in shape but tend to be equidimensional, whereas the voids in dispersed microfabrics are long and narrow. Therefore, for the same composition and density of the microfabric, flocculated fabrics are more permeable than dispersed fabrics. At the minifabric scale, a fabric wherein the clods have been remolded into a relatively homogeneous material is much less permeable than one in which the clods retain some of their individual identity and thus have relatively large interclod pores.

3. *As-compacted moisture condition and density.* Wetter cohesive soils have softer clods that are more easily remolded. For otherwise comparable compaction conditions, wetter compacted cohesive soils tend to have more dispersed microfabric and more homogeneous minifabric and therefore lower permeability. For the same method of compaction and compaction water content, increased density tends to reduce the permeability in two ways: (a) smaller interclod and intraclod void spaces, and (b) more dispersed microfabric. Isograms of  $k$  for laboratory specimens of silty clay prepared by kneading compaction are shown in water content-density space in Fig. 6A.109;  $k$  for this soil varied by over four orders of magnitude depending on the compaction water content and as-compacted density. (Note: Not all permeability data for the silty clay is reflected in Fig. 6A.109; see Mitchell et al., 1965 for additional data.) Wet of optimum ( $S_r > S_{opt}$ ), the permeability of the soil was primarily a function of degree of saturation and was little affected by density. Note also the rapid decrease in  $k$  with increasing  $S_r$ . Density played a more substantial role dry of optimum, but  $S_r$  was still the primary factor affecting  $k$ . To achieve low permeability in compacted clay liners, the soil should be compacted wet of the line of optimums. Other engineering characteristics of the soil—such as shear strength and shrinkage potential—may also be important, so a moisture-density zone should be specified that meets all the important criteria (Fig. 6A.110).

## 6.146 SOIL IMPROVEMENT AND STABILIZATION

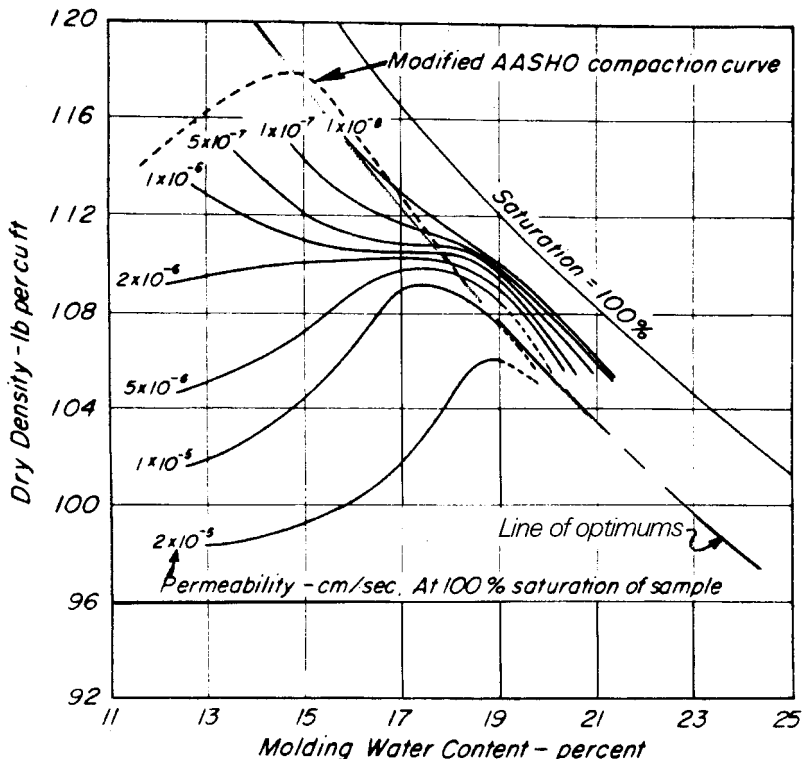


**FIGURE 6A.109** Isograms of coefficient of permeability for specimens of silty clay prepared by kneading compaction (from Mitchell et al., 1965).

4. *Method of compaction.* Very dry of optimum, the method of compaction generally has little influence on the fabric of the compacted soil. Wet of optimum, increasing the shearing strain induced in the soil during compaction tends to produce a more dispersed microfabric and greater remolding of the clods. Therefore, kneading compaction results in lower permeability than does static compaction for otherwise comparable conditions, and impact compaction produces an intermediate permeability. A comparison of permeability for kneading and statically compacted specimens of a silty clay is shown in Fig. 6A.111. All kneading rollers (sheepsfoot, tamping foot, and rubber-tired) can remold a wet cohesive borrow material into a relatively homogeneous mass for low permeability applications. However, unless good bonding is achieved between lifts, hydraulic defects in adjacent lifts may be hydraulically connected to each other. To produce good interfacial bonding in compacted clay liners, sheepsfoot rollers with feet longer than the lift thickness are usually specified. Heavier rollers are needed in drier soils to break down the clods; in wet soils, lighter rollers should be used that do not become bogged down in the soft soil.

5. *Compactive effort.* Increased compactive effort generally results in higher density, greater dispersion of the microfabric, and increased remolding of clods, all of which result in lower permeability. At some point, additional passes of the compaction equipment will produce no significant changes in the compacted soil. In some soft cohesive soils, additional passes beyond a certain number may produce loosening and weakening of the soil and a concomitant increase in permeability.

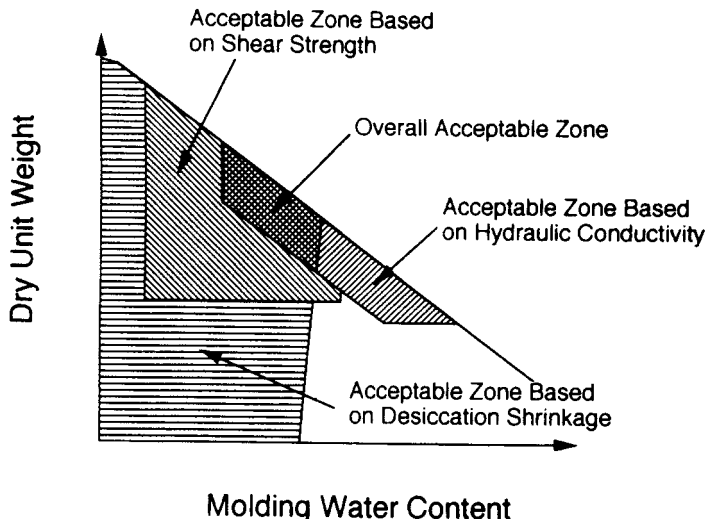


**FIGURE 6A.110** Overall acceptable moisture-density zone based on hydraulic conductivity, shear strength, and shrinkage upon desiccation (from Daniel, 1993).

6. *Compaction water content and moisture conditioning period.* The water content of the soil and the distribution of moisture within the clods determine to a great extent the amount of remolding that will occur during compaction for a given method of compaction. Very dry clods can be extremely hard and brittle and will not remold but may be broken during compaction, and the permeability of dry-compacted cohesive soils is relatively high owing to flocculated microfabrics and large interclod pores. Wet clods are soft and are easily remolded, and wet-compacted soils have relatively low permeabilities because of dispersed microfabrics and small interclod pores. The distribution of moisture within the clods also influences the as-compacted fabric. Long periods of time—up to several weeks in some cases—may be required to achieve moisture equilibrium within highly plastic clods, with the required length of time increasing with the size of the clods. If an adequate moisture conditioning time is not used, the outer portions of the clods will be wet and soft, and the inner portions will remain dry and hard. For this reason—and because of potential problems with postcompaction shrinkage and swelling (see number 9 below)—highly plastic borrow materials are not recommended for use in compacted clay liners. The water content of the borrow material for compacted clay liners should be wet and soft enough to allow easy remolding of the clods but not so wet that the compaction and construction equipment have inadequate traction to function properly.

7. *Clod size.* Laboratory studies have shown that the size of the clods may affect  $k$  by several orders of magnitude (Benson and Daniel, 1990; Daniel, 1984; Houston and Randeni, 1992) and that  $k$  tends to increase with increasing size of clods, as illustrated in Fig. 6A.112. The influence of clod size on  $k$  decreases with increasing compaction water content, as shown in Fig. 6A.113. Because of this effect, a maximum clod size of about 0.75 in (19 mm) should be specified for compacted clay liners.

8. *Lift thickness.* The lift thicknesses for cohesive soils are usually in the range of 4 to 12 in (0.1 to 0.3 m). If the lift thickness is too large for the borrow soil and compaction equipment being used, the lower portions of the lift will not be properly compacted, resulting in a lift with lower  $k$  near the top and higher  $k$  near the bottom.

## 6.148 SOIL IMPROVEMENT AND STABILIZATION

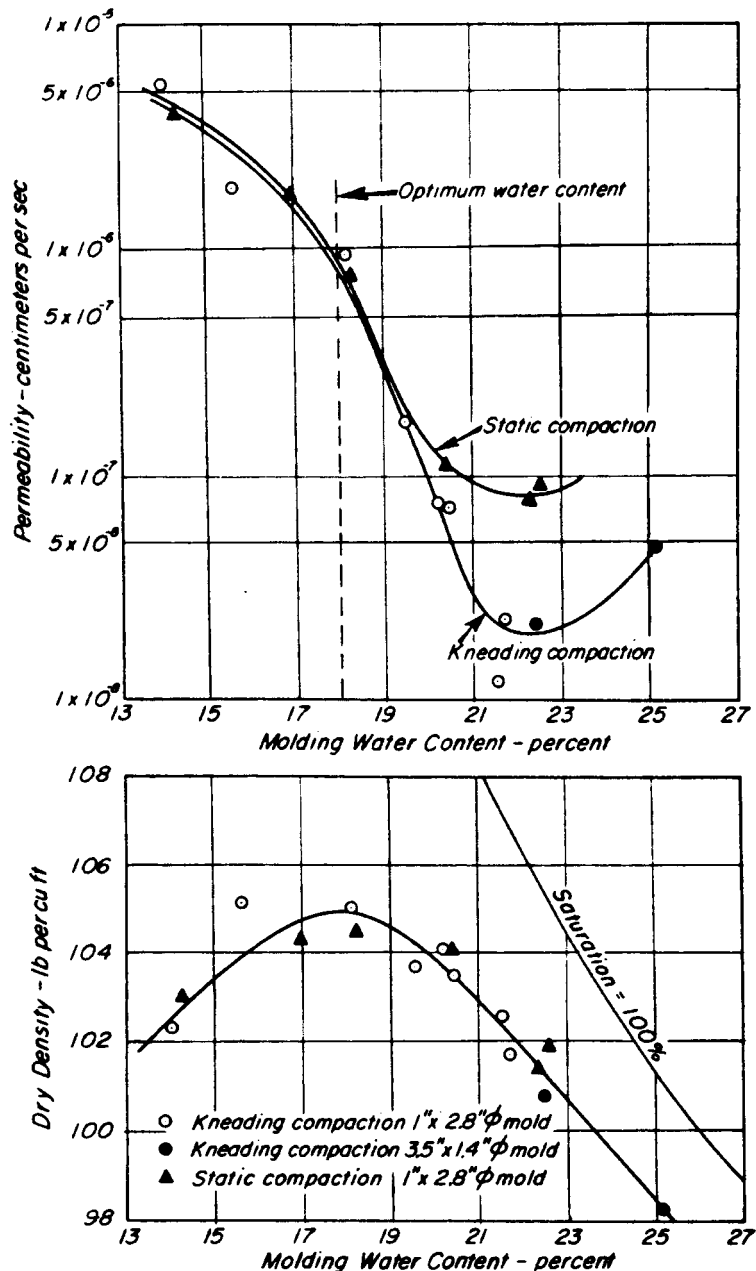
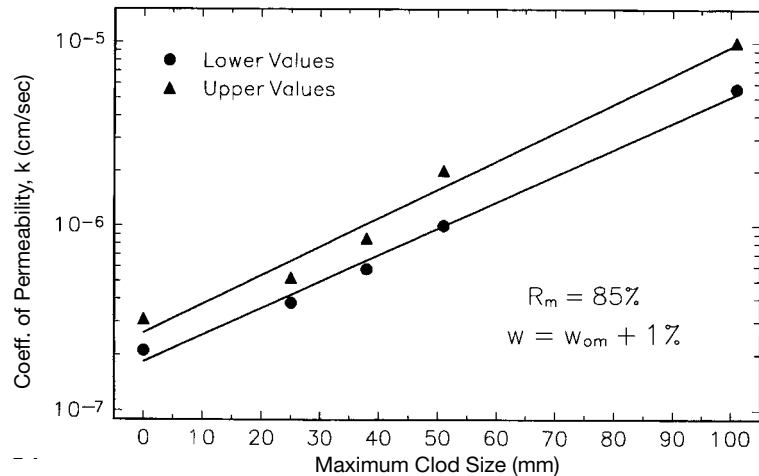
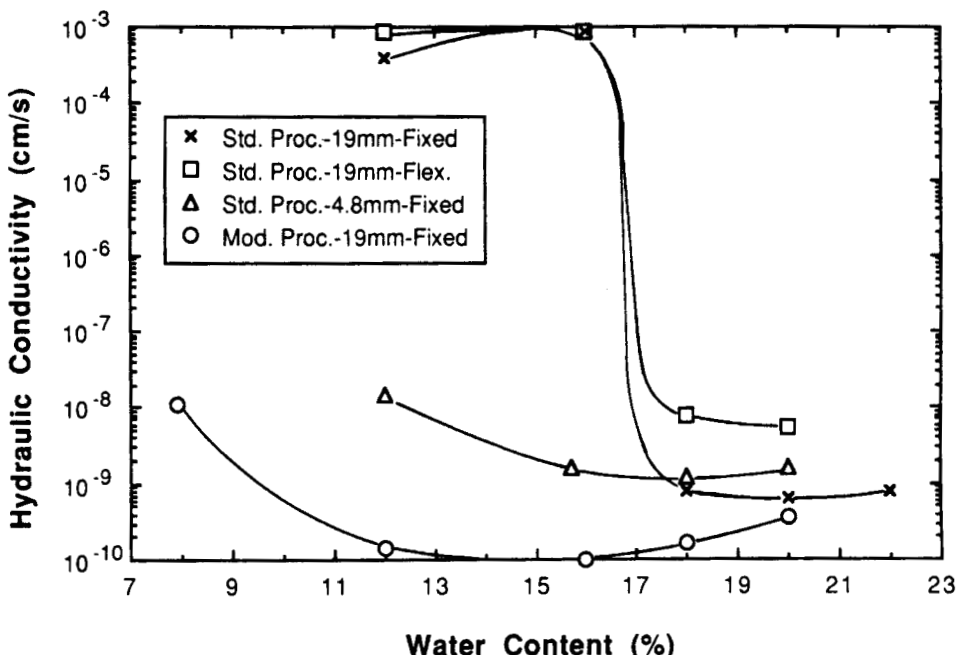


FIGURE 6A.111 Effect of method of compaction on the permeability of silty clay (from Mitchell et al., 1965).



**FIGURE 6A.112** Influence of clod size on the permeability of a compacted lean clay (data from Houston and Randeni 1992).



**FIGURE 6A.113** Influence of clod size, compactive effort, and method of testing on the hydraulic conductivity of highly plastic, compacted clay (from Benson and Daniel, 1990).

**6.150** SOIL IMPROVEMENT AND STABILIZATION

9. *Postcompaction moisture changes.* Postcompaction wetting and drying of the compacted soil may result in changes in permeability, especially in highly plastic soils. Wetting may result in swelling and increased  $k$  owing to decreased density. Drying may produce cracks that can penetrate compacted cohesive soils to a depth of several inches in just a few hours, with a substantial increase in  $k$  (Boynton and Daniel, 1985). In low-permeability applications, it is especially important that swelling and shrinkage be prevented to the extent possible. Shrinkage cracking can be prevented by lightly spraying the surface of each compacted lift with water as needed to prevent drying, but care should be taken not to add so much water that swelling is induced. The compacted soil can also be protected from shrinkage by covering it with a light-color plastic liner. If heavy rain is expected, the soil should be covered with a plastic liner to prevent swelling and erosion. To prevent postcompaction drying of the compacted clay liner in composite liner systems, the geomembrane liner should be placed as quickly as possible after proofrolling the final lift of the clay liner.

10. *Postcompaction freeze-thaw cycles.* Postcompaction freezing and thawing of compacted cohesive soils may produce cracking and an increase in permeability of about 5 to 1000 times that of the as-compacted soil. The effect of freeze-thaw on four compacted clays is shown in Fig. 6A.114. The change in permeability caused by freezing and thawing appears to increase with increasing compaction water content. From the results of permeability tests conducted on a glacial clay (Fig. 6A.115), it can be seen that five freeze-thaw cycles increased the permeability by about 2 to 6 times for specimens compacted dry of optimum and about 100 to 250 times for specimens compacted wet of optimum (Kim and Daniel, 1992). Field tests conducted on a test pad constructed of compacted clay in which the uninsulated portion of the pad underwent up to 10 cycles of freeze-thaw showed that the permeability of the soil within the depth of frost penetration ( $0.5\text{ m} = 1.6\text{ ft}$ ) increased by approximately 50 to 300 times compared to its as-compacted condition (Benson et al. 1995). However, because the frost penetrated only about 30% of the total thickness ( $1.5\text{ m} = 4.9\text{ ft}$ ) of the test pad, the overall hydraulic conductivity of the liner was not affected by the freeze-thaw cycles. Compacted clay liners in cold climates should be insulated to protect them from the potential effects of freeze-thaw.

11. *Macrofabric.* It is obvious from the preceding discussions that cracks produced by such phenomena as desiccation shrinkage and freeze-thaw cycles can substantially increase the permeability of a compacted cohesive soil. Macroscopic hydraulic channels can also be opened by other

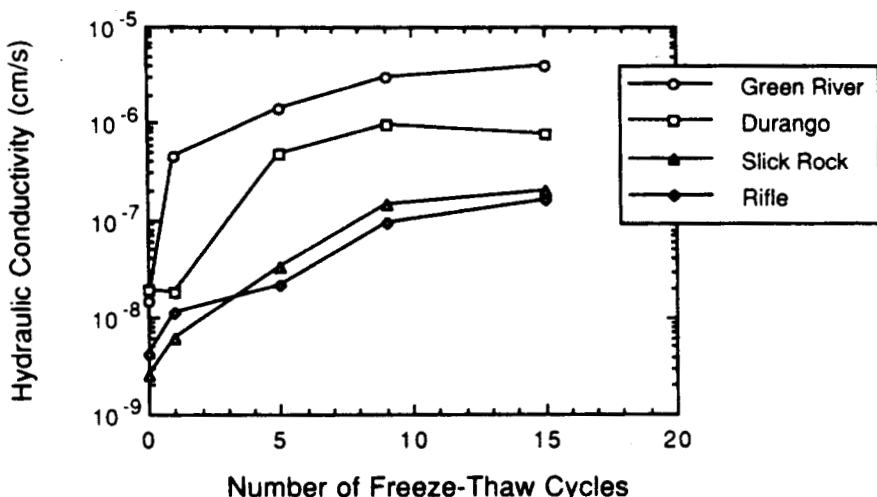


**FIGURE 6A.114** Effect of freeze-thaw on the hydraulic conductivity of four compacted clays (from Kim and Daniel, 1992, data from Chamberlain et al., 1990).

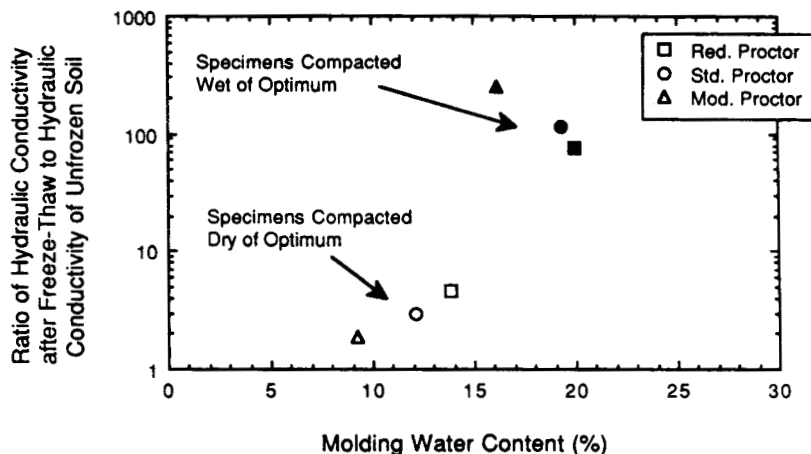


**FIGURE 6A.115** Ratio of average hydraulic conductivity after five cycles of freeze-thaw to hydraulic conductivity of unfrozen soil for a glacial clay (from Kim and Daniel, 1992).

phenomena, including burrowing animals, erosion by wind or water, penetration of plant roots, dissolution of water-soluble coarse-grained particles (e.g., gypsum), and chemical dissolution of soil particles.

12. *Degree of saturation during flow.* The influence of degree of saturation during flow on the permeability of a compacted silty clay is shown in Fig. 6A.116. The increase in permeability with increasing degree of saturation is expected because of the increased pore volume through which water can flow (Mitchell et al., 1965). Theory and experimental results suggest that the permeability varies approximately as the cube of degree of saturation ( $k \propto S^3$ ).

13. *Stress level.* The permeability of compacted cohesive soils decreases with increasing compressive stress level owing to an increase in density and perhaps some increase in dispersion of the microfabric, as depicted in Fig. 6A.117 (Boynton & Daniel 1985). Because field permeability tests are usually conducted on test pads at essentially zero overburden stress and therefore overestimate the in situ permeability, the results from field permeability tests should be corrected for stress level based on the results of laboratory permeability tests performed over a range of compressive stresses, as shown in Fig. 6A.118 (Daniel, 1993). Higher stress levels also tend to "heal" desiccation cracks, as illustrated in Fig. 6A.117. The data indicate that the cracks began to close at confining pressures of about 4 psi (28 kPa) and that the cracks were essentially closed at confining pressures greater than about 8 psi (55 kPa).

14. *Aging.* The effect of 21 days of aging on specimens of a compacted silty clay stored at constant water content and density is shown in Fig. 6A.119. This increase in permeability with aging was ascribed to an increase in flocculation of clay particles at the microscale (Mitchell et al., 1965). Boynton and Daniel (1985) reported that the permeability of the fire clay they studied increased for storage times up to 2 months and then decreased up to a storage time of 6 months. Thus, the effect of aging on the permeability of cohesive soils is not completely understood. Additional details on the effects of aging on the engineering characteristics of soils can be found in Sec. 6A.3.4.3.

*Liquefaction.* Both laboratory tests and field performance data indicate that the great majority of clayey soils will not liquefy during earthquakes (Seed et al., 1983). However, clayey soils with the following characteristics may be vulnerable to severe loss of strength from earthquake shaking:

## 6.152 SOIL IMPROVEMENT AND STABILIZATION

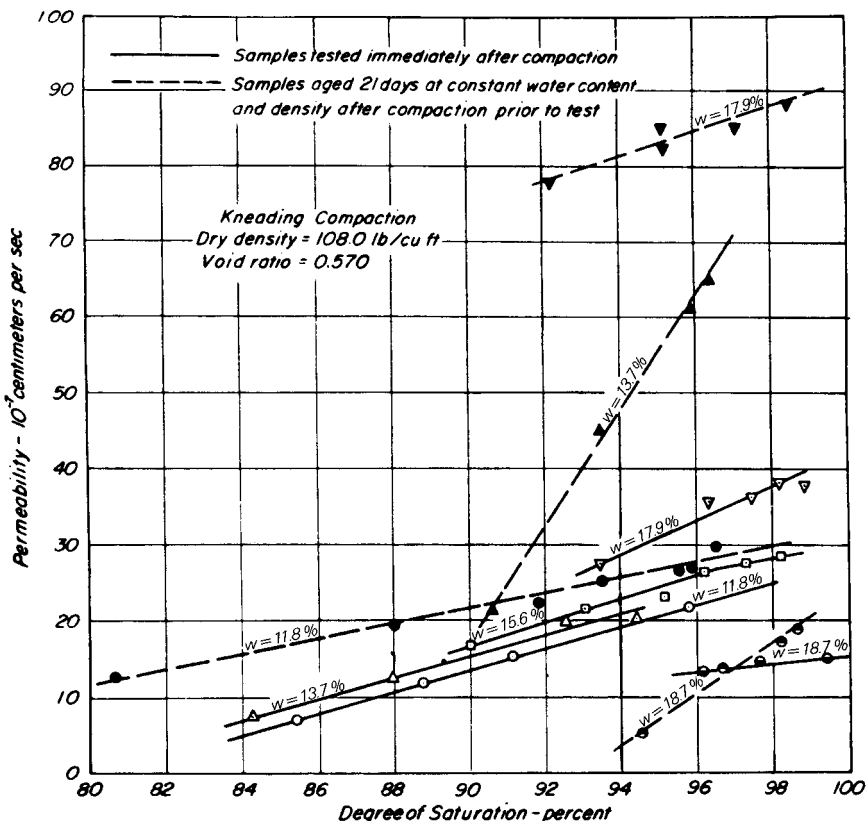


**FIGURE 6A.116** Effect of degree of saturation during flow on the permeability of compacted silty clay (from Mitchell et al., 1965).

Percent finer than 0.005 mm < 15%

Liquid limit < 35

Water content >  $0.9 \times$  liquid limit

A rough estimate of the liquefaction potential for these soils may be obtained using the procedures given previously for sands and silty sands, but the best means of determining their cyclic load characteristics is by test.

#### 6A.3.4.3 Aging, Thixotropy, and Cementation

Changes occur in the engineering properties of many compacted soils as the soils age. In general, the strength, stiffness, and permeability of compacted soils increase with aging, whereas the potentials for liquefaction, swelling, and shrinkage typically decrease. Examples of these changes are given in Figs. 6A.119 to 6A.123. Although the reasons for these changes are not completely understood, the following phenomena have been suggested as likely contributors: thixotropy, secondary compression, particle interference, clay dispersion, and cementation. Each of these phenomena is described in limited detail below. The reader is referred to Mitchell (1960) for additional details on thixotropy and to Schmertmann (1991) for further information about mechanical aging.

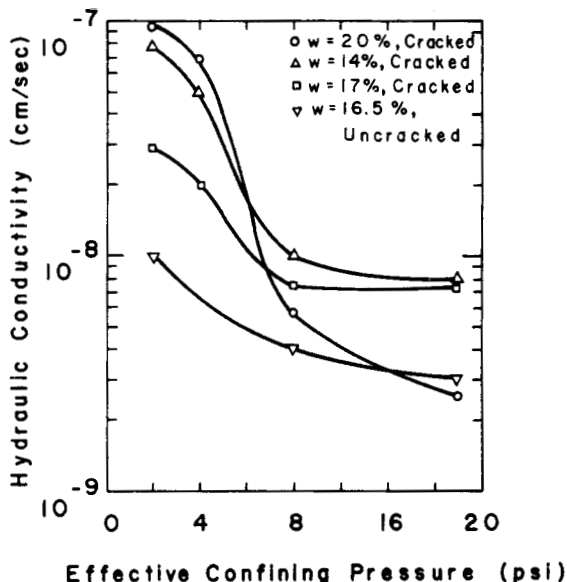


**FIGURE 6A.117** Hydraulic conductivity versus effective confining pressure for uncracked and desiccation-cracked specimens of fire clay compacted at various molding water contents (from Boynton and Daniel, 1985).

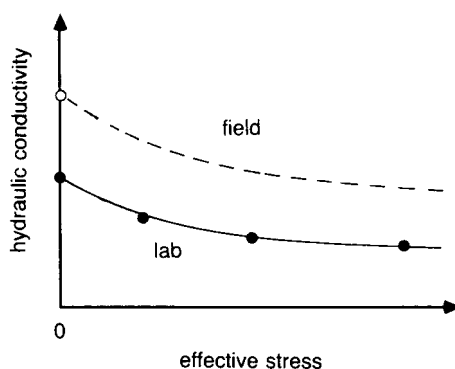


**FIGURE 6A.118** Procedure for adjusting the hydraulic conductivity measured in the field on a test pad for the influence of compressive stress (from Daniel, 1993).

## 6.154 SOIL IMPROVEMENT AND STABILIZATION

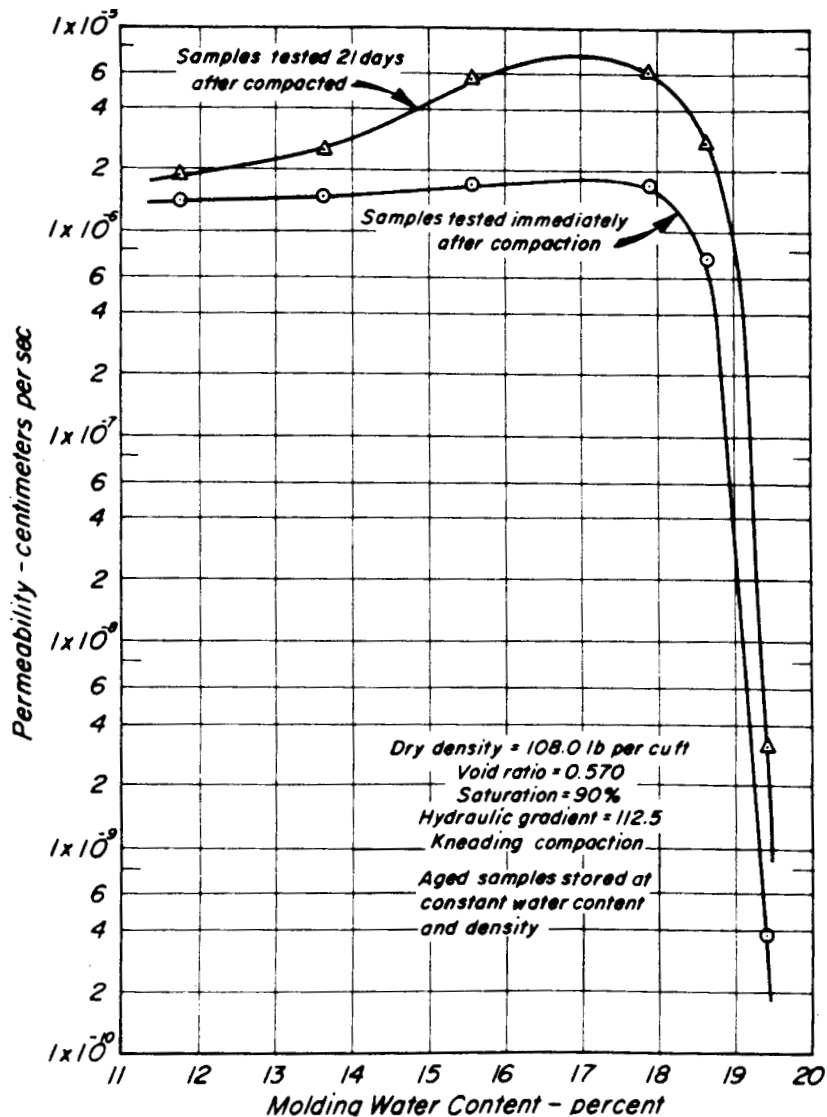
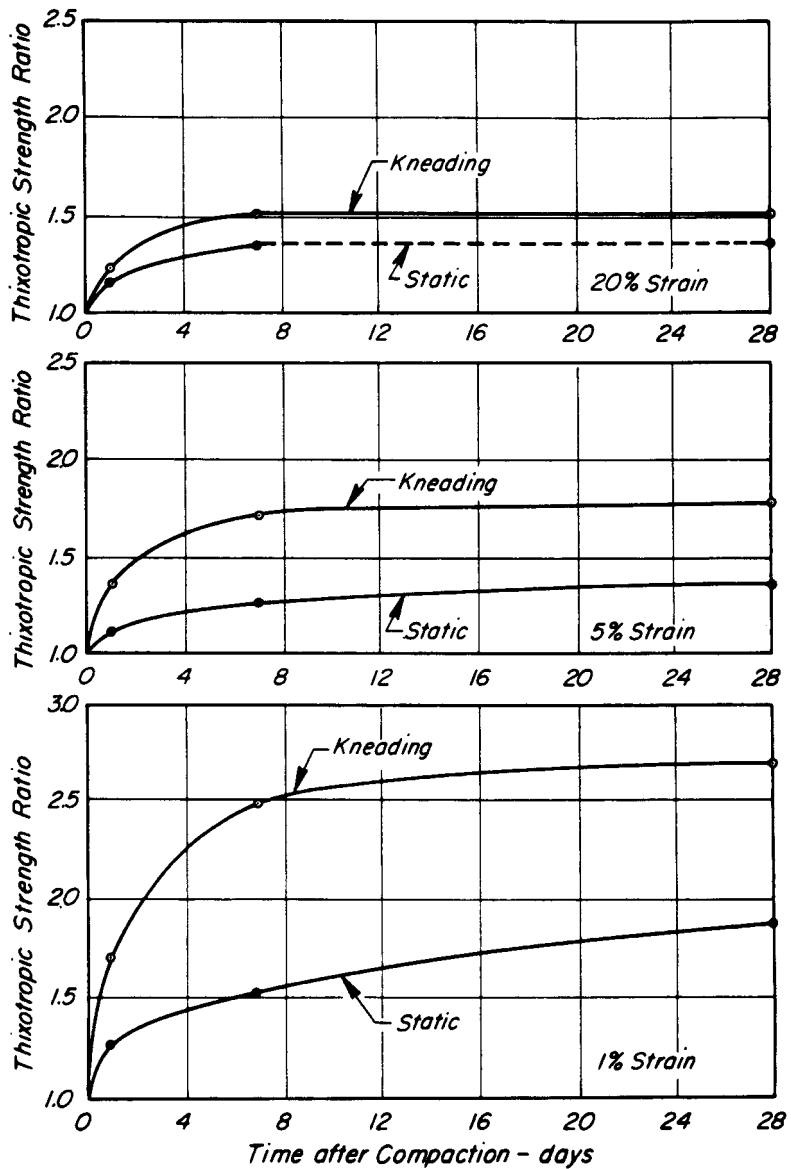


FIGURE 6A.119 Influence of aging at constant water content and density on the permeability of a compacted silty clay (from Mitchell et al., 1965).

*Thixotropy.* There is no universally accepted definition of *thixotropy* in soil mechanics. Mitchell (1960) defines thixotropy as an isothermal, reversible, time-dependent process occurring under conditions of constant composition and volume whereby a cohesive soil stiffens while at rest and softens upon remolding. Simply stated, thixotropy is an increase in flocculation (randomness) of a cohesive soil fabric in undrained (constant-volume) conditions. The properties of a purely thixotropic material are given in Fig. 6A.124.



**FIGURE 6A.120** Effect of method of compaction on the thixotropic strength ratio for a compacted silty clay (from Mitchell, 1960).

## 6.156 SOIL IMPROVEMENT AND STABILIZATION

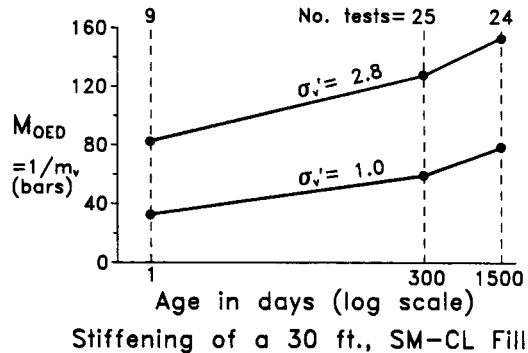


FIGURE 6A.121 Aging-induced increase in oedometer modulus of a compacted, cohesive fill (from Schmertmann, 1991).

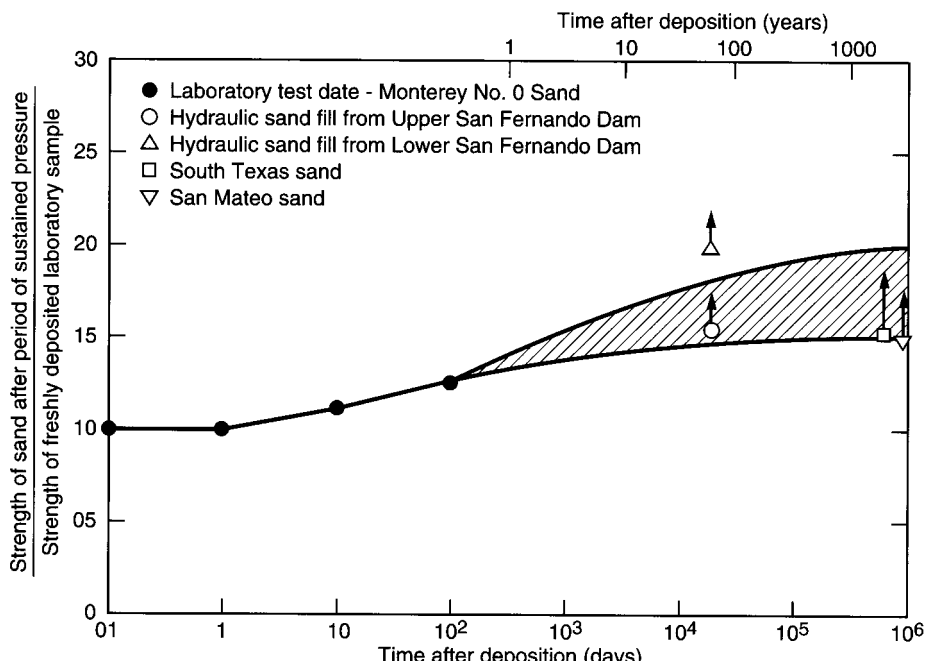
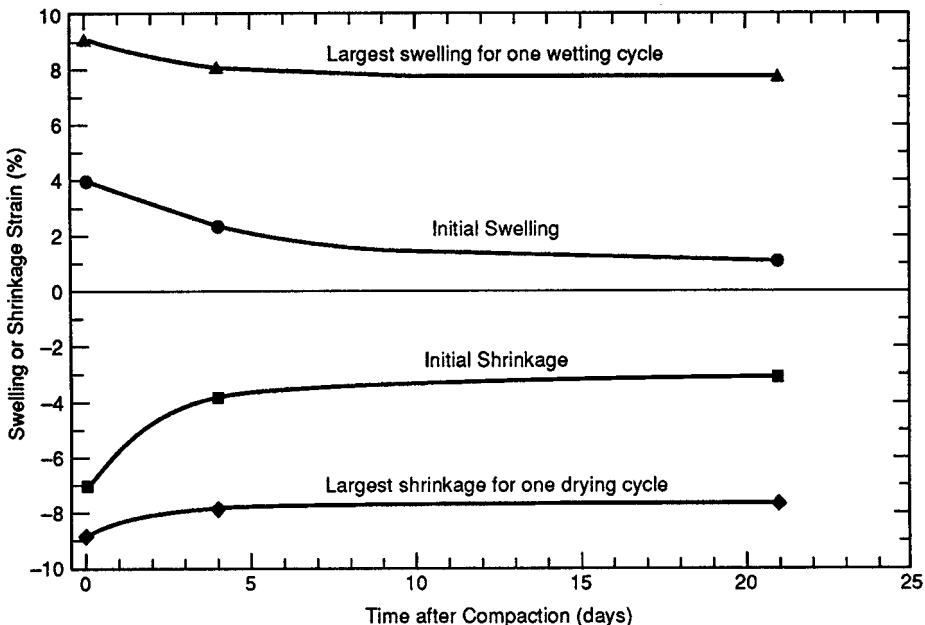
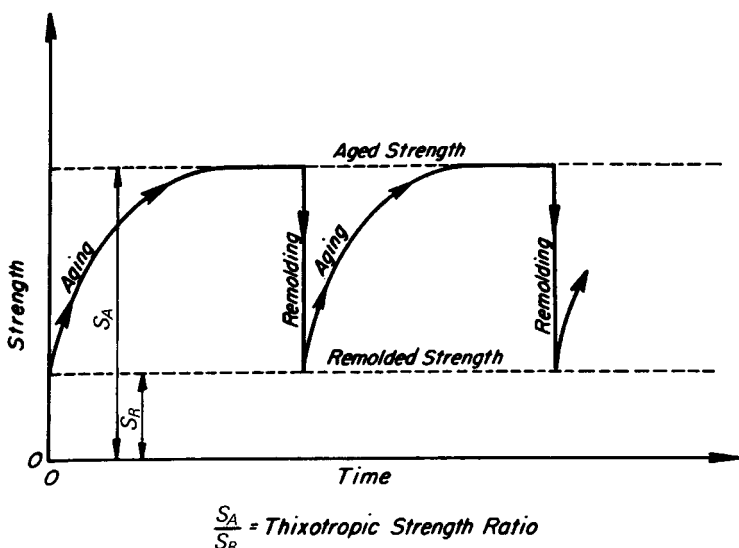


FIGURE 6A.122 Influence of aging under sustained pressure on the stress ratio causing liquefaction of sand (from Seed, 1979).



**FIGURE 6A.123** Effect of aging on the swelling and shrinkage of a compacted silty clay (data from Day, 1994).



**FIGURE 6A.124** Properties of a purely thixotropic material (from Mitchell, 1960).

**6.158** SOIL IMPROVEMENT AND STABILIZATION

The energy that drives thixotropy comes from the forces of attraction and repulsion between clay particles. A cohesive soil will exhibit thixotropy if the following two conditions exist (Mitchell 1960):

1. The net interparticle force balance is such that the clay particles will flocculate if given the chance.
2. The flocculation is not so strong, however, that the particles cannot be dispersed by applied shearing strains.

Mitchell (1960) has postulated that the mechanism of thixotropy may occur in the following manner:

1. When a thixotropic soil is compacted, a portion of the compactive shearing energy acts with the repulsive forces between platy particles to produce a more parallel arrangement. During compaction, the energy of interaction between particles is at a level commensurate with the externally applied compactive forces, and the adsorbed water layers and ions are distributed according to this high energy level. The net result is a structure similar to that shown schematically in Fig. 6A.125(a).
2. When compaction ceases, the externally applied energy drops to zero, and the net repulsive force decreases; that is, the attractive forces exceed the repulsive forces for the particular arrangement of particles and distribution of water, and the structure attempts to adjust itself to a lower energy condition. The dissipation of energy may be accompanied by changes in particle arrangements, adsorbed water structure, and distribution of ions. These structural changes are time-dependent, because physical movement of particles, water, and ions must take place. Since the process occurs at constant volume, the particle movements are probably small and of a rotational nature. A schematic diagram of the structure at some intermediate time after compaction is given in Fig. 6A.125(b).
3. After some time, the soil will achieve an equilibrium structure, as depicted in Fig. 6A.125(c). The time required to reach equilibrium is related to such factors as water content, particle size distribution, particle shape, the ease of displacement of adsorbed water molecules, pore water chemistry, and the magnitude of effective stress during aging.

Nalezy and Li (1967) suggested that thixotropic flocculation may result from Brownian motion that brings some clay particles close enough to flocculate.

Available evidence suggests that all compacted cohesive soils may undergo thixotropy under certain conditions. The following factors may affect the magnitude of the gain in strength and stiffness that occurs during thixotropy (Mitchell, 1960; Seed et al., 1960):

1. *As-compacted fabric.* Little or no thixotropic hardening occurs in soils with an initially flocculated fabric, such as those produced by compaction to dry-of-optimum saturation. Thixotropic hardening increases with increasing dispersion (all other factors being the same).
2. *Water content.* The influence of compaction water content on thixotropic hardening of a kneading-compacted silty clay after 6 days of aging is shown in Fig. 6A.126 (Mitchell 1960). The thixotropic strength ratio is defined as the strength of the aged soil to the strength of the as-compacted soil. Dry of optimum ( $w < 17.7\%$ ), the fabric is essentially flocculated, and the thixotropic strength ratio is small. Wet of optimum, the thixotropic strength ratio increases with increasing water content up to about 28 to 29%, beyond which the strength ratio decreases with increasing water content. The disparity between the induced and equilibrium structures is apparently as great as it can be for this soil and method of compaction at a water content of about 28 to 29%. The decrease in thixotropic effect at higher water contents may be attributable to the natural dispersing tendency of the soil at these water contents.
3. *Magnitude of strain.* The thixotropic increase in strength is greater at low strains and decreases with increasing strain (Fig. 6A.126) and is attributable to progressive destruction during shearing of the thixotropically formed structure.

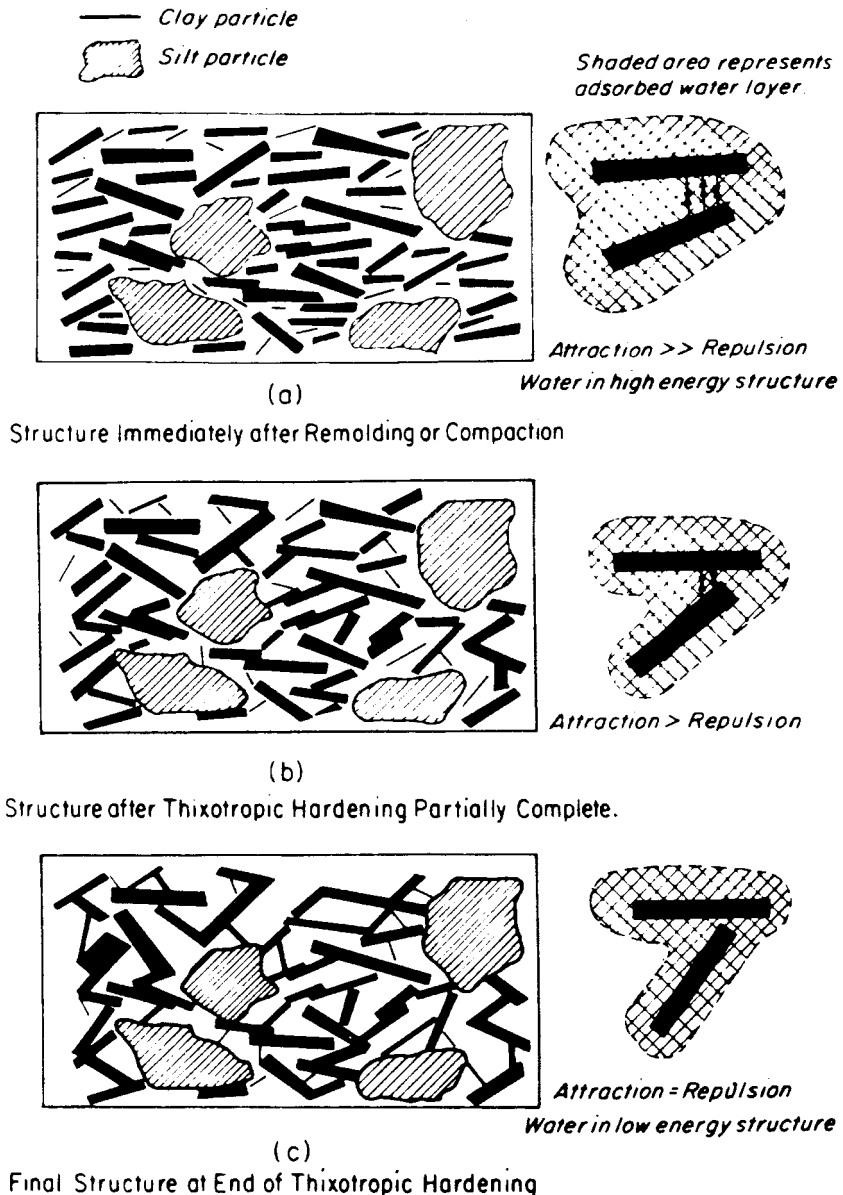


**FIGURE 6A.125** Schematic diagram of thixotropic change in structure for a fine-grained soil (from Mitchell, 1960).

## 6.160 SOIL IMPROVEMENT AND STABILIZATION

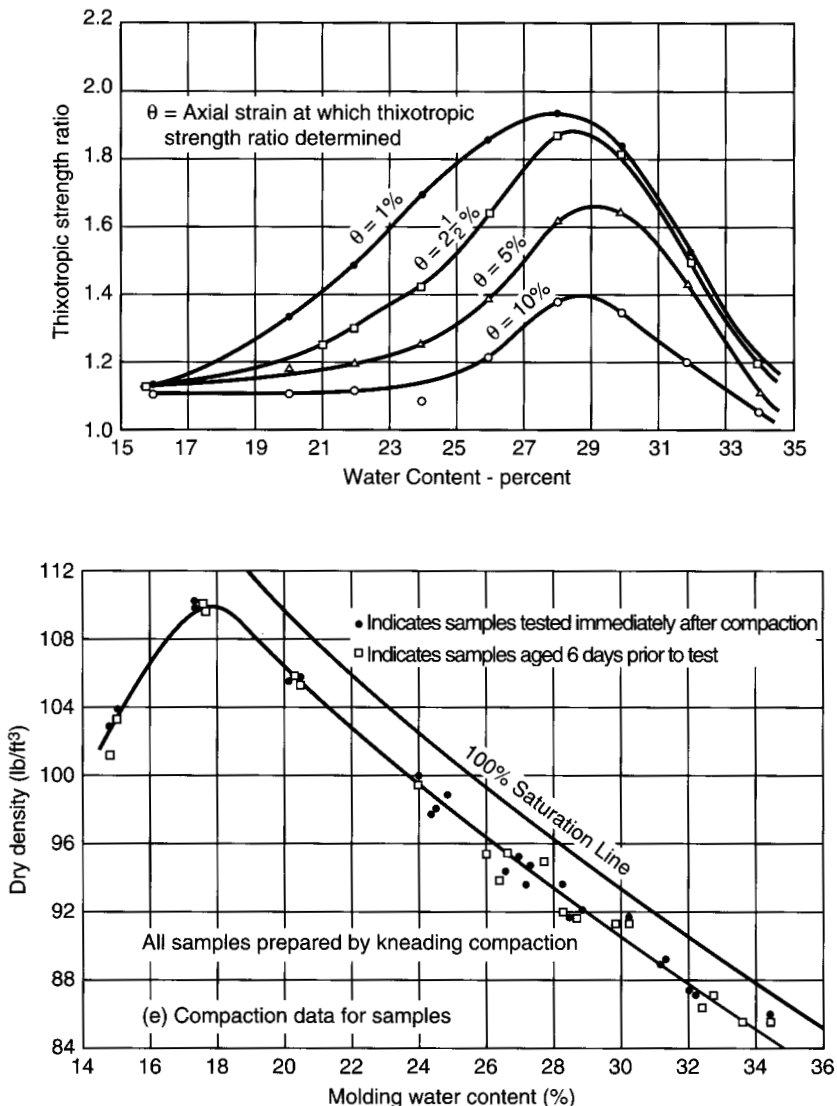


**FIGURE 6A.126** Thixotropic strength ratio for a silty clay as a function of molding water content and axial strain (from Mitchell, 1960).

4. *Method of compaction.* The effect of method of compaction on thixotropic strength ratio for the same silty clay is shown in Fig. 6A.120. As expected, the kneading-compacted soil is more thixotropic than the statically compacted soil because of the greater dispersion-and hence greater tendency toward thixotropic flocculation—produced by kneading compaction.

*Secondary Compression.* Secondary compression, which is a creep-type rearrangement of particles into a slightly denser fabric, is closely associated with aging effects (Schmertmann 1991). The

driving energy for secondary compression is supplied by the in situ effective stresses acting on the soil. Although some engineers believe that aging effects can be fully explained in terms of secondary compression, the magnitude of aging-induced changes in engineering behavior cannot be entirely attributed to the small changes in density that occur from secondary compression. Thus, secondary compression is one of several phenomena that contribute to aging effects in soils.

*Particle Interference.* The term *particle interference* is used to describe the tendency of aged soils to show increased dilation during shearing (see Fig. 6A.127). This increased dilatancy probably results from small slippages of particles during secondary compression, which produce additional particle-to-particle interlocking (Schmertmann, 1991).

*Clay Dispersion and Internal Arching.* The drained movements associated with secondary compression tend to disperse plate-shaped particles in cohesive soils, which leads to an increased basic frictional capability of the soil. Schmertmann (1991) has presented two possible mechanisms of internal arching by which this increased frictional resistance may occur:

1. As parts of the fabric of the soil stiffen owing to dispersion under drained conditions during aging, the stresses may arch to these stiffer parts.
2. The dispersive movements may occur primarily in the weaker, softer parts of the fabric and cause an arching stress transfer to the stiffer parts.

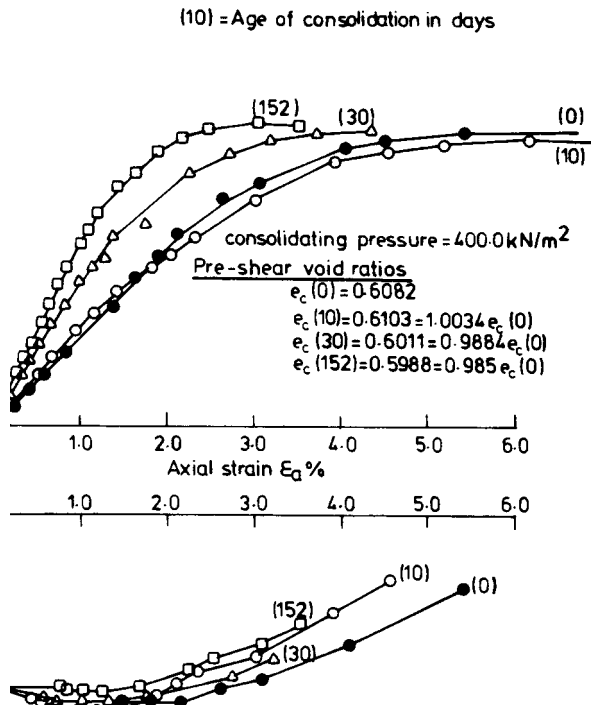


**FIGURE 6A.127** Effect of aging on the triaxial stress-strain and volume change characteristics of Ham River sand (from Daramola, 1980).

**6.162 SOIL IMPROVEMENT AND STABILIZATION**

In either case the arching is assumed to occur internally at the minifabric level, with the average effective stress remaining constant.

*Cementation and Bonding.* Although Schmertmann (1991) has shown that substantial increases in stiffness and strength can occur with aging in the absence of any measurable cementation, postcompaction cementation may play a significant role in aging effects for some soils, especially those containing carbonates, iron oxide, alumina, and organic matter. The decrease in swelling potential with aging shown in Fig. 6A.123 cannot be explained by any combination of factors that excludes cementation or some other form of bonding. Day (1994) suggested that the decrease in swelling potential for the silty clay he studied may be partially related to bonds that develop during aging. These bonds were manifested in the form of an aging-induced increase in effective cohesion intercept at zero effective stress, with  $c'$  ( $\sigma'_v = 0$ ) increasing from zero for no aging to 45 psf (2.2 kPa) after 21 days of aging (see Day, 1992). The nature of this bonding was not determined. Nalezny and Li (1967) also reported experimental evidence that showed swelling potential decreased with aging in the highly expansive clay they studied, which they attributed to an increase in cross-linking of clay particles. This additional cross-linking—which results from Coulombic and van der Waals attractive forces that develop at edge-to-face contacts—is assumed to occur with aging as Brownian motion brings some clay particles close enough to flocculate. Note, however, that increasing flocculation in freshly compacted soils tends to increase the swelling potential (compare the results for the kneading and statically compacted specimens shown in Fig 6A.100). Therefore, if the aging-induced decrease in swelling potential is produced entirely by cross-linking, the reduction in swelling potential caused by the cross-linking must be greater than the increase in swelling potential resulting from increased flocculation. Whatever its nature, some form of bonding occurs in cohesive soils with aging that contributes not only to a reduction in swelling potential but also to the other aging-induced changes in engineering behavior.

*Summary.* Aging effects have been reported in virtually all types of remolded and compacted soils. Aging effects in sands appear to result from increased density and particle interlocking as a consequence of secondary compression. Cementation may also be a contributing factor in some cases. In clays, aging effects may also be associated with thixotropy, dispersion, and some form of bonding. Schmertmann (1991) estimates that for most soils, the aging-induced improvement in many key soil properties is on the order of 50 to 100% during engineering times. Unfortunately, the mechanisms by which these improvements occur are not completely understood, and the beneficial effects of these improvements are seldom considered in engineering practice. However, because the potential degree of improvement is significant, a substantial savings in foundation costs may be realized on some projects involving compaction of bearing soils by performing laboratory and field tests to determine the extent of this improvement for important properties of the borrow soils or in situ soils to be compacted.

**6A.3.5 Quality Control and Assurance**

To ensure that a compacted soil has the desired engineering characteristics, a two-step quality control and assurance process is commonly employed that consists of compaction specifications and postcompaction testing of the compacted soil. The compaction specifications are usually written by a geotechnical engineer and become part of the legal construction documents. The primary purpose of the compaction specifications is to provide guidelines that assist the compaction contractor in achieving the desired engineering product. The postcompaction testing program is used to verify that compacted soil with appropriate engineering properties has been constructed.

**6A.3.5.1 Compaction Specifications**

Most compaction specifications fall into one of two general categories—*end product specifications* or *method specifications*. In end product specifications, the desired characteristics of the compacted soil are specified, and the compaction contractor may use any equipment and procedures to produce

compacted soil that meets the requirements. In method specifications, the methods and equipment that the contractor must use to compact the soil are prescribed. In some instances, combination end product and method specifications are provided.

*End Product Specifications.* The desired engineering characteristics for a compacted soil depend significantly on the use to which the soil will be put and therefore may vary considerably from project to project and at different locations within the same project. For the bearing soils beneath a building, the most important properties (in decreasing order of importance for most projects) are (a) volume change characteristics, (b) strength, and (c) permeability. Section 6A.3.4 provided a detailed discussion of these characteristics for compacted soils.

In many end product specifications, either a criterion for dry density or criteria for density and compaction water content are furnished. These specifications are based on the assumption that the desired engineering characteristics—usually low compressibility and high strength—are related to water content and/or density. Density and water content specifications are commonly used primarily for economic reasons, that is, it is much faster and cheaper to verify that density and water content specifications have been met than to verify, for example, that compressibility and strength specifications have been met. However, the engineer writing the specifications should remember that in some instances the desired characteristics may not be achieved even if the density and water content criteria are met.

*DENSITY SPECIFICATIONS* Dry density specifications are generally given in terms of *relative compaction* (or *percent compaction*),  $R$ , defined as

$$R(\%) = \frac{\gamma_d}{\gamma_{d\max}} \cdot 100 \quad (6A.41)$$

where  $\gamma_d$  = dry density of the compacted soil

$\gamma_{d\max}$  = "maximum" dry density of the same soil

Relative compaction specifications are used rather than density specifications in most fills because of the inherent variability of the borrow soils, for which small changes in size and gradation may result in significant changes in absolute values of maximum dry density and optimum water content (Hilf, 1991). The test method from which  $\gamma_{d\max}$  is to be determined should be specified because the value of  $\gamma_{d\max}$  for any soil depends on the method of compaction and compactive effort, as discussed in Sec. 6A.3.2. The most common tests used to determine  $\gamma_{d\max}$  are the standard and modified Proctor tests (ASTM D698 and D1557, or equivalent). The same dry density specifications can be given using  $\gamma_{d\max}$  from either test, and in the United States the preferred test varies from region to region. Poulos (1988) recommends using the modified Proctor test because the test errors are likely to be smaller than for the standard Proctor test.

The importance of specifying the method from which  $\gamma_{d\max}$  is to be determined cannot be overemphasized. If the required method is not given in the specifications, the compaction contractor can legally use any reasonable method she or he wishes. The author knows of several projects in which the method was not specified, and the contractor assumed standard Proctor  $\gamma_{d\max}$  (to the contractor's advantage) when the specifying engineer intended modified Proctor  $\gamma_{d\max}$ . In these cases, either the contractor was paid more than his or her bid price to compact the soil according to modified Proctor  $\gamma_{d\max}$ , or the soil was compacted using standard Proctor  $\gamma_{d\max}$  and the compacted soil did not meet the desired criteria (which resulted in either expensive litigation or removal and replacement of the unacceptable material). The net result in each case was that more money than necessary was paid to compact the soil, an expense that could have been avoided if the engineer writing the compaction specifications had simply specified the method for determining  $\gamma_{d\max}$  rather than assume that everyone would understand what was meant.

Density requirements for clean granular soils are sometimes given in terms of *relative density* ( $D_r$ ) rather than relative compaction. Relative density can be calculated in terms of either void ratios or dry densities using one of the following equations:

**6.164** SOIL IMPROVEMENT AND STABILIZATION

$$D_r(\%) = \frac{e_{\max} - e}{e_{\max} - e_{\min}} \cdot 100 \quad (6A.42a)$$

$$D_r(\%) = \frac{\gamma_{d\max} - \gamma_d}{\gamma_{d\max} - \gamma_{d\min}} \cdot 100 \quad (6A.42b)$$

where  $e$  = void ratio of the compacted soil

$e_{\min}$  = "minimum" void ratio for the same soil

$e_{\max}$  = "maximum" void ratio for the same soil

$\gamma_{d\min}$  = "minimum" dry density for the same soil

$\gamma_{d\max}$  = "maximum" dry density for the same soil

$e_{\min}$  and  $e_{\max}$  (or  $\gamma_{d\min}$  and  $\gamma_{d\max}$ ) are commonly determined from laboratory tests as described in Sec. 6A.3.3.4. and the method on which they are to be based should be specified (usually ASTM D4253 and D4254). Nominal values of relative density vary from 0% for a soil in its "loosest" condition to 100% for a soil in its "densest" state. However, note that, because  $\gamma_{d\min}$  and  $\gamma_{d\max}$  are generally based on laboratory tests that do not exactly model field compaction, the actual values of relative density for naturally deposited and compacted soils may be less than 0 or greater than 100%. Compacted soils never have  $D_r$  less than 0% but may have  $D_r$  greater than 100% depending on the method of compaction and the procedure used to determine  $e_{\min}$  or  $\gamma_{d\max}$  (refer also to Sec. 2A).

A statistical investigation by Lee and Singh (1971) of data found in the literature for 47 granular soils has shown that values for relative density and relative compaction for any soil are related. By assuming that the values of  $\gamma_{d\max}$  in Eqs. (6A.41) and (6A.42) are the same, they obtained the following equation relating  $D_r$  to  $R$ :

$$R = \frac{R_0}{1 - D_r(1 - R_0)} \quad (6A.43)$$

where

$$R_0 = \frac{\gamma_{d\min}}{\gamma_{d\max}} \quad (6A.44)$$

The term  $R_0$  has the physical meaning of being the relative compaction at zero relative density. The mean value of  $R_0$  for the soils studied was 81.8. Inserting this value of  $R_0$  in Eq. (6A.43) yields

$$R = \frac{0.818}{1 - 0.182D_r} \quad (6A.45)$$

Sixty-seven percent of the data fell within  $\pm 1$  standard deviation. Unfortunately, the values for  $\gamma_{d\max}$  and  $\gamma_{d\min}$  from which the mean value of  $R_0$  was calculated were obtained using a wide variety of test methods, and frequently the procedures used were not adequately described in the literature. Thus, Eq. (6A.45) is of limited practical use because the bases for calculating  $R$  and  $D_r$  are not standardized to particular methods.

According to the obsolete standard ASTM D2049 (replaced by D4253 and D4254), relative density rather than relative compaction should be used if the soil contains less than 12% fines. Lee and Singh (1971) recommend using relative density for granular soils because small deviations in field density appear as large numbers (a change in relative compaction of one percentage point is approximately equivalent to a change in relative density of five percentage points) and thus tend to convey the severity of the differences to the compaction contractor. However, there appears to be a growing trend among engineers toward using relative compaction for all types of soils. For example, Poulos

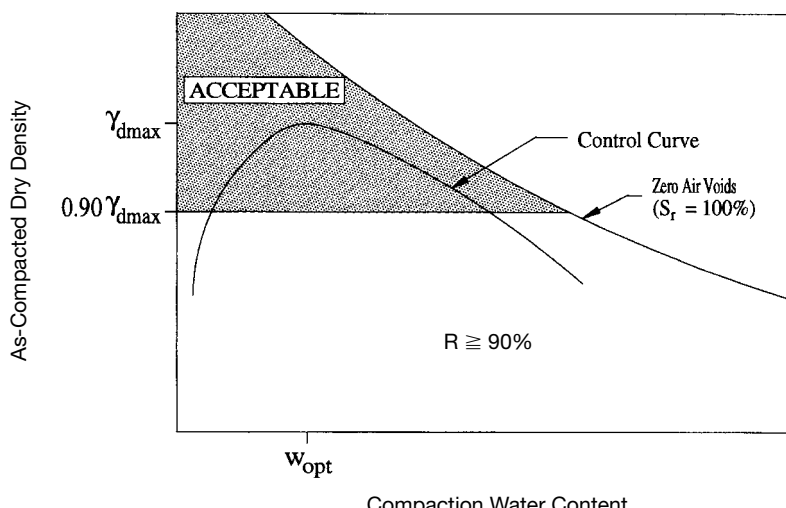
(1988) recommends against the use of relative density for compaction control of granular soils for the following reasons:

1. Both  $\gamma_{d\min}$  and  $\gamma_{d\max}$  are functions of soil composition (gradation, particle shape, mineralogy, etc.) and are linearly related (with some scatter) for most granular soils. Therefore, only one of the two factors is needed for controlling the compaction of granular soils.
2.  $\gamma_{d\min}$  is not of great interest in engineering practice.
3. Relative compaction appears to be a slightly better index of engineering properties than relative density.

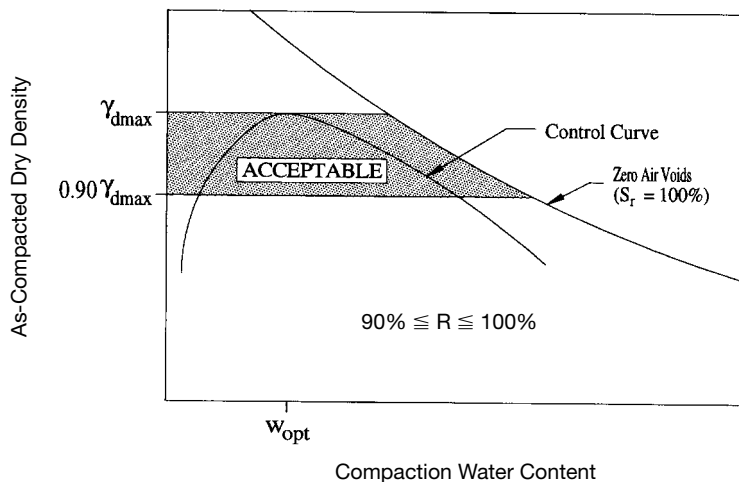
In most density specifications, only a minimum acceptable relative compaction or relative density is prescribed, which results in an allowable moisture-density range as shown in Fig. 6A.128. It may also be prudent in some instances to include a maximum acceptable relative compaction specification, as indicated in Fig. 6A.129. Typical values of relative compaction specification for different applications are summarized in Table 6A.9 and are provided only as general guidelines. Actual specifications should be based on the desired engineering characteristics and economics.

*MOISTURE CONDITION SPECIFICATIONS* The moisture condition of the soil during and after compaction determines, to a great extent, the maximum density that can be achieved with a given compaction roller, as well as the engineering characteristics of the as-compacted soil. The moisture condition of soils can be described in terms of either water content or degree of saturation. In many projects, therefore, it is imperative that the compaction specifications include some requirements as to the moisture condition of the soil during compaction. The moisture condition can be specified in terms of water content, degree of saturation, or both. In addition, because of the potential for volume changes owing to changes in the availability of free moisture, especially in compacted cohesive soils, it may be necessary to specify methods for preventing excessive drying or wetting of the compacted soil either prior to compaction of the next lift or after the compaction process is completed.

Compaction moisture condition is nearly always specified as a water content range, usually referenced to either standard or modified Proctor optimum water content. Typical water content speci-



**FIGURE 6A.128** Acceptable moisture-density region for specified minimum relative compaction.

**6.166** SOIL IMPROVEMENT AND STABILIZATION

**FIGURE 6A.129** Acceptable moisture-density region for specified minimum and maximum relative compaction.

fications for various applications are provided in Table 6A.9. When water content specifications are combined with relative compaction specifications, the resultant acceptable moisture-density zone is depicted in Fig. 6A.130. However, because of the confusion regarding optimum water content and optimum moisture condition (line of optimums) discussed in Sec. 6A.3.2, moisture condition specifications given in terms of water content only may not result in compacted soil with the desired engineering properties. For example, the permeability of a compacted clay may be several orders of magnitude lower when compacted wet of optimum than when compacted dry of optimum (see Fig. 6A.109). Optimum moisture condition refers to the line of optimums rather than one value of optimum water content referenced to some standard test. An example is given in Fig. 6A.131 showing the permeabilities that would be achieved in a compacted silty clay by specifying moisture condition as a water content range (Benson and Daniel, 1990). Because the specified water content range is above "optimum" water content, some engineers would believe that the given specifications would result in permeabilities less than the specified maximum value of  $1 \times 10^{-7} \text{ cm/s}$  ( $3 \times 10^{-4} \text{ ft/day}$ ). As can be seen in Fig. 6A.131, the actual permeabilities within some portions of the specified moisture-density zone are more than 100 times the desired maximum value.

In most compacted soils it is desirable to control more than one property. For example, in a compacted clay liner, low permeability is the dominant consideration, but moderate strength and low shrinkage potential are also desirable characteristics. An acceptable moisture-density range that would result in a compacted soil with all the desired characteristics can be established by delineating acceptable zones separately for each characteristic, as illustrated in Fig. 6A.110. Moisture-density specifications that meet the desired objectives in this type of situation can be given in terms of relative compaction and degree of saturation, as shown in Fig. 6A.132. Since many compaction personnel are familiar with the concept of water content but not degree of saturation, a water content range can also be specified to alleviate somewhat any concern they may have because of their unfamiliarity with degree of saturation, but the specifications must be clearly written to emphasize that the requirement for degree of saturation must also be met. It may also be prudent when working with cohesive soils to specify a maximum water content so that the soil remains dry enough that the hauling, spreading, and compaction equipment have sufficient traction to operate efficiently. The engineering properties of many compacted cohesive soils are better correlated with degree of satu-

**TABLE 6A.9** Typical Density, Water Content, and Lift Thickness Specifications\*

Use for compacted soil	Relative compaction <sup>†</sup> standard	Relative compaction <sup>†</sup> modified	Water content range <sup>‡‡</sup>	Lift thickness, in (mm)
Bearing soils for structures	98–100	92–95	–2 to +2	6–10 (152–254)
Lining for canal or reservoir	95	90	–2 to +2	6 (152)
Low earth dam	95	90	–1 to +3	6–12 (152–305)
High earth dam	98	93	–1 to +2	6–12 (152–305)
Highway or airfield	95	90	–2 to +2	6–12 (152–305)
Backfill surrounding structures	95–98	90–93	–2 to +2	6–10 (152–254)
Backfill in pipe or utility trenches	95–98	90–93	–2 to +2	6–8 (152–203)
Drainage blanket or filter	98	93	Thoroughly wetted	10 (254)
Subgrade of excavation for structure	98	93	–1 to +2	—
Rock fill	—	—	Thoroughly wetted	24–36 (610–914)

\*After NAVDOCKS (1961).

<sup>†</sup>All values for relative compaction and water content in percent.

<sup>‡‡</sup>Referenced to optimum water content (either standard or modified).

ration than water content. Hence, the desired engineering behavior frequently will be better achieved by specifying the as-compacted moisture condition in terms of degree of saturation rather than compaction water content.

Many compaction contractors are resistant to specifications that include degree of saturation because it cannot be measured directly but must be calculated indirectly from phase relations using an equation of the following form:

$$S_r = \frac{w}{(\gamma_w/\gamma_d) - (1/G_s)} \quad (6A.46)$$

Therefore, to calculate degree of saturation,  $\gamma_d$  and  $w$  must be measured, and  $G_s$  either estimated or determined from laboratory tests. Since  $\gamma_d$  and  $w$  are normally measured during the construction control process anyway, the only additional factor needed is  $G_s$ , which can be estimated or measured fairly easily. Because each of these three terms has an inherent variability associated with measuring it, the calculated value of  $S_r$  has a greater variability associated with it than any of the three terms from which it was calculated. This inherent variability in calculated values for degree of saturation must be considered when performing quality control and assurance checks on the compacted soil (Schmertmann, 1989). For example, this variability will result in a certain percentage of calculated values for  $S_r$  plotting above the zero air voids line, indicating that  $S_r > 100\%$ , which is physically impossible. Routinely rejecting moisture-density tests simply because they plot above the zero air

## 6.168 SOIL IMPROVEMENT AND STABILIZATION

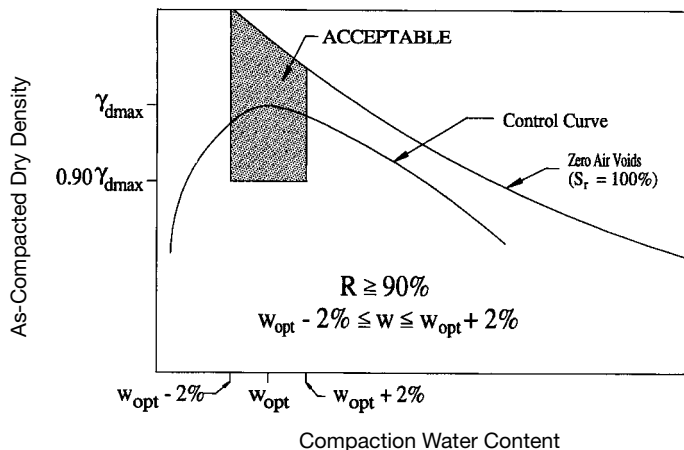


**FIGURE 6A.130** Acceptable moisture-density region for specified minimum relative compaction and water content range.

voids line may result in a fill that has a higher  $S_r$  than intended and the fill may therefore be weaker, more compressible, and more susceptible to developing high pore water pressures during construction. A detailed procedure for using test data with  $S_r > 100\%$  is given by Schmertmann (1989) (refer also to Sec. 2A).

**OTHER END PRODUCT SPECIFICATIONS** Although end product specifications are generally given in terms of dry density and water content, it is also possible—and sometimes more effective—to specify other criteria for quality control and assurance of compacted soil. The types of tests that may be used include the following:

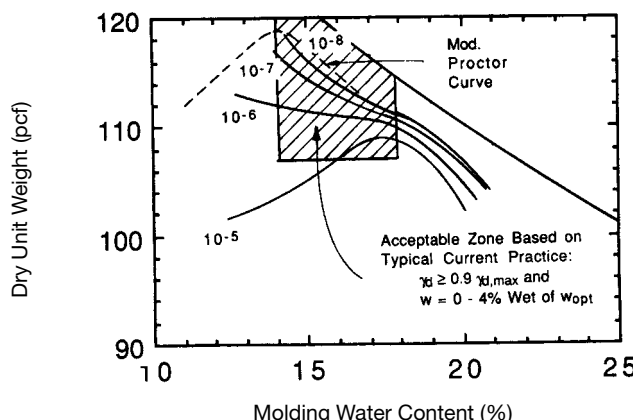


**FIGURE 6A.131** Acceptable moisture-density zone based on typical current practice superimposed on isograms of coefficient of permeability for a silty clay prepared by kneading compaction (from Daniel and Benson, 1990).

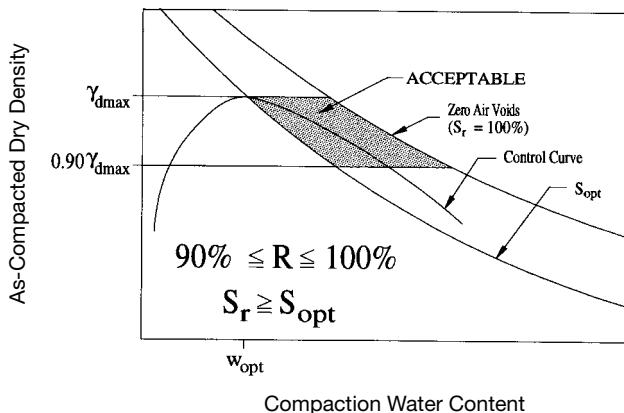


**FIGURE 6A.132** Acceptable moisture-density region for specified minimum and maximum relative compaction and minimum degree of saturation.

- Proctor penetrometer (ASTM D1558)
- Plate load test (ASTM D1194, D1195, D1196)
- California bearing ratio (CBR) test (ASTM D4429)
- Dynamic penetration test
- Unconfined compression test (ASTM D2166)
- One-dimensional compression test (ASTM D2435 and D4186)
- Triaxial compression test (ASTM D2850 and D4767)
- Standard penetration test (ASTM D1586)
- Cone penetration test (ASTM D3441)
- Sealed double ring infiltration test (ASTM D5093)
- One-dimensional swelling/collapse test (ASTM D4546)
- Laboratory permeability test (ASTM D2434 and D5084)
- Suction measured using tensiometer

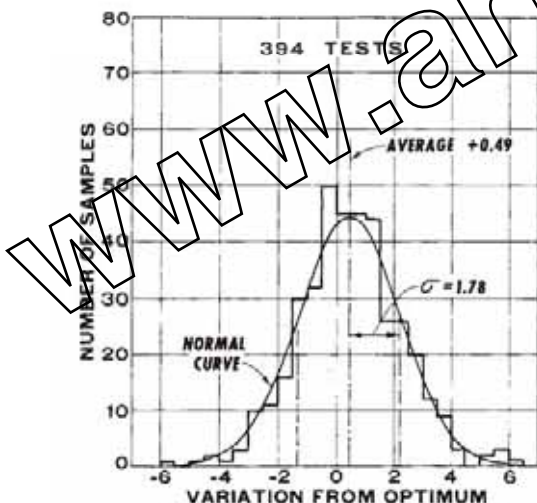
Although many of these tests are more expensive to conduct than density/water content tests, they frequently will provide better correlations with the desired engineering characteristics. For example, if settlement of a building is the primary consideration, results from plate load tests will give a better indication of the compressibility of the compacted soil than density/water content tests. Hausmann (1990) has reported that in Europe it is not uncommon to have acceptability of compacted soil specified in terms of the reload modulus determined by the plate load test. For compacted clay liners for waste containment facilities, it is often required that a sealed double ring infiltration test be performed on a field test pad constructed using the same equipment and procedures to be used on the actual liner. Laboratory permeability tests on samples taken from the actual liner are also typically required. Therefore, it is the responsibility of the engineer writing the specifications to ensure that the quality control/assurance testing procedures will result in a compacted soil that has the desired engineering characteristics. This cannot always be accomplished with density/water content criteria only, and in those instances the engineer should specify supplemental testing criteria that will assist in reliably assessing the appropriate engineering characteristics of the compacted soil.

## 6.170 SOIL IMPROVEMENT AND STABILIZATION

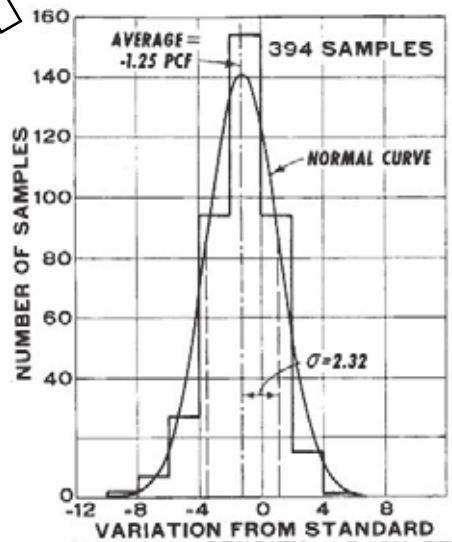
**TESTING VARIABILITY AND STATISTICAL SPECIFICATIONS** In traditional compaction specifications wherein only a minimum acceptable value or a range of acceptable values is specified for each parameter (density, water content, and so on), the acceptability of any compacted lift or portion of a lift is judged strictly by whether all measured values of that parameter fall within the acceptable range. If not, that lift or portion of the lift is deemed unsuitable and must be either recompacted in place to a greater density (if the water content is acceptable) or removed, moisture conditioned, and recompacted to meet the specifications. However, these traditional specifications do not consider the inherent variability of the soil and the variation between measured values and true values. Therefore, in recent years it has become more common to base compaction specifications and quality control on statistical considerations of soil and testing variability.

Compacted soil masses, whether compacted fills or natural soil deposits compacted at their original location, often vary considerably in terms of their composition and engineering characteristics. In addition, all tests conducted on the field-compacted soil or on samples taken therefrom all have some inherent inaccuracies, that is, the measured values will always vary from the "true" value by some amount. The more accurate the test, the less deviation between measured and true values. The accuracy of a particular test depends on random errors and systematic errors related to the particular equipment being used and the operator (Hausmann, 1990). Because of the many variables associated in testing compacted soils, the results of water content and density tests tend to be normally distributed (Turnbull et al., 1966; Hausmann, 1990). As an example, the distribution of water content variation from optimum and dry density variation from maximum dry density for the impervious fill of Ferrells Bridge dam are shown in Fig. 6A.133.

In a statistical approach to specification and control, it is recognized that measured values of density and water content will vary from the desired values. If the measured values are normally distributed about the desired value, every undervalue is balanced by an overvalue, and if the stan-



(a)



(b)

**FIGURE 6A.133** Variation in (a) compaction water content and (b) as-compacted dry density for the impervious fill of Ferrells Bridge dam (from Turnbull et al., 1966).

dard deviation is relatively small, the overall behavior of the compacted soil is not likely to be much different than if the entire soil had been compacted to the desired value. Therefore, some deviation from the desired value may be acceptable, so long as there is no large, contiguous zone of material for which the minimum acceptable value is not met.

The following abbreviated specifications for Cutler Dam illustrate the use of statistical control of compaction based on frequency distribution concepts (from Hilf, 1991). Note that these specifications are referenced to optimum water content and maximum dry density from the modified Proctor test.

1. *Moisture control.* The moisture content of the earthfill prior to and during compaction shall be distributed uniformly throughout each layer of the material. In addition, the moisture content of the compacted earthfill determined by testing shall be within the following limits.
  - a. If  $w < w_{opt} - 3.5\%$  or  $w > w_{opt} + 1.0\%$ , the material shall be removed or reworked until the water content is between these limits.
  - b. No more than 20% of the samples shall be drier than  $w_{opt} - 3\%$ , and no more than 20% of the samples shall be wetter than  $w_{opt} + 0.5\%$ .
  - c. The average water content of all accepted embankment material shall be between  $w_{opt} - 1.0\%$  and  $w_{opt} - 0.5\%$ .
  - d. As far as practicable, the material shall be brought to the proper water content in the borrow pit before excavation. Supplementary water, if required, shall be added to the material by sprinkling on the earthfill on the embankment, and each layer of the earthfill shall be conditioned so that the moisture is uniform throughout the layer.
2. *Density control.* The dry density of the compacted material shall conform to the following limits:
  - a. Material will be rejected if  $R < 96.0\%$ . Rejected material shall be rerolled until  $R \geq 96.0\%$ .
  - b. No more than 20% of the samples shall have  $R < 97.0\%$ .
  - c. The average density of all material shall be greater than or equal to  $R = 100\%$ .

*Method Specifications.* Method specifications typically prescribe the type of equipment to be used, the thickness of the lift to be compacted, and the number of passes of the equipment per lift (Hilf, 1991). Moisture requirements and a maximum size of material may also be specified. The most important advantages and disadvantages of method specifications are summarized as follows (Holtz and Kovacs, 1981):

1. An expensive field testing program generally must be conducted to determine the most efficient and economical methods and equipment for obtaining a compacted soil with the desired characteristics. Method specifications, therefore, are normally used only on major compaction projects such as earth dams.
2. A major part of the uncertainty associated with compaction will be eliminated for the contractor. Therefore, the contractor should be able to estimate the construction costs more accurately, and a substantial savings in earthwork costs should be realized.
3. The owner or owner's engineer has the major portion of the responsibility for the quality of the earthwork rather than the contractor. If the contractor follows the specifications but the compacted material does not meet the desired characteristics, the contractor will be paid extra for any work needed to make the material meet the requirements.

#### **6A.3.5.2 Postcompaction Testing and Verification**

*Moisture-Density Tests.* The most common type of postcompaction testing and verification program consists of density and water content tests conducted at random locations within the compacted material. In many fills, at least several tests are conducted on each lift. The frequency with which moisture-density tests are conducted in compacted fills varies considerably, with typical values as follows (after Hausmann 1990 and Hilf 1991):

**6.172** SOIL IMPROVEMENT AND STABILIZATION

Type of fill	Volume of fill per test, yd <sup>3</sup> or m <sup>3</sup>
Embankment	500–4000
Impermeable liner	200–1000
Subgrade	500–1500
Base course	500–1000
Backfill	100–500

Additional tests should be conducted when the borrow material changes significantly. If the surface of the most recent lift is uneven (e.g., sheepfoot or tamping foot roller) or some densification may occur during compaction of overlying lifts (e.g., sand), testing should be done one or two lifts below the top lift. To avoid potential bias of testing personnel, the locations for moisture-density testing should be randomly selected (that is, each location should have the same chance for being chosen). This can be accomplished using a table of random numbers such as that shown in Table 6A.10 or by generating random numbers on a computer or handheld calculator. The following example is given to illustrate the procedure for randomly selecting locations for testing (from Sherman et al., 1967):

A compacted lift is 30,000 ft (9,144 m) long and 26 ft (7.92 m) wide, and 50 moisture-density tests will be conducted. Starting at any point in the random number table and proceeding up or down (but not omitting any numbers), 50 pairs of numbers are read. For example, starting at the top of column 4, the following pairs of numbers are read: (.732, .721); (.153, .508); (.009, .420); . . . (.698, .539). The first or A number in each pair is multiplied by the length, and the second or B number in each pair is multiplied by the width to establish the locations for testing. Using the first pair of numbers, a moisture-density test would be conducted at (21,960 ft, 19 ft) or (6693 m, 5.7 m). The locations of the 50 tests are then plotted and numbered in the order in which they will be performed. Should two locations be so close together that they both could not be tested properly, the second one is discarded and the next pair of numbers in the table is substituted.

*SAND CONE AND RUBBER BALLOON TESTS* Moisture-density tests can be either destructive (fill material is excavated and removed) or nondestructive (density and water content are determined indirectly). The most common destructive tests are the sand cone test (ASTM D1556) and the rubber balloon method (ASTM D2167) (Fig. 6A.134). The following steps are used in these tests (after Holtz and Kovacs, 1981):

1. A hole is excavated in the compacted fill at the desired elevation. The size of the hole depends on the maximum size of included particle in the excavated material (ASTM D1556 and D2167):

Sand cone				Rubber balloon			
Maximum particle size		Minimum test hole volume		Maximum particle size		Minimum test hole volume	
in	mm	ft <sup>3</sup>	cm <sup>3</sup>	in	mm	ft <sup>3</sup>	cm <sup>3</sup>
½	12.5	0.05	1420	No.4 sieve	4.75	0.04	1130
1	25	0.075	2120	¾	19.0	0.06	1700
2	50	0.1	2830	1½	37.5	0.10	2840

The mass or weight of the excavated material is determined in the field using a scale or balance.

2. The water content is determined from either the total excavated material or a representative sample taken from the excavated material. The standard water content procedure consists of oven drying the sample at 110°C (230°F) (ASTM D2216). If the total excavated material is not used, requirements for minimum mass of the representative sample are given in ASTM D2216. The material is dried in the oven until a constant mass is reached. The time required to obtain con-

**TABLE 6A.10** Random Numbers for Selecting Locations of Field Testing (from Sherman et al., 1967)

1		2		3		4		5	
A	B	A	B	A	B	A	B	A	B
.576	.730	.430	.754	.271	.870	.732	.721	.998	.239
.892	.948	.858	.025	.935	.114	.153	.508	.749	.291
.669	.726	.501	.402	.231	.505	.009	.420	.517	.858
.609	.482	.809	.140	.396	.025	.937	.310	.253	.761
.971	.824	.902	.470	.997	.392	.892	.957	.640	.463
.053	.899	.554	.627	.427	.760	.470	.040	.904	.993
.810	.159	.225	.163	.549	.405	.285	.542	.231	.919
.081	.277	.035	.039	.860	.507	.081	.538	.986	.501
.982	.468	.334	.921	.690	.806	.879	.414	.106	.031
.095	.801	.576	.417	.251	.884	.522	.235	.398	.222
.509	.025	.794	.850	.917	.887	.751	.608	.698	.683
.371	.059	.164	.838	.289	.169	.569	.977	.796	.996
.165	.996	.356	.375	.654	.979	.815	.592	.348	.743
.477	.535	.137	.155	.767	.187	.579	.787	.358	.595
.788	.101	.434	.638	.021	.894	.324	.871	.698	.539
.566	.815	.622	.548	.947	.169	.817	.472	.864	.466
.901	.342	.873	.964	.942	.985	.123	.086	.335	.212
.470	.682	.412	.064	.150	.962	.925	.355	.909	.019
.068	.242	.667	.356	.195	.313	.396	.460	.740	.247
.874	.420	.127	.284	.448	.215	.833	.652	.601	.326
.897	.877	.209	.862	.428	.117	.100	.259	.425	.284
.875	.969	.109	.843	.759	.239	.890	.317	.428	.802
.190	.696	.757	.283	.666	.491	.523	.665	.919	.146
.341	.688	.587	.908	.865	.333	.928	.404	.892	.696
.846	.355	.831	.218	.945	.364	.673	.305	.195	.887
.882	.227	.552	.077	.454	.731	.716	.265	.058	.075
.464	.658	.629	.269	.069	.998	.917	.217	.220	.659
.123	.791	.503	.447	.659	.463	.994	.307	.631	.422
.116	.120	.721	.137	.263	.176	.798	.879	.432	.391
.836	.206	.914	.574	.870	.390	.104	.755	.082	.939
.636	.195	.614	.486	.629	.663	.619	.007	.296	.456
.630	.673	.665	.666	.399	.592	.441	.649	.270	.612
.804	.112	.331	.606	.551	.928	.830	.841	.602	.183
.360	.193	.181	.399	.564	.772	.890	.062	.919	.875
.183	.651	.157	.150	.800	.875	.205	.446	.648	.685

stant mass depends on such factors as type of material, size of specimen, and oven type and capacity. As a general rule of thumb, sands will dry to constant mass in about 4 h, whereas highly plastic soils may require 16 h or more. For most compaction projects, even 4 h is unacceptable for proper control of compacted fills, and one of the following faster but approximate methods are commonly used (after Hilf, 1991):

- a. The Proctor penetration needle, used to determine the field-compacted water content by comparing the penetration resistance of the field-compacted soil with a calibration curve of penetration resistance versus water content from tests on Proctor specimens. (Additional details are given below.)

## 6.174 SOIL IMPROVEMENT AND STABILIZATION

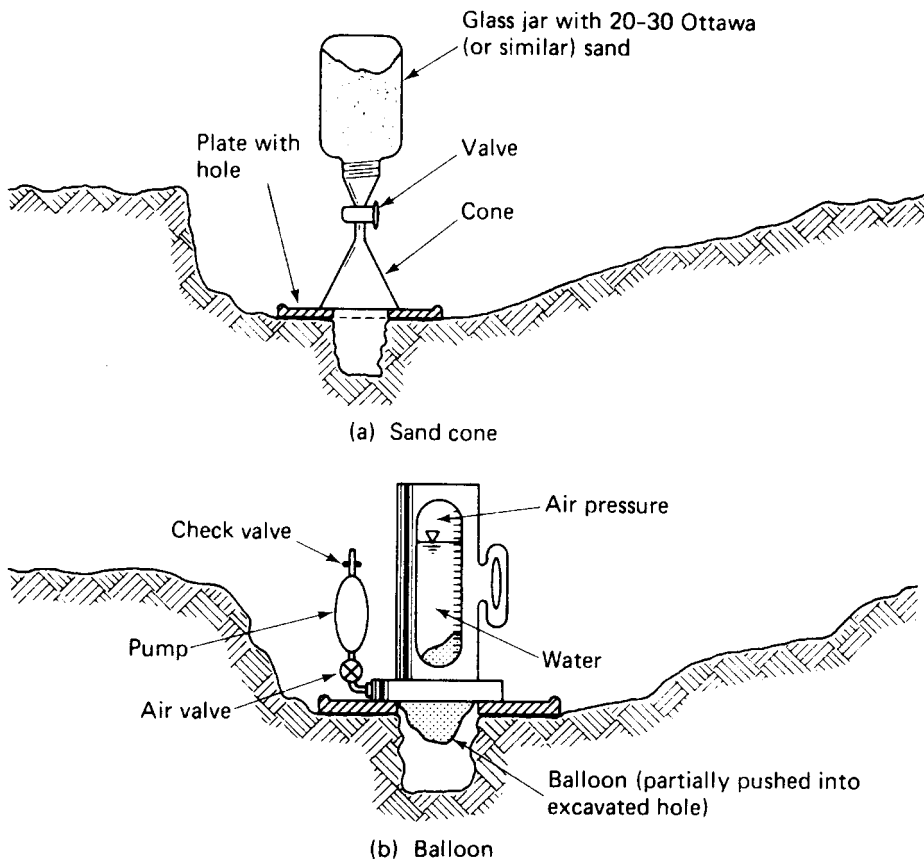


**FIGURE 6A.134** Schematic illustrations of sand cone and rubber balloon tests (from Holtz and Kovacs, 1981).

- b. Alcohol burning method (HRB, 1952).
  - c. Bouyoucos alcohol method using a hydrometer (Bouyoucos 1931).
  - d. A moisture meter using calcium carbide to generate acetylene in a closed container connected to a pressure gauge (Reinhold 1955; ASTM D4944).
  - e. Drying the soil in a container using any of a variety of types of direct heating equipment, such as a hotplate, stove, or blowtorch (ASTM D4959).
  - f. Drying the soil in a microwave oven (ASTM D4643).
- If one or more of these approximate methods are used, they must somehow be correlated with the oven-drying method. Usually this involves testing duplicate samples at selected intervals using the oven-drying method, and comparing the result with the result from the approximate method being used.
3. The original volume of the excavated material is determined by measuring the volume of the hole.
    - a. *Sand cone*. Clean, dry, uniform sand of known “loose” density is allowed to flow through a cone-shaped pouring device into the hole. The volume of the hole is calculated from the

weight of the sand in the hole (by weighing the sand container before and after placing the sand) and the calibrated loose dry density of the sand. Care must be taken to ensure that the loose sand is not densified by vibrations from any source, such as construction vehicles, nearby pile driving or blasting operations, or personnel walking near the hole. In soft soils, volume changes of the hole may occur by deformations induced by personnel (including those performing the test) who walk or stand close to the hole. In dry, cohesionless soils, raveling of the sides of the hole may occur by personnel or vibrations.

- b. *Rubber balloon.* The volume of the hole is determined by expanding the balloon directly into the hole and reading the change in volume of the water in the apparatus directly from the calibration marks. As with the sand cone test, care must be exercised to avoid deformation of the hole in soft soils or raveling of the sides of the hole in loose, dry, cohesionless soils.
4. Compute the total density and dry density of the compacted soil ( $\gamma_{\text{field}}$  and  $\gamma_{d\text{-field}}$ ) from the total mass or weight of material excavated from the hole, the volume of the hole, and the water content.
5. Compare  $\gamma_{d\text{-field}}$  with  $\gamma_{d\text{max}}$  and calculate relative compaction ( $R$ ).

The following destructive methods are also sometimes used.

*DRIVE-CYLINDER METHOD (ASTM D2937)* This method involves driving a short, thin-walled cylinder into the soil using a special drop-hammer sampler. The cylinder is dug from the ground, excess soil is removed from the sides of the cylinder, and the ends of the sample are trimmed flush with the ends of the cylinder using a sharpened straightedge. The volume of the sample is equal to the inner volume of the cylinder. The total mass is determined by separately weighing the cylinder only (usually before sampling) and the cylinder with the trimmed sample. Water content tests are also performed, from which the dry density is calculated. This method is not appropriate for organic soils, very hard soils, soils of low plasticity that will not readily stay in the cylinder, or soils which contain appreciable amounts of coarse material.

*SLEEVE METHOD (ASTM D4564)* The sleeve method is used primarily for soils that are predominantly fine gravel size, with a maximum of about 5% fines, and a maximum particle size of 0.75 in (19 mm). The density is obtained by rotating a metal sleeve into the soil, removing the soil from the sleeve, and calculating the dry mass of soil removed per linear inch (per linear 25 mm). The mass per inch is correlated with the dry density of the in-place material using a calibration equation that has been predetermined for the soil being tested. Details can be found in ASTM D4564.

*TEST PIT METHODS (ASTM D4914 AND D5030)* In these methods, a test pit is excavated in materials containing particles larger than about 3 in (75 mm). Test pit methods are generally limited to unsaturated materials and are not recommended for materials that are soft or friable or where water will seep into the excavated hole. Two methods are used which differ primarily by the manner in which the volume of the test pit is determined. In the *sand replacement method*, calibrated sand is poured into the excavated hole, and the mass of sand within the pit is determined. The volume of the hole is determined from the calibrated density of the sand and the total mass of sand within the hole in the same manner as for the sand cone test. In the *water replacement method*, an impervious liner is placed on the surface of the test pit, water is poured into the pit up to the appropriate level, and the mass or volume of the water within the pit is measured. Comparisons for the two tests are given below:

	Sand replacement	Water replacement
Maximum particle size	3–5 in (75–125 mm)	>5 in (>125 mm)
Excavated volume	1–6 ft <sup>3</sup> (0.03–0.17 m <sup>3</sup> )	3–100 ft <sup>3</sup> (0.08–2.83 m <sup>3</sup> )

*NUCLEAR METHODS* The use of nondestructive nuclear methods for moisture density testing of soils (ASTM D2922) has become increasingly popular in recent years because both density and water content readings can be obtained within a few minutes, which allows rapid feedback on the quality of the compacted soil. Density is determined by the emission of electromagnetic radiation (gamma rays or photons) from a radioactive source (usually either radium or cesium), as shown in Fig.

**6.176** SOIL IMPROVEMENT AND STABILIZATION

6A.135. Some of the gamma rays are absorbed by the soil particles while others are reflected. The number of photons reaching the detector (usually a Geiger-Mueller tube) is an indication of the total density of the soil; a lesser number of photons reaching the detector indicates a denser soil. Three modes of operation can be used. In the *backscatter* mode, the source and detector are on the bottom of the gauge and only about the top 2 to 3 in (50 to 75 mm) of the soil is tested. The backscatter technique is very sensitive to surface roughness and quality of site preparation (U.S. Army, 1985) and is not recommended for general use in soils. The gamma source is lowered into the ground through a hole punched into the soil in the *direct transmission* mode, which is therefore a pseudonondestructive technique. The depth of measurement can be varied in 1- or 2-in (25- or 50-mm) increments on most gauges, allowing a better measurement of the average density in a lift. The air gap mode, in which an open space is maintained between the bottom of the gauge and the ground surface, may also be used. Density calibration is achieved using standard blocks consisting of mate-

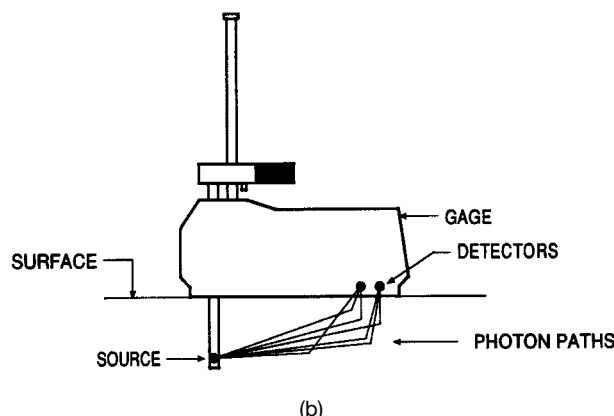
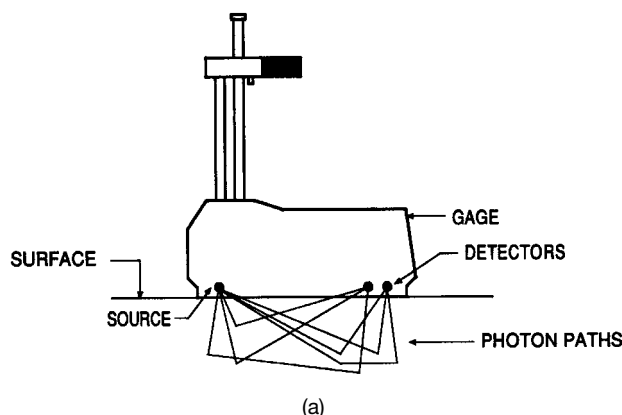


**FIGURE 6A.135** Measurement of density using a nuclear density meter: (a) backscatter; (b) direct transmission (after Troxler Electronic Laboratories, Inc., Research Triangle Park, NC).

rials of known density. Best calibration occurs using blocks of uniform rock because these materials best simulate those found in soils (Hausmann, 1990). Limestone and granite blocks are recommended in ASTM D2922. The gauge should be calibrated every day prior to testing. Sand cone or rubber balloon tests are commonly conducted at selected intervals of nuclear testing to provide comparison with the density and moisture results obtained from the nuclear gauges.

The measurement of moisture is nondestructive and is accomplished in the backscatter mode by emitting fast neutrons from a radioactive source (usually americium mixed with beryllium) located in the base of the gauge. The detector (usually a boron trifluoride or helium 3 tube) can only detect slow (thermal) neutrons and is also located in the base at some distance from the source. Hydrogen is the only atom normally found in soils that can slow down the neutrons to a level where they can be detected, and thus the moisture detector is really a hydrogen analyzer (U.S. Army, 1985). The moisture per unit volume of the soil is related to the total hydrogen content of the soil, and the water content (per unit mass of dry solids) can be calculated if the density is known. If hydrogen is present in the soil in any form other than free water, errors in measuring the water content will occur. Such errors may occur from the presence of various forms of hydrogen, including the following (U.S. Army, 1985; Hausmann, 1990):

1. Water of hydration in the mineral matrix
2. Organic matter
3. Oil or bitumen
4. Geosynthetics which contain hydrogen

Another factor which affects the accuracy of water content determined from a nuclear gauge is absorption interaction (Ballard and Gardner, 1965). Certain elements—particularly boron and cadmium, and to a lesser extent chlorine and iron—will absorb thermal neutrons to a very high degree. Thus, the presence of these elements in significant quantities may substantially affect the accuracy of the measured water content.

The major advantages and disadvantages of using nuclear gauges for moisture-density determination are summarized as follows (after Holtz and Kovacs, 1981 and Hausmann, 1990). Advantages of nuclear gauges are:

1. Tests can be performed quickly and results obtained within minutes. If necessary, corrective action can be taken before much additional fill has been placed.
2. Better statistical control of the fill is obtained because more tests can be conducted in the same amount of time.
3. The use of nuclear gauges on large projects or over extended periods is often more economical than other alternatives.

Disadvantages of nuclear gauges include:

1. The use of nuclear gauges is regulated by governmental agencies concerned with radiation safety. A radiation license must be obtained by the organization using the nuclear equipment.
2. Personnel using and supervising the use of nuclear gauges must be licensed and trained.
3. Operators are exposed to very small amounts of radiation and must wear film badges that monitor their exposure to radiation.
4. Extraordinary care must be taken during storage and transport of the gauges. If the seal containing the radioactive source is broken or is possibly broken, such as by a construction accident, a large area surrounding the gauge must be evacuated and the appropriate governmental agency notified. This may result in the shutdown of the entire construction project—and possible evacuation of nearby buildings and shutdown of nearby roads—for several hours or days while the status of the radioactive source is determined and necessary remedial measures taken.
5. Excessive concern or fear of the uninformed public and some transportation authorities when the radiation warning labels are sighted.

**6.178** SOIL IMPROVEMENT AND STABILIZATION

6. The initial cost of a nuclear gauge is relatively high compared to other moisture-density testing equipment.
7. There are differences in measured values of density and water content obtained using nuclear gauges versus the traditional tests (sand cone or rubber balloon for density, oven drying for moisture). Since some engineers consider the values obtained from the traditional tests to be "correct" even though those tests are also subject to inaccuracies, some engineers and governmental agencies have prohibited the use of nuclear gauges on some projects.
8. As discussed previously, there are some problems associated with determining density and moisture content indirectly using nuclear methods for certain soils and conditions. In some instances, therefore, the nuclear gauges simply will not give reliable or correctable answers. However, in most cases, if comparisons are made at selected intervals with the method specified as the standard, reliable values for density and water content can be obtained directly from the gauges or by applying corrections based on comparison with the values obtained from the specified standard test.

*HILF'S RAPID METHOD* Because of the problems associated with determining the water content of field-compacted cohesive soils—the long time required for oven drying and the differences in values obtained by the faster methods compared to those obtained by oven drying—Hilf (1959) developed a method that rapidly gives an exact value for standard Proctor relative compaction ( $R_s$ ) and a close approximation of the field water content relative to the standard Proctor optimum water content ( $w_{os}$ ). This method has been used satisfactorily on about 150 earth dams since 1957 and has been adopted for control of all compacted cohesive soils on U.S. Bureau of Reclamation projects (Hilf, 1991). The theoretical background and procedure for using this rapid method of field control is given as follows (after Hilf, 1991):

1. Excavate a field density hole in the compacted soil, weigh the excavated material, and determine the volume of the hole. Calculate the total density of the field-compacted soil ( $\gamma_f$ ) from the total weight and total volume. The amount of material removed should be enough to perform two reliable oven-dried water content tests and at least three standard Proctor tests without reusing any of the excavated material.
2. Perform a water content test by placing the excavated material in an oven at the site immediately after weighing it and drying the soil in the oven for a minimum of 16 h at 110°C (230°F) (preferred), or by placing the soil in an airtight container and transferring it to a laboratory for oven drying.
3. Conduct a minimum of three Proctor tests on the excavated material—one at the field water content and at least two others at different water contents.
4. Plot the results from the Proctor tests as total density ( $\gamma$ ) versus added water in percentage of the total weight of the soil ( $Z$ ), as shown by curve A in Fig. 6A.136.  $Z$  may be either positive or negative; that is, the water content of the soil during the Proctor tests can be either greater than or less than the water content of the field-compacted soil. Note that  $\gamma_t = \gamma_d(1 + w_p)$ , where  $w_p$  is the water content of the field-compacted soil. A relationship between  $Z$  and  $w$  (the water content of the soil for any Proctor test) can be developed as follows:

$$\Delta W_w = W_s \cdot \Delta w = W_s \cdot (w - w_f) \quad (6A.47)$$

$$W_f = W_s \cdot (1 + w_f) \quad (6A.48)$$

$$Z = \frac{\Delta W_w}{W_f} = \frac{W_s \cdot (w - w_f)}{W_s \cdot (1 + w_f)} = \frac{w - w_f}{1 + w_f} \quad (6A.49)$$

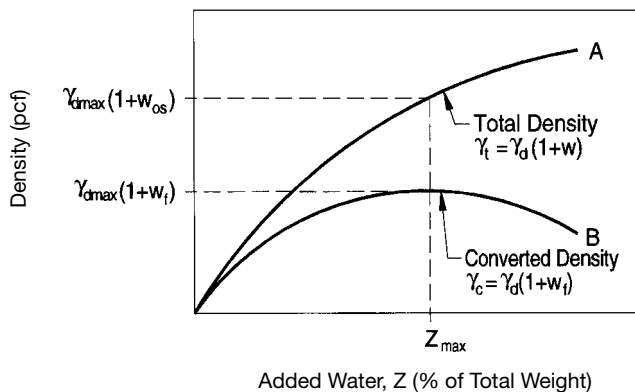


**FIGURE 6A.136** Compaction curves for Hilf's rapid method of control (after Hilf, 1990).

where  $\Delta W_w$  = weight of water added or removed from soil

$W_s$  = weight of the solids (dry weight of the soil)

$\Delta w$  = change in water content of the soil

$w_f$  = water content of the field-compacted soil

$W_{tf}$  = total weight of the soils at  $w_f$

5. Calculate the converted density ( $\gamma_c$ ) for each of the Proctor tests as follows:

$$\gamma_c = \frac{\gamma_t}{1 + Z} = \frac{\gamma_d \cdot (1 + w)}{1 + \frac{w - w_f}{1 + w_f}} = \frac{\gamma_d \cdot (1 + w)}{\frac{1 + w}{1 + w_f}} = \gamma_d \cdot (1 + w_f) \quad (6A.50)$$

Plot a curve of  $\gamma_c$  versus  $Z$  (curve  $B$  in Fig. 6A.136). Curve  $B$  can be drawn with only three data points by assuming that the curve is parabolic and using the method shown in Fig. 6A.137.

6. Obtain  $Z_{\max}$  as the abscissa at the peak point of curve  $B$ . Since  $w_f$  is a constant for every point on curve  $B$ , the maximum ordinate of curve  $B$  must have the value of  $\gamma_{d\max}(1 + w_f)$ . Dividing this value into  $\gamma_t$  gives the desired value of relative compaction as follows:

$$R_s = \frac{\gamma_t}{\gamma_{d\max} \cdot (1 + w_f)} = \frac{\gamma_{df} \cdot (1 + w_f)}{\gamma_{d\max} \cdot (1 + w_f)} = \frac{\gamma_{df}}{\gamma_{d\max}} \quad (6A.51)$$

7. Estimate  $w_{os}$  from Fig. 6A.138, which shows a best-fit curve of  $\gamma_t$  versus  $w_{os}$  based on data from 1300 specimens. Estimate  $(w_{os} - w_f)$  and  $w_{os}$  from the following equation:

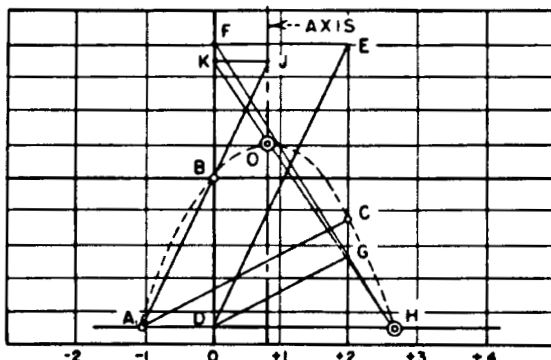
$$w_{os} - w_f = Z_{\max} \cdot (1 + w_f) = \frac{Z_{\max} \cdot (1 + w_{os})}{1 + Z_{\max}} \quad (6A.52)$$

$$w_{os} = w_f + (w_{os} - w_f) \quad (6A.53)$$

The estimate of  $(w_{os} - w_f)$  obtained in this manner is usually very close to the actual value and can be used to determine the acceptability of the field-compacted soil in terms of moisture con-

**Parabola Method**

Graphical solution for vertex, O, of a parabola whose axis is vertical, given three points A, B, and C. If more than three points are available, use the three closest to optimum.



1. Draw horizontal base line through the left point, A, and draw vertical lines through points B and C.
2. Draw line DE parallel to AB, point E lies on the vertical line through point C, project E horizontally to establish point F on the vertical line through B.
3. Draw line DG parallel to AC, point G lies on the vertical line through point C.
4. Line FG intersects the base line at H. Axis of parabola bisects AH, draw the axis.
5. Intersection of line AB with the axis is at J, project J horizontally to K, which lies on the vertical line through point B.
6. Line KH intersects the axis at O, the vertex.

**NOTE:** If points A, B, and C are equally spaced horizontally (this is true when 2 points are obtained by adding water or when soil is dried exactly 2 percent) steps 2 and 3 above are eliminated. Point F coincides with point B and point G is halfway between the base line and point C. Hence, point H is obtained by drawing BG and point O is obtained by steps 5 and 6 as usual. See graph below.

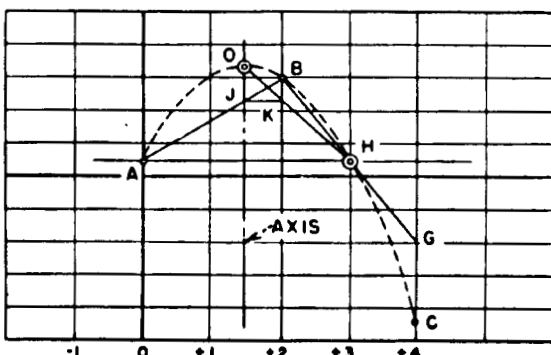


**FIGURE 6A.137** Hilf's parabolic method for obtaining the peak point for the curve of converted density versus added water based on three data points (from Hilf, 1991).

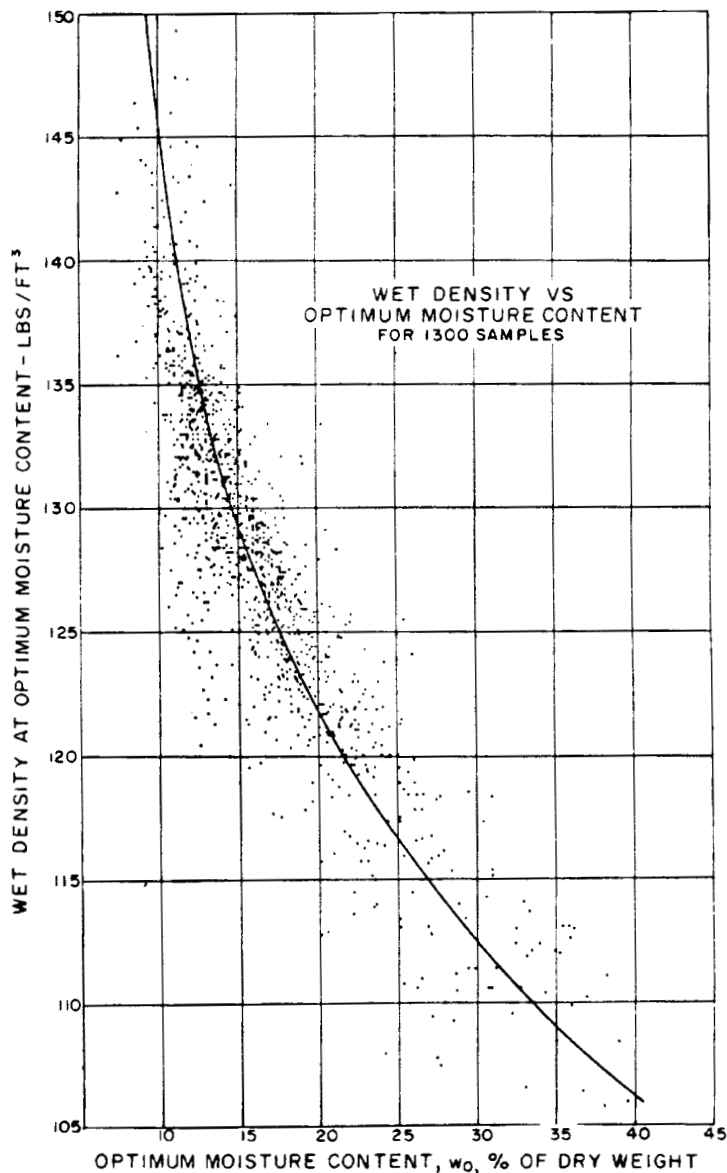


**FIGURE 6A.138** Best-fit curve for total (wet) density versus standard Proctor optimum water content based on data from 1300 specimens (from Hiltf, 1991).

**6.182** SOIL IMPROVEMENT AND STABILIZATION

dition only when the moisture condition is specified in terms of a range of water contents referenced to  $w_{os}$ . The value of  $w_{os}$  obtained from Eqs. (6A.52) and (6A.53) is an approximation only and may vary significantly from the actual value of  $w_{os}$ .

8. After the oven-dried water content has been determined, calculate the actual values of  $R_s$  and  $(w_{os} - w_f)$  and compare with the estimated values determined previously. Both values of  $R_s$  should be the same, and the actual value of  $(w_{os} - w_f)$  should be close to the estimated value.

The following is an abbreviated example given to illustrate the procedure (from Hilf, 1991): From a field density test we have  $\gamma_{tf} = 127.5$  pcf (20.03 kN/m<sup>3</sup>), and from standard Proctor tests on excavated material we have these values:

Point	Z, %	$\gamma_t$		$\gamma_c$	
		pcf	kN/m <sup>3</sup>	pcf	kN/m <sup>3</sup>
1	0	123.4	19.39	123.4	19.39
2	2	128.6	20.20	126.1	19.81
3	4	124.6	19.57	119.8	18.82

By the parabolic method:

$$Z_{\max} = 1.6\%$$

$$\gamma_{d\max}(1 + w_f) = 126.3 \text{ pcf (19.84 kN/m}^3)$$

From Eq. (6A.51):

$$R_s = \frac{127.5}{126.3} \cdot 100 = 101.0\%$$

From Fig. 6A.138:

$$w_{os} \cong 16.0\%$$

From Eq. (6A.52):

$$w_{os} - w_f = \frac{1.6 \cdot (1 + 0.160)}{1 + 0.016} = +1.8\% \text{ (dry of } w_{os})$$

After oven-drying water content specimens, the actual values are calculated as follows:

$$w_f = 15.0\%$$

$$\gamma_{df} = \frac{\gamma_{tf}}{1 + w_f} = \frac{127.5}{1 + 0.150} = 110.9 \text{ pcf (17.42 kN/m}^3)$$

$$\gamma_{d\max} = \frac{\gamma_{d\max} \cdot (1 + w_f)}{1 + w_f} = \frac{126.3}{1 + 0.150} = 109.8 \text{ pcf (17.25 kN/m}^3)$$

$$R_s = \frac{\gamma_{df}}{\gamma_{dmax}} = \frac{110.9}{109.8} \cdot 100 = 101.0\% \text{ (checks exactly with previous value)}$$

$$w_{os} - w_f = Z_{\max} \cdot (1 + w_f) = 1.6 \cdot (1 + 0.150) = 1.8\% \text{ (checks exactly with previous value)}$$

$$w_{os} = w_f + (w_{os} - w_f) = 15.0 + 1.8 = 16.8\% \text{ (compared to estimated 16.0\%)}$$

*Other Verification Tests.* As noted in Section 6A.3.5.1, many different types of tests may be used to verify that the compacted soil will be acceptable from an engineering standpoint. Some of these tests are discussed in more detail here.

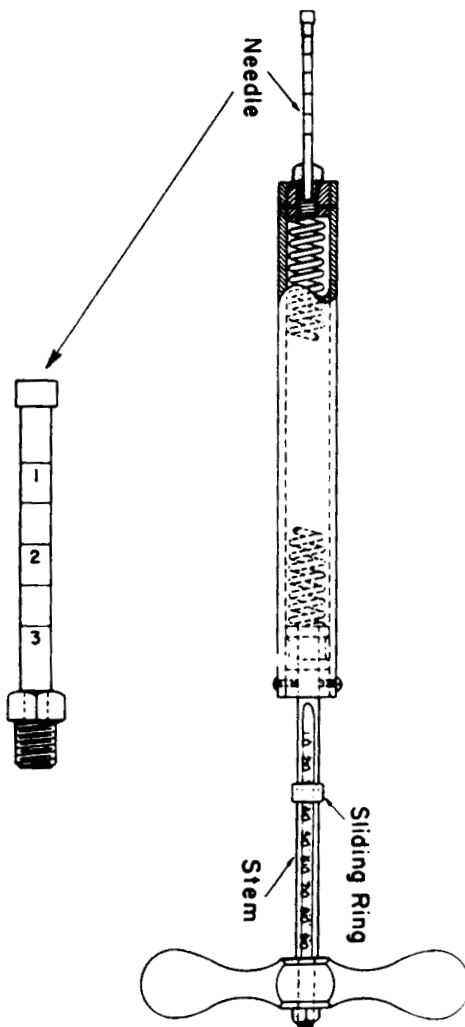
*PROCTOR PENETROMETER (ASTM D1558)* Proctor (1933) developed the soil plasticity needle—now more commonly known as the *Proctor penetrometer*—to assist in evaluating the suitability of compacted soils for use in earth dam construction. A modern version of the penetrometer is depicted in Fig. 6A.139 and can be used in the field and the laboratory. It consists of a special spring dynamometer with a pressure-indicating stem on the handle that is graduated to 90 lb in 2-lb divisions with a line encircling the stem at each 10-lb interval (or 45 kg in 1-kg divisions with a line at each 5-kg interval). The needle is pushed into the field-compacted soil or laboratory-compacted specimen at a rate of 0.5 in/s (13 mm/s) for a distance of at least 3 in (76 mm). As the spring deflects under load, a sliding ring on the stem indicates the developed force and remains at the maximum value as the force decreases during additional penetration beyond the point where the maximum force is developed. Interchangeable needles with heads varying in area from 0.025 in<sup>2</sup> (0.16 cm<sup>2</sup>) to 1 in<sup>2</sup> (6.45 cm<sup>2</sup>) are available so that the maximum force in any soil can be measured within a consistent range (40 to 80 lb or 10 to 20 kg according to ASTM D1558). The maximum penetration resistance is calculated as the maximum force divided by the area of the head.

The procedure used to determine the acceptability of field-compacted soils is as follows:

1. Establish the relationship between maximum penetration resistance and compaction water by conducting tests on Proctor specimens compacted in the laboratory or field, or on field-compacted test pad sections, for the soil compacted at various water contents with the same method and energy. A minimum of three tests at different water contents is specified by ASTM D1558, but at least five tests are recommended by the author.
2. Plot the results of the penetrometer tests on the same graph with the moisture-density results, as illustrated in Fig. 6A.140. Conduct laboratory or field tests to correlate penetration resistance with the desired engineering properties. Establish an acceptable range of penetration resistances. For bearing situations where strength and settlement are the most important engineering characteristics, a minimum value of penetration resistance is usually prescribed. The specifications can also be in the form of a range of values.
3. Conduct penetrometer tests at random locations within each compacted lift using a procedure for selecting testing locations similar to that given previously for density-water content testing. Compare the measured penetration resistance with the allowable criteria to determine the acceptability or unacceptability of the compacted soil.

*PLATE LOAD TEST (ASTM D1194, D1195, D1196)* The plate load test can be used to determine the stiffness and/or bearing capacity of a compacted soil. The steps performed in a plate load test are as follows (see Fig. 6A.141):

1. A steel plate [commonly 12 in (305 mm) in diameter] or a small concrete footing is placed at the desired depth within the compacted soil.
2. Vertical load is applied to the plate or footing by jacking against a reaction beam, a dead weight loading frame, or an axle of a heavy construction vehicle. The magnitude of the load is usually determined from a pressure gauge located on a hydraulic jack that has been calibrated

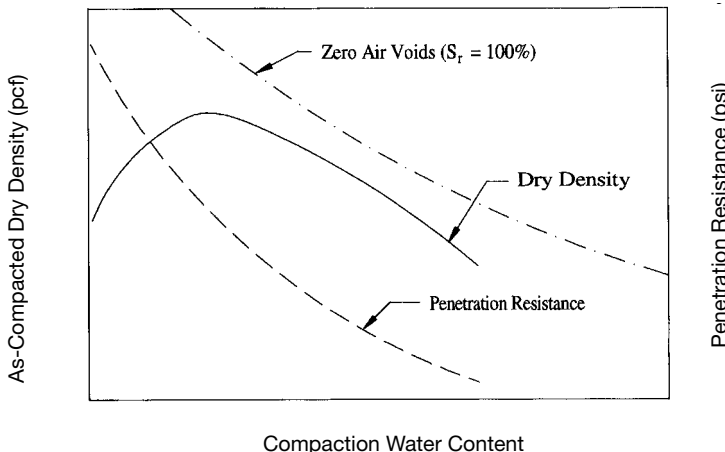
**6.184** SOIL IMPROVEMENT AND STABILIZATION

**FIGURE 6A.139** Schematic illustration of Proctor penetrometer (from ASTM D1558).

to indicate applied force or is read directly from an electronic load cell. The load is increased until a predetermined load or the maximum load for the setup has been reached or until failure has occurred.

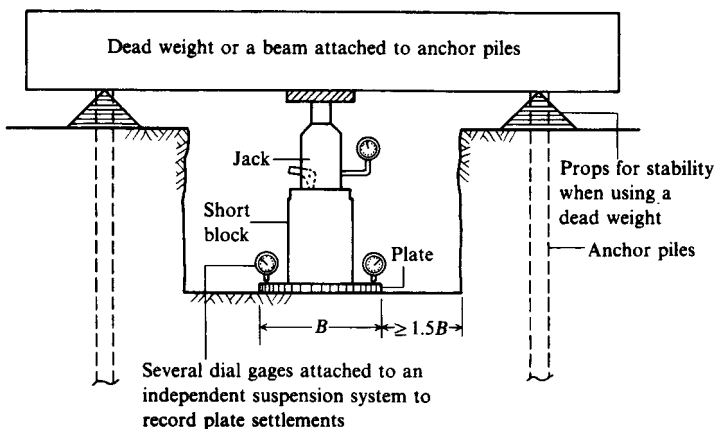
- Vertical settlement of the plate is measured at various times after the application of each loading increment. Settlement readings are taken at one or more locations on the plate or footing using a dial gauge or electronic distance transducer attached to an independent reference beam.

The results from a plate load test are plotted as settlement,  $S$ , versus average applied pressure,  $q_0$  (Fig. 6A.142), from which the subgrade modulus ( $k_s = \Delta q_0 / \Delta S$ ) and ultimate bearing capacity ( $q_{ult}$ ,

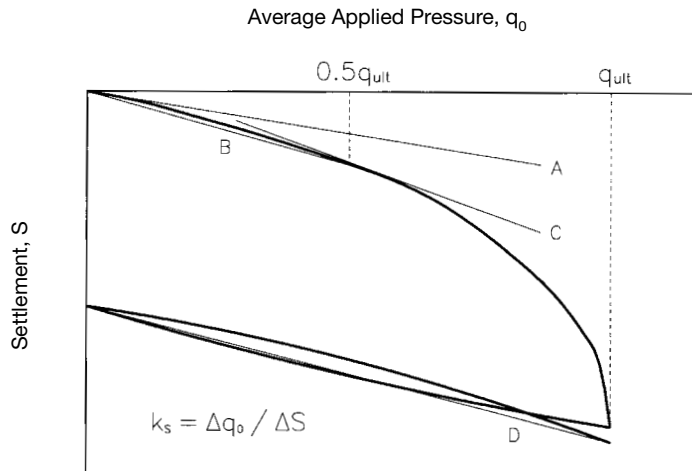


**FIGURE 6A.140** Proctor penetration resistance and as-compacted dry density as a function of compaction water content.

if loaded to failure) can be calculated. Because soils have nonlinear stress-deformation characteristics, a variety of methods can be used to calculate  $k_s$ , so the method to be used must be stated in the compaction specifications. Common methods for calculating  $k_s$  are shown in Fig. 6A.142 and include the initial tangent modulus (line A), secant modulus between zero and one-half the maximum or ultimate applied pressure (line B), tangent modulus at one-half the maximum or ultimate applied pressure (line C), or reload secant modulus from zero to the maximum or ultimate applied pressure (line D). The reload curve is often deemed to give better prediction of the stiffness of the field-compacted soil than the curve for first loading because problems associated with bedding errors are reduced or eliminated on reloading.



**FIGURE 6A.141** Schematic diagram of a typical setup for a plate load test (from Bowles, 1988).

**6.186** SOIL IMPROVEMENT AND STABILIZATION**FIGURE 6A.142** Typical results from a plate load test.

Because the subgrade modulus is a function of the width and shape of the loaded area, a scaling relationship is needed to extrapolate the results of plate load tests to full field scale (e.g., the width and shape of the footings for a building). It is best to establish this scaling relationship at the site for the actual soils and conditions. This can be accomplished by conducting a series of plate load tests, wherein the size of the plates or small footings are varied but are of the same shape as the actual foundation. For example, if the actual footings will be square, a series of tests using square plates with widths of 12, 18, and 24 in (305, 407, and 610 mm) could be conducted at stress levels comparable to those expected in the actual foundation. From the results of these tests,  $k_s$  can be plotted as a function of plate width and the curve extrapolated to obtain an estimate of  $k_s$  for the actual foundation width. It is desirable from an engineering standpoint to conduct tests at full field scale, but this is seldom done because of the cost and time needed to perform full-scale tests.

In the absence of data obtained for the particular site and soil, the scaling laws established by Terzaghi (1955) are often used. Terzaghi considered two types of soils: (1) Those whose stiffness is proportional to the effective confining pressure (e.g., sands and most partially saturated soils of all types), and (2) those whose stiffness is independent of the confining pressure (e.g., saturated, undrained clays). The following relationships were developed for estimating subgrade modulus for a full-scale footing based on the results of plate load tests on 1 ft (0.3 m) wide square plates.

For sands and square or rectangular foundations:

$$k_s = k_{s1} \cdot \left( \frac{B + 1}{2B} \right)^2 \text{ for } B \text{ in units of ft} \quad (6A.54a)$$

$$k_s = k_{s1} \cdot \left( \frac{B + 0.3}{2B} \right)^2 \text{ for } B \text{ in units of m} \quad (6A.54b)$$

where  $k_s$  = subgrade modulus for a foundation of width  $B$

$k_{s1}$  = subgrade modulus for a 1-ft (0.3-m) square plate

$B$  = width of actual foundation

For saturated, undrained clays and rectangular foundations:

$$k_s = \frac{k_{s1}}{B} \cdot \frac{n + 0.5}{1.5n} \text{ for } B \text{ in ft} \quad (6A.55a)$$

$$k_s = \frac{0.3k_{s1}}{B} \cdot \frac{n + 0.5}{1.5n} \text{ for } B \text{ in m} \quad (6A.55b)$$

where  $n = L/B$

$L$  = length of actual foundation

For a square foundation ( $n = 1$ ), Eq. (6A.55) reduces to

$$k_s = \frac{k_{s1}}{B} \text{ for } B \text{ in units of ft} \quad (6A.56a)$$

$$k_s = \frac{0.3k_{s1}}{B} \text{ for } B \text{ in units of m} \quad (6A.56b)$$

and for a strip or continuous foundation ( $n \approx \infty$ ), Eq. (6A.55) reduces to

$$k_s \cong \frac{2}{3} \cdot \frac{k_s}{B} \text{ for } B \text{ in units of ft} \quad (6A.57a)$$

$$k_s \cong \frac{1}{5} \cdot \frac{k_s}{B} \text{ for } B \text{ in units of m} \quad (6A.57b)$$

These relationships are valid for applied stresses less than one-half the ultimate bearing capacity of the actual footing.

These scaling laws were developed for relatively homogeneous soils, and one should exercise caution when the depth of influence for the actual foundation (approximately  $2B$ ) extends into a stratum or strata that are not influenced during the plate load test. This concept is illustrated in Fig. 6A.143 for the case of a dense sand overlying a soft clay layer wherein the depth of influence for the plate load test is entirely within the sand layer, while the depth of influence for the actual footing extends into the soft clay layer. Therefore, extrapolating the results from the plate load test to field scale using Terzaghi's scaling relationships would substantially overestimate the subgrade modulus, which would not be conservative.

Some engineers prefer to use stress-strain modulus ( $E_s$ ) for the soil rather than  $k_s$ . An average value of  $E_s$  for the actual foundation can be estimated from the equations for settlement based on elastic theory for a uniformly loaded foundation on a semi-infinite, homogeneous, linearly elastic material. These equations for settlement are of the following general form:

$$S = \frac{q_0 \cdot B \cdot (1 - v^2)}{E_s} \cdot I_s \cdot I_d \quad (6A.58)$$

where  $q_0$  = applied pressure

$B$  = width or diameter of loaded area

$v$  = Poisson's ratio

## 6.188 SOIL IMPROVEMENT AND STABILIZATION

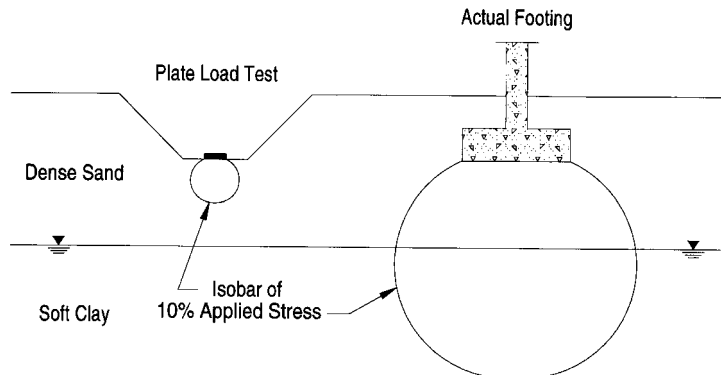


**FIGURE 6A.143** Comparison of depth of influence for a plate load test and an actual footing.

$E_s$  = stress-strain modulus for the soil

$I_s$  = influence factor that accounts for the shape and rigidity of the foundation, and the location where settlement is calculated

$I_d$  = correction factor for depth of embedment ( $D$ )

Using the secant value of subgrade modulus ( $k_s = q_0/S$ ), Eq. (6A.58) can be rearranged to solve for  $E_s = f(k_s)$  as follows:

$$E_s = k_s B(1 - v^2) I_s I_d \quad (6A.59)$$

When calculating  $E_s$  for the actual foundation, the value of  $k_s$  input into Eq. (6A.59) should be the field scale  $k_s$ . Equations or values of  $I_s$  for either rigid or flexible foundations of circular or rectangular shape can be found in a number of reference books (e.g., Poulos and Davis, 1974; Das, 1983). Selected values of  $I_s$  for circular and square foundations—the most common shapes used in plate load tests—are given in Table 6A.11. The plates in most plate load tests are quite rigid. If the plate is wide, usually a stack of increasingly narrower plates is placed on the bearing plate to increase the rigidity of the system. Thus, values of  $I_s$  for rigid foundations generally should be used. For example,  $I_s = 0.79$  for a rigid, circular foundation on a homogeneous half-space, and this value is commonly used for circular plate load tests. If the compressible layer or layers being tested are underlain by a hard layer, a value of  $I_s$  for a finite height of compressible layer ( $H_c$ ) should be used. E. Fox (1948) presented equations to calculate  $I_d$  for rectangular foundations embedded in a homogeneous half-space, and charts for estimating  $I_d$  based on these equations are given in Fig. 6A.144. Equations for calculating  $I_d$  for circular foundations can be found in Nishida (1966). Figure 6A.144 can also be used for circular foundations with little loss of accuracy by converting to an equivalent square based on area. Note that the values of  $I_d$  in Fig. 6A.144 are not strictly applicable to finite-height compressible layers but may be used as approximations. In tests conducted below the ground surface, the bottom of the excavated pit is typically several times wider than the width of the plate, so the use of a correction factor for embedment in these cases is probably not justified.  $v$  is usually estimated based on the soil type and moisture condition, but also can be determined from triaxial testing either directly by measuring radial deformations using a Poisson's ratio clamp or Hall effect transducers or indirectly by measuring the changes in height and total volume of the specimen and assuming that the specimen retains the shape of a right circular cylinder during the testing.

**TABLE 6A.11** Selected Values of Settlement Influence Factor  $I_s$  for Circular and Square Foundations

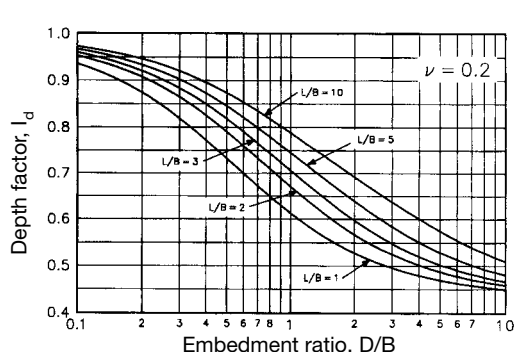
Shape	$v$	$H_c/B$	Rigid	$I_s$	
				Flexible	
				Center	Edge
Circular	0 to 0.5	$\infty$	0.79	1.00	0.64
		3		0.80	0.47
		2		0.77	0.43
		1		0.61	0.29
		3		0.85	0.50
		2		0.81	0.46
		1		0.67	0.34
		3		0.86	0.51
		2		0.83	0.47
		1		0.70	0.36
Square	0 to 0.5	$\infty$	0.89	1.12	0.56
		5		1.00	0.43
		2	0.77	0.82	0.29
		1	0.57	0.57	0.14
		5		1.01	0.45
		2		0.84	0.31
		1		0.61	0.17
		5		1.01	0.45
		2		0.86	0.32
		1		0.64	0.19
		5		1.02	0.46
		2		0.87	0.33
		1		0.67	0.20

The advantages of the plate load test over moisture-density testing can be summarized as follows (after Hausmann, 1990):

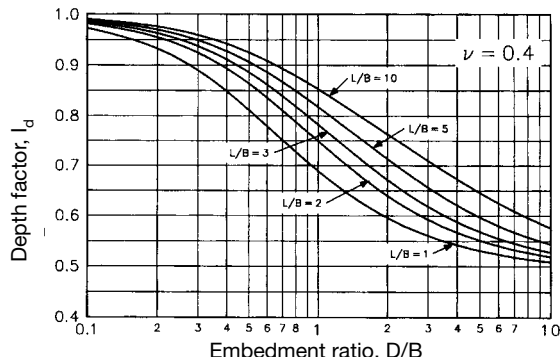
1. The stiffness and strength of the compacted soil are evaluated directly.
2. The results are available immediately.
3. No laboratory testing (e.g., compaction tests) is needed.
4. The test is suitable for a wide range of soil types and maximum particle sizes.
5. Once established as a routine test, the plate load test can be conducted rapidly at low cost.

*CALIFORNIA BEARING RATIO (CBR) TEST (ASTM D4429)* In the CBR test, a 1.95 in (49.6 mm) diameter piston with a flat head is slowly pushed into the soil, and the resisting force developed at various depths of penetration is measured. CBR value is calculated at penetrations of 0.1 and 0.2 in (2.54 and 5.08 mm) by dividing the calculated bearing stress by the appropriate standard stress (which varies as a function of penetration), and multiplying by 100. The higher of the two values is reported as the CBR value. If the piston is penetrated deeply enough, failure occurs in the soil beneath the piston, and the test is essentially a miniature bearing capacity test.

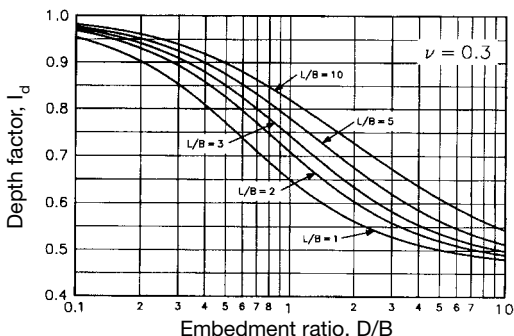
CBR value is an indication of the stiffness and strength of the soil and is widely used in the design and control of subsoils beneath pavements. By correlating CBR value with the desired strength and compressibility requirements for a particular compacted soil through laboratory testing or em-

**6.190** SOIL IMPROVEMENT AND STABILIZATION

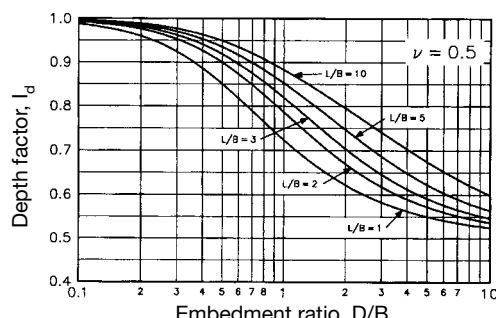
(a)



(c)



(b)



(d)

**FIGURE 6A.144** Charts for estimating settlement correction factor for depth of embedment ( $I_d$ ) for rectangular foundations based on E. Fox's (1948) equations: (a)  $v = 0.2$ ; (b)  $v = 0.3$ ; (c)  $v = 0.4$ ; and (d)  $v = 0.5$  (format adapted from Bowles, 1988).

pirical data on similar soils, the CBR test can, in some circumstances, provide a rapid and effective method for assessing the suitability of compacted soils.

The CBR test is similar to the plate load test in the type of results (penetration or settlement versus stress) that are obtained. In fact, one can easily calculate subgrade modulus from the CBR data. The primary difference in the two tests is the width of the loaded area—approximately 2 in (51 mm) in the CBR test and commonly 12 in (305 mm) in the plate load test—with a depth of influence of about 4 in (102 mm) in the CBR test and about 24 in (610 mm) in the plate load test. Therefore, the plate load test is suitable for a wider range of soils. However, for thin lifts (no more than about 8 in = 203 mm) and soils for which particles larger than medium sand size are only a small fraction of the soil, CBR tests often can be conducted faster and cheaper in many instances than can plate load tests, usually with equivalent success.

**STANDARD PENETRATION TEST (ASTM D1586)** The standard penetration test (SPT) is seldom used for quality control of compacted fills for the following reasons: (a) The test is conducted over a depth of 12 in (305 mm), so that it would be valid only for this lift thickness or greater; (b) the setup time and cost for performing one test per location is excessive; and (c) the results are reliable only

for granular soils with little or no particles gravel-size or larger. The main application for the SPT in compacted soils is for checking the degree of improvement in compacted in situ soils (primarily deep methods such as dynamic compaction and vibrocompaction).

*CONE PENETRATION TEST (ASTM D3441)* The cone penetration test (CPT) has limited application in near-surface compacted soils primarily because of setup time and cost. The CPT is not applicable in stiff or hard clays or soils that contain appreciable amounts of gravel or larger particles and is primarily applicable for establishing the improvement in both deeply compacted sands and silty sands.

*SEALED DOUBLE RING INFILTRATION TEST (ASTM D5093)* The sealed double-ring infiltration (SDRI) test has become increasingly popular in recent years for determining the field coefficient of permeability (hydraulic conductivity) of compacted clay liners. It was developed to eliminate the two major problems associated with using other field hydraulic conductivity tests on low permeability soils—difficulties in measuring small changes in elevation of the water surface (caused by low flow rates and evaporation) and separating lateral flow from vertical flow (Trautwein 1993).

The SDRI consists of an open outer ring and a sealed inner ring (Fig. 6A.145). The rings may be either circular or square, but square rings are usually used because they make it easier to excavate straight trenches in the soil. The most common sizes for the rings are 12 ft (3.7 m) and 5 ft (1.5 m) square for the outer and inner rings, respectively.

The general procedure for conducting an SDRI test is summarized as follows (ASTM D5093; Trautwein, 1993):

1. The rings are embedded in trenches excavated in the soil and the trenches are sealed with grout to prevent water loss.
2. The outer ring is filled with water to a level such that the inner ring is completely submerged.
3. The rate of flow is measured by connecting a flexible bag filled with a known weight of water to a port on the inner ring. As water from the inner ring infiltrates into the ground, an equal amount of water flows from the flexible bag into the inner ring. The flexible bag is removed after a known interval of time and weighed. The volume of water that has infiltrated the ground is determined from the weight loss of the flexible bag.
4. The infiltration rate  $I$  is calculated from the following equation:

$$I = \frac{Q}{At} \quad (6A.60)$$

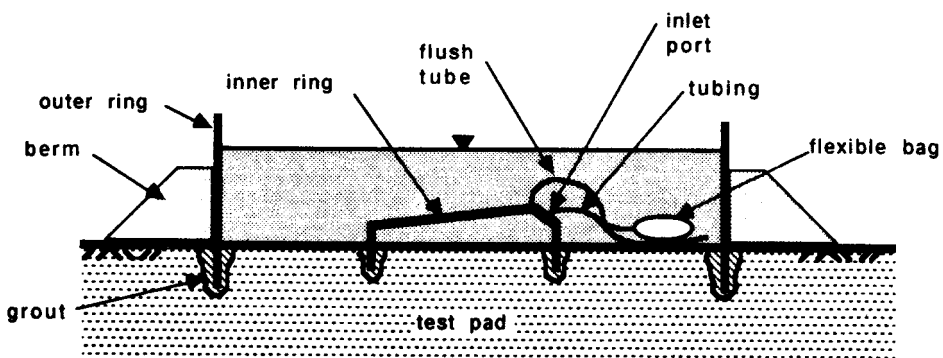


**FIGURE 6A.145** Schematic illustration of a typical setup for a sealed double ring infiltration test (from ASTM D5093).

**6.192** SOIL IMPROVEMENT AND STABILIZATION

where  $Q$  = volume of infiltrated water

$A$  = area of the inner ring

$t$  = time interval over which  $Q$  is determined

5. The process is repeated, and a plot is constructed of infiltration rate versus time. The test is continued until the infiltration rate becomes steady or until it becomes less than or equal to a specified value.
6. The coefficient of permeability  $k$  is calculated as follows:

$$k = \frac{Q}{iAt} = \frac{I}{i} \quad (6A.61)$$

where  $i$  = hydraulic gradient  $\Delta H/\Delta L$

$\Delta H$  = total head loss

$\Delta L$  = length of flow path for which  $\Delta H$  is measured

This equation for  $k$  assumes steady state, vertical, one-dimensional flow under saturated conditions.

Although Eq. (6A.61) seems simple, the calculation of  $i$  is complex because the flow is transient and the soil is usually unsaturated at the start of testing. The problem of transient flow is overcome by waiting for quasi-steady-state conditions to be reached, which unfortunately results in long testing times. The unsaturated flow makes it difficult to determine the gradient, but this can be alleviated by making some simplifying assumptions. Three methods are commonly used for calculating  $i$  (refer to Fig. 6A.146 for illustration of parameters).

**Apparent Hydraulic Conductivity Method** This is the simplest method, and it yields the most conservative (highest) value of  $k$ . It is assumed that the wetting front has passed completely through the compacted liner, which means that the depth of the wetting front is equal to the thickness of the liner ( $D_w = H_L$ ) and that the suction head at the bottom of the liner is zero ( $H_s = 0$ ). This results in  $\Delta H = H_w + H_L$ , and  $\Delta L = H_L$ . The advantage of this method is that neither the location of

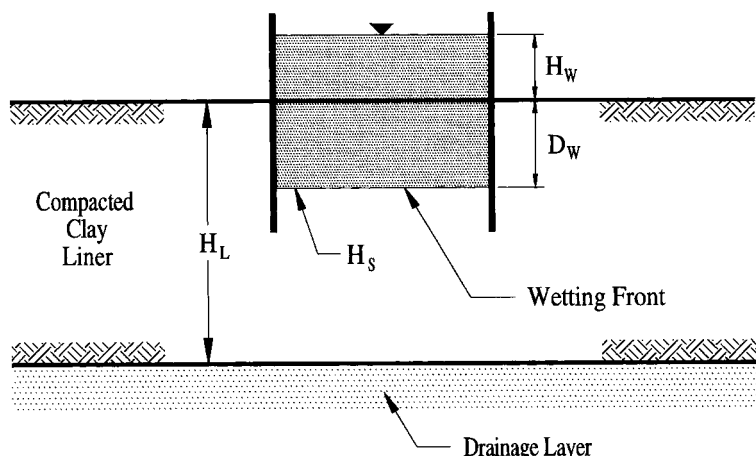


**FIGURE 6A.146** Parameters for calculating hydraulic gradient for the sealed double-ring infiltration test (after Trautwein, 1993).

the wetting front nor the suction at the wetting front need be known. The disadvantage is that the correct value of  $k$  is calculated only if the wetting front has passed through the test zone; otherwise,  $k$  is overestimated. Therefore, this method can be used to determine compliance with the specified maximum acceptable value of  $k$  ( $k \leq k_{\max}$ ) but cannot be used to determine noncompliance ( $k > k_{\max}$ ).

**Suction Head Method** In this method it is assumed that  $H_s$  is equal to the ambient suction in the soil below the wetting front, and the location of the wetting front and the ambient soil suction must be known. For this method,  $\Delta H = H_w + D_w + H_s$ , and  $\Delta L = D_w$ . Unfortunately, the basic assumption appears to be incorrect. Although the suction below the wetting front may have some impact on infiltration rate, this impact is apparently offset by low hydraulic conductivity in the unsaturated transition zone between the wetting front and the unaffected unsaturated soil, which restricts downward flow. This method is not recommended because it can yield highly unconservative (low) values of  $k$ .

**Wetting Front Method** This method is based on the assumption that the suction head at the wetting front is zero ( $H_s = 0$ ) and requires that the location of the wetting front be known. With this assumption and a known  $D_w$ ,  $\Delta H = H_w + D_w$  and  $\Delta L = D_w$ . Because ambient suction may have a small effect on infiltration (and hence  $k$ ), this method is considered to be conservative. Recent research suggests that the wetting front method is the best of the three methods, and it is the recommended procedure.

The location of the wetting front and changes in suction within the compacted soil as the water advances can be monitored by installing tensiometers in the compacted soil. Typically nine tensiometers are used per test, three at each depth of 6, 12, and 18 in (152, 305, 457 mm). If desired, tensiometers can also be installed in the native soil to measure and monitor ambient suctions.

The SDRI test is the best test currently available for determining the hydraulic conductivity of low-permeability in situ soils. Many governmental agencies now require the SDRI test to establish the acceptability of compacted clay liners for containing waste and hazardous materials. The disadvantages of SDRI testing include lack of overburden, long test times (a few weeks to several months), and high cost (\$8000 to \$15,000 per test).

## **6A.4 DEEP COMPACTION**

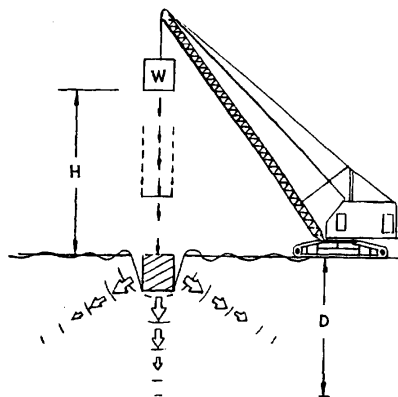
---

The methods for compacting near-surface soils described in Section 6A.3 can be used to a maximum depth of about 10 ft (3 m) under highly favorable circumstances and generally much less than this depth. Techniques for compacting soil to greater depths include dynamic compaction, vibrocompaction, and blasting. These three methods are discussed in the following sections.

### **6A.4.1 Dynamic Compaction**

Dynamic compaction consists of repeatedly raising and dropping heavy tampers onto the ground surface to compact the underlying soil deposits to typical depths of improvement ( $D$ ) of about 10 to 35 ft (3.0 to 10.7 m) (Lukas 1986, 1995). With special lifting equipment and a heavy tamper, the ground can be affected to depths as great as 100 ft (30.5 m). This process is illustrated in Figs. 6A.147 and 6A.148 and has also been referred to as pounding, dynamic consolidation, dynamic pre-compaction, impact densification, and heavy tamping. The weight of the tampers ( $W$ ) is generally in the range of 6 to 30 tons (5.4 to 27.2 MN), with usual drop heights ( $H$ ) of 40 to 100 ft (12.2 to 30.5 m).

Although this technique was used long ago by the Romans and as early as the 1870s in the United States (Kerisel 1985), it was resurrected and systematically developed in the early 1970s by the

**6.194** SOIL IMPROVEMENT AND STABILIZATION

**FIGURE 6A.147** Schematic illustration of the dynamic compaction process (modified from Lukas 1995).

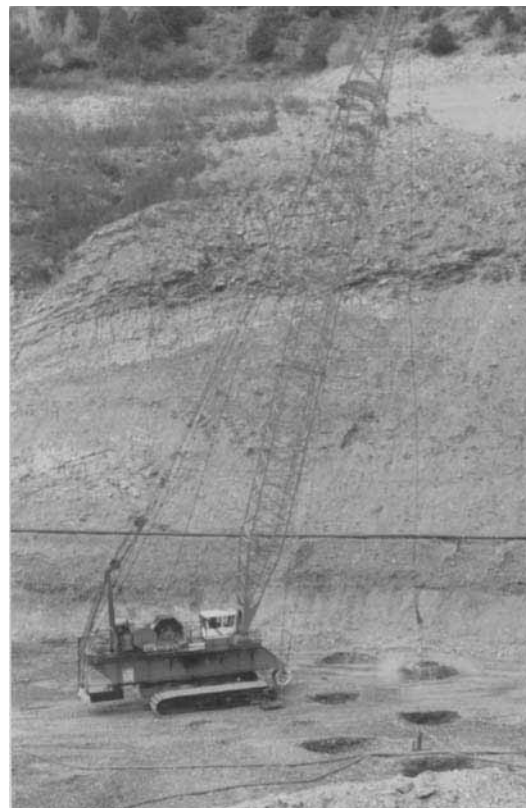


**FIGURE 6A.148** Dynamic compaction showing tamper at impact.

Frenchman Louis Menard (Welsh 1986). This method has seen considerable growth in the last decade, with over 500 projects completed in the U.S. (ASCE 1997).

Dynamic compaction has been successful in improving many types of weak ground deposits, including the following (Lukas 1995):

1. Loose, naturally occurring soils such as alluvial, flood plain, and hydraulic fill deposits
2. Recent and old landfill deposits
3. Deposits of construction debris and building rubble
4. Spoil from strip mines
5. Partially saturated clay fill deposits that are located above the groundwater table
6. Formations where large voids are present close to final grade; for example, karst topography and sinkholes
7. Saturated loose sands and silts to reduce liquefaction potential

#### **6A.4.1.1 Equipment**

Tampers with weights of 25 tons (220 kN) or less are generally raised and dropped with a conventional heavy crawler crane using a single cable with a free spool to allow the drop to be nearly free fall. For heavier tampers, either conventional equipment is modified to reinforce certain components or specially designed equipment is used to raise and drop the tamper. A summary is given in Table 6A.12 of required crane and cable sizes as a function of tamper weight.

The tampers are typically constructed of steel or steel shells filled with sand or concrete (Mayne et al. 1984). Reinforced concrete tampers have also been used but tend to fall apart after repeated use. The bases of the tampers are typically square, circular, or octagonal. The craters formed during the primary phase eventually assume a circular shape, so circular or octagonal bases are best suited for this phase. Square bases are best suited for the ironing phase where the tamper is dropped on a contiguous or overlapping pattern to densify the surficial soils only. A steel tamper with a circular base is shown in Fig. 6A.149.

#### **6A.4.1.2 General Procedures**

The spacing of the impact points, the energy per drop (combination of weight of tamper and drop height), and the chronological sequence of energy application depend primarily on the following factors:

1. Depth and thickness of the compressible layer or layers
2. Depth to the groundwater table
3. Permeability and moisture condition of the compressible materials

In general, there are at least two phases of the treatment process, which are normally called passes. The first phase—called the *primary phase* or *high-energy phase*—is intended to improve the deeper portions of the compressible zone. Impact points are widely spaced in this phase to prevent the creation of a dense zone of material at an intermediate depth. If an intermediate dense zone is created,

**TABLE 6A.12** Equipment Requirements for Different Weights of Tampers (from Lukas, 1986)

Tamper weight		Crawler crane size		Cable size	
tons	kN	tons	kN	in	mm
6 to 8	53 to 71	40 to 50	360 to 440	3/4 to 7/8	19 to 22
8 to 14	71 to 120	50 to 100	440 to 890	7/8 to 1	22 to 25
15 to 18	130 to 160	100 to 125	890 to 1,100	1 to 1 1/8	25 to 29
18 to 25	160 to 220	150 to 175	1,300 to 1,600	1 1/4 to 1 1/2	32 to 38

**6.196** SOIL IMPROVEMENT AND STABILIZATION

**FIGURE 6A.149** Steel tamper with a circular base.

it tends to spread the induced pressures over a wider area, lessening the magnitude of the energy transmitted beneath it. This makes it difficult or impossible to densify the underlying materials. A general rule of thumb is that the spacing of impact points in the primary phase should be at least equal to the depth to the bottom of the compressible layer or the maximum depth to be improved. Also, the spacing should be at least 1.5 to 2.5 times the diameter or width of the tamper and usually not less than about 10 ft (3 m). There may be more than one pass at the same impact points during the primary phase. The craters are backfilled after each pass (see Figs. 6A.150 through 6A.152), normally with nearby site materials. In this case, the ground surface is lowered by an amount commensurate with the degree of densification achieved during that pass. In some situations, for example when the groundwater table is high, it may be desirable to keep the ground surface at the same elevation, which necessitates the use of imported materials to backfill the craters and the intermediate areas that have settled.

The final phase is called the *ironing phase* or *low energy* phase and is intended to densify the surficial soils to a depth of about 6 ft (2 m). A square tamper, low drop height, and low contact pressure are typical for this phase. The whole treated area is densified on a contiguous or overlapping pattern. If the depth of the craters is less than about 1.5 ft (0.5 m), the surficial soils generally can be densified by conventional compaction rollers rather than by dropping tampers.

If the compressible layer or layers is deep, it is sometimes necessary to use one or more *intermediate phases* to densify the intermediate depths. If one intermediate phase is used, the intermediate drop points are centered between the primary drop points.

#### **6A.4.1.3 Soil Type and Moisture Condition**

The following characteristics of the soil significantly influence the effectiveness of dynamic compaction:

1. Classification, geologic origin, and layering of the soil mass to be compacted
2. The moisture condition (degree of saturation) of the soil
3. For saturated soil, the permeability of the soil and length of drainage paths, which control the rate of dissipation of induced excess pore water pressures

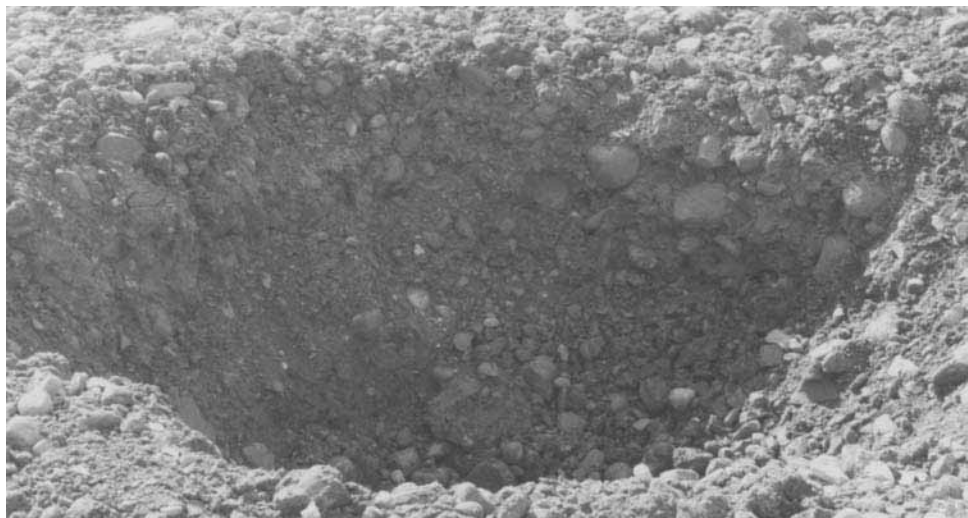


**FIGURE 6A.150** Crater created during primary phase.

Lukas (1986) has classified the suitability of soil for dynamic compaction into the following three zones based on grain-size distribution (Fig. 6A.153): Pervious soils (Zone 1), semipervious soils (Zone 2), and impervious soils (Zone 3).

Soils with high degrees of saturation, high permeabilities, and good drainage are best suited for dynamic compaction. The method is generally effective in all types of soils that are partially saturated with a continuous air phase within the voids. When energy from the tamper impacting the surface is transmitted within the ground, densification of the soil occurs as air is squeezed from the voids.



**FIGURE 6A.151** Dumping backfill into crater.

**6.198** SOIL IMPROVEMENT AND STABILIZATION

**FIGURE 6A.152** Leveling backfilled crater.

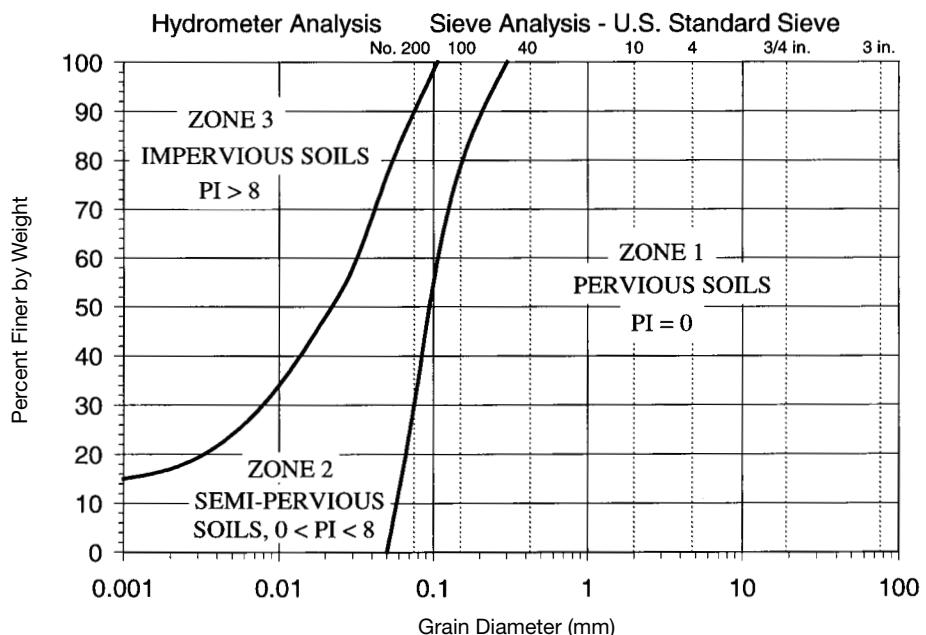


**FIGURE 6A.153** Grouping of soils according to effectiveness of dynamic compaction (redrawn from Lukas 1986).

Air rather than water is squeezed from soils with a low degree of saturation because the viscosity of air is several orders of magnitude lower than the viscosity of water. A continuous air phase typically exists within the voids of a soil when the degree of saturation is less than about 70 to 95%, with the lower values usually representative of sandy soils and higher values representative of clayey soils. At higher degrees of saturation, the air in the voids occurs as bubbles trapped within water in the voids and the soil behaves as if it is saturated. (See Fig. 6A.85 and the related discussion for further clarification.)

Zone 1 materials are pervious, with typical values of coefficient of permeability ( $k$ ) greater than  $1 \times 10^{-3}$  cm/sec (3 ft/day). Soil particle sizes range from boulders to sands. Also included within this category are deposits consisting of building rubble, construction debris, coarser mine spoils, some industrial waste fill such as slag and clinker, and decomposed refuse deposits. Dynamic compaction is effective in all Zone 1 deposits, even if saturated, because the permeability is sufficiently high to dissipate excess pore water pressures almost immediately. Hence densification is also nearly immediate.

Zone 3 materials are nearly impervious to water [generally,  $k < 1 \times 10^{-6}$  cm/sec (3  $\times 10^{-3}$  ft/day)] and are generally not suitable for dynamic compaction if saturated or nearly saturated. Soils included in this category consist of clays or clayey soils with clay content higher than about 25% and plasticity index (PI) greater than 8. Induced excess pore pressures in these soils typically require long periods of time to dissipate, and densification is unduly delayed. Exceptions to this rule may occur when the drainage paths are very short, such as occurs in varved clays and where macroscopic features (animal burrows, holes resulting from decomposition of organic material, etc.) allow faster drainage. Some improvements have been achieved in partially saturated clays where the water content is less than the plastic limit. Densification will occur until the deposit becomes essentially saturated by the compaction process. No further improvement will be produced after saturation occurs, regardless of the amount of energy that is applied.

Zone 2 materials are semipervious with values of  $k$  usually ranging from  $1 \times 10^{-3}$  to  $1 \times 10^{-6}$  cm/sec (3  $\times 10^{-3}$  to  $3 \times 10^0$  ft/day). These materials include silts, sandy silts, silty sands, and clayey silts with PI < 8. Densification generally occurs readily in these materials when partially saturated. However, when saturated, induced excess pore water pressures may require days or weeks to dissipate completely. Therefore, tamping operations must be planned and conducted carefully. It is prudent to perform permeability tests beforehand to establish the suitability of these materials for dynamic compaction. Usually, the energy must be applied in multiple phases or multiple passes, with sufficient time in between to allow excess pore water pressures to dissipate. Alternately, wick drains can be used to facilitate drainage, but the cost-effectiveness of this combined method has not been established relative to other improvement techniques (Dise et al. 1994).

Obviously, there are soils that will not fall entirely within one of the three zones. In these cases, permeability tests should be conducted on the soil because permeability is a better indicator than grain-size distribution of the behavior of the soil during dynamic compaction.

Rollins et al. (1998) showed that the concept of optimum moisture content (OMC) is valid for dynamic compaction. This is to be expected, since dynamic compaction is an impact method similar to that used in Proctor tests. The following conclusions were drawn from their research:

1. OMC increases with depth because the compactive energy produced by the dynamic compaction decreases with depth.
2. The depth of improvement increased somewhat as the moisture content increased.
3. The crater depth increased as the moisture content increased. At moisture contents above optimum, crater depths became excessive and did not always reflect greater improvement.

These results suggest that the efficiency of dynamic compaction can be improved by controlling the moisture condition of the soils being treated. However, owing to the difficulty in controlling moisture content in the field for the large volumes of soils typically treated in any dynamic compaction, this may not be feasible for many dynamic compaction projects.

**6.200** SOIL IMPROVEMENT AND STABILIZATION**6A.4.1.4 Design Guidelines**

The five steps shown below need to be undertaken during the design process for any dynamic compaction project (Lukas 1995). Other steps may be needed for particular projects.

1. Selection of tamper weight, shape, and drop height to achieve the desired depth of treatment
2. Determination of the applied energy required over the project site to obtain the desired improvement
3. Selection of the area(s) to be treated
4. Determination of the grid spacing along with the number and chronological sequence of phases, and the number of passes in each phase
5. Determining if a surface stabilizing layer is needed

Each of these steps is described in more detail in the following sections.

**Tamper Characteristics and Drop Height.** The weight of the tamper and the height of drop are not independent parameters, as shown in Fig. 6A.154. The theoretical energy applied by one drop of the tamper is equal to  $W \times H$ . However, there are energy losses associated with cable drag and wind resistance on the order of about 10% of the theoretical energy. Therefore, the actual applied energy is about 90% of the theoretical energy. The energy required to achieve a particular depth of treatment at a site can be achieved by infinite combinations of  $W$  and  $H$ .

Mayne et al. (1984) established an empirical trend between apparent maximum depth of improvement ( $D_{\max}$ ) and theoretical energy per blow ( $WH$ ) shown in Fig. 6A.155 based on data from numerous projects. From this data, the following equation can be used to estimate  $D_{\max}$ :

$$D_{\max} = n \sqrt{\frac{WH}{f}} \quad (6A.62)$$

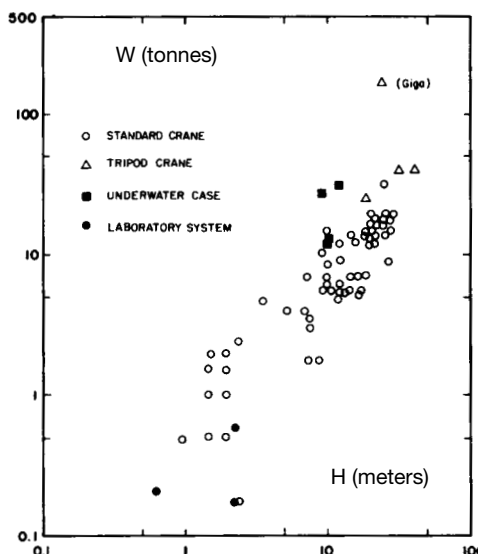


**FIGURE 6A.154** Relationship between weight of tamper and drop height (from Mayne et al., 1984).

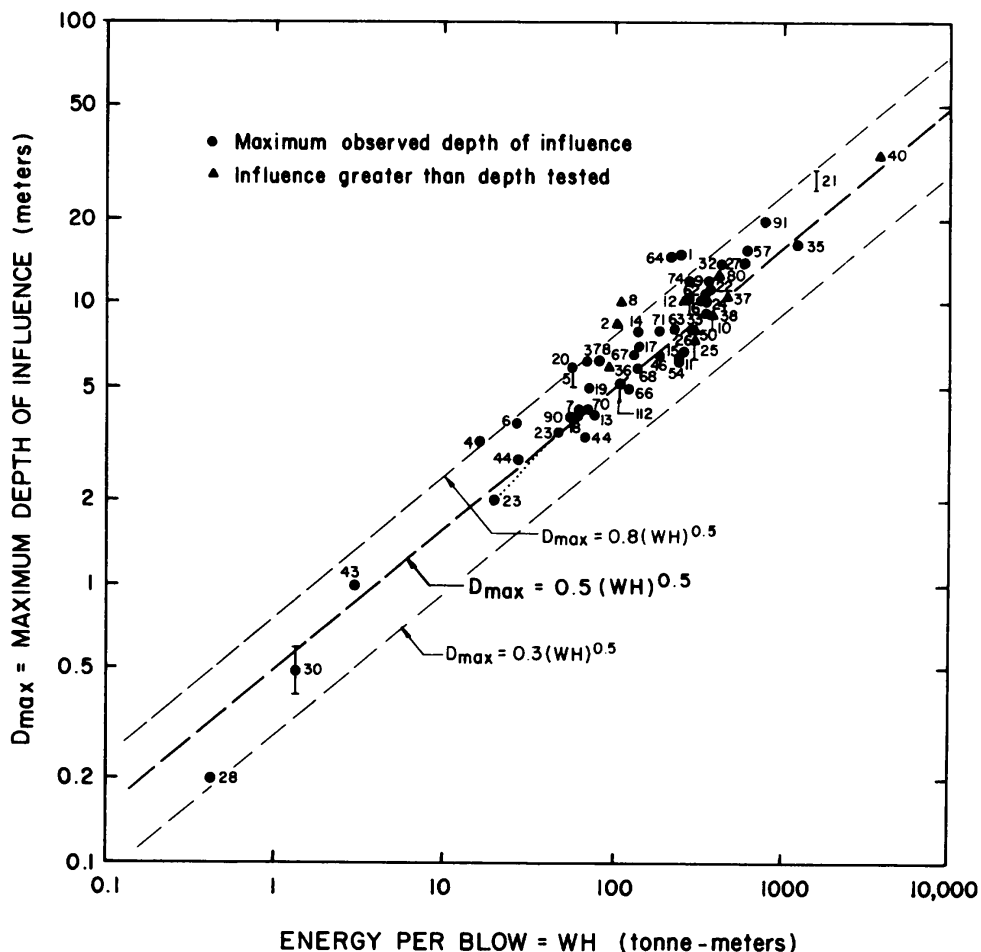


**FIGURE 6A.155** Trend between apparent maximum depth of influence and theoretical energy per blow (from Mayne et al., 1984).

where  $n$  = empirical coefficient ranging from 0.3 to 0.8, averaging about 0.5  
 $f$  = units factor = 1.0 tonne/m = 9.807 kN/m = 672 lb/ft

The variation in  $n$  can be attributed to the following factors (Lukas 1995):

1. Efficiency of the drop mechanism of the crane
2. Magnitude of total applied energy
3. Types and layering of soil being densified
4. Possible presence of energy absorbing layers
5. Presence of a hard layer below or above the material being treated
6. Contact pressure induced by the tamper on the ground

**6.202** SOIL IMPROVEMENT AND STABILIZATION

Lukas (1995) provided recommended values of  $n$  as a function of soil type and degree of saturation, which are summarized in Table 6A.13.

There is a critical depth at which the improvement is the greatest ( $D_c$ ), which occurs at about one-half the maximum depth of improvement:

$$D_c \approx 0.5D_{\max} \quad (6A.63)$$

Use of values of  $n$  from Table 6A.13 in Eq. 6A.62 generally provide a reasonable estimate of  $D_{\max}$ . However, the following factors may affect the maximum depth of improvement actually achieved and, if present on a particular project, may require adjustment of the tamper characteristics and drop height to ensure the soil is densified to the desired depth:

1. The tamper used during the high energy phases generally should have a flat bottom and a contact pressure (tamper weight divided by area of base) in the range of 800 to 1,550 lb/ft<sup>2</sup> (40 to 75 kPa). If the contact pressure is significantly higher, the tamper could punch into the ground with little densification of the underlying soils. Smaller contact pressures generally produce densification of the surficial soil only and should only be used during the ironing phase.
2. Weak saturated clay layers tend to absorb energy. Depending on the thickness of these energy-absorbing layers and their location within the zone to be treated, some reduction in  $D_{\max}$  may occur. If the weak layer is thick and located near the middle of the zone to be treated, the soils underlying this layer will not be improved. If the weak layer is thin and located near the ground surface, it is possible that the tamper will penetrate this layer and densify the underlying materials. The influence of a weak layer or layers on the depth of improvement is best determined by field tests wherein *in situ* tests are conducted after trial dynamic compaction to ascertain the effect of the weak layer(s).
3. Hard or cemented layers tend to distribute the impact load over a larger area, lessening the energy transmitted to underlying layers. If located near the ground surface, the harder layer will need to be loosened prior to tamping. A hard layer located immediately below the zone to be improved has the beneficial effect of increasing the effectiveness of the treatment by reflecting energy back into the loose materials.
4. If the groundwater table is within about 6 ft (2 m) of the ground surface, effectiveness of the tamping will be reduced. Water can rise up into the craters as a result of induced excess pore water pressures. Repeated tamping may cause liquefaction within the surficial soils. This weak upper zone will not densify and will not efficiently transmit energy beneath it. The water table can be controlled either by lowering it through pumping or by placing fill to raise the ground surface.

**TABLE 6A.13** Recommended Values of Empirical Coefficient  $n$  for Different Types of Soil and Degrees of Saturation (from Lukas 1986)

Soil type	Degree of Saturation	Recommended value of $n^a$
Zone 1—Pervious granular soils	High	0.5
	Low	0.50 to 0.60
Zone 2—Semipervious primarily silts with PI < 8	High	0.35 to 0.40
	Low	0.40 to 0.50
Zone 3—Impervious primarily clays with PI > 8	High	Not recommended
	Low	0.35 to 0.40 <sup>b</sup>

<sup>a</sup>For an applied energy of 1 to 3 MJ/m<sup>2</sup> (69 to 206 ft-kips/ft<sup>2</sup>) and a tamper drop using a single cable with a free spool drum.

<sup>b</sup>Soils should be at a water content less than the plastic limit.

**Applied Energy.** The energy applied per unit volume of treated soil ( $E$ ) can be calculated from the following equation:

$$E = \frac{NWHP}{S_{d\max}^2} \quad (6A.64)$$

where  $N$  = number of drops at each drop point

$P$  = number of passes

$S$  = spacing of drop points on a square grid pattern

Guidelines for applied energy requirements as a function of type of deposit to be treated are given in Table 6A.14. The range in values in Table 6A.14 accounts for the initial relative density of the deposit to be treated and the required degree of improvement. The higher values in any range should be used for loose deposits or a high required degree of improvement and the lower values for dense deposits or a low required degree of improvement. The energy per unit area to be applied to the surface of the deposit can be obtained by multiplying the selected value of  $E$  by the thickness of the deposit to be densified.

**Characteristics of Phases.** Dynamic compaction undertaken on Zone 1 materials with any degree of saturation or Zone 2 materials with low degrees of saturation can generally be completed in one high-energy phase. Saturated Zone 2 materials and Zone 3 materials with low degrees of saturation usually required two or three high-energy phases. In the first phase, tamping is conducted at every second or third drop point. In the second or third phases, tamping is performed at intermediate points after the excess pore water pressures have dissipated significantly. Piezometers should be installed in the treated ground and monitored to determine when additional tamping can be conducted.

It is usually economical to use between about 7 and 15 drops at each impact point for any pass of a high-energy phase. The number of drops required at each impact point can be determined from Eq. 6A.64. If the required number of drops does not fall within the economical range, the spacing of the impact points can be adjusted.

The number of drops that can be applied at any impact point may be controlled by the development of excess pore water pressures or the depth of the craters. In general, the crater depth should be no more than the height of the tamper plus about 1 ft (0.3 m) for the following reasons (Lukas 1995):

1. Extracting the tamper from a deep crater is difficult because suction forces may develop and loose debris may fall on top of the tamper. This may result in cable damage and lost production time.
2. After extraction of the tamper, the sides of the crater may cave in, causing two types of problems: (a) the caved soil cushions additional impacts, and (b) the tamper may strike the caved material that accumulates along the sides, lessening the amount of energy that is transmitted deeper.
3. Applying the energy at a deeper level may generate higher excess pore water pressures.

**TABLE 6A.14** Guidelines for Applied Energy Requirements (from Lukas 1986)

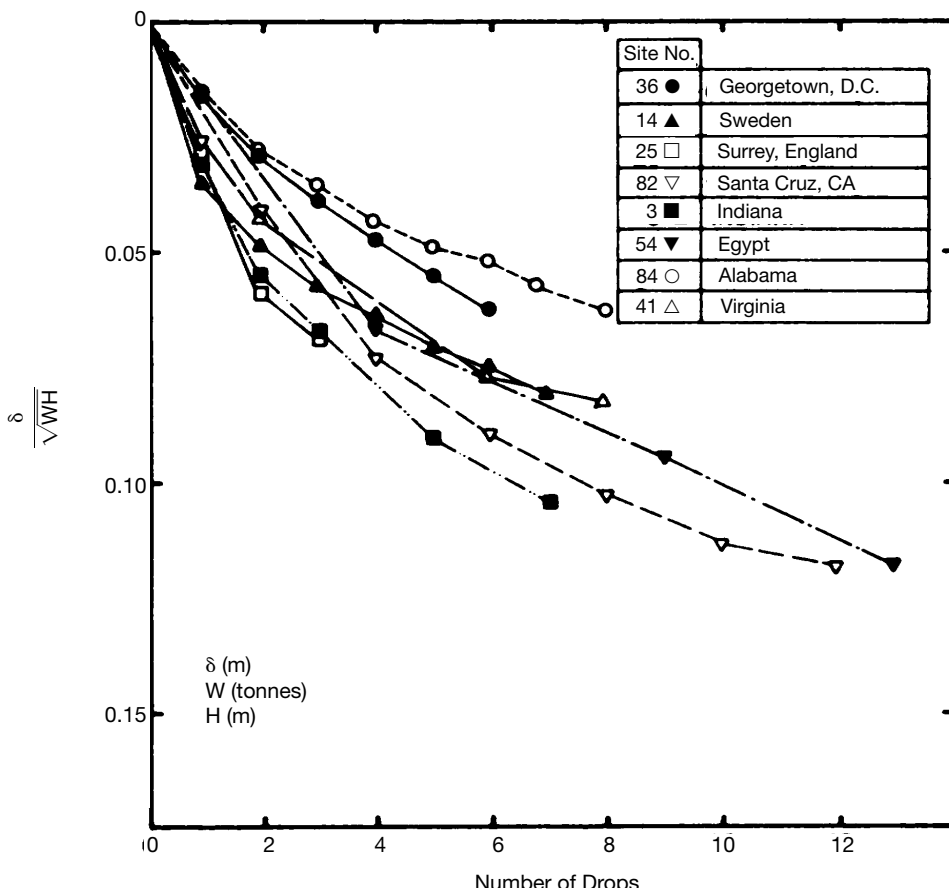
Type of deposit	Required $E$	
	ft-kips/ft <sup>3</sup>	kJ/m <sup>3</sup>
Zone 1	4.2 to 5.2	200 to 250
Zone 2; Zone 3 above the groundwater table	5.2 to 7.3	250 to 350
Landfills	12.5 to 23.0	600 to 1,100

**6.204** SOIL IMPROVEMENT AND STABILIZATION

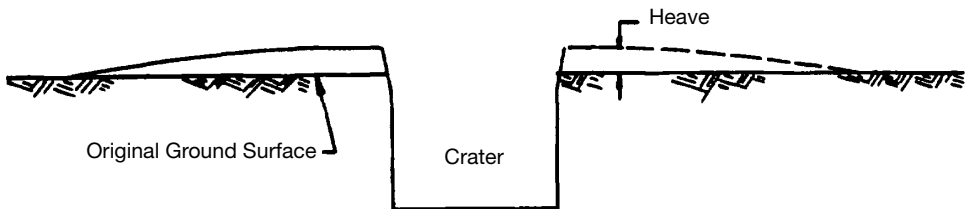
4. The loosened soil above the base of the crater requires that a higher level of energy be used during the ironing phase.

Fig. 6A.156 can be used to estimate a range in expected crater depths ( $\delta$ ) as a function of the theoretical applied energy ( $WH$ ) and the number of drops at each impact point.

In saturated Zone 2 and Zone 3 materials, which have moderate to low permeabilities, significant excess pore water pressures can be generated, which may require days or weeks to dissipate. These excess pore water pressures are sometimes sufficient to cause surface boils, and may result in water rising into the craters or ground heave adjacent to the craters. When high excess pore water pressures develop, additional applied energy primarily produces distortion of the soil mass (change in shape without change in volume). Hence, no significant densification occurs. Heaving of the ground surface, as illustrated in Fig. 6A.157, is an indication that distortion rather than densification is occurring and that tamping should be stopped at that location. In this case, the energy should be applied in multiple passes to allow dissipation of the excess pore water pressures prior to additional tamping at those impact points.



**FIGURE 6A.156** Normalized crater depths (from Mayne et al., 1984).



**FIGURE 6A.157** Heaving of ground surface adjacent to a crater (from Lukas, 1995).

**Treated Area.** In many projects, the treated area is larger than the area used for foundation support. In general, the distance the treated area extends beyond the edges of the loaded area is between one-half to one times the thickness of the weak deposit being treated. In some cases, the treated area may need to be larger than this. For example, when an embankment is constructed on a dynamically compacted area where slope stability is a concern, it is necessary to densify the soil beyond the toe a distance greater than the distance at which the potential critical failure surface will intersect the ground surface. If some areas are to be more heavily loaded than others, additional tamping can be performed at these locations after the entire grid area has already been tamped. For example, additional tamping has been conducted on some building projects at the column locations after tamping of the entire treated area has been completed.

**Surface Stabilizing Layer and Control of Groundwater.** When the surficial soils are soft, a granular stabilizing layer should be placed on the surface to provide a working mat. This mat serves two primary purposes—it prevents sticking of the tamper and it limits the depth of penetration of the tamper into the soft material. The thickness of the stabilizing layer should be determined such that the mat provides adequate stability but does not significantly reduce the magnitude of energy transmitted to the soil to be treated.

When the groundwater table is less than about 6 ft (2 m) from the ground surface, the bottom of the craters may reach below the water table, reducing the effectiveness of the dynamic compaction. In this case, three methods of control can be used: (1) Raise the grade by adding a granular layer, (2) dewater the site to lower the groundwater table before tamping commences, or (3) pump water from the craters between tamps and then add granular material to keep the impact elevation higher.

#### 6A.4.1.5 *Ground Vibrations, Lateral Displacements, and Airborne Debris*

When a tamper impacts the ground, vibrations are transmitted through the ground in all directions, as illustrated in Fig. 6A.147. Vibrations transmitted along and near the ground surface may travel large distances and affect nearby structures and occupants of adjacent buildings. The magnitude of the vibrations and the distance they travel increase with increasing impact energy. It has been determined that damage to structures and annoyance to people is more closely associated with particle velocity than either displacement or acceleration (Nicholls et al. 1971). Therefore, peak particle velocity (PPV) is the parameter generally used to estimate the magnitude of potential problems from vibrations. However, frequency of vibration also is an important factor in damage and annoyance. The frequency of ground vibrations from dynamic compaction is generally in the range of 6 to 10 Hz (Lukas 1995).

The expected magnitude of PPV from dynamic compaction should be estimated beforehand at any location where potential damage to adjacent structures or annoyance to occupants of nearby buildings may occur. Fig. 6A.158, which shows PPV as a function of scaled energy factor for various types of ground materials, can be used for this purpose. In addition, the following equation can be used to estimate a conservative upper limit of PPV as a function of energy and distance (Mayne et al. 1984):

## 6.206 SOIL IMPROVEMENT AND STABILIZATION

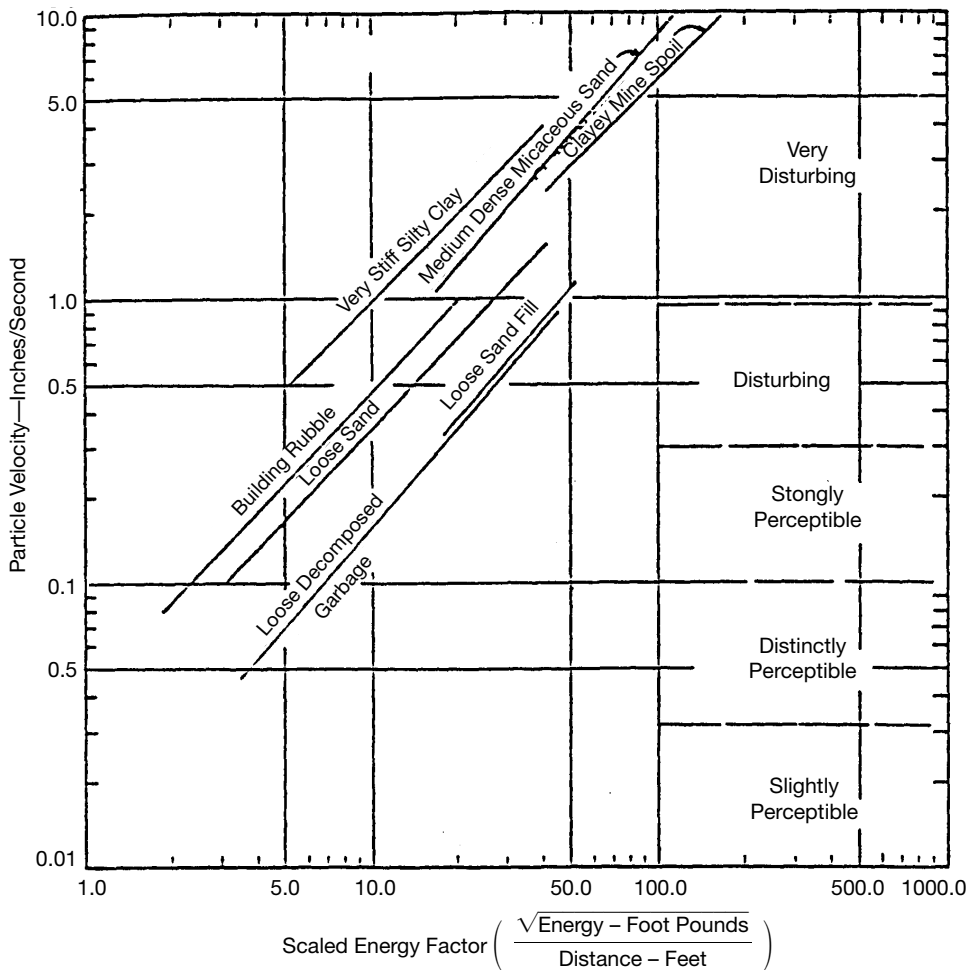


**FIGURE 6A.158** PPV versus scaled energy factor for various types of ground materials (from Lukas 1986).

$$PPV \text{ (in/sec)} \leq 3.64 \left( \frac{\sqrt{WH}}{d} \right)^{1.4} \quad \text{for } W \text{ in kips, and } H \text{ and } d \text{ in ft} \quad (6A.65a)$$

$$PPV \text{ (mm/sec)} \leq 70 \left( \frac{\sqrt{WH}}{d} \right)^{1.4} \quad \text{for } W \text{ in tonnes, and } H \text{ and } d \text{ in m} \quad (6A.65b)$$

where  $d$  is the distance from the impact point. It has also been found that PPV tends to increase with the number of blows from a tamper at a particular location as the underlying materials densify.

Levels of annoyance to people are given in Fig. 6A.158 as a function of particle velocity, with categories ranging from slightly perceptible to very disturbing. Within the normal range of vibration

frequencies produced by dynamic compaction, cracking of plaster and drywall in structures occur at particle velocities of about 0.5 in (13 mm) and 0.75 in (19 mm), respectively (Lukas 1995). Structural damage occurs at particle velocities greater than about 2 in (51 mm). In some cases, the ground vibrations can be substantially reduced by digging a trench to a depth of about 6 to 10 ft (2 to 3 m) between the impact point and the structure or area of concern (for example, see Thompson and Herbert 1978). An open trench is most effective in reducing vibrations but may be unacceptable for many reasons. In situations where an open trench is not feasible, the trench should be filled with loose granular soil or some other compressible material.

An assessment of preexisting cracking of adjacent houses and other structures should be conducted prior to beginning dynamic compaction, in conjunction with the owners of these structures, if it is expected that damage might occur. Actual PPVs produced by dynamic compaction should also be measured on the ground by adjacent structures using a portable field seismograph. If these steps are not taken, it may be impossible to determine whether cracking of these structures occurred before or during dynamic compaction and may cause unnecessary legal problems for the contractor.

Some permanent lateral displacements occur adjacent to the impact point. Although no reliable method has yet been established to predict the magnitude and distribution of lateral displacements with distance from the impact zone, some general relationships have been established (Lukas 1986, 1995):

1. Lateral displacements decrease with distance from the point of impact.
2. PPVs up to 3 in/sec (76 mm/sec) have not damaged buried utilities. Pressure pipelines have withstood PPVs of 10 to 20 in/sec (250 to 500 mm/sec) without distress.
3. For tampers in the range of 33 to 66 kips (147 to 294 kN), dynamic compaction should not be conducted within 25 ft (7.6 m) of any buried structure located within the upper 30 ft (9.1 m) of the ground mass if movement could cause damage.

Debris sometimes becomes airborne when the tamper impacts the ground. Rubble fills and landfills may produce substantial amounts of flying debris, owing to the large particles being impacted. Fine-grained soils may produce dust if dry or flying mud if wet. There are generally little or no problems with airborne debris in granular soils. Mitigation measures include the wearing of hard-hats for all on-site personnel, maintaining a safe distance from the impact point, and erecting protective shields adjacent to the impact location.

#### ***6A.4.1.6 Verification of Improvement***

Verification of the degree of improvement obtained by the dynamic compaction process is generally determined from in situ testing performed before and after the treatment. The most common methods are the standard penetration test (SPT), cone penetration test (CPT), and the pressuremeter test (PMT). Other methods that have been used include measurement of the increase in unit weight from samples, measurement of the deceleration of the tamper during impact using an accelerometer, load-deformation data from load tests, and measurement of increase in shear velocity from the cross-borehole seismic test.

The SPT and CPT are relatively insensitive to changes in stiffness of the soil compared to the PMT. Therefore, the PMT is generally a better test to provide information on the degree of improvement obtained by the treatment process. In many cases, the primary purpose of the dynamic compaction is to increase the stiffness of the soil, which is directly measured in the PMT. Another good method for determining the increase in stiffness of the soil is from load tests such as the plate load test (see section 6A.3.5.2 for additional details) and larger-scale load tests.

Since dynamic compaction remolds the treated soil, the strength and stiffness of the soil will increase with aging after the treatment ceases. On average, an increase in strength and stiffness on the order of 50 to 100% owing to aging can be expected during engineering times. Further details on the effects of aging on compacted soils can be found in section 6A.3.4.3. Much of the aging-induced improvement occurs in a few weeks in many cases but can continue for months and years afterward. In moderate and low permeability saturated soils, improvement also occurs as excess pore water

**6.208** SOIL IMPROVEMENT AND STABILIZATION

pressures dissipate. Thus, it is advisable to delay post-treatment testing as long as possible. If testing is performed immediately after treatment, additional testing should be performed a month or more later. The ideal posttreatment testing pattern is to test immediately after treatment, then 1, 2, 4, 8, 16, 32, etc. days afterward so that the long-term effects can be predicted from statistically reliable short-term data. Unfortunately, this is not always economically or logically feasible.

**6A.4.1.7 Case History**

The following case history is condensed from Lukas (1995) to illustrate some important aspects of dynamic compaction. Additional details can be found in the reference.

A three-story structure was to be constructed on an 86,000 ft<sup>2</sup> (8,000 m<sup>2</sup>) site in Florida. Although the structural loads were relatively light, the initial subsurface exploration indicated that sinkholes and voids caused by dissolution of limestone formations were present at the site. The geologic profile was relatively heterogeneous. The predominant soil type was a silty fine sand grading to a fine sand with seams of sandy clay. At some locations there was some cementation in the silty sand, making it substantially stiffer and stronger than the uncemented zones. Preliminary analyses indicated that settlement across the structure would range from 0.9 to 2.9 in. (23 to 74 mm), assuming that no voids or sinkholes were present within the bearing soils. The predicted differential settlement of 2.0 in. (51 mm) was considered to be unacceptable from a structural standpoint. Furthermore, the possible presence of large voids within the bearing materials was considered to be an unacceptable risk. Therefore, dynamic compaction was undertaken to improve the foundation bearing materials, eliminate voids to depths of 25 to 30 ft (7.6 to 9.1 m) below ground surface, reduce total settlements, and reduce differential settlements of the shallow foundations.

The dynamic compaction contractor used a 16.5 ton (147 kN) tamper and a drop height of 66 ft (20 m). From Eq. 6A.62, backcalculated values of  $n$  from 0.44 to 0.53 would be required to produce densification to the required depth of 25 to 30 ft (7.6 to 9.1 m). These values of  $n$  are reasonable. Since the soils at the site were predominantly Zone 2 materials, multiple passes and phases were needed to allow induced excess pore water pressures to dissipate. In addition, additional energy was applied at two locations where large ground depressions occurred, which was indicative of the presence of voids or sinkholes at those locations. Details of the dynamic compaction procedures and resulting induced settlements are summarized in Table 6A.15.

The total applied energy per unit area was approximately 111 ft-kips/ft<sup>2</sup> (1.63 MJ/m<sup>2</sup>). Dividing the energy per unit area by the desired maximum depth of improvement of 30 ft (9.1 m) yields a value of energy per unit volume of 3.7 ft-kips/ft<sup>3</sup> (180 kJ/m<sup>3</sup>), which falls below the recommended range of 5.2 to 7.3 ft-kips/ft<sup>3</sup> (250 to 350 kJ/m<sup>3</sup>) given in Table 6A.14 for Zone 2 materials. Pressuremeter tests conducted before dynamic compaction and 21 days after the treatment was completed showed that the dynamic compaction produced substantial increases in both limit pressure and pressuremeter modulus at all depths (Fig. 6A.159).

**TABLE 6A.15** Details of Dynamic Compaction Procedures Used in Florida Project

Phase	Pass	Spacing of impact points		Blows per point	Energy		Induced settlement	
		ft	m		ft-kips/ft <sup>2</sup>	kJ/m <sup>2</sup>	in	mm
1	1	30	9.1	8	19.4	284	4.8	121
1	2	30	9.1	9	21.8	320	3.9	98
1	3	30	9.1	9	21.8	320	2.8	70
2	1	30	9.1	9	21.8	320	3.8	97
2	2	30	9.1	10	24.2	355	3.7	93
Ironing	7	Overlapping	Overlapping	1	2.42	35.5	3.5	89
		Sinkhole locations	Sinkhole locations					

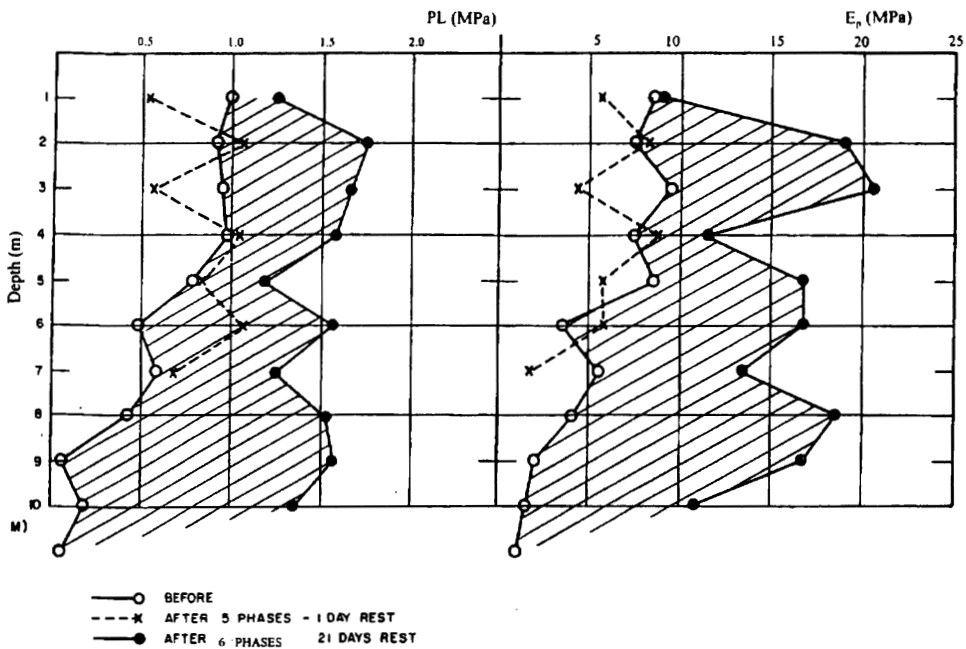


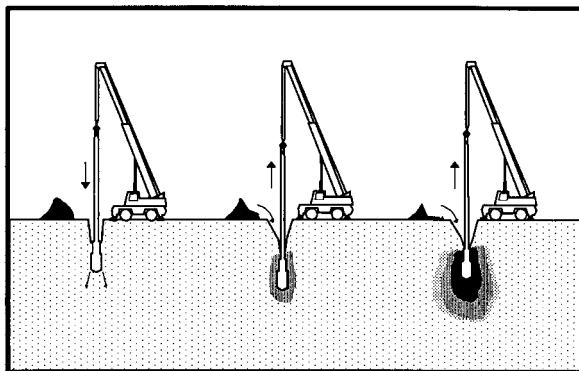
**FIGURE 6A.159** PMT values before and after dynamic compaction (from Lukas 1995).

#### 6A.4.2 Vibro-Compaction

In vibro-compaction, a vibratory probe is inserted into granular soils to densify them at depth below the ground surface. A schematic illustration of a typical vibro-compaction process is given in Fig. 6A.160. Typical depths of densification range from 10 to 50 ft (3 to 15 m), but can be as shallow as 3 ft (1 m) and as deep as 120 ft (36 m) (ASCE 1997). Horizontal spacing of the compaction points depends on the type of soil being densified, the amount of densification desired, and the characteristics of the probe. Usual horizontal spacings are in the range of 5 to 12 ft (1.5 to 4 m). Applications of this method include increasing bearing capacity, reducing settlement, increasing shear strength in foundation soils for embankments and hydraulic fills, and reducing liquefaction potential of loose saturated sands and silts.

##### 6A.4.2.1 Equipment and Procedures

The probe vibrates either horizontally or vertically to densify the granular soil. The most common type of vibro-compaction is called vibro-flotation and was developed in Germany in the 1930s and brought to the U.S. in the 1940s. Vibro-flotation involves the use of a torpedo-shaped probe called a vibroflot, which densifies the soil by horizontal motion from the probe while in the ground. The vibroflot is a hollow steel tube with an eccentric weight inside that rotates to develop large horizontal forces. Typical vibroflots are 12 to 18 in (300 to 460 mm) in diameter, 6 to 16 ft (2 to 5 m) in length, vibrate at frequencies of 1200 to 3000 rpm with amplitudes of 0.5 to 1.5 in (13 to 38 mm), and weigh about 3 to 5 kips (13 to 22 kN). Extension tubes are slightly smaller in diameter than the probe and allow the treatment process to be taken to greater depths. The vibroflot is normally suspended from a 60 to 100 ton (530 to 900 kN) crawler crane. A flexible coupling is used to isolate the vibroflot from the extension tubes so that the vibrations are not transmitted up the tubes to the crane.

**6.210** SOIL IMPROVEMENT AND STABILIZATION

**FIGURE 6A.160** Schematic illustration of typical vibro-compaction process (courtesy of Hayward Baker Inc., Odenton, Maryland).

The typical procedure used to densify the soil at depth is as follows:

1. The vibroflot is lowered to the desired depth by vibration, sometimes with the assistance of pressurized air or water jets located in the nose of the probe.
2. The vibroflot continues to vibrate at one depth, creating a cavity around the probe. This cavity is continuously filled with granular soil introduced either from the ground surface (top-feed method) as shown in Fig. 6A.160 or through feeder tubes directed to the tip of the probe (bottom-feed method). In the top-feed method, upper water jets can be used to facilitate getting the fill soil to the bottom of the cavity.
3. The vibroflot is retracted at about 1 ft (0.3 m) intervals, leaving a densified column of granular soil.
4. This procedure is repeated at other specified locations. The treated area can consist of isolated locations (for example to support individual footings) or full treatment of the area by compacting the soil on a grid pattern that allows overlapping of the densified zones.

Several other techniques use a top pile-driving vibrator that imparts vertical vibrations to the ground. Techniques utilizing this method include Terra-Probe, Vibro-Wing, and Tri-Star or Y-Probe (ASCE 1997). For example, the Terra-Probe method transmits vertical vibrations down an attached pipe with a diameter of about 30 in. (760 mm). Vertical vibration is generally less efficient than horizontal vibration, especially in finer-grained granular soils, and typically requires closer spacing of the compaction points.

#### **6A.4.2.2 Soil Types and Technical Considerations**

Vibro-compaction works best in loose granular soils, particularly clean sands and silty sands with less than about 20% fines and less than about 3% clay. The approximate range of grain-size distribution curves of granular soils suitable for densification by vibro-compaction is shown in Fig. 6A.161. The same procedures can be used in other types of soils with gravel as the backfill material, resulting in the creation of vibro-stone columns. Vibro-stone columns are described in Section 6A.5.

The radial extent of the densified soil depends on the characteristics of the soil being treated and the applied energy. The relative density of the treated material is highest at the periphery of the probe and decreases radially outward. Typical ranges of treated area per compaction probe as a function of the relative density obtained are shown in Fig. 6A.162. If treatment is conducted to the ground surface, the upper 3 to 6 ft (1 to 2 m) may require additional densification by surface rolling.

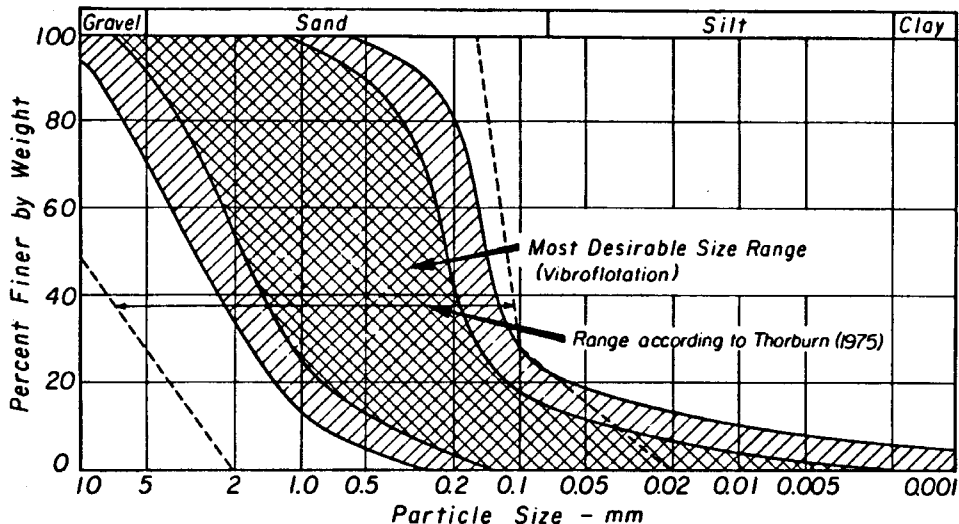


**FIGURE 6A.161** Range of particle size distributions suitable for densification by vibro-compaction (from Mitchell 1981).

Verification of the effectiveness of the treatment is done by conducting pretreatment and posttreatment SPTs or CPTs.

#### 6A.4.3 Blast Densification

The detonation of buried explosives can provide a rapid and sometimes economical means of densifying deep deposits of granular soils. This process is called blast densification or explosive compaction. Saturated loose sands and loessial soils are particularly suited to densification by blasting.

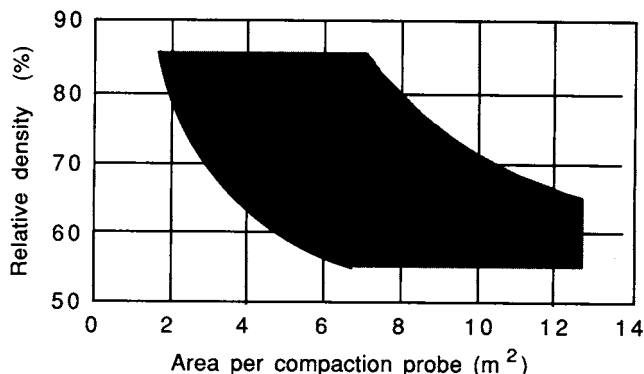


**FIGURE 6A.162** Envelope for spacing of vibro-compaction centers in clean granular soils (from Hausmann 1990).

**6.212 SOIL IMPROVEMENT AND STABILIZATION**

Although this technique has been used successfully for over 60 years in many different soil types under a variety of site and environmental conditions, it has not achieved general acceptance in civil engineering (Narin van Court and Mitchell 1995).

***6A.4.3.1 Mechanisms of Explosion and Densification***

To densify the soil effectively, the explosion must create sufficient energy to destroy the existing structure of the soil and rearrange the particles into a denser configuration. The explosion and densification process is summarized below from Narin van Court and Mitchell (1995). Additional details can be found in the reference.

The energy from the explosion is released in two forms—shock energy and gas energy. Shock energy is produced because the rate of reaction in the explosion is greater than the speed of sound in the soil, thereby forming a shock that impacts the surrounding soil. The stress applied to the soil by the shock wave is called detonation pressure. Gas energy is generated as the gaseous reaction products expand from their initial volume (volume of the charge) to an equilibrium volume dictated by the weight of the explosive charge and the confining pressure provided by the soil. The stress applied to the soil by the expanding gases is called the gas or explosion pressure. Gas energy typically accounts for 85% of the useful energy released by the explosive in rock blasting, and in soils the proportion may be higher.

Densification of granular soils occurs by many mechanisms, including compression, volumetric strains, shearing, and induction of liquefaction resulting from generated excess pore water pressures. The generation of excess pore water pressures is an important part of the densification process. During liquefaction, the soil particles are suspended and then settle out into a denser configuration as the excess pore water pressures dissipate. Ivanov (1983) has indicated that full liquefaction (excess pore water pressures equal to the effective confining pressure) is necessary to achieve maximum densification. According to Barendsen and Kok (1983), the excess pore water pressure generated by the blasting should be greater than 80% of the effective overburden pressure for optimum densification. Vertical drains can be used to accelerate the rate of dissipation of excess pore water pressures (see Section 6A.6). The effect of shearing can be improved by setting off subsequent adjacent detonations while some excess pore water pressures remain. When adjacent charges are detonated while the soil is in this weakened state, the shear waves generated by subsequent blasts can readily cause additional particle movements and hence compaction.

***6A.4.3.2 Procedures***

The typical procedure used to densify soils by blasting is as follows

1. Pipes are installed at specified locations and depths by jetting, vibration, or other suitable means.
2. Charges are placed in the pipes.
3. The holes are backfilled.
4. The charges are detonated according to a pre-established pattern.

Three types of charges can be used: concentrated (point) charges, columnar charges that extend the full height of the soil layer, and short columnar charges called deck charges. The blasting procedure, layout, and timing of detonation of the charges are mostly empirical, owing to the many unpredictable factors involved.

Hansbo (1983) provided the following guidelines for the densification of loose, saturated sands by blasting:

1. The charges should be placed at approximately  $\frac{1}{2}$  to  $\frac{3}{4}$  the desired depth of compaction, and in no case less than  $\frac{1}{4}$  the depth.
2. The spacing between detonation holes should be about 15 to 50 ft (5 to 15 m), and in no case less than 10 ft (3 m).
3. The number of coverages is usually 2 to 3, which are separated by hours or days.

#### **6A.4.3.3 Design Considerations**

For blast densification to be effective, the soils must be cohesionless, loose, saturated, and freely draining. Narin van Court and Mitchell (1995) recommend using average normalized cone penetration tip resistance ( $q_{c1}$ ) before treatment to determine the looseness of the soil and its suitability to be densified by blasting.  $q_{c1}$  is given by the following equation:

$$q_{c1} = q_{c,\text{avg}} \cdot C_n \quad (6A.66)$$

where

$$C_n = \left( \frac{\sigma_{\text{atm}}}{\sigma_{\text{eff}}} \right)^{1/2} \leq 1.7 \quad (6A.67)$$

$q_{c,\text{avg}}$  = average CPT tip resistance in 3 ft (1 m) intervals

$\sigma_{\text{atm}}$  = atmospheric pressure in units consistent with  $\sigma_{\text{eff}}$

$\sigma_{\text{eff}}$  = effective confining stress at the middle of the interval

Estimation of the effectiveness of blast densification is based on initial (pretreatment) values of  $q_{c1}$ , designated  $q_{c1i}$ . Explosive compaction is nearly always effective when values of  $q_{c1i} \leq 157$  ksf (7.5 MPa) and is generally ineffective when  $q_{c1i} \geq 522$  ksf (25 MPa). At intermediate values of  $q_{c1i}$ , blast densification is sometimes effective and sometimes ineffective.

After determining that a site is suitable for blast densification, an engineer needs to develop a blast design that ensures the entire soil mass receives sufficient energy. The explosive energy input to the soil at any location is influenced by the strength of the charge, the distance from the detonation, and the confining pressure acting on the charge. The following equation can be used to estimate the magnitude of  $q_{c1}$  following treatment (designated  $q_{c1f}$ ):

$$q_{c1f} = 3.20 q_{c1i} (E_{i,\text{total}})^{0.149} \quad (6A.68)$$

$$E_{i,\text{total}} = \sum E_i \quad (6A.69)$$

$$E_i = \frac{W_e^{1/2}}{R_e \cdot \sigma_t} \quad (6A.70)$$

where  $E_i$  = explosive energy input for one charge

$E_{i,\text{total}}$  = explosive energy input for all charges

$W_e$  = weight of the charge, in equivalent weight of TNT

$R_e$  = radial distance from the point of the explosion

$\sigma_t$  = total confining stress at the depth of the charge, in kPa

Barendsen and Kok (1983) have indicated that the magnitude of generated excess pore water pressure and the degree of densification are related to Hopkinson's number ( $N_h$ ) as follows:

$$N_h = 2.52 \frac{W_e^{1/3}}{R_e} \quad \text{for } W_e \text{ in lb and } R_e \text{ in ft} \quad (6A.71a)$$

$$N_h = \frac{W_e^{1/3}}{R_e} \quad \text{for } W_e \text{ in kg and } R_e \text{ in m} \quad (6A.71b)$$

Little or no liquefaction is expected to occur when  $N_h$  is less than about 0.09 to 0.15. This criterion

**6.214 SOIL IMPROVEMENT AND STABILIZATION**

and Eq. 6A.66 can be used to estimate the safe distance from the explosion. The following relationships can be used to estimate the settlement of the ground surface ( $\Delta h$ ) and the magnitude of the induced excess pore water pressure:

$$\frac{\Delta h}{h} = 2.73 + 0.9 \ln N_h \quad (6A.72)$$

$$\frac{u_e}{\sigma'_v} = 1.65 + 0.65 \ln N_h \quad (6A.73)$$

where  $h$  = height of the soil layer affected by the explosion

$\sigma'_v$  = effective overburden stress

**6A.4.3.4 Other Considerations**

Other considerations in blast densification are summarized as follows:

1. Blasting can cause high PPVs and therefore may damage adjacent structures or cause annoyance to occupants of adjacent buildings. Values of PPV higher than 12 in/sec (0.3 m/sec) have been reported from blast densification.
2. Zones of soil that are initially dense may be weakened by the blasting. However, if these dense zones are a small portion of the overall soil profile affected by the blasting, the resultant overall condition is likely to be satisfactory.
3. Settlement of the ground surface occurs almost immediately, with little additional settlement with time.
4. The surficial soil may be poorly compacted and may need to be excavated or compacted by some other method.
5. Gains in strength may continue with time after the blasting is complete, and even after all excess pore water pressures have dissipated. The majority of the gain in strength occurs within a few months after blasting, but may continue for several years after. This effect has not been observed at all sites treated by blast densification.

**6A.5 GRANULAR COLUMNS**

Several types of granular columns are currently used to improve bearing soils for shallow foundations in one or more of the following ways: (a) increase ultimate bearing capacity, (b) reduce compressibility, (c) increase the rate of settlement in saturated soils, (d) reduce liquefaction potential, (e) increase lateral resistance, and (f) increase uplift capacity. Granular columns can also be used to increase the stability of natural or fill slopes. The applicability of each type of granular column is summarized in Table 6A.16.

Although the methods of installation and types of columnar materials can vary significantly among the different types of granular columns, all types have the following basic features:

1. A single vertical, cylindrical column or group of columns consisting of granular or chemically stabilized granular material are created within the ground. Typically, about 10 to 40% of the volume of the native soil is replaced or displaced by the granular columns within the reinforced zone.
2. The columns are usually stronger, stiffer, and more permeable than the preexisting natural or fill soil into which they are installed (hereinafter called *matrix* or *native soil*).
3. When large areal coverage is provided, such as beneath a long embankment or a mat foundation, a triangular pattern is typically used (Fig. 6A.163). Sometimes a square pattern is used.

**TABLE 6A.16** Comparison of Engineering Properties Improved by Various Granular Columns

Type of granular column	Type of improvement						
	Increase ultimate bearing capacity	Reduce magnitude of settlement	Increase rate of settlement	Provide uplift resistance	Increase lateral resistance	Reduce liquefaction potential	Increase slope stability
Stone column	Significant	Significant	Significant	None	Moderate	Significant	Significant
Sand column	Significant	Significant	Significant	None	Some	Significant	Significant
Geopier	Significant	Significant	Significant	Significant	Significant	Significant	Significant
Gravel drain	Some	Some	Significant	None	Not applicable	Significant	Not applicable
Sand drain	Some	Some	Significant	None	Not applicable	Significant	Not applicable

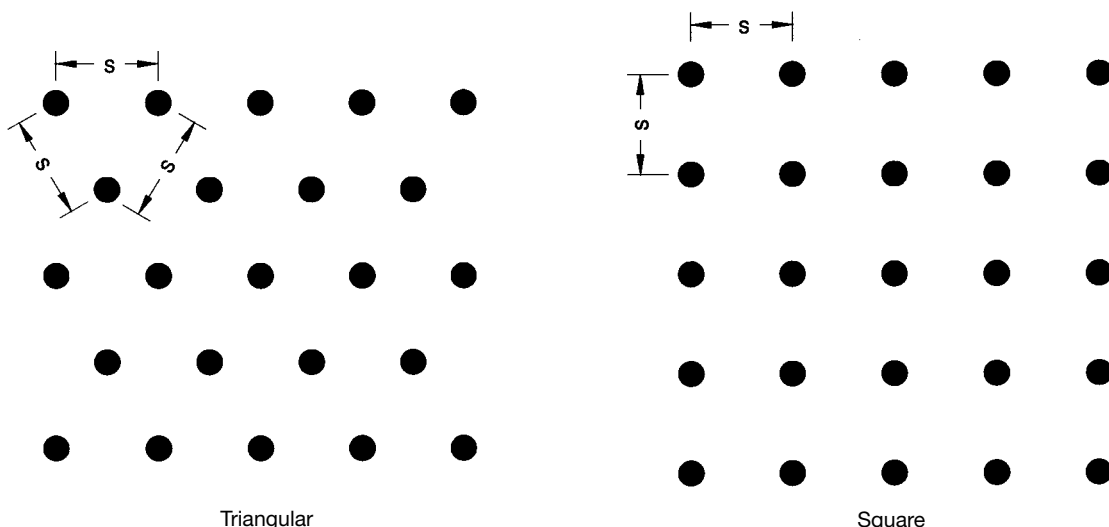
4. For support of individual footings, a variety of patterns can be used, depending on the shape and size of the footing, as well as the types and degrees of improvement needed in the soil. Some common patterns for individual footings are illustrated in Fig. 6A.164.

### 6A.5.1 Types of Granular Columns

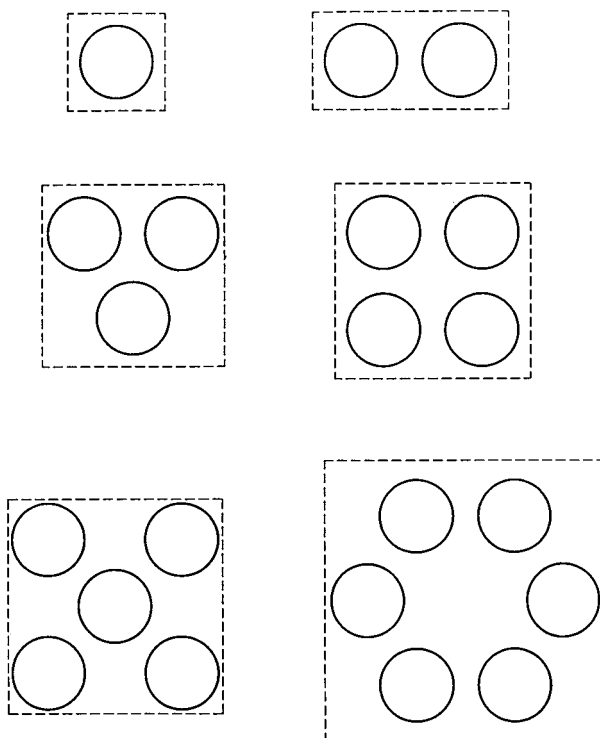
The primary types of granular columns in common use today are *stone columns*, *sand columns*, *geopiers*, *gravel drains*, and *sand drains*. The important characteristics of each of these types are described in the following sections.

#### 6A.5.1.1 Stone Columns

Stone columns are installed using either vibratory, rotary, or ramming techniques. The conventional stone column method was developed in Germany in the 1950s as an extension of the vibro-compaction process and is the most predominant technique in current use.



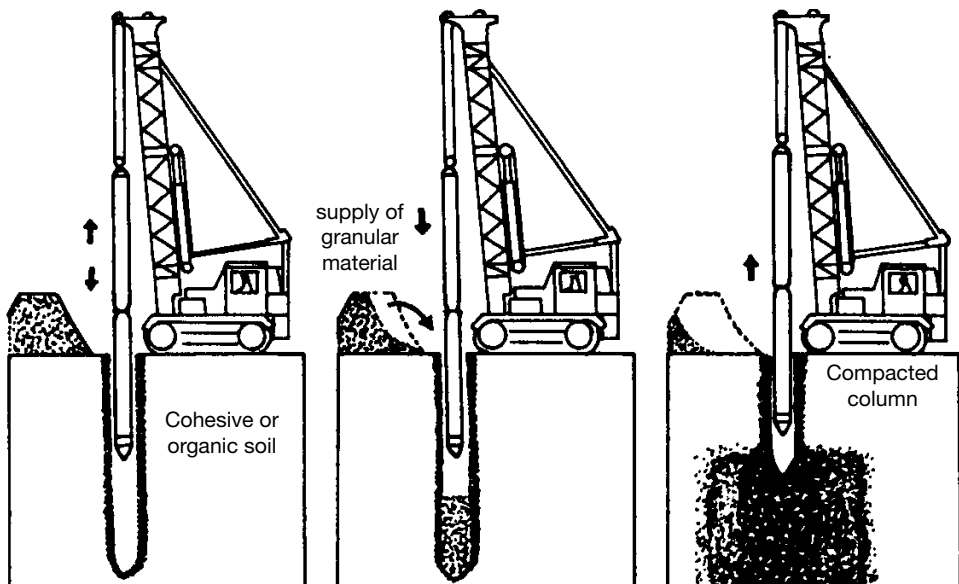
**FIGURE 6A.163** Triangular and square patterns of columnar reinforcement.

**6.216** SOIL IMPROVEMENT AND STABILIZATION

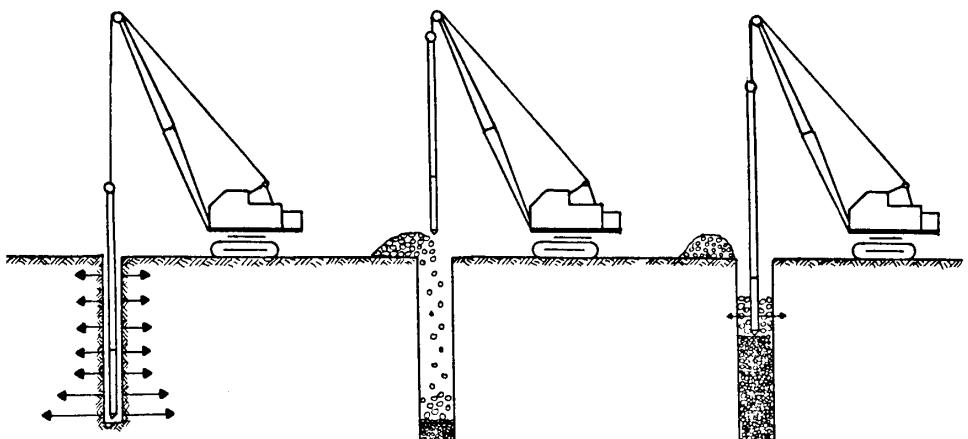
**FIGURE 6A.164** Some common patterns of granular columns to support individual footings (from Geopier Foundation Company 1998).

Conventional stone columns are installed using the same type of horizontally vibrating probe used in vibro-compaction (see Section 6A.4.2). Either replacement (wet) or displacement (dry) techniques can be used. In the *vibro-replacement* method (Fig. 6A.165a), a hole is created in the ground to the desired depth by water jetting from the vibratory probe (ASCE 1987). The uncased hole is flushed out and stone is added in increments through the annular space between the probe and the enlarged hole. The stone is compacted in about 12 to 48 in (0.3 to 1.2 m) thick lifts by a combination of vibration from the probe and ramming the probe into the stone. During this process, soft matrix soils may collapse into the hole. If so, the continuing water upflow carries the collapsed material to the ground surface, allowing the stone to expand farther outward until equilibrium is reached. The diameter of the column varies with depth, generally being larger at the top, bottom, and at softer soil layers. Vibro-replacement is best suited for sites with soils having undrained shear strengths in the range of about 300 to 1000 psf (15 to 50 kPa) and a high groundwater table. In the 1970s and early 1980s, vibro-replacement was the only method used to construct stone columns in the United States, although dry methods were used elsewhere (Barksdale and Bachus 1983, Goughnour 1997). However, since that time environmental constraints have complicated the disposal of the large amounts of silt and clay-laden effluents generated during the wet process. An additional problem is the ponding of water on the ground surface, which can disrupt work and slow production. In response to these constraints and problems, the use of dry techniques is now common in the United States.

In the vibro-displacement technique, the vibrating probe displaces the soil laterally as it is ad-



(a)



Soil Displacement

Stone Backfill

Compacted Column

(b)

**FIGURE 6A.165** Construction of a stone column by top-feed (a) vibro-replacement (from Baumann and Bauer 1974), and (b) vibro-displacement (from Barksdale and Dobson 1983).

**6.218** SOIL IMPROVEMENT AND STABILIZATION

vanced into the ground, usually with the aid of compressed air through the tip of the probe (ASCE 1987). In the top-feed method illustrated in Fig. 6A.165b, the probe is removed from the hole after reaching the desired depth, backfill is dropped in the annular space between the probe and enlarged hole, and the probe is lowered again to displace the stone laterally and downward. This process is repeated in lifts to create the compacted stone column. This top-feed dry method is best suited for sites with a deep groundwater table and firm soils with undrained shear strengths from about 600 to 1200 psf (30 to 60 kPa) and low sensitivity. Beginning about 1976, bottom-feed equipment and methods were developed to extend the use of vibro-displacement methods to soft and loose saturated soils (Jebe and Bartels 1983). In the bottom-feed methods, the probe remains in the hole while the stone is discharged through the probe. The columns created by the dry techniques are usually smaller in diameter than those created by the wet process because no matrix material is removed from the hole in the dry process.

The rotary method of installing stone columns was developed as an alternate technique for use in soft cohesive soils and loose silty or clayey sands (Goughnour 1997). This method was developed to reduce the problems associated with contamination of the stone by intermixing with matrix soil that occur in vibratory installation methods. The heart of this system is an impeller that consists of two symmetrically located logarithmic spiral sections (Fig. 6A.166). The impeller is driven by a centrally placed drive shaft and fits closely beneath the bottom of a feed pipe. Stone is fed down the annular space between the feed pipe and the shaft. During rotation of the impeller, stone is thrown radially outward while additional stone falls from the feed pipe into the pockets behind the logarithmic spiral sections. The main components of the machine used to install rotary stone columns (Fig. 6A.167a) are a carrier (crane) and mast (construction leads), a hopper and winch arrangement for stone delivery, a probe that includes a vibratory driver/extractor, a rotary hydraulic motor, an airlock and chute, and an impeller fitted at the bottom. The top portion of the probe is shown in Fig. 6A.167b.

The normal procedures used to build a rotary stone column are as follows (Goughnour 1997):

1. The feed pipe and the impeller are positioned over the location where the stone column is to be installed.
2. The feed pipe is lowered into the ground. During this process air pressure is applied to the in-

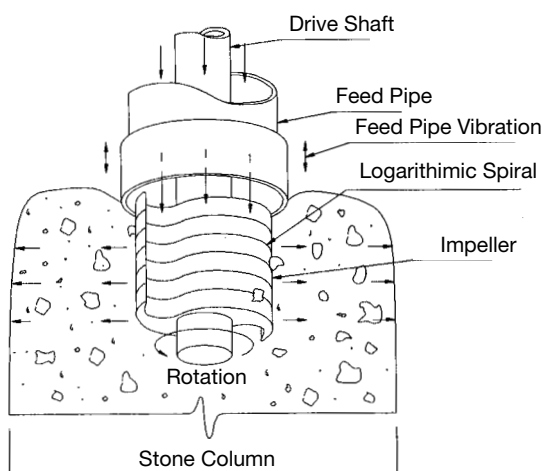


**FIGURE 6A.166** Perspective view of impeller used in construction of rotary stone columns (from Goughnour 1997)

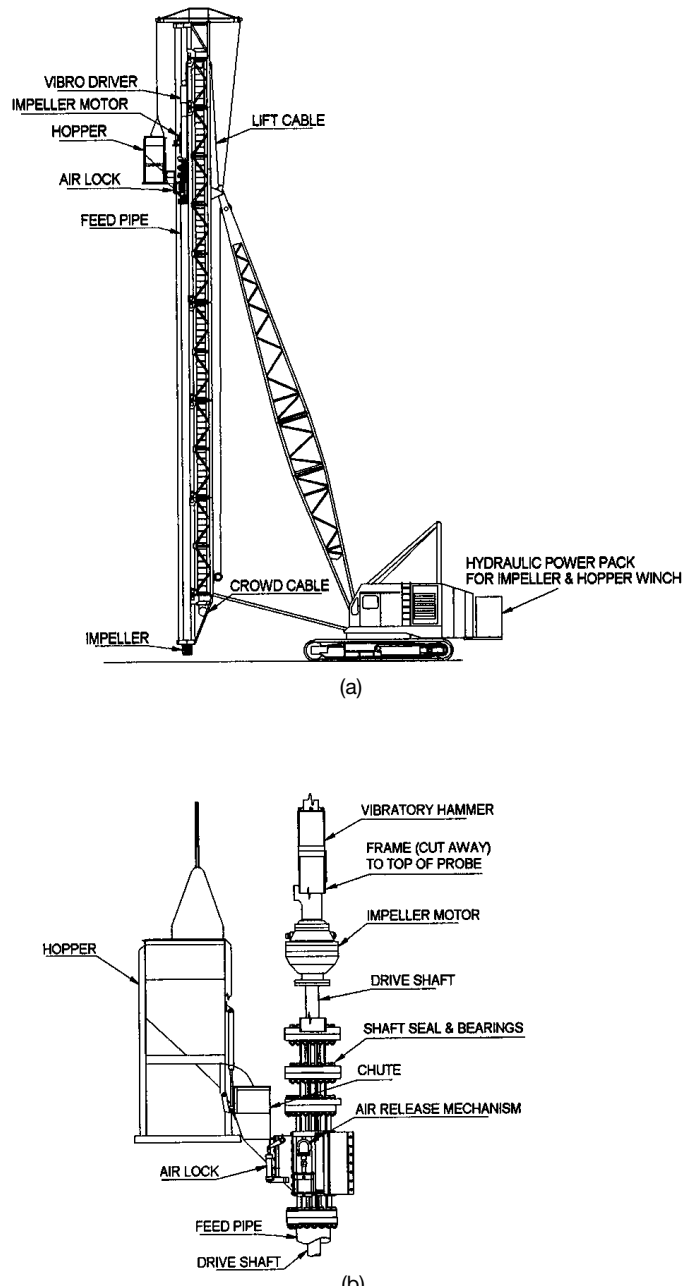


**FIGURE 6A.167** Equipment used to construct rotary stone columns (from Goughnour 1997): (a) Overall view of rig, and (b) detail of top part of probe.

**6.220** SOIL IMPROVEMENT AND STABILIZATION

terior of the empty feed pipe, the impeller is rotating, and the vibratory driver/extractor is turned on.

3. When the desired depth is reached, the penetration, vibration, and impeller rotation are all stopped.
4. The loaded hopper is positioned for discharge into the airlock.
5. The air pressure from the feed pipe is released, the airlock is opened, and stone is fed from the hopper through the airlock into the feed pipe.
6. The airlock is closed and air pressure is re-established within the feed pipe.
7. With the impeller rotating and vibration applied as necessary, the feed pipe is raised in response to hydraulic pressure on the impeller motor. The pressure must be maintained as closely as possible to the target pressure, which is site-specific and depends on field conditions and desired column diameter. The target pressure may be varied if field conditions change on site.
8. When the feed pipe is empty, the hydraulic pressure on the impeller motor drops and does not rebuild. At this point the pipe is no longer lifted, and the vibration and impeller are stopped.
9. Steps 4 through 8 are repeated until the column is constructed to the desired elevation.

Stone columns have also been installed using a technique called *dynamic replacement*, which is a combination of stone columns and dynamic compaction, as shown in Fig. 6A.168 (Gambin 1984, Liausu 1984). In this method, stone is placed in a layer on the ground surface and compacted using a heavy tamper in the manner described for dynamic compaction (section 6A.4.1). Soil improvement occurs not only at the location of the stone columns, but also between column locations, owing to horizontal densification of the soil.

**6A.5.1.2 Sand Columns**

Sand columns—also known as sand compaction piles—have been used extensively in Japan and other parts of Asia to reinforce soft and loose soils. The methods of installation used to create sand columns can be classified into the following three primary types (Japanese Geotechnical Society 1998):

1. Vertical vibration and compaction with enlargement of the column diameter by repeatedly supplying sand and then pulling and repenetrating the casing pipe (Fig. 6A.169a).
2. Vertical vibration and compaction with enlargement of the column diameter by a hydraulic compaction device at the end of the casing pipe (Fig. 6A.169b).
3. Vertical vibration and compaction with enlargement of the column diameter by horizontal vibration of the end of the casing pipe (Fig. 6A.169c).

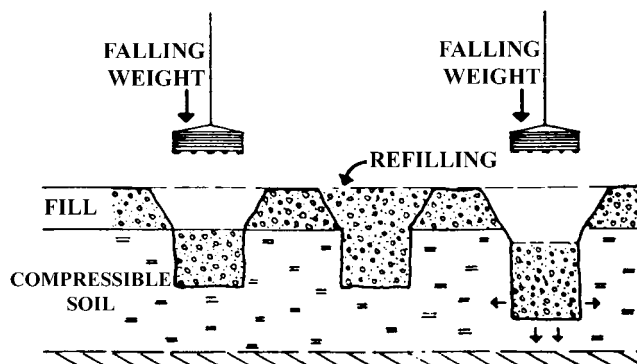


**FIGURE 6A.168** Construction of stone columns by dynamic replacement (modified from Liausu 1984).

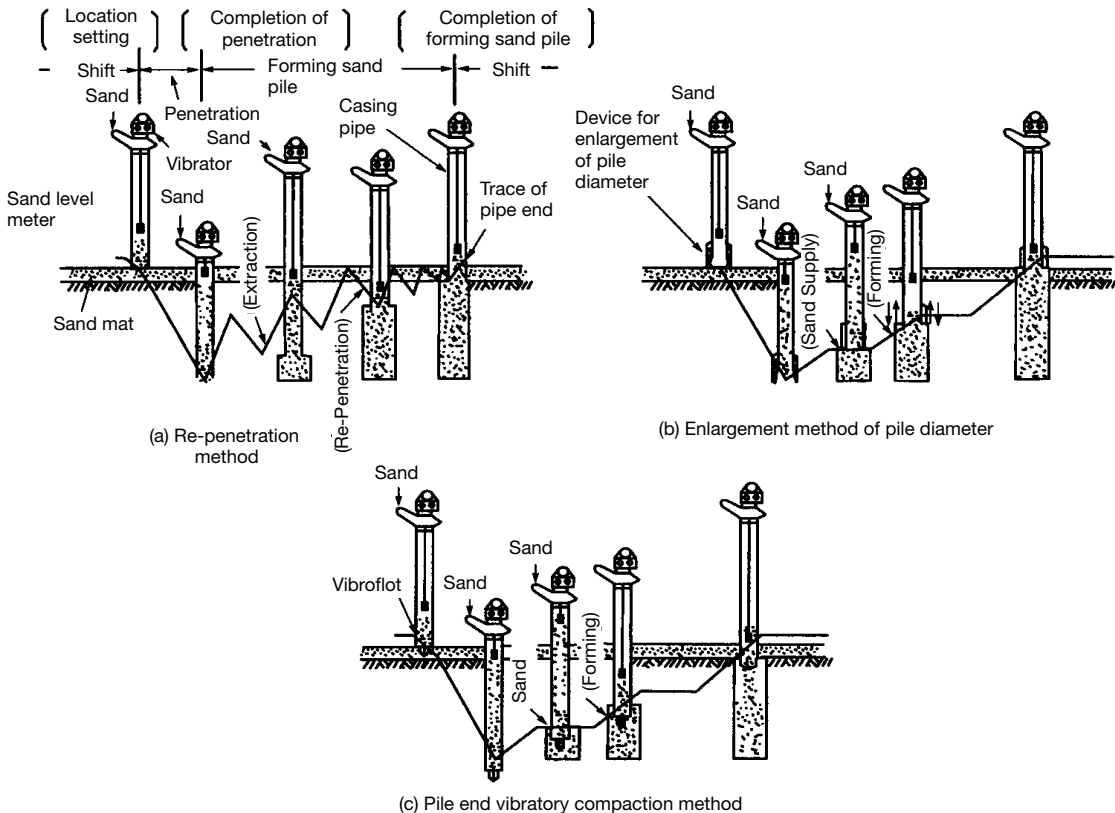


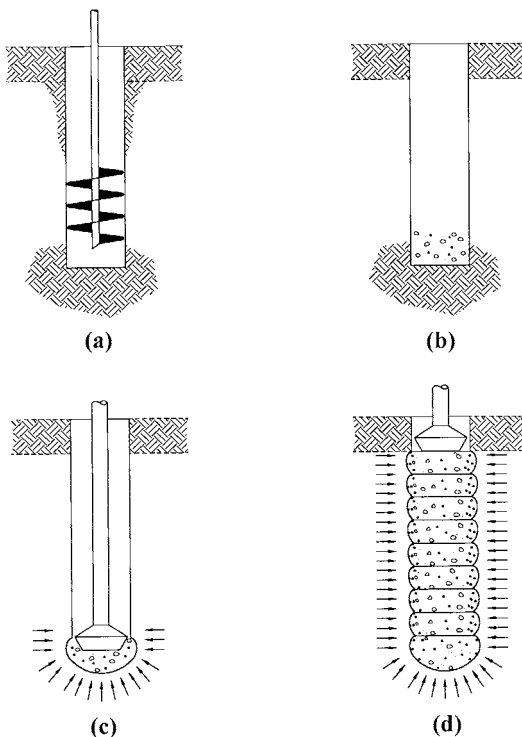
**FIGURE 6A.169** Common methods used to install sand columns (from Japanese Geotechnical Society 1998).

#### 64.5.1.3 Geopiers

There are two primary types of geopiers—compressive and uplift. The major steps used to construct compressive geopiers are illustrated in Fig. 6A.170 and summarized as follows:

1. A cylindrical cavity is formed in the soil using an auger (Fig. 6A.170a). The diameter of the cavity is typically in the range of 24 to 36 in (0.61 to 0.91 m).
2. Aggregate is placed at the bottom of the hole and is compacted by repeated ramming using a specially designed tamper with a beveled head (Fig. 6A.170b,c). High-frequency, low-amplitude energy for this process is supplied by a skid loader, a backhoe, or an excavator (Fig. 6A.171). The “bulb” created from this process provides a firm foundation on which to construct the remainder of the geopier and is especially important in soft and loose soils.
3. The main body of the geopier is then constructed in a similar manner by placing loose aggregate in the hole and compacting it in 12 in (0.30 m) or thinner lifts to the desired height (Fig. 6A.170d). The height of a geopier is typically two to five times its diameter.

An uplift geopier is constructed in a similar manner with the following additional steps. After the bottom bulb is constructed (step 2), an uplift assembly consisting of a horizontal steel plate and attached vertical threaded steel bars (Fig. 6A.172) is set in hole and rests on the bottom bulb. A spac-

**6.222** SOIL IMPROVEMENT AND STABILIZATION

**FIGURE 6A.170** Steps in construction of a compressive geopier.

er is used to hold the threaded bars apart during construction of the main body of the geopier in the same manner as described in step 3 above. In permanent applications, the uplift plate and threaded bars are galvanized to reduce long-term corrosion of the steel. The uplift bars or dowels spliced to the uplift bars extend upward into a reinforced concrete footing and are bonded to the concrete, forming an integral foundation system with the footing. Uplift geopiers also provide substantial resistance to compressive and lateral forces and displacements.

Well-graded gravelly sand (normally highway base course material) is typically used as the geopier aggregate above the groundwater table, with open-graded gravel normally used below the groundwater table. Owing to the confinement provided by the adjacent matrix soil and the high energy used to compact the geopiers, high densities are achieved within the compacted geopier aggregate (typically more than 100% of modified Proctor maximum dry density). In addition, the adjacent matrix soils are substantially prestressed and prestrained. Measurements in matrix soils adjacent to geopiers have shown that installation of a geopier can increase the horizontal stresses as far away as 10 ft (3 m) or more, and that the horizontal stresses immediately adjacent to the geopiers can reach the limiting passive condition.

Linear geopiers can also be constructed by first excavating a trench using a backhoe or excavator. Aggregate is then compacted to fill the trench in thin lifts using the same procedures described above for columnar geopiers. Linear geopiers are used to support walls and long, thin rectangular foundations and typically have nominal widths of 18 to 30 in (0.46 to 0.76 m).



**FIGURE 6A.171** Installation of a geopier with an excavator supplying the energy.

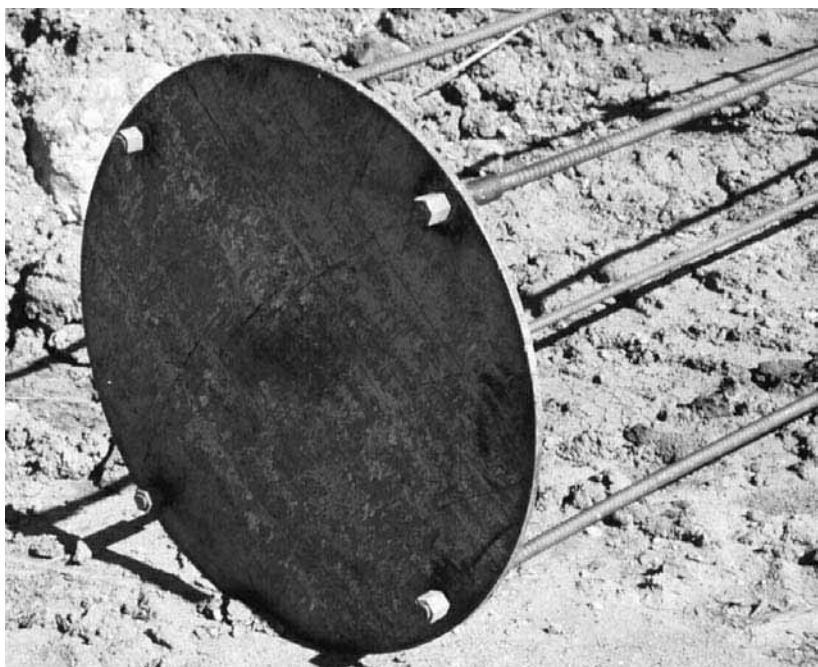


**FIGURE 6A.172** Anchor plate with threaded steel bars used in uplift geopiers.

**6.224** SOIL IMPROVEMENT AND STABILIZATION**6A.5.1.4 Sand and Gravel Drains**

The main purpose of sand and gravel drains is to provide rapid drainage of a saturated soil during pre-compression (section 6A.6), earthquakes, or other phenomena in which significant excess pore water pressures may develop. Sand and gravel drains are typically 8 to 20 in (200 to 500 mm) in diameter and are spaced anywhere from 5 to 20 ft (1.5 to 6.0 m). Since drainage is the primary desired engineering characteristic, compaction of the sand or gravel is not a priority; on the contrary, excessive compaction may reduce the permeability and hence reduce drainage capability of the drain. Therefore, only sufficient compaction necessary to ensure continuity of the drain is typically undertaken.

Many methods of installation are used to construct sand and gravel drains, which are generally classified into two groups (displacement and nondisplacement). The equipment used to install these types of drains include closed-ended mandrel, screw-type auger, continuous flight hollow stem auger, internal jetting, rotary jet, and Dutch jet-bailer. Additional details on the installation can be found in Ladd (1986).

**6A.5.2 Engineering Characteristics, Response, and Behavior****6A.5.2.1 Stress Concentration**

When compressive loads are applied to a bearing soil reinforced with granular or chemically stabilized columns, the vertical stress induced on top of the substantially stiffer columns is much greater than on the more compressible matrix soil at the same level. This concept is illustrated using a spring analogy in Fig. 6A.173 for a centric vertical load applied to a rigid foundation. In this analogy, each spring represents the force generated over the same amount of contact area. It is well known from basic physical laws that the force induced in a linearly elastic spring is equal in magnitude to the spring constant times the amount of deflection of the spring and acts in the direction opposite to the direction of the spring deflection ( $F = -K\delta$ ). For the conditions shown in Fig. 6A.173, the footing will settle the same amount at all points. Hence the force induced in the stiff spring representing a granular column will be substantially greater than the forces generated in the springs representing the matrix soil. The sum of these spring forces must equal the applied load  $P$ . If these forces are divided by the same contact area, it is concluded that the stresses induced on the columns

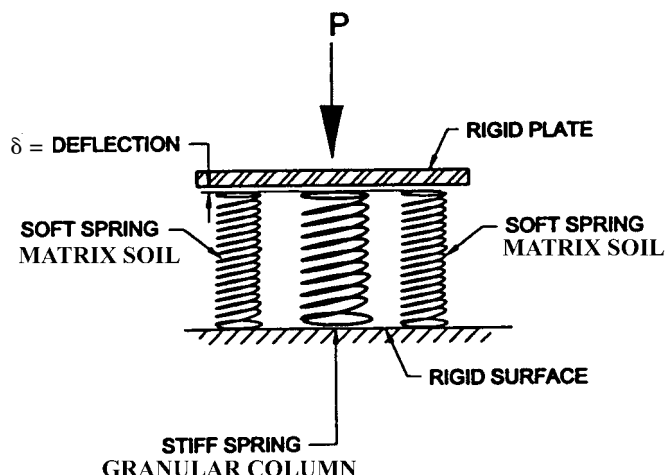


**FIGURE 6A.173** Spring analogy illustrating stress concentration on granular columns (modified from Geopier Foundation Company 1998).

are greater than those induced on the matrix soil. Stress concentration also occurs beneath flexible foundations but to a lesser degree. Concentration of stresses on the stiffer columns is a key factor in controlling foundation settlement, increasing lateral resistance of footings, and stabilizing slopes with columnar reinforcement.

The concepts of unit cell, area replacement ratio, and stress concentration are illustrated in Fig. 6A.174 for columnar reinforcement arranged in a large square array at a center-to-center spacing of  $s$ . The unit cell is comprised of a single column and the corresponding tributary matrix soil. The boundaries of the unit cells are shown with dashed lines in Fig. 6A.174a. The area of a column is designated  $A_c$ , the area of the matrix soil within the unit cell  $A_m$ , and the total area of the unit cell  $A$ . The area replacement ratio ( $R_a$ ) and the stress concentration ratio ( $R_s$ ) are given by the following equations:

$$R_a = \frac{A_c}{A} \quad (6A.74)$$

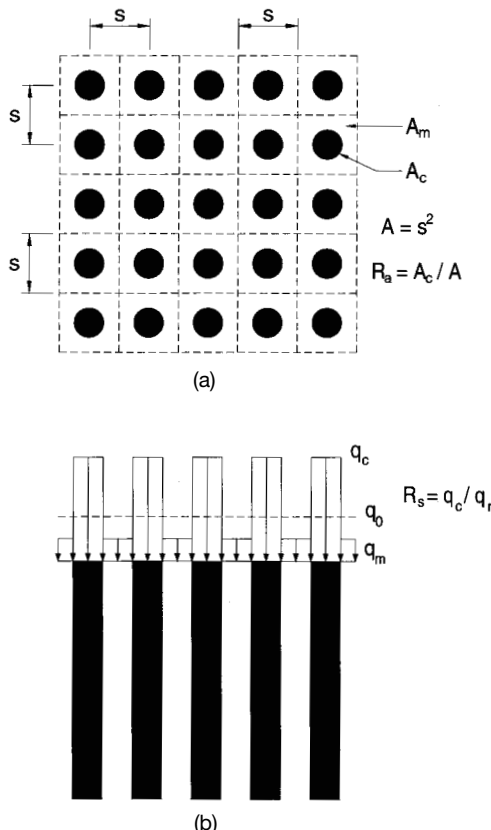


**FIGURE 6A.174** Illustration of (a) unit cell and area replacement ratio (horizontal section), and (b) stress concentration and stress concentration ratio (vertical section).

**6.226** SOIL IMPROVEMENT AND STABILIZATION

$$R_s = \frac{q_c}{q_m} \quad (6A.75)$$

For an individual footing,  $A_c$  is the area of all the columns supporting the footing and  $A$  is the total area of the footing. If the footing is rigid, as is the case for most individual footings composed of reinforced concrete,  $R_s = k_{sc}/k_{sm}$ , where  $k_s$  is vertical subgrade modulus (Lawton et al. 1994). Since  $k_s$  varies as a function of the width of the loaded area (see Eqs. 6A.54–6A.57), the values of  $k_{sc}$  and  $k_{sm}$  used must correspond to the appropriate loaded areas of the columns and the matrix soil.  $k_{sc}$  can be obtained by performing a plate load test on top of a test or production column, with the diameter of the plate the same as the nominal diameter of the column.  $k_{sm}$  can be estimated by performing a similar plate bearing test on the matrix soil at the elevation of the top of the columns and using established scaling laws to calculate  $k_{sm}$  for the width and shape of the actual footing.  $k_{sm}$  can also be estimated from the results of in situ or laboratory tests on the matrix soil (see Bowles 1975, pp. 516–518).

The following equations for the stresses induced on the top of columns ( $q_c$ ) and the matrix soil ( $q_m$ ) as a function of the average applied stress ( $q_0$ ) can be obtained by summing forces in the vertical direction and satisfying static equilibrium (Aboshi et al. 1979):

$$q_c = q_0 \frac{R_s}{R_a(R_s - 1) + 1} = q_0 \cdot \mu_c \quad (6A.76)$$

$$q_m = q_0 \frac{1}{R_a(R_s - 1) + 1} = q_0 \cdot \mu_m \quad (6A.77)$$

Both  $q_c$  and  $q_m$  depend on  $R_s$ , which must be estimated. The following theoretical equations from Aboshi et al. (1979) can be used to estimate the stress concentration ratio at yield ( $R_{sy}$ ).

For friction-only columnar and matrix materials ( $\phi' = 0$ ,  $c' = 0$ ):

$$\tan^2(45^\circ + \phi'_c/2) \leq R_{sy} \leq \tan^2(45^\circ + \phi'_c/2) \cdot \tan^2(45^\circ + \phi'_c/2) \quad (6A.78)$$

For friction-only columnar material ( $\phi'_c = 0$ ,  $c'_c = 0$ ) and a saturated cohesive matrix soil in the unconsolidated-undrained condition ( $\phi_m = 0$ ,  $c_m = s_{um}$ ):

$$R_{sy} \leq \tan^2(45^\circ + \phi'_c/2) \cdot (1 + 2s_{um}/q_m) \quad (6A.79)$$

In a design situation where settlement is to be estimated, these equations are of limited value because the actual state of stress should be well below the level at which failure occurs.

Typical values of  $R_s$  vary depending on the type of granular columns, applied stress level, duration of the load, stiffness of the matrix soil, and flexibility of the foundation applying the load to the columns. Measured values of  $R_s$  for stone columns and sand columns generally range from 2.5 to 5.0 for typical values of applied stress. In design,  $R_s$  is usually conservatively assumed to be about 2 or 3. There are less data available for measured values of  $R_s$  for geopiers. In recent tests with rigid foundations, measured stress concentration ratios varied from about 10 to 40 at typical applied stress levels (Lawton 1999).  $R_s$  for the design of geopier foundations is usually conservatively estimated to be about 10 to 15. It appears that  $R_s$  increases with increasing applied load up to a critical value of applied stress where it reaches a maximum (Han and Ye 1991). At stresses higher than the critical value,  $R_s$  decreases with increasing load. Furthermore,  $R_s$  usually increases with time at constant applied stress, probably owing to greater secondary compression within the matrix soil than the granular columns.

**6A.5.2.2 Settlement**

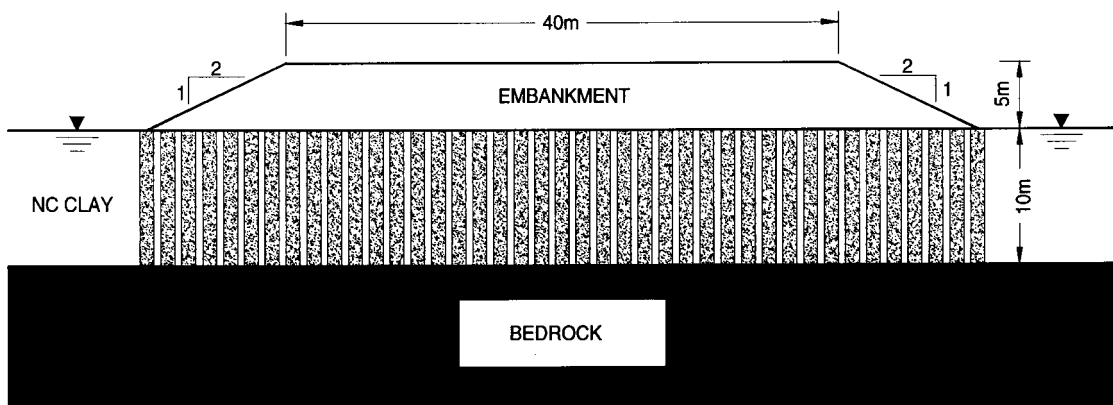
The inclusion of columnar reinforcement reduces the magnitude of settlement and generally increases the rate of settlement compared to the unreinforced soil. Numerous methods varying in complexity from simple approximations to sophisticated numerical analyses have been used to estimate the magnitude of settlement for foundations bearing on columnar-reinforced soil. Some of these methods are used exclusively for certain types of columnar reinforcement. Only a general overview of some of the most commonly used methods will be described here. Discussions of additional methods can be found, for example, in ASCE (1987) and Barksdale and Bachus (1983).

One of the simplest methods for estimating the settlement of structures founded on column-reinforced bearing soil is the *equilibrium method*. Although this method was originally developed to estimate primary consolidation settlement of saturated clays reinforced with sand columns (Aboshi et al. 1979), it can be applied to any type of matrix soil and drainage conditions. However, the equilibrium method is valid only where the columnar reinforcement extends throughout the entire depth of the compressible material or throughout the depth where most of the strain occurs (approximately two times the width of a circular or a square foundation and about four times the width of a strip foundation). The steps in the equilibrium method are summarized as follows:

1. Estimate the stress induced on the matrix soil at the bearing level ( $q_m$ ) using Eq. 6A.77.
2. Calculate the settlement of the structure as if there is no columnar reinforcement and the average stress at the bearing level is  $q_m$  rather than  $q_0$ . Use the actual dimensions and shape of the foundation.

The following example is given to illustrate the method.

**Example Problem 6A.2** A proposed highway embankment will be 40 m (131 ft) wide at its crest and 5 m (33 ft) tall ( $H_e$ ) with 2H:1V side slopes and an average unit weight ( $\gamma_e$ ) of 20 kN/m<sup>3</sup> (127 pcf). The embankment will be constructed on the surface of a normally consolidated clay stratum that is 10 m (33 ft) thick with an average buoyant unit weight ( $\gamma'$ ) of 7.0 kN/m<sup>3</sup> (45 pcf), an existing average void ratio of 1.30, and a virgin compression index ( $C_v$ ) of 0.30. The clay stratum is underlain by hard and impervious bedrock. The properties of the clay stratum will be assumed constant throughout the clay layer to simplify the calculations. Reinforcing columns 1.0 m (3.3 ft) in diameter will be arranged in a square array at a spacing ( $s$ ) of 1.5 m (4.9 ft) and will extend the entire height of the clay stratum. The stress concentration ratio ( $R_s$ ) is estimated to be 5. Estimate the ultimate primary consolidation settlement ( $S_c$ ) of this embankment along its centerline both without and with the columnar reinforcement.



**6.228** SOIL IMPROVEMENT AND STABILIZATION

**Solution:  $S_c$  without columnar reinforcement**  $S_c$  for the clay layer without reinforcement will be calculated by subdividing the clay stratum into ten 1.0-m (3.3-ft) thick sublayers and calculating and summing  $S_{ci}$  for each sublayer. In equation form:

$$S_c = \sum_{i=1}^{i=n} S_{ci}$$

where  $n$  is the total number of sublayers (ten in this case) and  $i$  identifies individual sublayers. The solution is shown in tabular form below. It should be noted that in real practice, a greater number of sublayers should be used, which can be easily accomplished using a spreadsheet program. Only ten sublayers are used here because of space limitations. For simplicity, buoyancy effects produced by submergence of the lower portion of the embankment as settlement occurs will be ignored (these effects are usually minor).

For a normally consolidated clay:

$$S_{ci} = \frac{C_{ci}}{1 + e_{0i}} \cdot H_{0i} \cdot \log \frac{\sigma'_{vf}}{\sigma'_{v0}}$$

where  $H_{0i}$  = initial height of sublayer  $i$

$\sigma'_{v0i}$  = initial effective vertical stress at the midheight of sublayer  $i$  =  $\gamma' \cdot z_i$

$\sigma'_{vf}$  = final effective vertical stress at the midheight of sublayer  $i$  =  $\sigma'_{v0i} + \Delta\sigma_{vi}$

$\Delta\sigma_{vi}$  = total vertical stress induced by load from embankment

$z_i$  = depth from top of the clay layer to the midheight of sublayer  $i$

$\Delta\sigma_v$  will be calculated using the following equation (Osterberg 1957):

$$\Delta\sigma_v = \frac{2q_0}{\pi} \left[ \frac{m+n}{m} \cdot \tan^{-1}(m+n) - \frac{n}{m} \tan^{-1}n \right]$$

where  $m = a/z$

$n = b/z$

$a$  = horizontal width of one slope = 10 m (33 ft)

$b$  = half the width of the embankment crest = 20 m (66 ft)

$q_0$  = applied stress at the bottom of the embankment =  $\gamma_e \cdot H_e$  = (20)(5) = 100 kPa (2.09 ks)

$i$	$H_{0i}$ (m)	$z_i$ (m)	$\sigma'_{v0i}$ (kPa)	m	n	$\Delta\sigma_{vi}$ (kPa)	$\sigma'_{vf}$ (kPa)	$S_{ci}$ (m)
1	1	0.5	3.5	20.00	40.00	100.00	103.50	0.1919
2	1	1.5	10.5	6.67	13.33	99.99	110.49	0.1333
3	1	2.5	17.5	4.00	8.00	99.95	117.45	0.1078
4	1	3.5	24.5	2.86	5.71	99.88	124.38	0.0920
5	1	4.5	31.5	2.22	4.44	99.74	131.24	0.0808
6	1	5.5	38.5	1.82	3.64	99.54	138.04	0.0723
7	1	6.5	45.5	1.54	3.08	99.26	144.76	0.0656
8	1	7.5	52.5	1.33	2.67	98.89	151.39	0.0600
9	1	8.5	59.5	1.18	2.35	98.44	157.94	0.0553
10	1	9.5	66.5	1.05	2.11	97.89	164.39	0.0513
								$\sum S_{ci} = 0.9103$

Therefore,  $S_c = 0.91$  m (3.0 ft) without reinforcement.

**Solution:  $S_c$  with columnar reinforcement**  $S_c$  for the clay layer with reinforcement will be calculated in the same manner except that  $q_m$  will be used in place of  $q_0$ . First, the area replacement ratio ( $R_a$ ) will be calculated using the unit cell concept because the columnar reinforcement is of large areal extent.

$$A = s^2 = (1.5)^2 = 2.25 \text{ m}^2 (24.2 \text{ ft}^2)$$

$$A_c = 0.25\pi(1.0)^2 = 0.7854 \text{ m}^2 (8.45 \text{ ft}^2)$$

$$R_a = A_c/A = 0.7854/2.25 = 0.3491$$

Now calculate  $q_m$  using Eq. 6A.77:

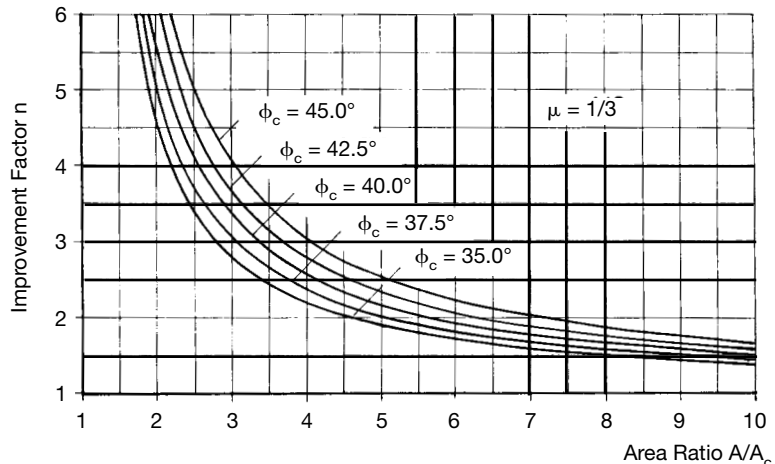
$$q_m = 100 \cdot \frac{1}{0.3491(5 - 1) + 1} = 100(0.4173) = 41.73 \text{ kPa (872 psf)}$$

The solution is set up in the same tabular form as before.

$i$	$H_{0i}$ (m)	$z_i$ (m)	$\sigma'_{v0i}$ (kPa)	m	n	$\Delta\sigma_{vi}$ (kPa)	$\sigma'_{vi}$ (kPa)	$S_{ci}$ (m)
1	1	0.5	3.5	20.00	40.00	41.73	45.23	0.1450
2	1	1.5	10.5	6.67	13.33	41.73	52.23	0.0909
3	1	2.5	17.5	4.00	8.00	41.71	59.21	0.0690
4	1	3.5	24.5	2.86	5.71	41.68	66.18	0.0563
5	1	4.5	31.5	2.22	4.44	41.62	73.12	0.0477
6	1	5.5	38.5	1.82	3.64	41.54	80.04	0.0415
7	1	6.5	45.5	1.54	3.08	41.42	86.92	0.0367
8	1	7.5	52.5	1.33	2.67	41.27	93.77	0.0329
9	1	8.5	59.5	1.18	2.35	41.08	100.58	0.0297
10	1	9.5	66.5	1.05	2.11	40.85	107.35	0.0271
								$\Sigma S_{ci} = 0.5767$

Therefore, using columnar reinforcement would result in an estimated 58% reduction in stress induced in the matrix soil. The ultimate primary consolidation settlement is expected to be reduced from 0.91 m (3.0 ft) to 0.58 m (1.9 ft), a 36% reduction. Note that the reduction in  $S_c$  is less than the reduction in stress because  $S_c$  is proportional to the reduction in the logarithm of induced stress rather than the reduction in induced stress. For very small values of induced stress and very high values of initial effective stress (deep compressible layers), the percent reduction in settlement approaches the average percent reduction in induced stress (Barksdale and Bachus 1983). Note also that the magnitude of settlement for thick embankments constructed on soft clays is significant even for substantial reinforcement. Generally the columnar reinforcement will also substantially increase the rate at which the settlement occurs. This increase in the rate of settlement is especially important in embankment and fill construction wherein most of the settlement must be allowed to occur before any structures (pavement systems, bridge abutments, buildings, etc.) are founded on or within the embankment or fill.

Priebe (1988) has developed design charts for estimating the reduction in settlement for long granular columns. Charts were provided for both one-dimensional and three-dimensional settlement (Figs. 6A.175 to 177). The charts for one-dimensional settlement (Figs. 6A.175 and 6A.176) are appropriate when the width of the loaded area ( $B$ ) is very large in comparison to the height of the com-

**6.230** SOIL IMPROVEMENT AND STABILIZATION

**FIGURE 6A.175** Priebe's chart for reduction in settlement for an infinite array of infinitely stiff granular columns (from Moseley and Priebe 1993).

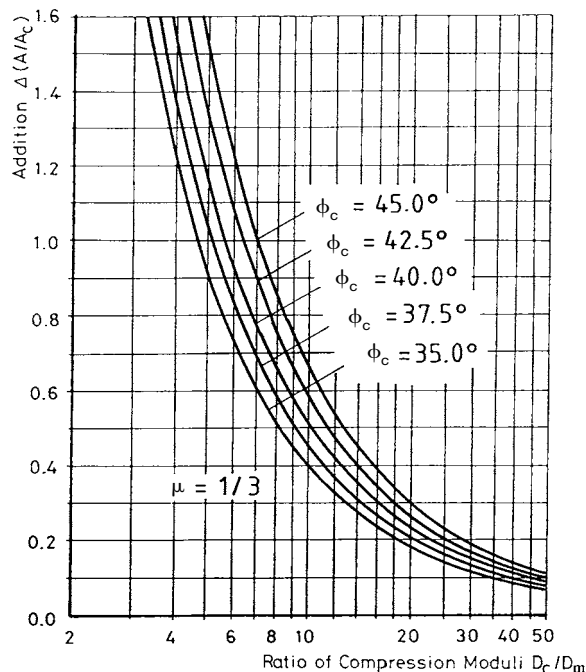


**FIGURE 6A.176** Priebe's chart for additional area ratio to account for compressibility of the granular columns (from Moseley and Priebe 1993).

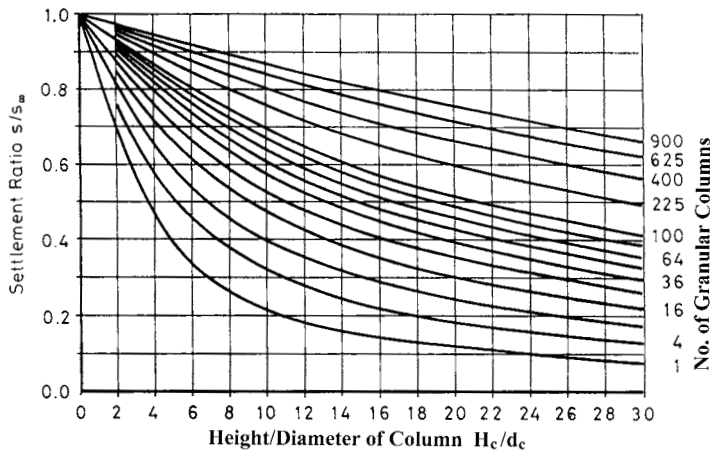


**FIGURE 6A.177** Priebe's chart to estimate settlement of an isolated footing supported by granular columns (modified from Moseley and Priebe 1993).

pressible layer, and the columns extend throughout the height of the compressible layer. Fig. 6A.177 applies to isolated footings supported by granular columns.

**One-Dimensional Settlement.** One-dimensional settlement occurs when the width of the loaded area is infinitely wide. One-dimensional settlement is also approximated when the width of the loaded area is very large in comparison to the height of the compressible layer. The results in Fig. 6A.175 are based on the assumption that the granular columns are incompressible, which is obviously not the case. Fig. 6A.176 is used to correct for the compressibility of the granular columns. The procedure for estimating settlement for this case is as follows:

1. Determine the ratio of one-dimensional compression moduli for the columnar material to the matrix soil ( $D_c/D_m$ ). This value can be estimated (it is approximately equal to the stress concentration ratio,  $R_s$ ), or one-dimensional compression tests can be conducted on specimens of the two materials.
2. From Fig. 6A.176 with  $D_c/D_m$  and  $\phi_c$ , determine the additional area ratio  $\Delta(A/A_c)$ .
3. Add the value of  $\Delta(A/A_c)$  calculated in step 2 to the true area ratio ( $A/A_c$ ).
4. With the combined value of  $A/A_c$  calculated in step 3 and  $\phi_c$ , determine the settlement improvement factor ( $n$ ) using Fig. 6A.175.  $n$  is defined as the ratio of the settlement without granular columns to the settlement with granular columns.
5. Divide the value of settlement for no granular columns (calculated using any appropriate method) by the value of  $n$  found in step 4. This value is the estimated settlement with granular columns.

**Three-Dimensional Settlement.** Three-dimensional settlement occurs when the width of the loaded area is small in comparison to the height of the compressible layers. This commonly occurs when individual footings are supported by granular columns. The procedure for estimating settlement for this case is as follows:

1. Determine the number of granular columns in the group and the height-to-diameter ratio of the columns ( $H_c/d_c$ ). With these values, find the settlement ratio  $S/S_\infty$  using Fig. 6A.177.  $S/S_\infty$  is de-

**6.232** SOIL IMPROVEMENT AND STABILIZATION

fined as the settlement of the finite group (3-D settlement) divided by the settlement for an infinitely wide group (1-D settlement) under the same conditions.

2. Estimate  $S_\infty$  using the method described above for one-dimensional settlement.
3. Multiply  $S/S_\infty$  from step 1 by  $S_\infty$  from step 2 to obtain an estimate of the settlement for the finite group.

**6.4.5.2.3 Ultimate Bearing Capacity**

In most instances, the bearing soil for a foundation is supported by a group of reinforcing columns. The mechanisms by which failure occurs for a group of columns is quite complex and involves several types of interaction. Sometimes a foundation is supported by a single column, for which the mechanisms of failure are more straightforward. Thus, ultimate bearing capacity for single columns will be discussed first, which will then provide the basis to understand the more complex situation for groups of columns.

**Single Columns.** There are three possible mechanisms of failure for a single reinforcing column in a homogeneous soil mass, as illustrated in Fig. 6A.178. The type of failure that would occur in any situation depends on characteristics of the columnar material and the matrix soil, and the area over which the load is applied (Fig. 6A.179).

**Bulging:** Failure of a single granular column in weak matrix soil such as a soft clay will occur by bulging. Granular columns have little or no internal cohesion and therefore depend on lateral resistance provided by the matrix soil. As load is applied to the top of the column, the column will tend to push outward within the upper portion of the column. If the matrix soil is weak, bulging will occur within a height of about two to three times the diameter of the column if the matrix soil is relatively homogeneous within this zone. If the upper portion of the matrix soil consists of layers of relatively strong and weak soils, bulging may occur only in the weaker layers. If the load is applied over an area greater than the area of the column (Fig. 6A.179a), the ultimate bearing capacity is increased in two ways: (a) Some of the load is carried by the matrix soil, lessening the load carried by the column; and (b) the stress carried by the matrix soil increases the confinement on the upper portion of the column.

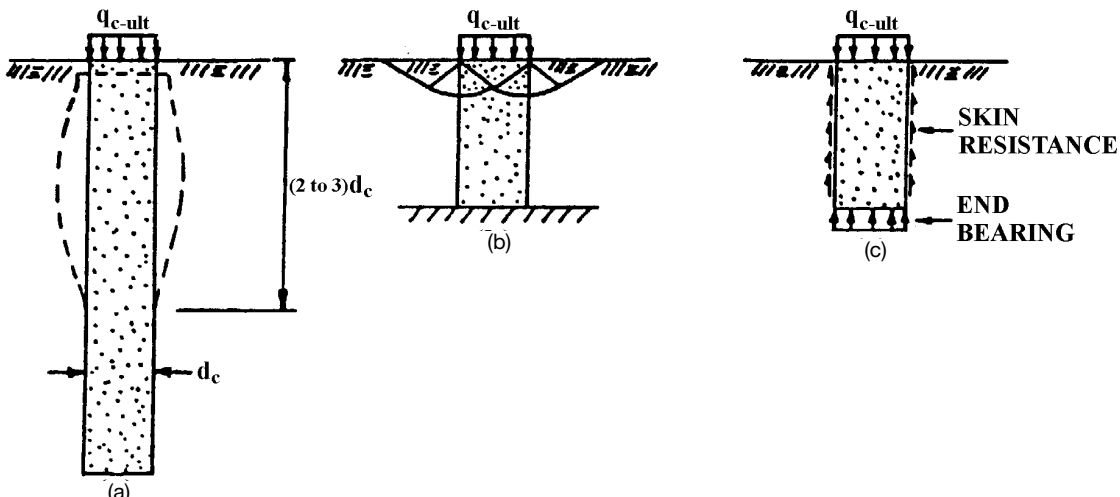


**FIGURE 6A.178** Mechanisms of failure for single reinforcing columns: (a) Bulging, (b) general or local shear, and (c) punching.

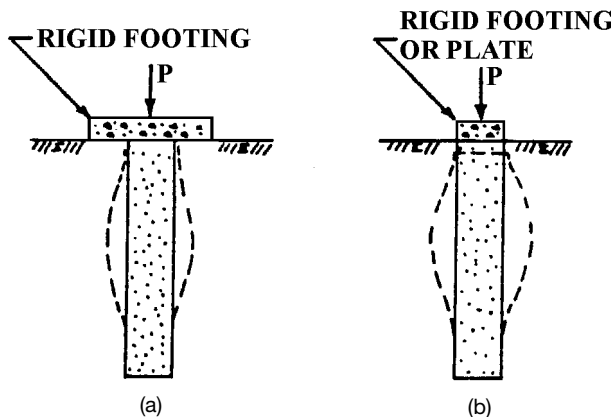


**FIGURE 6A.179** Types of loading for single reinforcing column: (a) Footing larger than column, (b) footing same size as column.

*General or Local Shear:* It is unlikely that a single column will fail by general or local shear failure, but it may occur under the following conditions: (a) a very short column [ $H_c < (2 \text{ to } 3)d_c$ ] bearing on a rigid base, or (b) the columnar material is not significantly stronger than the matrix soil. Neither situation occurs very often in practice. These types of failure are similar to those that occur for shallow foundations bearing on homogeneous unreinforced soils.

*Punching:* Punching or pile-like failure will occur in columns with substantial internal cohesion, such as lime-cement, jet grouted, vibratory concrete, and rammed cement columns. This mechanism of failure may also predominate in very short granular columns [ $H_c < (2 \text{ to } 3)d_c$ ] floating in the matrix soil (not bearing on a rigid base). Resistance to the applied load develops as skin resistance (shearing stresses) along the interface of the column and matrix soil, end bearing (normal stresses) at the bottom of the column, or a combination of both.

The best method to determine the ultimate bearing capacity of a single column is to load a prototype to failure. This is generally accomplished by conducting a plate load test (see Section 6A3.5.2 for details). However, this is an expensive and time-consuming process that typically requires generating about 100 to 500 kips (450 to 2200 kN) of reactive force. Thus, ultimate bearing capacity is usually estimated.

The following empirical formula can be used to estimate the ultimate bearing capacity of a single granular column within a matrix of soft clay (bulging failure):

$$q_{c\text{-ult}} = N_{sc} \cdot s_{um} \quad (6A.80)$$

where  $N_{sc}$  = bearing capacity factor for a single column

$s_{um}$  = undrained shear strength of the clay matrix

For vibro-replacement stone columns,  $N_{sc}$  has been found to range from about 18 to 25 (Barksdale and Bachus 1983, Mitchell 1981).

Many theories and analytical methods have been developed for the ultimate compressive capacity of a single granular column in saturated clay under undrained conditions. Summaries of many of these methods can be found in ASCE (1987), Barksdale and Bachus (1983), and Brauns (1978). Two theories will be described here for illustrative purposes.

Bell's (1915) method is the simplest and most conservative and is illustrated in Fig. 6A.180. In

## 6.234 SOIL IMPROVEMENT AND STABILIZATION

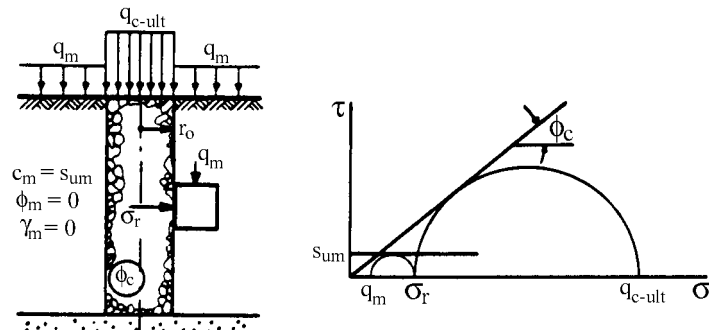


**FIGURE 6A.180** Bell's (1915) Method for the ultimate bearing capacity of a single granular column within undrained clay matrix (modified from Brauns 1978).

this method, the weight of the matrix soil and the shear stresses that develop along the column–matrix interface are ignored, as well as the distribution of stress within the columnar and matrix soils. Hence, the principal stresses in both the column and matrix soil adjacent to the interface are assumed to act in the vertical and horizontal directions. In the column adjacent to the interface, the major principal stress is in the vertical direction ( $q_{c\text{-ult}}$ ) owing to the high stress concentration on the column. The minor principal stress therefore acts in the radial direction and is designated  $\sigma_r$ . For a granular column, the cohesion intercept ( $c_c$ ) is zero, and the following equation can be written based on the geometry of the Mohr's circle at failure in the column:

$$q_{c\text{-ult}} = \sigma_r \cdot \tan^2(45^\circ + \phi_c/2) \quad (6A.81)$$

The corresponding equation at failure in the clay adjacent to the interface is as follows:

$$\sigma_r = q_m + 2s_{um} \quad (6A.82)$$

Inserting Eq. 6A.82 into Eq. 6A.81 gives:

$$q_{c\text{-ult}} = (q_m + 2s_{um}) \cdot \tan^2(45^\circ + \phi_c/2) \quad (6A.83)$$

Normalized values of ultimate bearing capacity ( $N_{sc} = q_{c\text{-ult}}/s_{um}$ ) are plotted versus  $\phi_c$  for Bell's method assuming  $q_m = 0$  in Fig. 6A.181. Note that Bell's method is very conservative compared to the other methods shown and compared to the typical range of values of  $N_{sc}$  reported in the literature (see previous discussion).

Hughes and Withers (1974) considered bulging failure of a single column to be similar to the expansion of a pressuremeter probe against the sides of a borehole. In a pressuremeter test, the radial resistance of the soil reaches a limiting value ( $\sigma_{rl}$ ) at which indefinite expansion occurs. If the soil is idealized as an elasto-plastic material, the limiting radial stress can be estimated from the following equation (Gibson and Anderson 1961):

$$\sigma_{rl} = \sigma_{r0} + s_{um} \left[ 1 + \ln \frac{E_m}{2s_{um}(1 + \nu_m)} \right] \quad (6A.84)$$

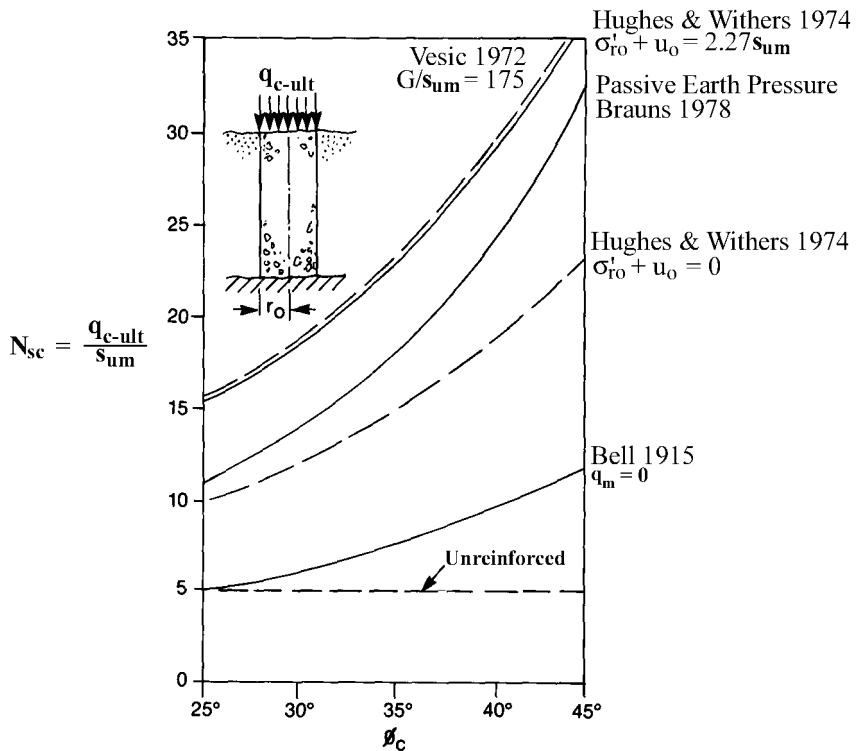


**FIGURE 6A.181** Comparison of predicted values by various methods of ultimate bearing capacity for a single granular column within an undrained clay matrix (modified from Brauns 1978).

where  $\ln$  is the natural logarithm,  $\sigma_{r0}$  is the initial radial stress in the matrix soil (prior to conducting the pressuremeter test), and  $s_{um}$ ,  $E_m$ , and  $\nu_m$  are the undrained shear strength, elastic modulus, and Poisson's ratio of the matrix soil, respectively. The following empirical equation for  $\sigma_r$  determined from the results of many quick-expansion pressuremeter tests can also be used:

$$\sigma_r = \sigma'_{r0} + 4s_{um} + u_0 \quad (6A.85)$$

where  $\sigma'_{r0}$  is the initial effective radial stress and  $u_0$  is the initial excess pore water pressure. Because the granular columnar material acts as a drain,  $u_0$  can be reasonably taken as zero with little or no error introduced. Of course,  $\sigma_r$  can also be determined from pressuremeter tests conducted within the range of depths where bulging is expected occur (upper two to three diameters of the column).

Ignoring the shearing stresses that develop along the interface of the columnar and matrix soils and any stress carried by the matrix soil at the bearing level ( $q_m$ ), the ultimate bearing capacity can be calculated as follows:

$$q_{c-ult} = \sigma_r \cdot \tan^2(45^\circ + \phi_c/2) \quad (6A.86)$$

**6.236** SOIL IMPROVEMENT AND STABILIZATION

Curves of  $q_{c\text{-ult}}/s_{um}$  versus  $\phi_c$  are shown in Fig. 6A.181 using Eqs. 6A.85 and 6A.86 and two values of  $(\sigma'_{r0} + u_0)$ : zero and  $2.27s_{um}$ .

Madhav and Vitkar's (1978) method can be used to estimate the ultimate bearing capacity for general shear failure within a long granular trench (rectangular prism) and an undrained clay matrix supporting a foundation. This method is described in Section 6A.2.1. So far as the author knows, there is no method available for general shear failure for a single reinforcing column. Established methods for estimating the ultimate bearing capacity of piles can be extended to single reinforcing columns that fail by punching. These methods can be found in any standard foundation engineering book (for example, see Section 4C) and will not be discussed here.

**Groups of Columns.** Hughes and Withers (1974) indicated that groups of granular columns within soft cohesive soils act independently when the center-to-center spacing of the columns is greater than about  $2.5d_c$ . This criterion also seems reasonable for other types of columns and matrix soils. For this case, the average ultimate stress that can be carried by the group ( $q_{ult}$ ) is given by the following expression:

$$q_{ult} = \frac{q_{c\text{-ult}} \cdot A_c + q_m \cdot A_m}{A} = q_{c\text{-ult}} \cdot R_a + q_m(1 - R_a) \quad (6A.87)$$

It should be noted that many of the methods developed for single columns ignore the confining pressure provided by  $q_m$  that in a group of columns helps to resist bulging. This contribution may be significant in some instances and should not be arbitrarily ignored.

For larger spacings the columns act with the matrix soil as a composite material, and the group action of the reinforced zone must be considered. It is useful in some instances to consider this composite zone to have a single set of Mohr–Coulomb strength parameters calculated as follows:

$$\phi_{comp} = \tan^{-1}[\mu_c \cdot R_a \cdot \tan \phi_c + \mu_m(1 - R_a) \tan \phi_m] \quad (6A.88)$$

$$c_{comp} = c_c \cdot R_a + c_m(1 - R_a) \quad (6A.89)$$

Note that the effects of stress concentration are included in Eq. 6A.88 for  $\phi_{comp}$ . If stress concentration does not occur, such as when columnar reinforcing is used to stabilize natural slopes (to be discussed subsequently), values of  $\mu_c = \mu_m = 1$  must be used in Eq. 6A.88.

If the height of the columns is relatively short compared to the width of the foundation ( $H_c \leq 1.5B$ ),  $q_{ult}$  for the group can be estimated using the composite strength parameters and the method developed for overexcavation/replacement (Section 6A.2.1). For taller columns ( $H_c > 1.5B$ ), the failure mechanism suggested by Barksdale and Bachus (1983), as illustrated in Fig. 6A.182, may be appropriate. In this method, the major principal plane at the bearing level is assumed to be horizontal, with the result that failure is initiated at one corner of the foundation and the failure surface extends underneath the foundation at an angle of  $\beta = 45^\circ + \phi_{comp}/2$  relative to horizontal to a point directly beneath the opposite corner of the foundation. This sliding wedge is resisted by passive lateral resistance within the adjacent matrix soil. This passive resistance is assumed to be the major principal stress in the matrix soil ( $\sigma_{1m}$ ) and the minor principal stress in the composite reinforcing zone ( $\sigma_{3c}$ ), and  $q_{ult}$  is the major principal stress for the composite reinforced zone. If the weight of the sliding wedge is ignored, which is conservative, the corresponding equations are as follows:

$$\sigma_{1m} = \sigma_{3c} = (\bar{q} + 0.5\gamma_m B \tan \beta) \tan^2(45^\circ + \phi_m/2) + 2c_m \tan(45^\circ + \phi_m/2) \quad (6A.90)$$

$$q_{ult} = \sigma_{3c} \tan^2 \beta + 2c_{comp} \tan \beta \quad (6A.91)$$

where  $\bar{q}$  is the effective vertical surcharge pressure at the bearing level. The term  $(\bar{q} + 0.5\gamma_m B \tan \beta)$  corresponds to the average vertical normal stress acting along the vertical face of the sliding wedge

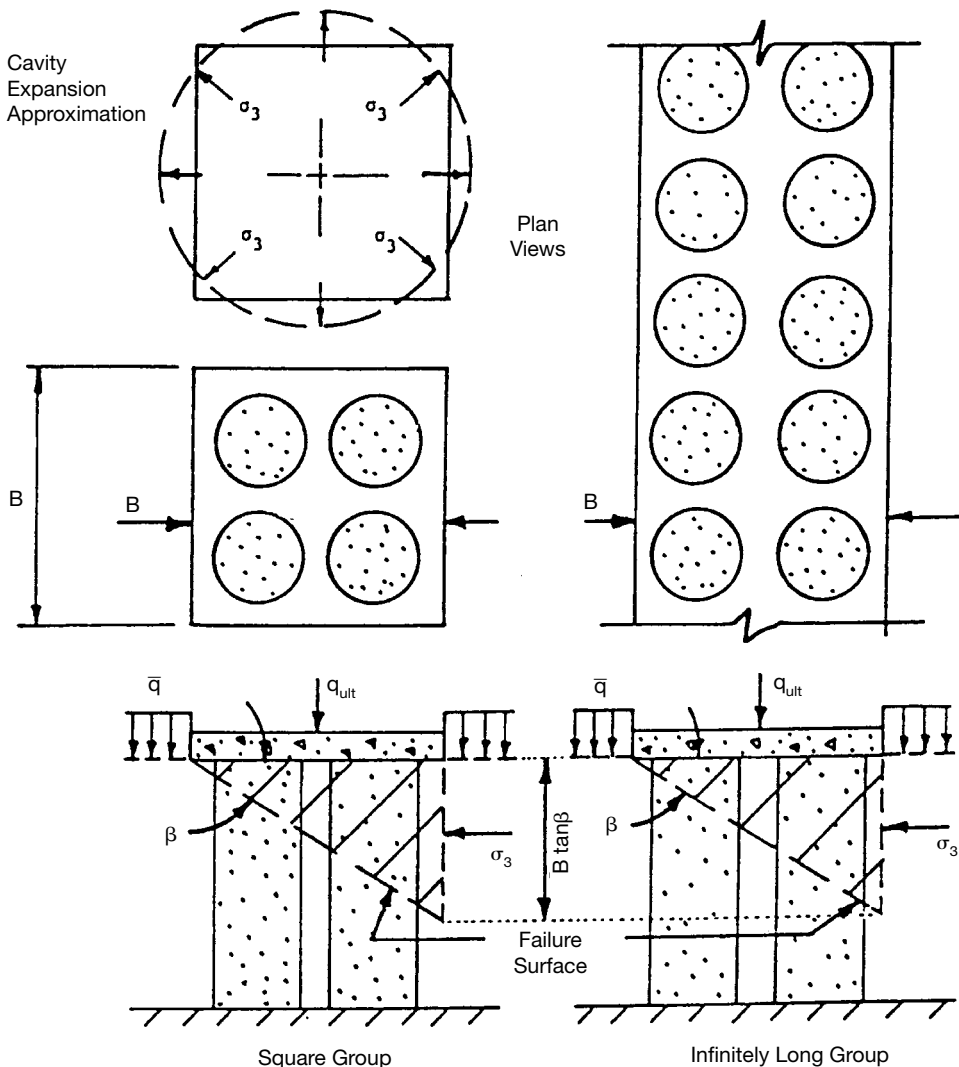


**FIGURE 6A.182** Barksdale and Bachus' (1983) method to estimate the ultimate bearing capacity of a foundation supported by a group of reinforcing columns.

and is valid for either a shallow or deep groundwater table. The value of  $\gamma_m$  used in these cases should correspond to the appropriate groundwater and drainage conditions. That is, the saturated unit weight should be used for a shallow groundwater table and undrained (short-term) conditions; the effective (buoyant) unit weight should be used for a shallow groundwater table and drained (long-term) conditions; and the total (wet) unit weight should be used for a deep groundwater table. If the groundwater table is located within the height of the sliding wedge, the appropriate value of average vertical stress along the vertical face owing to the weight of the matrix soil below the bearing level should be used in place of  $0.5 \gamma_m B \tan \beta$  and added to  $\bar{q}$ . Total vertical stress should be used

**6.238** SOIL IMPROVEMENT AND STABILIZATION

for undrained conditions and effective vertical stress for drained conditions, with the exception that  $\bar{q}$  should be the *effective* surcharge pressure for undrained and drained conditions.

**64.5.2.4 Liquefaction Potential**

Columnar reinforcement can mitigate the potential for liquefaction of saturated granular matrix soils in the following four ways (Baez 1995):

1. Columns act as drainage wells to reduce the buildup of excess pore water pressures
2. Increase the density the matrix soil adjacent to the columns
3. Increase the stress levels in the matrix soil adjacent to the columns
4. Reduce the shear stress carried by the matrix soil

The effectiveness of each type of granular column in reducing liquefaction potential by the four possible ways described above is summarized in Table 6A.17.

Granular columns must meet three requirements if they are to reduce significantly the excess pore water pressures generated in potentially liquefiable saturated granular soils during an earthquake (Seed and Booker 1976, Sonu et al. 1993): (1) To act as a free drain, the columnar material must have a permeability of at least 200 times that of the matrix soil; (2) the columns must effectively filter the matrix soil to prevent clogging by intrusion of finer particles into the columns; and (3) the columns must have sufficient void space to handle the volume of inflowing water required to keep the excess pore water pressures to an acceptably low level.

The increase in density of the matrix soil adjacent to stone columns can be significant. This also occurs in other types of granular columns to a lesser extent (see Table 6A.17). Baez (1995) evaluated this effect for vibratory stone columns at 18 sites based on an evaluation of nearly 400 sets of pretreatment and posttreatment data from standard penetration and cone penetration tests. Empirical correlations were developed for posttreatment normalized SPT blowcounts as a function of pretreatment values for area replacement ratios from 5 to 20%. Results of the empirical study are presented graphically in Fig. 6A.183 and are valid for uniform to medium silty sands with less than 15% fines and little or no clay content. When used in conjunction with Seed's method, this design chart can be used to estimate the area replacement ratio needed to achieve a desired factor of safety against liquefaction (see discussion of liquefaction potential in Section 6A.3.4.1).

The increase in horizontal stresses within the matrix soil adjacent to geopiers can be significant. This also occurs in other types of granular columns to a much lesser extent (see Table 6A.17). There

**TABLE 6A.17** Comparison of effectiveness of various types of granular columns in controlling liquefaction potential

Type of granular column	Method of controlling liquefaction potential			
	Reduce buildup of excess pore water pressures by providing radial drainage	Increase density of adjacent matrix soil	Increase stress levels in adjacent matrix soil	Reduce shear stresses in matrix soil
Stone column	Significant <sup>a</sup>	Significant	Moderate	Moderate
Sand column	Significant <sup>a</sup>	Moderate	Some	Moderate
Geopier	Significant <sup>a</sup>	Some	Significant	Significant
Gravel drain	Significant <sup>a</sup>	Slight	Slight	Some
Sand drain	Significant <sup>a</sup>	Slight	Slight	Some

<sup>a</sup>Significant so long as the permeability of the column is greater than 200 times the permeability of the matrix soil, the column material acts as a filter (prevents intrusion of finer particles into the column), and there is sufficient void space in the columns to handle the volume of inflowing water required to keep the excess pore water pressures at a sufficiently low level.

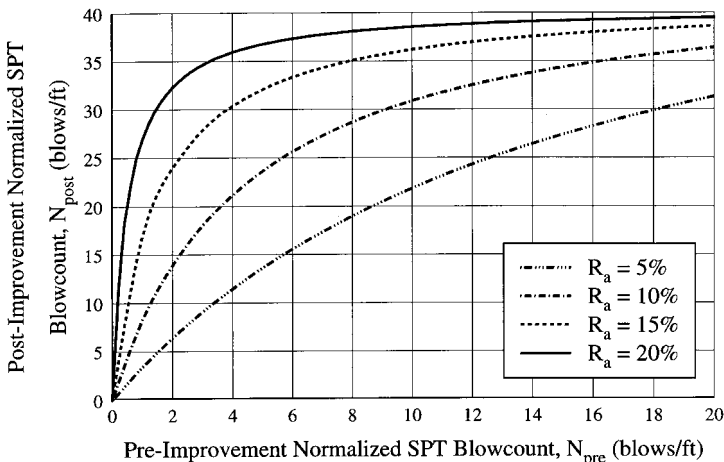


**FIGURE 6A.183** Prediction of postimprovement normalized SPT blowcount as a function of preimprovement normalized SPT blowcount for uniform fine to medium silty sands with less than 15% fines and little or no clay content (from Baez 1995).

may also be some minor increases in the vertical stresses. This increase in stress level helps to reduce the potential for liquefaction by increasing the confining stresses, particularly for vertical shaking (see Fig. 6A.64).

During horizontal ground shaking, lateral shear stresses are generated in the soil. Within a columnar reinforced soil, a concentration of shear stresses on the columns occurs, similar to the concentration of normal stresses for vertical loads discussed previously. This results in a reduction in the shear stresses within the potentially liquefiable matrix soil. The magnitude of this reduction depends on the area replacement ratio and the ratio of the shear modulus for the granular columns to that for the matrix soil ( $R_G = G_c/G_m$ ), according to the following equation:

$$\tau_m = \tau \frac{1}{R_a(R_G - 1) + 1} \quad (6A.92)$$

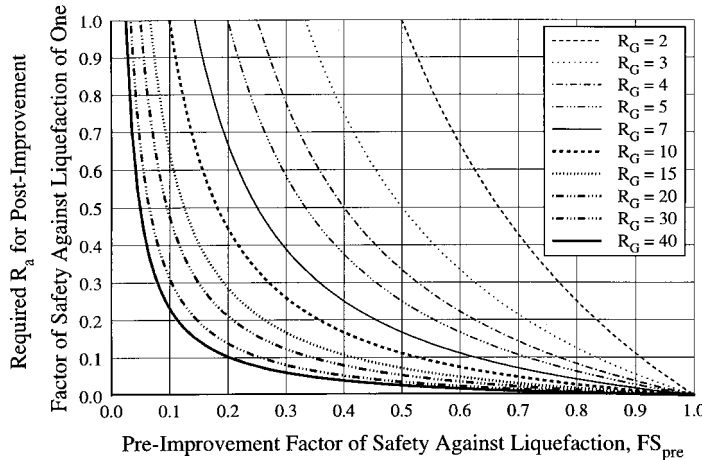
where  $\tau$  is the average shear stress generated by the earthquake. Eq. 6A.92 can be rearranged to solve for area replacement ratio:

$$R_a = \frac{1}{R_G - 1} \left( \frac{\tau}{\tau_m} - 1 \right) \quad (6A.93)$$

The factor of safety against liquefaction is generally defined as the available cyclic shear strength divided by the cyclic shear stress expected to be generated by the earthquake (Eq. 6A.20). The preimprovement factor of safety ( $FS_{\text{pre}}$ ) can be introduced into Eq. 6A.93 as  $\tau_m/\tau$ , resulting in the following equation for the area replacement ratio required to produce a posttreatment factor of safety of one:

$$R_a = \frac{1}{R_G - 1} \left( \frac{1}{FS_{\text{pre}}} - 1 \right) \quad (6A.94)$$

Eq. 6A.94 is shown graphically in Fig. 6A.184.

**6.240** SOIL IMPROVEMENT AND STABILIZATION

**FIGURE 6A.184** Required area replacement ratio to achieve a posttreatment factor of safety of one against liquefaction considering shear stress redistribution only (from Baez 1995).

#### 6A.5.2.5 Slope Stability

Columnar reinforcement can be used to increase the stability of man-made and natural slopes. In situations where fill or other load is placed on top of the columns, such as occurs when stabilizing a soil deposit and then placing an embankment on top of the reinforced soil (for example, see Example Problem 6A.2), the concentration of stress on the columns provides a very efficient and cost-effective reinforced zone. When stabilizing natural slopes or landslides, however, stress concentrations generally do not occur and the method is less efficient but still technically effective.

Most slope stability analyses conducted in engineering practice involve the use of a two-dimensional computer program. Although all slope stability problems are three-dimensional, two-dimensional analyses are usually conducted for three primary reasons:

1. Many slopes are long in comparison to their height and width and thus are reasonably represented as two-dimensional problems.
2. Three-dimensional analyses require about an order of magnitude more time to perform than two-dimensional analyses.
3. Use of a two-dimensional analysis is nearly always conservative.

Two methods for performing slope stability analyses involving columnar reinforcement are the *composite strength method* and the *profile method*. Either method can be used with standard slope stability computer programs. In the composite strength method, which is valid only when no stress concentration is present, the reinforced zone is treated as a single composite material with one set of Mohr–Coulomb strength parameters ( $\phi_{\text{comp}}$  and  $c_{\text{comp}}$ ) and a composite unit weight ( $\gamma_{\text{comp}}$ ). Some judgment is required to determine how far outside the edge of the outermost row of columns the reinforced zone should extend.  $c_{\text{comp}}$  can be calculated from Eq. 6A.89 and  $\phi_{\text{comp}}$  from Eq. 6A.88 with  $\mu_c = \mu_m = 1$ .  $\gamma_{\text{comp}}$  can be calculated from the following equation:

$$\gamma_{\text{comp}} = \gamma_c R_a + \gamma_m (1 - R_a) \quad (6A.95)$$

The values used for  $\gamma_c$  and  $\gamma_m$  should correspond to the location of the groundwater table and type of strength analysis being conducted. Use total unit weights for soils above the groundwater and sat-

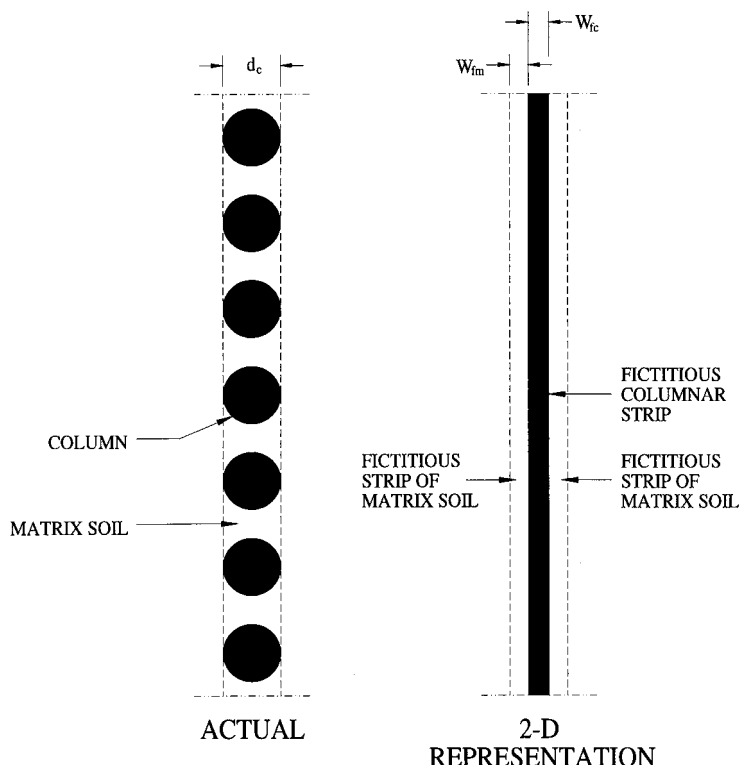
urated unit weights for undrained conditions below the water table. Use effective (buoyant) unit weights for drained conditions below the groundwater table. The composite strength method should not be used when  $c_c = 0$  and  $\phi_m = 0$ , which occurs for static loads, granular columns, and saturated clay as the matrix soil in the unconsolidated–undrained condition.

The profile method is preferred by the author for most cases. In this method, each row of columns and the matrix soil between the columns within that row are converted into three fictitious two-dimensional strips of materials: a strip of columnar material in the center sandwiched between a strip of matrix material on each side. This conversion is illustrated in Fig. 6A.185. The corresponding equations for the width of the fictitious columnar strip ( $W_{fc}$ ) and the width of each fictitious matrix strip ( $W_{fm}$ ) are as follows:

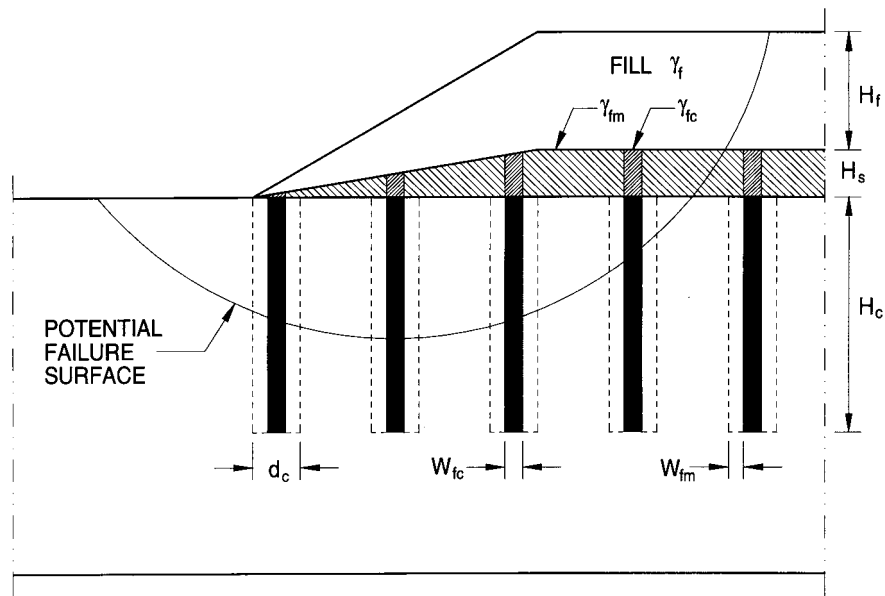
$$W_{fc} = R_a d_c \quad (6A.96)$$

$$W_{fm} = 0.5(1-R_a) d_c \quad (6A.97)$$

When stress concentrations are present, they are accounted for by placing a zone of fictitious strips between the fill and the underlying soil as illustrated in Fig. 6A.186. The fictitious strips above the columns have a positive unit weight to account for the additional stress carried by the columns



**FIGURE 6A.185** Plan view of long row of columns with matrix soil and two-dimensional representation using profile slope stability method.

**6.242** SOIL IMPROVEMENT AND STABILIZATION**FIGURE 6A.186** Accounting for stress concentration in the profile method.

$(\Delta\sigma_c)$ . The fictitious strips above the matrix soil have a negative unit weight to account for the corresponding reduction in stress on the matrix soil ( $\Delta\sigma_m$ ). Equations for  $\Delta\sigma_c$  and  $\Delta\sigma_m$  can be written in the following form:

$$\Delta\sigma_c = \sigma_c - \sigma = \mu_c\sigma - \sigma = \sigma(\mu_c - 1) \quad (6A.98)$$

$$\Delta\sigma_m = \sigma_m - \sigma = \mu_m\sigma - \sigma = \sigma(\mu_m - 1) \quad (6A.99)$$

The corresponding unit weights of the fictitious strips above the columns ( $\gamma_{fc}$ ) and the fictitious strips above the matrix soil ( $\gamma_{fm}$ ) are given as follows:

$$\gamma_{fc} = \frac{\Delta\sigma_c}{H_s} = \frac{\sigma(\mu_c - 1)}{H_s} = \frac{\gamma_f H_f (\mu_c - 1)}{H_s} \quad (6A.100)$$

$$\gamma_{fm} = \frac{\Delta\sigma_m}{H_s} = \frac{\sigma(\mu_m - 1)}{H_s} = \frac{\gamma_f H_f (\mu_m - 1)}{H_s} \quad (6A.101)$$

where  $\gamma_f$  = unit weight of the fill

$H_f$  = height of the fill

$H_s$  = height of the fictitious strip

The thickness of the fictitious strips should be small to avoid changing the geometry of the problem. Barksdale and Bachus (1983) recommended using a maximum value of  $H_s$  in the range

of 0.25 to 0.5 ft (75 to 100 mm). The ratio  $H_s/H_f$  should be constant for all the fictitious strips, tapering to zero at the edge of an embankment as shown in Fig. 6A.186. In addition, the fictitious strips must be assigned zero shear strength ( $\phi = 0$  and  $c = 0$ ) or else very small values if zeroes are not allowed by the computer program. Furthermore, if allowed by the program, limits should be placed on the generated failure surfaces so that the critical failure surface is not controlled by the weak, fictitious strips. If limits are not possible, a final check of the critical failure surface should be made to ensure that a significant part of it does not go through the zone of fictitious strips. Potential failure surfaces not meeting this criterion should be eliminated from consideration because they are not realistic.

#### **64.5.2.6 Lateral Sliding Resistance**

For most types of columnar reinforcement, the resistance to lateral sliding of footings bearing on soil reinforced with columns comes from two sources: shearing resistance along the bottom of the footing and passive resistance of the soil adjacent to the side of the footing. The passive resistance of the adjacent soil is unaffected by the reinforcement unless the columns extend outside the footprint of the footing and above the bearing level. Traditional methods can be used to estimate this passive resistance. The shearing resistance along the bottom of the footing is significantly enhanced by the concentration of stress on the stronger columns. The maximum horizontal resisting force that can be developed from shearing along the bottom of the footing ( $R_{h\text{-max}}$ ) can be estimated from the following equation:

$$R_{h\text{-max}} = A_c (a_c + q_c \tan \delta_c) + A_m (a_m + q_m \tan \delta_m) \quad (6A.102)$$

where  $A_c$  = area of columns at the bearing level within the footprint of the footing

$A_m$  = area of matrix soil at the bearing level within the footprint of the footing

$a_c$  = maximum adhesive stress for sliding along the columnar material

$a_m$  = maximum adhesive stress for sliding along the matrix soil

$\delta_c$  = angle of friction for sliding of the footing along the columnar material

$\delta_m$  = angle of friction for sliding of the footing along the matrix soil

If the bottom of the footing is rough, which is generally the case for concrete cast directly against the ground,  $\delta_c$ ,  $\delta_m$ ,  $a_c$ , and  $a_m$  are approximately equal to  $\phi_c$ ,  $\phi_m$ ,  $c_c$ , and  $c_m$ , respectively. Stronger materials generally achieve peak lateral resistance at smaller displacements of the footing than do weaker soils. If the columnar material is dilative at the expected level of  $q_c$ , the columnar adhesive and frictional resistance may reach a peak and drop into the residual range before peak resistance is achieved in the matrix soil. Therefore, Eq. 6A.102 may be somewhat unconservative for these conditions. However, in many cases the contribution of the matrix soil to the total sliding resistance is small so that this error is insignificant. So long as a reasonable factor of safety is applied to Eq. 6A.102 to obtain an allowable or design value of  $R_h$ , use of this equation is acceptable. If desired, laboratory direct shear tests can be conducted on the columnar and matrix materials at appropriate vertical stress levels to determine if stress-displacement incompatibility is a potential problem.

When uplift geopiers are used, additional lateral resistance results from passive pressure generated on the uplift bars as they are pushed into the geopier material. The results from full-scale tests and numerical analyses conducted on footings supported by uplift geopiers indicate that this phenomenon may produce as much as 40% of the total lateral resistance at large displacements of the footings (Lawton 1999).

#### **64.5.2.7 Uplift Capacity of Geopiers**

The results of a study on the behavior of single geopiers during uplift has been reported by Hsu (2000). Based on the results of a series of uplift tests conducted on geopiers, methods to predict the maximum pullout force ( $T_{\text{max}}$ ) of a single geopier have been developed. These methods can also be extended to groups of uplift geopiers supporting a footing.

**6.244** SOIL IMPROVEMENT AND STABILIZATION

The following key factors were found to affect the uplift capacity of geopier foundations:

1. During installation of geopiers, the horizontal stresses in the adjacent matrix soil are increased to limiting passive pressures to a depth of about 6 ft (2 m) below the top of the geopier. Below this depth, the horizontal stresses are increased but not to full limiting passive values.
2. In cohesive soils, remolding of the matrix soil occurs, resulting in a complete loss of the cohesion intercept. It is believed that in the long-term, the cohesive soil will regain strength owing to thixotropy and the full cohesion intercept will be redeveloped. However, additional research is needed to verify that this occurs.
3. During uplift loading, the horizontal stress along the interface of the geopier and the matrix soil decreases by about 1 psi (7 kPa) from the initial condition (just prior to loading) to failure.
4. Possible shapes of the potential failure surfaces can take two forms: (a) the surface of a cylinder, or (b) the surface of a cylinder in the lower portion transitioning to the surface of a truncated cone in the upper portion.

Based on these factors and assuming the failure surface occurs along the surface of the geopier, the following equations can be used to estimate  $T_{\max}$  for a single geopier when the Mohr–Coulomb strength parameters ( $\phi$  and  $c$  or  $\phi'$  and  $c'$ ) are known for all layers of the matrix soil adjacent to the geopiers.

For a height of geopier ( $H_g$ )  $\leq$  6 ft (1.8 m):

$$T_{\max}(\text{single}) = W' + \pi d_g \sum_{i=1}^{i=l} (K_{pi} \cdot \sigma'_{vi} - \Delta\sigma_h) H_i \cdot \tan \phi'_i \quad (6A.103)$$

For  $H_g > 6$  ft (1.8 m):

$$T_{\max}(\text{single}) = W' + \pi d_g \left[ \sum_{j=1}^{j=m} (K_{pj} \cdot \sigma'_{vj} - \Delta\sigma_h) H_j \cdot \tan \phi'_j + \sum_{k=1}^{k=n} [0.5(K_{0k} + K_{pk})\sigma'_{vk} - \Delta\sigma_h] H_k \cdot \tan \phi'_k \right] \quad (6A.104)$$

where  $W'$  = effective weight of the geopier =  $0.25\pi d_g^2 (\gamma_g H_{ga} + \gamma'_g H_{gb})$

$d_g$  = nominal diameter of the geopier

$\gamma_g$  = total unit weight of the geopier above the groundwater table

$\gamma'_g$  = effective unit weight of the geopier below the groundwater table

$H_{ga}$  = height of the geopier above the groundwater table

$H_{gb}$  = height of the geopier below the groundwater table

$H_i$  = height of the  $i$ th layer of matrix soil

$i, j, k$  = summation variables referring to the numbering of the matrix soil layers

$l$  = number of layers of matrix soil adjacent to a geopier when  $H_g < 6$  ft (1.8 m)

$m$  = number of layers of matrix soil adjacent to a geopier for the upper 6 ft (1.8 m) when  $H_g > 6$  ft (1.8m)

$n$  = number of layers of matrix soil adjacent to a geopier for the portion below 6 ft (1.8 m) from the top of the geopier when  $H_g > 6$  ft (1.8 m)

$K_{pi}$  = Rankine's coefficient of passive earth pressure for the  $i$ th layer of matrix soil =  $\tan^2(45^\circ + \phi_i'/2)$

$K_{0k}$  = coefficient of lateral earth pressure at rest for the  $k$ th layer of matrix soil

$\phi'_i$  = coefficient of internal friction for the  $i$ th layer of matrix soil

$\sigma'_{vi}$  = average vertical overburden pressure for the  $i$ th layer of matrix soil

$\Delta\sigma_h$  = reduction in horizontal stress during uplift loading = 1 psi = 0.144 ksf = 7 kPa

If there is soil above the top of the geopier and it will remain throughout the design life of the structure, the weight of this soil can be added into the equations for  $T_{\max}$  (single). However, generally this

weight is insignificant compared to the other components. It is recommended that the borehole shear test (Handy and Fox 1967) be used to obtain the strength parameters of the matrix soil layers because the shearing action during this test simulates the shearing action in the matrix soil that occurs during uplift of a geopier.

$T_{\max}$  can also be estimated from CPT data when it is available using the following equations.  
For all soils:

$$T_{\max}(\text{single}) = W' + 1.6\pi d_g \sum_{i=1}^{i=n} f_{si} H_i \quad (6A.105)$$

where  $f_{si}$  is the average CPT sleeve resistance for the height increment  $H_i$ .

For cohesionless soils:

$$T_{\max}(\text{single}) = W' + \frac{\pi d_g}{47} \sum_{i=1}^{i=n} q_{ci} H_i \quad (6A.106)$$

For cohesive soils:

$$T_{\max}(\text{single}) = W' + \frac{\pi d_g}{23} \sum_{i=1}^{i=n} q_{ci} H_i \quad (6A.107)$$

where  $q_{ci}$  is the average CPT tip resistance for the height increment  $H_i$ .

This method can be extended to calculate the uplift capacity of a group of geopiers supporting a footing by assuming that the failure surface is vertical and, in plan view, takes the shape of the geometric figure determined by drawing straight lines between the outermost points on the geopier group. This technique is illustrated in Fig. 6A.187 for 2 by 2 and 3 by 4 groups of geopiers. The capacity determined in this manner cannot be more than the total uplift capacity of the geopiers in the group assuming that each geopier behaves individually. A similar technique is commonly used in the analysis of the uplift capacity of groups of piles. This method is described in equation form as follows.

For  $H_g \leq 6$  ft (1.8 m):

$$T_{\max}(\text{group}) = W' + W_f + p \sum_{i=1}^{i=l} (K_{pi} \cdot \sigma'_{vi} - \Delta\sigma_h) H_i \cdot \tan \phi'_i \leq W_f + N_g \cdot T_{\max}(\text{single}) \quad (6A.108)$$

For  $H_g > 6$  ft (1.8 m):

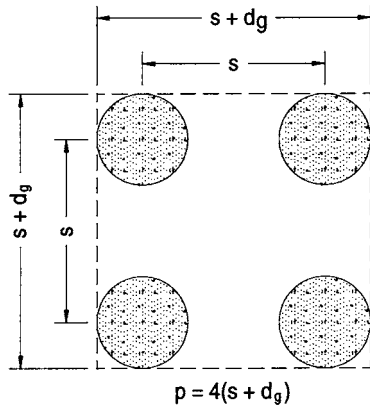
$$\begin{aligned} T_{\max}(\text{group}) &= W' + W_f + p \left[ \sum_{j=1}^{j=m} (K_{pj} \cdot \sigma'_{vj} - \Delta\sigma_h) H_j \cdot \tan \phi'_j + \sum_{k=1}^{k=n} [0.5(K_{0k} + K_{pk})\sigma'_{vk} - \Delta\sigma_h] H_k \cdot \tan \phi'_k \right] \\ &\leq W_f + N_g \cdot T_{\max}(\text{single}) \end{aligned} \quad (6A.109)$$

where  $W'$  = effective weight of geopiers and matrix soil within group mass

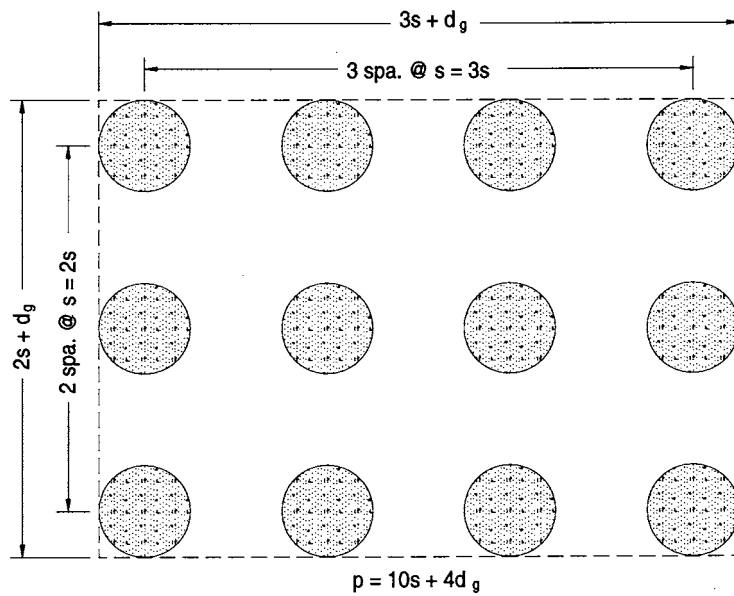
$W_f$  = weight of footing

$p$  = perimeter length of group mass

$T_{\max}(\text{single})$  is the maximum uplift capacity for a single geopier, from Eqs. 6A.103 through 6A.107

**6.246** SOIL IMPROVEMENT AND STABILIZATION

(a)



(b)

**FIGURE 6A.187** Determination of geopier group perimeter length for (a) 2 by 2 group, and (b) 3 by 4 group.

For all soils:

$$T_{\max}(\text{group}) = W' + W_f + 1.6p \sum_{i=1}^{i=n} f_{si} H_i \quad (6A.110)$$

For cohesionless soils:

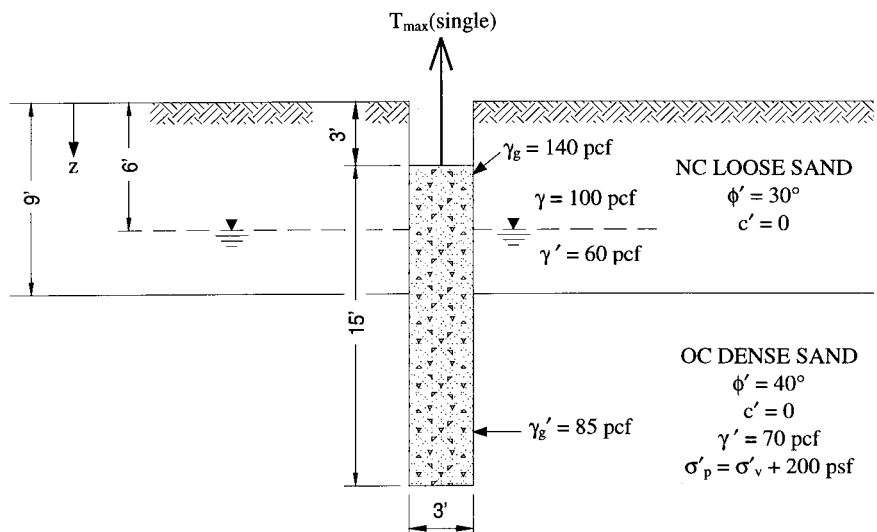
$$T_{\max}(\text{group}) = W' + W_f + \frac{p}{47} \sum_{i=1}^{i=n} q_{ci} H_i \quad (6A.111)$$

For cohesive soils:

$$T_{\max}(\text{group}) = W' + W_f + \frac{p}{23} \sum_{i=1}^{i=n} q_{ci} H_i \quad (6A.112)$$

If there is soil above the top of the footing and it will remain throughout the design life of the structure, the weight of this soil can be added into the equations for  $T_{\max}$  (group). However, generally this weight is insignificant compared to the other components. The use of the equations to estimate  $T_{\max}$  (single) and  $T_{\max}$  (group) are illustrated in the following examples.

**Example Problem 6A.3** Estimate the maximum uplift capacity of the single geopier shown in the diagram below. The geopier is 3 ft (0.91 m) in diameter, 15 ft (4.57 m) tall, has a total unit weight above the groundwater table ( $\gamma_g$ ) of 140 pcf (22.0 kN/m<sup>3</sup>), and an effective (buoyant) unit weight below the groundwater table ( $\gamma'_g$ ) of 85 pcf (13.4 kN/m<sup>3</sup>). The top of the geopier is 3 ft (0.91 m) below the ground surface. The soils at the site consist of two layers. The upper layer consists of normally consolidated, loose sand that is 9 ft (2.74 m) thick with a total unit weight ( $\gamma$ ) of 100 pcf (15.7 kN/m<sup>3</sup>), an effective unit weight ( $\gamma'$ ) of 60 pcf (9.43 kN/m<sup>3</sup>), an effective friction angle ( $\phi'$ ) of 30°, and an effective cohesion intercept ( $c'$ ) of zero. This upper layer is underlain by a deep, overconsolidated, dense sand layer with  $\gamma' = 70$  pcf (11.0 kN/m<sup>3</sup>),  $\phi' = 40^\circ$ , and  $c' = 0$ . The dense sand layer is overconsolidated owing to removal of overburden at some time in the past, with the preconsolidation pressure ( $\sigma'_p$ ) equal to the effective vertical stress ( $\sigma'_v$ ) plus 200 psf (9.6 kPa). The groundwater table is 6 ft (1.83 m) below the ground surface.  $z$  is defined as the depth below the ground surface.



**6.248** SOIL IMPROVEMENT AND STABILIZATION

**Solution:** For purposes of analysis, the matrix soils will be divided into three layers: Layer 1 is loose sand from the top of the geopier to the groundwater table ( $z = 3$  to  $6$  ft = 0.91 to 1.83 m); Layer 2 is loose sand from the groundwater table to the bottom depth where full passive pressures are assumed to develop ( $z = 6$  to  $9$  ft = 1.83 to 2.74 m); and Layer 3 from the top of the dense sand to the bottom of the geopier ( $z = 9$  to  $18$  ft = 2.74 to 5.49 m). Since  $H_g = 15$  ft (4.6 m) > 6 ft (1.8 m), Eq. 6A.104 will be used to calculate  $T_{\max}$  (single).

**Layer 1:** This layer is completely within the zone where full passive pressures are assumed to develop in the matrix soils adjacent to the geopiers.

$$K_{p1} = \tan^2(45^\circ + \phi'_1/2) = \tan^2(45^\circ + 30^\circ/2) = 3$$

$$\sigma'_{v1}(z = 4.5 \text{ ft}) = \gamma z = (100)(4.5) = 450 \text{ psf} = 0.45 \text{ ksf} (21.5 \text{ kPa})$$

$$\Delta\sigma_h = 0.144 \text{ ksf} (7.0 \text{ kPa})$$

$$H_1 = 3 \text{ ft (0.91 m)}$$

$$\begin{aligned} \text{Maximum uplift shearing force} &= \pi d_g (K_{p1} \sigma'_{v1} - \Delta\sigma_h) H_1 \tan \phi'_1 = \pi(3)[(3)(0.45) - 0.144](3) \tan 30^\circ \\ &= 19.7 \text{ kips (87.6 kN)} \end{aligned}$$

$$W'_1 = 0.25 \pi d_g^2 \gamma_g H_1 = 0.25 \pi(3)^2(0.140)(3) = 3.0 \text{ kips (13.2 kN)}$$

$$T_{\max} \text{ (single) for Layer 1} = 19.7 + 3.0 = 22.7 \text{ kips (101 kN)}$$

**Layer 2:** This layer is also completely within the zone where full passive pressures are assumed to develop in the matrix soils adjacent to the geopiers.

$$K_{p2} = K_{p1} = 3$$

$$\sigma'_{v2}(z = 7.5 \text{ ft}) = (100)(6) + (60)(1.5) = 690 \text{ psf} = 0.69 \text{ ksf} (33.0 \text{ kPa})$$

$$H_2 = 3 \text{ ft (0.91 m)}$$

$$\text{Maximum uplift shearing force} = \pi(3)[(3)(0.69) - 0.144](3) \tan 30^\circ = 31.4 \text{ kips (140 kN)}$$

$$W'_2 = 0.25 \pi d_g^2 \gamma_g' H_2 = 0.25 \pi(3)^2(0.085)(3) = 1.8 \text{ kips (8.0 kN)}$$

$$T_{\max} \text{ (single) for Layer 2} = 31.4 + 1.8 = 33.2 \text{ kips (148 kN)}$$

**Layer 3:** This layer is within the zone where the pressures are assumed to be halfway between at-rest and full passive conditions.

$$\sigma'_{v3}(z = 13.5 \text{ ft}) = (100)(6) + (60)(3) + (70)(4.5) = 1,095 \text{ psf} = 1.095 \text{ ksf (52.4 kPa)}$$

$$\sigma'_{p3}(z = 13.5 \text{ ft}) = \sigma'_{v3} + 200 = 1,095 + 200 = 1,295 \text{ psf} = 1.295 \text{ ksf (62.0 kPa)}$$

$$\text{Overconsolidation Ratio, OCR} = \sigma'_{p3}/\sigma'_{v3} = 1.295/1.095 = 1.183$$

$$K_{03} = (1 - \sin \phi'_3) \text{ OCR}^{0.5} = (1 - \sin 40^\circ)(1.183)^{0.5} = 0.388$$

$$K_{p3} = \tan^2(45^\circ + 40^\circ/2) = 4.599$$

$$H_3 = 9 \text{ ft (2.74 m)}$$

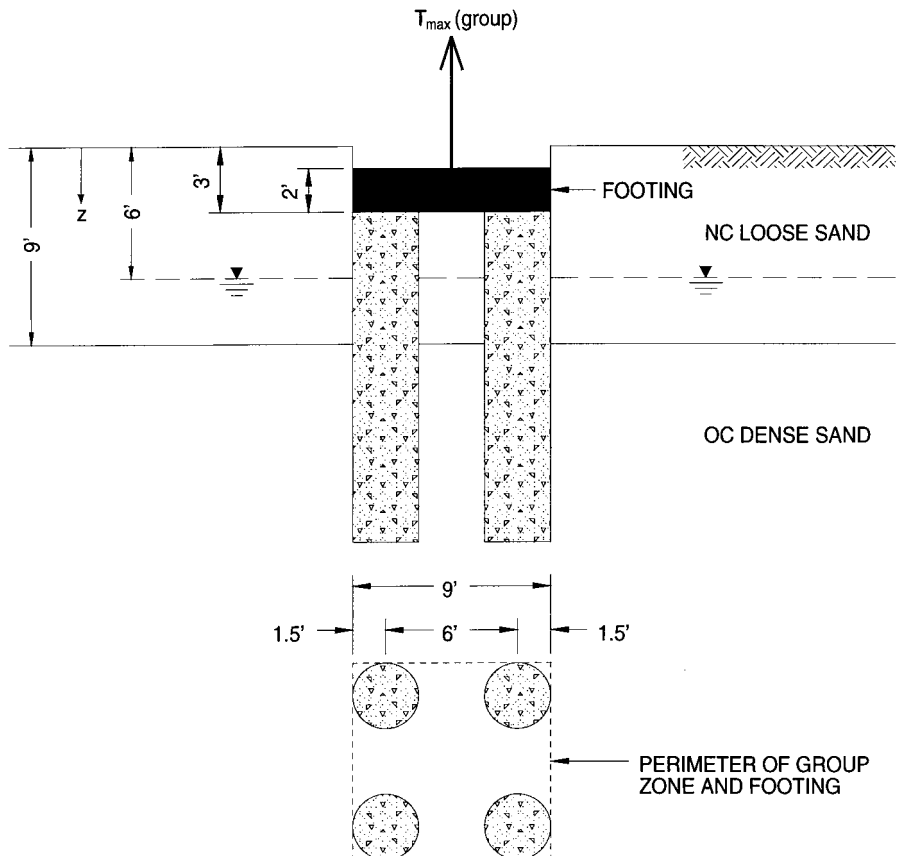
$$\text{Maximum uplift shearing force} = \pi d_g [0.5(K_{03} + K_{p3}) \sigma'_{v1} - \Delta\sigma_h] H_3 \tan \phi'_3 = \pi(3)[0.5(0.388 + 4.599)(1.095) - 0.144](9) \tan 40^\circ = 184.1 \text{ kips (87.6 kN)}$$

$$W'_3 = 0.25 \pi(3)^2(0.085)(9) = 5.4 \text{ kips (24.1 kN)}$$

$$T_{\max} \text{ (single) for Layer 1} = 184.1 + 5.4 = 189.5 \text{ kips (843 kN)}$$

$$\text{All Three Layers: } T_{\max} \text{ (single)} = 22.7 + 33.2 + 189.5 = 245 \text{ kips (1,090 kN)}$$

**Example Problem 6A.4** Estimate the maximum uplift capacity of a group of four geopiers with the same dimensions and soil conditions as in Example Problem 6A.3. The four geopiers will support a 9-ft (2.74-m) square footing with a thickness of 2 ft (0.61 m) as shown in the figure below. The unit weight of the footing ( $\gamma$ ) is assumed to be 150 pcf (23.6 kN/m<sup>3</sup>).



**Solution:** Since  $H_g > 6$  ft (1.8 m), Eq. 6A.109 will be used to calculate  $T_{\max}$  (group). The same three layers used in Example Problem 6A.3 will be used for the group.

#### Layer 1:

$$p = 4(s + d_g) = 4(6 + 3) = 36 \text{ ft (11.0 m)}$$

$$\text{Maximum uplift shearing force} = p(K_p \sigma'_{v1} - \Delta \sigma_h) H_1 \tan \phi'_1 = 36[(3)(0.45) - 0.144](3) \tan 30^\circ = 75.2 \text{ kips (335 kN)}$$

$$\text{Area of geopiers, } A_g = N_g (0.25 \pi d_g^2) = 4[0.25 \pi (3)^2] = 28.27 \text{ ft}^2 (2.63 \text{ m}^2)$$

$$\text{Area of matrix soil, } A_m = 9^2 - 28.27 = 52.73 \text{ ft}^2 (2.63 \text{ m}^2)$$

$$W'_1 = H_1(A_g \gamma_g + A_m \gamma) = 3[(28.27)(0.140) + (52.73)(0.100)] = 27.7 \text{ kips (123 kN)}$$

$$T_{\max} \text{ (group) for Layer 1} = 75.2 + 27.7 = 103 \text{ kips}$$

#### Layer 2:

$$\text{Maximum uplift shearing force} = 36[(3)(0.69) - 0.144](3) \tan 30^\circ = 120.1 \text{ kips (534 kN)}$$

$$W'_2 = H_2(A_g \gamma'_g + A_m \gamma') = 3[(28.27)(0.085) + (52.73)(0.060)] = 16.7 \text{ kips (123 kN)}$$

$$T_{\max} \text{ (group) for Layer 2} = 120.1 + 16.7 = 137 \text{ kips (657 kN)}$$

**6.250 SOIL IMPROVEMENT AND STABILIZATION****Layer 3:**

Maximum uplift shearing force =  $p[0.5(K_{03} + K_{p3}) \sigma'_{v3} - \Delta\sigma_h] H_3 \tan \phi'_3 = 36[0.5(0.388 + 4.599)(1.095) - 0.144](9) \tan 40^\circ = 703.2$  kips (3,130 kN)

$$W'_2 = 9[(28.27)(0.085) + (52.73)(0.070)] = 54.8 \text{ kips (244 kN)}$$

$$T_{\max} \text{ (group) for Layer 3} = 703.2 + 54.8 = 758 \text{ kips (3,370 kN)}$$

**Weight of Footing:**

$$W_f = (9)^2(2)(0.150) = 24.3 \text{ kips (108 kN)}$$

**Total Uplift Capacity for Group:**

$$T_{\max} \text{ (group)} = 103 + 137 + 758 + 24 = 1,022 \text{ kips (4,550 kN)} \leq W_f + N_g T_{\max} \text{ (single)} = 24 + 4(245) = 1,004 \text{ kips (4,470 kN)}$$

So single action controls and  $T_{\max}$  (group) = 1,004 kips (4,470 kN)

**6A.6 PRECOMPRESSION**

*Precompression* or *preloading* of weak and compressible soils to increase their strength and stiffness is one of the oldest and most widely used methods of soil improvement (Mitchell 1981). In its simplest form, the technique involves increasing the effective stress within the bearing soils at a site to the anticipated final level under the structure to be built there. In some instances, the time required for the precompression to occur may be longer than desired or acceptable, in which case the process can be accelerated using *surcharging*, *vertical drains*, or both. Surcharging involves the application of an additional load beyond that necessary to achieve the final effective stresses. Vertical drains are used in saturated, fine-grained soils to hasten the rate at which primary consolidation occurs. Details of these procedures are provided in subsequent sections.

Precompression is especially well suited for use when the bearing soils will undergo large volume decreases and strength increases under sustained static loads, and when there is adequate time for the required compressions to occur. The types of soils that meet these requirements are generally normally consolidated or lightly overconsolidated, loose granular or soft cohesive soils.

**6A.6.1 Types of Preloads**

The effective stresses in the bearing soils can be increased by either increasing the total stress, decreasing the pore air or water pressures, or a combination thereof. Generally, the increase in effective stress is accomplished by adding weight to the ground surface to increase the total stress within the underlying soils. The added weight is usually in the form of an earthen embankment, but can also be in many other forms including water in tanks, water in lined ponds, concrete highway barriers, and rubble. The total stress can also be increased by jacking against an anchored reaction system. If the groundwater table is at or near the ground surface, a drainage medium is usually needed on the ground surface to provide surface drainage for the water that is squeezed from the underlying soils. The drainage medium typically consists of a geotextile or granular drainage layer. These total stress methods are generally simple in execution but can cause stability problems in the underlying soils, especially in soft, saturated, cohesive soils if the loads are applied quickly.

Lowering the groundwater table at a site increases the effective stresses by reducing the pore water pressures and reducing slightly the total stress owing to a decrease in unit weight of the soils above the lowered groundwater table. Applying a vacuum beneath an impervious membrane—called *vacuum preloading*—reduces the pore air pressure in an unsaturated soil or reduces the pore water pressure in a saturated soil, which results in an increase in effective stress. Additional details on this technique can be founded in Holtz and Wager (1975), Pilot (1977), and Cognon et al. (1994).

In electro-osmosis, water is removed from saturated, fine-grained soils by application of a direct current field, producing increases in effective stress with the treated soil mass. If stabilizing chemicals are injected into the soil while water is being removed, the process is called electro-kinetic injection. Further information on electro-osmosis and electro-kinetic injection can be found in Mitchell (1981, 1993), Esrig (1968), Wan and Mitchell (1976), Mitchell and Wan (1977), and Pilot (1977). Although preloading by lowering the groundwater table, vacuum, or electro-osmosis eliminates the problem with stability of the bearing soils, these methods are substantially more complex to design, execute, and monitor than the total stress methods.

### 6A.6.2 Simple Precompression

The term *simple precompression* is used for the case where a preload equal to a future site load is applied (Hausmann 1990). When primary compression or consolidation is nearly complete, the preload is removed and the new structure is built. This process is illustrated in Fig. 6A.188 for the case

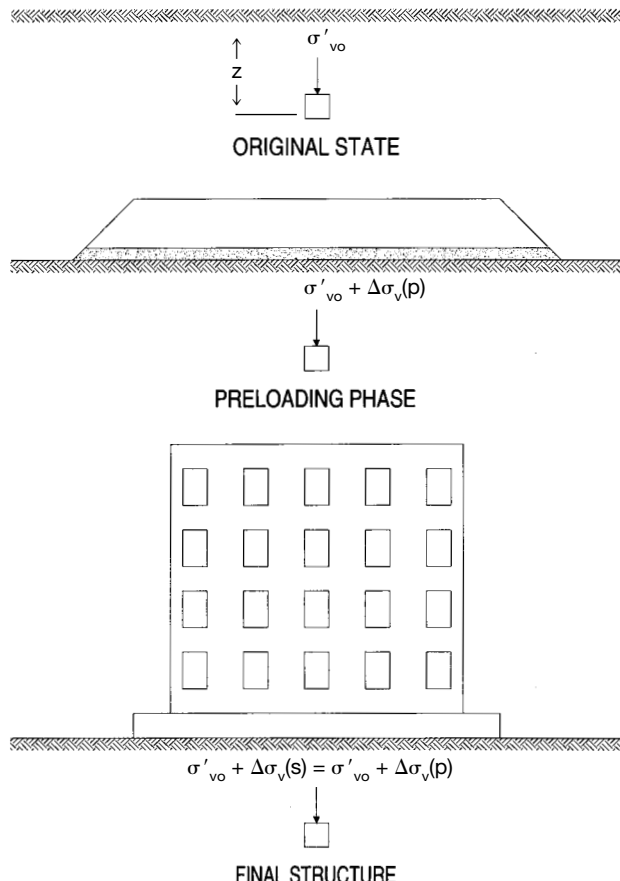


**FIGURE 6A.188** Illustration of simple precompression (modified from Hausmann 1990).

**6.252** SOIL IMPROVEMENT AND STABILIZATION

of preloading with an earthen fill at a site where a building supported on a mat foundation will be constructed. In this case, the increase in total stress at any location within the bearing soil caused by the preload [ $\Delta\sigma_v(p)$ ] is equal to the expected increase in total stress to be caused by the structure at the same point [ $\Delta\sigma_v(s)$ ].

If the preload could be removed instantaneously and the structure built instantaneously, the primary compression settlement ( $S_c$ ) under the load of the structure [ $\Delta\sigma_v(s)$ ] would theoretically be zero. In reality, the magnitude of  $S_c$  resulting from  $\Delta\sigma_v(s)$  is approximately equal to the amount of primary heave that occurs upon removal of the preload. The magnitude of primary heave depends on the rate at which it occurs and how long it takes to remove the preload and build the structure. The rate of primary heave is primarily a function of the moisture condition and permeability of the soil, and the lengths of the drainage paths if the soil is saturated. For example, a coarse sand is highly permeable regardless of its moisture condition and primary heave will be complete within a few days after the preload is removed. On the opposite extreme, the primary heave for a saturated, low-permeability clay with long drainage paths may require many years to complete, and thus the magnitude of primary heave would be very small for typical removal and construction times.

Soils that are overconsolidated behave essentially elastically when loaded to stresses up to the preconsolidation pressure ( $\sigma'_p$ ). Precompression is ineffective in overconsolidated soils when the final stress under the load of the structure [ $\sigma'_{vo} + \Delta\sigma_v(s)$ ] is less than the preexisting  $\sigma'_p$  and full primary heave occurs upon removal of the preload. That is, the magnitude of  $S_c$  (and the strength of the soil) will be about the same whether or not precompression is performed. Therefore, precompression should only be considered when at least one of the following conditions is present:

1. The soil is normally consolidated
2. The soil is overconsolidated but  $\sigma'_{vo} + \Delta\sigma_v(s)$  is somewhat greater than the preexisting  $\sigma'_p$ .
3. The amount of rebound that will occur between removal of the overburden and completion of the structure will be small.

The total settlement or heave ( $S_t$ ) that the structure will undergo throughout its design life is given by the following equation:

$$S_t = S_i + S_c + S_s + S_m \quad (6A.113)$$

where  $S_i$  = immediate distortion settlement

$S_c$  = settlement from secondary compression

$S_s$  = settlement or heave caused by changes in moisture condition (swelling, shrinkage, or collapse)

Precompression is generally not a viable treatment method for soils with high potential for  $S_m$ . Highly expansive clays generally are chemically stabilized to reduce problems from swelling and shrinkage. Highly collapsible soils are generally densified using dynamic compaction or other densification techniques, or chemically stabilized, to reduce collapse potential. Thus, for precompression, Eq. 6A.113 is generally reduced to one of the following equations, depending on the time required for primary consolidation to be nearly complete ( $t_{pr}$ ) in relation to the design life of the structure ( $t_d$ ).

For  $t_{pr} \leq t_d$ :

$$S_t = S_i + S_c(t_{pr}) + S_s(t_d) \quad (6A.114a)$$

For  $t_{pr} > t_d$ :

$$S_t = S_i + S_c(t_d) \quad (6A.114b)$$

$S_i$  results primarily from distortion of the soil mass (change in shape without change in volume) at the edges of the loaded area, and generally increases in significance as the width of the loaded area decreases in relation to the height of the compressible layer.  $S_i$  is theoretically equal to zero for true one-dimensional compression.

Although secondary compression occurs during primary consolidation, it is difficult to determine the magnitudes of the two phenomena. Therefore, it is generally assumed that secondary compression does not occur until primary consolidation is essentially complete.  $S_s$  is usually calculated from the following equation:

$$S_s = \frac{C_{ae}}{1 + e_{pr}} H_{pr} \log \frac{t_d}{t_{pr}} \quad (6A.115)$$

where  $C_{ae} = -\frac{\Delta e}{\Delta(\log t)}$

$e_{pr}$  = void ratio at  $t_{pr}$

$H_{pr}$  = height of the compressible layer at  $t_{pr}$

$e_{pr}$  can be difficult to determine for three-dimensional loading conditions, so it can be assumed that  $H_{pr}/(1 + e_{pr}) \approx H_0/(1 + e_0)$ , with little error generally introduced by this assumption. One of the additional benefits of precompressing a normally consolidated clay is that it reduces  $C_{ae}$  to about 10 to 50% of the normally consolidated value (Hausmann 1990).

$S_c$  in saturated, fine-grained soils is typically estimated from one of the following equations.

For virgin compression:

$$S_c \sum_{i=1}^{i=n} = \frac{C_{cei}}{1 + e_{1i}} H_{1i} \log \frac{\sigma'_{v2i}}{\sigma'_{v1i}} \quad (6A.116a)$$

For rebound or recompression to  $\sigma'_{v2} \leq \sigma'_p$ :

$$S_c \sum_{i=1}^{i=n} = \frac{C_{rei}}{1 + e_{1i}} H_{1i} \log \frac{\sigma'_{v2i}}{\sigma'_{v1i}} \quad (6A.116b)$$

For recompression to  $\sigma'_{v2} > \sigma'_p$ :

$$S_c \sum_{i=1}^{i=n} = \frac{C_{rei}}{1 + e_{1i}} H_{1i} \log \frac{\sigma'_{pi}}{\sigma'_{v1i}} + \sum_{i=1}^{i=n} \frac{C_{cei}}{1 + e_{pi}} H_{pi} \log \frac{\sigma'_{v2i}}{\sigma'_{pi}} \quad (6A.116c)$$

where  $i$  = integer summation variable

$n$  = number of sublayers into which the compressible layer is divided

$C_{cei}$  = virgin compression index based on void ratio for the  $i$ th sublayer

$C_{rei}$  = recompression/rebound index based on void ratio for the  $i$ th sublayer

$H_{1i}$  = height of the  $i$ th sublayer when loading begins

$H_{pi}$  = height of the  $i$ th sublayer when  $\sigma'_{vi} = \sigma'_{pi}$

$e_{1i}$  = void ratio of the  $i$ th sublayer when loading begins

$e_{pi}$  = void ratio of the  $i$ th sublayer when  $\sigma'_{vi} = \sigma'_{pi}$

$\sigma'_{pi}$  = preconsolidation pressure of the  $i$ th sublayer

$\sigma'_{v1i}$  = effective vertical stress at the midheight of the  $i$ th sublayer when loading begins

$\sigma'_{v2i}$  = effective vertical stress at the midheight of the  $i$ th sublayer when the soil comes to equilibrium under the load from the structure

log = logarithm to the base 10

**6.254** SOIL IMPROVEMENT AND STABILIZATION

The rate at which  $S_c$  occurs is usually predicted beforehand using Terzaghi's one-dimensional consolidation theory. Unfortunately, there are a number of assumptions in this theory that invalidate its use in some preloading situations. Details of some of these assumptions and limitations can be found in Duncan (1993). The following assumptions most often invalidate its use in practice:

1. All compression occurs in the direction the load is applied or removed; that is, there is no lateral compression. This assumption is reasonably correct only if the applied stress is relatively uniform; the bearing soil consists of nearly horizontal, uniform layers; and the width of the loaded area is much greater than the thickness of the compressible layer.
2. The strains resulting from primary consolidation are small. In precompression, the soils being treated are frequently soft clays that undergo large strains when precompressed, which invalidates this assumption.
3. The change in void ratio of the consolidating soil is directly proportional to the change in effective stress:  $\Delta e \propto \Delta \sigma'_v$ . For one-dimensional compression, this is tantamount to assuming that the strains are constant throughout the compressible layer. It has been found from experience that for most saturated, fine-grained soils,  $\Delta e \propto \Delta(\log \sigma'_v)$ , as indicated by the log terms in Eq. 6A.116. So in reality, the strains are greatest in the upper portions of the compressible layer and decrease with depth within the layer.

According to Terzaghi's theory, the primary consolidation settlement at any time ( $t$ ) after a load has been applied can be estimated from the following equation:

$$S_c(t) = U_v \cdot S_c(t = \infty) \quad (6A.117)$$

where  $U_v$  is called the average degree of vertical consolidation within the compressible layer and can be determined from the following equation:

$$U_v = 1 - \sum_{m=0}^{m=\infty} \frac{2}{M^2} \cdot e^{-M^2 T_v} \quad (6A.118)$$

where  $m$  = integer summation variable starting at zero

$$M = \frac{\pi}{2}(2m + 1)$$

$$T_v = \frac{c_v t}{H_{dp}^2}$$

$c_v$  = coefficient of consolidation (usually obtained from 1-D consolidation tests)

$H_{dp}$  = height of the longest vertical drainage path

In actuality,  $U_v$  is the average degree of dissipation of excess pore water pressure within the compressible layer rather than the average degree of primary consolidation settlement. This discrepancy is related to the inconsistency of assumption number 3 discussed above. Duncan (1993) gives an example where the use of Eq. 6A.117 to estimate  $S_c(t)$  gives unrealistic results. **Hence, Eq. 6A.117 is not correct and should not be used in practice.**

Terzaghi's theory can be used to give reasonable estimates of  $S_c(t)$  in many cases if the following procedure is used:

1. The compressible layer should be subdivided into at least ten sublayers and  $S_c(t)$  calculated using Eq. 6A.116.
2. The increase in total stress at the midheight of each sublayer ( $\Delta\sigma_{vi}$ ) should not be assumed to be equal to the applied stress unless one-dimensional compression conditions are closely approximated. Instead,  $\Delta\sigma_{vi}$  should be calculated using a method that accounts for the finite width of the loaded area, embedment of the foundation (if any), and layering of the bearing soils.

3.  $\sigma'_{v2i}$  should be replaced in Eq. 6A.116 with  $\sigma'_{vi}(t)$ , with  $\sigma'_{vi}(t)$  calculated as follows:

$$\sigma'_{vi}(t) = \sigma'_{v1i} + U_{zi} \cdot \Delta\sigma'_{vi} \quad (6A.119)$$

where  $U_{zi}$  is the consolidation ratio at the midheight of the  $i$ th sublayer, which can be calculated as

$$U_z = 1 - \sum_{m=0}^{m=\infty} \frac{2}{M^2} \cdot \sin \frac{Mz_i}{H_{dp}} \cdot e^{-M^2 T_v} \quad (6A.120)$$

where  $z_i$  is the depth from the top of the clay layer to the midheight of the  $i$ th sublayer.

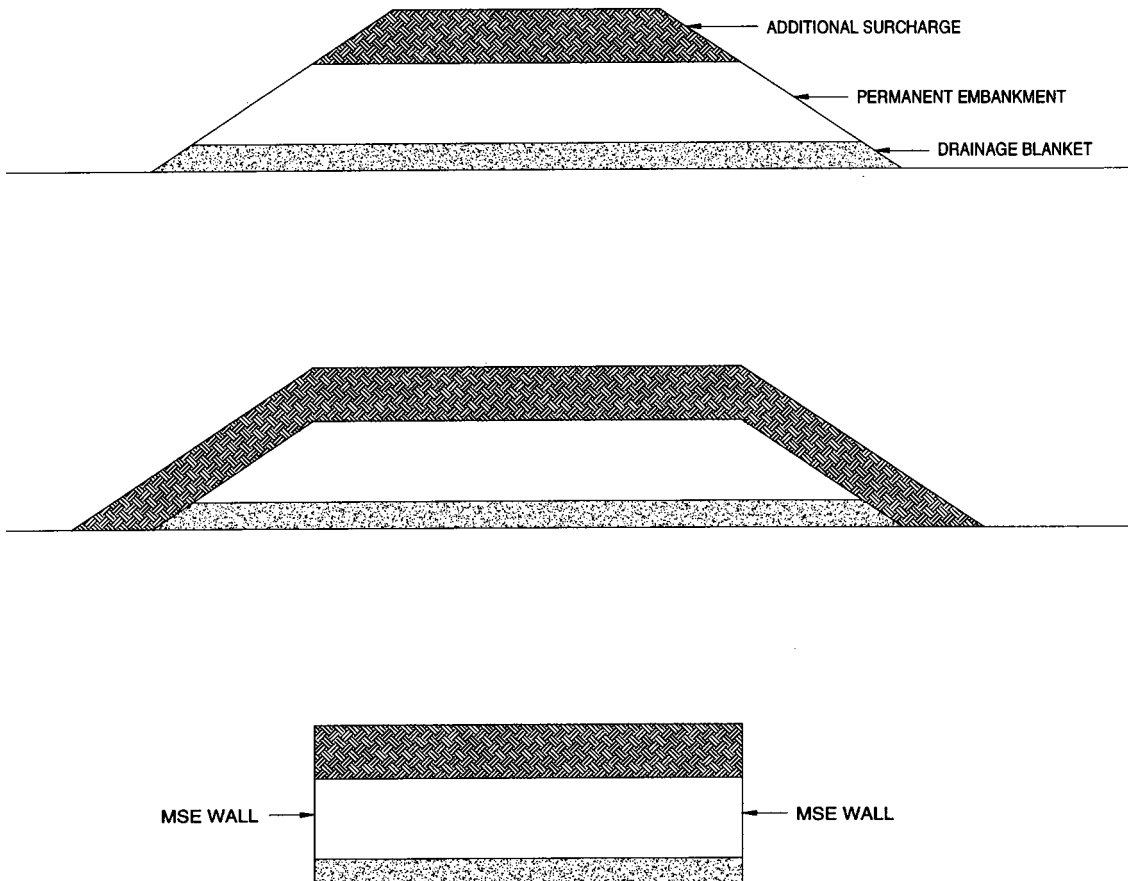
It is sometimes difficult to determine  $H_{dp}$  reliably, especially in highly stratified soils containing alternating layers of cohesive and cohesionless soils, such as varved clays. In these types of soils, it must be determined whether or not the cohesionless layers are continuous across the site. This determination requires that extensive boring and sampling be conducted. If the cohesionless layers are continuous, they will act as drainage layers and  $H_{dp}$  will be considerably reduced. Otherwise their effect on  $H_{dp}$  will be minimal unless vertical drains are installed.

### **6A.6.3 Precompression with Additional Surcharge**

The precompression process can be achieved much quicker in saturated clays if additional surcharge is used above that required for simple precompression. This method is especially attractive when the structure to be built on the site is a permanent embankment, such as for highway and railroad applications. Three possible ways to construct the additional surcharge are illustrated in Fig. 6A.189.

The critical factor in successful application of this technique is determining the appropriate time when the surcharge should be removed ( $t_{sr}$ ). Proper determination of  $t_{sr}$  depends on a thorough understanding how the pore pressures and effective stresses change in the clay layer as the permanent and surcharge embankments are constructed, while the additional surcharge is in place, and after the surcharge is removed.

Total vertical stress ( $\sigma'_v$ ), pore water pressure ( $u$ ), and effective vertical stress ( $\sigma'_e$ ) profiles in the clay layer at various times are illustrated in Fig. 6A.190 for the idealized case of perfect one-dimensional compression of a normally consolidated clay layer, instantaneous construction and removal times, the top of the clay layer and the groundwater table both coinciding with the ground surface, and double drainage. The applied stress at the ground surface from the permanent embankment is designated  $\Delta p$ , and the corresponding stress from the additional surcharge is designated  $\Delta s$ . Just before construction of the permanent and surcharge embankments ( $t_0^-$ ),  $\sigma'_v$ ,  $u$ , and  $\sigma'_e$  are zero at the top of the clay layer and increase linearly with depth ( $z$ ) in proportion to the saturated unit weight of the clay ( $\gamma_{sat}$ ), the unit weight of the water ( $\gamma_w$ ), and the effective unit weight of the clay ( $\gamma'$ ), respectively. Just after the permanent and surcharge embankments are constructed instantaneously ( $t_0^+$ ), the combined applied stress ( $\Delta p + \Delta s$ ) is carried entirely by the pore water as excess pressure. Therefore, at time  $t_0^+$  the effective vertical stresses in the clay layer have not changed from their initial values and no primary consolidation settlement has occurred. As time elapses after construction, the excess pore water pressures dissipate. At the drainage boundaries, the excess pore pressures dissipate completely in a short time. The rate of dissipation decreases with distance from the boundaries and is slowest at the elevation farthest from the drainage boundaries (midheight of the clay layer in this case). Since the total stresses have not changed once construction was completed, the effective stresses increase by the same amounts that the excess pore water pressures decrease ( $\Delta\sigma'_e = -\Delta u$ ). At time  $t_1$ , corresponding to some time after construction, the stress profiles take the shapes shown in Fig. 6A.190. Profiles at later times  $t_2$  and  $t_3$  are also shown. As time elapses with the additional surcharge, the pore water pressures are decreasing toward their equilibrium condition (same

**6.256** SOIL IMPROVEMENT AND STABILIZATION

**FIGURE 6A.189** Three possible configurations of permanent embankment with additional surcharge.

as initial condition assuming the groundwater table stays at the same elevation), while the effective vertical stresses are increasing toward their equilibrium condition ( $\sigma'_{v0} + \Delta p + \Delta s$ ).

At the instant the additional surcharge is removed,  $\sigma'_v$  and  $u$  at all depths decrease by  $-\Delta s$ , while  $\sigma'_v$  at all depths does not change. The equilibrium condition for  $u$  remains the same, while the equilibrium condition for  $\sigma'_v$  decreases by  $\Delta s$  and is now equal to  $\sigma'_{v0} + \Delta p$ . If the surcharge is removed at time  $t_1$ , the pore water and effective stress profiles are as shown in Fig. 6A.191.  $t_1^-$  denotes just before the surcharge is removed,  $t_1^+$  denotes just after the surcharge is removed, and  $t_\infty$  denotes the equilibrium condition under the permanent embankment. The central portion of the clay layer is *normally consolidated-underconsolidated* (NC-UC, normally consolidated and still compressing but now only under the permanent embankment load), while the top and bottom portions of the clay layer are *overconsolidated-underconsolidated* (OC-UC, precompressed and now rebounding owing to removal of the additional surcharge). The excess pore water pressures are indicated by the hatched regions. The excess pore water pressures in the upper and lower portions are negative, and in the middle portion they are positive. At equilibrium under the permanent embankment, the net vertical movement of the clay layer from  $t_{sr}$  to  $t_\infty$  may be either settlement (downward) or heave (upward) depending on the magnitude of the compression or rebound that occurs within each portion of

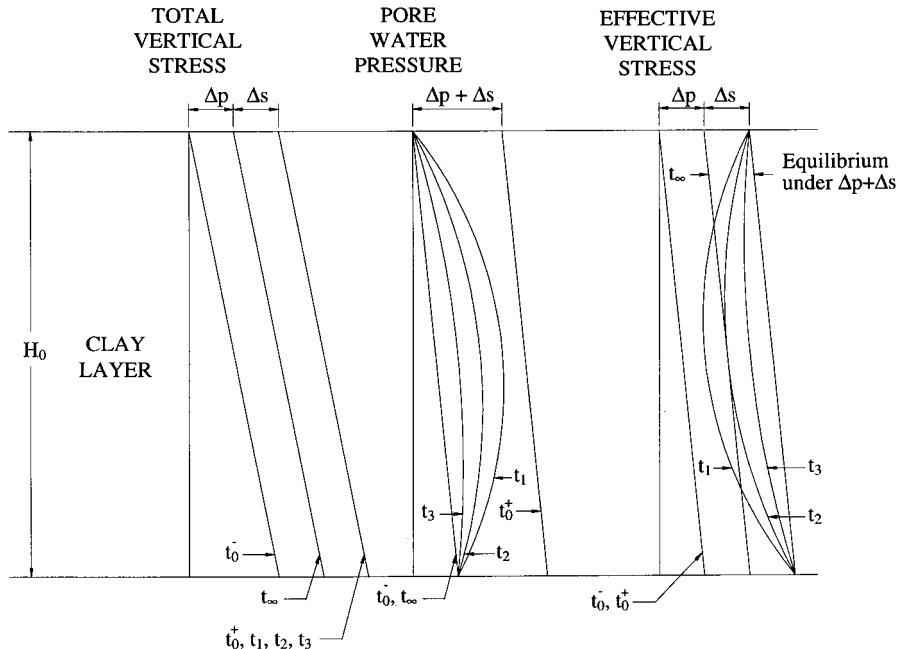


**FIGURE 6A.190** Stress profiles within a doubly drained clay layer before, during, and after precompression.

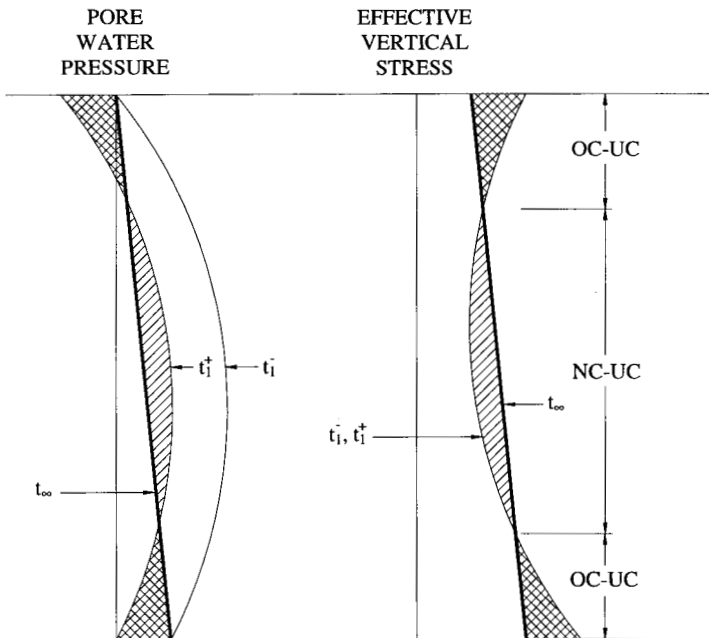


**FIGURE 6A.191** Pore water and effective vertical stress profiles within a doubly drained clay layer if additional surcharge is removed at time  $t_1$ .

**6.258** SOIL IMPROVEMENT AND STABILIZATION

the clay layer. It is theoretically possible to time the surcharge removal such that the net vertical movement of the clay layer at equilibrium is zero, but this is difficult to do in practice. Furthermore, the rates at which virgin compression and rebound occur are different. Virgin compression is typically much slower than either recompression or rebound. Hence, there would be net vertical movement of the clay layer between  $t_{sr}$  and  $t_\infty$  even if the net vertical movement at equilibrium is zero.

If the additional surcharge is removed at time  $t_2$ , the pore water and effective stress profiles are as shown in Fig. 6A.192. The entire clay layer is precompressed (OC-UC), except at its midheight, which is the location where the water has the longest vertical distance to drain in this case. This critical location is in equilibrium (primary consolidation is complete). If the clay layer is singly drained (drainage at the top only), the critical location will be at the bottom of the layer. When controlling the magnitude of primary consolidation settlement is the primary goal of the precompression process, this method of determining when the surcharge should be removed is preferred by most engineers, and a small amount of primary consolidation heave will occur after the surcharge is removed. The procedure used to determine  $t_{sr}$  for zero excess pore water pressure at the critical location is as follows:

1. Calculate  $\Delta\sigma_v$  for the load from permanent embankment only ( $\Delta p$ ) at the critical depth ( $z_{cr}$ ) using an appropriate method. If true one-dimensional compression conditions exists,  $\Delta\sigma_v(z_{cr}, \Delta p) = \Delta p$ .
2. Calculate  $\Delta\sigma_v$  for the load from permanent embankment plus the additional surcharge ( $\Delta p + \Delta s$ ) at the critical depth ( $z_{cr}$ ) using an appropriate method. If true one-dimensional compression conditions exists,  $\Delta\sigma_v(z_{cr}, \Delta p + \Delta s) = \Delta p + \Delta s$ .

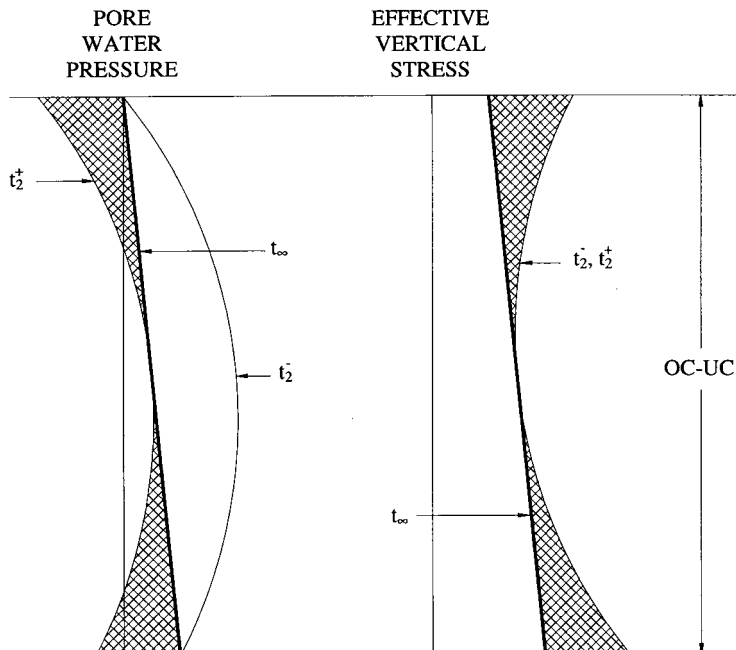


**FIGURE 6A.192** Pore water and effective vertical stress profiles within a doubly drained clay layer if additional surcharge is removed at time  $t_2$ .

3. Set the consolidation ratio at the critical depth ( $U_{z-cr}$ ) equal to the value calculated in step 1 divided by the value calculated in step 2. That is,

$$U_{z-cr} = \frac{\Delta\sigma_v(z_{cr}, \Delta p)}{\Delta\sigma_v(z_{cr}, \Delta p + \Delta s)} \quad (6A.121)$$

4. Assume a value of  $T_{v-sr}$  and solve for  $U_{z-cr}$  using Eq. 6A.120. If the values of  $U_{z-cr}$  calculated from Eqs. 6A.120 and 6A.121 are not the same, assume other values of  $T_{v-sr}$  until the two values are the same. This is the correct value of  $T_{v-sr}$ .
5. Calculate  $t_{sr}$  from the following equation:

$$t_{sr} = \frac{T_{v-sr} \cdot H_{dp}^2}{c_v} \quad (6A.122)$$

Because the theory is based on many simplifying assumptions that may deviate significantly from reality, and there are errors associated with determining the input parameters for the soil, the value of  $t_{sr}$  determined using this method should be considered an approximation only. In practice, the pore water pressures at various depths and locations beneath the preloaded area should be monitored at regular intervals to ascertain when the additional surcharge should be removed.

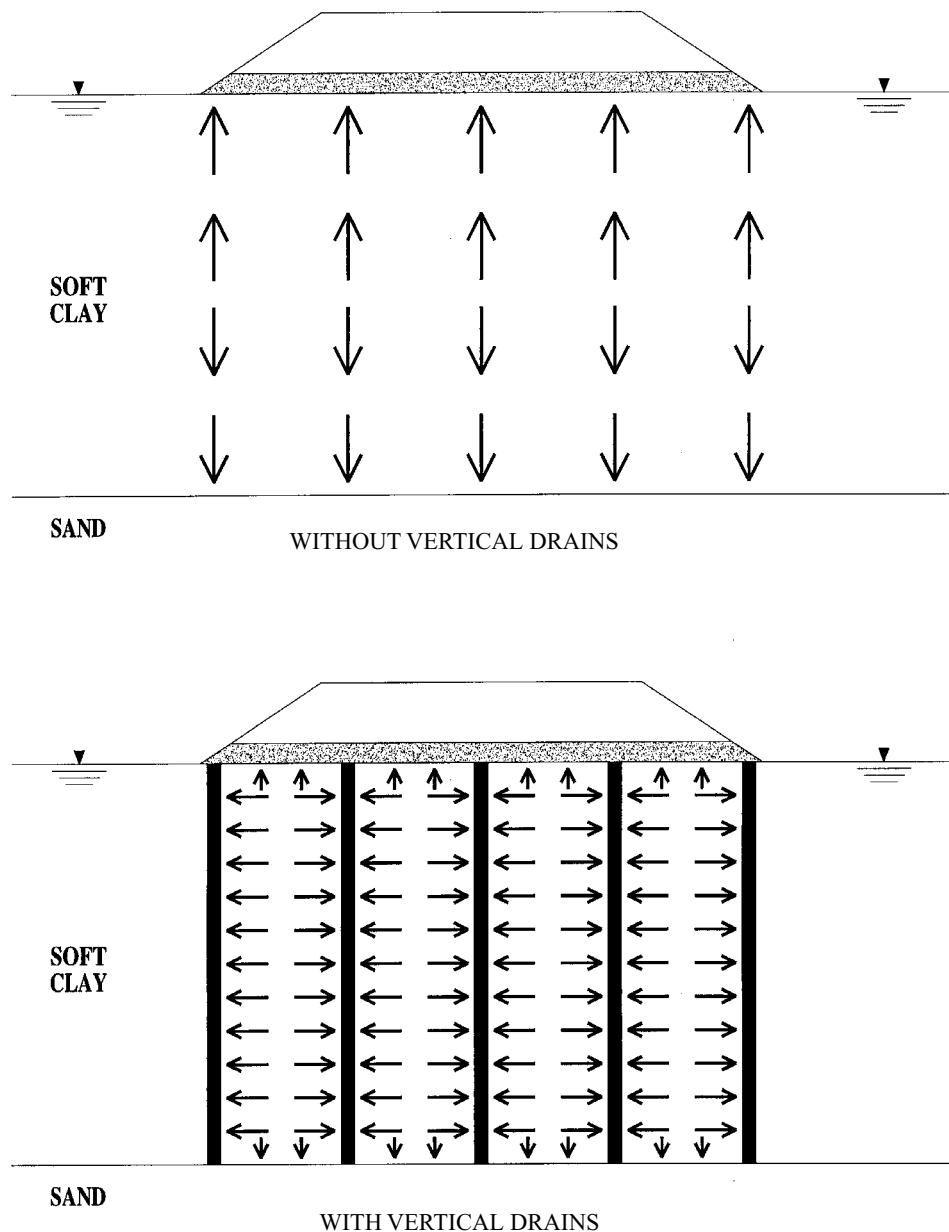
If the additional surcharge is not removed until time  $t_3$ , the preloaded soil will be precompressed beyond the level needed to ensure that primary consolidation settlement will be controlled. This will result in additional primary heave above that which will occur if  $t_{sr} = t_2$ . In some instances, this may be desirable to reduce post-preloading settlements resulting in soils such as highly organic clays and peats where secondary compression is the dominant mechanism of settlement. In soils where secondary compression is to be controlled, the equation for  $U_{z-cr}$  that is analogous to Eq. 6A.121 is as follows:

$$U_{z-cr} = \frac{S_c(\Delta p, t_{pr}) + C_{ae}H_p \log(t_d/t_{pr})}{S_c(\Delta p + \Delta s, t_\infty)} \quad (6A.6.123)$$

Once  $U_{z-cr}$  is calculated,  $t_{sr}$  can be determined in the same manner described above for controlling primary consolidation settlement.

#### **6A.6.4 Precompression with Vertical Drains**

Vertical drains can be used in many cases to accelerate the rate of primary consolidation settlement within the preloaded zone, whether or not additional surcharge is used. However, they are ineffective in soils such as highly organic clays and peats whose settlement behavior is dominated by secondary compression, owing to the small amount of water squeezed from these soils during second compression. Vertical drains allow drainage to take place horizontally in addition to vertically, as illustrated in Fig. 6A.193. In typical applications where vertical drains are used, most of the drainage will occur horizontally rather than vertically for two reasons: (a) the horizontal drainage path is generally shorter than the vertical drainage path for most of the compressible layer, and (b) most clay deposits have greater permeability in the horizontal direction than in the vertical direction. Representative values of horizontal to vertical permeability ( $k_h/k_v$ ) for soft clays (undrained shear strength less than 1 ksf = 48 kPa) are given in Table 6A.18. Actual values of  $k_h/k_v$  for any given soil should be verified by the designer.

**6.260** SOIL IMPROVEMENT AND STABILIZATION

**FIGURE 6A.193** Comparison of drainage during precompression without and with vertical drains.

**TABLE 6A.18** Representative Values of  $k_h/k_v$  for Soft Clays (from Rixner et al. 1986)

Description	$k_h/k_v$
No evidence of layering (partially dried clay has completely uniform appearance)	1.0 to 1.4
No or only slightly developed macrofabric (e.g., sedimentary clays with discontinuous lenses and layers of more permeable soil)	1.0 to 1.5
Slight layering (e.g., sedimentary clays with occasional silt dustings to random silty lenses)	2 to 5
Fairly well to well developed macrofabric (e.g., sedimentary clays with discontinuous lenses and layers of more permeable material)	2 to 4
Varved clays in Northeastern United States	5 to 15
Varved clays and other deposits containing embedded and more or less continuous permeable layers	3 to 15

#### 6A.6.4.1 Types of Vertical Drains

Sand drains were used to accelerate primary consolidation in early precompression applications in the United States (Rixner et al. 1986). A U.S. patent for a sand drain system was granted in 1926. Since that time, sand drains have been used successfully worldwide on a large number of precompression projects. Gravel drains have also been used successfully. Details on sand and gravel drains can be found in Section 6A.5.1.4.

Prefabricated sand drains have also been used. These drains consist of sand prepacked in a fabric sock.

In the late 1930s, the first prefabricated vertical (PV) drain was developed in Sweden and patented (Kjellman 1948). This drain, called a *cardboard wick*, was band-shaped (rectangular cross-section) with a width of about 4 in (100 mm) and a thickness of about 3 mm (0.13 in). It came in continuous strips about 1,300 ft (400 m) long and was rolled on a drum.

Most modern PV drains have many of the same general characteristics as the cardboard wick but are made of different materials. They are typically band-shaped with widths of about 4 in (100 mm) and thicknesses varying from about 0.08 to 0.25 in (2 to 6 mm). The main components typically consist of a plastic core surrounded by a synthetic geotextile jacket, as shown in Fig. 6A.194. Configuration of four types of PV drains are illustrated in Fig. 6A.195. The primary functions of the core and jacket are summarized as follows (Ladd 1986).

##### Jacket

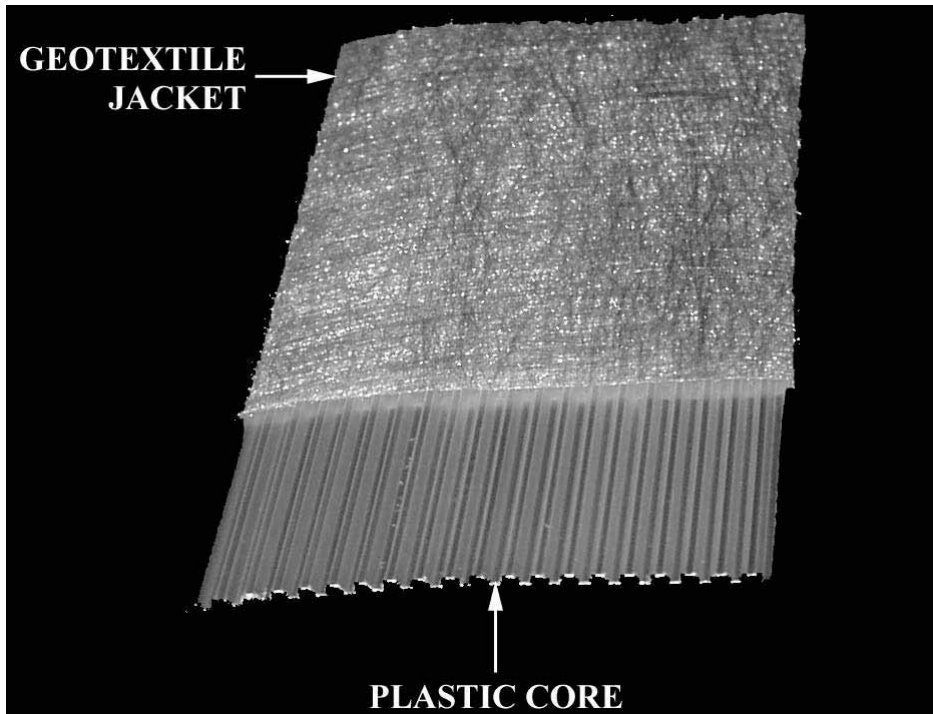
1. Separate the flow channels of the core from the surrounding fine-grained soils
2. Act as a filter to allow easy passage of water into the core while preventing the intrusion of soil
3. Prevent closure of internal drain flow paths under lateral soil pressure

##### Core

1. Provide internal flow paths along the drain
2. Maintain drain configuration and shape
3. Provide resistance to buckling and longitudinal stretching of the drain

The major advantages of PV drains compared to sand drains are simplicity and speed of installation, less disturbance to the soil mass, and usually lower cost. Because of these advantages, the use of PV drains has largely replaced sand drains for most preloading applications.

PV drains are usually installed using equipment similar to that shown schematically in Fig. 6A.196. The drain is enclosed within a mandrel and attached to an anchor plate at the bottom of the

**6.262** SOIL IMPROVEMENT AND STABILIZATION

**FIGURE 6A.194** Typical band-shaped PV drain in common use today.

mandrel. The mandrel is then pushed, driven, or vibrated into the soil to the desired depth. The anchor plate holds the drain in the soil while the mandrel is extracted. The drain is then cut off, a new anchor plate installed, and the process repeated at another location. PV drains are typically installed in a triangular pattern at a spacing ranging from about 3 to 30 ft (1 to 10 m) to depths up to about 160 ft (50 m).

Band-shaped PV drains are more commonly referred to as *wick drains* in the United States. However, this term is a misnomer because “wick” suggests that water is absorbed by and rises within the drain owing to capillary action. In fact, the excess pore water pressure generated by the pre-load increases the hydraulic head and causes the water to flow into the PV drain and then either upward or downward to a drainage layer. Thus, use of the term wick drain is not recommended, but because its use has been prevalent for a long period of time within the construction and civil engineering industries, usage of the term may well continue. Koerner (1994) reported that his attempts in the United States to change usage from wick drain to strip drain were unsuccessful.

Detailed information regarding using, designing, and specifying PV drains can be found in a number of sources. Good references on this topic include Bergado et al. (1996), Holtz et al. (1991), and Rixner et al. (1986).

#### **6A.6.4.2 Radial and Combined Drainage**

Barron (1948) provided the first comprehensive theory for vertical consolidation resulting from axisymmetric radial drainage into a cylindrical drain well. Barron’s theory was based on the same simplifying assumptions as Terzaghi’s one-dimensional consolidation theory, and thus suffers from the same limitations discussed in Section 6A.6.2.

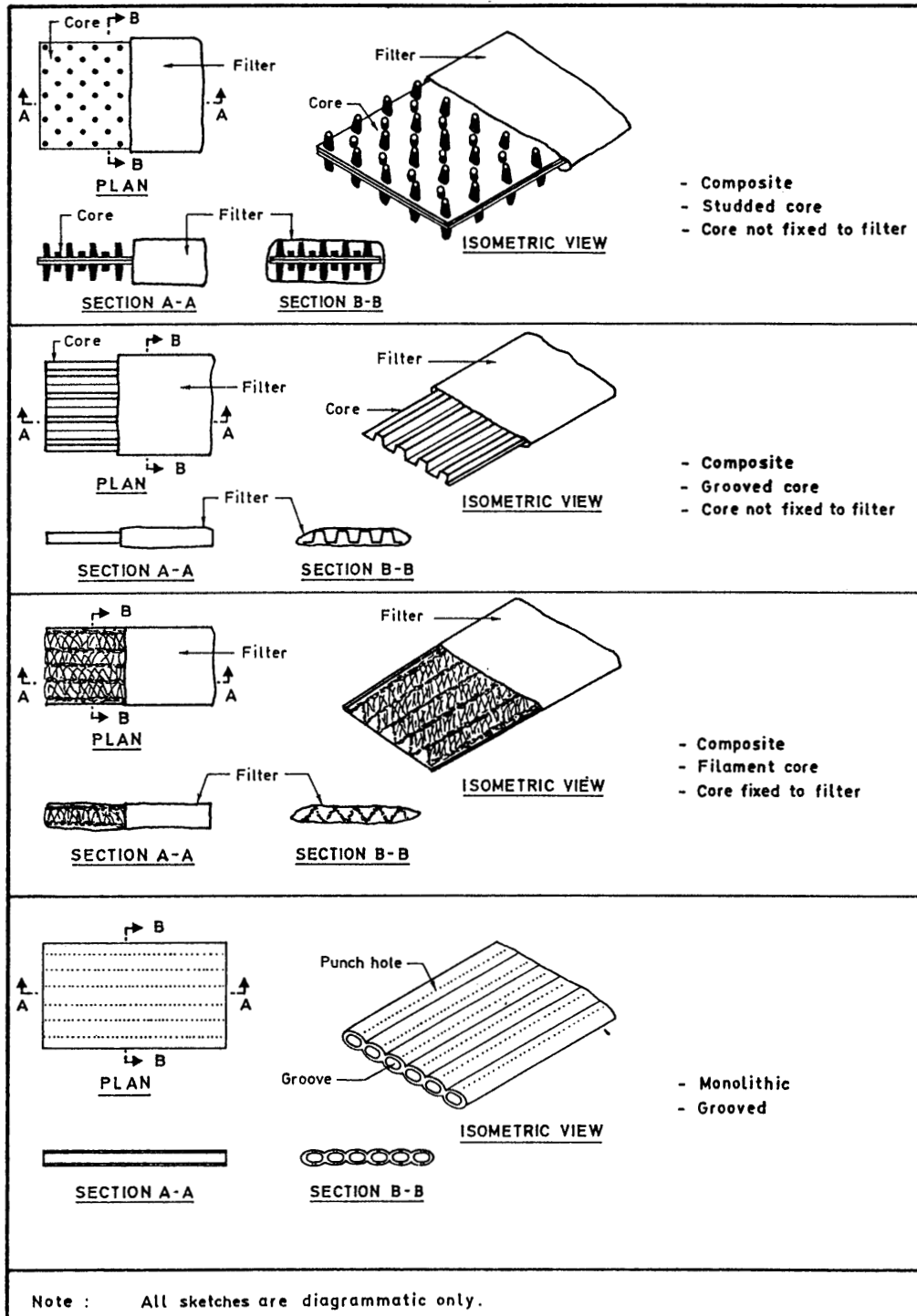
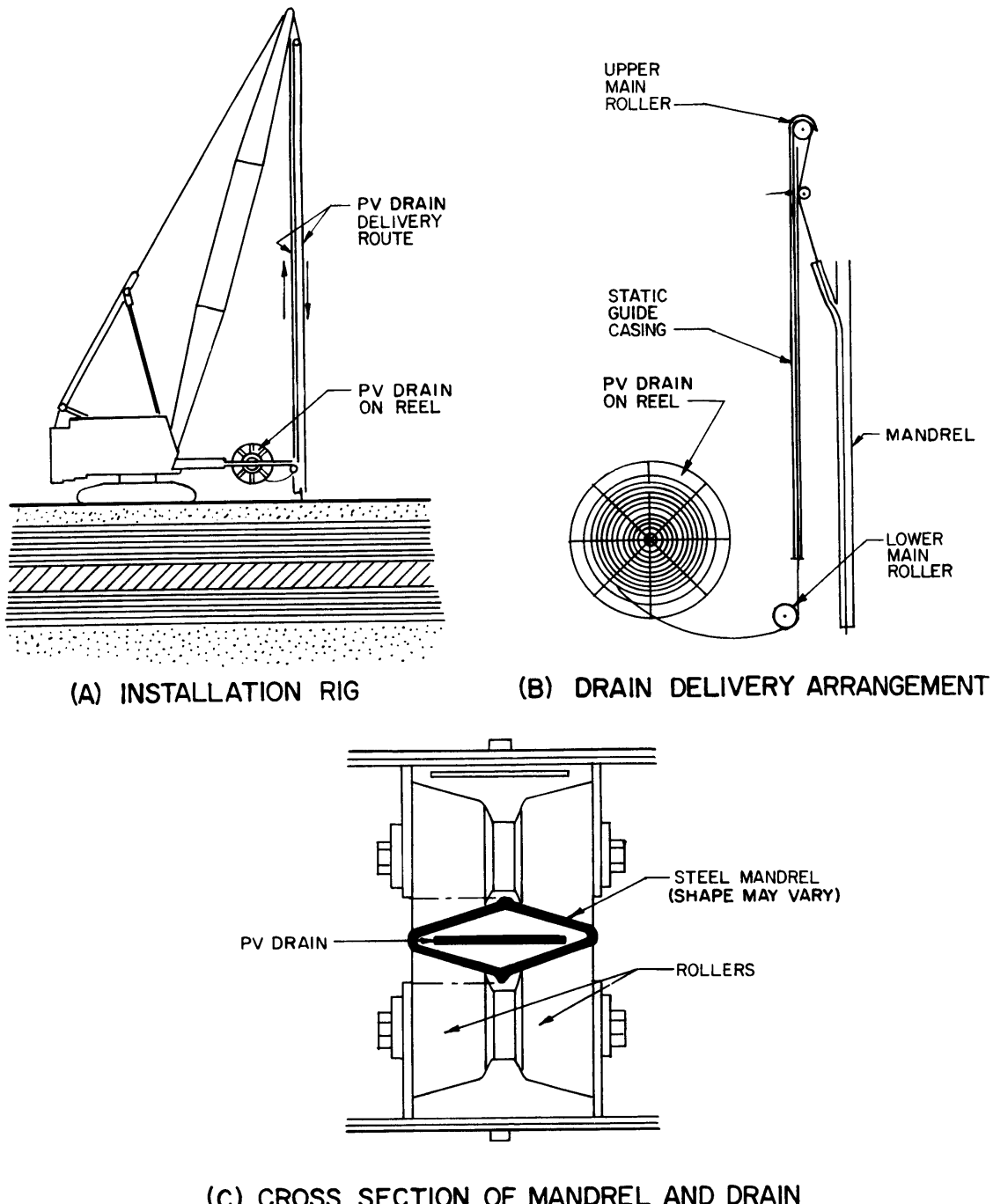


FIGURE 6A.195 Configuration of different types of PV drains (from Bergado et al., 1996).

**6.264** SOIL IMPROVEMENT AND STABILIZATION

**FIGURE 6A.196** Schematic illustration of typical equipment used to install PV drains (from Rixner et al., 1986).

Barron developed theories for two cases of vertical strain: (a) free strain, corresponding to a flexible foundation such as a soil embankment, and (b) equal strain, corresponding to a rigid foundation such as a thick, reinforced concrete footing. Although the free strain theory is more applicable to most preloading projects, Barron found that the two theories generally give similar results. Since the solution to the equal-strain theory is simpler to use, it is preferred in practice. Furthermore, settlement observations in the field strongly support the assumption of equal vertical strains (Hansbo 1979).

For the idealized case of no soil disturbance and no resistance to flow within the drain, the following differential equation governs consolidation for equal vertical strains and radial flow only:

$$\frac{\partial u_e}{\partial t} = c_h \left( \frac{1}{r} \cdot \frac{\partial u_e}{\partial r} + \frac{\partial^2 u_e}{\partial r^2} \right) \quad (6A.124)$$

where  $u_e$  = average excess pore water pressure at any point and time

$t$  = time after instantaneous application of the preload

$r$  = radial distance from the center of the drain

$c_h$  = horizontal coefficient of consolidation

The solution to Eq. 6A.124 is as follows:

$$u_e = \frac{u_i}{r_c^2 \cdot \mu} \left[ r_c^2 \ln\left(\frac{r}{r_d}\right) - \frac{r^2 - r_d^2}{2} \right] e^\lambda \quad (6A.125)$$

where  $u_i$  = initial excess pore water pressure caused by the preload

$r_c$  = radius of equivalent soil cylinder from which radial drainage occurs

$r_d$  = radius of a sand or gravel drain, or equivalent radius of a PV drain (see subsequent discussion)

$$\mu = \frac{n^2}{n^2 - 1} \cdot \ln(n) - \frac{3n^2 - 1}{4n^2}$$

$$n = r_c/r_d = d_c/d_d$$

$d_c = 2r_c = 1.05s$  for triangular pattern of drains = 1.13s for square pattern of drains (see Fig. 6A.163), where  $s$  is the center-to-center spacing of the drains

$$d_d = 2r_d$$

$$\lambda = -8T_r/F(n)$$

$$T_r = c_h t / d_c^2 = \text{dimensionless time factor for radial drainage}$$

$\ln$  = natural logarithm = logarithm to the base  $e$

From Eq. 6A.125, it can be seen that at any time  $t$ ,  $u_e$  increases with radial distance ( $r$ ) from the drain, as would be expected.

The average radial consolidation ratio ( $U_r$ ) within the zone of drainage for each vertical drain is given by the following equation:

$$U_r = 1 - \frac{u_{e-av}}{u_i} = 1 - e^\lambda \quad (6A.126)$$

where  $u_{e-av}$  = average excess pore water pressure with the drainage zone at any time.

It is important to note that  $U_r$  is the same at all depths within the clay layer ( $z$ ) for the simplifying assumptions of the theory.

A number of methods have been used to calculate the equivalent diameter of a band-shaped PV drain. Of these methods, two are used predominantly in practice. The first method was proposed by Kjellman (1948) and is based on the assumption that the drainage capacity of the drain depends on

**6.266** SOIL IMPROVEMENT AND STABILIZATION

the area of contact with the soil. With this assumption, the perimeter of a PV drain with a thickness of  $a$  and a width  $b$  is set equal to the perimeter of an equivalent circular with a diameter of  $d_d$ . Solving for the equivalent diameter  $d_d$  of the PV drain gives

$$d_d = \frac{2(a + b)}{\pi} \quad (6A.127a)$$

Finite element analyses and other studies have indicated that the following equation provides a better estimate of  $d_d$  (Rixner et al. 1986):

$$d_d = \frac{a + b}{2} \quad (6A.127b)$$

Hansbo (1987) also supported the use of this second equation. Eq. 6A.127b is the more conservative of the two equations and is recommended for use in practice.

Two important factors can slow the rate of water drainage from the soil into the drain: (a) disturbance of the fabric of the soil adjacent to the drain during installation of the drain, also known as *smear*; and (b) resistance to flow of water within the drain itself. A schematic diagram illustrating both effects is depicted in Fig. 6A.197. Hansbo et al. (1981) proposed the following equation for the average degree of radial consolidation that accounts for smear and resistance to flow ( $U_{r-sr}$ ):

$$U_{r-sr} = 1 - e^{-8T_r/\mu_{sr}} \quad (6A.128)$$

where  $\mu_{sr} = \ln \frac{n}{m} + \frac{k_h}{k_s} \ln m - \frac{3}{4} + \pi z_d (2L_{dp} - z_d) \frac{k_h}{q_d}$

$$m = d_s/d_d$$

$d_s$  = diameter to the outer perimeter of the smear zone

$k_s$  = coefficient of horizontal permeability for the smeared zone

$z_d$  = vertical distance from the closest end of the drain where drainage occurs

$L_{dp}$  = length of the longest drainage path along the vertical drain =  $L$  for drainage at one end  
only =  $L/2$  for drainage at both ends

$q_d$  = discharge capacity of the drain under a hydraulic gradient of one =  $k_d A_d$

$k_d$  = axial coefficient of permeability for the drain

$A_d$  = cross-sectional area of the drain

It can be seen in Eq. 6A.128 that when the resistance of flow within the drain is finite, the value of average radial consolidation varies with depth within the clay layer.

The size of the smear zone and the degree of disturbance depend significantly on the type of drain and the method of installation. For sand and gravel drains, displacement methods of installation result in greater disturbance than nondisplacement methods. The size of the smear zone is also a function of the diameter of the drain. For PV drains, the disturbance depends mostly on the size and shape of the mandrel and the shoe, the soil macrofabric, and the installation procedure. Typical shapes of mandrels and shoes are shown in Figs. 6A.198 and 6A.199. In general, it appears that the amount of disturbance increases with increasing cross-sectional area of the mandrel (Bergado et al. 1991). Therefore, the mandrel cross-sectional area should be the smallest possible that allows clearance for the PV drain and gives adequate stiffness for installation. The shape of the mandrel tip and anchor should be as tapered as possible to reduce disturbance. The outer diameter of the smear zone ( $d_s$ ) can be estimated from the following equation (Jamiolkowski and Lancellotta 1981, Hansbo 1987):

$$d_s = (2 \text{ to } 3)d_m \quad (6A.129)$$

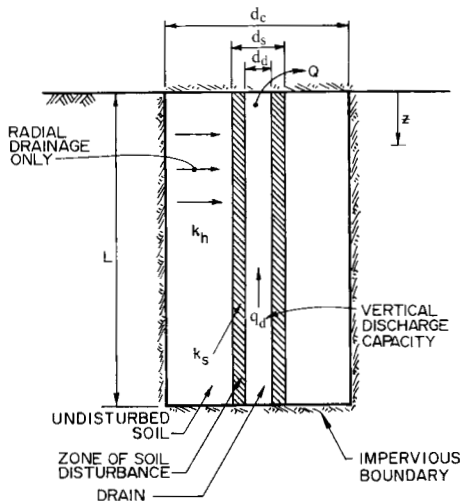


**FIGURE 6A.197** Schematic of vertical drain with drain resistance and soil disturbance (from Rixner et al., 1986).

where  $d_m$  is the diameter of a circle with an area equal to the cross-sectional area of the mandrel. The effect of disturbance on the coefficient of horizontal permeability of the soil is less well known. It appears that values of  $k_h/k_s$  range from about 1 to 10 (Rixner et al. 1986, Holtz et al. 1991). It should be recognized, however, that the disturbance is not uniform throughout the smeared zone; rather, it transitions from greater disturbance near the drain to less disturbance near the outer perimeter of the smear zone.

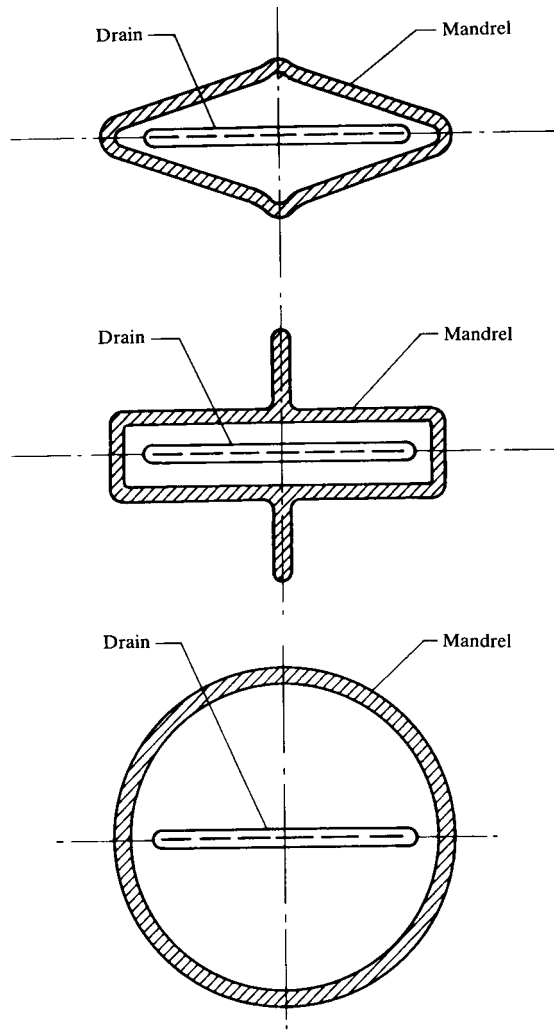
If the discharge capacity of the drain ( $q_d$ ) is reached during consolidation, the overall consolidation process will be slowed. The discharge capacity of sand and gravel drains depends on the permeability of the sand or gravel. Clean sand or gravel should be used in these drains. The discharge capacity of PV drains varies considerably depending on the make of the drain and decreases with increasing lateral pressure, as shown in Fig. 6A.200. Therefore, long drains are more susceptible to reduction in consolidation rate owing to drain resistance. Accurate measurement of  $q_d$  requires sophisticated laboratory or field testing and is time consuming. It is also almost always less significant than spacing of the drains and disturbance factors. Therefore,  $q_d$  is usually estimated rather than measured. Although values of  $q_d$  are generally reported by PV drain manufacturers, the test procedures are not standardized. In general,  $q_d$  can be conservatively assumed to be  $3500 \text{ ft}^3/\text{yr}$  ( $100 \text{ m}^3/\text{yr}$ ) (Rixner et al. 1986).

$c_h$  is usually estimated from the following equation:

$$c_h = \frac{k_h}{k_v} c_v \quad (6A.130)$$

Values of  $k_h/k_v$  can be estimated (see Table 6A.18) or determined from laboratory or field tests. Alternately,  $c_h$  can be determined from the following equation:

$$c_h = \frac{k_h}{m_v \gamma_w} \quad (6A.131)$$

**6.268** SOIL IMPROVEMENT AND STABILIZATION

**FIGURE 6A.198** Typical shapes of mandrels for band-shaped PV drains (from Holtz et al., 1991).

where  $m_v$  is the one-dimensional coefficient of volume change and  $\gamma_w$  is the unit weight of water.  $m_v$  is generally obtained from laboratory one-dimensional consolidated tests and  $k_h$  is usually determined by small-scale pumping tests in piezometers or from self-boring permeameters. A number of other methods can be used to determine  $c_h$ . Some of these methods are summarized in Ladd and Foott (1977) and Rixner et al. (1986).

There is still considerable uncertainty about the influence of smear and drain resistance on the effectiveness of vertical drains. In addition, it is frequently difficult to determine accurate values of  $q_d$ ,  $d_s$ , and  $k_s$  to use in Eq. 6A.128. Hence, many engineers prefer to use reduced values of  $c_h$ .

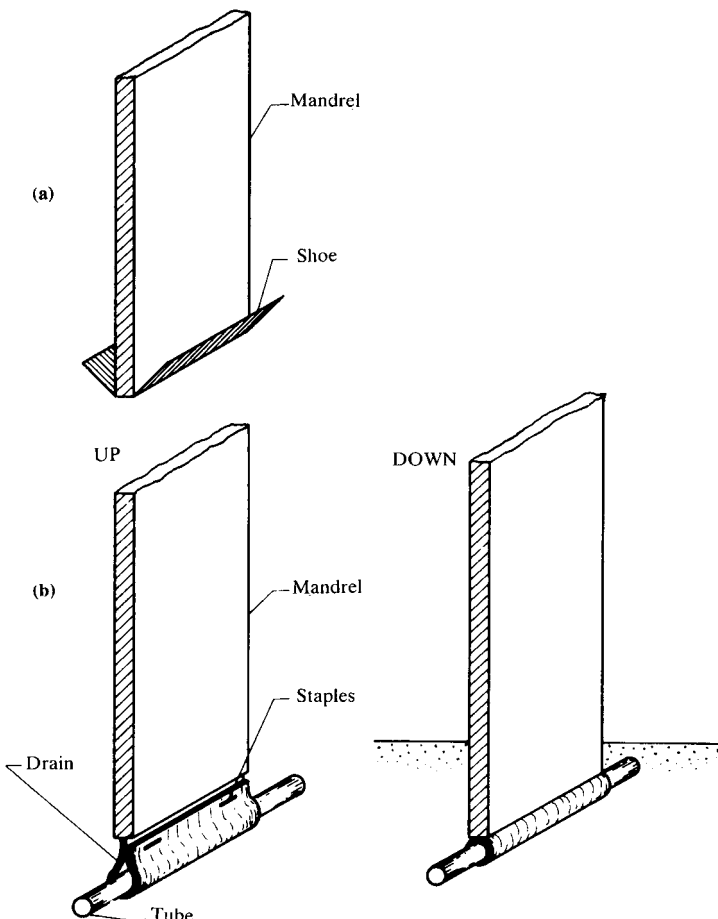


**FIGURE 6A.199** Typical detachable shoes used with mandrels for band-shaped PV drains (from Holtz et al., 1991).

$d_d$  or both in the simpler Eq. 6A.126 to account for the possible negative effects of these phenomena.

Buckling and kinking of PV drains has been observed in the laboratory and the field. It is very difficult to predict when and where these phenomena will occur, and if they do occur, how they will affect the discharge capacity of the drains.

In a typical design situation, the engineer must determine the required spacing of vertical drains to achieve a specified degree of consolidation (usually 90 or 95%) within a certain amount of time usually dictated by various aspects of the construction process. If vertical consolidation is ignored, which is sometimes done to be conservative, either Eq. 6A.126 or 6A.128 can be used in a trial and error process to find the appropriate spacing. In this iterative process, a spacing is assumed for the pattern of the wick drains to be used, and the corresponding value of  $d_c$  is calculated. Then, using Eq. 6A.126 or 6A.128, a corresponding value of  $U_r$  is calculated. If the calculated value of  $U_r$  is not equal to the desired value of  $U_r$ , the process is repeated until the calculated and desired values are the same.

## 6.270 SOIL IMPROVEMENT AND STABILIZATION

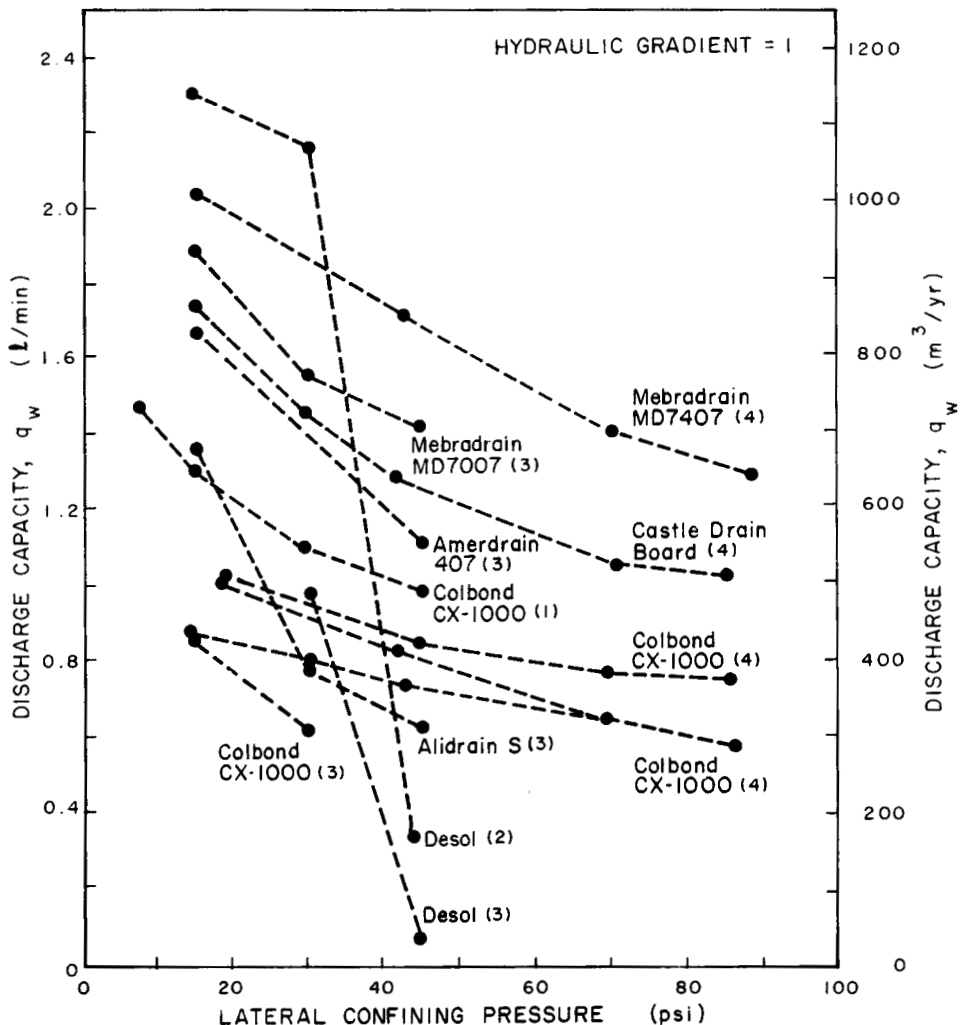


**FIGURE 6A.200** Effect of confining pressure on vertical discharge capacity of some typical PV drains (from Rixner et al. 1986). Note: Data from sources other than (3) not verified. Test methods vary. Data Sources: (1) Colbond promotional literature; (2) Desol internal report; (3) Reference 8; (4) Jamiolkowski and Lancellotta, unpublished.

If both vertical and radial drainage are considered, the combined degree of consolidation ( $U_{vr}$ ) can be found from the following equation (Carillo 1942):

$$U_{vr} = 1 - (1 - U_v)(1 - U_r) \quad (6A.6.132a)$$

A trial and error process is also required to determine the required spacing of the vertical drains for combined drainage. First,  $U_v$  is calculated for the desired time ( $t$ ) from Eq. 6A.118. Next, the re-

quired value of  $U_r$  to provide the desired value of  $U_{vr}$  is determined by rearranging Eq. 6A.6.132a to solve for  $U_r$ :

$$U_r = 1 - \frac{1 - U_{vr}}{1 - U_v} \quad (6A.6.132b)$$

A trial and error process similar to that described above for radial drainage only is then used to determine the spacing of drains that will give the value of  $U_r$  obtained from Eq. 6A.132b in time  $t$ .

It is important to note that the values of consolidation ratio calculated for  $U_v$ ,  $U_r$ , and  $U_{vr}$  are not the portion of the ultimate primary consolidation settlement that will occur in time  $t$ . Instead, these values are the average degree of dissipation of excess pore pressure within the clay layer.

#### **6A.6.5 Strength Considerations**

Since precompression is typically conducted on soft, saturated clays, and the preloads can be large, strength is an important consideration in the process. In the short-term, large positive excess pore water pressures can be generated that may lead to bearing capacity failure or large deformations near the perimeter of the preloaded area. As the excess pore water pressures dissipate and primary consolidation occurs, the soil becomes stronger. Therefore, potential strength problems can be alleviated by preloading in stages, where a portion of the total preload is applied and allowed to consolidate some prior to the application of additional preload. Vertical drains can also be used to accelerate the consolidation process, and hence the strengthening process. Sand drains, gravel drains, or other granular columns can also provide an increase in strength and reduction in vertical and lateral deformations (see Section 6A.5).

#### **6A.6.6 Monitoring Field Performance**

The performance of the precompression in the field should always be monitored. The deformations of the soil (settlement and horizontal movement) should be determined, as well as the pore water pressures in the soil if it is saturated and fine-grained. Settlement is usually monitored using settlement plates, gauges, and leveling points. The horizontal movements are monitored using alignment stakes and vertical inclinometers. Pore water pressures are monitored using piezometers. Details on the instrumentation and monitoring of the preloading process can be found in many references (e.g., Hanna 1973 and Mitchell 1981). Variations in performance can be determined and adjustments made, as necessary, to the time required to leave the surcharge in place, the magnitude of the preload, or any other aspects of the preloading process.

#### **6A.7 CHEMICAL STABILIZATION\***

The mechanical properties of a soil can be improved by chemical stabilization, which involves the injection or mixing of a chemical agent or agents into the soil. Chemical stabilization can be used on in situ soils or on borrow or excavated materials prior to compaction. The two most common types of chemical reactions used to stabilize soils are cation or base exchange reactions with clay particles and cementitious or pozzolanic reactions. Commonly used chemical agents for cementitious and pozzolanic stabilization include Portland cement, lime, fly ash, sodium silicate, polyacrylamides, and bituminous emulsions. Chemicals used for base exchange include inorganic cations

---

\*Coauthored by Robert Wade Brown.

**6.272 SOIL IMPROVEMENT AND STABILIZATION**

such as  $\text{Ca}^{2+}$  and organic products such as polyquaternaryamines. Engineering properties of a soil that may be intentionally altered during chemical stabilization, or that may occur as a by-product of the stabilization process, include the following:

1. Strength
2. Compressibility
3. Permeability
4. Expansiveness
5. Collapsibility
6. Potential for liquefaction
7. Erodability

Because of environmental concerns and regulations, an engineer must consider the potentially adverse impact that chemical stabilization may have on the soil and local groundwater. Before any chemical stabilization is conducted, the appropriate local, state, and federal environmental regulatory agencies should be consulted to ensure that the chemicals to be used are not prohibited.

**6A.7.1 Chemicals and Reactions**

This section discusses chemicals that are commonly used to stabilize soils, along with the reactions that may occur and the manner in which the chemicals stabilize the soil.

***6A.7.1.1 Cation and Base Exchange with Clay Particles***

*Clay Mineralogy, Clay-Water Interaction, and Cation Exchange.* The near-surface clay minerals are basically composed of various hydrated oxides of silicon, aluminum, iron, and to a lesser extent potassium, sodium, calcium, and magnesium (Brown, 1992). Since clays are produced from the weathering of certain rocks, the particular origin of a clay determines its nature and properties. Chemical elements present in a clay are aligned or combined in a specific geometric pattern referred to as structural or crystalline lattice, which is generally sheetlike in appearance. This structure, coupled with ionic substitution, accounts principally for both the various clay classifications and their specific physical and chemical behavior.

Owing to their loose crystalline structure, most clays exhibit the properties of ion exchange and moisture absorption and adsorption. Among the more common clays, the activity of the clays—defined in general terms as the capacity for electrochemical interaction with water and chemicals in the soil—decreases in the following order: montmorillonite, illite, attapulgite, chlorite, and kaolinite. A specific clay may adsorb and absorb water to varying degrees—from a single layer to six or more layers—depending on such factors as its structural lattice, presence of exchange ions, temperature, and environment. The moisture taken on by a clay may be described as one of three basic forms: interstitial or pore water, surface adsorbed water, or crystalline interlayer water. This combined moisture accounts for the differential movement (e.g., swelling and shrinkage) problems encountered with expansive soils. If this movement is to be controlled, each of these forms of moisture must be controlled and stabilized.

Interstitial water and surface adsorbed water both occur within the soil mass external to individual soil grains and are generally accepted as capillary moisture. The interstitial water is held by interfacial tension, whereas the surface adsorbed water is held by molecular attraction between the clay particles and the dipolar water molecules. Variations in this combined moisture are believed to account for the principal volume change potential of the soil (see also Sec. 1).

Interlayer moisture is the water situated within the crystalline layers of the clay. The amount of this water that can be accommodated by a particular clay depends on three primary factors: crystalline spacing, elements present in the crystalline structure, and presence of exchange ions. For example, bentonite (sodium montmorillonite) will swell approximately thirteen times its original vol-

ume when saturated in fresh water. If the same clay is added to water containing sodium chloride ( $\text{NaCl}$ ), the expansion is reduced to about threefold. If the bentonite is added to a calcium hydroxide [ $\text{Ca}(\text{OH})_2$ ] solution, the expansion is suppressed even further, to less than twofold. This reduction in swelling is produced principally by ion exchange within the crystalline lattice of the clay. The absorbed sodium ions ( $\text{Na}^+$ ) or calcium ions ( $\text{Ca}^{2+}$ ) limit the space available to the water and cause the clay lattice to collapse and further decrease the capacity.

As a rule (and as indicated by the preceding example), the divalent cations such as  $\text{Ca}^{2+}$  produce a greater collapse of the lattice than the monovalent ions such as  $\text{Na}^+$ . Exceptions to this rule may be found with potassium ( $\text{K}^+$ ) and hydrogen ( $\text{H}^+$ ) ions. The potassium ion, owing to its atomic size, is believed to fit almost exactly within the cavity on the oxygen layer. Consequently, the structural layers of the clay are held more closely and more firmly together. As a result, the  $\text{K}^+$  becomes abnormally difficult to replace by other exchange ions.

The hydrogen ion, for the most part, behaves like a divalent or trivalent ion, probably because of its relatively high bonding energy. Therefore, in most cases the presence of  $\text{H}^+$  interferes with the cation exchange capacity of most clays. This has been verified by several authorities. Orcutt and coworkers (1955) showed that sorption of  $\text{Ca}^{2+}$  by halloysite was increased by a factor of 9 as the pH was increased from 2 to 7. Although these data are limited and qualitative, they are sufficient to establish a trend. Grim (1953, 1962) indicated that this trend would be expected to continue to a pH range of 10 or higher. Stabilization of clays with cement or lime represents one condition in which clays are subjected to  $\text{Ca}^{2+}$  at high pH (see Secs. 6A.7.1.2 and 6A.7.1.3). Under any conditions, as the concentration of exchanged ions within the clay increases, the capacity of a soil for ion exchange decreases, and hence the potential for moisture sorption and desorption (swelling/shrinkage) also decreases.

The preceding discussions have referred to changes in the potential for volumetric expansion caused by induced cation exchange. In nature, various degrees of exchange preexist, giving rise to widely variant soil behavior even among soils containing the same type and amount of clay. For example, soils containing  $\text{Na}^+$  substituted montmorillonite will be more volatile (expansive) than will soils containing montmorillonite with equivalent substitution of  $\text{Ca}^{2+}$  or  $\text{Fe}^{3+}$ .

To this point, the discussion has been limited to inorganic ion exchange. However, available data suggest that organic ion adsorption might have even more practical importance to construction problems (McLaughlin et al., 1976). The exchange mechanism for organic ions is basically identical to that discussed above except that, in all probability, more organic sorption occurs on the surface of the clays than in the interlayers, and once attached is more difficult to exchange. Giesecking (1939) reported that montmorillonitic clays lost or reduced their tendency to swell in water when treated with several selected organic cations. The surface that surrounds the clay platelets can be removed or reduced by certain organic chemicals. When this layer shrinks, the clay particles tend to pull closer together (flocculate) and create macropores or shrinkage cracks (fractures in the macrofabric). The effect of this cracking is to increase the permeability of the soil (Foreman and Daniel, 1986), which can be helpful to reduce runoff and ponding and to facilitate penetration by chemicals for stabilization. The extent of these benefits would depend on the performance of the specific chemical product. From a broad viewpoint, certain chemical qualities—such as high pH, high OH substitution, low ionic radii, high molecular size, high polarity, high valence (cationic), and highly polar vehicles—tend to help stabilize active clays. Examples of organic chemicals that possess a combination of these features include polyacrylamides, polyvinylalcohols, polyglycolethers, polyamines, polyquaternaryamines, pyridine, collidine, and certain salts of each.

Because none of the organic chemicals listed above possess all the desired qualities, they are often blended with other additives to enhance their performance. For example, the desired pH can be attained by the addition of hydrated lime [ $\text{Ca}(\text{OH})_2$ ], hydrochloric acid (HCl), or acetic acid ( $\text{C}_2\text{H}_3\text{OOH}$ ); the polar vehicle is generally satisfied by dilution with water; high molecular size can be accomplished by polymerization; and surfactants can be used to improve penetration of the chemical through the soil. Additional details concerning the chemical reactions of base exchange in montmorillonite are given in the next two sections.

Organic chemicals generally can be formulated to be far superior to lime with respect to stabi-

**6.274** SOIL IMPROVEMENT AND STABILIZATION

lization of clay. The organic products can be rendered soluble in water for easy introduction into the soil. Chemical characteristics can be more finitely controlled, and the stabilization process is more nearly permanent. About the only advantages lime has over specific organics, at present time, are lower treatment cost, more widespread usage (general knowledge), and greater availability.

*Chemistry of Cation Exchange.* The chemistry of cation exchange and moisture capacity within a particular clay is neither exact nor predictable. A given clay under seemingly identical circumstances will often indicate variations in cation exchange, as well as the extent to which a particular cation is exchanged. The specifics with this exchange capacity dictate the affinity for water and bonding to the structure of the clay.

*Chemical Bonding in Cation Exchange.* The principal conditions that create the affinity of a clay to cation bonding include the following:

1. *Broken bonds around the edges of the silica-alumina units.* These broken bonds give rise to unsatisfied negative charges that can be balanced by adsorbed cations. In montmorillonite, this accounts for about 20% of the cation exchange capacity.
2. *Substitutions of cations within the crystalline lattice.* Examples include  $\text{Al}^{3+}$  for  $\text{Si}^{4+}$  in the tetrahedral sheet, and ions of lower valence, particularly  $\text{Mg}^{2+}$  for  $\text{Al}^{3+}$ , in the octahedral sheet. The latter substitution results in unbalanced negative charges within the structural units of the clay (see Fig. 6A.201). These exchanges account for about 80% of the total cation exchange capacity of montmorillonite.
3. *Hydrogens of exposed hydroxyl groups that are replaced by exchangeable cations.* There is some doubt that this occurrence is substantial in the cation exchange reaction, since it seems that the hydrogen bond to the hydroxyl group would resist the exchange reaction (Grim 1962).

A simplified relationship between the exchanged cation and the substituted cation, as well as that relationship to adsorbed water, is also shown in Fig. 6A.201. Water held directly on the surface of the unit is in a physical state different from liquid water. Generally, the thickness of the nonliquid layer is restricted to 3 to 10 molecular layers of interlayer water (Brown, 1989).

The manner in which adsorbed ions on the surface of clay affect the adsorption of water can be described in simple terms as follows:

1. Adsorbed ions may serve as a bond to hold the clay mineral units together or limit the distance over which they can be separated. Either phenomenon would resist the intrusion of water.
2. The adsorbed cations may become hydrated (that is, develop an envelope of water molecules), and then might either interfere with or influence the configuration of adjacent adsorbed water molecules.
3. The size and geometry of the adsorbed ion may influence the manner in which it fits into the configuration of the adsorbed water molecules. This would thereby influence the nature of the configuration of the adsorbed water molecules and the extent to which the configuration could develop.

Hence it follows that the type of bonding (or the energy required to break this bond) suggests the ease by which water can be removed or exchanged from the clay. Temperature is generally the source of that energy. Water lost at various levels of temperature can be categorized as (a) water in the pores (interstitial), on the surface, and on the surface and around the edges of the clay mineral particles (surface adsorbed); (b) interlayer water between the unit-cell layers of the minerals; and (c) the water that occurs within the tubular openings between elongated structural units (sepiolite, attapulgite, polygorskite). Type *a* water is easily removed, substantially in its entirety, with little energy such as drying at slightly above room temperature. Types *b* and *c* water require definite energy for their removal. Specifically, in the case of montmorillonite, temperatures in the range of about 100°C (212°F) are required for the removal of interlayer water. Some clay minerals—montmorillonite in particular—rehydrate with great difficulty if the dehydration is absolutely complete but with great ease if only trace amounts of water remain between unit layers.

The amount of energy required to liberate a water molecule depends on the strength of the bond

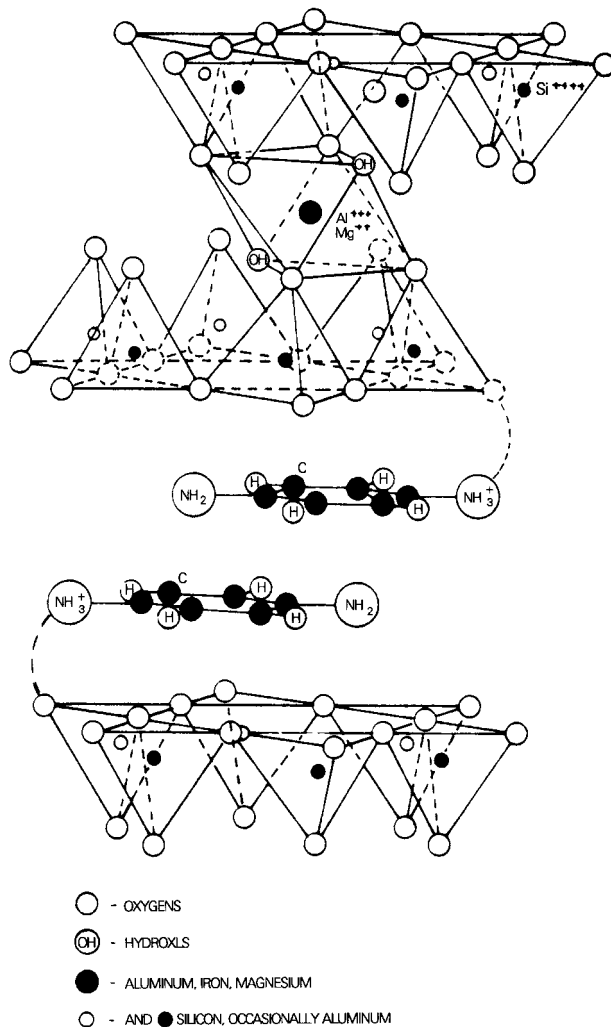


**FIGURE 6A.201** Cationic substitution within clay crystalline structure (from Brown, 1992).

between that molecule and the clay particle. These bonds typically involve intermolecular electrostatic forces rather than the more conventional ionic or covalent bonds. [Ionic bonds (typical of salts) result from the complete transfer of electrons. Covalent bonds result from the sharing of a pair of electrons, one supplied by each atom forming the bond. (Shared electrons must be of opposite spin.)] The electrostatic (coulombic) forces generally develop from some variation of hydrogen bonding, ion-dipole attraction, or dipole-dipole attraction. A dipole is said to exist when two equal and opposite charges are separated in space. In a pictorial representation (see Fig. 6A.202), one end of the molecule bears a partial negative charge whereas the other end has a positive charge of equal value. Molecular shapes plays an important role in determining polarity, as bond polarity alone does

**6.276** SOIL IMPROVEMENT AND STABILIZATION

not necessarily lead to a polar molecule. It is entirely possible for a molecule to contain polar bonds but for the entire molecule to be nonpolar, as is the case for CO<sub>2</sub>. The two C–O bond dipoles in the linear CO<sub>2</sub> molecule cancel each other, and therefore their combined effects cancel. Hydrogen bonding is an exceptionally strong dipole-dipole attraction and results from the situation where a hydrogen atom serves as a bridge between two electronegative atoms. The hydrogen is held by a rather strong covalent bond (about 75 to 100 kcal/mol depending on the electronegative atom) and by a hydrogen bond (4 to 10 kcal/mol) of purely electrostatic forces. For hydrogen bonding to become predominate, both electronegative atoms must come from the group F, O, or N (Fig. 6A.202).

In the absence of a true dipole moment, electrons in constant movement can, at any instant, exist in an unequal distribution, thus creating in effect a net dipole. The electrostatic forces so produced are referred to as van der Waals forces. The larger the molecule, the stronger the van der Waals forces. This, at least in part, gives rise to the organic treatment or modification of clay.

*Organic Modification of Clay.* Many clay units have a natural attraction to specific organic ions through van der Waals and coulombic forces. Larger organic ions are difficult, if not impossible, to replace by smaller ions owing to the intensity of the van der Waals forces. Furthermore, whereas smaller ions are absorbed only up to the exchange capacity, larger ions may be absorbed to a greater extent and are not disassociated.

The dipolar nature of water (plus its capacity for hydrogen bonding) makes it an excellent vehicle for the implementation of cation exchange or organic modification. The most important reactions for modification of clays include absorption, cation exchange, and interlocation (Evans and Pancoski, 1989). Interlocation refers to the process of absorption owing to the pillaring of clay. Pillaring is the process whereby the clay platelets are forced apart, thereby creating greater porosity. Both effects provide greater access to the surface for organic cations to replace exchangeable inorganic cations (see Fig. 6A.203). The organic cations are more restrictive to the inclusion of water than are the inorganic cations. In fact, the organically modified clays become organophilic (hydrophobic) rather than hydrophilic when treated with long-chain organic amines. The structure of smectite modified by an organic amine is depicted in Fig. 6A.203.

In addition to the foregoing, many organic chemicals tend to shrink the double diffuse layer that surrounds the clay particles, causing the clay particles to flocculate and the soil skeleton to shrink. The net result is the formation of cracks referred to as syneresis cracks. The combination of these effects, coupled with attendant desiccation, increases the permeability of the clay (Broderick and Daniel, 1990). The exposure of greater surface area may further facilitate the base exchange of certain organic molecules (Jordan, 1949).

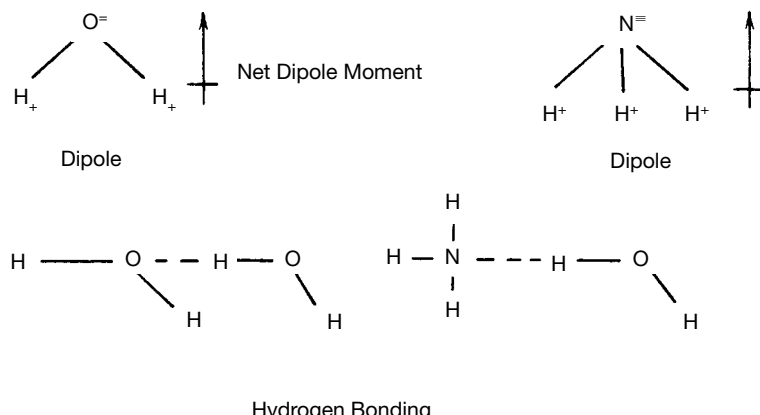


**FIGURE 6A.202** Dipole moments and hydrogen bonding (from Brown, 1992).

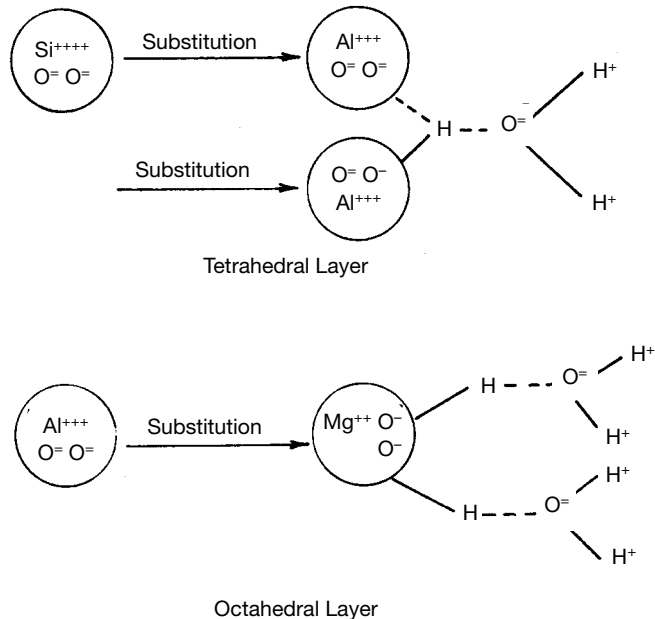


**FIGURE 6A.203** Structure of organically modified smectite layers (from Grim, 1968).

#### 6A.7.1.2 Cement

The most common application of cement-stabilized soils is for roadway and airfield pavement systems, but cement stabilization has also been used successfully in many other types of applications, including the following:

1. Strengthening and stiffening bearing soils to support structures by the overexcavation/replacement method (Sec. 6A.2)
2. Reducing the potential for swelling and shrinkage in expansive soils
3. Reducing the potential for liquefaction in liquefiable sand and silty sand deposits
4. Slope protection (erosion control) for embankments, dams, canals, reservoirs, etc.
5. Strengthening of embankment materials to allow steeper side slopes
6. Repairs of failed slopes

Except for grouting techniques, which are discussed in Sec. 6B, cement stabilization is achieved by wetting or drying the soil to an appropriate moisture condition, mixing the cement into the soil, and compacting the stabilized soil into place. The soil to be stabilized may be either an *in situ* soil that is excavated and replaced in the same location or a borrow material that is used in a fill.

Cement can be used to stabilize all types of soils except organic soils containing more than about 1 to 2% organic matter (Ingles and Metcalf, 1973). Fat (highly plastic) clays are difficult to stabilize with cement for two reasons: (a) It is difficult to mix the cement into the clay in the field, and (b) high percentages of cement are required to effect a significant change in engineering properties. Pretreatment of fat clays with a small percentage (2 to 3%) of either hydrated lime or cement is a common method used to overcome these difficulties. The pretreatment, also called *modification*, reduces the plasticity of the soil and renders the soil more workable. After a curing period of 1 to 3

**6.278** SOIL IMPROVEMENT AND STABILIZATION

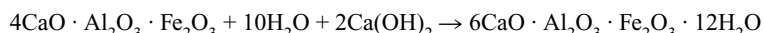
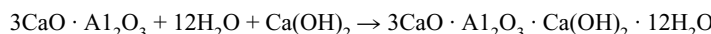
days, the modified soil is stabilized with cement in the usual way. Certain salt solutions, especially sulfates, can disrupt the structure of the cement and thus reduce the effectiveness of the cement. This problem can be overcome in most cases by increasing the cement content. Some salts, if present in the soil-cement mixture at the time the cementitious reactions occur, may have a beneficial effect (e.g., Lambe et al., 1960).

Portland cement, because it is readily available and is relatively inexpensive, is the most widely used type of cement for stabilizing soils, but any type of cement may be used. Ordinary Portland cement (type I) and air-entraining cement (type IA) have been used extensively and have given about the same results (Little et al., 1987). Type II cement, because of its greater resistance to sulfates, has been used more frequently in recent years. High early strength cement (type III) has produced higher strengths in some soils. Subsequent discussions about cement will be limited to Portland cement, because it is used predominantly in stabilizing soils.

Portland cements are hydraulic cements—that is, they set and harden by reacting with water (hydration). The four principal compounds in Portland cement are the following (PCA, 1968):

Name of compound	Chemical formula	Abbreviation
Tricalcium silicate	$3\text{CaO} \cdot \text{SiO}_2$	$\text{C}_3\text{S}$
Dicalcium silicate	$2\text{CaO} \cdot \text{SiO}_2$	$\text{C}_2\text{S}$
Tricalcium aluminate	$3\text{CaO} \cdot \text{Al}_2\text{O}_3$	$\text{C}_3\text{A}$
Terracalcium aluminoferrite	$4\text{CaO} \cdot \text{Al}_2\text{O}_3 \cdot \text{Fe}_2\text{O}_3$	$\text{C}_4\text{AF}$

The primary reactions that occur when water is added to Portland cement can be summarized as follows:



where  $\text{CaO}_2 \cdot \text{SiO}_2 \cdot 3\text{H}_2\text{O}$  = calcium silicate hydrate (tobermorite gel)

$\text{Ca}(\text{OH})_2$  = calcium hydroxide (hydrated lime)

$\text{CaO} \cdot \text{Al}_2\text{O}_3 \cdot \text{Ca}(\text{OH})_2 \cdot 12\text{H}_2\text{O}$  = calcium aluminate hydrate

$\text{CaO} \cdot \text{Al}_2\text{O}_3 \cdot \text{Fe}_2\text{O}_3 \cdot 12\text{H}_2\text{O}$  = calcium aluminoferrite hydrate

$\text{C}_3\text{S}$  hardens quickly and is primarily responsible for initial set and early strength.  $\text{C}_2\text{S}$  hardens slowly and contributes mainly to strength increase at ages beyond 1 week.  $\text{C}_3\text{A}$  liberates a large amount of heat during the first few days of hardening and contributes slightly to early strength development. Sulfate-resistant cements have less than 8% of  $\text{C}_3\text{A}$ . The formation of  $\text{C}_4\text{AF}$  during manufacturing reduces the clinkering temperature and thus assists in the manufacturing process.  $\text{C}_4\text{AF}$  hydrates rather rapidly but contributes very little to strength. A detailed discussion on the chemistry, preparation, and properties of concrete can be found in Sec. 3A.

Unhydrated Portland cements contain particles in the range of 0.5 to 100  $\mu\text{m}$ , with a mean of about 20  $\mu\text{m}$  (Ingles and Metcalf, 1973). Calcium silicate hydrate (CSH), also known as *tobermorite*, is the predominant cementing compound in hydrated Portland cement. Although the specific surface of dry portland cement powder is only about  $0.3 \text{ m}^2/\text{g}$  ( $1460 \text{ ft}^2/\text{lb}$ ), the tobermorite gel after hydration has a specific surface of about  $300 \text{ m}^2/\text{g}$  ( $1.46 \times 10^6 \text{ ft}^2/\text{lb}$ ) (Little et al., 1987). In predominately coarse-grained soils, this large specific surface is responsible for the cementing action of cement pastes owing to adhesion forces to adjacent surfaces of particles. In fine-grained soils, the clay phase may also contribute to the stabilization through solution in the high-pH envi-

ronment and reaction with free lime from the cement to form additional CSH. The crystallization structure formed by the hardened cement is primarily extraneous to the soil particles. This structure can be disrupted by subsequent swelling of soil particle groups (clods) if insufficient cement is used.

The amount of cement needed for treatment depends on the type of soil being treated and the intended use and desired engineering characteristics of the treated soil. The extent of treatment can be classified by two general categories—modification and stabilization. *Modification* occurs when a low percentage of cement is incorporated within a soil that improves its workability owing to a reduction in plasticity and an agglomeration of particles. If a high percentage of cement is mixed with the soil, the surface molecular properties of the soil are changed and the grains are cemented together. Typical values of cement content used to stabilize soils according to their AASHTO and USCS group symbols are given in Table 6A.19, which can be used as a general guideline to estimate the amount of cement that may be required to stabilize a particular soil.

As a general rule, the cement requirement increases as the fine-grained fraction increases. The one exception to this rule is that poorly graded (uniform) sands require more cement than sandy soils containing some silt and clay.

The actual proportion of cement to be used on any particular project should be determined from an appropriate mixture design evaluation. The mixture design procedure typically consists of Proctor tests on the cement-stabilized soil to determine the approximate optimum water content and maximum dry density for either standard or modified energy, followed by a series of laboratory tests on cement-stabilized specimens with varying cement contents to determine the minimum cement content that will achieve the desired engineering properties. For example, if strength is the primary requirement, the general procedures for a typical mixture design would be as follows:

1. Establish a minimum desired strength based on rational engineering procedures. In soil–cement applications, the minimum strength is typically specified as unconfined compressive strength. In applications where the cement-stabilized soil will be subjected to significant confining pressures, it is more appropriate to specify strength in terms of friction angle and cohesion intercept determined by triaxial or other appropriate strength tests.
2. Estimate the required cement content based on personal experience or guidelines provided by others (such as Table 6A.19).
3. Conduct a series of Proctor tests on the cement-stabilized soil at three cement contents—the estimated value from step 2 and one value above and one value below the estimated value. It is com-

**TABLE 6A.19** Typical Cement Requirements According to AASHTO and USCS Soil Groups

AASHTO group symbol	Corresponding USCS group symbols*	Usual range in cement requirement†	
		Percent by volume	Percent by weight
A-1-a	GW, GP, GM, SW, SP, SM	5 to 7	3 to 5
A-1-b	GM, GP, SM, SP	7 to 9	5 to 8
A-2	GM, GC, SM, SC	7 to 10	5 to 9
A-3	SP	8 to 12	7 to 11
A-4	ML, CL-ML	8 to 12	7 to 12
A-5	ML, MH, CH	8 to 12	8 to 13
A-6	CL, CH	10 to 14	9 to 15
A-7	OH, MH, CH	10 to 14	10 to 16

\*Based on correlation presented by Air Force.

†For most *A* horizon soils, the cement content should be increased by 4 percentage points if the soil is dark gray to gray, and by 6 percentage points if the soil is black.

**6.280** SOIL IMPROVEMENT AND STABILIZATION

mon practice to use 1% increments for estimated cement contents of 5% or less and 2% increments for estimated cement contents of 6% or more. As an illustration, if the estimated cement content is 8%, the Proctor tests typically would be conducted at cement contents of 6, 8, and 10%. Determine the optimum water content and maximum dry density for each of the three cement contents.

4. Perform a series of unconfined compression tests on specimens compacted at the corresponding optimum water content to the corresponding maximum dry density for each of the three cement contents used in step 3. Cement-stabilized specimens are generally stored (cured) at room temperature in a relative humidity of approximately 100% for periods of 2, 7, and 28 days and then immersed in water for 4 h prior to testing (see ASTM D1632 and D1633). Usually at least three replicate specimens are tested for each cement content and curing period.
5. Three situations are possible depending on how the measured values of strength obtained in step 4 compare with the specified minimum value developed in step 1.
  - a. The measured values of unconfined compressive strength at the three cement contents are both above and below the specified minimum value. The actual (design) cement content to be used can be determined as the lowest cement content that yields strengths greater than or equal to the minimum desired value. In cases where a small difference in cement content would significantly affect the economics of the project, steps 2 and 3 could be repeated at intermediate cement contents to better establish the most economical cement content for the desired strength characteristics.
  - b. The measured values of strength at all three cement contents are less than the specified minimum value. Repeat steps 2 to 4 at three cement contents higher than the previous maximum value.
  - c. The measured values of strength at all three cement contents are greater than the specified minimum value. Repeat steps 2 to 4 at three cement contents lower than the previous minimum value.
6. Additional testing can be conducted to determine if other important engineering characteristics are met for the preliminary design cement content established in steps 2 through 5. If the other criteria are met, the preliminary design cement content is the final design cement content. If not, the final design cement content is determined based on the results of the additional tests, ensuring that the strength requirement is also met. For example, in soil-cement applications in pavement systems, wet-dry and freeze-thaw tests (ASTM D559 and D560) are also conducted. In applications for building foundations, compressibility and liquefaction resistance are also important engineering properties.

The presence of organic material or sulfates in a soil may inhibit the proper hydration of the cement. Organics with low molecular weights, such as nucleic acid and dextrose, retard hydration and reduce strength (Clare and Sherwood, 1954). Certain types of organics, such as undecomposed vegetation, may not adversely affect cement stabilization. For situations where organics are present in the soil, Little and coworkers (1987) recommend conducting a pH test on a 10:1 mixture (by weight) of soil and cement. If the pH of the soil-cement 15 min after mixing is at least 12.1, the organic content probably will not interfere with normal hardening. One method by which organics repress the hydration of cement is absorption of calcium ions liberated during the hydrolysis of the calcium silicates and aluminates in the cement grains (Clare and Sherwood, 1954, 1956). These ions are subsequently not available to form the compounds constituting the set cement matrix. The addition of a material with readily available calcium, such as calcium chloride ( $\text{CaCl}_2$ ) or hydrated lime, may satisfy the adsorptive capacity of the organic matter before hydration of the bulk of the cement has begun, thus enabling the soil to be successfully stabilized with cement. For the calcium additive to be effective, it must be present in a sufficient quantity to completely satisfy the adsorptive capacity of the organic matter, as illustrated by the following data from Clare and Sherwood (1956) for an otherwise clean silica sand stabilized with 10% ordinary Portland cement:

Additive (by weight of dry soil)	Unconfined compressive strength	
	psi	kPa
None (clean silica sand)	355	2450
0.01% tartaric acid	285	1970
0.02% tartaric acid	190	1310
0.03% tartaric acid	150	1030
0.04% tartaric acid	25	172
0.05% tartaric acid	10	69
0.10% tartaric acid + 0.25% calcium chloride	10	69
0.10% tartaric acid + 0.50% calcium chloride	10	69
0.10% tartaric acid + 1.00% calcium chloride	260	1793

Research by Sherwood (1962) has shown that the presence of sulfates can significantly affect the durability, integrity, and strength of cement-stabilized cohesive soils but has relatively little influence on cement-stabilized granular soils. These trends are illustrated in Fig. 6A.204, which shows how immersion in magnesium sulfate solutions of different concentrations affected the unconfined

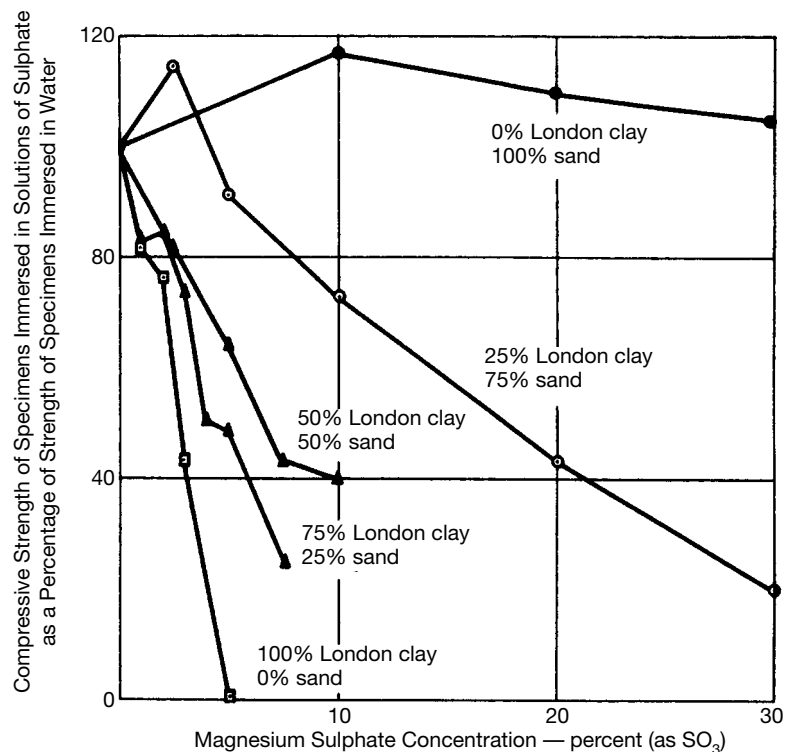


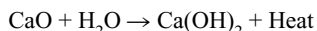
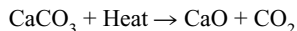
**FIGURE 6A.204** Effect of immersion in magnesium sulfate solution on the unconfined compressive strength of London clay-silica sand mixtures stabilized with 10% ordinary Portland cement (from Sherwood, 1962).

**6.282** SOIL IMPROVEMENT AND STABILIZATION

compressive strength of cement-stabilized specimens of London clay, silica sand, and various mixtures of the two soils. The presence of magnesium sulfate in the immersion water reduced the strength of all specimens containing London clay except one. In contrast, the strengths of the 100% silica sand specimens were somewhat greater when immersed in magnesium sulfate solutions than when immersed in water without magnesium sulfate. Note that 0.5% magnesium sulfate was sufficient to cause complete disintegration of the stabilized London clay. Similar trends were found for the same soils immersed in calcium sulfate solutions. Owing to the problems that sulfates can cause in cement-stabilized cohesive soils, Little and colleagues (1987) suggest that the use of cement be avoided for fine-grained soils containing more than about 1% sulfates.

**64.7.1.3 Lime**

Two types of lime are commonly used to stabilize cohesive soils—CaO (calcium oxide, also known as *quicklime*) and Ca(OH)<sub>2</sub> (calcium hydroxide, also referred to as *hydrated lime* or *construction lime*). Hydrated lime is the most frequently used lime product for soil stabilization in the United States, and quicklime is used more often in Europe (Bell, 1988). Both quicklime and hydrated lime are produced by burning limestone (CaCO<sub>3</sub>, calcium carbonate), as illustrated by the following reactions (Fox, 1968):



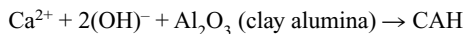
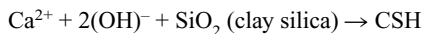
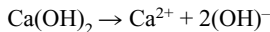
Less pure forms of lime are also sometimes used to stabilize soils. These alternate forms include monohydrated dolomitic lime [Ca(OH)<sub>2</sub> · MgO], dolomitic quicklime (CaO · MgO), and by-product limes (Little et al., 1987). Ground limestone (CaCO<sub>3</sub>), also known as *lime dust* or *agricultural lime*, is ineffective in chemically stabilizing soils but is sometimes used as a filler to increase the fines content of a soil, which modifies the gradation of the soil for better compaction and sometimes enhances stabilization by other chemicals.

Treatment with lime is generally effective in soils with plasticity indices in the range of 10 to 50 (Bell, 1988). Lime stabilization is typically ineffective in soils with little or no clay content because the primary improvements in engineering behavior are produced by reactions between the lime and the clay minerals. All clay minerals react with lime, with the strength of the reaction generally increasing in proportion to the amount of available silica. Thus, the three-layer clay minerals (e.g., montmorillonite, illite, chlorite) are more reactive than the two-layer clay minerals (e.g., kaolinite). The availability of the silica in the clay minerals is also important. Hence, illite and chlorite are much less reactive than montmorillonite because their silicas are bound to other silicas by ions that are not readily exchangeable.

Four basic types of reactions occur in cohesive soils treated with lime: (a) carbonation, (b) cation exchange, (c) flocculation-agglomeration, and (d) pozzolanic cementation. Carbonation occurs if carbon dioxide from the air or stagnant water gains entry into the lime-soil matrix and converts the lime back to calcium carbonate. Calcium carbonate is a weak cement because it is soluble in acidic water. Carbonation is undesirable because it reduces that amount of lime available to produce the primary cementitious reactions, which are pozzolanic. Carbonation can be prevented by using appropriate construction techniques.

Lime mixed with water results in free calcium cations that may replace other cations within the exchange complex of the soil. In some instances the exchange complex may be saturated with Ca<sup>2+</sup> before the addition of lime, yet cation exchange may still occur, since the capacity for cation exchange increases as the pH increases (TRB, 1987). Cation exchange is at least partially responsible for the flocculation and agglomeration of clay particles that occur in lime-treated soils (Herzog and Mitchell, 1963). The rapid formation of calcium aluminate hydrate cementing materials probably significantly assists in the flocculation-agglomeration process (Diamond & Kinter 1965). The net result of flocculation and agglomeration is a change in texture of the soil as the clay particles clump together into larger clods.

The pozzolanic reactions that occur in lime-treated soils, although not completely understood, are similar to those that occur in cement-treated soil (see Sec. 6A.7.1.2). We know that the lime and water react with silica and alumina in the soil to form various cementitious compounds (TRB, 1987). Typical sources of alumina and silica in soils include clay minerals, quartz, feldspars, micas, and similar silicate or alumino-silicate materials (either crystalline or amorphous). The addition of lime also raises the pH of the soil, which is beneficial because it increases the solubility of the silica and alumina present in the soil. If a significant amount of lime is added to the soil, the pH may reach 12.4, which is the pH of saturated lime water. The following is an oversimplification of the reactions that occur in a lime-treated soil (TRB, 1987):



where C = CaO

S = SiO<sub>2</sub>

A = Al<sub>2</sub>O<sub>3</sub>

H = H<sub>2</sub>O

These reactions occur only if water is present and able to bring Ca<sup>2+</sup> and (OH)<sup>-</sup> to the surfaces of the clay particles (that is, while the pH is still high) (Bell, 1988). Hence, the reactions will not occur in dry soils and will cease in a previously wet soil if it dries out. The primary characteristics of a soil that determine the effectiveness of lime treatment include the following (TRB, 1987):

1. Type and amount of clay minerals
2. Silica-alumina ratio
3. Silica-sesquioxide ratio
4. pH
5. Organic carbon content
6. Natural drainage
7. Degree of weathering
8. Presence of carbonates, sulfates, or both
9. Extractable iron

Caution is needed when one is considering lime stabilization of soils that contain sulfates and carbonates. Sherwood (1962) provided experimental results showing that lime-stabilized soils can be deleteriously affected by sulfates in a similar manner to cement-stabilized soils. A first set of experiments was conducted in which specimens of London clay were stabilized with 10% lime and cured at constant water content for 7 days. The specimens were then immersed in solutions of either sodium sulfate or magnesium sulfate at concentrations ranging from 0 to 1.5%. In all cases, the specimens immersed in the sulfate solutions cracked and swelled to the extent that they were too weak to be tested in unconfined compression. A second series of experiments was then performed in which varying amounts of calcium, sodium, and magnesium sulfates were mixed with the soil before adding 10% lime. Two sets of specimens were made for each sulfate concentration and were cured at constant moisture content. After 7 days of curing, one set of specimens was immersed in water while the other set was allowed to continue curing at constant moisture content. At the end of a second 7-day period, both sets of specimens were tested in unconfined compression. The following trends can be observed from the results of these tests, which are given in Fig. 6A.205.

## 6.284 SOIL IMPROVEMENT AND STABILIZATION

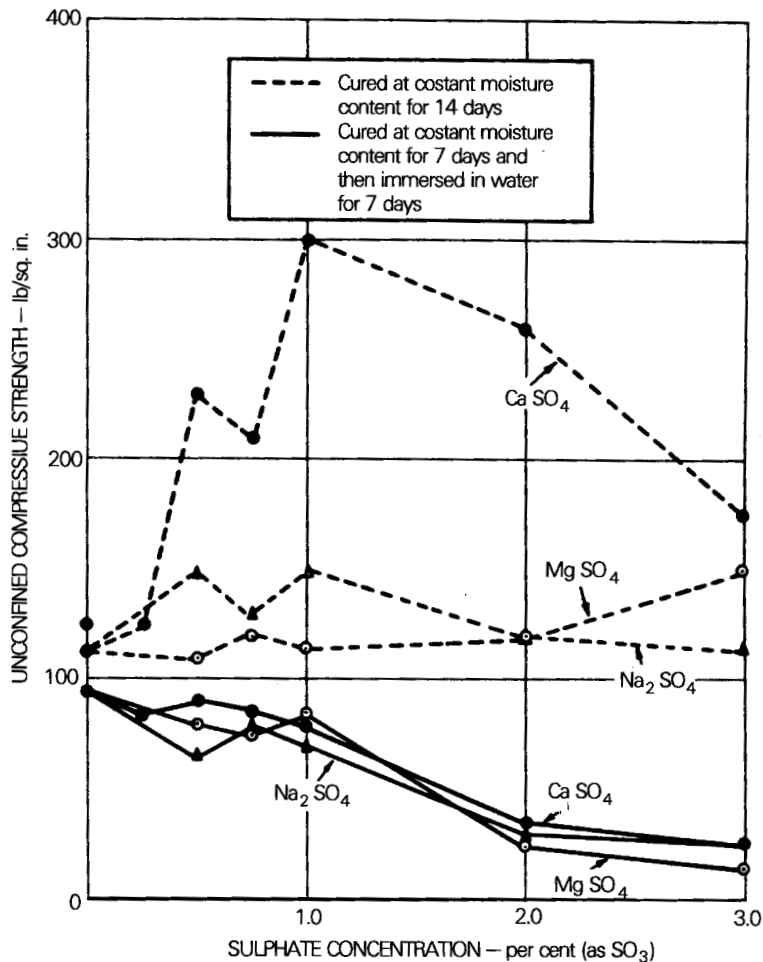


**FIGURE 6A.205** Influence of sulfates on the unconfined compressive strength of London clay stabilized with 10% hydrated lime (from Sherwood, 1962).

- For the specimens cured at constant moisture condition for 14 days, the calcium sulfate had a substantial beneficial effect, and the magnesium sulfate and sodium sulfate had no significant influence.
- All the immersed specimens containing sulfates swelled and cracked, resulting in a loss in strength, with a general trend of decreased strength with increased sulfate content. At the higher sulfate concentrations (2%), the losses in strength were considerable, ranging from about 65 to 85%.

Poststrength testing analyses of the 2% calcium sulfate specimens indicated that the calcium sulfate had reacted with the clay and that ettringite  $\{\text{Ca}_6 \cdot [\text{Al}(\text{OH})_6]_2 \cdot (\text{SO}_4)_3 \cdot 26\text{H}_2\text{O}\}$  had been formed as a result of the reaction. Ettringite is a very expansive material that is one of the materials responsible for the deterioration of concrete by sulfate attack.

Mitchell (1986) presented a case history in which the presence of sodium sulfate in the soil contributed to the failure of lime-stabilized subbases in Las Vegas, Nevada. The results of postmortem investigations that showed the effect of the sulfates can be summarized as follows:

1. The untreated soil contained up to 1.5% soluble sodium sulfate.
2. The lime-treated soil in the failed zones had swelled more than untreated soils also exposed to water.
3. Calcium silicate hydrates (CSH), the cementitious material produced during successful lime stabilization, were not found in specimens from the failed zones. This lack of cementation was attributed to the low pH of the treated soils (8 to 10.5), well below the minimum pH of 12.4 necessary for the pozzolanic reactions to occur.
4. Significant amounts of ettringite and thaumasite  $\{Ca_6 \cdot [Si(OH)_6]_2 \cdot (SO_4)_2 \cdot (CO_3)_2 \cdot 24H_2O\}$  were found in the failed zones. Thaumasite also is very expansive and is known to contribute to the deterioration of concrete by sulfate attack.
5. Negligible amounts of ettringite and thaumasite were found in treated samples from locations where failure had not occurred.

Owing to problems such as these, Mitchell (1986) recommended that lime stabilization not be used for soils containing more than 5000 ppm (0.5%) of soluble sulfates. Petry and Little (1992) indicated that the minimum level of sulfates that may represent potential problematic situations depends on the method used to extract the sulfates from the soil and may be as low as 500 ppm (0.05%) for 1:1 soil-to-water ratios to 2000 ppm (0.2%) for 1:10 soil-to-water ratios. Additional case histories in which sulfates in lime-treated soils resulted in swelling and structural damage to pavements related to the formation of ettringite and thaumasite can be found in Hunter (1988), Grubbs (1990), and Penn (1992). Hunter (1988) also provided a geochemical model for the formation of ettringite and thaumasite.

Note that lime stabilization in expansive soils with high sulfate contents is possible. This is confirmed by the fact that lime has been used successfully to stabilize sulfate-bearing soils in Texas for over 30 years (Petry and Little, 1992). Unfortunately, the construction and application techniques responsible for successful stabilization have yet to be identified. The following methods have been studied or are currently being evaluated as potential techniques to overcome the detrimental aspects of sulfates in lime-treated soils:

- Pretreatment of the soils with compounds of barium (Little and Deuel, 1989; Ferris et al., 1991).
- Double applications of lime
- Use of compounds to sustain high pH values and thus promote pozzolanic reactions
- Addition of materials to enhance pozzolanic reactions

The amount of lime needed for treatment depends on the characteristics of the soil being treated and the intended use and desired engineering characteristics of the treated soil. As with cement stabilization, the treatment of soils with lime can be divided into two general classes (Ingles and Metcalf, 1973): (a) modification, which reduces plasticity, improves workability, increases resistance to deflocculation and erosion, and produces a rapid increase in strength as a construction expedient and (b) stabilization, which provides permanent increases in strength and stiffness to increase bearing capacity, reduce settlement, and so on (Table 6A.20).

Several lime-soil mixture design methods have been developed. TRB (1987) summarizes eight procedures. These procedures are of two general types—those relating to soil modification and those pertaining to soil stabilization. The Illinois procedure will be summarized below to illustrate the basic concepts for both modification and stabilization (from TRB, 1987).

*Modification.* The mixture design procedure for modification is based on the effect that the lime has on the plasticity index (PI) of the soil. CBR testing can also be performed but is optional.

**6.286** SOIL IMPROVEMENT AND STABILIZATION**TABLE 6A.20** Typical range of hydrated lime content for modification and stabilization of various types of soils (from Ingles and Metcalf, 1973)

Type of soil	Typical range of hydrated lime content, % by dry weight of soil	
	Modification	Stabilization
Fine crushed rock*	2 to 4	Not recommended
Well-graded clayey gravels	1 to 3	Approximately 3
Sands†	Not recommended	Not recommended
Sandy clay	Not recommended	Approximately 5
Silty clay	1 to 3	2 to 4
Heavy clay	1 to 3	3 to 8
Very heavy clay	1 to 3	3 to 8
Organic soils	Not recommended	Not recommended

\*Lime only effective if fines are plastic.

†Lime used in bitumen stabilization for promoting adhesion; quicklime in loessial materials.

1. The liquid limit (LL), plastic limit (PL), and PI of the soil treated with various percentages of lime are determined. The soil-lime-water mixtures are loose-cured (conditioned) for 1 h before the LL and PL tests are conducted.
2. A plot is prepared of PI versus lime content. The design lime content may be based on one of the following criteria: (a) The lime content above which no additional appreciable reduction in PT occurs; or (b) the minimum lime content that produces an acceptable reduction in the PI.
3. If desired, CBR tests may also be performed to assess the stability or swelling potential of the soil, or both. Depending upon the objectives of the lime treatment, curing and soaking the CBR specimens before testing is optional. If the results of the CBR tests indicate that a higher lime content is required for successful modification, the design lime content is changed accordingly.
4. The design lime content for field construction is increased by 0.5 to 1% to offset the effects of variability in soil properties and construction procedures.

*Stabilization.* The mixture design procedure for stabilization is based on the results of unconfined compressive strength tests:

1. Standard Proctor tests (AASHTO T-99, ASTM D698) are conducted on the natural soil and soil-lime mixtures at various lime contents to determine the optimum water content and maximum dry density for the natural soil and each of the soil-lime mixtures.
2. Specimens 2 in (51 mm) in diameter and 4 in (102 mm) in height of the natural soil and soil-lime mixtures are prepared at the corresponding optimum water content and corresponding maximum dry density. The soil-lime mixtures are cured at 120°F (48.9°C) for 48 h before testing.
3. The unconfined compressive strength of the soil-lime mixture containing 3% lime must be at least 50 psi (345 kPa) greater than that of the natural soil. If not, the soil is considered unsuitable for lime stabilization. If the criterion for 3% lime is met, the design lime content is the value above which additional lime does not produce a significant increase in strength. Minimum strength requirements are 100 psi (690 kPa) for use as a subbase and 150 psi (1030 kPa) for use as a base course.
4. The design lime content for field construction is increased by 0.5 to 1% to offset the effects of variability in soil properties and construction procedures.

**TABLE 6A.21** Typical ranges in values for the chemical composition of fly ash (from NCHRP, 1976)

Principal constituent	Content by weight, %
SiO <sub>2</sub>	28 to 52
Al <sub>2</sub> O <sub>3</sub>	15 to 34
Fe <sub>2</sub> O <sub>3</sub>	3 to 26
CaO	1 to 40
MgO	0 to 10
SO <sub>3</sub>	0 to 4

combination with lime, cement, or both in soil stabilization, (d) as a fill material in the form of lime–fly ash-aggregate (LFA), cement-fly ash-aggregate (CFA), or lime-cement-fly ash-aggregate (LCFA) mixtures, and (e) as a drying agent to facilitate compaction of overly wet soils.

The chemical and physical properties of fly ash vary widely and depend primarily on the mineralogy and purity of the coal and the process and equipment used to burn the coal and recover the fly ash. Owing to variations in the properties of the coal burned at any power plant, fly ash within the same stockpiles can be quite heterogeneous. The primary chemical components of fly ash are silica (SiO<sub>2</sub>), alumina (Al<sub>2</sub>O<sub>3</sub>), ferric oxide (Fe<sub>2</sub>O<sub>3</sub>), and calcium oxide (CaO), and the secondary constituents include magnesium oxide (MgO), titanium oxide (TiO<sub>2</sub>), alkalies (Na<sub>2</sub>O and K<sub>2</sub>O), sulfur trioxide (SO<sub>3</sub>), phosphorous oxide (P<sub>2</sub>O<sub>5</sub>), and carbon (Hausmann, 1990). Typical chemical compositions and physical properties of fly ashes are given in Tables 6A.21 and 6A.22. Fly ash is classified as either class F (pozzolanic properties only) or class C (pozzolanic and some cementitious properties) depending primarily on its CaO content (ASTM C618). Type F fly ashes are generally produced by burning anthracite or bituminous coal, and type C fly ashes are normally derived from the combustion of subbituminous or lignite coal. In the United States, characteristics of the fly ashes from the major coal-producing regions can be broadly summarized as follows (Little et al., 1987; refer to Fig. 6A.206):

- Fly ashes from the bituminous coals of the Appalachian region generally behave as true Pozzolans, with little or no inherent cementitious properties.
- Fly ashes from the midcontinent coals, which are mostly bituminous, have some inherent cementitious properties owing to the CaO present in the ash.
- Fly ashes from the subbituminous and lignite coals of the northern and western plains states have a high natural CaO content and are highly cementitious even without the addition of lime.

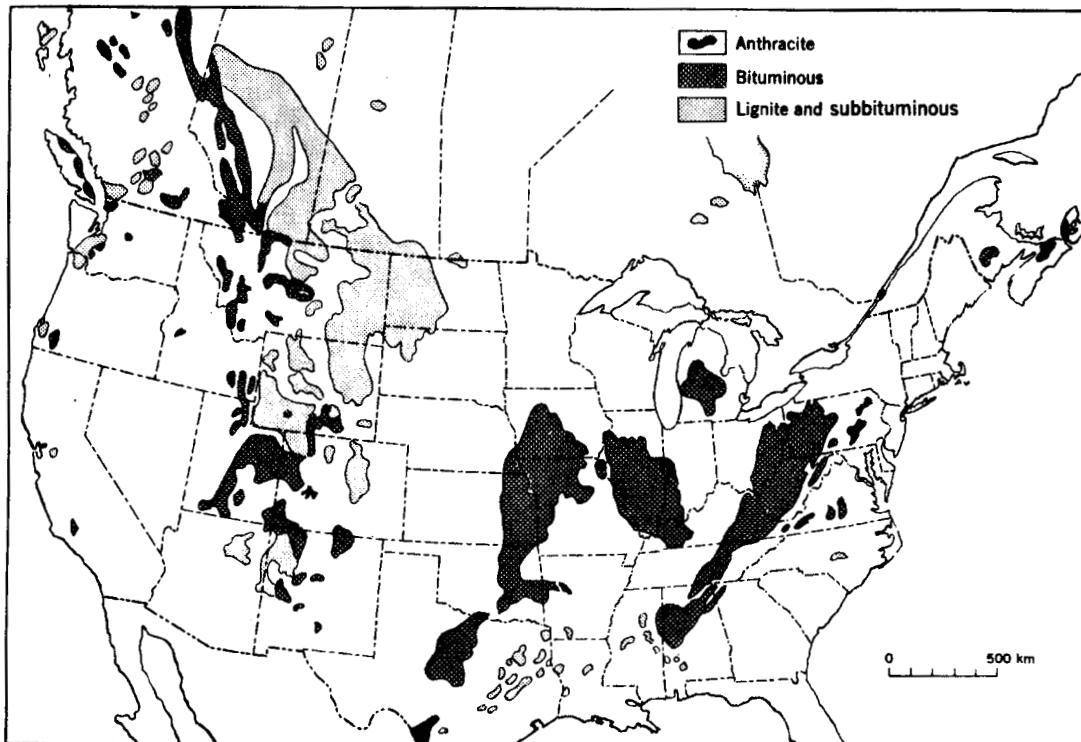
Several kinds of chemical reactions occur in naturally cementitious fly ash and lime–fly ash mixtures. These reactions are complex, owing in part to the heterogeneous nature of fly ash and have not been completely defined. The principal cementitious reactions are similar to those that

**TABLE 6A.22** Typical physical properties for fly ash (from NCHRP, 1976)

Property	Description or typical range in values
Color	Usually light gray, but can vary from light tan through black
Shape	Spherical, solid, or hollow
Glass content (amorphous material)	71 to 88%
Size	1 to 80 $\mu\text{m}$ ( $3.9 \times 10^{-5}$ to $3.1 \times 10^{-3}$ in)
Specific surface	0.2 to 0.8 $\text{m}^2/\text{g}$ (8800 to 35,000 $\text{in}^2/\text{oz}$ )

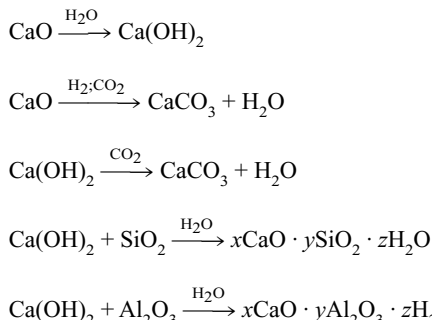
#### 6A.7.1.4 Fly Ash

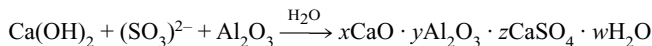
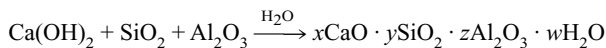
Two waste products are produced by the burning of powdered coal—fly ash and bottom ash (boiler slag). Bottom ash collects at the base of the furnace, and fly ash is collected from the flue gases by mechanical and/or electrostatic precipitation. The particles in bottom ash range in size from fine sand to gravel, and bottom ash serves well as structural fill in road construction (Hausmann, 1990). Fly ash is powdery and of predominantly silt size and is used for a variety of purposes, including (a) as a stand-alone cement, (b) as a partial replacement for cement in concrete, (c) in combination with lime, cement, or both in soil stabilization, (d) as a fill material in the form of lime–fly ash-aggregate (LFA), cement-fly ash-aggregate (CFA), or lime-cement-fly ash-aggregate (LCFA) mixtures, and (e) as a drying agent to facilitate compaction of overly wet soils.

**6.288** SOIL IMPROVEMENT AND STABILIZATION

**FIGURE 6A.206** Coal fields of the United States and southern Canada (from Skinner and Porter, 1987).

take place in cement and lime-treated soils (see Secs. 6A.7.1.2 and 6A.7.1.3): Alumina and silica in the fly ash react with lime (either naturally occurring in the fly ash or added quicklime or hydrated lime), in the presence of water, to produce calcium silicate hydrates and calcium aluminosilicate hydrates. An illustrative list of some reactions that may occur is given as follows (Minnick, 1967):





Note that  $\text{Mg}^{2+}$  may be substituted for  $\text{Ca}^{2+}$  in all equations.

Not all fly ashes are reactive even when lime is added, so the procedures provided in ASTM C593 can be used to evaluate the suitability of a fly ash for use in lime–fly ash mixtures. Low temperatures, high organic content, and high sulfate content can have deleterious effects on the cementitious reactions. These reactions are retarded at low temperatures and are almost nonexistent at temperatures below about 40°F (14°C) (Leonard and Davidson, 1959; Little et al., 1987). The organics probably affect the cementitious reactions in fly ash in a similar manner as in Portland cement, primarily by absorbing calcium ions. If high organic content is suspected, loss-on-ignition tests (ASTM C114) can be conducted to determine carbon content. Fly ashes having sulfate contents of 5 to 10% appear to have lower rates of initial hydration (Ferguson 1993). For high sulfate contents, high initial strengths have been observed, but durability appears to be substantially reduced. The formation of ettringite, which is highly expansive, is also a potential problem when using fly ashes with high sulfate content.

The amount of fly ash used in any application depends on a variety of factors such as the desired engineering characteristics of the stabilized material, and the properties of the fly ash, the additives (if any), and the soil to be stabilized. For applications where self-cementing fly ash is used without additives, more fly ash is required to achieve the same stabilizing effect as that produced by Portland cement, with typical fly ash requirements on the order of 15 to 25%. In LFA, CFA, and LCFA applications, the stabilizer is defined by designating the total amount of stabilizer (fly ash plus additives) and the lime-to-fly-ash ratio or the cement-to-fly-ash ratio (or both). For example, an LFA mixture of 5% lime, 15% fly ash, and 80% aggregate would be specified as 20% lime plus fly ash with a 1:3 lime-to-fly-ash ratio. Lime-plus-fly-ash contents generally range from 12 to 30%, with fine-grained soils requiring higher percentages and well-graded granular soils requiring lower percentages (NCHRP 1976). The lime-plus-fly-ash content generally increases with increasing angularity and roughness of the particles. Lime-to-fly-ash ratios normally range from 1:10 to 1:2, with ratios of 1:3 to 1:4 being common. Factors that tend to increase the lime requirement are greater fines content, increased PI, and increased pozzolanic reactivity of the fly ash.

Because of the unique characteristics of each stockpile of fly ash and the complex chemical reactions that occur in fly ash-stabilized soils, mixture proportions cannot be established from separate analyses of the components (fly ash, soil, additives). Proportions are properly determined using laboratory or field-based design procedures with representative samples of the component materials to be incorporated into the field mixture. Mixture design procedures for fly ash stabilization are similar to those used for cement or lime-treated soils (Secs. 6A.7.1.2 and 6A.7.1.3) but are somewhat more complicated when additives are used, because the optimal content for the fly ash and the additive(s) must be determined. Figure 6A.207 illustrates a typical mixture design procedure for LFA when strength and durability are the most important engineering properties.

#### **6A.7.1.5 Emulsions, Sodium Silicates, and Other Chemicals**

A variety of other chemicals—including emulsions, sodium silicates, polyacrylamides, phosphoric acid, and iron and aluminum oxides—have been successfully used to stabilize soils. The use of these other chemicals in foundation applications has been limited and thus will be only briefly discussed here. A discussion of some of the less frequently used chemicals can be found in ASCE (1987).

An emulsion is a fluid formed by the suspension of a very finely divided oily or resinous liquid in another liquid. Various emulsions have been used to stabilize soils, of which the most common types are bituminous. The principal component of bituminous emulsions is bitumen, which refers to a class of cementitious substances composed mainly of hydrocarbons with high molecular weights. Included in the class of bitumens are asphalts, tars, pitches, and asphaltites. Bituminous emulsions

## 6.290 SOIL IMPROVEMENT AND STABILIZATION

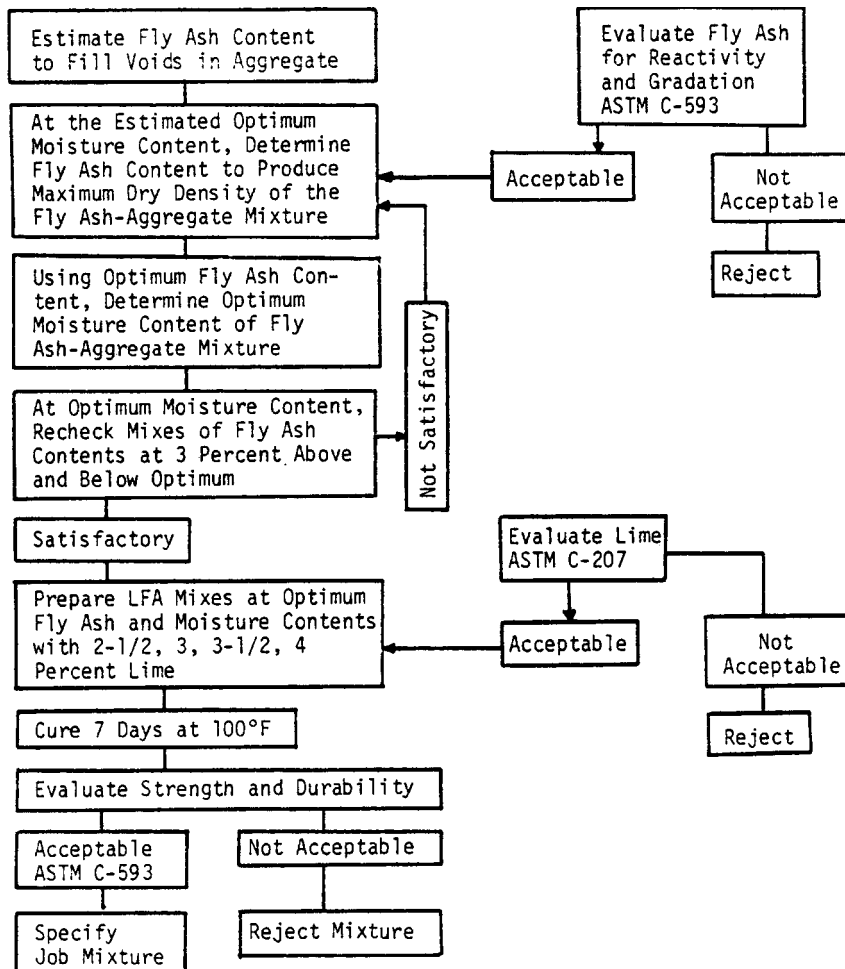


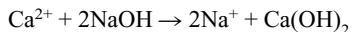
**FIGURE 6A.207** Mixture design flow chart for lime-fly-ash-aggregate (LFA) mixtures (from Little et al., 1987).

are typically either anionic or cationic, depending on the predominance of the type of charges on the discontinuous phase, and are incorporated into the soil using either hot or cold mixing methods. A number of nonbituminous emulsions have been developed to stabilize soils, many of which are proprietary. The primary use for emulsions in treating soils has been in pavement applications (stabilization of soils for use in subgrade, subbase, and base courses). Detailed discussions of bituminous stabilization of soils are given in Ingles and Metcalf (1973) and Little and coworkers (1987), among others.

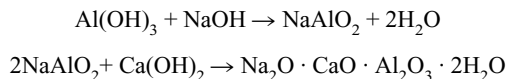
Details on the use of sodium silicates and acrylamides in grouting applications are given in Section 6B. The difference between the usage of these materials for grouting and chemical stabilization

is the nature of the chemical reactions. In solution grouting, the basic chemical is combined with a hardener that, upon setting, produces a solid material that fills the pore spaces of the soil. Thus, the chemical reaction in grouting is external to the soil particles; that is, the reaction is between the primary component and the hardener. In contrast, when used in chemical stabilization, sodium silicates and polyacrylamides react chemically with the soil particles to produce the characteristics of stabilization (reduced swelling potential, increased strength and stiffness, and so on). Sodium silicates and polyacrylamides are injected as solutions into the soil.

The cementitious reactions that occur between sodium silicate and the clay fraction of a soil can be summarized as follows (Sokolovich and Semkin, 1984). Adsorbed calcium cations are exchanged with sodium cations from the introduced reagent:



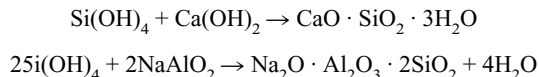
Hydrated alumina interact with liberated calcium hydroxide:



as well as



Interaction of hydrated silica with calcium hydroxide and sodium aluminate is as follows:



Because the permanence of sodium silicate grouts has been questioned, caution should be exercised when considering the use of sodium silicate for soil stabilization.

### **6A.7.2 Engineering Properties and Behavior of Chemically Stabilized Soils**

In many instances, chemical stabilization of a soil produces significant and often dramatic changes in the engineering properties and behavior of the soil compared to its natural condition. Although the magnitude of the changes produced in any soil depend on the type and amount of chemicals used, the qualitative features of these changes in successfully stabilized soils are often similar for all the types of chemicals commonly used. In this section, results illustrating the nature and magnitude of these changes will be presented and discussed according to the different engineering properties that may be affected by the stabilization process. Most of the data and results presented will be for soils treated with cement, lime, and fly ash because of the vast amount of information publicly available for these stabilizers and the dearth of data available for most other chemicals.

#### **6A.7.2.1 Plasticity and Workability**

As discussed in Sec. 6A.7.1, chemical modification using admixtures involves mixing a relatively small amount of a chemical stabilizer into a cohesive soil to improve its workability from a construction standpoint—primarily resulting in a reduction in plasticity and an agglomeration of particles into larger clods. The net result of successful modification is a friable soil with a silty texture.

**6.292** SOIL IMPROVEMENT AND STABILIZATION

These changes are visually illustrated in Fig. 6A.208 in which a highly plastic clay is shown in its natural state and after modification with hydrated lime.

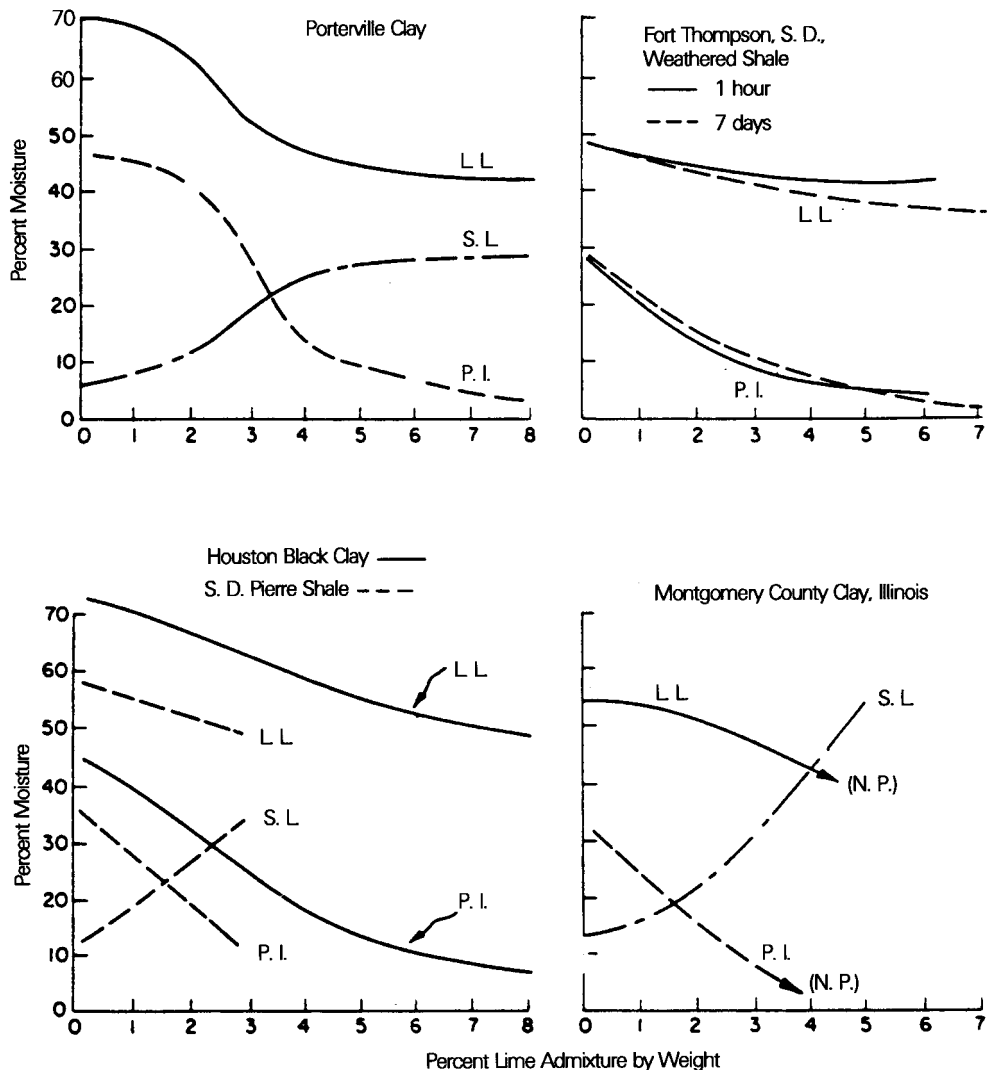
Quantitative changes in the liquid limit (LL), plastic limit (PL), plasticity index (PI), and shrinkage limit (SL) are shown in Figs. 6A.209 and 6A.210 for lime and cement-treated soils, respectively, as a function of stabilizer content. In general, chemical modification of a cohesive soil reduces the liquid limit and increases the plastic limit, with both changes producing a reduction in the plasticity of the soil as indicated by a decrease in plasticity index. The reduction in plasticity can be extensive; for example, the PI of Porterville Clay (Fig. 6A.209) was reduced from 47 to 3 with the addition of 8% lime. The reduction in plasticity increases with increasing stabilizer content up to a certain content, above which little or no additional effect occurs. Many, but not all, soils can be made nonplastic through chemical stabilization (at contents typically used in practice), and generally the amount of a particular stabilizer required to effect a nonplastic state increases with increasing PI of the natural soil. The changes in plasticity are also time-dependent, as depicted in Fig. 6A.211. In most cases, a considerable reduction in PI occurs within the first 24 h, and most of the reduction occurs within the first week. However, the process may continue for years.

**6A.7.2.2 Swelling**

Areas of the United States that have a general and local abundance of high-clay, expansive soils are shown in Fig. 6A.212. The darker areas indicate those regions suffering most seriously from problems related to expansive soils. These data indicate that eight states have extensive, highly active soils and nine others have sufficient distribution and content to be considered serious. An additional 10 to 12 states have problems that are generally viewed as relatively limited. As a rule, the 17 “problem” states have soil containing montmorillonite, which is, of course, the most expansive clay mineral. The 10 to 12 states with so-called limited problems (represented by the lighter shading) gener-



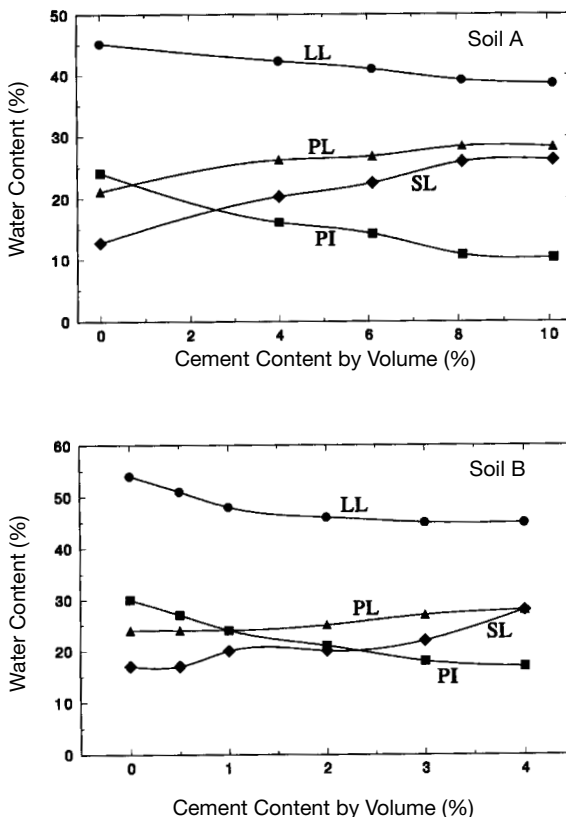
**FIGURE 6A.208** Modification of highly plastic clay with lime in Vietnam in 1967, illustrating the reduction in plasticity and agglomeration of particles into clods (courtesy of Dr. Nathaniel S. Fox, Geopier Foundation Company, Scottsdale, Arizona).



**FIGURE 6A.209** Effect of lime on the plasticity characteristics of montmorillonitic clays (from TRB, 1987; after Holtz, 1969).

ally have soils which contain clays of lesser volatility such as illite and/or attapulgite, or montmorillonite in lesser abundance.

Chemical stabilization is the most effective and permanent method available for controlling the swelling potential of expansive soils. In new construction where controlled, intimate mixing with the expansive soil is feasible, hydrated lime  $[Ca(OH)_2]$  is the most commonly used stabilizer for controlling swelling. Data illustrating the effectiveness of lime in reducing the swelling potential of a number of soils are given in Table 6A.23. Other stabilizers such as cement, fly ash, lime-fly ash,

**6.294** SOIL IMPROVEMENT AND STABILIZATION

**FIGURE 6A.210** Effect of cement content on the consistency limits of two cohesive soils (data from PCA, 1971).

and organic chemicals can also be used but are generally more expensive than lime. In remedial applications, such as stabilizing the soil beneath an existing structure, lime has inherent shortcomings. Lime is difficult to introduce into the soil matrix with any degree of uniformity, penetration, or saturation largely because (a) lime is sparsely soluble in water and (b) the expansive soil needing stabilization is both impermeable and heterogeneous. In addition, the presence of sulfates or organics in the soil may produce detrimental side effects when lime, cement, fly ash, or lime-fly ash are used (see Secs. 6A.7.1.2, 6A.7.1.3, and 6A.7.1.4).

For the reasons cited in the previous paragraph, organic chemicals are the preferred stabilizer for remedial applications. As early as 1965, certain surface-active organic chemicals were evaluated and utilized with some degree of success. One chemical used in the late 1960s and early 1970s was unquestionably successful in stabilizing the swell potential of montmorillonitic clay. The chemical was relatively inexpensive and easily introduced into the soil. However, the product maintained a “nearly permanent” offensive aroma which chemists were never able to mask. Generally, this product was a halide salt of the pyridine-collidine-pyrrillidene family. In the late 1970s, the quest began to focus more on the potential use of polyamines, polyethanol glycolethers, polyacrylamides, and so on, generally blended and containing surface-active agents to enhance soil penetration (Williams

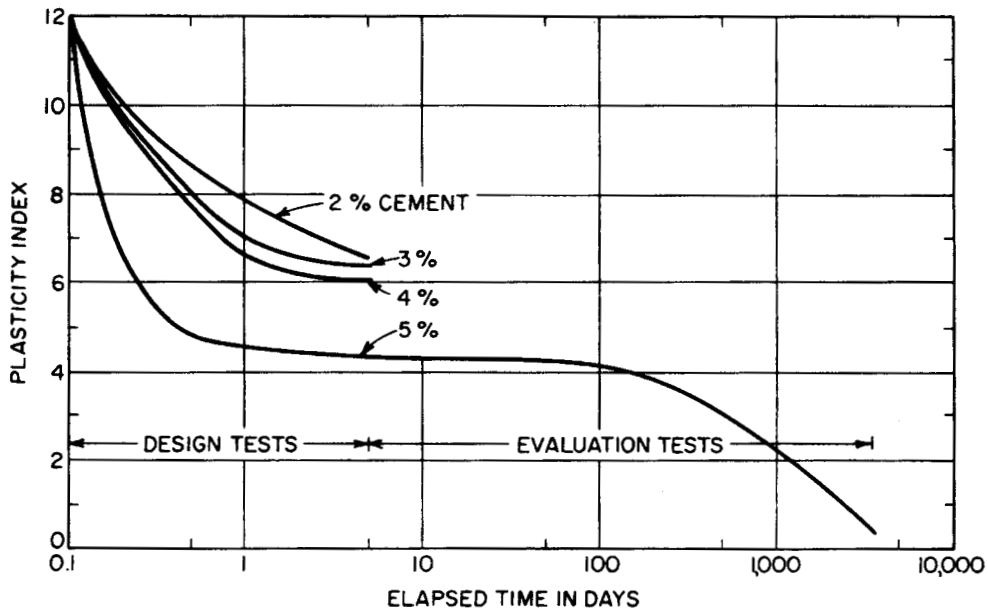


**FIGURE 6A.211** Influence of aging on the plasticity index of cement-treated soil mixes from Hot Springs, Arkansas (from Redus, 1958).

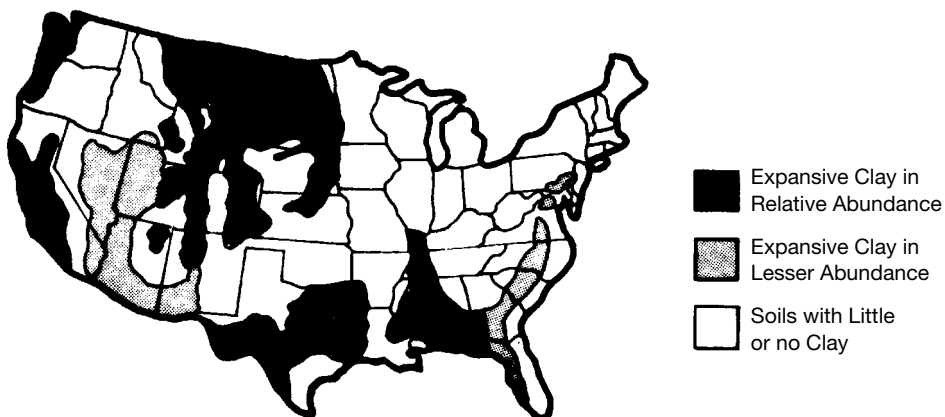


**FIGURE 6A.212** Areas in the United States with expansive soils (from Godfrey, 1978).

**6.296** SOIL IMPROVEMENT AND STABILIZATION**TABLE 6A.23** Values of Swell for Selected Soils and Soil-Lime Mixtures (Data from Thompson, 1969)

Name of soil	Natural soil	Swell, %		
		Soil-lime mixtures		Lime content, %
		No curing*	48-h curing at 120°F (48.9°C)	
Accretion Gley 2	2.1	0.1	0.0	5
Accretion Gley 3	1.4	0.0	0.1	5
Bryce B	5.6	0.2	0.0	3
Champaign Co. till	0.2	0.5	0.1	3
Cisne B	0.1	0.1	0.1	5
Cowden B	1.4	—	0.0	3
Cowden B	2.9	0.1	0.1	5
Cowden C	0.8	0.0	0.0	3
Darwin B	8.8	1.9	0.1	5
East St. Louis clay	7.4	2.0	0.1	5
Fayette C	0.0	0.0	0.1	5
Illinoian B	1.8	0.0	0.0	3
Illinoian till	0.3	0.1	0.0	3
Illinoian till	0.3	0.9	0.1	3
Sable B	4.2	0.2	0.0	3
Fayette B	1.1	0.0	0.0	3
Miami B	0.8	0.0	0.0	3
Tama B	2.0	0.2	0.1	3

\*Specimens were placed in 96-h soak immediately after compaction.

and Undercover, 1980). Certain combinations of chemicals seemed to be synergistic in behavior (the combined product achieved superior results to those noted for any of its constituents). Such a product is Soil Sta (proprietary to Robert Brown); similar laboratory and field data are not publicly available for any other organic stabilizer. Organic stabilizers function differently from lime, and no standardized testing procedures existed for the evaluation of these type products. The following discussions and data should prove beneficial to others wishing to evaluate an organic chemical stabilizer. All descriptive information was supplied through the courtesy of Brown Foundation Repair & Consulting, Inc., Dr. Cecil Smith, Professor of Civil Engineering, Southern Methodist University, Dr. Tom Petry, Professor of Civil Engineering, University of Texas, Arlington, all of Dallas, Texas, and Dr. Malcom Reeves, Soil Survey of England and Wales, London, England.

Soil Sta is basically a mixture of surfactant, buffer, inorganic cation source, and polyquaternaryamine in a polar vehicle. By virtue of its chemical nature, Soil Sta would be expected to have a lesser influence on kaolinite or illite than on the more expansive clays such as montmorillonite. Prior research had also indicated that soils exhibiting LL less than 35 or PI less than 23 (montmorillonite content less than about 10% by weight) would not swell appreciably (Sherif et al., 1982). Hence, the soils used in the laboratory tests and field applications contained at least 10% montmorillonite.

Soil Sta was first subjected to laboratory evaluation in 1982, and field testing commenced in mid-1983. The laboratory tests indicated that Soil Sta:

- Reduced the free swell potential of montmorillonitic clay (see Fig. 6A.213)
- Appeared stable to repeated cycles of weathering (a simulated period of 50 years)
- Increased shear strengths in some soils by 2-fold

- Increased soil permeabilities up to 40-fold
- Reduced soil shrinkage by amounts varying from 11 to 50% (Petry and Brown, 1987; Brown, 1989)

By 1991 Soil Sta had been subjected to literally thousands of field applications with few, if any, failures. That is, less than 1% of the foundations treated with the chemical experienced recurrent movement, and, in a goodly proportion of those, there was a serious question as to the cause.

Some interesting points are illustrated in Fig. 6A.213:

1. At moisture contents above about 10.5%, the chemical treatment of these particular montmorillonitic soils reduced the free swell potential to levels often considered as "tolerable." Free swell potential was essentially nil above in situ moisture contents of about 18%.
2. The untreated soil is somewhat moisture-stabilized (against swell) at natural moisture contents above about 21% and would be totally stabilized against swell at natural moisture contents above about 27%.
3. The PL of this soil was 30%; hence, the moisture stabilization (against swell) occurs several percentage points below the PL.
4. Even at natural moisture contents below 10.5%, the effective abatement of swell is still profound, nearly fourfold. However, in the "real world," the natural soil moisture in foundation bearing soils (expansive in nature) is seldom found to be materially less than 10.5%.

Again, the principal intended function for this particular product (Soil Sta) is to abate swell. Under certain conditions, recurrent settlement could be a persistent problem. For example, Soil Sta is not designed to prevent soil shrinkage resulting from either soil moisture losses (evaporation or transpiration), compaction, or consolidation.

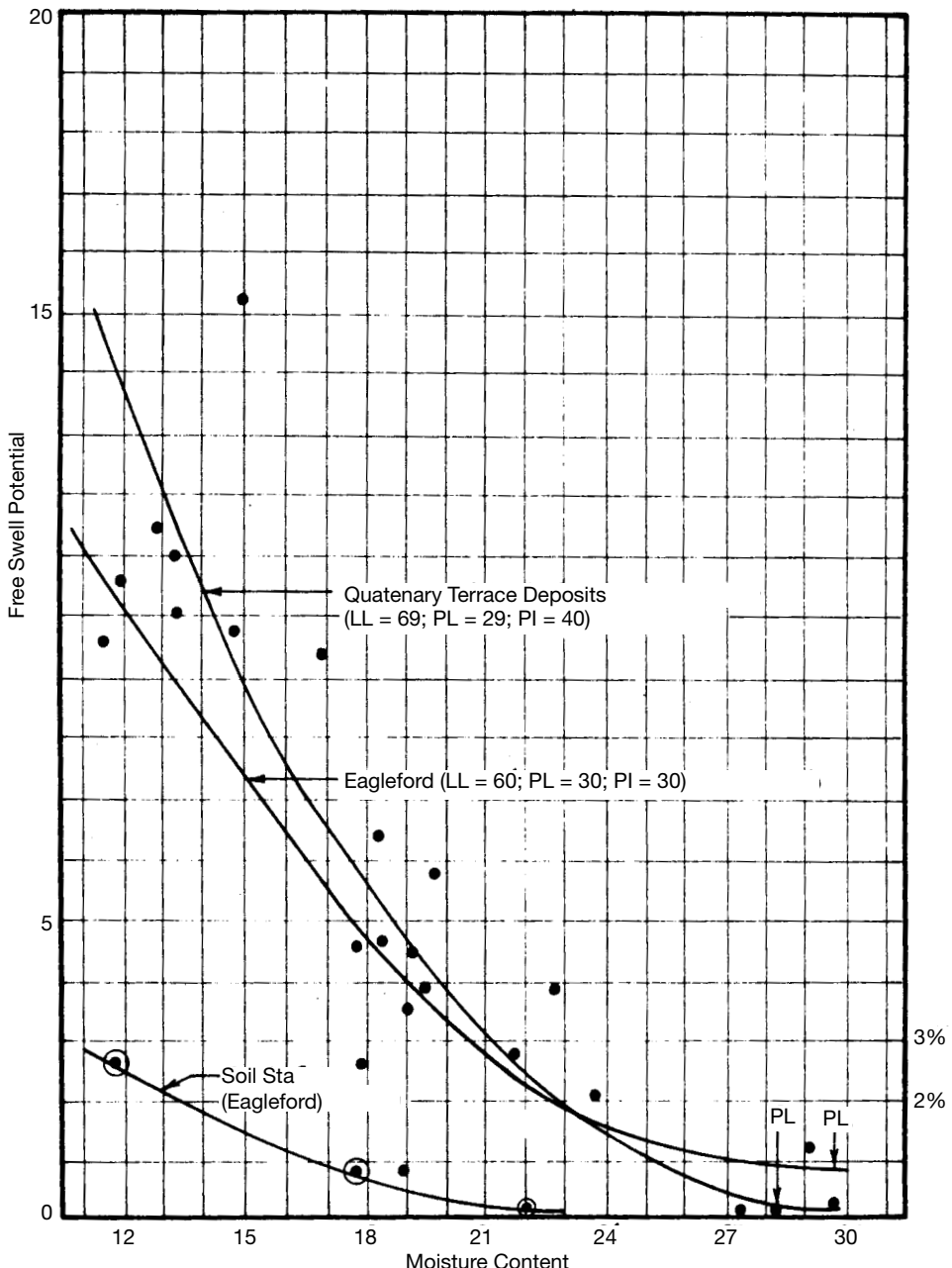
#### **6A.7.2.3 Shrinkage**

Successful chemical stabilization of expansive soils results in reduced shrinkage potential. This reduction in shrinkage potential is illustrated in Figs. 6A.209 and 6A.210 by the increase in the SL for the stabilized soils compared to the natural soils and by the data for linear shrinkage of three cement-stabilized cohesive soils provided in Fig. 6A.214. Natural granular (cohesionless) soils do not shrink because of a lack of clay content, but cement-stabilized granular soils will shrink because the cement shrinks owing to increased cohesion associated with the cementing action.

Shrinkage of properly stabilized soils is usually of little or no significance in most foundation applications. The magnitude of the shrinkage is generally so small that little or no settlement will occur in foundations bearing on chemically stabilized soils. For example, data from Nakayama and Handy (1965) showed that the total shrinkage was less than 1% for four soils (two sands, a silt, and a clay) treated with various levels of cement and tested under a variety of curing and drying conditions. The cement-stabilized sands shrank very little (<0.1%). Shrinkage may produce minor cracking of the stabilized soil, which may result in some small but probably insignificant reduction in strength. Perhaps the most important potential problem related to shrinkage-induced cracking is that it may subject the stabilized soil to greater attack from sulfates that are leached from adjacent sulfate-bearing soils by providing easier access into the interior of the stabilized mass.

#### **6A.7.2.4 Collapse**

The preconstruction collapse potential of both naturally deposited and compacted soils can be substantially reduced or eliminated by chemical stabilization. Naturally deposited collapsible soils can be chemically treated either by adding the chemical in an aqueous solution to the soil via either injection or ponding or by excavating the soil, mixing lime or cement with the soil at an appropriate water content, and recompacting the soil in place (Clemence and Finbarr, 1981). The collapse potential of compacted fills can be controlled by mixing the stabilizer with the borrow soil prior to compaction (Lawton et al., 1993). To the authors' knowledge, there are no methods of chemical stabilization currently available for remedial applications in collapsible soils.

**6.298** SOIL IMPROVEMENT AND STABILIZATION

**FIGURE 6A.213** Effectiveness of Soil Sta in reducing the free swell potential of montmorillonitic clays (from Brown, 1992).

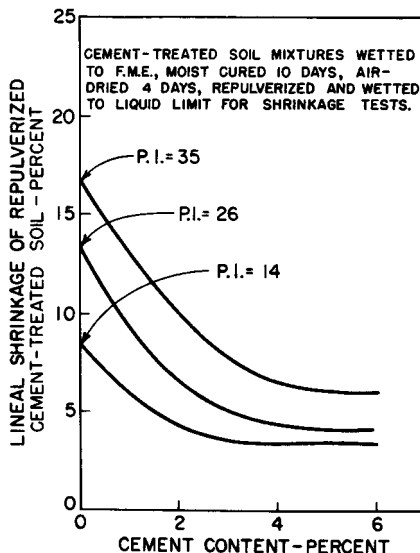


**FIGURE 6A.214** Influence of cement content on the linear shrinkage of repulverized cement-treated soil (from HRB, 1961).

The stabilization of naturally deposited collapsible soils using sodium silicate has been demonstrated by laboratory and field tests conducted in the former Soviet Union and in the United States. Sokolovich and Semkin (1984) reported the results of laboratory collapse tests conducted on specimens of loess that had been prewetted in the field by injecting either water or a 2% solution of sodium silicate in water. The prewetted soil was allowed to dry for several months before samples were taken from the field at depths of 4 m and 6 m (13 ft and 20 ft). Upon wetting in the laboratory (applied stress not given), the specimens prewetted with water collapsed an average of 4.1%, whereas those prewetted with the sodium silicate solution collapsed an average of 0.26%. Rollins and Rogers (1994) conducted a series of full-scale field load tests to evaluate the effectiveness of different treatment methods in reducing the collapse potential of a deposit of clayey sandy silt located in an alluvial fan. One of the test sections was prewetted with a 2% sodium silicate solution that was ponded on the ground surface and allowed to percolate into the ground. After periods of 1.5 months for curing and drying and two weeks for sampling, a 1.5 m (4.9 ft) square reinforced concrete footing was built and loaded to an average bearing stress of 85 kPa (1.8 ksft). The site was then wetted with water. The resulting collapse settlement was less than 27 mm (1.1 in), compared to an average settlement of 280 mm (11 in) for the untreated soil. Furthermore, the treatment with sodium silicate reduced the creep settlement after 6 months from 12 mm (0.47 in) to 9 mm (0.35 in).

Laboratory results provided by Lawton and coworkers (1993) have demonstrated the effectiveness of lime and cement in substantially reducing the collapse potential of compacted cohesive soils. One-dimensional collapse tests were conducted on comparable untreated and treated specimens of compacted clayey sand wherein the dry density and water content of the soil exclusive of the stabilizer were the same. By comparing the results of the collapse tests on these comparable untreated and treated specimens, which are provided in Table 6A.24, the fundamental influence of the stabilizer on the collapse potential can be determined. In all instances where there was sufficient free water in the soil for complete hydration of the stabilizer (a compaction water content of at least 8.8% in these tests), the reduction in collapse was significant, and the magnitude of collapse was

**6.300** SOIL IMPROVEMENT AND STABILIZATION**TABLE 6A.24** Results from Single Oedometer Collapse Tests on Comparable Untreated and Chemically Stabilized Specimens Consisting of 70% Silica Sand and 30% Kaolin (from Lawton et al., 1993)\*

Stabilizer†	$\gamma_d^{*‡}$		$\sigma_v$			$\varepsilon_{vw}$ , %	
	Mg/m <sup>3</sup>	pcf	w‡, %	$S_r^‡$ , %	kPa	ksf	
None	1.50	94	8.8	30	400	8.4	-17.04
5% cement	1.50	94	8.8	30	400	8.4	-0.02
None	1.60	100	12.5	50	400	8.4	-0.60
2% cement	1.60	100	12.5	50	400	8.4	-0.08
None	1.60	100	7.5	30	400	8.4	-13.47
5% lime	1.60	100	7.5	30	400	8.4	-4.04
None	1.67	104	10.0	45	400	8.4	-0.31
0.5% cement	1.67	104	10.0	45	400	8.4	-0.01
None	1.67	104	10.0	45	800	16.7	-0.06
0.5% cement	1.67	104	10.0	45	800	16.7	-0.01
None	1.67	104	7.0	31	400	8.4	-13.06
2% cement	1.67§	104§	7.0§	31§	400	8.4	-13.51
None	1.67	104	7.0	31	800	16.7	-11.28
2% cement	1.67	104	7.0	31	800	16.7	-9.56

\*  $\gamma_d$  = dry density of soil (exclusive of stabilizer);  $w$  = compaction water content of soil (exclusive of stabilizer);  $S_r$  = degree of saturation of soil (exclusive of stabilizer);  $\sigma_v$  = applied (total) vertical stress;  $\varepsilon_{vw}$  = wetting-induced strain.

† Cement = Portland cement; lime hydrated lime [Ca(OH)<sub>2</sub>].

‡ Values given are nominal. Actual values for all specimens, except as noted below, were close to their nominal values.

§ Actual  $\gamma_d = 1.60 \text{ Mg/m}^3 = 100 \text{ pcf}$ ; actual  $w = 6.4\%$ ; actual  $S_r = 25\%$

small ( $\leq 0.08\%$ ). The most dramatic example of reduction in collapse was from 17.04 to 0.02% by the addition of 5% cement (by weight) at a dry density of 1.50 Mg/m<sup>3</sup> (93.6 pcf), a water content of 8.8%, and an applied stress of 400 kPa (8.4 ksf). For a compaction water content  $\leq 7.5\%$ , the hydration of the stabilizer was incomplete, and, although collapse was generally reduced, the magnitude of collapse was still quite high ( $\geq 4.04\%$ ) and unacceptable from a design standpoint.

The addition of chemical stabilizers also substantially reduced the time to the end of collapse ( $t_c$ ) as illustrated in Fig. 6A.215. For  $\gamma_d = 1.60 \text{ Mg/m}^3$  (100 pcf),  $w = 7.5\%$ , and  $\sigma_v = 400 \text{ kPa}$  (8.4 ksf),  $t_c$  for the 5% lime specimen was 4 min compared to 60 min for the untreated specimen. Similarly, for  $\gamma_d = 1.67 \text{ Mg/m}^3$  (104 pcf),  $w = 7.0\%$ , and  $\sigma_v = 800 \text{ kPa}$  (16.7 ksf), the addition of 2% cement reduced  $t_c$  from 240 min to 60 min. Similar reductions in  $t_c$  occurred in the other treated specimens.

The chemically treated soils also exhibited significantly less postcollapse creep strain than the comparable untreated soils. For example, for the same specimens discussed in the preceding paragraph, the modified secondary compression index [ $C_{as} = -\Delta\varepsilon_v/\Delta(\log t)$ ] decreased from 0.094 to 0.025% for the lime-treated specimen and decreased from 0.36 to 0.014% for the cement-treated specimen. This trend was consistent in all treated specimens.

#### 6A.7.2.5 Stress-Strain-Strength Behavior

The general effect of chemical stabilization on soils is to increase both the strength and stiffness of the soil while making the soil more brittle. Where the stabilization occurs primarily by cation and base exchange with clay particles, the changes in these characteristics are generally modest. For example, as noted in Sec. 6A.7.2.2, the increases in shear strength of montmorillonitic soils produced

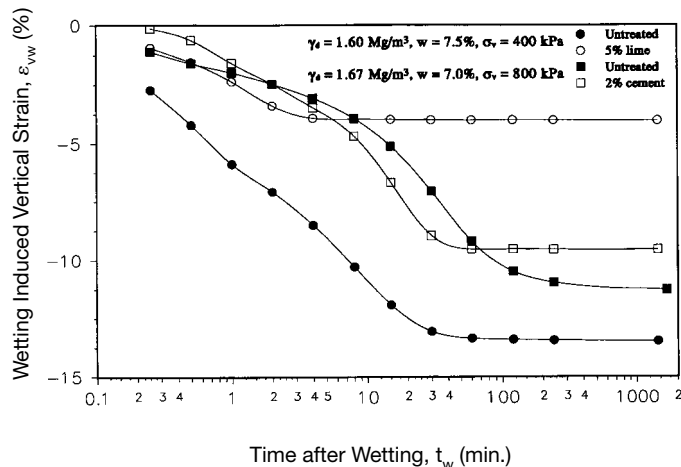


**FIGURE 6A.215** Effect of lime and cement on the time rate of collapse of compacted specimens consisting of 70% silica sand and 30% kaolin (from Lawton et al., 1993).

by Soil Sta, an organic stabilizer designed to control swelling potential, are typically a maximum of about 100% (that is, it doubles the shear strength of the natural soil). In contrast, cementitious or pozzolanic stabilizers may produce 50-fold or greater increases in stiffness and strength. To illustrate the substantial changes in stiffness and strength that may occur from chemical stabilization, the results of triaxial compression tests on untreated and cement-treated specimens of a micaceous silty sand are presented in Fig. 6A.216. At a confining pressure ( $\sigma_3$ ) of 30 psi (207 kPa), the maximum deviator stress increased from 78.7 psi (543 kPa) for the untreated soil to 971 psi (6.70 MPa) for the same soil treated with 10% cement (by dry weight), an increase of more than 12-fold. The stiffness

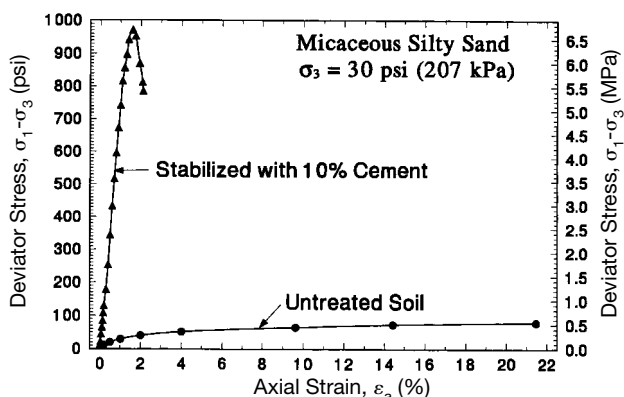


**FIGURE 6A.216** Influence of cement stabilization on the triaxial stress-strain characteristics of a micaceous silty sand.

**6.302** SOIL IMPROVEMENT AND STABILIZATION

of the cemented-treated specimen, as measured by the secant modulus at 50% of the maximum deviator stress ( $E_{50}$ ), was about 37 times that of the natural soil: 73.9 ksi (510 MPa) for the cement-stabilized soil compared to 2.0 ksi (13.8 MPa) for the untreated soil. Note also that the stress-strain behavior changed from ductile for the untreated soil to brittle for the cement-treated soil. The cement stabilization also produced substantial increases in the strength parameters. For  $\sigma_3$  ranging from 5 to 30 psi (34 to 207 kPa), the friction angle ( $\phi$ ) increased from 33° to 64°, and the cohesion intercept increased from 1.4 psi (9.7 kPa) to 60 psi (410 kPa).

In general, an increase in stabilizer content will produce an additional increase in stiffness and strength so long as the additional stabilizer produces further cementitious or pozzolanic reactions in the soil. Thus, cement-stabilized soils will continue to increase in strength and stiffness with increased cement content so long as there is sufficient water for hydration of the cement (up to the point where the cement constitutes a vast majority of the material and the strength of the mixtures is essentially equal to the strength of the cement). In contrast, the maximum strength and stiffness of lime-treated soils is achieved at a specific lime content that depends primarily on the amount of clay available in the soil for pozzolanic reactions. The addition of lime beyond this point produces no further pozzolanic reactions and may result in a decrease in strength and stiffness. The minimum lime content that produces the maximum benefit in terms of strength and stiffness is about 8% for most clayey soils (Ingles and Metcalf, 1973). Typical characteristics of compressive strength versus stabilizer content for both cement and lime are given in Fig. 6A.217.

Because the cementitious and pozzolanic reactions are time-dependent, the strength and stiffness of stabilized soils generally increases with time for at least several years. Typical results showing the effect of aging on the strength and stiffness of cement-stabilized soils are provided in Figs. 6A.218 and 6A.219. Aging can have a significant effect on both strength and stiffness. For example, for Soil 2 treated with 14% cement in Figs. 6A.218 and 6A.219, the unconfined compressive strength increased from 1400 psi (9650 kPa) after 7 days of curing to 2300 psi (15,900 kPa) after 90 days of curing, while the compressive secant modulus at one-third of the ultimate load increased from 2000 ksi (13,800 MPa) to 2,800 ksi (19,300 MPa) during the same period of time. Similar effects of aging on the stress-strain-strength characteristics of a lime-treated silty clay are shown in Fig. 6A.220. That the increase in strength and stiffness may occur over long periods of aging is demonstrated in Fig. 6A.221 for two cement-treated soils.

When chemical stabilizers are mixed with the soil, a delay between the time of mixing and the time of compaction may result in a substantial decrease in strength and stiffness of the treated soil. Thus, many specifications require that compaction be completed within a short time after mixing, usually less than 1 or 2 h. A delay in compaction reduces the strength and stiffness in two ways:

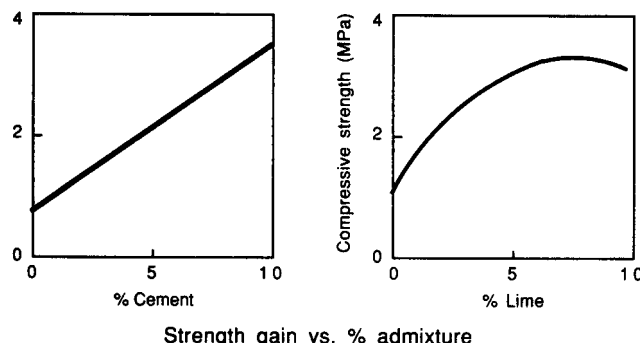


**FIGURE 6A.217** Typical characteristics of gain in strength versus admixture content for cement and lime (from Hausmann, 1990).

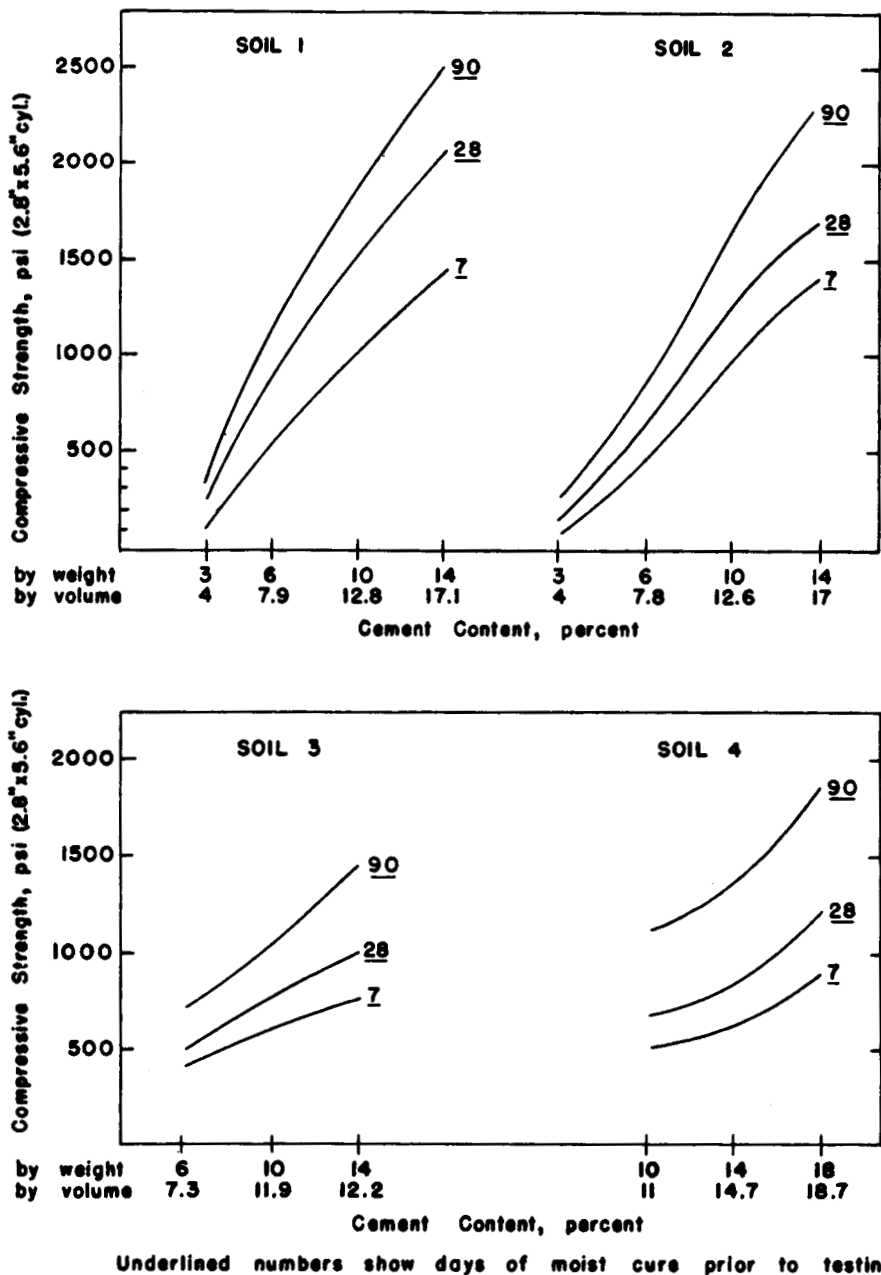
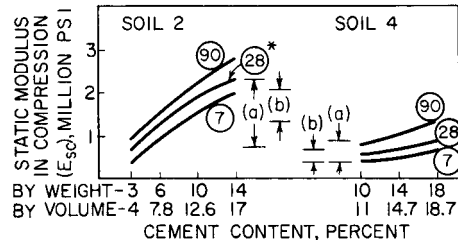
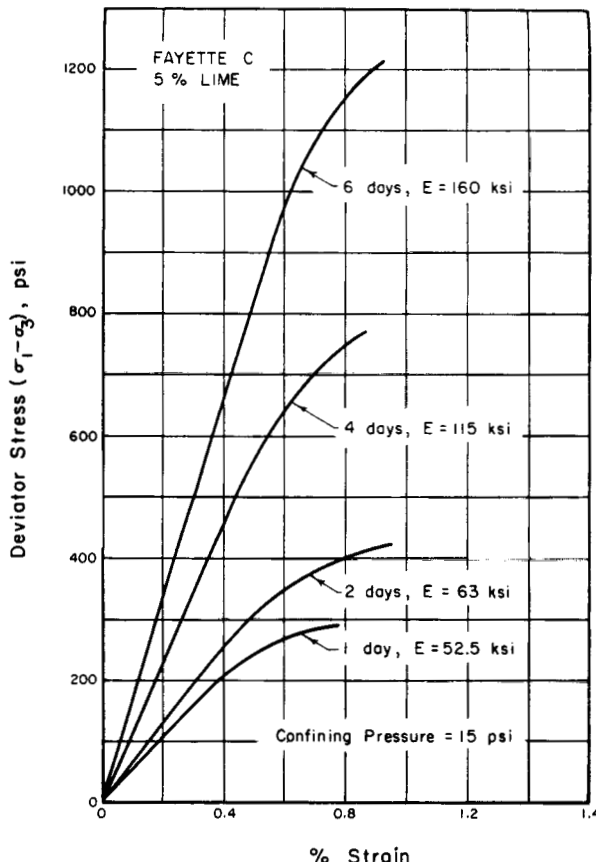


FIGURE 6A.218 Influence of aging and cement content on unconfined compressive strength (from HRB, 1961; after Felt and Abrams, 1957).

## 6.304 SOIL IMPROVEMENT AND STABILIZATION



**FIGURE 6A.219** Effect of aging and cement content on static unconfined compressive modulus (from HRB, 1961; data from Felt and Abrams, 1957).



**FIGURE 6A.220** Influence of aging on the stress-strain properties of a lime-treated cohesive soil (from Thompson, 1966).

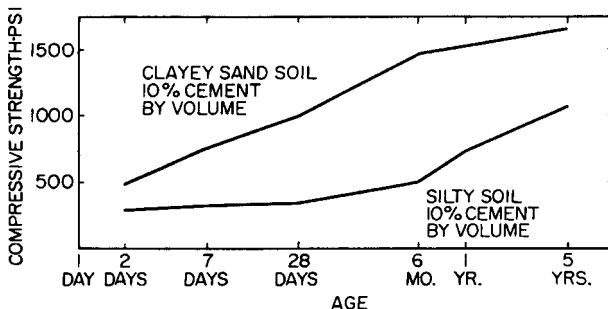


**FIGURE 6A.221** Influence of long-term aging on the unconfined compressive strength of two specimens of soil-cement (from HRB, 1961; after Leadabrand, 1956).

1. Cementitious products (clods) are formed that harden with time. These clods must be broken down or remolded if the material is to be densified. For the same compactive effort, the density will decrease with increasing delay in compaction, as shown in Fig. 6A.222 for a soil stabilized with self-cementing fly ash.
2. As clods form and harden with increasing delay, the effective area of contact between clods in the compacted soil decreases. The result is that a smaller volume of stabilized soil is cemented together because cementation between clods occurs only along the interclod contact areas. In contrast, a well-mixed, chemically treated soil that is compacted immediately after compaction will be relatively homogeneous with cementation occurring throughout the treated mass. Thus, a delay in compaction means that a portion of the stabilizer is lost to the clodforming process and is unavailable for cementation of the entire mass.

The loss in strength resulting from a delay in compaction can be significant. For example, a 2-h delay in compaction of the fly-ash-treated material shown in Fig. 6A.222 reduced the maximum strength for a given compactive effort from about 2300 kPa (330 psi) to about 700 kPa (100 psi)—a decrease of 70%. This magnitude of reduction in strength is typical for class C (cementitious) fly ashes, which “flash-set” when water is added. To counteract this characteristic, set retarders often must be added to the mixture to delay the cementitious reactions for about 2 h to permit hauling, placing, and compaction of the treated material (ASCE, 1987). A delay in compaction may also be a significant problem in cement-treated soils, as illustrated in Fig. 6A.223, but is generally not a significant problem in soils treated with pozzolanic stabilizers (typically lime and lime-fly ash).

Temperature affects the rate at which the cementitious or pozzolanic reactions take place and thus the strength and stiffness of the soil. In general, higher temperatures produce faster gains in strength and stiffness, as illustrated in Fig. 6A.224 for various soils treated with lime and cement, and in Fig. 6A.225 for an LFA mixture. At temperatures below about 40°F (4°C), the cementitious or pozzolanic reactions are severely retarded. Thus, during the winter, the cementitious reactions will be minimal when temperatures drop below 40°F (4°C) but will resume when the weather warms, as illustrated in Fig. 6A.226. Low temperatures, including long periods of freezing, seem to have no permanent effect on the strength that will eventually be achieved.

Some typical guidelines for estimating the stress-strain-strength relationships of soils stabilized with lime, cement, and fly ash have been developed. The typical shape of a stress-strain plot for these types of chemically treated soils is as shown in Fig. 6A.227. In general, the stress-strain relationship is approximately linear up to about 50 to 70% of the peak strength, beyond which the relationship is nonlinear (strain-softening) up to failure.

## 6.306 SOIL IMPROVEMENT AND STABILIZATION

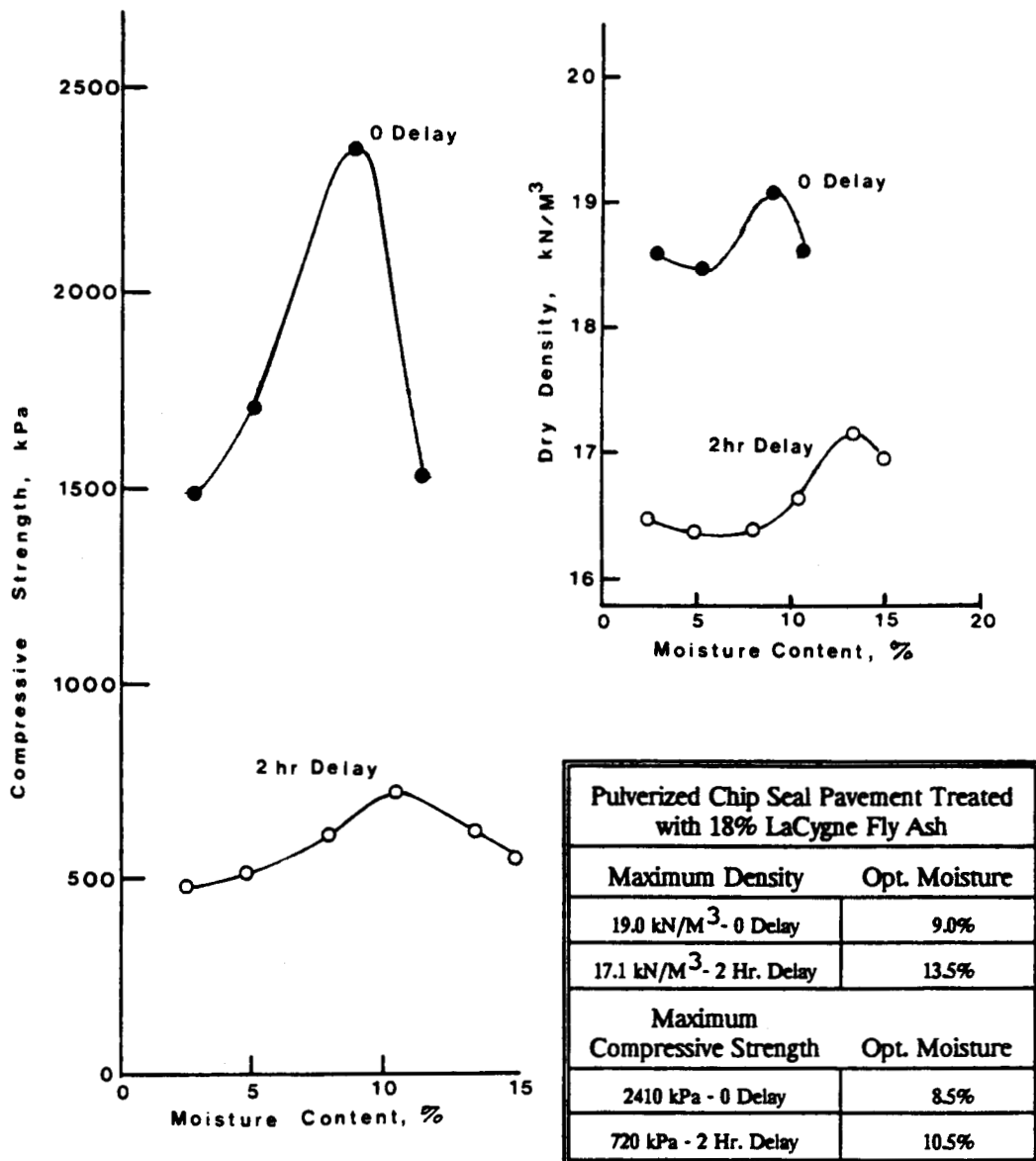
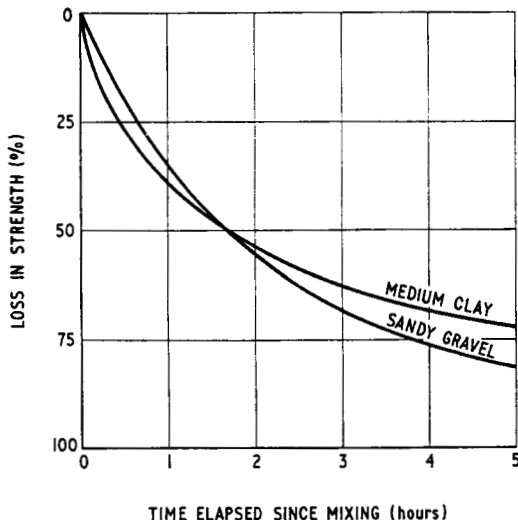
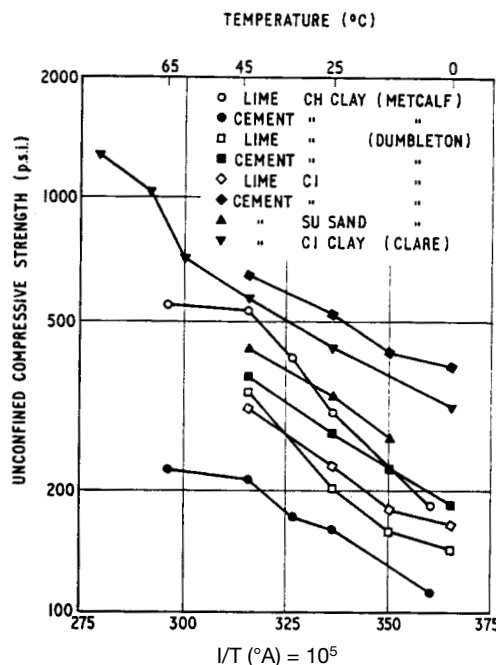


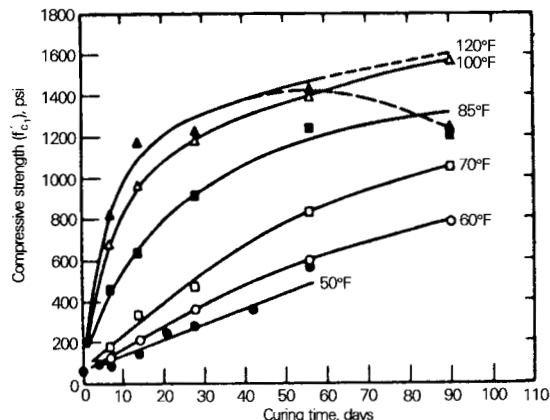
FIGURE 6A.222 Moisture-density and moisture-strength relationships for a fly-ash-treated material (from Ferguson, 1993).



**FIGURE 6A.223** Loss in strength caused by delay in compaction for two soils stabilized with 10% cement (standard Proctor compaction) (from Ingles and Metcalf, 1973; after West, 1959)



**FIGURE 6A.224** Relationship between the rate of gain in strength and curing temperature for lime and cement-stabilized soils (from Ingles and Metcalf, 1973).

**6.308** SOIL IMPROVEMENT AND STABILIZATION

**FIGURE 6A.225** Effect of curing time and temperature on the strength development of a lime-fly ash-aggregate mixture (from NCHRP, 1976; after MacMurdo and Barenberg, 1973).

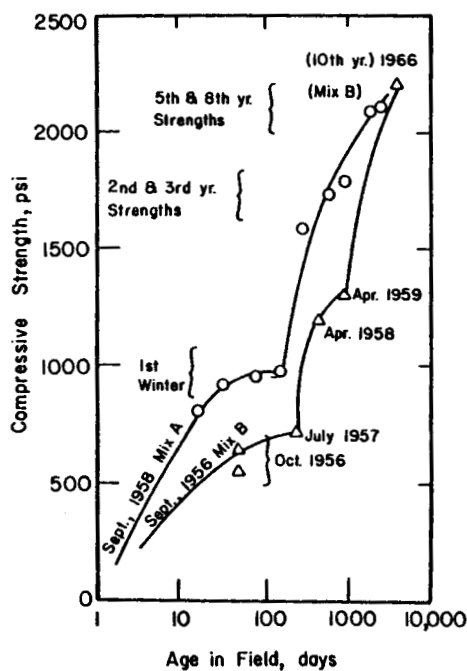


**FIGURE 6A.226** Age-strength relationships of lime-fly ash-aggregate mixtures (from Little et al., 1987; after FHWA, 1979).

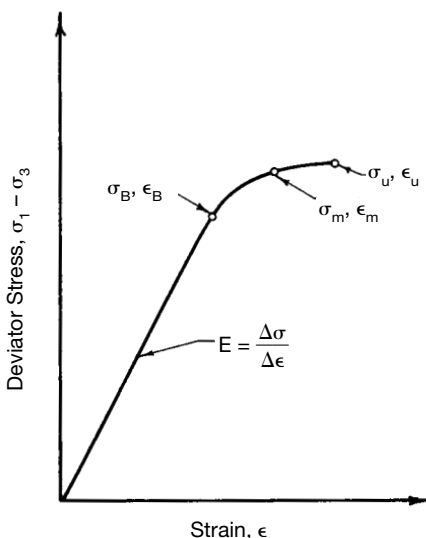


**FIGURE 6A.227** Idealized stress-strain curve for lime-stabilized soils (from Thompson, 1966).

Typical relationships between unconfined compressive strength ( $q_u$ ) and stabilizer content have been established for cement-stabilized soils. Data illustrating these relationships are provided in Fig. 6A.228, from which the following approximate equations have been developed for estimating  $q_u$  based on cement content ( $C$  in percent by dry weight) for coarse-grained and fine-grained soils. For coarse-grained soils, the equations are

$$q_u(\text{psi}) = (80 \text{ to } 150) \cdot C \quad (6A.133a)$$

$$q_u(\text{kPa}) (550 \text{ to } 1030) \cdot C \quad (6A.133b)$$

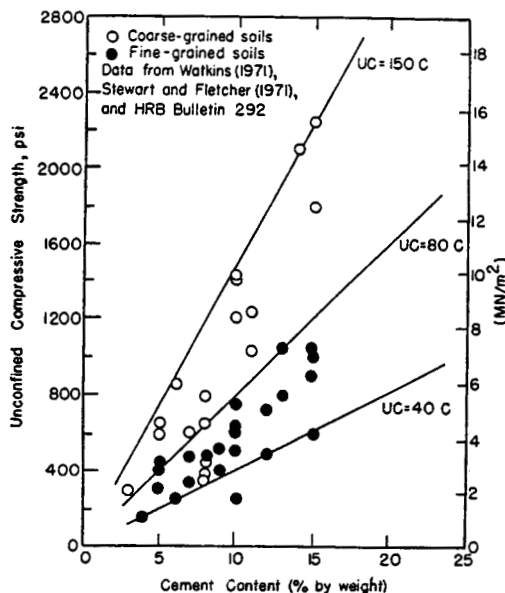
For fine-grained soils the equations are

$$q_u(\text{psi}) = (40 \text{ to } 80) \cdot C \quad (6A.134a)$$

$$q_u(\text{kPa}) = (275 \text{ to } 550) \cdot C \quad (6A.134b)$$

Note that Eqs. (6A.133) and (6A.134)-as well as the rest of the equations given in this section—should be used only to estimate values, not to obtain values for design or analysis.

Typical values of  $q_u$  for lime-fly-ash-stabilized materials are given in Table 6A.25 according to general soil type. An equation for estimating  $q_u$  for cement-stabilized soils at a later age ( $d$  = number of days) based on a known value of  $q_u$  at a certain age ( $d_0$ ) is given as follows (Little et al., 1987; Mitchell, 1981):

**6.310** SOIL IMPROVEMENT AND STABILIZATION

**FIGURE 6A.228** Relationship between cement content and unconfined compressive strength for soil-cement mixtures (from Little et al., 1987; after FHWA, 1979).

$$(q_u)_d = (q_u)_{d_0} + F \cdot \log\left(\frac{d}{d_0}\right) \quad (6A.135)$$

where  $F = 70C$  for coarse-grained soils and  $q_u$  in psi

$F = 480C$  for coarse-grained soils and  $q_u$  in kPa

$F = 10C$  for fine-grained soils and  $q_u$  in psi

$F = 70C$  for fine-grained soils and  $q_u$  in kPa

The stiffness and strength of a chemically stabilized soil are obviously interrelated. The following equation gives an approximate relationship between compressive modulus ( $E_c$ ) at a confining

**TABLE 6A.25** Ranges of unconfined compressive strength for lime-fly-ash-stabilized materials (from NCHRP, 1976).

Type of soil	28-day immersed unconfined compressive strength	
	psi	kPa
Gravels	400 to 1300	2800 to 9000
Sands	300 to 700	2100 to 4800
Silts	300 to 700	2100 to 4800
Clays	200 to 500	1400 to 3400
Crushed stones and slag	1400 to 2000	10,000 to 14,000

pressure of 15 psi (100 kPa) and unconfined compressive strength for lime-treated soils (Thompson, 1966):

$$E_c(\text{ksi}) = 10 + 0.124 \cdot q_u(\text{psi}) \quad (6A.136a)$$

$$E_c(\text{MPa}) = 70 + 0.124 \cdot q_u(\text{kPa}) \quad (6A.136b)$$

Values of  $E_c$  for cement-stabilized soils are typically within the range of 1000 to 5000 ksi (7000 to 35,000 MPa) for coarse-grained soils and 100 to 1000 ksi (700 to 7000 MPa) for fine-grained soils.  $E_c$  depends on the confining pressure and can be expressed in the following form based on an assumed hyperbolic shape of the stress-strain relationship (Duncan et al., 1980):

$$E_{tc} = K \cdot P_a \cdot \left( \frac{\sigma_3}{P_a} \right)^n \cdot \left[ 1 - \frac{0.75(1 - \sin\phi)(\sigma_1 - \sigma_3)}{2(c \cdot \cos\phi + \sigma_3 \cdot \sin\phi)} \right]^2 \quad (6A.137)$$

where  $E_{tc}$  = tangent compressive modulus at a given stress level ( $\sigma_1 - \sigma_3$ )

$\phi$  = angle of internal friction

$c$  = cohesion intercept

$P_a$  = atmospheric pressure

$n$  = modulus exponent (typically 0.1 to 0.5 for cement-stabilized soils)

$K$  = modulus number (typically 1000 to 10,000 for cement-stabilized soils)

$E_c$  for lime-fly-ash-stabilized soils generally varies from about 500 to 2500 ksi (3500 to 17,500 MPa) (Little et al., 1987).

Values of the Mohr-Coulomb strength parameters, angle of internal friction ( $\phi$ ) and cohesion intercept ( $c$ ), vary considerably for chemically stabilized soils depending primarily upon the type of soil, the amount of stabilizer, and the amount and type of curing. Typical values of  $\phi$  for soils treated with cement, lime, and lime-fly ash are given in Table 6A.26. For cement-stabilized soil,  $c$  may be as high as a few hundred psi (a few thousand kPa) (FHWA, 1979; Mitchell, 1981). The following equation can be used to estimate  $c$  based on  $q_u$  for lime-stabilized soils (Thompson, 1966):

$$c(\text{psi}) = 9.3 + 0.292 \cdot q_u(\text{psi}) \quad (6A.138a)$$

$$c(\text{kPa}) = 64 + 0.292 \cdot q_u(\text{kPa}) \quad (6A.138b)$$

For the lime-fly ash-stabilized gravels evaluated by Hollon and Marks (1962),  $c$  varied from 55 to 128 psi (380 to 880 kPa).

**TABLE 6A.26** Typical Ranges of Values for Angle of Internal Friction for Soil Stabilized with Cement, Lime, and Lime-Fly Ash

Stabilizer	Typical values of $\phi$ (degrees)	
	Coarse-grained	Fine-grained
Cement	40 to 60	30 to 40
Lime	N.A.*	25 to 35
Lime-fly ash	49 to 53†	N.A.*

\*N.A. indicates not available or not applicable.

†Based on limited data for gravel (Hollon and Marks, 1962).

**6.312** SOIL IMPROVEMENT AND STABILIZATION

Although few data in the literature address values of Poisson's ratio ( $\nu$ ) for chemically stabilized soils, some general guidelines can be given for soils stabilized with cement, lime, and fly ash. Values of static  $\nu$  for chemically stabilized soils are typically smaller than for natural soils. In general,  $\nu$  is relatively constant within the linear stress-strain range for a given stabilized soil and confining pressure, as shown in Fig. 6A.229 for a lime–fly ash-stabilized gravel. Values of  $\nu$  within this range of stresses typically vary from about 0.08 to 0.15 for granular soils and 0.15 to 0.20 for cohesive soils. Thus, these values are typical for the normal range of stresses that a stabilized soil would be subjected to during its service life. At higher stresses levels,  $\nu$  increases with increasing stress up to values at failure of about 0.20 to 0.30 for granular soils and 0.25 to 0.35 for cohesive soils. Values of dynamic Poisson's ratio appear to be somewhat higher. In a study of four soils stabilized with cement (Felt and Abrams, 1957), values of dynamic  $\nu$  were found to range from 0.22 to 0.27 for two granular soils, 0.24 to 0.31 for a silty soil, and 0.30 to 0.36 for a clayey soil.

**6A.7.2.6 Compaction Moisture-Density Relationships**

The addition of a chemical stabilizer usually alters the compaction moisture-density relationships of a soil. The moisture-density curves for a loess treated with varying amounts of quicklime compacted 24 h after mixing are shown in Fig. 6A.230. For nearly all cohesive soils, the addition of lime produces the same types of changes to the moisture-density relationships illustrated in Fig. 6A.230—a decrease in maximum dry density ( $\gamma_{d\max}$ ) and an increase in optimum water content ( $w_{opt}$ ) for the same method of compaction and compactive effort. In addition,  $\gamma_{d\max}$  typically decreases and  $w_{opt}$  normally increases with increasing stabilizer content. These changes can be explained in simplified terms as follows:

1. Some cementitious or pozzolanic reactions occur immediately upon hydration. This cementing effect produces a resistance to compaction that results in a decrease in  $\gamma_{d\max}$ .
2. Extra water (in addition to that needed to facilitate rearrangement of the soil particles during compaction) is required to hydrate the lime and produce the pozzolanic reactions. Hence,  $w_{opt}$  is increased.

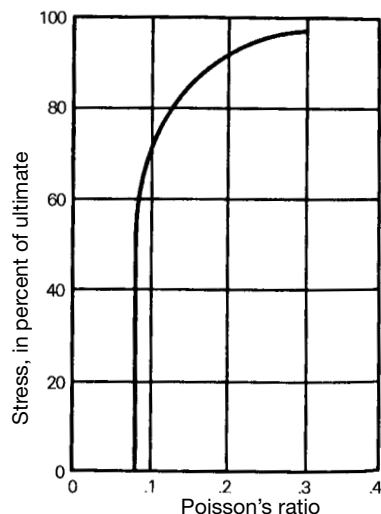


**FIGURE 6A.229** Effect of stress level on Poisson's ratio for a lime–fly ash–gravel mixture (from NCHRP, 1976; after Ahlberg and Barenberg, 1965).

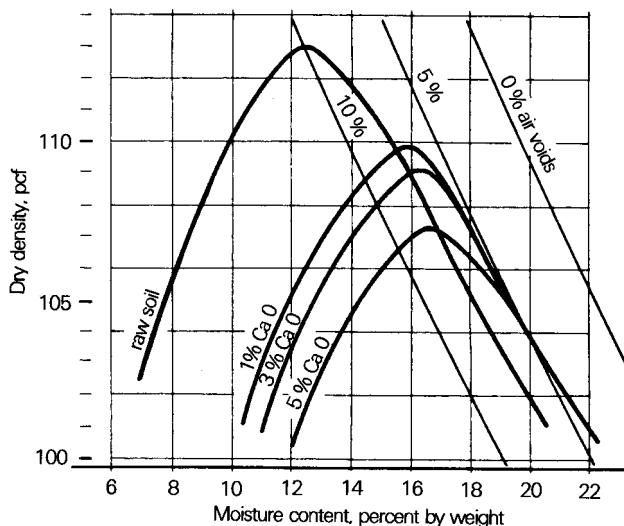


**FIGURE 6A.230** Influence of quicklime content on the standard Proctor moisture-density relationship of a loess (from Brand and Schoenberg, 1959).

In soils treated with cement,  $\gamma_{d\max}$  and  $w_{opt}$  may either increase or decrease (HRB, 1961). Increases in  $\gamma_{d\max}$  usually occur for sands and sandy soils and sometimes to a small degree for heavy clays. Little or no change in  $\gamma_{d\max}$  generally occurs for light to medium clays. Decreases in  $\gamma_{d\max}$  may occur in silts;  $w_{opt}$  normally decreases for clays, increases for silts, and changes little for sands and sandy soils. Typical values for changes in  $w_{opt}$  and  $\gamma_{d\max}$  compared to the values for the comparably compacted untreated soil, are summarized in Table 6A.27 according to type of soil for the normal range of cement contents. The reasons for the wide variation in the changes in  $w_{opt}$  and  $\gamma_{d\max}$  that occur in soils because of cement stabilization are not completely understood. The diversity of changes in  $\gamma_{d\max}$  may relate to the opposing trends caused by the high specific gravity of Portland cement ( $G_s \cong 3.15$ ) compared to that for the soil particles (typical average  $G_s \cong 2.65$  to 2.75),

**TABLE 6A.27** Maximum dry densities and optimum water contents for cement-treated soils compared to the corresponding values for untreated soils (from HRB, 1961)

Type of soil	Change in $\gamma_{d\max}$		Change in $w_{opt}$ , %
	pcf	kN/m <sup>3</sup>	
Sandy loams	0 to +3	0 to +0.5	-1 to +1
Sands	0 to +6	0 to +0.9	0 to -1
Silts and loams	0 to -6	0 to -0.9	0 to +3
Silts	-3 to +1	-0.5 to +0.2	0 to -3
Medium clays	0 to +1	0 to +0.2	0 to -2
Heavy clays	-1 to +2	-0.2 to +0.3	0 to -4

**6.314** SOIL IMPROVEMENT AND STABILIZATION

which tends to increase the density, and the resistance to compaction produced by the cementitious reactions, which tends to decrease the density.

As the length of the delay between mixing and compaction increases, the characteristics of the treated soil, including the moisture-density relationships, continuously changes as the cementitious or pozzolanic reactions occur with time. The effect of a 2-h delay on the moisture-density relationships of a pulverized chip seal pavement stabilized with a cementitious fly ash is illustrated in Fig. 6A.222. In general,  $\gamma_{d\max}$  decreases and  $w_{opt}$  increases with increasing length of the delay. The effect of delay in compaction is usually much less important in pozzolanic stabilizers (lime and lime-fly ash) than in self-cementing stabilizers (cement and class C fly ash), as illustrated in Fig. 6A.231. Because the length of the delay may significantly affect the engineering characteristics of the stabilized soil (for example, see the reduction in strength shown in Fig. 6A.222), it is essential that when preparing laboratory specimens for testing, the delay between mixing and compaction match the delay expected during the actual field construction. Sometimes retarders are used with cement or class C fly ash to inhibit the cementitious reactions during the anticipated delay between mixing and compaction.

**6A.7.2.7 Permeability**

The changes in permeability that occur because of chemical stabilization depend on the type of soil, the amount of stabilizer, the process used to add the stabilizer (injection versus mixing), and the density achieved during compaction (admixture-stabilized soil). Unfortunately, the data available in the literature regarding the permeability of chemically stabilized soils is rather limited, with most of the information pertaining to soils treated with cement and lime. Data reflecting changes in permeability produced by the chemical stabilization of particular soils can be found in HRB (1961), Townsend and Klym (1966), Ingles and Metcalf (1973), Poran and Ahtchi-Ali (1989), Bowders and colleagues (1990), and Taki and Yang (1991), among others.

In general, chemical stabilization increases the permeability of soils with very low natural permeabilities and reduces the permeability of soils with moderate to high natural permeabilities. Ex-

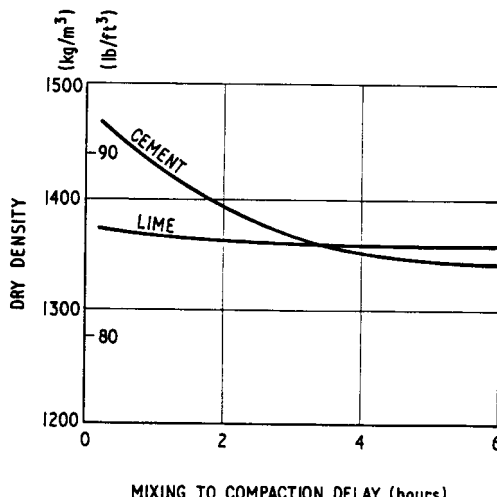


**FIGURE 6A.231** Effect of delay in compaction on the as-compacted density of a heavy clay treated with 10% stabilizer (from Ingles and Metcalf, 1973; after Dumbleton, 1962).

amples illustrating these two general trends are given as follows: (a) Soil Sta, an organic chemical stabilizer that is injected into expansive soils to control swelling potential (see Sec. 6A.7.2.2), increases the permeability of montmorillonitic soils by as much as 40-fold; and as shown in Fig. 6A.232, the treatment of two fine sands with cement reduced their permeabilities by more than two orders of magnitude. Ingles and Metcalf (1973) have indicated the following general trends for cement stabilization regarding how the permeability changes for different types of soils:

Permeability is generally decreased	Permeability is generally increased
Well-graded gravel	Silt
Well-graded sand	Silty clay
Well-graded gravel-sand-clay	Very poorly graded soil
Sand and gravel	Heavy clay
Poorly graded sand	Organic and sulfate-rich soil
Silty sand	
Sandy clay	
Silty-sandy clay	

Deviations from these general trends may occur, particularly for the borderline soil types (sandy clay, silty-sandy clay, silt, and silty clay), but deviations for the extreme soil types (clean coarse-grained soils and highly plastic clays) are unlikely. These trends are also applicable to other chemical admixtures (lime, lime-fly ash, and fly ash). The effect of the stabilizer on permeability usually increases with increasing stabilizer content, as illustrated in Fig. 6A.232, up to a limiting value of stabilizer content above which little or no additional change occurs.

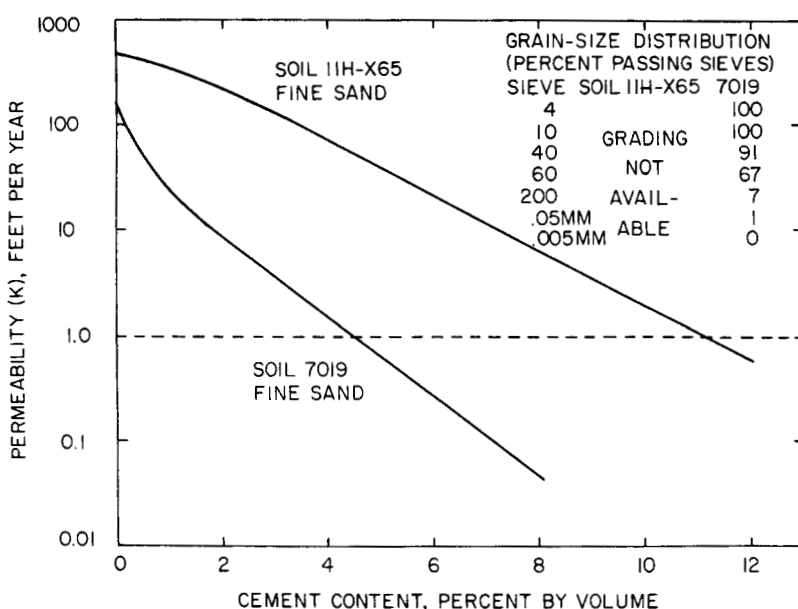


**FIGURE 6A.232** Permeability versus cement content for two cement-treated sands (from HRB, 1961; after Leadabrand, 1956).

## 6.316 SOIL IMPROVEMENT AND STABILIZATION

### 6A.7.2.8 Liquefaction Potential

For many years it has been recognized that cementation in saturated granular soils, whether occurring naturally or induced artificially, tends to inhibit liquefaction when the soil is subjected to seismic loading. In a laboratory study conducted by Clough and coworkers (1989), the following results and conclusions were determined regarding the liquefaction resistance of sands treated with cement:

1. For the sands studied, when the unconfined compressive strength ( $q_u$ ) exceeded 100 kPa (14.5 psi), the soil was, for practical purposes, not liquefiable.
2. When  $q_u$  for the cemented sand was greater than 60 kPa (8.7 psi), differences in unit weight had little influence on the resistance to liquefaction.
3. The addition of small amounts of cement (1 and 2%) to the sands substantially reduced the potential for liquefaction (see Fig. 6A.233)

Although the use of chemical stabilization to control liquefaction potential is technically viable, it has been used only infrequently in practice. No case histories have been found in the literature in which an entire liquefiable mass beneath a structure has been chemically stabilized. In two recent projects, in situ soil mixing techniques (see Sec. 6A.7.3) were used to reduce the potential for damage from liquefaction by containing the liquefiable soil within cells formed by cement-stabilized walls. In the Jackson Lake Dam modification project, cement-stabilized walls arranged in a hexagonal shape (Fig. 6A.234) were built within the liquefiable soils beneath the earth dam (Taki and Yang, 1991). Research has shown that soil-cement walls constructed in a cellular arrangement can reduce seismically generated pore pressures within loose granular soils by as much as 90%. In a similar application, soil-cement walls were constructed in a circular pattern beneath the walls of two spill tanks for a paper mill (Broomhead and Jasperse, 1992). The soil-cement walls were intersected by cross-drains at regular intervals to allow water generated by the dissipation of excess pore water pressures to drain to the exterior of the tanks (Fig. 6A.235). The cross-drains were connected by a continuous perimeter drain inside the wall footing, which in turn was connected to a gravel drainage blanket beneath the entire floor slab.

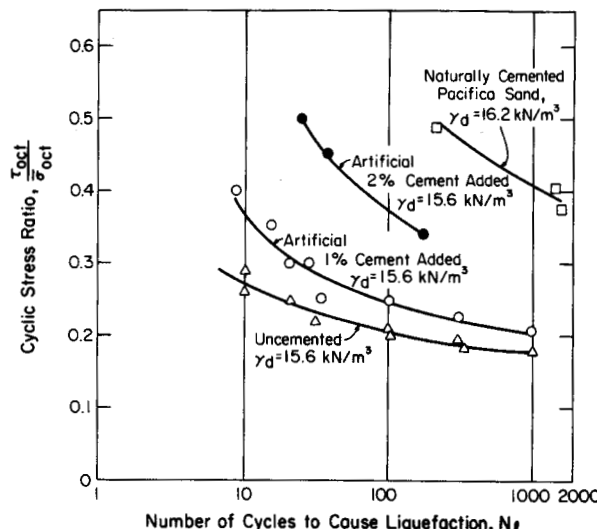


**FIGURE 6A.233** Influence of cementation on the number of cycles required to cause liquefaction of cemented sands (from Clough et al., 1989).

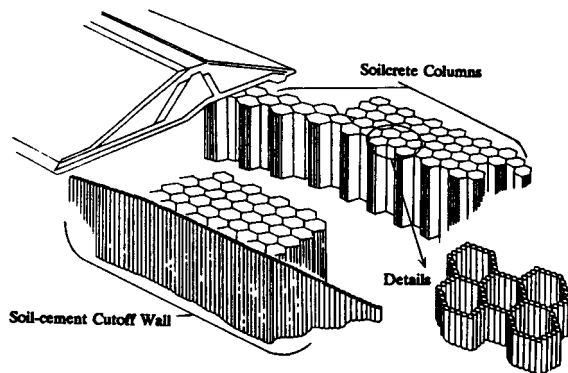


**FIGURE 6A.234** Schematic illustration of the soil-cement walls used to control liquefaction potential in the Jackson Lake Dam modification project (from Taki and Yang, 1991).

### 6A.7.3 Construction Methods

Numerous methods can be used to incorporate chemical stabilizers within soils. These methods can be divided into two general categories—*injection* and *mixing*. The information provided in this section is meant not as a complete treatment of the subject but as a summary of the principles, techniques, and equipment used to effect chemical stabilization of soils. Additional details on this topic can be found in NCHRP (1976), PCA (1979), Boynton and Blacklock (1985), Little and coworkers (1987), TRB (1987), and Broms (1993).

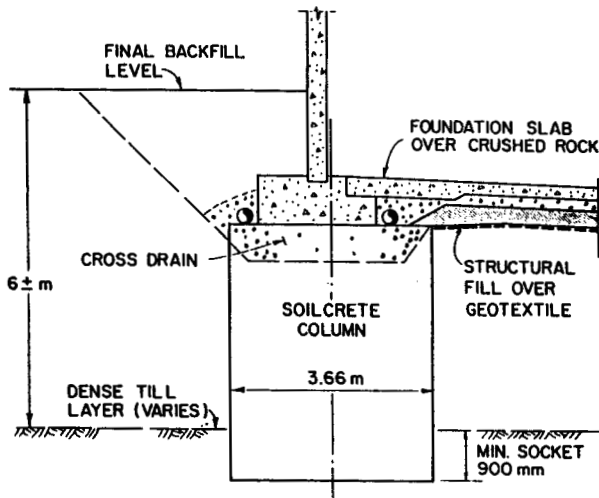


**FIGURE 6A.235** Foundation details showing soil-cement walls used to control liquefaction potential beneath two spill tanks (Broomhead and Jasperse, 1992).

**6.318** SOIL IMPROVEMENT AND STABILIZATION**6A.7.3.1 Injection**

Chemical stabilizers contained within solutions or suspensions (slurries) can be injected into the soil through the openings (void spaces and cracks). Many techniques have been used to inject chemical stabilizers into soils, some of which are similar or the same as those used for grouting (see Sec. 6B). In the following discussions, a technique is described to inject Soil Sta, a proprietary organic chemical stabilizer (refer to Sec. 6A.7.2.2). Bear in mind that Soil Sta is used almost exclusively in remedial applications to stabilize expansive soils beneath existing foundations, and the following discussions are necessarily aimed toward that application.

In special cases in the United States and for most applications within the United Kingdom, chemical injection is performed through a specially designed stem. In the system utilized, Soil Sta is injected under pressure to some depth—usually 4 to 6 ft (1.2 to 1.8 m). Penetration of the stem is accomplished by pumping through the core and literally washing the tool down. Once positioned, the hand valves are switched to close the core and divert flow into the annular space and out the injection ports (Fig. 6A.236).

In some instances, a particular soil might tend to resist penetration by Soil Sta. Both the rate of penetration and the volume of chemical placed can be enhanced by utilizing hydraulic pulsation (high pressure of short duration) during the injection phase. Alternatively, the stem can be equipped with a packer assembly to isolate selective zones (Fig. 6A.237). This equipment permits higher injection pressures and also allows some zone selectivity.

From a practical viewpoint, minimal concern should be given to the exact volume of chemical injected into a specific hole. The primary intent is to distribute the stabilizer volume reasonably uniformly over the area to be treated. Time (days, weeks, or months—depending on the specific site conditions) will produce a nearly equal distribution.

A similar analysis would be true for depth interval injection. Within a short depth (that is, 6 ft  $\approx$  2 m or less), chemical penetration can be fairly uniform given time, although placement of the stinger might vary a foot (0.3 m) or so one way or the other. This condition could change if two factors coexisted: (a) The depth of penetration is increased substantially, that is, 15 to 20 ft (4.6 to 6 m), and (b) packers or other positive seal methods are used to isolate each zone to be injected. Even in the latter example, true penetration of the zone may not occur if the placement pressure or specific soil characteristics favor communication between zones. No matter what precautions might be taken, the normal heterogeneous and fractured nature of the soil would tend to preclude exact placement of a specified volume.

At a pressure differential of about 3.5 psi (24 kPa), the system in Fig. 6A.236 would theoretically place about 12 gal/min (45 L/min) *neglecting line friction*. Hence, 10 s would theoretically place 2 gal (7.6 L) of chemical through the stinger perforations. [This volume equates to  $\frac{1}{8}$  gal/ $\text{ft}^2$  (5 L/ $\text{m}^2$ ) on a 4-ft (1.2-m) spacing pattern.] By timing the period of injection and maintaining a reasonably constant supply pressure, an acceptably uniform treatment spread would result. Carelessness in either timing or pressure would not be disastrous so long as it was not excessive. [In field practice, a pressure differential of about 60 psi (414 kPa) delivered 2 gal (7.6 L) of chemical in 30 s through the stinger and approximately 60 ft (18.3 m) of  $\frac{1}{2}$ -in (12.7-mm) ID hose.] The following equations are used to calculate velocities and pressure differentials:

Annular velocity is

$$V_a = \frac{Q}{A} \quad (6A.139)$$

which for an annular area,  $A = 0.175 \text{ in}^2$  ( $113 \text{ mm}^2$ ) reduces, to

$$V_a(\text{ft/s}) = 1.83 Q \text{ for } Q \text{ in gal/min} \quad (6A.140a)$$

$$V_a(\text{m/s}) = 0.148 Q \text{ for } Q \text{ in L/min} \quad (6A.140b)$$

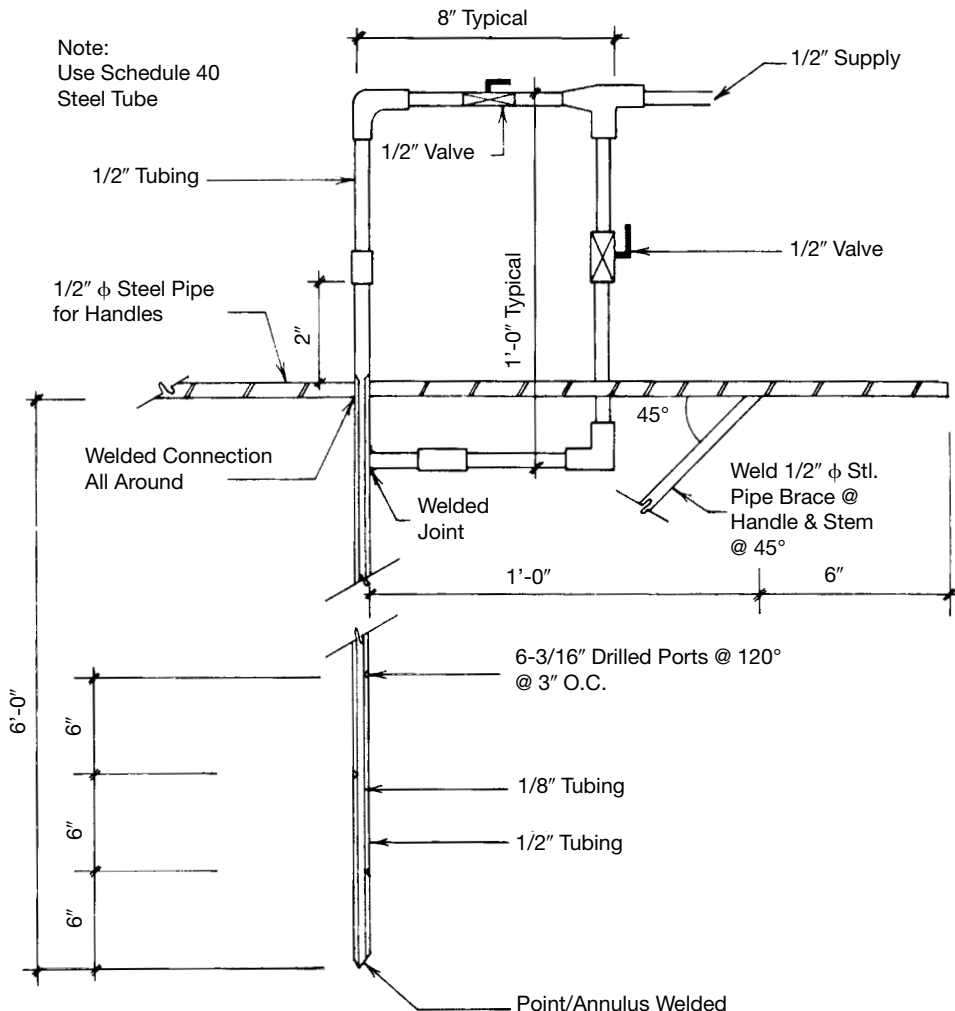


**FIGURE 6A.236** Pressure injection stem (from Brown, 1992).

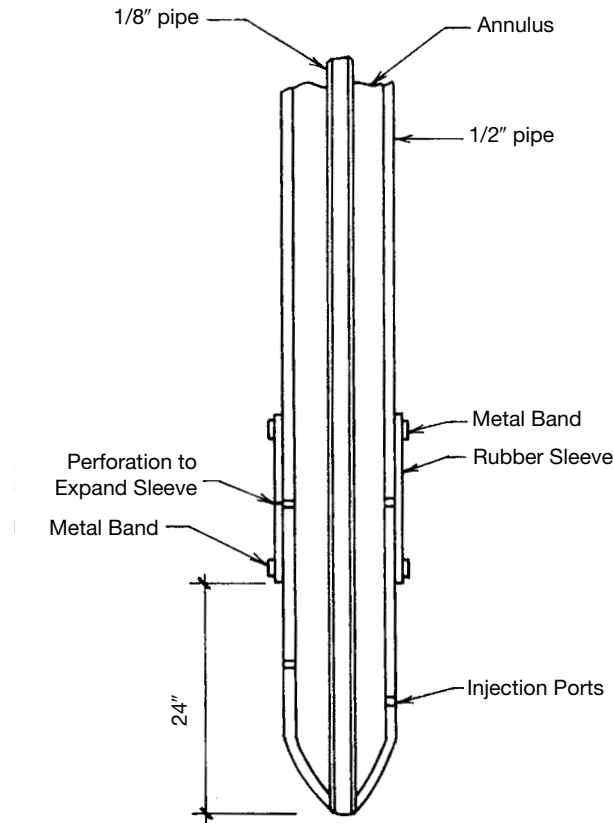
Port velocity

$$V_p = \frac{Q}{A_p C_D} = \frac{4Q}{D_p^2 \pi n C_D} \quad (6A.141)$$

which for  $D_p = \frac{3}{16}$  in (4.8 mm), the number of ports,  $n = 6$ , and the discharge coefficient  $C_D = 0.8$  (Brown and Gilbert, 1957), reduces to

$$V_p (\text{ft/s}) = 2.42 Q \text{ for } Q \text{ in gal/mm} \quad (6A.142a)$$

$$V_p (\text{m/s}) = 0.195 Q \text{ for } Q \text{ in L/min} \quad (6A.142b)$$

**6.320** SOIL IMPROVEMENT AND STABILIZATION

**FIGURE 6A.237** Injection stinger with pack-off (from Brown, 1992).

The pressure differential is represented as

$$\Delta P = \frac{\gamma_f(V_p^2 - V_a^2)}{2g} = \frac{\rho_f(V_p^2 - V_a^2)}{2} \quad (6A.143)$$

where  $\gamma_f$  = unit weight (weight density) of the fluid ( $= 62.43 \text{ pcf} = 9.807 \text{ kN/m}^3$  for water)

$\rho_f$  = mass density of the fluid ( $= 1.0 \text{ Mg/m}^3 = 1000 \text{ kg/m}^3$  for water)

$g$  = acceleration owing to gravity  $= 32.17 \text{ ft/s}^2 = 9.807 \text{ m/s}^2$

For  $V_p$  and  $V_a$  in ft/s [from Eqs. (6A.140a) and (6A.142a), Eq. (6A.143) can be represented as

$$\Delta P (\text{psi}) = \frac{G_f(V_p^2 - V_a^2)}{148} \quad (6A.144a)$$

where  $G_f$  is the specific gravity of the fluid ( $= 1.0$  for water).

For  $V_p$  and  $V_a$  in m/s [from Eqs. (6A.140b) and (6A.142b), Eq. (6A.143) can be represented as

$$\Delta P \text{ (kPa)} = \frac{G_f(V_p^2 - V_a^2)}{2} \quad (6A.144b)$$

Force developed from the hydraulic pressure is

$$F = PA \quad (6A.145)$$

where  $F$  = force

$P$  = pressure

$A$  = area

Equation (6A.145) illustrates the factors that create a lifting force on a foundation. Generally, pressure injection of chemical soil stabilizers does not involve lifting, as mudjacking or pressure grouting would. In fact, as a rule, chemical injection pressures are limited to prevent lifting. The safe operating pressure could then be estimated from the rearrangement of Eq. (6A.145) as follows:

$$P = \frac{F}{A} \quad (6A.146)$$

#### 6A.7.3.2 Mixing

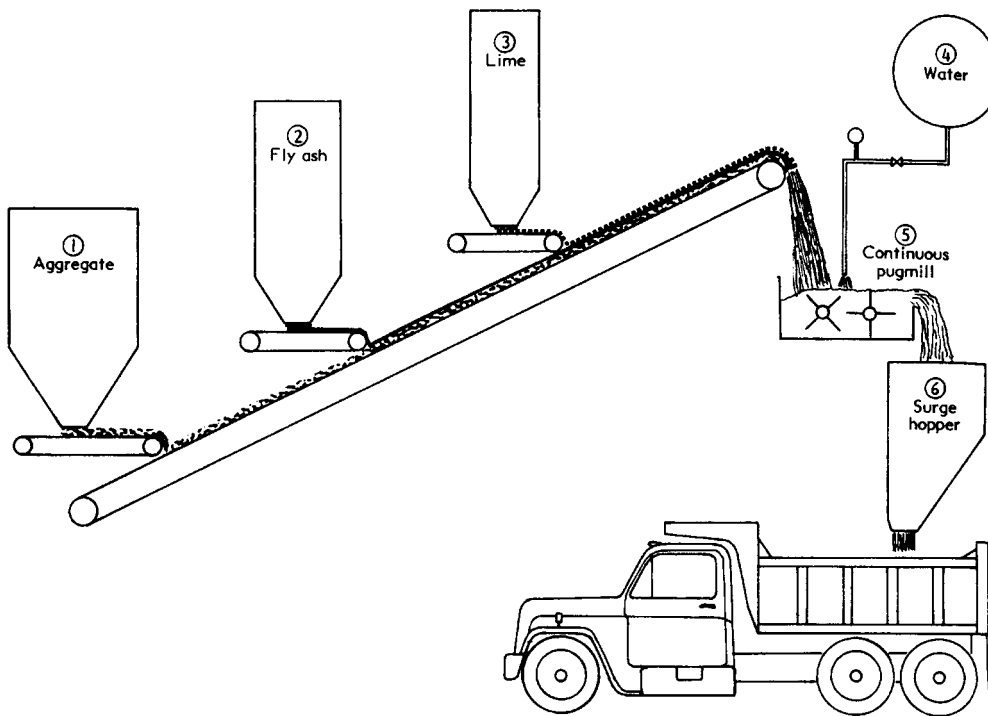
The primary objective of all mixing techniques is to obtain a thorough mixture of soil and stabilizer at an appropriate moisture content. There are three main types of mixing methods, broadly categorized as off-site, on-site, and deep in situ mixing. A general overview of these mixing methods will be given in the following subsections.

*Off-Site Mixing.* In off-site mixing techniques, excavated or borrow material is brought to the mixing site, stabilizers and water (if required) are thoroughly mixed with the soil, and the mixture is then hauled to the site for spreading and compaction. Depending upon preference or performance, the soil can be brought to the compaction moisture content either during the off-site mixing process or on-site with the soil remixed to distribute thoroughly the additional water. If the haul distances are very long or if there is a long delay between the off-site mixing and on-site compaction of the material, the soil should be brought to the compaction water content on-site to avoid potentially substantial losses in strength and stiffness of the stabilized material (see Sec. 6A.7.2.5).

Off-site mixing can be performed either in pads or in a central plant. When prepared in a mixing pad, the soil is spread on the ground surface and the stabilizer is added in either a dry or wet condition. If applied wet, the stabilizer is contained within either a thick suspension (slurry) or a solution depending on the chemical nature of the stabilizer and the primary fluid (usually water). Mixing is accomplished using a disc harrow, a grader, or a traveling mixing machine (see below for discussion of different types of mixing equipment).

The most common type of off-site mixing is conducted in a central plant. A typical layout of a plant for lime–fly ash mixtures is shown schematically in Fig. 6A.238, which is also typical of the plants used for lime and cement stabilization except only one stabilizer is added instead of two. The main components of a mixing plant are as follows (NCHRP, 1976):

1. Conveyor system
2. Aggregate hopper with belt feeder
3. Hoppers for stabilizers with feed control devices
4. Water storage tank with calibrated pump
5. Surge hopper for temporary storage of soil-stabilizer mixture

**6.322** SOIL IMPROVEMENT AND STABILIZATION

**FIGURE 6A.238** Schematic diagram of typical plant layout for lime–fly ash–aggregate (LFA) mixtures (from NCHRP, 1976).

As soon as possible after mixing, the soil-stabilizer mixture is hauled to the site in open-bed or bottom dump trucks. If the haul distances are long, or if drying or scattering of the material en route is a problem, the trucks should be covered with tarpaulins or other suitable covers.

Some soils, particularly highly plastic clays, cannot be adequately pulverized and mixed in central mixing plants unless the soils are modified beforehand with a small amount of stabilizer to reduce plasticity and increase agglomeration. If feasible, however, central plant mixing accomplishes the most thorough and uniform mixing and reduces safety problems associated with the chemicals (for example, health problems for workers caused by the causticity of lime).

*On-Site Mixing.* On-site mixing can be accomplished in test pads, in a plant, or in portable mechanical mixers or through use of mixed-in-place techniques. Details on mixing in test pads or a central plant are given in the previous section. Mixing in pads is usually conducted off-site rather than on-site owing to a lack of sufficient on-site open space in most cases. On-site mixing plants are similar in concept and equipment to off-site plants but are usually smaller and hence cannot produce mixing at the same volumetric rate. The portable mechanical mixers used to mix soil and stabilizer are the same as or similar to the portable mixers used for concrete.

Mixed-in-place methods can be used on excavated materials, borrow materials, or in situ surficial soils. When borrow or excavated materials are mixed in place, the soil is first spread in either uniform layers or windrows. Wet or dry stabilizer is then added to the soil. Dry stabilizer can be added either in bags (lime or cement) or in bulk from pneumatic tanker trucks or mechanical spreaders. Bags are typically spotted by hand by dropping them at previously marked locations from a slowly moving truck. The bags are then slit open and the contents dumped into piles or

transverse windrows across the area to be stabilized. The cement or lime is leveled by hand raking, or using a spike-tooth harrow, a nail drag, or a length of chain-link fence pulled by a tractor or truck. When both lime and fly ash are used, they can be spread separately, or if dry they can be preblended before being added to the soil. After lime (but not cement or lime–fly ash) is placed, the surface is usually sprinkled with water to reduce dusting. Either hydrated lime or quicklime can be added to the soil as a slurry. Lime and water are mixed in a central mixing tank, jet mixer, or tank truck and spread by either gravity or pressure spraying from a tank truck through spray bars.

Many different types of equipment can be used to mix soil and stabilizer in place. Pugmill travel plants can be used on excavated or borrow materials only. When hopper-type pugmill travel plants are used, soil is dumped into a hopper from a dump truck, and stabilizer and water (if desired) are added prior to mixing. Water can also be added after the soil-stabilizer mixture has been placed. For windrow-type pugmill travel plants, soil is placed in windrows and stabilizer added using one of the methods described in the previous paragraph. Rotary mixers, graders, and disc harrows can be used on excavated, borrow, or *in situ* surficial soils.

The difficulty of *in-place* mixing increases with increasing fineness and plasticity of the soils being treated. A double application of lime (modification of the soil with a small amount of lime followed by a suitable period for curing and then a second treatment for stabilization) or modification with lime prior to stabilization with cement or lime–fly ash, is often required when highly plastic clays ( $PI \geq 50$ ) are to be stabilized. In general, compaction should begin as soon as possible after mixing is completed.

After mixing, accomplished by any of the off-site or on-site methods, and placement, the stabilized soil must be compacted. The same equipment and methods used for near-surface compaction (see Sec. 6A.3.1 for details) can also be used for chemically stabilized soils. For cohesive soils, tamping foot or sheepfoot rollers are typically used. Static or vibratory rubber-tired or smooth-drum rollers are generally used to compact granular soils or chemically modified cohesive soils that behave essentially as granular materials. When a relatively smooth surface finish is desired, smooth drum rollers can be used to proof-roll the material.

Compaction should commence as soon as possible after uniform mixing of soil, stabilizer, and water has taken place. It is common to specify that the chemically treated materials be compacted within 2 h after mixing. Because the reactions associated with lime stabilization are slow compared to those that occur in cement and lime–fly ash stabilization, additional time may be available between mixing and compaction for lime-treated soils.

A typical density specification for a chemically treated soil is a minimum relative compaction of 95% based on standard Proctor maximum dry density. However, the actual specification given on any project should be based on criteria that will yield the desired engineering characteristics. The reference Proctor tests should be conducted on samples of the soil treated with the same percentage of stabilizer used in the field and allowing the same delay between mixing and compaction as the average (or maximum) delay that occurs in the field. The specifications for compaction moisture condition are critical to successful stabilization. If the soil is too dry when compacted, incomplete hydration of the stabilizer may occur, resulting in engineering properties that may not meet the requirements for the project. In general, the compaction water content should not be less than standard Proctor optimum water content, which may be several percentage points higher than modified Proctor optimum water content. The specifications for compaction water content ideally should be based on the results of laboratory or field tests conducted to establish the range in water contents that will produce the desired engineering characteristics.

*Deep in Situ Mixing.* Although deep *in situ* soil mixing techniques originated in the United States in the 1950s, the major development of these methods has occurred over the last two decades in Japan and Sweden (Broomhead and Jasperse, 1992; Hausmann, 1990). Although the techniques were developed almost concurrently in Japan and Sweden and are similar in concept, they are generally referred to by different names—*deep soil mixing* for the Japanese method and *lime columns* for the Swedish method. In general, unslaked lime (quicklime,  $CaO$ ) is used as the primary stabilizer in the Swedish method, and cement is used most frequently in the Japanese method. Other stabi-

**6.324** SOIL IMPROVEMENT AND STABILIZATION

lizers and additives that have been used include fly ash, furnace slag, gypsum, hydroxyalumininum, potassium chloride, and bentonite (Broomhead and Jasperse, 1992; Broms, 1993).

Lime columns are used only in soft clays and silts. The mixing tool, which is shaped like a giant dough mixer (see Fig. 6A.239), is rotated down to the depth that corresponds to the desired length of the columns (Broms 1993). The direction of rotation is then reversed, and the mixing tool is slowly withdrawn as quicklime is forced into the soil by compressed air pushing through holes located just above the horizontal blades of the mixing tool. The blades are inclined so that the stabilized soil will be compacted during the withdrawal of the tool. The rotary table and kelly are on a mast, which

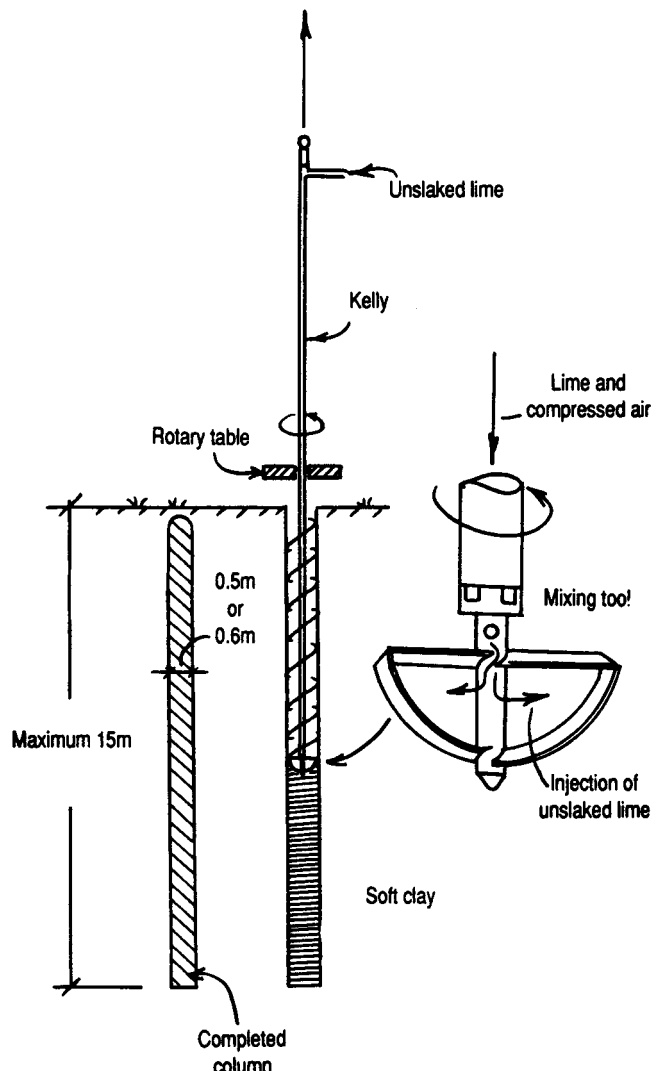


**FIGURE 6A.239** Typical equipment used to manufacture lime columns (from Broms, 1993).

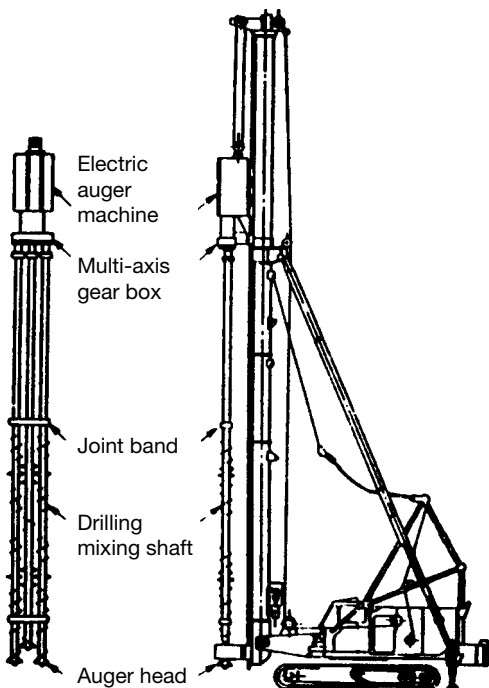


**FIGURE 6A.240** Typical equipment used to manufacture deep soil-cement mixed columns (from Taki requiring the soil to be kept moist are to and Yang, 1991).

is mounted on either a standard front wheel loader or on a special off-road vehicle. The lime-stabilized columns are typically 0.5 to 0.6 m (1.6 to 2.0 ft) in diameter and can be constructed up to about 30 m (100 ft) in length.

Deep soil mixing can be used in soils ranging from soft clays to gravels (Broomhead and Jasperse, 1992; Taki and Yang, 1991). The equipment used in deep soil mixing consists of a crane-supported set of leads that guide a series of one to eight hydraulically driven mixing augers, as illustrated in Fig. 6A.240. The augers are typically 0.45 to 1.0 m (1.5 to 3.3 ft) in diameter, and columns of more than 60 m (200 ft) in length can be constructed. Each auger shaft is mounted with discontinuous auger flights and mixing paddles. The purposes of the discontinuous auger flights are to provide some vertical displacement for soil mixing and to prevent the transportation of soil to the surface. As penetration by the auger flights occurs, the soil is broken loose and the cement slurry is injected into the soil through the tip of the hollow-stemmed augers. The auger flights lift the soil and slurry to the mixing paddles where the materials are blended. As the auger continues to advance, the soil and slurry are remixed by additional paddles attached to the shaft. When multiple augers are used, overlapped soil-cement columns are created that can be extended to form any geometric shape or pattern.

Lime columns have been used extensively in Sweden, Norway, and Finland, with some applications in the United States, for the following purposes (Broms, 1993):

- To improve the total and differential settlements of light structures
- To increase the settlement rate and control the settlements of relatively heavy structures
- To improve the stability of embankments, slopes, trenches, and deep cuts
- To reduce the vibrations from, for example, traffic, blasting, pile driving

More than 3,000,000 m (10,000,000 ft) of lime columns have been installed in Sweden alone since 1975, with a production rate (1990) of about 600,000 m/yr (2,000,000 ft/yr).

Deep soil mixing has been used on more than 1500 projects in Japan and the Far East and was reintroduced in the United States in 1986 (Broomhead and Jasperse, 1992; Taki and Yang, 1991).

Soil-cement walls constructed by deep soil mixing have been used in the following applications:

- Cutoff walls for ground-water control
- Walls for excavation support
- Stabilization of soft or liquefiable soils

A spinoff technology to deep soil mixing has recently been developed and has been dubbed shallow soil mixing (Broomhead and Jasperse, 1992). This process uses a single auger 1.0 to 3.7 m (3 to 12 ft) in diameter and can be used to stabilize soils to a depth of 10 m (33 ft) or less. Shallow soil mixing has been used for both geotechnical and geoenvironmental applications.

*Curing.* Three conditions are needed for proper curing of soils stabilized with cementitious or pozzolanic admixtures:

1. *Favorable temperatures.* Temperatures greater than 40°F (4°C) are needed for the cementitious or pozzolanic reactions to occur at a reasonable rate. Therefore, construction of admixture stabi-

**6.326** SOIL IMPROVEMENT AND STABILIZATION

lized soils should not commence if the temperatures during the month or so following the completion of the construction will drop below the minimum required temperature for extended periods.

2. *Passage of time.* Usually at least a 3- to 7-day undisturbed curing period is specified before any appreciable load can be applied.
3. *Moist conditions.* The primary purposes for requiring the soil to be kept moist are to ensure that adequate moisture is available for hydration of the stabilizer and to keep the shrinkage cracking to a minimum. In lime-stabilized soils, moist conditions are also needed to prevent carbonation. If the stabilized soil is backfilled immediately after construction, no special measures are required for adequate curing. If the stabilized soil is exposed to the atmosphere for more than a few hours following construction, appropriate procedures should be taken to ensure that complete curing will occur. The procedures used are of two general types—moist or asphaltic curing. In *moist curing*, the surface is sprinkled with water to keep it damp. On small jobs, the stabilized soil may also be covered with plastic sheets. Light compaction with small smooth drum rollers or vibratory plate compactors may be used, as needed, to keep the surface knitted together. *Asphaltic curing* involves sealing the surface with a coat of cutback asphalt or bituminous emulsion.

*Quality Control and Assurance.* For admixture-stabilized soils prepared by off-site or onsite mixing methods, the procedures for quality control and assurance are similar to those for compacted untreated soils (Sec. 6A.3.5), with the additional requirements that the stabilizer content and uniformity of mixing be checked. The control of stabilizer content is a two-step process involving monitoring and spot-checking the amount of stabilizer that is added to the soil and conducting tests on samples obtained from the material immediately after mixing is completed. Standard chemical analyses for determining the cement or lime content of freshly mixed, treated soils are given in ASTM D2901 and D3155, respectively.

The uniformity of cement-stabilized soils can be checked by visually inspecting the exposed soil within a trench dug across the width of the treated area and to the desired depth of treatment. A satisfactory mixture will exhibit a uniform color throughout, and a streaked appearance indicates a nonuniform mixture. Checking the uniformity of lime-soil mixtures is more difficult because the visual appearances of the untreated soil and the treated soil are the same. Phenolphthalein, a color-sensitive indicator solution, can be used to check that the minimum lime content required for soil treatment is present. When the solution is sprayed on the soil, the soil will turn a reddish pink color if free lime is available ( $\text{pH} = 12.5$ ). Short-cut strength methods can also be used.

The quality control and assurance procedures used for deep *in situ* mixing are necessarily complex because the soil is stabilized to substantial depths. Details regarding the methods used for lime columns are given in Broms (1993).

**6A.8 MOISTURE BARRIERS\***

As implied by their names, the intended purpose of horizontal or vertical moisture barriers is to prevent the seepage of moisture into or out of an expansive soil located beneath a foundation. Moisture barriers have been used as both preventive and remedial measures. Unfortunately, moisture barriers are frequently ineffective in controlling swelling in expansive soils for the following reasons (Jones and Jones, 1987):

1. Moisture may enter the protected area from below the barrier, such as by upward migration of water vapor from an underlying ground-water table.
2. Variations in moisture content of the protected soil will still occur in covered soils owing to changes in soil temperature (called hydrogenesis). Even in dry climates the air has some mois-

---

\*Coauthored by Robert Wade Brown.

ture, which enters the subgrade soil. As the ground temperatures cool at shallow depths, the moisture in the air condenses and accumulates in areas that are covered.

3. Moisture barriers cannot prevent moisture flow through shrinkage cracks, slickensides, or permeable inclusions below the barriers.

The use of moisture barriers is not a viable preventative or remedial measure for expansive soils because the money spent could be better spent on an alternative solution that is both more effective and more permanent.

#### **6A.8.1 Horizontal Barriers**

Horizontal moisture barriers are intended to prevent or substantially reduce the moisture loss from an area of soil resulting primarily from evaporation. A typical design of a horizontal barrier using a polyethylene membrane overlain by a thin layer of gravel is depicted in Fig. 6A.241. Membranes made from polyvinyl chloride (PVC) and polypropylene have also been used. These plastic membranes typically range from about 4 to 20 mils (0.2 to 0.8 mm) in thickness. Other materials that have been used to make the impervious barrier include concrete and asphalt. Regardless of the type of barrier material used, construction techniques are important to the effectiveness of the barriers (Nelson and Miller, 1992). Care should be taken to seal joints, seams, rips, or holes in the barrier.

Jones and Jones (1987) indicate that the effectiveness of horizontal barriers can be improved in the following ways:

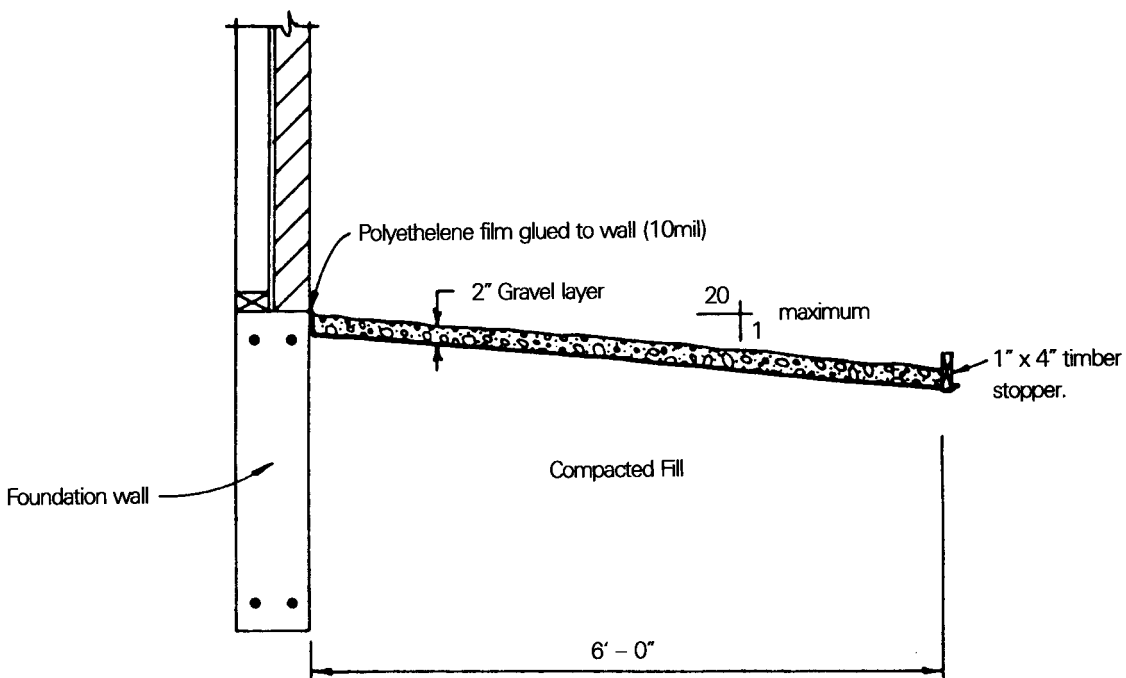


**FIGURE 6A.241** Horizontal moisture barrier consisting of a polyethylene membrane overlain by a thin gravel layer (from Chen, 1988).

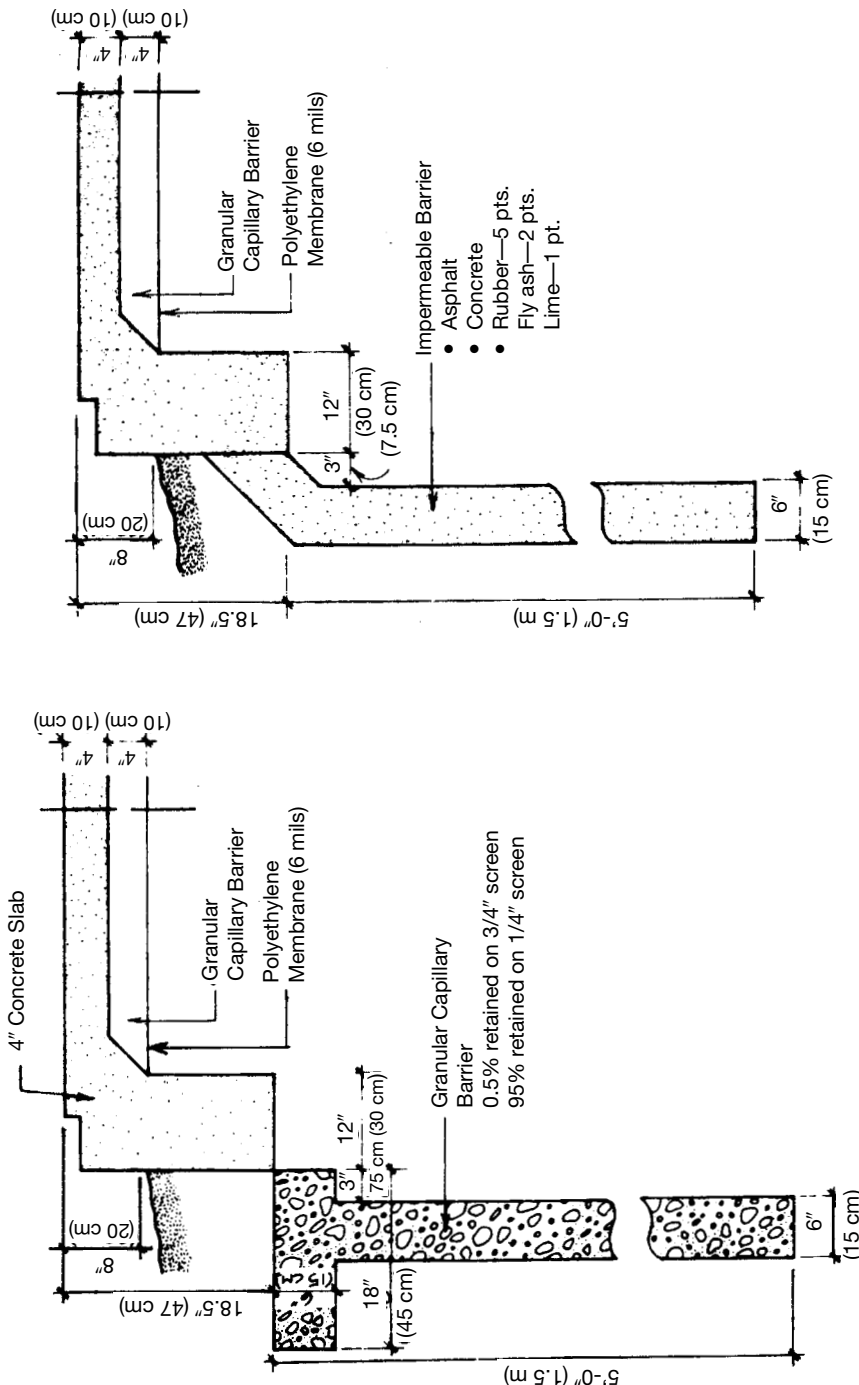


FIGURE 6A.242 Typical permeable and impermeable vertical moisture barriers (from Brown, 1992).

1. The barriers should be placed at least 2 ft (0.6 m) below the ground surface because at this depth, the daily variations in soil temperature are negligible.
2. The preconstruction moisture condition of the bearing soil and the soil underlying the barrier should be controlled to maintain a high water content that is uniform throughout the soil.
3. Open areas surrounding the barriers should be irrigated regularly using a sprinkler system to sustain a consistently high water content.

Even if the measures outlined above are taken, the behavior of a horizontal barrier is not reliably predictable. Discussions of data reflecting the success or benefit in using horizontal barriers can be found in Chen (1988) and Nelson and Miller (1992). Both sources seem to agree that a horizontal barrier does little to prevent or lessen the increase in moisture (heave) within a foundation soil over several years. However, the presence of a barrier does seem to cause the buildup in moisture to develop more slowly and to be more uniform. The pertinent question is whether these benefits justify the cost.

#### **6A.8.2 Vertical Barriers**

Vertical moisture barriers are intended to avoid or substantially limit the lateral transfer of water between the foundation bearing soils and those outside the perimeter. The theory is that if expansive soils are maintained at a constant level of moisture, no volumetric changes occur. The vertical barrier can consist of an excavated trench lined or filled with any impermeable material such as polyethylene membrane, fiberglass, asphalt, concrete, semihardening slurries, or sometimes even tar paper (see Fig. 6A.242). If polyethylene membrane is used, it should be sufficiently thick and durable to resist puncturing and tearing during installation. The trench should ideally extend as deep as the zone of seasonal changes in moisture (active zone). Sometimes a horizontal barrier is used with a vertical barrier to prevent wetting of the soil between the vertical barrier and the building.

The published data dealing with the effectiveness of impermeable vertical barriers are similar to those described for horizontal barriers. Vertical barriers tend to reduce increases in soil moisture (heave) during the first year or so; however, after 4 or 5 years, the results become nearly the same with or without the barrier. As with horizontal barriers, the rate of increase in moisture is generally slower and more uniform when a vertical barrier is used. Again the question arises: Does the result justify the cost? As stated by Chen (1988), "... in view of the high cost involved in the installation of a vertical moisture barrier, especially where great depth is required, it is doubtful that such an installation is of sufficient merit to warrant the expense."

A variation of this design is the permeable, vertical soil barrier, also shown in Fig. 6A.242. This technique is primarily intended to prevent or minimize external water from entering the bearing soil matrix, somewhat similar to a French drain. Published information on the performance of permeable vertical barriers is not readily available.

#### **REFERENCES**

---

- Aboshi, H., Ichimoto, E., Enoki, M., and Harada, K. (1979). "The 'Compozer'—a Method to Improve Characteristics of Soft Clays by Inclusion of Large Diameter Sand Columns." *Proceedings of the International Conference on Soil Reinforcement*, Paris, Vol. 1, pp. 211–216.
- Ahlberg, H. L., and Barenberg, E. J. (1965). "Pozzolanic Pavements." *Bulletin 473*, Engineering Experiment Station, University of Illinois, Urbana.
- Alwail, T. A., Ho, C. L., and Fragaszy, R. J. (1992). "Collapse Mechanisms of Low Cohesion Compacted Soils." *Bulletin of the Association of Engineering Geologists*, Vol. 29, No. 4, pp. 345–353.
- ASCE (1987). *Soil Improvement—A Ten Year Update*, Geotechnical Special Publication No. 12, edited by J. P. Welsh.

**6.330** SOIL IMPROVEMENT AND STABILIZATION

- ASCE (1997). *Ground Improvement, Ground Reinforcement, Ground Treatment: Developments 1987–1997*, Geotechnical Special Publication No. 69, Edited by V. R. Schaefer, American Society of Civil Engineers.
- ASTM (1991). *Annual Book of Standards, Volume 04.08: Soil and Rock; Dimension Stone; Geosynthetics*, American Society for Testing and Materials, Philadelphia.
- Baez, J. I. (1995). "A Design Model for the Reduction of Soil Liquefaction by Vibro-Stone Columns." Ph.D. Dissertation, University of Southern California, Los Angeles, California.
- Ballard, L. F., and Gardner, R. P. (1965). "Density and Moisture Content Measurements by Nuclear Methods." *National Cooperative Highway Research Program Report No. 14*, Highway Research Board, Washington, D.C.
- Barden, L., and Pavlakis, G. (1971). "Air and Water Permeability of Compacted Unsaturated Cohesive Soil." *Journal of Soil Science*, Vol. 22, No. 3, pp. 302–317.
- Barden, L., and Sides, G. R. (1970). "Engineering Behavior and Structure of Compacted Clay." *Journal of the Soil Mechanics and Foundations Division*, ASCE, Vol. 96, No. SM4, July, pp. 1171–1200.
- Barendsen, D. A., and Kok, L. (1983). "Prevention and Repair of Flow Slides by Explosion." *Proceedings of the Eighth European Conference on Soil Mechanics and Foundation Engineering*, pp. 205–208.
- Barksdale, R. D., and Bachus, R. C. (1983). "Design and Construction of Stone Columns—Volume 1." *Report No. FHWA/RD-83/026*, Federal Highway Administration, Washington, D.C.
- Barksdale, R. D., and Dobson, T. (1983). "Improvement of Marginal Urban Sites Using Stone Columns and Rigid Concrete Columns." Presented at the 34th Annual Highway Geology Symposium, Stone Mountain, Georgia, May.
- Baumann, V., and Bauer, G. E. A. (1974). "The Performance of Foundations on Various Soils Stabilized by the Vibro-Compaction Method." *Canadian Geotechnical Journal*, Vol. 11, pp. 509–530.
- Bell, F. G. (1988). "Stabilization and Treatment of Clay Soils with Lime: Part 1—Basic Principles." *Ground Engineering*, British Geotechnical Society, London, Vol. 21, No. 1, January, pp. 10–15.
- Benson, C. H., Abichou, T. H., Olson, M. A., and Bosscher, P. J. (1995). "Winter Effects on Hydraulic Conductivity of Compacted Clay." *Journal of Geotechnical Engineering*, ASCE, Vol. 121, No. 1, January, pp. 69–79.
- Benson, C. H., and Daniel, D. E. (1990). "Influence of Clods on the Hydraulic Conductivity of Compacted Clay." *Journal of Geotechnical Engineering*, ASCE, Vol. 116, No. 8, August, pp. 1231–1248.
- Benson, C. H., Abichou, T. H., Olson, M. A., and Bosscher, P. J. (1995). "Winter Effects on Hydraulic Conductivity of Compacted Clay." *Journal of Geotechnical Engineering*, ASCE, Vol. 121, No. 1, January, pp. 69–79.
- Bergado, D. T., Anderson, L. R., Miura, N., and Balasubramaniam, A. S. (1996). "Prefabricated Vertical Drains." Chapter 4 in *Soft Ground Improvement in Lowland and Other Environments*, ASCE, New York, pp. 88–185.
- Bergado, D. T., Asakami, H., Alfaro, M. C., and Balasubramaniam, A. S. (1991). "Smear Effects of Vertical Drains on Soft Bangkok Clay." *Journal of Geotechnical Engineering*, ASCE, Vol. 117, No. 10, October, pp. 1509–1530.
- Bishop, A. W. (1959). "The Principle of Effective Stress." *Teknisk Ukeblad*, Vol. 39, pp. 859–863.
- Bishop, A. W., Alpan, I., Blight, G. E., and Donald, I. B. (1960). "Factors Controlling the Strength of Partly Saturated Cohesive Soils." *Proceedings of the Research Conference on Shear Strength of Cohesive Soils*, ASCE, Boulder, Colorado, pp. 503–532.
- Bishop, A. W., and Eldin, A. K. G. (1953). "The Effect of Stress History on the Relation between  $\phi$  and Porosity in Sand." *Proceedings of the Third International Conference on Soil Mechanics and Foundation Engineering*, Zurich, Switzerland, Vol. 1, pp. 100–105.
- Blight, G. E. (1965). "A Study of Effective Stresses for Volume Change." *Moisture Equilibria and Moisture Changes in Soils beneath Covered Areas*, edited by U. D. Aitchison, Butterworths, Sydney, Australia.
- Booth, A. R. (1976). "Compaction and Preparation of Soil Specimens for Oedometer Testing." *Soil Specimen Preparation for Laboratory Testing*, ASTM STP 599, American Society for Testing and Materials, Philadelphia, Pennsylvania, pp. 216–228.
- Booth, A. R. (1977). "Collapse Settlement in Compacted Soils." *CSIR Research Report 324*, Council for Scientific and Industrial Research, Pretoria, South Africa.
- Bouyoucos, G. J. (1931). "The Alcohol Method for Determining the Water Content for Soils." *Soil Scientist*, Vol. 32, pp. 173–179.
- Bowders, J. J., Jr., Gidley, J. S., and Usman, M. A. (1990). "Permeability and Leachate Characteristics of Stabilized Class F Fly Ash." *Transportation Research Record No. 1288: Geotechnical Engineering 1990*, Transportation Research Board, Washington, D.C., pp. 70–77.
- Bowles, J. E. (1975). "Combined and Special Footings." Ch. 16 in *Foundation Engineering Handbook*, edited by H. F. Winterkorn and H.-Y. Fang, Van Nostrand Reinhold, New York, pp. 504–527.

- Bowles, J. E. (1987). "Elastic Foundation Settlements on Sand Deposits." *Journal of Geotechnical Engineering*, ASCE, Vol. 113, No. 8, pp. 846–860.
- Bowles, J. E. (1988). *Foundation Analysis and Design*, 4th ed., McGraw-Hill, New York.
- Boynton, R. S., and Blacklock, J. R. (1985). "Lime Slurry Pressure Injection Bulletin." *Bulletin No. 331*, National Lime Association, Arlington, Virginia.
- Boynton, S. S., and Daniel, D. E. (1985). "Hydraulic Conductivity Tests on Compacted Clay." *Journal of Geotechnical Engineering*, ASCE, Vol. 111, No. 4, April, pp. 465–478.
- Brand, W., and Schoenberg, W. (1959). "Impact of Stabilization of Loess with Quicklime on Highway Construction." *Highway Research Board Bulletin No. 231: Lime and Lime-Flyash as Soil Stabilizers*, Washington, D.C., pp. 18–23.
- Brauns, J. (1978). "Initial Bearing Capacity of Stone Columns and Sand Piles." *Proceedings of the Symposium on Reinforcing and Stabilizing Techniques*, Sydney, Australia, pp. 477–496.
- Broderick, G. P., and Daniel, D. E. (1990). "Stabilizing Compacted Clay against Chemical Attack." *Journal of Geotechnical Engineering*, ASCE, Vol. 116, No. 10, October, pp. 1549–1567.
- Broms, B. B. (1993). "Lime Stabilization." Chapter 4 in *Ground Improvement*, edited by M. P. Moseley, CRC Press, Boca Raton, Florida, pp. 65–99.
- Broms, B. B., and Forssblad, L. (1969). "Vibratory Compaction of Cohesionless Soils." *Proceedings of the Seventh International Conference on Soil Mechanics and Foundation Engineering*, Specialty Session No. 2, pp. 101–118.
- Broomhead, D., and Jasperse, B. H. (1992). "Shallow Soil Mixing—a Case History." *Grouting, Soil Improvement and Geosynthetics*, edited by R. H. Borden, R. D. Holtz, and I. Juran, ASCE Geotechnical Special Publication No. 30, Vol. 1, pp. 564–576.
- Brown, R. W. (1989). *Design and Repair of Residential and Light Commercial Foundations*, McGraw-Hill, New York.
- Brown, R. W. (1992). *Foundation Behavior and Repair: Residential and Light Commercial*, 2d ed., McGraw-Hill, New York.
- Brown, R. W., and Gilbert, B. (1957). "Pressure Drop Perforations Can Be Computed." *Petroleum Engineer*, September.
- Bureau of Reclamation (1968). *Earth Manual*, rev. ed., U.S. Bureau of Reclamation, Denver, Colorado.
- Burland, J. B., and Burbidge, M. C. (1985). "Settlement of Foundations on Sand and Gravel." *Proceedings of the Institution of Civil Engineers*, part 1, Vol. 78, December, pp. 1325–1381.
- Burnister, D. M. (1945). "The General Theory of Stresses and Displacements in Layered Soil Systems." *Journal of Applied Physics*, Vol. 16, No. 2, pp. 89–96; No. 3, pp. 126–127; No. 5, pp. 296–302.
- Burnister, D. M. (1958). "Evaluation of Pavement Systems of the WASHO Road Test by Layered System Methods." *Highway Research Board Bulletin 177*, Washington, D.C., pp. 26–54.
- Burnister, D. M. (1962). "Application of Layered System Concepts and Principles to Interpretations and Evaluations of Asphalt Pavement Performances and to Design and Construction." *Proceedings of the International Conference on Structural Design of Pavements*, University of Michigan, Ann Arbor, pp. 441–453.
- Butt, G. S., Demirel, T., and Handy, R. L. (1968). "Soil Bearing Tests Using a Spherical Penetration Device." *Highway Research Record No. 243: Soil Properties from in Situ Measurements*, Highway Research Board, Washington, D.C., pp. 62–74.
- Carillo, N. (1942). "Simple Two- and Three-Dimensional Cases in the Theory of Consolidation of Soils." *Journal of Mathematics and Physics*, Vol. 21, No. 1, pp. 1–5.
- Carter, D. P., and Seed, H. B. (1988). "Liquefaction Potential of Sand Deposits under Low Levels of Excitation." *Report No. UCB/EERC-88/11*, University of California at Berkeley, College of Engineering.
- Casagrande, A. (1936a). "Characteristics of Cohesionless Soils Affecting the Stability of Slopes and Earth Fills." *Journal of the Boston Society of Civil Engineers*, January; reprinted in *Contributions to Soil Mechanics 1925–1940*, BSCE, pp. 257–276.
- Casagrande, A. (1936b). "The Determination of the Preconsolidation Load and Its Practical Significance." *Proceedings of the First International Conference on Soil Mechanics and Foundation Engineering*, Cambridge, Vol. 3, pp. 60–64.
- Casagrande, A. (1938). "Notes on Soil Mechanics—First Semester." Harvard University (unpublished), cited in Holtz, R. D. and Kovacs, W. D. (1981).
- Chamberlain, E. J., Iskander, I., and Hunsicker, S. E. (1990). "Effect of Freeze-Thaw Cycles on the Permeability and Macrostructure of Clays." *Proceedings of the International Symposium on Frozen Soil Impacts on Agricultural, Range, and Forest Lands, CRREL Special Report 90-1*, U.S. Army Corps of Engineers Cold Regions Research and Engineering Laboratory, Hanover, New Hampshire, pp. 145–155.
- Chen, F. H. (1988). *Foundations on Expansive Soils*, Elsevier Science Publishers, New York.
- Clare, K. E., and Sherwood, P. T. (1954). "The Effect of Organic Matter on the Setting of Soil-Cement Mix-

**6.332** SOIL IMPROVEMENT AND STABILIZATION

- tures." *Journal of Applied Chemistry*, Society of Chemical Industry, London, Vol. 4, November, pp. 625–630.
- Clare, K. E., and Sherwood, P. T. (1956). "Further Studies on the Effect of Organic Matter on the Setting of Soil-Cement Mixtures." *Journal of Applied Chemistry*, Society of Chemical Industry, London, Vol. 6, August, pp. 3 17–324.
- Clemence, S. P., and Finbarr, A. O. (1981). "Design Considerations for Collapsible Soils." *Journal of the Geotechnical Engineering Division*, ASCE, Vol. 107, No. GT3, March, pp. 305–317.
- Clifford, J. M. (1980). "An Introduction to Impact Rollers." *Proceedings of the International Conference on Compaction*, Paris, April, pp. 621–626.
- Clough, G. W., Iwabuchi, J., Rad, N. S., and Kuppusamy, T. (1989). "Influence of Cementation on Liquefaction of Sands." *Journal of Geotechnical Engineering*, ASCE, Vol. 115, No. 8, August, pp. 1102–1117.
- Cognon, J. M., Juran, I., and Thevanayagam, S. (1994). "Vacuum Consolidation Technology—Principles and Field Experience." *Vertical and Horizontal Deformations of Foundations and Embankments*, ASCE Geotechnical Special Publication No. 40, Vol. 2, pp. 1237–1248.
- D'Appolonia, D. J., Whitman, R. V., and D'Appolonia, E. D. (1969). "Sand Compaction with Vibratory Rollers." *Journal of the Soil Mechanics and Foundations Division*, ASCE, Vol. 95, No. SM1, January, pp. 263–284.
- Daniel, D. E. (1984). "Predicting Hydraulic Conductivity of Clay Liners." *Journal of Geotechnical Engineering*, ASCE, Vol. 110, No. 2, February, pp. 285–300.
- Daniel, D. E. (1993). "Clay Liners." Chapter 7 in *Geotechnical Practice for Waste Disposal*, edited by D. E. Daniel, Chapman & Hall, New York, pp. 137–163.
- Daniel, D. E., and Benson, C. H. (1990). "Water Content-Density Criteria for Compacted Soil Liners." *Journal of Geotechnical Engineering*, ASCE, Vol. 116, No. 12, December, pp. 1811–1830.
- D'Appolonia, D. J., Whitman, R. V., and D'Appolonia, E. D. (1969). "Sand compaction with vibratory rollers." *Journal of the Soil Mechanics and Foundations Division*, ASCE, Vol. 95, No. SM1, January, pp. 263–284.
- Daramola, O. (1980). "Effect of Consolidation Age on Stiffness of Sand." *Geoteknique*, Vol. 30, No. 2, June, pp. 213–216.
- Das, B. M. (1983). *Advanced Soil Mechanics*, Hemisphere Publishing, New York.
- Davis, R. E., Gailey, K. D., and Whitten, K. W. (1984). *Principles of Chemistry*, Saunders College Publishing, Philadelphia.
- Day, R. W. (1989). "Relative Compaction of Fill Having Oversize Particles." *Journal of Geotechnical Engineering*, ASCE, Vol. 115, No. 10, October, pp. 1487–1491.
- Day, R. W. (1991). "Expansion of Compacted Gravelly Clay." *Journal of Geotechnical Engineering*, ASCE, Vol. 117, No. 6, June, pp. 968–972.
- Day, R. W. (1992). "Effective Cohesion for Compacted Clay." *Journal of Geotechnical Engineering*, ASCE, Vol. 118, No. 4, April, pp. 611–619.
- Day, R. W. (1994). "Swell-Shrink Behavior of Compacted Clay." *Journal of Geotechnical Engineering*, ASCE, Vol. 120, No. 3, March, pp. 618–623.
- Diamond, S., and Kinter, E. B. (1965). "Mechanisms of Soil-Lime Stabilization, an Interpretive Review." *Highway Research Record No. 92: Lime Stabilization*, Highway Research Board, Washington, D.C., pp. 83–102.
- Disce, K., Stevens, M. G., and Von Thun, J. L. (1994). "Dynamic Compaction to Remediate Liquefiable Embankment Foundation Soils." *In-Situ Deep Soil Improvement*, ASCE Geotechnical Special Publication No. 45, K. M. Rollins, Ed., pp. 1–25.
- Douglas, B. J., Olsen, R. S., and Martin G. R. (1981). "Evaluation of Cone Penetrometer Test for SPT Liquefaction Assessment." *In Situ Testing to Evaluate Liquefaction Susceptibility*, Preprint 8 1–544, ASCE.
- Dumbleton, M. J. (1962). "Lime Stabilized Soil for Road Construction in Great Britain—A Laboratory Investigation." *Roads and Road Construction*, Vol. 40, November, pp. 321–325.
- Duncan, J. M. (1993). "Limitations of Conventional Analysis of Consolidation Settlement." *Journal of Geotechnical Engineering*, ASCE, 27th Terzaghi Lecture, Vol. 119, No. 9, pp. 1333–1359.
- Duncan, J. M., Byrne, P., Wong, K. S., and Mabry, P. (1980). "Strength, Stress-Strain, and Bulk Modulus Parameters for Finite Element Analyses of Stresses and Movements in Soil Masses." *Report No. UCB/GT/80-01*, University of California, Berkeley, August.
- Duncan, J. M., and Chang, C.-Y. (1970). "Nonlinear Analysis of Stress and Strain in Soils." *Journal of the Soil Mechanics and Foundations Division*, ASCE, Vol. 96, No. SMS, September, pp. 1629–1653.
- Duncan, J. M., and Seed, R. B. (1986). "Compaction-Induced Earth Pressures under  $K_0$ -Conditions." *Journal of Geotechnical Engineering*, ASCE, Vol. 112, No. 1, January, pp. 1–22.
- Esrig, M. I. (1968). "Pore Pressures, Consolidation, and Electrokinetics." *Journal of the Soil Mechanics and Foundations Division*, ASCE, Vol. 94, No. SM4, pp. 899–921.
- Evans, J. C., and Pancoski, S. E. (1989). "Organically Modified Clays." *Paper No. 880587*, Transportation Research Board, Washington, D.C., January.

- Felt, E. J., and Abrams, M. S. (1957). "Strength and Elastic Properties of Compacted Soil-Cement Mixtures." *Special Technical Publication No. 206*, ASTM.
- Ferguson, G. (1993). "Use of Self-Cementing Fly Ashes as a Soil Stabilization Agent." *Fly Ash for Soil Improvement*, ASCE Geotechnical Special Publication No. 36, pp. 1–14.
- Ferris, G. A., Eades, J. L., McClellan, G. H., and Graves, R. E. (1991). "Improved Characteristics in Sulfate Soils Pretreated with Barium Compounds Prior to Lime Stabilization." Paper presented at the 1991 Annual Meeting of the Transportation Research Board, Washington, D.C., January.
- FHWA (1979). *Soil Stabilization in Pavement Structures—A User's Manual*, Report No. FHWA-IP-80-2, Federal Highway Administration, Washington, D.C., October.
- Foreman, D. E., and Daniel, D. E. (1986). "Permeation of Compacted Clay with Organic Chemicals." *Journal of Geotechnical Engineering*, ASCE, Vol. 112, No. 7, July, pp. 669–681.
- Forssblad, L. (1981). *Vibratory Soil and Rock Fill Compaction*. Dynapac Maskin AB, Stockholm, Sweden.
- Foster, C. R. (1962). "Field Problems: Compaction." Chapter 12 in *Foundation Engineering*, edited by G. A. Leonards, McGraw-Hill, New York, pp. 1000–1024.
- Foster, C. R., and Ahlvin, R. G. (1954). "Stresses and Deflections Induced by a Uniform Circular Load." *Proceedings of the Highway Research Board*, Washington, D.C., Vol. 33, pp. 467–470.
- Fox, E. N. (1948). "The Mean Elastic Settlement of a Uniformly Loaded Area at a Depth below the Ground Surface." *Proceedings, Second International Conference on Soil Mechanics and Foundation Engineering*, Rotterdam, Netherlands, Vol. 1, pp. 129–132.
- Fox, L. (1948). "Computation of Traffic Stresses in a Simple Road Structure." *Proceedings of the Second International Conference on Soil Mechanics and Foundation Engineering*, Vol. 2, pp. 236–246.
- Fox, N. S. (1968). *Clay Stabilization in the Mekong Delta*, U.S. Army Report, 579th Engineer Detachment.
- Fragaszy, R. J., Su, J., and Siddiqi, F. H. (1992). "Effects of Oversize Particles on Density of Clean Granular Soils." *Geotechnical Testing Journal*, Vol. 12, No. 2, June, pp. 106–114.
- Fragaszy, R. J., Su, J., Siddiqi, F. H., and Ho, C. L. (1992). "Modeling Strength of Sandy Gravel." *Journal of Geotechnical Engineering*, ASCE, Vol. 118, No. 6, June, pp. 920–935.
- Fredlund, D. G., and Rahardjo, H. (1993). *Soil Mechanics for Unsaturated Soils*. John Wiley & Sons, New York.
- Fredlund, D. G., Morgenstern, N. R., and Widger, R. A. (1978). "The Shear Strength of Unsaturated Soils." *Canadian Geotechnical Journal*, Vol. 15, No. 3, pp. 313–321.
- Gambin, M. P. (1984). "Puits Ballastes a La Seyne—sur-Mer." *Proceedings of the International Conference on in Situ Soil and Rock Reinforcement*, Paris, pp. 139–144.
- Geopier Foundation Company (1998). *Geopier Foundation and Soil Reinforcement Manual*, Scottsdale, Arizona, September.
- Giesecking, J. E. (1939). "Mechanics of Cation Exchange in the Montmorillonite-Beidellite-Nontronite Type of Clay Mineral." *Soil Science*, Vol. 4, pp. 1–14.
- Godfrey, K. A. (1978). "Expansive and Shrinking Soils—Building Design Problems Being Attacked." *Civil Engineering*, ASCE, October, pp. 87–91.
- Goughnour, R. R. (1997). "Stone Column Construction by the Rotary Method." *Ground Improvement, Ground Reinforcement, Ground Treatment: Developments 1987–1997*, ASCE Geotechnical Special Publication No. 69, Edited by V. R. Schaefer, pp. 492–505.
- Grim, R. E. (1953). *Clay Mineralogy*, McGraw-Hill, New York.
- Grim, R. E. (1962). *Applied Clay Mineralogy*, McGraw-Hill, New York.
- Grim, R. E. (1968). *Clay Mineralogy*, 2nd Edition, McGraw-Hill, New York.
- Grubbs, B. R. (1990). "Lime-Induced Heave of Eagle Ford Clays in Southeast Dallas County." Presented at Texas Section ASCE Fall Meeting, El Paso, October 13.
- Hamed, J. T., Das, B. M., and Echelberger, W. F. (1986). "Bearing Capacity of a Strip Foundation on Granular Trench in Soft Clay." *Civil Engineering for Practicing and Design Engineers*, Pergamon Press, Vol. 5, pp. 359–376.
- Han, J., and Ye, S. (1991). "Analyses of Characteristics of Composite Grounds." *Proceedings of the First Young Asian Geotechnical Engineers Conference*, Bangkok, Thailand, January, pp. 197–206.
- Handy, R. L., and Fox, N. S. (1967). "A Soil Borehole Direct-Shear Test Device." *Highway Research News*, Vol. 27, pp. 42–51.
- Hanna, T. H. (1973). *Foundation Instrumentation*, Trans Tech Publications.
- Hanna, A. M. (1981). "Foundations on Strong Sand Overlying Weak Sand." *Journal of the Geotechnical Engineering Division*, ASCE, Vol. 107, No. GT7, pp. 915–927.
- Hansbo, S. (1979). "Consolidation of Clay by Band-Shaped Prefabricated Drains." *Ground Engineering*, Vol. 12, No. 5, July, pp. 16–25.
- Hansbo, S., Jamiolkowski, M., and Kok, L. (1981). "Consolidation by Vertical Drains." *Geotechnique*, March.
- Hansbo, S. (1983). "Technoeconomic Trend of Subsoil Improvement Methods in Foundation Engineering." *Pro-*

**6.334 SOIL IMPROVEMENT AND STABILIZATION**

- ceedings of the Eighth European Conference on Soil Mechanics and Foundation Engineering*, Helsinki, Finland, Vol. 3., pp. 1333–1343.
- Hansbo, S. (1987). "Design Aspects of Vertical Drains and Lime Column Installations." *Proceedings of the 9th Southeast Asian Geotechnical Conference*, Bangkok, Thailand, Vol. 2, pp. 8–12.
- Hausmann, M. R. (1990). *Engineering Principles of Ground Modification*, McGraw-Hill, New York.
- Herzog, A., and Mitchell, J. K. (1963). "Reactions Accompanying Stabilization of Clay with Cement." *Highway Research Record No. 36*, Highway Research Board, Washington, D.C., pp. 146–171.
- Hilf, J. W. (1959). *A Rapid Method of Construction Control for Embankments of Cohesive Soil*, Engineering Monograph No. 26, U.S. Department of the Interior, Bureau of Reclamation, Denver, Colorado.
- Hilf, J. W. (1991). "Compacted Fill." Chapter 8 in *Foundation Engineering Handbook*, 2d ed., edited by H.-Y. Fang, Van Nostrand Reinhold, New York, pp. 249–316.
- Hodek, R. J., and Lovell, C. W. (1979). "A New Look at Compaction Processes in Fills." *Bulletin of the Association of Engineering Geologists*, Vol. 16, No. 4, pp. 487–499.
- Hollon, G. W., and Marks, B. A. (1962). "A Correlation of Published Data on Lime-Pozzolan-Aggregate Mixtures for Highway Base Course Construction," Circular No. 72, Engineering Experiments Station, University of Illinois, Urbana.
- Holtz, R. D., Jamiołkowski, M. B., Lancellotta, R., and Pedroni, R. (1991). *Prefabricated Vertical Drains: Design and Performance*, Construction Industry Research and Information Association report, Butterworth-Heinemann, Oxford.
- Holtz, R. D., and Kovacs, W. D. (1981). *An Introduction to Geotechnical Engineering*, Prentice-Hall, Inc., Englewood Cliffs, New Jersey.
- Holtz, R. D., and Wager, O. (1975). "Preloading by Vacuum—Current Prospects." *Transportation Research Record No. 548*, Transportation Research Board, Washington, D.C., pp. 26–29.
- Holtz, W. G. (1969). "Volume Change in Expansive Clay Soils and Control by Lime Treatment." Presented at the Second International Research and Engineering Conference on Expansive Clay Soils, Texas A & M University, College Station, August.
- Houston, S. L., and Randeni, J. S. (1992). "Effect of Clod Size on Hydraulic Conductivity of Compacted Clay." *Geotechnical Testing Journal*, ASTM, Vol. 15, No. 2, June, pp. 123–128.
- Houston, S. L., and Walsh, K. D. (1993). "Comparison of Rock Correction Methods for Compaction of Clayey Soils." *Journal of Geotechnical Engineering*, ASCE, Vol. 119, No. 4, April, pp. 763–778.
- HRB (1952). *Highway Research Board Bulletin No. 58: Compaction of Embankments, Subgrades, and Bases*, Washington, D.C.
- HRB (1961). *Highway Research Board Bulletin No. 292: Soil Stabilization with Portland Cement*. Washington, D.C.
- Hsu, C.-L. (2000). "Uplift Capacity of Geopier Foundations" Master of Science Thesis, University of Utah, Department of Civil & Environmental Engineering.
- Huges, J. M. O., and Withers, N.J. (1974). "Reinforcing of Soft Cohesive Soils with Stone Columns." *Ground Engineering*, May, pp. 42–49.
- Hunter, D. (1988). "Lime-Induced Heave in Sulfate-Bearing Clay Soils." *Journal of Geotechnical Engineering*, ASCE, Vol. 114, No. 2, February, pp. 150–167.
- Ingles, O. G., and Metcalf, J. B. (1973). *Soil Stabilization: Principles and Practice*, John Wiley & Sons, New York.
- Ivanov, P. L. (1983). "Prediction and Control Techniques to Compact Loose Soils by Explosions." *Proceedings of the Eighth European Conference on Soil Mechanics and Foundation Engineering*, Helsinki, Finland, Vol. 1.
- Jaky, J. (1948). "Influence of Ground Water Level Oscillation on Subsidence of Structures." *Proceedings of the Second International Conference on Soil Mechanics and Foundation Engineering*, Rotterdam, pp. 148–150.
- Jamiołkowski, M., and Lancellotta, R. (1981). "Consolidation by Vertical Drains—Uncertainties Involved in Prediction of Settlement Rates." Panel Discussion, *Proceedings of the 10th International Conference on Soil Mechanics and Foundation Engineering*, Stockholm.
- Japanese Geotechnical Society (1998). *Remedial Measures Against Soil Liquefaction*. Edited by the Japanese Geotechnical Society, A. A. Balkema, Rotterdam.
- Jones, A. (1962). "Tables of Stresses in Three-Layer Elastic Systems." *Highway Research Board Bulletin 342: Stress Distribution in Earth Masses*, Washington, D.C., pp. 176–214.
- Jones, D. E. Jr., and Jones, K. A. (1987). "Treating Expansive Soils." *Civil Engineering*, ASCE, Vol. 57, No. 8, August, pp. 62–65.
- Jordan, J. W. (1949). "Alteration of the Properties of Bentonite by Reaction with Amines." *Journal of Mineralogical Society*, London, June.
- Kerisel, J. (1985). "The History of Geotechnical Engineering Up Until 1700." *Proceedings of the Eleventh Inter-*

- national Conference on Soil Mechanics and Foundation Engineering*, San Francisco, A. A. Balkema, Boston, pp. 3–93.
- Kim, W.-H., and Daniel, D. E. (1992). "Effects of Freezing on Hydraulic Conductivity of Compacted Clay." *Journal of Geotechnical Engineering*, ASCE, Vol. 118, No. 7, July, pp. 1083–1097.
- Kjellman, W. (1948). "Accelerating Consolidation of Fine-Grained Soils by Means of Card-Board Wicks." *Proceedings of the 2nd International Conference on Soil Mechanics and Foundation Engineering*, Rotterdam, Vol. 2, pp. 302–305.
- Koerner, R. M. (1994). *Designing with Geosynthetics*, 3rd edition, Prentice-Hall, Englewood Cliffs, New Jersey, p. 735.
- Kyulule, A. L. (1983). "Additional Considerations on Compaction of Soils in Developing Countries." No. 121, *Mitteilungen des Institutes fur Grundbau und Bodenmechanik Eidgenossische Technische Hochschule Zurich*.
- Ladd, C. C. (1986). "Stability Evaluation During Staged Construction." Terzaghi Lecture, ASCE Convention, Boston, October (as cited in Rixner, et al., 1986).
- Ladd, C. C., and Foott, R. (1977). "Foundation Design of Embankments on Varved Clays." *Report No. FHWA-TS-77-214*, Federal Highway Administration, Washington, D.C.
- Lade, P. V., and Lee, K. L. (1976). "Engineering Properties of Soils." *Report No. UCLA-ENG-7652*, University of California at Los Angeles.
- Lambe, T. W. (1958). "The Structure of Compacted Clay." *Journal of the Soil Mechanics and Foundations Division*, Proceedings of ASCE, No. SM2, May, pp. 1654–1 to 1654–34.
- Lambe, T. W. (1967). "Stress Path Method." *Journal of the Soil Mechanics and Foundations Division*, Proceedings of ASCE, No. SM6, November, pp. 309–331.
- Lambe, T. W., Michaels, A. S., and Mob, Z. C. (1960). "Improvements of Soil-Cement with Alkali Metal Compounds." *Highway Research Board Bulletin No. 241: Soil Stabilization with Asphalt, Portland Cement, Lime and Chemicals*, Washington, D.C., pp. 67–103.
- Lambe, T. W., and Whitman, R. V. (1979). *Soil Mechanics, SI Version*, Wiley, New York.
- Larson, C. T., Lawton, E. C., Bravo, A., and Perez, Y. (1993). "Influence of Oversize Particles on Wetting-Induced Collapse of Compacted Clayey Sand." *Proceedings of the 29th Symposium on Engineering Geology and Geotechnical Engineering*, Reno, Nevada, March, pp. 449–459.
- Lawton, E. C. (1986). "Wetting-Induced Collapse in Compacted Soil." Ph.D. thesis, Washington State University, Pullman, Washington.
- Lawton, E. C. (1999). "Performance of Geopier Foundations during Simulated Seismic Tests at South Temple Bridge on Interstate 15, Salt Lake City Utah." *Report No. UUCVEEN 99-06*, University of Utah, Department of Civil & Environmental Engineering, Salt Lake City.
- Lawton, E. C., Chen, J., Larson, C. T., Perez, Y., and Bravo, A. (1993). "Influence of Chemical Admixtures and Pore Fluid Chemistry on Wetting Induced Collapse of Compacted Soil." *Proceedings of the 29th Symposium on Engineering Geology and Geotechnical Engineering*, Reno, Nevada, March, pp. 425–448.
- Lawton, E. C., Fox, N. S., and Handy, R. L. (1994). "Control of Settlement and Uplift of Structures Using Short Aggregate Piers." *In-Situ Deep Soil Improvement*, ASCE Geotechnical Special Publication No. 45 (edited by K. M. Rollins), pp. 121–132.
- Lawton, E. C., Fragaszy, R. J., and Hardcastle, J. H. (1989). "Collapse of Compacted Clayey Sand." *Journal of Geotechnical Engineering*, ASCE, Vol. 115, No. 9, September, pp. 1252–1267.
- Lawton, E. C., Fragaszy, R. J., and Hardcastle, J. H. (1991). "Stress Ratio Effects on Collapse of Compacted Clayey Sand." *Journal of Geotechnical Engineering*, ASCE, Vol. 117, No. 5, May, pp. 714–730.
- Lawton, E. C., Fragaszy, R. J., and Hetherington, M. D. (1992). "Review of Wetting-Induced Collapse in Compacted Soil." *Journal of Geotechnical Engineering*, ASCE, Vol. 115, No. 9, September, pp. 1376–1394.
- Leadabrand, J. A. (1956). "Some Engineering Aspects of Soil-Cement Mixtures." Mid-South Section, ASCE, April 27.
- Lee, K. L. (1965). "Triaxial Compressive Strength of Saturated Sands under Seismic Loading Conditions." Ph.D. dissertation, University of California at Berkeley.
- Lee, K. L., and Seed, H. B. (1967a). "Cyclic Stress Conditions Causing Liquefaction of Sand." *Journal of the Soil Mechanics and Foundations Division*, ASCE, Vol. 93, No. 1, January, pp. 47–70.
- Lee, K. L., and Seed, H. B. (1967b). "Drained Strength Characteristics of Sands." *Journal of the Soil Mechanics and Foundations Division*, ASCE, Vol. 93, No. SM6, November, pp. 117–141.
- Lee, K. L., and Seed, H. B. (1967c). "Effect of Moisture on the Strength of a Clean Sand." *Journal of the Soil Mechanics and Foundations Division*, ASCE, Vol. 93, No. SM6, November, pp. 17–40.
- Lee, K. L., and Singh, A. (1971). "Compaction of Granular Soils." *Proceedings of the Ninth Annual Symposium on Engineering Geology and Soils Engineering*, Boise, Idaho, pp. 161–174.
- Lee, P. Y., and Suedkamp, R. J. (1972). "Characteristics of Irregularly Shaped Compaction Curves of Soils."

**6.336** SOIL IMPROVEMENT AND STABILIZATION

- Highway Research Record No. 381: Compaction and Stabilization*, Highway Research Board, Washington, D.C., pp. 1–9.
- Leonard, R. J., and Davidson, D. T. (1959). "Pozzolanic Reactivity Study of Flyash." *Highway Research Board Bulletin No. 231: Lime and Lime-Flyash as Soil Stabilizers*, Washington, D.C., pp. 1–14.
- Leonards, G. A., and Narain, J. (1963). "Flexibility of Clay and Cracking of Earth Dams." *Journal of the Soil Mechanics and Foundations Division*, ASCE, Vol. 89, No. 2, pp. 47–98.
- Liausu, P. (1984). "Renforcement de Couches de Sol Compressibles par Substitution Dynamique (Compressible Soil Layers Reinforcement by Means of Dynamic Replacement)." *Proceedings of the International Conference on in Situ Soil and Rock Reinforcement*, Paris, pp. 151–155.
- Lin, P. S., and Lovell, C. W. (1981). "Compressibility of Field Compacted Clay." *Joint Highway Research Project Report No. 81-14*, Purdue University, West Lafayette, Indiana.
- Lin, P. S., and Lovell, C. W. (1983). "Compressibility of Field Compacted Clay." *Transportation Research Record No. 897*, Transportation Research Board, Washington, D.C., pp. 51–60.
- Little, D. N., and Deuel, L. (1989). "Evaluation of Sulfate-Induced Heave at Joe Pool Lake." Report Prepared for Chemical Lime Company, June.
- Little, D. N., Thompson, M. R., Terrell, R. L., Epps, J. A., and Barenberg, E. J. (1987). "Soil Stabilization for Roadways and Airfields." Report No. ESL-TR-86-19, Air Force Engineering and Services Center, Tyndall AFB, Florida, July.
- Lukas, R. G. (1986). "Dynamic Compaction for Highway Construction, Volume I: Design and Construction Guidelines." *Report No. FHWA/RD-86/133*, Federal Highway Administration, Washington, D.C., July.
- Lukas, R. G. (1995). "Dynamic Compaction." *Report No. FHWA-SA-95-037*, Geotechnical Engineering Circular No. 1, Federal Highway Administration, Washington, D.C., October.
- MacMurdo, F. D., and Barenberg, E. J. (1973). "Determination of Realistic Cutoff Dates for Late-Season Construction with Lime-fly Ash and Lime-Cement-Fly Ash Mixtures." *Highway Research Record No. 442*, Highway Research Board, Washington, D.C., pp. 92–101.
- Madhav, M. R., and Vitkar, P. P. (1978). "Strip Footing on Weak Clay Stabilized with a Granular Trench or Pile." *Canadian Geotechnical Journal*, Vol. 15, pp. 605–609.
- Mahmood, A., and Mitchell, J. K. (1974). "Fabric-Property Relationships in Fine Granular Soils." *Clays and Clay Minerals*, Vol. 22, nos. 5/6, pp. 397–408.
- Marsal, R. J., and Ramírez de Arellano, L. (1967). "Performance of El Infiernillo Dam, 1963–1966." *Journal of the Soil Mechanics and Foundations Division*, ASCE, Vol. 93, No. SM4, July, pp. 265–298.
- Mayne, P. W., Jones, Jr., J. S., and Dumas, J. C. (1984). "Ground Response to Dynamic Compaction." *Journal of Geotechnical Engineering*, ASCE, Vol. 110, No. 6, June, pp. 757–774.
- McLaughlin, H. C., et al. (1976). "Aqueous Polymers for Treating Clays." *SPE Paper No. 6008*, Society of Petroleum Engineers, Bakersfield, California.
- Meehan, R. L. (1967). "The Uselessness of Elephants in Compacting Soil." *Canadian Geotechnical Journal*, Vol. 4, No. 3, September, pp. 358–360.
- Meyerhof, G. G. (1951). "The Ultimate Bearing Capacity of Foundations." *Geotechnique*, Vol. 2, No. 4, pp. 301–331.
- Meyerhof, G. G. (1956). "Penetration Tests and Bearing Capacity of Cohesionless Soils." *Journal of the Soil Mechanics and Foundations Division*, ASCE, Vol. 82, No. SM1, pp. 1–19.
- Meyerhof, G. G. (1963). "Some Recent Research on the Bearing Capacity of Foundations." *Canadian Geotechnical Journal*, Vol. 1, No. 1, September, pp. 16–26.
- Meyerhof, G. G. (1965). "Shallow Foundations." *Journal of the Soil Mechanics and Foundations Division*, ASCE, Vol. 91, No. SM2, pp. 21–31.
- Meyerhof, G. G., and Hanna, A. M. (1978). "Ultimate Bearing Capacity of Foundations on Layered Soils under Inclined Load." *Canadian Geotechnical Journal*, Vol. 15, No. 4, pp. 565–572.
- Minnick, L. J. (1967). "Reactions of Hydrated Lime with Pulverized Coal Fly Ash." *Proceedings of the Fly Ash Utilization Conference*. Bureau of Mines Information Circular 8348.
- Mitchell, J. K. (1960). "Fundamental Aspects of Thixotropy in Soils." *Journal of the Soil Mechanics and Foundations Division*, ASCE, Vol. 86, No. SM3, pp. 19–52.
- Mitchell, J. K. (1981). "Soil Improvement: State-of-the-Art." *Proceedings of the Tenth International Conference on Soil Mechanics and Foundation Engineering*, Stockholm, Sweden, Vol. 4, pp. 509–565.
- Mitchell, J. K. (1986). "Practical Problems from Surprising Soil Behavior." *Journal of Geotechnical Engineering*, ASCE, Vol. 112, No. 3, March, pp. 259–289.
- Mitchell, J. K. (1993). *Fundamentals of Soil Behavior*, 2d ed., Wiley, New York.
- Mitchell, J. K., Hooper, D. R., and Campanella, R. G. (1965). "Permeability of Compacted Clay." *Journal of the Soil Mechanics and Foundations Division*, ASCE, Vol. 91, No. SM4, July, pp. 41–65.

- Mitchell, J. K., and Wan, T. Y. (1977). "Electro-Osmotic Consolidation—Its Effect on Soft Soils." *Proceedings of the Ninth International Conference on Soil Mechanics and Foundation Engineering*, Vol. 1, pp. 219–224.
- Morgenstern, N. R. (1979). "Properties of Compacted Soils." *Proceedings of the Sixth Pan-American Conference on Soil Mechanics and Foundation Engineering*, Lima, Peru, Vol. 3, pp. 349–354.
- Moseley, M. P. and Priebe, H. J. (1993). "Vibro Techniques." Chapter 1 in *Ground Improvement*, Edited by M. P. Moseley, Blackie Academic and Professional, Boca Raton, Florida, pp. 1–19.
- Nakayama, H., and Handy, R. L. (1965). "Factors Influencing Shrinkage of Soil-Cement." *Highway Research Record No. 86: Soil-Cement Stabilization*, Highway Research Board, Washington, D.C., pp. 15–27.
- Nalezy, C. L., and Li, M. C. (1967). "Effect of Soil Structure and Thixotropic Hardening on the Swelling Behavior of Compacted Clay Soils." *Highway Research Record No. 209: Physicochemical Properties of Soils*, Highway Research Board, Washington, D.C., pp. 1–19.
- Narin van Court, W. A., and Mitchell, J. K. (1995). "New Insights into Explosive Compaction of Loose, Saturated Cohesionless Soils." *Soil Improvement for Earthquake Hazard Mitigation*, ASCE Geotechnical Special Publication No. 49, Edited by R. D. Hryciw, pp. 51–65.
- NAVDOCKS (1961). "Design Manual: Soil Mechanics, Foundations, and Earth Structures." *NAVDOCKS DM-7*, Department of the Navy, Washington, D.C.
- NCEER (1997). "Summary Report." *Proceedings of the NCEER Workshop on Evaluation of Liquefaction Resistance of Soils*, Technical Report No. NCEER-97-0022, Edited by T. L. Youd and I. M. Idriss, National Center for Earthquake Engineering Research, State University of New York at Buffalo, pp. 1–40.
- NCHRP (1976). *Lime-Fly Ash-Stabilized Bases and Subbases*, National Cooperative Highway Research Program Synthesis of Highway Practice No. 37, Transportation Research Board, Washington, D.C.
- Nelson, J. D., and Miller, D. J. (1992). *Expansive Soils: Problems and Practice in Foundation and Pavement Engineering*, Wiley, New York.
- Nicholls, H. R., Johnson, C. F., and Duvall, W. I. (1971). "Blasting Vibrations and Their Effects on Structures." *Bulletin 656*, U.S. Bureau of Mines.
- Nishida, Y. (1966). "Vertical Stress and Vertical Deformation of Ground under a Deep Circular Uniform Pressure in the Semi-Infinite." *Proceedings of the First Congress of the International Society of Rock Mechanics*, Lisbon, Portugal, Vol. 2, pp. 493–497.
- Noorany, I. (1987). "Precision and Accuracy of Field Density Tests in Compacted Soils." *Research Report*, Department of Civil Engineering, San Diego State University, San Diego, California.
- Noorany, I., and Stanley, J. V. (1994). "Settlement of Compacted Fills Caused by Wetting." *Vertical and Horizontal Deformations of Foundations and Embankments*, ASCE Geotechnical Special Publication No. 40, Vol. 2, pp. 15 16–1530.
- NRC (1985). *Liquefaction of Soils during Earthquakes*, National Research Council, National Academy Press, Washington, D.C.
- Oda, M. (1972). "Initial Fabrics and Their Relations to Mechanical Properties of Granular Material." *Soils and Foundations*, Vol. 12, No. 1, March, pp. 17–36.
- Olsen, H. W. (1962). "Hydraulic Flow through Saturated Clays." *Clays and Clay Minerals*, Vol. 9, No. 2, pp. 131–161.
- Orcutt, R. G., et al. (1955). "The Movement of Radioactive Strontium through Naturally Porous Media." *Atomic Energy Commission Report*, November 1.
- Osterberg, J. O. (1957). "Influence Values for Vertical Stresses in a Semi-Infinite Mass Due to an Embankment Loading." *Proceedings of the Fourth International Conference on Soil Mechanics and Foundation Engineering*, London, Vol. 1, pp. 393–394.
- PCA (1968). *Design and Control of Concrete Mixtures*, 11th ed., Portland Cement Association, Skokie, Illinois, July.
- PCA (1971). *Soil-Cement Laboratory Handbook*, Portland Cement Association, Skokie, Illinois.
- PCA (1979). *Soil-Cement Construction Handbook*, Portland Cement Association, Skokie, Illinois.
- Peattie, K. R. (1962). "Stress and Strain Factors for Three-Layer Elastic Systems." *Highway Research Board Bulletin 342: Stress Distribution in Earth Masses*, Washington, D.C., pp. 215–253.
- Penn, L. L. (1992). "Expansion of Lime-Treated Clays Containing Sulfates." *Proceedings of the Seventh International Conference on Expansive Soils*, Dallas, Texas, August, Vol. 1, pp. 409–414.
- Petry, T. M., and Brown, R. W. (1987). "Laboratory and Field Experiences Using Soil Sta Chemical Soil Stabilizer." ASCE Paper Presented at San Antonio, Texas, October 3, 1986. *Texas Civil Engineer*, February 1987, pp. 15–19.
- Petry, T. M., and Little, D. N. (1992). "Update on Sulfate Induced Heave in Treated Clays; Problematic Sulfate Levels." *Transportation Research Record No. 1362: Aggregate and Pavement-Related Research*, Transportation Research Board, Washington, D.C., pp. 51–55.

**6.338 SOIL IMPROVEMENT AND STABILIZATION**

- Pilot, G. (1977). "Methods of Improving the Engineering Properties of Soft Clay: State of the Art." *Proceedings of the Symposium on Soft Clay*, Bangkok.
- Poesch, H., and Ikes, W. (1975). *Verdichtungstechnik und Verdichtungsgeräte in Erdbau (Compaction Techniques and Compaction Equipment in Earth Construction)*, in German, Wilhelm Ernst & Sohn, Berlin.
- Poran, C. J., and Abtehi-Ali, F. (1989). "Properties of Solid Waste Incinerator Fly Ash." *Journal of Geotechnical Engineering*, ASCE, Vol. 115, No. 8, August, pp. 1118–1133.
- Poulos, H. G., and Davis, E. H. (1974). *Elastic Solutions for Soil and Rock Mechanics*. Wiley, New York.
- Poulos, S. J. (1988). "Compaction Control and the Index Unit Weight." *Geotechnical Testing Journal*, ASTM, Philadelphia, Vol. 11, No. 2, June, pp. 100–108.
- Priebe, H. J. (1988). "On Assessing the Behavior of a Soil Improved by Vibro-Replacement." *Bautechnik*, Vol. 65, No. 1, pp. 23–26.
- Proctor, R. R. (1933). "Fundamental Principles of Soil Compaction." *Engineering News-Record*, Vol. 111, Nos. 9, 10, 12, and 13.
- Redus, J. F. (1958). "Study of Soil-Cement Base Courses on Military Airfields." *Highway Research Board Bulletin No. 198: Cement-Soil Stabilization*, Washington, D.C., pp. 13–19.
- Reinhold, F. (1955). "Soil-Cement Methods for Residential Streets in Western Germany." *World Construction*, March-April, p. 41.
- Rixner, J. J., Kraemer, S. R., and Smith, A. D. (1986). "Prefabricated Vertical Drains: Volume I, Engineering Guidelines." *Report No. FHWA/RD-86/168*, Federal Highway Administration, Washington, D.C.
- Rizkallah, V., and Hellweg, V. (1980). "Compaction of Non Cohesive Soils by Watering." *Proceedings of the International Conference on Compaction*, Paris, April, pp. 357–361.
- Robertson, P. K., and Campanella, R. G. (1985). "Liquefaction Potential of Sands Using the CPT." *Research Report R69-15*, Department of Civil Engineering, Massachusetts Institute of Technology, Cambridge, Massachusetts.
- Rollins, K. M., Jorgensen, S. J., and Ross, T. E. (1998). "Optimum Moisture Content for Dynamic Compaction of Collapsible Soils." *Journal of Geotechnical and Geoenvironmental Engineering*, ASCE, Vol. 124, No. 8, August, pp. 699–708.
- Rollins, K. M., and Rogers, G. W. (1994). "Mitigation Measures for Small Structures on Collapsible Alluvial Soils." *Journal of Geotechnical Engineering*, ASCE, Vol. 120, No. 9, September, pp. 1533–1553.
- Schmertmann, J. H. (1970). "Static Cone to Compute Settlement over Sand." *Journal of the Soil Mechanics and Foundations Division*, ASCE, Vol. 96, No. SM3, pp. 1011–1043.
- Schmertmann, J. H. (1978). "Guidelines for Cone Penetration Test Performance and Design." *Report No. FHWA-TS-78-209*, U.S. Department of Transportation, Federal Highway Administration, Washington, D.C., July.
- Schmertmann, J. H. (1989). "Density Tests above Zero Air Voids Line." *Journal of Geotechnical Engineering*, ASCE, Vol. 115, No. 7, July, pp. 1003–1018.
- Schmertmann, J. H. (1991). "The Mechanical Aging of Soils." *Journal of Geotechnical Engineering*, ASCE, Vol. 117, No. 9, September, pp. 1288–1330.
- Schmertmann, J. H., Hartman, J. P., and Brown, P. R. (1978). "Improved Strain Influence Factor Diagrams." *Journal of the Geotechnical Engineering Division*, ASCE, Vol. 104, No. GT8, pp. 1131–1135.
- Seed, H. B. (1979). "Soil Liquefaction and Cyclic Mobility Evaluation for Level Ground during Earthquakes." *Journal of the Geotechnical Engineering Division*, ASCE, Vol. 105, No. GT2, February, pp. 201–255.
- Seed, H. B. (1986). "Design Problems in Soil Liquefaction." *Report No. UCB/EERC-86/02*, University of California at Berkeley, February.
- Seed, H. B., and Chan, C. K. (1959a). "Structure and Strength Characteristics of Compacted Clays." *Journal of the Soil Mechanics and Foundations Division*, ASCE, Vol. 85, No. SM5, October, pp. 87–128.
- Seed, H. B., and Chan, C. K. (1959b). "Undrained Strength of Compacted Clays after Soaking." *Journal of the Soil Mechanics and Foundations Division*, ASCE, Vol. 85, No. SM6, December, pp. 31–47.
- Seed, H. B., and Idriss, I. M. (1967). "Analysis of Soil Liquefaction: Nigata Earthquake." *Journal of the Soil Mechanics and Foundations Division*, ASCE, Vol. 93, No. SM3, May, pp. 83–108.
- Seed, H. B., and Idriss, I. M. (1971). "Simplified Procedure for Evaluating Soil Liquefaction Potential." *Journal of the Soil Mechanics and Foundations Division*, ASCE, Vol. 97, No. SM9, September, p. 1249.
- Seed, H. B., and Idriss, I. M. (1982). "Ground Motions and Soil Liquefaction During Earthquakes." Earthquake Engineering Research Institute, Berkeley, California.
- Seed, H. B., Idriss, I. M., and Arango, I. (1983). "Evaluation of Liquefaction Potential Using Field Performance Data." *Journal of Geotechnical Engineering*, Vol. 109, No. 3, March, pp. 458–482.
- Seed, H. B., and Lee, K. L. (1966). "Liquefaction of Saturated Sands during Cyclic Loading." *Journal of the Soil Mechanics and Foundations Division*, ASCE, Vol. 92, No. SM6, November, pp. 105–134.

- Seed, H. B., Mitchell, J. K., and Chan, C. K. (1960). "The Strength of Compacted Cohesive Soil." *Proceedings of the Research Conference on Shear Strength of Cohesive Soils*, ASCE, Boulder, Colorado, June.
- Seed, H. B., Tokimatsu, K., Harder, L. F., and Chung, R. M. (1985). "Influence of SPT Procedures in Soil Liquefaction Resistance Evaluations." *Journal of Geotechnical Engineering*, ASCE, Vol. 111, No. 12, December, pp. 1425-1445.
- Selig, E. T., and You, T.-S. (1977). "Fundamentals of Vibratory Roller Behavior." *Proceedings of the Ninth International Conference on Soil Mechanics and Foundation Engineering*, Tokyo, Vol. 2, pp. 375-380.
- Shelley, T. L., and Daniel, D. E. (1993). "Effect of Gravel on Hydraulic Conductivity of Compacted Soil Liners." *Journal of Geotechnical Engineering*, ASCE, Vol. 119, No. 1, January, pp. 54-68.
- Sherard, J. L., Woodward, R. J., Gizienski, S. F., and Clevenger, W. A. (1963). *Earth and Earth-Rock Dams*, Wiley, New York.
- Sherif, M. A., et al. (1982). "Swelling of Wyoming Montmorillonite and Sand Mixtures." *Journal of Geotechnical Engineering*, ASCE, Vol. 108, No. GT1, January, pp. 33-45.
- Sherman, G. B., Watkins, R. O., and Prysock, R. H. (1967). "A Statistical Analysis of Embankment Compaction." *Highway Research Record No. 177: Symposium on Compaction of Earthwork and Granular Bases*, Highway Research Board, Washington, D.C., pp. 157-185.
- Sherwood, P. T. (1962). "Effect of Sulfates on Cement- and Lime-Stabilized Soils." *Highway Research Board Bulletin No. 353: Stabilization of Soils with Portland Cement*, Washington, D.C., pp. 98-107. Also in *Roads and Road Construction*, Vol. 40, February, pp. 34-40.
- Siddiqi, F. H., Seed, R. B., Chan, C. K., Seed, H. B., and Pyke, R. M. (1987). "Strength Evaluation of Coarse-Grained Soils." *Report No. UCB/EERC-87/22*, University of California, Berkeley.
- Skempton, A. W., and Bjerrum, L. (1957). "A Contribution to the Settlement Analysis of Foundations on Clay." *Geotechnique*, Vol. 7, No. 4, pp. 168-178.
- Skinner, B. J., and Porter, S. C. (1987). *Physical Geology*, Wiley, New York.
- Skopek, J. (1961). "The Influence of Foundation Depth on Stress Distribution." *Proceedings of the Fifth International Conference on Soil Mechanics and Foundation Engineering*, Paris, France, Vol. 1, p. 815.
- Sokolovich, V. E., and Semkin, V. V. (1984). "Chemical Stabilization of Loess Soils." *Soil Mechanics and Foundation Engineering*, Vol. 21, No. 4, July-August, pp. 8-11.
- Sonu, C. J., Ito, K., and Hiroshi, O. (1993). "Harry Seed, Liquefaction and the Gravel Drain." *Civil Engineering*, ASCE, December, pp. 58-60.
- Sowers, G. F., Williams, R. C., and Wallace, T. S. (1965). *Proceedings of the Sixth International Conference on Soil Mechanics and Foundation Engineering*, Montreal, Vol. 2, pp. 561-565.
- Spangler, M. G., and Handy, R. L. (1982). *Soil Engineering*, 4th ed., Harper & Row, New York.
- Taki, O., and Yang, D. S. (1991). "Soil-Cement Mixed Wall Technique." *Geotechnical Engineering Congress 1991*, edited by F. G. McLean, D. A. Campbell, and D. W. Harris, ASCE Geotechnical Special Publication No. 27, Vol. 1, pp. 298-309.
- Terdich, G. M. (1981). "Prediction and Control of Field Swell Pressures of Compacted Medium Plastic Clay." *Joint Highway Research Project Report No. 81-4*, Purdue University, West Lafayette, Indiana.
- Terzaghi, K. (1955). "Evaluation of Coefficients of Subgrade Reaction." *Geotechnique*, Vol. 5, No. 4, December, pp. 297-326.
- Terzaghi, K., and Peck, R. B. (1967). *Soil Mechanics In Engineering Practice*, 2d ed., Wiley, New York.
- Themn de Barros, S. (1966). "Deflection Factor Charts for Two and Three-Layer Elastic Systems." *Highway Research Record No. 145*, Highway Research Board, Washington, D.C., pp. 83-108.
- Thompson, G. H., and Herbert, A. (1978). "Compaction of Clay Fills in-Situ by Dynamic Consolidation." *Proceedings of the Conference on Clay Fills*, Institution of Civil Engineers, London, pp. 197-204.
- Thompson, M. R. (1966). "Shear Strength and Elastic Properties of Lime-Soil Mixtures." *Highway Research Record No. 139: Behavior Characteristics of Lime-Soil Mixtures*, Highway Research Board, Washington, D.C., pp. 1-14.
- Thompson, M. R. (1969). "Engineering Properties of Soil-Lime Mixtures." *Journal of Materials*, ASTM, Vol. 4, No. 4, December.
- Townsend, D. L., and Klym, T. W. (1966). "Durability of Lime-Stabilized Soils." *Highway Research Record No. 139: Behavior of Lime-Soil Mixtures*, Highway Research Board, Washington, D.C., pp. 25-41.
- Trautwein, S. J. (1993). "Field Hydraulic Conductivity Testing." *Permeability of Soil Liners for Waste Containment Facilities*, Notes for Short Course, Reno, Nevada, March.
- TRB (1987). *Lime Stabilization: Reactions, Properties, Design, and Construction*, State of the Art Report 5, Transportation Research Board, Washington, D.C.
- Turnbull, W. J., Compton, J. R., and Ahlvin, R. G. (1966). "Quality Control of Compacted Earthwork." *Journal of the Soil Mechanics and Foundations Division*, ASCE, Vol. 92, No. SM1, January, pp. 93-103.

**6.340** SOIL IMPROVEMENT AND STABILIZATION

- Ueshita, K., and Meyerhof, G. G. (1967). "Deflection of Multilayer Soil Systems." *Journal of the Soil Mechanics and Foundations Division*, ASCE, Vol. 93, No. SM5, pp. 257–282.
- U.S. Army (1985). "Operator's and Organizational Maintenance Manual for Tester, Density and Moisture (Soil and Asphalt), Nuclear Method." *Technical Manual (TM) 5-6635-386-12&P*, U.S. Department of the Army.
- Uzan, J., Ishai, I., and Hoffman, M. S. (1980). "Surface Deflexion in a Two-Layer Elastic Medium Underlain by a Rough Rigid Base." *Geotechnique*, Vol. 30, No. 1, pp. 39–47.
- Valsangkar, A. J., and Meyerhof, G. G. (1979). "Experimental Study of Punching Coefficients and Shape Factor for Two-Layered Soils." *Canadian Geotechnical Journal*, Vol. 16, No. 4, November, pp. 802–805.
- Vesic, A. S. (1975). "Bearing Capacity of Shallow Foundations." Chapter 3 in *Foundation Engineering Handbook*, edited by H. F. Winterkorn and H.-Y. Fang, Van Nostrand Reinhold, New York, pp. 121–147.
- Wacker (1987). *Soil Compaction and Equipment for Confined Areas*, Wacker Corporation, Menomonee Falls, Wisconsin.
- Waidelich, W. C. (1990). "Earthwork Construction." Chapter 4 in *Guide to Earthwork Construction*, State of the Art Report 8, Transportation Research Board, Washington, D.C., pp. 25–48.
- Walsh, K. D., Houston, W. N., and Houston, S. L. (1993). "Evaluation of in-Place Wetting Using Soil Suction Measurements." *Journal of Geotechnical Engineering*, ASCE, Vol. 119, No. 5, May, pp. 862–873.
- Wan, T. Y., and Mitchell, J. K. (1976). "Electro-Osmotic Consolidation of Soils." *Journal of the Geotechnical Engineering Division*, ASCE, Vol. 102, No. GT5, pp. 473–491.
- Welsh, J. P. (1986). "In Situ Testing for Ground Modification Techniques." *Proceedings of in Situ '86*, Blacksburg, Virginia, American Society of Civil Engineers, pp. 322–335.
- West, G. (1959). "A Laboratory Investigation into the Effect of Elapsed Time after Mixing on the Compaction and Strength of Soil-Cement." *Geotechnique*, Vol. 9, pp. 22–28.
- Williams, L. H., and Undercover, D. R. (1980). "New Polymer Offers Effective, Permanent Clay Stabilization Treatment." *Society of Petroleum Engineers Paper No. 8797*, January.
- Wilson, S. D. (1970). "Suggested Method of Test for Moisture-Density Relations of Soils Using Harvard Compaction Apparatus." *STP No. 479*, ASTM, pp. 101–103.
- Wimberley, P. L. III, Mazzella, S. G., and Newman, F. B. (1994). "Settlement of a 15-Meter Deep Fill Below a Building." *Vertical and Horizontal Deformations of Foundations and Embankments*, ASCE Geotechnical Special Publication No. 40, edited by A. T. Yeung and G. Y. Felio, Vol. 1, pp. 398–416.
- Yi, F. (1991). "Behavior of Compacted Collapsible Soils Subjected to Water Infiltration." Doctor of Engineering thesis, University of Tokyo, Tokyo, Japan.
- Youd, T. L. (1993). "Liquefaction-Induced Lateral Spread Displacement." *NCEL Technical Note*, Naval Civil Engineering Laboratory, Port Hueneme, California.
- Zeller, J., and Wullimann, R. (1957). "The Shear Strength of Shell Materials for the Goschenalp Dam, Switzerland." *Proceedings of the Fourth International Conference on Soil Mechanics and Foundation Engineering*, London, England, Vol. 2, pp. 399–404.